IEEE
CONFERENCE RECORD — ABSTRACTS

1997 IEEE International Conference on Plasma Science



19970909 125

19 – 22 May 1997

San Diego, California

Sponsored by

Plasma Science and Applications Committee
of
The IEEE Nuclear and Plasma Sciences Society

DTIC QUALITY INSPECTED 3

DISTRIBUTION STATEMENT A
Approved for public release;
Distribution Unlimited

IEEE CONFERENCE RECORD—ABSTRACTS
1997 IEEE INTERNATIONAL CONFERENCE ON PLASMA SCIENCE

Copyright and Reprint Permission: Abstracting is permitted with credit to the source. Libraries are permitted to photocopy beyond the limit of U.S. Copyright law for private use of patrons those articles in this volume that carry a code at the bottom of the first page, provided that per-copy fee indicated in the code is paid through Copyright Clearance Center, 222 Rosewood Drive, Danvers, MA 01923. For other copying, reprint or reproduction permission write to: IEEE Copyrights Manager, IEEE Service Center, 445 Hoes Lane, PO Box 1331 Piscataway, NJ 08855-1331. All rights reserved. Copyright ©1997 by the Institute of Electrical and Electronics Engineers, Inc.

IEEE Catalog Number:	97CH36085
ISBN	0-7803-3990-8 (Softbound Edition)
ISBN	0-7803-3991-6 (Casebound Edition)
ISBN	0-7803-3992-4 (Microfiche Edition)
Library of Congress:	81-644315
ISSN	0730-9244

Additional copies of this Conference Record are available from
IEEE Service Center
445 Hoes Lane
Piscataway, NJ 08854-1331
1-800-678-IEEE

TABLE OF CONTENTS *

An Invitation to ICOPS'97 1

Catamaran Resort Hotel Floor Plans 2

IEEE Nuclear and Plasma Sciences Society

NPSS Administrative Committee 3

Plasma Science and Applications Executive Committee 4

1997 IEEE International Conference On Plasma Science

Conference Information

Conference Organizing Committees 5
Session Topics and Organizers 8
Conference Registration 10
Mini-Course On High-Energy-Density Plasma Diagnostics 12
Women in Plasma Science 12
Companion Program 13
Hotel and Travel Information 16
Tour of General Atomics DIII-D Fusion Facility 18
Conference Management 18
Future ICOPS Conferences 18
IEEE Membership Information 19
Placement Center 20
Conference Sponsors 21

Summary of Technical Sessions 22

Conference Record—Abstracts 113

Index by Author 341

Previous Conferences 357

1998 Conference— 358

San Diego Map 359

* An up-to-date version of the material presented in the Program Schedule will be maintained on the Conference Web Site: <http://www.jetlink.net/~ktw/ICOPS97.html>

24th IEEE INTERNATIONAL CONFERENCE ON PLASMA SCIENCE



Catamaran Resort Hotel
San Diego, California
May 19-22, 1997

Sponsored by

Plasma Science and Applications Committee
of the
IEEE Nuclear and Plasma Sciences Society

An Invitation to ICOPS 1997 . . .

You are cordially invited to join us for the 24th IEEE International Conference on Plasma Science in San Diego. The Conference will be held at the Catamaran Resort Hotel, Monday through Thursday, May 19-22, 1997.

The four day conference will include plenary, oral and poster sessions. Plenary sessions will highlight recent advances in plasma science. On Monday morning, Professor Roald Z. Sagdeev of the University of Maryland will deliver the Keynote Address entitled "Changes in the Nature of Science in the Post-Cold War Era," and on Tuesday afternoon, Dr. Wallace M. Manheimer of NRL will moderate a panel of distinguished academic, industrial and government-laboratory scientists to further explore this subject.

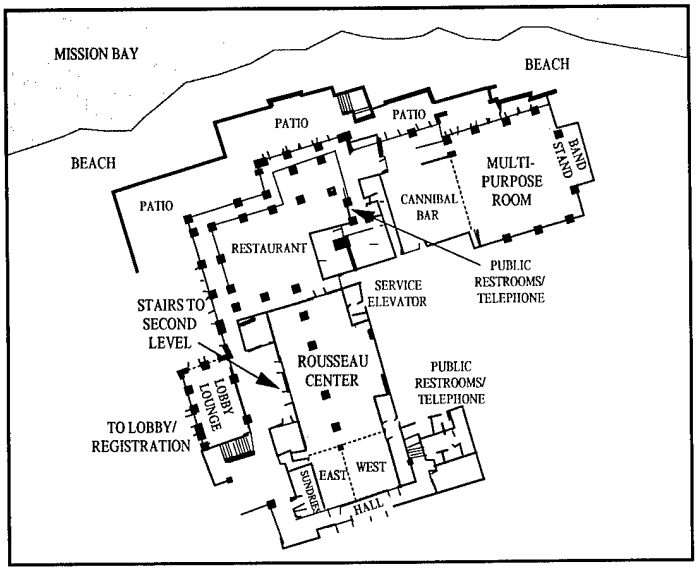
The Conference Hotel is located on the white-sand beach at the north end of Mission Bay—a block away from the Pacific Ocean and a couple of miles from Sea World. The second largest city in California, San Diego is located 120 miles south of Los Angeles and 15 miles north of Tijuana, Mexico. The wide variety of attractions include the world famous San Diego Zoo, the nearby Wild Animal Park, the city of Tijuana itself, and, for the touring scientist, the University of California at San Diego and General Atomics are both located in nearby La Jolla.

Our banquet will be held Tuesday night in the Grand Ballroom at the historic U.S. Grant Hotel located in San Diego's Gaslamp Quarter across the street from the architecturally unique Horton Plaza shopping center. An outstanding Companion Program has been arranged for the conference period, but there's so much more to see and do that you might choose to remain over the weekend for a pleasurable mini-vacation.

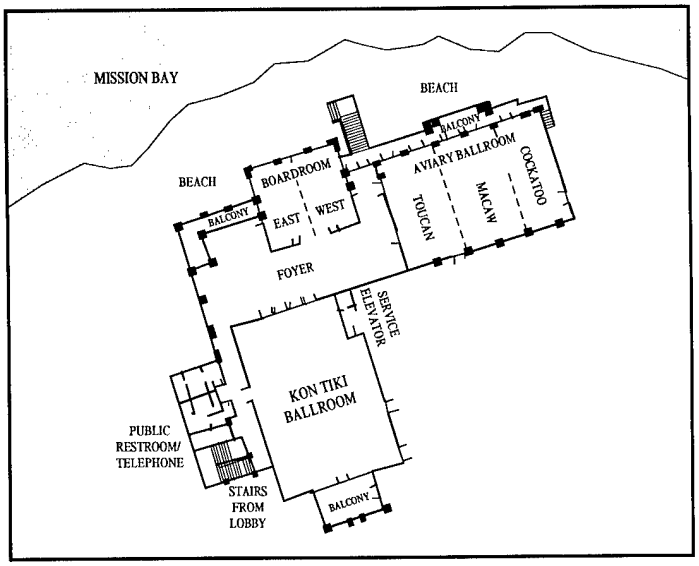
We thank the Program Committee, the International Organizing Committee, the Local Organizing Committee, the Technical Area Coordinators, and the Session Organizers for their work that will make ICOPS '97 a success. We look forward to seeing and welcoming you to San Diego.

Jay Hyman
Conference Chair, ICOPS '97 Conference

Noah Hershkowitz
Chairman, Plasma Science and Applications Committee
IEEE Nuclear and Plasma Sciences Society



First Floor



Second Floor

Catamaran Hotel Meeting Rooms

IEEE NUCLEAR AND PLASMA SCIENCES SOCIETY

Administrative Committee

Officers

President	Ronald Jaszczak
Vice President	William M. Bugg
Secretary	Alberta M. Dawson Larsen
Treasurer	Edward J.Lampo
Most Recent Past President	Peter N. Clout

Elected Representatives

Terms Expiring in 1997
William M. Bugg
Victor L. Granatstein
Erik Heijne
Burr Passenheim

Terms Expiring in 1998
James R. Coss
Ronald J. Jaszczak
Bob Schafer
James P. Spratt

Terms Expiring in 1999
Igor Alexeff
M. (Kris) Kristiansen
George H. Miley
William M. Moses

Terms Expiring in 2000
Gary T. Alley
Jes Asmussen, Jr.
Bruce C. Brown
Roy I. Cutler

PLASMA SCIENCE AND APPLICATIONS COMMITTEE

Executive Committee

Officers

Chairman	Noah Hershkowitz
Vice Chairman	Anthony L. Peratt
Secretary	Ronald M. Gilgenbach
Most Recent Past Chairman	Gerald L. Rogoff

Elected Representatives

Terms Expiring in 1997
Noah Hershkowitz
Osamu Ishihara
Andrew Ng
Anthony Peratt
John Siambis
Frank C. Young

Terms Expiring in 1998
Barbara Abraham-Shrauner
Jennifer M. Butler
Donald J. Rej
Norman F. Roderick
Cha-Mei Tang
Amy E. Wendt

Terms Expiring in 1999
Carter M. Armstrong
Virginia M. Ayres
Robert J. Barker
James N. Benford
Robert J. Commisso
Thomas W. Hussey

24th IEEE International Conference on Plasma Science

May 19-22, 1997
Catamaran Resort Hotel, San Diego, California

Conference Chair	**Dr. Jay Hyman** Hughes Research Laboratories
Program Committee	**Dr. Robert J. Barker** Air Force Office of Scientific Research
	Professor Chung Chan Northeastern University
	Professor Robert W. Conn University of California at San Diego
	Professor John Gilligan North Carolina State University
	Dr. Steven Gold Naval Research Laboratory
	Dr. Sidney L. Ossakow Naval Research Laboratory
	Dr. Anthony L. Peratt US Department of Energy
	Dr. Gerald L. Rogoff OSRAM Sylvania Inc.

Local Committee

Ms. Gloria Christian

Dr. Dan Goebel

Dr. Dan Gregoire

Dr. Robin Harvey

Ms. Bobbi Hyman

Dr. Jesse Matossian

Mr. Ron Robson

Dr. Joe Santoru

Dr. Tod Williamson

Hughes Research Laboratories
3011 Malibu Canyon Road
Malibu CA 90265

International Committee

Professor Kwo Ray Chu
Department of Physics
National Tsing Hua University
Hsinchu, Taiwan
Republic of China

Professor Paul K. Chu
City University of Hong Kong
Kowloon, Hong Kong

Professor Kyu-Sun Chung
Hanyang University
Soul 133-791, Korea

Dr. Valentin V. Danilov
Krasnoyarsk State University
Svbodny, 79
Krasnoysrsk 41, Russia

Dr. R.A.J. Keijser
Philips Lighting B.V.
Eindhoven, The Netherlands

Dr. Fermin Castillo Mejia
Instituto De Ciencias Nucleares
UNAM
A P 70543
04510 Mexico, D.F. Mexico

Dr. Andrew Ng
Univ. of British Columbia
6224 Agricultural Rd.
Vancouver, BC V6T 1Z1 Canada

Professor Zhenkui Shang
Southwestern Institute of Physics
P.O. Box 432
Chengolu Sichuan, China

Dr. George Zissis
Centre de Physique des Plasmas
et Applications de Toulouse
118 Route de Narbonne
F-31062 Toulouse CEDEX,
France

Session Topics and Organizers

	TOPIC	ORGANIZER	INSTITUTION	TELEPHONE / E-MAIL	FAX
1	**Basic Processes in Fully and Partially Ionized Plasmas**	**Noah Hershkowitz**	**University of Wisconsin**	**708/230-4970 hershkowitz@engr.wisc.edu**	**708/265-2364**
1.1	Basic Processes in Fully Ionized Plasmas-Waves, Instabilities, Plasma Theory, Etc.	Osamu Ishihara	Texas Tech University	806/742-3430 oishihara@coe2.coe.ttu.edu	806/742-1245
1.2	Space Plasmas	Earl Scime	University of West Virgina	304/293-3422 scime@wvnvms.wvnet.edu	304/293-3422
1.3	Basic Phenomena In Partially Ionized Gases-Gaseous Electronics, Electrical Discharges	Mark Kushner	University of Illinois	217/244-5137 mjk@uiuc.edu	217/244-7097
1.4	Computational Plasma Physics	Glenn Joyce	Naval Research Laboratory	202/767-6785 joyce@ppd.nrl.navy.mil	202/767-0301
2	**Microwaves Generation and Microwave/Plasma Interaction**	**John Booske**	**University of Wisconsin**	**608/262-8548 booske@eceserv.ece.wisc.edu**	**608/262-1267**
2.1	Intense Beam Microwaves	Edl Schamiloglu	University of New Mexico	505/277-4423 edl@eece.unm.edu	505/277-1439
2.2	Fast Wave Devices	Baruch Levush	Naval Research Laboratory	202/767-0037 levush@mmace.nrl.navy.mil	202/767-1280
2.3	Vacuum Microelectronics	Kevin Jensen	Naval Research Laboratory	202/767-3114 kevin.jensen@nrl.navy.mil	202/767-1280
2.4	Slow Wave Devices	William Menninger	Hughes Electronics	310/517-6271 wmenning@igate1.hac.com	310/517-5117
2.5	Microwave Systems	Glenn Scheitrum	Stanford Linear Accelerator	415/926-2628 glenn@slac.stanford.edu	415/926-3654
2.6	Microwave-Plasma Interactions	Tom Katsouleas	University of Southern California	213/740-0194 katsoule@usc.edu	213/740-7581
3	**Intense Electron and Ion Beams**	**Ron Gilgenbach**	**University of Michigan**	**313/730-1261 rongilg@engin.umich.edu**	**313/730-4540**
3.1	Plasma Ion and Electron Sources	Jes Asmussen, Jr.	Michigan State University	517/355-4620 asmussen@ee.msu.edu	517/353-1980
3.2	Intense Ion and Electron Beams	Peter Menge	Sandia National Laboratories	505/845-7418 prmenge@sandia.gov	505/845-7864
4	**High Energy Density Plasmas and their Applications**	**Jim Degnan**	**Air Force Phillips Laboratory**	**505/846-1235 degnan@plk.af.mil**	**505/846-9853**
4.1	Laser Produced Plasma	Robert Peterkin, Jr.	Air Force Phillips Laboratory	505/846-0259 bob@ppws07.plk.af.mil	505/846-9103

Session Topics and Organizers

TOPIC		ORGANIZER	INSTITUTION	TELEPHONE / E-MAIL	FAX
4.2	Inertial Confinement Fusion	James Hammer	Lawrence Livermore National Laboratory	510/422-9829 hammer@lll.llnl.gov	510/423-3484
4.3	Magnetic Confinement Fusion	Carlos Ordonez	University of Northern Texas	817/565-4870 cordonez@sol.acs.unt.edu	817/565-2515
4.4	Dense Plasma Focus	Gerald Kiuttu	Air Force Phillips Laboratory	505/846-0683 kiuttu@plk.af.mil	505/846-9103
4.5	Fast Z-Pinches and X-Ray Lasers	Melissa Douglas	Sandia National Laboratories	505/845-7472 mrdougl@sandia.gov	505/284-4135
4.6	Spherical Configurations / Ball Lightning	Uri Shumlak	University of Washington	206/616-1986 shumlak@aa.washington.edu	206/543-4719
5	**Industrial / Commercial Applications of Plasmas**	**Voitek Byszewski**	**OSRAM Sylvania, Inc.**	**508/750-1551 byszewsk@rd.sylvania.com**	**505/7501799**
5.1	Non-Equilibrium Plasma Processing	Blake Wood	Los Alamos National Laboratory	505/665-6524 bwood@lanl.gov	505/665-3552
5.2	Thermal Plasma Processing	Evelio Sevillano	Applied Science and Technology, Inc.	617/937-5129 sevillano@astex.com	617/933-0750
5.3	Plasma For Lighting	Timothy Sommerer	General Electric CRD	518/387-6440 sommerer@crd.ge.com	518/387-5714
5.4	Flat Panel Displays	Cha-Mei Tang	National Institute of Standards and Technology	301/975-4272 ctang@nist.gov	301/975-3038
5.5	Environmental / Energy Issues In Plasma Science	Loucas Christophorou	National Institute of Standards and Technology	301/975-2432 christo@eeel.nist.gov	301/948-5796
6	**Plasma Diagnostics**	**Ramon Leeper**	**Sandia National Laboratories**	**505/845-7185 rjleepe@sandia.gov**	**505/854-7820**
7	**Pulsed Power and Other Plasma Technology Applications**	**Kenneth Ware**	**Defense Special Weapons Agency**	**703/325-6734 wareke@hqg.dswa.mil**	**703/325-0249**
7.1	MHD and EM/ETH Launchers	Rex Richardson	SAIC	619/546-6404 rex_d_richardson@cpqm.saic.com	619/546-6584
7.2	Plasma Closing Switches	Ian Roth	Physics International Company	510/577-7214 isroth@corp.olin.com	510/577-7247
7.3	Fast Opening Switches	William Rix	Maxwell Laboratories, Inc.	619/576-7720 rix@maxwell.com	619/576-7659

Conference Registration

All attendees must register. Cash, checks (personal & travelers), money orders and credit cards (VISA and MasterCard only) will be accepted. The registration fee includes the Sunday Reception, Refreshment Breaks, the Tuesday Cocktail Cruise, and Conference Proceedings and materials.

Registration and general information will be available on the second-floor foyer of the Catamaran-Hotel Conference Center on the following days and times:

Sunday	May 18 4:00 p.m .- 8:00 p.m.
Monday	May 19 7:30 a.m. - 4:30 p.m.
Tuesday	May 20 7:30 a.m. - 4:30 p.m.
Wednesday	May 21 7:30 a.m. - 4:30 p.m.
Thursday	May 22 7:30 a.m. - 1:30 p.m.

Conference Registration Fees

IEEE Member	$275
Non-Member*	$375
Retired or Unemployed	$35
Student*	$35
Banquet Ticket	$25

* Registrants in these two categories (Non-Member and Student) are eligible for the free Introductory IEEE membership described in a later section.

CONFERENCE REGISTRATION FORM

CONFERENCE REGISTRATION: (please type or print)

NAME _____
Last Name First Name Middle Initial

NAME TO APPEAR ON BADGE _____

AFFILIATION/COMPANY _____

MAILING ADDRESS _____

CITY _____

STATE/PROVINCE _____

COUNTRY _____ ZIP CODE _____

TELEPHONE _____

FAX _____

E-MAIL _____

❑ I am an IEEE Member. _____
Membership Number

❑ I am not an IEEE Member.

Nonmembers must register at the nonmember rate but if you join during the conference, you will receive a free half-year introductory membership.

❑ I wish to join the IEEE.

There will be IEEE membership material in the Registration Area.

Notes:

- Early registration discount fees are valid only if **FULL PAYMENT ACCOMPANYING THIS FORM** is received by 18 April 1997
- Forms received after May 12th will be processed at the Conference.

Mail this form, or a copy, together with your remittance payable to:

ICOPS '97 Registration Manager
c/o: Concepts Meeting and Trade Show Management, Inc.
6540 Lusk Blvd., Suite C-124
San Diego, CA 92121
Phone: (619) 535-0050
FAX: (619) 535-8252
E-mail:<planners@conceptsmeet.com>

CONFERENCE FEES:

	On or Before 18 April 1997		After 18 April 1997	
IEEE Member	$225	❑	$275	❑
Non-Member	$320	❑	$375	❑
Retired or Unemployed	$30	❑	$35	❑
Student	$30	❑	$35	❑

BANQUET FEE:

Banquet $25 x _____ ❑

Buses will Depart Starting at 5:30 p.m.

MINI-COURSE FEES:

Deadline: April 4, 1997

High-Energy-Density Plasma Diagnostics $500 ❑

FEE SUMMARY:

Conference Registration	$_____
Banquet @ $25/Ticket	$_____
Mini-Course Fee	$_____
TOTAL AMOUNT	$_____

METHODS OF PAYMENT:

All payments must be in U.S. dollars. Only checks drawn on or payable through U.S. Banks may be used. Travelers checks, money orders and credit cards listed below are acceptable.

❑ Check or money order enclosed. (Make payable to IEEE 1997 ICOPS)

(❑ MasterCard ❑ Visa Only) Exp. Date _____

CREDIT CARD # _____

CARDHOLDER'S NAME _____
(print)

SIGNATURE _____

Mini-Course on High-Energy-Density Plasma Diagnostics

The two-day course is offered May 22-23, 1997 at the Catamaran Hotel. The course will be organized by Dr. James E. Bailey and Dr. Ramon J. Leeper of Sandia National Laboratories. The course will be taught by experts in the field including distinguished representatives of the National Laboratory and University communities.

Course Objectives: To educate academics, professionals, and students in the latest methods used to diagnose high-energy-density plasmas. We welcome both experimentalists and theoreticians wishing to expand their insight into practical tests of predictive capability. Topics will include X-ray, optical, and nuclear and particle diagnostics, as well as overviews of methods used for ICF and short-pulse laser-produced plasmas and Z-pinch plasmas.

Lectures: The emphasis will be on providing both the underlying physics and specific examples to enable researchers to evaluate and apply the techniques to their own situations. The instructors will discuss advantages and disadvantages of each technique for particular applications.

Materials Supplied: Copies of transparencies and lecture notes will be distributed at the course.

Mini-course registrations are still being accepted at the time of this publication. The registration fee for the mini-course is $500 per attendee.

Women in Plasma Science

There will be a Networking Gathering for Women in Plasma Science on Tuesday afternoon from 5:00 p.m. to 6:30 p.m. The room location will be available from the Conference Registration Desk. For more information please contact Cha-Mei Tang at e-mail: <ctang@nist.gov>, or by phone at (301) 975-4272. Additional information will be posted on the WWW site as it becomes available.

Companion Program

Companions will be pleased that this year's conference is being held in San Diego. So be sure to accompany your Plasma Scientist for this unusual vacation opportunity. For those with young families, bring the children along for a great vacation—and why not stay the weekend while you're at it.

Step outside the Catamaran Hotel and enjoy the white-sand beach and water sports of beautiful Mission Bay. Or, walk a block west and enjoy your stretch of the Pacific Ocean. Better still, sign up now for the Optional Companion Program. It will make all the difference in your enjoyment of the trip. San Diego offers easy access to Old Mexico on her southern border, the Pacific ocean to the west, and wide open spaces with nearby mountains to the north. There is Sea World, Wild Animal Park, the San Diego Zoo, museums, the Gaslamp Quarter, gourmet restaurants, and more. Days will be sunny with balmy breezes. For the evenings, a light sweater or wrap is always recommended; a jacket and tie is seldom required. And don't forget to bring your bathing suit for water sports of all kinds.

Schedule of Events:

Sunday May 18: Reception at the Kon Tiki Ballroom of the Catamaran Resort Hotel from 4:00 - 8:00 p.m. for registered attendees and companions. There will be a no-host bar with a wide variety of excellent culinary selections.

Breakfast: Companions gather for complimentary Breakfast in the Companions' Room Monday, Wednesday, and Thursday from 8:30 - 10:00 a.m. We urge you to come meet new friends and get together with long-time friends.

Companion Program Cont'd

Monday, May 19: Visit the world famous San Diego Zoo in the a.m. Cost for entrance fee and tour is $41 per adult and $31 per child. In the evening, join the conference attendees for a night to remember aboard the William D. Evans sternwheeler; we'll have complimentary hors d'oeuvres and drinks with music and a tour of the bay.

Tuesday, May 20: Nordstrom at Horton Plaza invites us for complimentary breakfast at 8:30 a.m. along with a fashion seminar including "make up," "make overs" and personal shoppers. There is limited space and this is Nordstrom's gift, so sign up early. At 6:30 p.m. we'll join conference attendees at the historic U.S. Grant Hotel in San Diego's Gaslamp Quarter for cocktails in the Crystal Room followed by a Banquet in the Grand Ballroom. The cost of the banquet is $25.00 per person (see Conference Registration Form) and we provide the transportation.

Wednesday, May 21: After breakfast in the Companions' Room, a tour of Tijuana, Mexico. We'll have our own guide, an air-conditioned bus, and lunch in a healthy, care-free restaurant. Our escorts speak several foreign languages. Remember U.S. citizens will need a photo-ID: U.S. driver's license or certified U.S. birth certificate. Non-U.S. citizens may need Visas and Passports—check with the Mexican Embassy. The cost, including lunch, is $43.00.

Thursday, May 22: Companion Breakfast and Awards for 1) Best Shopper, 2) Most Museums Visited, 3) Best Tan, 4) Best Child, and 5) Best Dancer, then a farewell to all. In the evening, we will gather for a Casual No-Host Dinner for those still in town.

Please fill out a Companion Program Registration Form at the Conference Registration Desk to participate.

COMPANION PROGRAM REGISTRATION FORM

(Tear Off and Take Home)

Mail or Fax to:

Ms. Christy Martin
Enjoy California Enterprises
3990 Old Town Avenue
Suite 101A
San Diego, CA 92110

Phone: (619) 681-0500
Fax: (619) 681-0505

CONFERENCE PARTICIPANT _____

AFFILIATION _____

NAME OF COMPANION _____

ADDRESS _____

CITY _____

STATE/PROVINCE _____ COUNTRY _____ ZIP CODE _____

TELEPHONE _____ FAX _____

PAYMENT – MAKE CHECK PAYABLE TO: ENJOY CALIFORNIA ENTERPRISES

❑ CHECK OR MONEY ORDER ENCLOSED

❑ VISA ❑ MASTERCARD CREDIT CARD # _____

EXP. DATE _____ CARDHOLDER'S NAME _____ (print)

SIGNATURE _____

ACTIVITIES	COST	NUMBER OF PERSONS	$ AMOUNT
	After April 18, 1997		
Companion Program Registration Fee: Includes Sunday Reception, Breakfasts and the Monday Evening Cocktail Cruise	**No Charge**	_____	
MONDAY, MAY 19:			
AM: Tour of the World Famous San Diego Zoo, Adult/Child	**$41/31**	_____	
PM: Cocktail Cruise	**No Charge**	_____	_____
TUESDAY, MAY 20:			
AM: Nordstroms	**No Charge**	_____	
PM: Banquet at U.S. Grant Hotel	**$25**	_____	_____
WEDNESDAY, MAY 21:			
AM: Guided Bus Tour of Tijuana, Mexico with Lunch Included	**$43**	_____	_____
		TOTAL $	_____

Hotel and Travel Information

Rooms have been reserved at the Catamaran Resort Hotel (designated Conference Hotel) and the Bahia Resort Hotel (1.5 miles away) at the discounted group rate for the Conference. Please complete hotel arrangements by April 23, 1997 to obtain the special conference rate. The group rate will be honored three days prior to and two days following the conference dates so plan to stay awhile and spend a vacation in this exciting area. To receive this rate you must mention that you are attending the IEEE International Conference on Plasma Science.

Boat transportation will be provided between the Bahia and Catamaran hotels by ferry each morning and evening. Additional ground shuttles will be provided on a driver-availability basis. Self-service parking is available at the Catamaran for $5 per day, and valet parking is available for $7 per day. Parking at the Bahia is free.

Catamaran Resort Hotel
3999 Mission Boulevard
San Diego, CA 92109

Phone Toll Free: (800) 288-0770
Phone: (619) 488-1081
FAX: (619) 488-1387

Group Rate Deadline: April 23, 1997

Rates	Catamaran	Bahia
Single	$90	$80
Double	$99	$89

Ground Transportation

Car Rental Discounts: Special discounted car rental arrangements with AVIS are available. For reservations, contact the IEEE Travel Services (1-800-TRY-IEEE), and identify yourself as an ICOPS '97 attendee.

Taxi Service: San Diego's Lindberg Field Airport is only 10 miles from the Conference hotels. A taxi will cost less than $20.

Bus Service: San Diego Bus No. 34 stops at the Catamaran Resort Hotel. It can take you as far as UCSD to the north and to the Bahia Hotel and on to Downtown San Diego to the south.

Airport Shuttle Service: Cloud Nine Shuttle (1-800-9-SHUTTLE) will be providing shuttleservice from the San Diego Airport to the hotel for the discounted rate of $7.00 per person. Please identify yourself as an attendee of ICOPS '97 to receive the discounted fare.

Airfare Discounts

Special discounted rates for travel to the Conference have been negotiated with United Airlines and Continental Airlines. They are offering a 10% discount on coach fares, and a 5% discount on the lowest available special supersaver fares, as well as other special fare reductions. Restrictions apply, and airfares are guaranteed to be the lowest available when ticketed.

Travel arrangements using the designated air carriers, or the carriers of your choice, can be made through the IEEE Travel Services by calling 1-800-TRY-IEEE within the U.S. Outside the U.S., call collect by dialing 1-908-562-5441 between the hours of 8:30 a.m. and 5:30 p.m. EST, Monday through Friday.

When calling, please advise the Travel Counselor that you are traveling in connection with ICOPS 97. You may call 1-800-TRY-IEEE, or FAX your requirements to the IEEE Travel Service at 1-908-562-8815. When faxing, please be sure to include your travel dates, departure time, and FAX numbers. A Travel Counselor will contact you as soon as possible.

Tour of General Atomics DIII-D National Fusion Facility

On Thursday, May 22, there will be a tour of the DIII-D National Fusion facility at General Atomics (GA) in San Diego, California. Tours will begin at 1:30 pm. tour will last approximately 1 hour. Please plan for a total of ~2 hours including transportation to and from GA for each tour. An overview of the DIII-D Research Program will be presented, followed by a tour of the DIII-D facility. Tour guides include Dr. Jim Luxon (Director of DIII-D Operations) and/or Dr. Tom Simonen (DIII-D Program Director). GA will provide complimentary pastries, coffee and tea, as well as transportation to and from GA.

Please sign up for these tours by 4:30 p.m., Tuesday, May 20, 1997 at the ICOPS Registration Desk, providing **name, affiliation, and citizenship**.

Conference Management

Dr. Jay Hyman
ICOPS '97 Conference Chair
Hughes Research Laboratories
3011 Malibu Canyon Road
Malibu, CA 90265
Phone: (310) 317-5495 Fax: (310) 317-5840
e-mail: <jhyman@hrl.com>

ICOPS '97 Registration Manager
c/o: Concepts Meeting & Trade Show Management, Inc.
6540 Lusk Blvd. Suite C-124
San Diego, CA 92121
Phone: (619) 535-0050 Fax: (619) 535-8252
e-mail: <planners@conceptsmeet.com>

Future ICOPS Conferences

1998 - June 1-3, Raleigh, NC
Chair: J. Gilligan,
North Carolina State University

1999 - June, Monterey, CA
Chair: C. Deeney,
Sandia National Laboratories

2000 - June, New Orleans, LA
Chair: M. Mazzola,
Mississippi State University

IEEE Membership Information

Free Introductory IEEE Membership

In order to encourage participation in the activities of the IEEE and the Plasma Science and Applications part of the IEEE Nuclear and Plasma Sciences Society, free half-year memberships will be given to all interested non-IEEE members (including students) registering for this conference. This free half-year membership includes a subscription to both the IEEE Spectrum and the Transactions on Plasma Science. The regular cost of a full year's membership is $128. To receive your free membership, fill out the application at the registration desk.

IEEE Membership includes:

- A subscription to Transactions on Plasma Science—a journal devoted to all aspects of plasma technology
- A subscription to Spectrum—a magazine covering engineering topics of general technical, economic, political, and social interest
- A subscription to Society Newsletter with news items about the Conference on Plasma Science, Particle Accelerator Conference, and Symposium on Fusion Engineering
- Eligibility to participate in a broad range of IEEE activities
- Opportunities for IEEE educational services such as video-conferences and individual learning packages
- Eligibility for group insurance, employment referral services, IRAs, and discounted auto rentals. Dental, auto, and homeowners insurance will be available the winter of 1997.

To join, visit the Registration Desk at this Conference for an application. Membership applications are available anytime by calling 1-800-678-IEEE.

Placement Center

A placement center will be set up at the conference. Individuals interested in employment opportunities in plasma physics and related areas should send their resumes to:

Professor Victor Granatstein
Institute For Plasma Research
University of Maryland
College Park, MD 20742
E-mail: <vlg@plasma.umd.edu>
Fax: 301/314-9437

or

Dr. Wallace M. Manheimer
Naval Research Laboratory
4555 Overlook Avenue, SW
Washington, DC 20375
E-mail: <manheime@nrlfs1.nrl.navy.mil>
Fax: 202/767-1607

The resumes should be marked ICOPS in the upper right-hand corner. Persons who have positions available should notify Dr. Manheimer or Professor Granatstein.

Interviews will be arranged at the conference. Applicants and employers who are interested in part-time and consulting positions are also encouraged to participate.

The Placement Center is a free, voluntary service.

Conference Sponsors



The support of the:

AIR FORCE OFFICE OF SCIENTIFIC RESEARCH,

THE NAVAL RESEARCH LABORATORY and

THE NATIONAL SCIENCE FOUNDATION

is also acknowledged.

	Location	Monday, 19 May 1997		Tuesday, 20 May 1997		Wednesday, 21 May 1997		Thursday, 22 May 1997	
		8:30 a.m.	1:30 p.m.	8:30 a.m.	1:30 p.m.	8:30 a.m.	1:30 p.m.	8:30 a.m.	1:30 p.m.
Plenary	Kon Tiki Ballroom	1) Welcome to Conference Participants 2) Keynote Address: Changes in the Nature of Plasma Science in the Post-Cold War Era	Plasma Propulsion for Deep-Space Missions	Trapped Plasmas with a Single Sign of Charge (An Overview)	Interaction of Ultra-Intense Lasers with Beams and Plasmas	NASA's International Solar Terrestrial Physics Program and the Roadmap Forward	PSAC Prize Address: Science and Applications of Energy Beam Ablation	Tokamak Fusion Science Research on the DIII-D Tokamak	Tour of General Atomics DIII-D Tokamak Facility
	Speaker(s)	1) Dr. Jay Hyman 2) Professor Roald Z. Sagdeev	Professor Roald Z. Sagdeev	Professor Thomas M. O'Neil	Dr. Phillip Sprangle	Dr. Robert L. Carovillano	Professor Ronald M. Gilgenbach	Dr. Thomas C. Simonen	Front of Catamaran Hotel
Oral Sessions	**Location**	**10:00 a.m.**	**3:00 p.m.**	**10:00 a.m.**	**3:00 p.m.**	**10:00 a.m.**	**3:00 p.m.**	**10:00 a.m.**	**3:00 p.m.**
A	Kon Tiki Ballroom	1A 1.1: Basic Processes in Fully Ionized Plasmas–Waves, Instabilities, Plasma Theory, etc. I	2A 5.1: Non-Equilibrium Plasma Processing II	3A 1.4: Computational Plasma Physics I	4A Special Panel Changing Career Opportunities in Plasma Science	5A 1.3: Basic Phenomena in Partially Ionized Gases...	6A 2.2: Fast wave Devices II	7A 2.7: Special Session Microwave Generation and Plasma Interactions	Unscheduled Papers
B	Board Room	1B 5.1: Non-Equilibrium Plasma Processing I	2B 1.1: Basic Processes in Fully Ionized Plasmas-Waves, Instabilities, Plasma Theory, etc. II	3B 2.1: Intense Beam Microwaves	—	5B 2.2: Fast Wave Devices I	6B 4.5: Fast Z-Pinches and X-Ray Lasers	7B 5.5: Environmental/ Energy Issues in Plasma Science	Unscheduled Papers
C	Toucan Room	1C 3.1: Plasma Ion and Electron Sources	2C 2.6: Microwave-Plasma Interactions	3C 3.2: Intense Ion and Electron Beams	—	5C 6: Plasma Diagnostics	6C 1.4: Computational Plasma Physics II	7C 5.4: Flat Panel Displays	Unscheduled Papers
D	Macaw Room	1D 4.1: Laser Produced Plasmas	2D 2.5: Microwave Systems 2.4: Slow Wave Devices I	3D 2.4: Slow Wave Devices II		5D 5.3: Plasma for Lighting	6D 4.4: Dense Plasma Focus II	7D 7.1: MHD and EM/ETH Launchers	Unscheduled Papers
E	Cockatoo Room	1E 2.3: Vacuum Microelectronics	2E 1.2: Space Plasmas	3E 4.4: Dense Plasma Focus I		5E 4.2: Inertial Confinement Fusion 4.3: Magnetic Confinement Fusion	6E 7.3: Fast Opening Switches	7E 4.6: Spherical Configurations / Ball Lightning	Unscheduled Papers
Poster Sessions	**Location**	**10:00 a.m.**	**3:00 p.m.**	**10:00 a.m.**	**3:00 p.m.**	**10:00 a.m.**	**3:00 p.m.**	**10:00 a.m.**	**3:00 p.m.**
P	Rousseau Center	1P 2.5: 1P01-07 2.6: 1P08-15	2P 4.1: 2P16-22 4.2: 2P23-28 4.3: 2P29-35 4.4: 2P36-44 4.5: 2P45-65	3P 1.1: 3P01-28	4P 2.2: 4P29-52	5P 2.1: 5P01-15 7.1: 5P16-19 7.2: 5P20-24 7.3: 5P25-28	6P 2.3: 6P29-32 5.2: 6P33-36 5.3: 6P37-46 5.5: 6P47-54	7P 1.4: 7P01-10 3.1: 7P11-25 3.2: 7P26-41	8P Unscheduled Papers
Q	Multipurpose Room	1Q 1-3a: 1Q01-09 1-3b: 1Q10-20 1-3c: 1Q21-32	—	3Q 5.1-Ia: 3Q01-15	4Q 5.1-IIb: 4Q16-21 5.1-IIc: 4Q22-28 5.1-IId: 4Q-29-32	5Q 1.2: 5Q01-12	6Q 2.2: 6Q13-14 2.4: 6Q15-23 6: 6Q24-44	—	—

Session	Topic	Oral Locations	Poster Locations
1.1 (I &II)	Basic Processes in Fully Ionized Plasmas–Waves, Instabilities, Plasma Theory, etc.	1A-I, 2B-II	3P
1.2	Space Plasmas	2E	5Q
1.3	Basic Phenomena in Partially Ionized Gases–Gaseous Electronics, Electrical Discharges	5A	1Q
1.3-a	Basic Phenomena in Partially Ionized Gases-... (High Pressure Discharges)	5A	1Q
1.3-b	Basic Phenomena in Partially Ionized Gases-... (Plasma Processing & Low Pressure Discharges)	5A	1Q
1.3-c	Basic Phenomena in Partially Ionized Gases-... (Electron & Ion Transport & Fundamental Data)	5A	1Q
1.4 (I & II)	Computational Plasma Physics	3A-I, 6C-II	7P
2.1	Intense Beam Microwaves	3B	5P
2.2 (I & II)	Fast Wave Devices	5B-I, 6A-II	4P, 6Q
2.3	Vacuum Microelectronics	1E	6P
2.4 (I & II)	Slow Wave Devices	2D-I, 3D-II	6Q
2.5	Microwave Systems	2D	1P
2.6	Microwave-Plasma Interactions	2C	1P
2.7	Microwave Generation and Plasma Interactions	7A	—
3.1	Plasma Ion and Electron Sources	1C	7P
3.2	Intense Ion and Electron Beams	3C	7P
4.1	Laser Produced Plasmas	1D	2P
4.2	Inertial Confinement Fusion	5E	2P

Session	Topic	Oral Locations	Poster Locations
4.3	Magnetic Confinement fusion	5E	2P
4.4 (I & II)	Dense Plasma Focus	3E-I, 6D-II	2P
4.5	Fast Z-Pinches and X-Ray Lasers	6B	2P
4.6	Spherical Configurations / Ball Lightning	7E	—
5.1 Ia	Non-Equilibrium Plasma Processing (Ion Implantation)	1B	3Q
5.1 IIb	Non-Equilibrium Plasma Processing (Atmospheric Discharges)	2A	4Q
5.1 IIc	Non-Equilibrium Plasma Processing (Deposition and Etching)	2A	4Q
5.1 IId	Non-Equilibrium Plasma Processing (ICP Modeling)	2A	4Q
5.2	Thermal Plasma Processing	—	6P
5.3	Plasma for Lighting	5D	6P
5.4	Flat Panel Displays	7C	—
5.5	Environmental / Energy Issues in Plasma Science	7B	6P
6	Plasma Diagnostics	5C	6Q
7.1	MHD and EM/ETH Launchers	7D	5P
7.2	Plasma Closing Switches	—	5P
7.3	Fast Opening Switches	6E	5P
8.0	Unscheduled Papers	—	8P

Poster Papers will be displayed all day in the Rousseau Center and Multipurpose Room, 10:00 a.m. - 5:30 p.m. Authors are to be present at their poster session in either the morning or afternoon session as noted in above schedule. Please take down posters at the end of the day. Poster board sizes are approximately 4' x 8'.

Technical Sessions

Monday Morning – 19 May, 1997
8:30 a.m. – Kon Tiki Ballroom

Welcome to Conference Participants

Dr. Jay Hyman, Conference Chair

Hughes Research Laboratories

Monday Morning – 19 May, 1997
8:45 a.m. – Kon Tiki Ballroom

Keynote Address:

Changes in the Nature of Plasma Science in the Post-Cold War Era

Professor Roald Z. Sagdeev

University of Maryland, College Park, MD, USA

Chair: Dr. Jay Hyman

Morning – 19 May, 1997
10:00 a.m. – Kon Tiki Ballroom

Oral Session 1A: 1.1 Basic Processes in Fully Ionized Plasmas – Waves, Instabilities, Plasma Theory, etc. I
Chair: O. Ishihara

1A01-02 *Invited*—**Helicon Waves in Theory and Experiment**
F.F. Chen
University of California at Los Angeles, Los Angeles, CA, USA

1A03 **Velocity-Shear Origin of Broadband Electrostatic Noise**
M.E. Koepke, J.J. Carroll III and M.W. Zintl
West Virginia University, Morgantown, WV, USA

1A04 **Experimental Study of Polarization of Lines, Emitted by the Plasma of Z-Pinch Devices**
E.O. Baronova
RRC Kurchatov Institute, Moscow, Russia

1A05 **Gyrobroadening of Fast Ion Energy Spectrum in Magnetized Plasma**
K.R. Chen
National Changhua University of Education, Changhua, Taiwan, ROC

1A06 **Influence of Density Gradient on Absorption of Upper Hybrid Pump Energy in Turbulent Plasma**
V.N. Pavlenko and V.G. Panchenko
Institute for Nuclear Research, Kiev, Ukraine

1A07 **Cross Correlation of the Low-Frequency Electromagnetic Excitations and Anomalous Diffusion in a Plasma**
M.O. Vakulenko
Institute for Theoretical Physics, Kiev, Ukraine

1A08 **Boundary Conditions for Use in Plasma Simulations**
C.A. Ordonez, K.F. Stephens II and R.E. Peterkin Jr.[1]
University of North Texas, Denton, TX, USA
[1]Phillips Laboratory, Kirtland AFB, NM, USA

1A09 **Self-Sustained Oscillations in Spatially Confined Beam-Plasma Systems**
V.P. Kovalenko and I.M. Parneta
National Academy of Sciences of Ukraine, Kiev, Ukraine

Monday Morning – 19 May, 1997
10:00 a.m. – Board Room

Oral Session 1B: 5.1 Non-Equilibrium Plasma Processing (Inductively Coupled Plasmas, Etching Plasmas and Modeling) I
Chair: B.P. Wood

1B01-02 *Invited*—**Simulation Tools for the Design and Analysis of Plasma Processing Equipment**
S. Rauf, M.J. Grapperhaus, R.J. Hoekstra and M.J. Kushner
University of Illinois, Urbana, IL, USA

1B03 **Real Time Characterization of Plasma Etch Selectivity**
M.K. Harper, M. Sarfaty, C. Baum and N. Hershkowitz
University of Wisconsin-Madison, Madison, WI, USA

1B04 **Real-Time Control and Modeling of Plasma Etching**
M. Sarfaty, C. Baum, M.K. Harper and N. Hershkowitz
University of Wisconsin-Madison, Madison, WI, USA

1B05 **Model Etch Profiles for Argon and Chlorine Ion Energy Distribution Functions in Inductively Coupled Discharge Plasmas**
W. Chen, B. Abraham-Shrauner and J.R. Woodworth[1]
Washington University, St. Louis, MO, USA
[1]Sandia National Laboratories, Albuquerque, NM, USA

1B06 **Characterization of Stationary and Rotating Magnetic Fields in an MERIE**
M.J. Buie and J.T.P. Pender
Applied Materials, Santa Clara, CA, USA

1B07 **Plasma-Ion Beam Treratment of AL for Enhanced Corrosion**
V.M. Bystritskii, Y.B. Yankelevich, A.V. Kharlov[1], E. Garate, V. Grigoriev[2], E. Lavernia and X. Dong
University of California at Irvine, Irvine, CA, USA
[1]Institute of Electrophysics, Ekaterinburg, Russia
[2]Institute of Nuclear Physics, Tomsk, Russia

1B08 **Ionized Physical Vapor Deposition Charactized for Ionization Fraction and Deposition Rate**
D.B. Hayden, D.R. Juliano and D.N. Ruzic
University of Illinois, Urbana, IL, USA

Monday Morning – 19 May, 1997
10:00 a.m. – Toucan Room

Oral Session 1C: 3.1 Plasma Ion and Electron Sources
Chair: J. Asmussen, Jr.

1C01-02 *Invited*—**Investigation of Diagnostic Sensors and Control Models for a Compact Ion Source**
M.-H. Tsai and T.A. Grotjohn
Michigan State University, East Lansing, MI, USA

1C03 **Laser-Driven Ion Sources for High-Brightness High-Purity Ion Beams**
A.B. Filuk, C.H. Ching, M.E. Cuneo, J.E. Bailey, M.A. Bernard, B.F. Clark, W.E. Fowler, P. Lake, J.S. Lash, J. McKenney, P.R. Menge, D. Cohen[1], and P. Wang[1]
Sandia National Laboratories, Albuquerque, NM, USA
[1]University of Wisconsin–Madison, Madison, WI, USA

1C04 **A Plasma Purification Method for Plasma Source Ion Implantation Doping of Semiconductors**
T.G. Snodgrass, D.E. Arnott, J.L. Shohet, J.H. Booske, and M.J. Kushner[1]
University of Wisconsin–Madison, Madison, WI, USA
[1]University of Illinois, Urbana, IL, USA

1C05 **Evaluation of the Resonant Mode Behavior of a Compact, End Feed, Microwave Plasma Source**
M. Perrin and J. Asmussen Jr.
Michigan State University, East Lansing, MI, USA

1C06 **Two-dimensional MHD Simulation of Plasma Closure in High Current-Density Diodes**
P.J. Turchi[1] and R.E. Peterkin Jr.
Phillips Laboratory, Kirtland AFB, NM, USA
[1]On leave from Ohio State University, Columbus, OH, USA

1C07 **Preliminary Design and Experimental Evaluation of Carbide Field Emitters in mTorr Pressure Environments**
C.M. Marrese, W.A. Mackie and A.D. Gallimore
University of Michigan, Ann Arbor, MI, USA

1C08 **Beam Discharge for New Technology**
M. Ghoranneviss, A. Abbaspour, M.R. Salami, S. Zorriasatin and A. Pouraslan
Plasma Physics Research Center of I.A.U., Tehran, Iran

1C09 **Thermal and Mechanical Loading of Particle and RF Transmission Windows Exposed to Atmospheric Pressure**
R.J. Vidmar
SRI International, Menlo Park, CA, USA

Monday Morning – 19 May, 1997
10:00 a.m. – Macaw Room

Oral Session 1D: 4.1 Laser Produced Plasmas
Chair: R.E. Peterkin, Jr.

1D01-02 *Invited*—**Production of X-rays from Laser Heated Gas Targets**
J. Grun, C.A. Back[1], J.L. Davis[2], A. Fisher, R. Burris, C.D. Decker[1], O.L. Landen[1], L.J. Suter[1] and R. Wallace[1]
Naval Research Laboratory, Washington, DC, USA
[1]Lawrence Livermore National Laboratory, Livermore, CA, USA
[2]Alme Associates, Alexandria, VA, USA

1D03 **Stochastic Theory of Dense Laser Produced Plasma**
V.I. Arefyev
Russian Space Agency, Moscow Region, Russia

1D04 **Collective Effects of Atomic Structures in Super Strong Fields**
V.S. Beliaev
Russian Space Agency, Moscow Region, Russia

1D05 **Laser Produced Plasma as Accelerator Fast Particles**
A.V. Komissarov
Russian Space Agency, Moscow Region, Russia

1D06 **Potential of Eximer Laser System with Pumping Power g-Pulse Radiation for Studying of Plasma Physics and 0.1-1.0 MJ ICF**
E.C. Bonuishkin, R.I. Il'kaev, A.P. Morovov, A.I. Pavlovski and B.V. Lashintsev
Russian Science Research Institute of Experimental Physics, Nizhnii, Novogorod Region, Russia

1D07 **RF from Two Pulse Laser Plasmas in Atmospheric Pressure Gas**
G.K. Chawla and C.W. von Rosenberg Jr.
Textron Systems Corporation, Wilmington, MA, USA

1D08 **When Air Becomes an Electrical Pathway**
K.R. Umstadter, D.L. Millard and R.C. Block
Rensselaer Polytechnic Institute, Troy, NY, USA

Monday Morning – 19 May, 1997
10:00 a.m. – Cockatoo Room

Oral Session 1E: 2.3 Vacuum Microelectronics
Chair: K.L. Jensen

1E01-02 *Invited*—**Arcing and Voltage Breakdown in Vacuum Microelectronics Microwave Devices Using Field Emitter Arrays. Causes and Possible Solutions**
F. Charbonnier
Linfield Research Institute, McMinnville, OR, USA

1E03 **Laser Produced Silicon Field Emission Arrays**
A.A. Evtukh, E.B. Kaganovich, V.G. Litovchenko, R.I. Marchenko,
S.V. Svechnikov and E.G. Manoilov
Institute of Semiconductor Physics, Kiev, Ukraine

1E04 **Fabrication of Field-Emitter Arrays for Inductive-Output Amplifiers**
R.A. Murphy, C.T. Harris, R.H. Mathews, C.A. Graves, M.A. Hollis, M.A. Kodis[1],
J. Shaw[1], M. Garven[1], M.T. Ngo[1], and K.L. Jensen[1]
Massachusetts Institute of Technology, Lincoln Laboratory, Lexington, MA, USA
[1]Naval Research Laboratory, Washington, DC, USA

1E05 **Application of Gated Field Emitter Arrays in Microwave Amplifier Tubes**
S.G. Bandy, M.C. Green[1], C.A. Spindt[2], M.A. Hollis[3], D. Palmer[4], B. Goplen[4]
and E.G. Wintucky[5]
Varian Associates, Palo Alto, CA, USA
[1]CPI MPTP,
[2]SRI International, Menlo Park, CA, USA
[3]Massachusetts Institute of Technology, Lincoln Laboratory, Lexington, MA, USA
[4] Mission Research Corporation, Newington, VA, USA
[5]NASA Lewis Research Center, Cleveland, OH, USA

1E06 **Field-Emitter-Array Development for Microwave Applications**
C.A. Spindt, C.E. Holland, P.R. Schwoebel and I. Brodie
SRI International, Menlo Park, CA, USA

1E07 **Analysis of Isotropic and Anistropic Etch Field Emitter Array Cathodes**
R.B. True, G.R. Good, T.A. Hargreaves and W.D. Palmer[1]
Litton Electron Devices Division, San Carlos, CA, USA
[1]MCNC Electronic Technologies Division, Research Triangle Park, NC, USA

1E08 **Microgun**
V.T. Binh, V. Semet, S.T. Purcell and D. Guillot
Université Claude Bernard Lyon 1, Villeurbanne, France

1E09 **Diamond Cold Cathodes**
M.W. Geis, J.C. Twichell, T.M. Lysczarz, K.E. Krohn and N.N. Efremow
Massachusetts Institute of Technology, Lincoln Laboratory, Lexington, MA, USA

1E10 **A Simplified FEA-Based TWT Model**
K.L. Jensen, E.G. Zaidman, K.T. Nguyen[1], M.A. Kodis and M. Garven
Naval Research Laboratory, Washington, DC, USA
[1]KN Research, Silver Springs, MD, USA

Monday Morning – 19 May, 1997
10:00 a.m. – Rousseau Center

Poster Session 1P01–07: 2.5 Microwave Systems

1P01 **Parametric Excitement of Surface Waves on Harmonics of Cyclotron Frequencies in External Pumping Electric Field**
V.O. Girka, V.I. Lapshin and I.V. Pavlenko
Kharkiv State University, Kharkiv, Ukraine

1P02 **Cold and High-Power Tests of a Multibunch X-Band Photoinjector**
G.P. Le Sage, C.V. Bennett, L.L. Laurent, J.R. VanMeter, V.V. Dinh, A.L. Troha, B.H. Kolner, F.V. Hartemann and N.C. Luhmann Jr.
University of California at Davis, Davis, CA, USA

1P03 **Frequency Response in Multipactor Discharge**
A. Valfells, R.A. Kishek, Y.Y. Lau and R.M. Gilgenbach
University of Michigan, Ann Arbor, MI, USA

1P04 **Initial Results from the Multi-Megawatt 110 GHz ECH System for the DIII-D Tokamak**
R.W. Callis, J. Lohr, R.C. O'Neill, D. Ponce, R. Prater and D. Zhang[1]
General Atomics, San Diego, CA, USA
[1]Institute of Plasma Physics, Hefei, Anhui, Peoples Republic of China

1P05 **Design and Characterisitics of a High T_c Superconducting Magnet for Electron Beam Control**
A.C. Day, W.P. Geren, M. Strasik, D. Garrigus and K.E. McCrary
Boeing Defense and Space Group, Seattle, WA, USA

1P06 **Rep-rate Modulator & Electron Gun for High Power Microwave Research Using Ferroelectric Cathodes**
J.D. Ivers, D. Flechtner, Cz. Golkowski, G.S. Kerslick and J.A. Nation
Cornell University, Ithaca, NY, USA

1P07 **Construction of a Multi-Cell Resonator for a 94 GHz Extended Interaction Klystron**
K.W. Zieher
Texas Tech University, Lubbock, TX, USA

Monday Morning – 19 May, 1997
10:00 a.m. – Rousseau Center

Poster Session 1P08–15: 2.6 Microwave Plasma Interactions

1P08 **Temporal Evolution of a Beam-Plasma Wave Spectrum**
V. Tkachenko and P. Turbin
Scientific Center of Physical Technologies, Kharkiv, Ukraine

1P09 **A Plasma of the Positive Column of Cs-Xe DC Gas Discharge as a Fast Highly Nonlinear Volumetric Medium for Microwaves**
M.S. Gitlin, N.A. Bogatov, D.A. Dikan and G.A. Luchinin
Institute of Applied Physics, Nizhny Novgorod, Russia

1P10 **Dynamics of a Laser Produced Plasma and its Properties for Microwave Reflection**
G. Ding, J.E. Scharer, K.L. Kelly, M.H. Bettenhausen and N.T. Lam
University of Wisconsin–Madison, Madison, WI, USA

1P11 **Microwave Reflections from a VUV Laser Produced Plasma Sheet**
K.L. Kelly, J.E. Scharer, G. Ding, M.H. Bettenhausen and N.T. Lam
University of Wisconsin–Madison, Madison, WI, USA

1P12 **Numerical Analysis of Microwave Propagation and Interaction with Plasma in Surface-Wave Plasma**
Q. Chen and M. Katsurai
University of Tokyo, Tokyo, Japan

1P13 **Interaction of an Air Plasma Layer Covering a Conducting Surface with Microwaves**
M. Laroussi
University of Tennessee, Knoxville, TN, USA

1P14 **On Phonomenon of Plasma-Loaded High-Power Backward Wave Oscillator**
G.I. Zaginaylov and P.V. Turbin[1]
Kharkiv State University, Kharkiv, Ukraine
[1]Scientific Center of Physical Technologies, Kharkiv, Ukraine

1P15 **Electrodynamics of Wide Spectrum Plasma Waveguide Surrounding with a Periodic Succession of Metallic Rings**
V.A. Balakirev, Yu.P. Bliokh, A.V. Borodkin, O.F. Kovpik, E.A. Kornilov, I.N. Onishchenko and G.V. Sotnikov
Kharkiv Institute of Physics & Technology, Kharkiv, Ukraine

Monday Morning – 19 May, 1997
10:00 a.m. – Multipurpose Room

Poster Session 1Q01-09: 1.3-a Basic Phenomena in Partially Ionized Gases - Gaseous Electronics, Electrical Discharges (High Pressure Discharges)

1Q01 **Stability Measurements of PPPL Atmospheric Pressure Arc**
M. Karasik, G. Lemunyan, L. Roquemore, S.J. Zweben and G.A. Wurden[1]
Princeton Plasma Physics Laboratory, Princeton, NJ, USA
[1]Los Alamos National Laboratory, Los Alamos, NM, USA

1Q02 **A New DC Electric Gas Breakdown Criterion**
V.A. Lisovskiy
Kharkiv State University, Kharkiv, Ukraine

1Q03 **Generalized Moment Method of an AC Plasma Display Panel Cell**
Y.B. Kim, Y.K. Shin, H.J. Lee and J.K. Lee
Pohang University of Science and Technology, Pohang, Korea

1Q04 **Electron Drift Velocity Determination in Air**
V.A. Lisovskiy and V.D. Yegorenkov
Kharkiv State University, Kharkiv, Ukraine

1Q05 **Control of Trichel Pulses of Corona by Geometric and Gasdynamic Factors**
Yu.S. Akishev, A.P. Napartovich, M.V. Pan'kin and N.I. Trushkin
Troitsk Institute for Innovation and Thermonuclear Research, Troitsk, Moscow Region, Russia

1Q06 **Study on Factors for the Starting Potential of Short Gap Discharge in N_2+NO Gas**
K. Itoyama, T. Nishimura and T. Yanobe[1]
Nagasaki University, Nagasaki, Japan
[1]Hokushin Industries Inc., Yokohama, Japan

1Q07 **An Electrostatic MHD Theory for Helical Instabiliites of Arc Discharges**
X. Wang
University of Iowa, Iowa City, IA, USA

1Q08 **Simulation of Microdischarges in a Dielectric Barrier Discharge**
J. Li and S.K. Dhali
Southern Illinois University, Carbondale, IL, USA

1Q09 **Stripping Properties of a Free Electron Target Produced in a Pseudospark Discharge**
M. Englebrecht, J. Kolb, R. Kowalewicz, J. Philipps and D.H.H. Hoffmann
University of Erlangen-Nürnberg, Erlangen, Germany

Monday Morning – 19 May, 1997
10:00 a.m. – Multipurpose Room

Poster Session 1Q10–20: 1.3-b Basic Phenomena in Partially Ionized Gases - Gaseous Electronics, Electrical Discharges (Plasma Processing and Low-Pressure Discharges)

1Q10 **Designing Planar Magnetron Cathodes: Analysis and Experiment**
M. Garcia
Lawrence Livermore National Laboratory, Livermore, CA, USA

1Q11 **One-Dimensional Continuum Modeling of Chlorine Radio-Frequency Discharges**
J.N. Baléo and M.J. Vignes[1]
Ecole des Mines de Nantes, Nantes, France
[1]Matra MHS, Nantes, France

1Q12 **Time-Dependent Global Model for Electronegative High-Density Plasma Discharges**
H.J. Yoon, T.H. Chung and J.K. Lee[1]
Dong-A University, Pussan, Korea
[1]Pohang University of Science and Technology, Pohang, Korea

1Q13 **Negative Ion Densities in Cl_2 and BCl_3 Inductively-Coupled Plasmas**
C.B. Fleddermann and G.A. Hebner[1]
University of New Mexico, Albuquerque, NM, USA
[1]Sandia National Laboratories, Albuquerque, NM, USA

1Q14 **Characterization of Pulse-Modulated Inductively Coupled Discharges in Argon and Chlorine**
G.A. Hebner and C.B. Fleddermann[1]
Sandia National Laboratories, Albuquerque, NM, USA
[1]University of New Mexico, Albuquerque, NM, USA

1Q15 **Operation Characteristics of an ICP Plasma Source**
K.C. Leou, T.L. Lin, C.H. Tsai, J.H. Li, S.C. Pan, S.L. Wu and J.L. Tsai
National Tsing Hua University, Hsinchu, Taiwan, ROC

1Q16 **Damage to Ferroelectric Cathodes from Surface Discharge and Mechanical Strain**
T. Cavazos and C.B. Fleddermann
University of New Mexico, Albuquerque, NM, USA

1Q17 **A Large Area ECR Plasma Source**
T.L. Lin, Y. Hu, K.C. Leou, J.H. Shiau and Y.C. Lan
National Tsing Hua University, Hsinchu, Taiwan, ROC

1Q18 **Stable Regimes, Mode Transitions and Discharge Disruptions in a Helicon Plasma Source**

K.P. Shamrai
Institute for Nuclear Research, Kiev, Ukraine

1Q19 **Basic Experimental Results of MCEBPS**

T.Y. Kim, K.H. Chung, Y.B. Kang[1], D.K. Ko[2], J.K. Jung[2] and S.J. Noh[3]
Seoul National University, Seoul, Korea
[1]Hanyang University, Seoul, Korea
[2]Joongang University, Seoul, Korea
[3]Dankook University, Seoul, Korea

1Q20 **Mass-Spectrometrical Study of Neutral Component of Plasma in Gas Discharge with Metal-Hydride Cathode**

V.V. Bobkov, V.N. Borisko, E.V. Klochko, D.L. Ryabchikov and Yu.V. Sidorenko
Kharkiv State University, Kharkiv, Ukraine

Monday Morning – 19 May, 1997
10:00 a.m. – Multipurpose Room

Poster Session 1Q21–32: 1.3-c Basic Phenomena in Partially Ionized Gases - Gaseous Electronics, Electrical Discharges (Electron and Ion Transport and Fundamental Data)

1Q21 **Electron Behavior in Inhomogeneous DC Discharges**
T. Kimura and K. Ohe
Nagoya Institute of Technology, Nagoya, Japan

1Q22 **Mode Transition and Nonlinear Dynamics in the Beam-Injected Plasma**
H.J. Lee, J.K. Lee, Y. Yang, M.S. Huh, Y.B. Kim, M. Yoon and T.H. Chung[1]
Pohang University of Science and Technology, Pohang, Korea
[1]Dong-A University, Pussan, Korea

1Q23 **Ion-Energy Distributions in Townsend Discharges of CHF_3 at High *E/N***
M.V.V.S. Rao, R.J. Van Brunt and J.K. Olthoff
National Institute of Standards & Technology, Gaithersburg, MD, USA

1Q24 **Secondary Electron Emission Influence on the RF Gas Breakdown**
V.A. Lisovskiy, N.Yu. Kropotov and V.I. Farenik[1]
Kharkiv State University, Kharkiv, Ukraine
[1]Scientific Center of Physics and Technology, Kharkiv, Ukraine

1Q25 **Ion Cyclotron Instability in Rotating Plasma**
M. Sosipatrov
Scientific Center of Physical Technologies, Kharkiv, Ukraine

1Q26 **Non-Local Electron Kinetics in a Weakly Ionized Plasma**
E. Furkal, A. Smolyakov and A. Hirose
University of Saskatchewan, Saskatoon, Canada

1Q27 **Acoustic Pulse Magnification at Its Propagation Along Structurally-Modified Zone of Radiation-Matter Interaction**
V.A. Deryuga, A.I. Kalinichenko, G.F. Popov, A.G. Ponomarev[1] and V.V. Uvarov[1]
Kharkiv State University, Kharkiv, Ukraine
[1]Institute of Physics and Technology, Kharkiv, Ukraine

1Q28 **The Ion Motion in the Field of Ion-Sound Surface Wave**
A.N. Azarenkov, O.A. Bizyukov, A.V. Gapon and I.B. Denisenko
Kharkiv State University, Kharkiv, Ukraine

1Q29 **The Dispersion Properties of Ion-Sound Surface Waves Propagating Between Two Parallel Metal Planes and Some Applications of These Waves**
A.N. Azarenkov, I.B. Denisenko and A.V. Gapon
Kharkiv State University, Kharkiv, Ukraine

1Q30 **Electron Interactions with C_2F_6**
L.G. Christophorou[1] and J.K. Olthoff
National Institute of Standards and Technology, Gaithersburg, MD, USA
[1]University of Tennessee, Knoxville, TN, USA

1Q31 **High-Accuracy Expressions for the Rotational-Vibrational Energies of the O_2, N_2, NO and CO Molecules**
F.J. Gordillo-Vázquez and J.A. Kunc
University of Southern California, Los Angeles, CA, USA

1Q32 **Spectroscopic Determination of W I and W II Oscillator Strengths**
B. Michelt, R. Sielker and J. Mentel
Ruhr-Universität Bochum, Bochum, Germany

Monday Afternoon – 19 May, 1997
1:30 p.m. – Kon Tiki Ballroom

Plenary Session

Plasma Propulsion for Deep-Space Missions

Professor Roald Z. Sagdeev
University of Maryland, College Park, MD, USA

Chair: S.L. Ossakow

Monday Afternoon – 19 May, 1997
3:00 p.m. – Kon Tiki Ballroom

Oral Session 2A: 5.1 Non-Equilibrium Plasma Processing II
Chair: B. Cluggish

2A01-02 *Invited*–**Surface Modification of Polyurethane and Silicane Rubber for Biomedical Applications**
Z. Jiang, C. Zheng and J. Ran
Sichuan Union University, Chengdu, Sichuan, Peoples Republic of China

2A03 **High Power Nitrogen-Incorporating Remote Plasma Oxidation Process for MOS Applications**
C.G. Parker, G. Lucovsky and J.R. Hauser
North Carolina State University, Raleigh, NC, USA

2A04 **Reaction Pathways for Nitrided Si-SiO_2 Interfaces by Remote Plasma Assisted Oxidation**
H. Niimi, K. Koh and G. Lucovsky
North Carolina State University, Raleigh, NC, USA

2A05 **Profile of Electric and Magnetic Field Strength in New Plasma Source Using Coaxially Symmetric Surface Wave in VHF Band**
S. Ikezawa, R. Miyano, J-I. Inaguma, Y. Shiraki, Y. Mikawa, K. Baba, K. Kida, A. Nishiwaki, M. Nagatsu[1], Y. Okamoto[2], S. Nonaka[3] and M. Kando[4]
Chubu University, Kasugai, Japan
[1]Nagoya University, Nagoya, Japan
[2]Toyo University, Kawagoe, Japan
[3]Toyota Technological Institute, Nagoya, Japan
[4]Shizuoka University, Hamamatsu, Japan

2A06 **Study of Plasma Chemistry in Plasma Doping Processes**
S. Qin, Y. Zhou, C. Chan, J. Shao[1] and S. Denholm[1]
Northeastern University, Boston, MA, USA
[1]Eaton Corporation, Beverly, MA, USA

2A07 **Hydrodynamic and Analytical Models for Plasma Immersion Ion Implantation with Dielectric Substrates**
Y. Zhou, S. Qin and C. Chan
Northeastern University, Boston, MA, USA

2A08 **A Theory of the Plasma Torch for Waste-Treatment**
H.S. Uhm and S.H. Hong[1]
Naval Surface Warfare Center, West Bethesda, MD, USA
[1]Seoul National University, Seoul, Korea

Monday Afternoon – 19 May, 1997
3:00 p.m. – Board Room

Oral Session 2B: 1.1 Basic Processes in Fully Ionized Plasmas – Waves, Instabilities, Plasma Theory, etc. II
Chair: D.K. Kalluri

2B01-02 *Invited*—**Heating and Melting of the Dusty Crystal in RF Discharge**
I.V. Schweigert and V.A. Schweigert[1]
Institute of Semiconductor Physics, Novosibirsk, Russia
[1]Institute of Theoretical and Applied Mechanics, Novosibirsk, Russia

2B03 **An Analytic Treatment for Radial Density Profiles of a Large ECR Source**
K.-S. Chung, S.M. Hwang[1], G.H. Kim[2], J.I. Kim, J.S. Chun, T.H. Noh and D.-H. Chang
Hanyang University, Seoul, Korea
[1]Korea Basic Science Institute, Daejeon, Korea
[2]Hanyang University, Ansan, Korea

2B04 **Sawtooth Oscillation in the IR-T1 Tokamak with Tomographic Reconstructions**
M. Ghoranneviss, M. Bakhtiary, M.R. Salami, A.K. Tafreshi, M. Zamani Mehr and J. Mirzaei
Plasma Physics Research Center of I.A.U., Tehran, Iran

2B05 **Narrow, Stationary and Stable Electric Field Spikes Produced by an Electron Beam in an Inhomogeneous Plasma**
H. Gunell, J.P. Verboncoeur, N. Brenning and S. Torvén
Royal Institute of Technology, Stockholm, Sweden

2B06 **On a Sphere of Applicability of the Vlasov Equation**
V.I. Erofeev
Siberian Branch of Russian Academy of Sciences, Novosibirsk, Russia

2B07 **Surface Waves Parametric Excitation in Planar Plasma Filled Waveguides**
A.N. Azarenkov, V.O. Girka and A. Sporov[1]
Kharkiv State University, Kharkiv, Ukraine
[1]National Academy of Sciences of Ukraine, Kharkiv, Ukraine

2B08 **Quantization Problems of Electromagnetic Field 2**
M. Mészáros
Institute of Physics, Budapest, Hungary

2B09 **Lyapunov Stability of MHD-Like Plasma with Flows**
V.I. Ilgisonis
RRC Kurchatov Institute, Moscow, Russia

Monday Afternoon – 19 May, 1997
3:00 p.m. – Toucan Room

Oral Session 2C: 2.6 Microwave-Plasma Interactions
Chair: T. Katsouleas

2C01-02 *Invited*—**Atmospheric Pressure Collisional Plasma Absorber: Theory, Experiments and Issues Relating to Efficient Production**
R.J. Vidmar
SRI International, Menlo Park, CA, USA

2C03 **VUV Laser Plasma Formation and Microwave Agile Mirror/Absorber**
J.E. Scharer, K.L. Kelly, G. Ding and M.H. Bettenhausen
University of Wisconsin–Madison, Madison, WI, USA

2C04 **Radiation Generation by an Ionization Front in a Gas-Filled Capacitor Array**
P. Muggli, R. Liou, C.H. Lai, T.C. Katsouleas, C. Joshi[1], W.B. Mori[1] and J. Dawson[1]
University of Southern California, Los Angeles, CA, USA
[1]University of California at Los Angeles, Los Angeles, CA, USA

2C05 **Time Domain Wave Phenomena in Rapidly Created Periodic Plasmas**
S.P. Kuo, J.C. Faith and E. Koretzky
Polytechnic University, Farmingdale, NY, USA

2C06 **Tunable Microwaves from Cerenkov Wakes in Magnetized Plasma**
J. Yoshii, C.H. Lai, T.C. Katsouleas, W.B. Mori[1] and C. Joshi[1]
University of Southern California, Los Angeles, CA, USA
[1]University of California at Los Angeles, Los Angeles, CA, USA

2C07 **Electromagnetic Wave Propogation Below Cutoff**
P. Sprangle, E. Esarey, B. Hafizi[1] and S.E. Harris[2]
Naval Research Laboratory, Washington, DC, USA
[1]Icarus Research Inc., Bethesda, MD, USA
[2]Stanford University, Stanford, CA, USA

2C08 **Gamma Ray Production in Colliding Laser Pulses**
F.V. Hartemann, J.R. VanMeter, N.C. Luhmann Jr. and A.K. Kerman[1]
University of California at Davis, Davis, CA, USA
[1]Massachusetts Institute of Technology, Cambridge, MA, USA

2C09 **Wave Propagation in a Transient Anisotropic Plasma Medium–Development of a Green's Function**
D.K. Kalluri and T. Huang
University of Massachusetts at Lowell, Lowell, MA, USA

Monday Afternoon – 19 May, 1997
3:00 p.m. – Macaw Room

Oral Session 2D: 2.5 Microwave Systems and 2.4 Slow Wave Devices I
Chair: G.P. Scheitrum

2D01 **Low Cost Infrared Temperature Measurement and Optimal Process Control in Microwave Sintering Systems**
J.P. Calame, Y. Carmel, E. Pert and D. Gershon
University of Maryland, College Park, MD, USA

2D02 **Sintering of Ceramic Compacts in a 35 GHz Gyrotron-Powered Furnace**
A.W. Fliflet, R.W. Bruce[1], R.P. Fischer, D. Lewis III, B.A. Bender, G.-M. Chow, R.J. Rayne, L.K. Kurihara and P.E. Schoen
Naval Research Laboratory, Washington, DC, USA
[1]SFA, Landover, MD, USA

2D03 **Rapid Waveguide System and Component Design Using Scattering Matrices and Computer Optimization**
L. Ives, J. Neilson and W.F. Vogler
Calabazas Creek Research, Inc., Saratoga, CA, USA

2D04 **Computer Analysis of the Effect of a Spectrum Anomaly on the RF System for the Cassini Mission**
J.A. Dayton Jr., J.D. Wilson and C.L. Kory[1]
NASA Lewis Research Center, Cleveland, OH, USA
[1]Analex Corporation/NASA Lewis Research Center, Cleveland, OH, USA

2D05 **Gyrotron-Based Millimeter-Wave Beams and their use in Material Processing**
T. Hardek, W. Cooke and D. Rees
Los Alamos National Laboratory, Los Alamos, NM, USA

2D06 **Millimeter-Wave Folded Waveguide TWT Development at Northrop Grumman**
D. Gallagher, J. Richards and C.M. Armstrong
Northrop Grumman Corporation, Rolling Meadows, IL, USA

2D07 **High-Perveance Electron Beams for High-Power, Slow-Wave Microwave Devices**
M.A. Basten, J.H. Booske, J.E. Scharer and L.J. Louis
University of Wisconsin–Madison, Madison, WI, USA

2D08 **Plasma Induced Gain Enchancement in Backward Wave Oscillators Using Pencil Beams**
A.T. Lin and C.-C. Lin
University of California at Los Angeles, Los Angeles, CA, USA

Monday Afternoon – 19 May, 1997
3:00 p.m. – Cockatoo Room

Oral Session 2E: 1.2 Space Plasmas
Chair: E.E. Scime

2E01-02 *Invited*—**Spacecraft Potential Control on the POLAR Satellite by the Plasma Source Instrument**
R.H. Comfort, T.E. Moore[1], P.D. Craven[1], C.J. Pollock[2], F.S. Mozer[3] and W.S. Williamson[4]
University of Alabama at Huntsville, Huntsville, AL, USA
[1]NASA, Marshall Spaceflight Center, Huntsville, AL, USA
[2]SWRI, San Antonio, TX, USA
[3]University of California at Berkeley, Berkeley, CA, USA
[4]Hughes Research Laboratories, Malibu, CA, USA

2E03 **Reactive Plasma System for On-Orbit Cleaning of Spacecraft Thermal Radiators**
W.S. Williamson, B.L. Drolen[1] and D.A. Kaufman[1]
Hughes Research Laboratories, Malibu, CA, USA
[1]Hughes Space and Communications Co., El Segundo, CA, USA

2E04 **Versatile Toroidal Facility (VTF) for Space Plasma Research**
M.C. Lee, R.J. Riddolls, D.T. Moriarty, M.J. Rowlands and N.E. Dalrymple
Massachusetts Institute of Technology, Cambridge, MA, USA

2E05 **A Laboratory Quiescent Plasma Device for Modeling Velocity Shear in Space**
M.W. Zintl, M.E. Koepke and J.J. Carroll III
West Virginia University, Morgantown, WV, USA

2E06 **"Space Experiments" in the Laboratory**
V.M. Antonov, A.G. Ponomarenko and Yu.P. Zakharov
Siberian Branch of the Russian Academy of Sciences, Novosibirsk, Russia

2E07 **Spacecraft Interactions With Beam Emissions**
S.T. Lai and J. Wang[1]
Phillips Laboratory, Hanscom AFB, MA, USA
[1]Jet Propulsion Laboratory, Pasadena, CA, USA

2E08 **Ion Bunching as a Source of Field-Aligned Currents in Space Plasmas**
N. Brenning
Royal Institute of Technology, Stockholm, Sweden

2E09 **Comparison Between Measured and Simulated Features of Current Collection by the Tethered Satellite**
N. Singh and W.C. Leung
University of Alabama at Huntsville, Huntsville, AL, USA

2E10 **Propagation of Electron Beam in Inhomogeneous Plasma**
E. Kontar, V. Lapshin and V. Mel'nik[1]
Kharkiv State University, Kharkiv, Ukraine
[1]Ukrainian Academy of Sciences, Kharkiv, Ukraine

Monday Afternoon – 19 May, 1997
3:00 p.m. – Rousseau Center

Poster Session 2P16-22: 4.1 Laser Produced Plasmas

2P16 **Reconstruction of Refraction Angle Topology from Laser Plasma Interferogram**
G.S. Sarkisov
P.N. Lebedev Physical Institute, Moscow, Russia and University of California at Irvine, Irvine, CA, USA

2P17 **Satellite Transitions near He_a Lines in a Dense Plasma Heated by 120 fsec Laser**
F.B. Rosmej, I.Yu. Skobelev[1], A.Ya. Faenov[1], T.A. Pikuz[1], M. Fraenkel[2] and A. Zigler[2]
Ruhr-Universitaet Bochum, Germany
[1]MISDC of VNIIFTRI, Moscow Region, Russia
[2]Hebrew University of Jerusalem, Jerusalem, Israel

2P18 **Characterisitcs of a YAG Triggered Plasma Shutter for a CO_2 Laser Beam**
R.L. Williams and K.N. Chase
Florida A & M University, Tallahassee, FL, USA

2P19 **Numerical Model for Plasma Electron Acceleration in Laser Wakefield Accelerators**
R.F. Hubbard, E. Esarey, A. Ting and P. Sprangle
Naval Research Laboratory, Washington, DC, USA

2P20 **Evidence for the Electromagnetic Decay Instability Driven by Two Plasmon Decay**
K.L. Baker, B.B. Afeyan, K.G. Estabrook and R.P. Drake
University of California at Davis, Davis, CA, USA and Lawrence Livermore National Laboratory, Livermore, CA, USA

2P21 **Simulation of Magnetic Field Generation in Laser Plasma Jet**
I.V. Glazyrin, O.V. Diyankov, S.V. Koshelev and V.A. Lykov
Russian Federal Nuclear Center, Snezhinsk, Chelyabinsk Region, Russia

2P22 **Threshold of Nonstationary Laser Supported Detonation Wave**
V. Semak
University of Tennessee Space Institute, Tullahoma, TN, USA

Monday Afternoon – 19 May, 1997
3:00 p.m. – Rousseau Center

Poster Session 2P23-28: 4.2 Inertial Confinement Fusion

2P23 **Analysis of Filtered Silicon Diode Data from MAGO/MTF Experiments**
R.C. Kirkpatrick and G.C. Idzorek
Los Alamos National Laboratory, Los Alamos, NM, USA

2P24 **Plasma Uniformity Issues in a 2 x 1 Plasma-Electrode Pockels Cell**
S. Fochs, M.A. Rhodes and C.D. Boley
Lawrence Livermore National Laboratory, Livermore, CA, USA

2P25 **Target Inserter Ablation Studies for ICF Reactors**
P.B. Parks, R.R. Peterson[1], R.B. Stephens and G.A. Moses[1]
General Atomics, San Diego, CA, USA
[1]University of Wisconsin–Madison, Madison, WI, USA

2P26 **Laser Plasma Interaction at High Intensities**
M. Asthana
Center for Advanced Technology, Indore (M.P.), India

2P27 **Scattering of Laser Radiation at the Heating of Low Density Foam Targets**
S.Y. Guskov, Y.S. Kas'anov[1], M.O. Koshevoi, V.B. Rozanov, A.A. Rupasov and A.S. Shikanov
P.N. Lebedev Physical Institute, Moscow, Russia
[1]General Physics Institute, Moscow, Russia

2P28 **Plasma Formation Dynamics for Laser Interaction with Near Critical Foam Matter**
S.Y. Guskov, Y.S. Kas'anov[1], M.O. Koshevoi, V.B. Rozanov, A.A. Rupasov and A.S. Shikanov
P.N. Lebedev Physical Institute, Moscow, Russia
[1]General Physics Institute, Moscow, Russia

Monday Afternoon – 19 May, 1997
3:00 p.m. – Rousseau Center

Poster Session 2P29-35: 4.3 Magnetic Confinement Fusion

2P29 **Poloidal Current Drive by Rotating Magnetic Field**
Y. Maeda[2], A. Okino[1], M. Maeyama and E. Hotta
Tokyo Institute of Technology, Yokohama, Japan
[1]Saitama University, Urawa, Japan
[2]Tokyo Institute of Technology, Tokyo, Japan

2P30 **A Novel Technique for Disruption Simulation and Accident Analysis Using an ET Plasma Source**
J.P. Sharpe, M.A. Bourham and J.G. Gilligan
North Carolina State University, Raleigh, NC, USA

2P31 **Measurement of Edge Plasma Parameters in KT-1 Tokamak by Single/Mach Probes**
D.-H. Chang, K.-S. Chung, B.-H. Oh[1], K.-W. Lee[1] and S.-K. Kim[1]
Hanyang University, Seoul, Korea
[1]Korea Atomic Energy Research Institute, Seoul, Korea

2P32 **Fast Adiabatic Compression of a Toroidal Plasma to Thermonuclear Ignition**
C.A. Ordonez and R.E. Peterkin Jr.[1]
University of North Texas, Denton, TX, USA
[1]Phillips Laboratory, Kirtland AFB, NM, USA

2P33 **Steady-State Plasma Current Production in a Discharge Device with Magnetic Field Confinement**
W. Luo, H.-S. Li, S. Xu and S. Lee
Nanyang Technological University, Singapore

2P34 **On the Possibility of the Iter Machine to Reach Ignition**
E. Panarella
University of Tennessee, Knoxville, TN, USA and Advanced Laser and Fusion Technology, Inc., Hull, Canada

2P35 **A Heavy Ion Beam Probe for the Madison Symmetric Torus**
K.A. Connor, U. Shah, Y. Dong, P.M. Schoch, T.P. Crowley and J. Lei
Rensselaer Polytechnic Institute Institute, Troy, NY, USA

Monday Afternoon – 19 May, 1997
3:00 p.m. – Rousseau Center

Poster Session 2P36-44: 4.4 Dense Plasma Focus

2P36 **On the Plasma Focus-Produced Spheromak-Like Magnetic Configuration for Jet Propulsion**
A.B. Kukushkin and V.A. Rantsev-Kartinov
RRC Kurchatov Institute, Moscow, Russia

2P37 **Heavy Ion Beam Generation In PF-Systems**
N.V. Filippov and T.I. Filippova
RRC Kurchatov Institute, Moscow, Russia

2P38 **Studies of a Plasma Focus Operated at Higher D_2 Filling Pressure**
M-F. Lu
Chinese Academy of Sciences, Beijing, China

2P39 **Modification of Polyester Film by High Energy Density Plasmas**
M-F. Lu, S.-Z. Yang and C-Z. Liu
Chinese Academy of Sciences, Beijing, China

2P40 **Modified Thomson Spectrometer for the Detection of Low Energy (1keV) High Power Ion Beams**
M-F. Lu, S.-Z. Yang and C-Z. Liu
Chinese Academy of Sciences, Beijing, China

2P41 **X-ray Emission from PF-1000 Plasma-Focus Device Admixtured with Argon**
M. Scholz, M. Borowiecki, L. Karpinski, R. Miklaszewski, W. Stepniewski, M. Sadowski[1], A. Szydlowski[1], V.M. Romanova[2], S.A. Pikuz[2], and A.Ya. Faenov[3]
Institute of Plasma Physics and Laser Microfusion, Warsaw, Poland
[1]Soltan Institute for Nuclear Studies, Warsaw, Poland
[2] P.N. Lebedev Physical Institute, Moscow, Russia
[3]MISDC of VNIIFTRI, Moscow Region, Russia

2P42 **Influence of Electrode Structure on Neutron Emission in PF-40**
M. Han, M-F. Lu, T.C. Yang and X.X. Wang
Tsinghua University, Beijing, China

2P43 **Electron Beam and Neutron Yields in Dependence on Initial Parameters of Plasma Focus**
V.V. Vikhrev and E.O. Baronova
RRC Kurchatov Institute, Moscow, Russia

2P44 **Preliminary Estimations of a Possibility of Creation of Inductive Current Source with a Power 10^{12} W for a Large Plasma Focus Device with Energy ~ 100MJ**
A. P. Lototzky, E.A. Azizov, M.K. Krylov and N.V. Filippov[1]
TRINITI, Moscow Region, Troitsk, Russia
[1]RRC Kurchatov Institute, Moscow, Russia

Monday Afternoon – 19 May, 1997
3:00 p.m. – Rousseau Center

Poster Session 2P45-65: 4.5 Fast Z-Pinches and X-Ray Lasers

2P45 **Laser Probing Experiments with X-Pinches**
G.S. Sarkisov, S.A. Pikuz, T.A. Shelkovenko and V.M. Romanova
P.N. Lebedev Physical Institute, Moscow, Russia

2P46 **Expectations for Hohlraum Environment Driven By Spatially Compressed Flying Radiation Case At Intermediate Currents**
R.L. Bowers, J. Brownell and H.H. Rogers
Los Alamos National Laboratory, Los Alamos, NM, USA

2P47 **Measurements of Z-Pinch Plasma Parameters With Crystal Spectroscopy on PBFAZ and Saturn**
T.J. Nash, C. Deeney, T.W.L. Sanford, G.A. Chandler, R.B. Spielman, D.O. Jobe, J.F. Seamen, T. Gilliland, J.S. McGurn, J.J. MacFarlane[1], J.P. Apruzese[2], K.G. Whitney[2], P.E. Pulsifer[2], J. Davis[2], B. Failor[3], P.D. LePell[3], B. Whitton[3], J.C. Riordan[3] and E.J. Yadlowsky[4]
Sandia National Laboratories, Albuquerque, NM, USA
[1]University of Wisconsin–Madison, Madison, WI, USA
[2]Naval Research Laboratory, Washington, D.C., USA
[3] Primex Physics International, San Leandro, CA, USA
[4] HYTECH Research Co., Washington, DC, USA

2P48 **Determining the Effects of Wire Diameter in Tungsten Wire Array Implosions**
C. Deeney, M.R. Douglas, D.L. Peterson[1], R.B. Spielman, T.J. Nash, G.A. Chandler, D.L. Fehl, J.F. Seamen, K.W. Struve, W.A. Stygar, J.S. McGurn, D.O. Jobe, T. Gilliland, J.A. Torres, R.C. Mock, T.W.L. Sanford and M.K. Matzen
Sandia National Laboratories, Albuquerque, NM, USA
[1]Los Alamos National Laboratory, Los Alamos, NM, USA

2P49 **Method to Unfold the Density Distribution of Any Axially Symmetric Liner from Radiographic Data**
H. Lee
Los Alamos National Laboratory, Los Alamos, NM, USA

2P50 **Compression and Heating History of an Imploding Z-Pinch Plasma**
G. Davara, L. Gregorian, E. Kroupp, V. Fisher and Y. Maron
Weizmann Institute of Science, Rehovot, Israel

2P51 **Wire-Array Initiation and Interwire-Plasma Merger Concerns in PBFA-Z Tungsten Z-Pinch Implosions**

T.W.L. Sanford, R. B. Spielman, G.O. Allshouse, B.M. Marder, K.W. Struve, G.A. Chandler, C. Deeney, D.L. Fehl, T.J. Nash, W.A. Stygar, R.C. Mock, J.F. Seamen, J.S. McGurn, D.O. Jobe, T. Gilliland, A.R. Moats, J.A. Torres, M. Vargas, M.K. Matzen and D.L. Peterson[1]
Sandia National Laboratories, Albuquerque, NM, USA
[1]Los Alamos National Laboratorym, Los Alamos, NM, USA

2P52 **Monochromatic X-ray Backlighting of Dense Z-pinch Plasmas Using an X-pinch X-ray Source**

S.A. Pikuz, T.A. Shelkovenko, D.A. Hammer[1] and D.F. Acton[1]
P.N. Lebedev Physical Institute, Moscow, Russia
[1]Cornell University, Ithaca, NY, USA

2P53 **Shear Flow Stabilization of the Hydromagnetic Rayleigh-Taylor Instability**

N.F. Roderick, U. Shumlak[1], M.R. Douglas[2], R.E. Peterkin Jr.[3] and E.L. Ruden[3]
University of New Mexico, Albuquerque, NM, USA
[1]University of Washington, Seattle, WA, USA
[2]Sandia National Laboratories, Albuquerque, NM, USA
[3]Phillips Laboratory, Kirtland AFB, NM, USA

2P54 **Two-Dimensional MHD Numerical Simulation of Radiating Exploding Wire Plasma Dynamics**

W. Stepniewski, R. Miklaszewski and M. Scholz
Institute of Plasma Physics and Laser Microfusion, Warsaw,Poland

2P55 **Stepping-Up of a Generation of High Intensity X Radiation In Liner Systems**

S.V. Zakharov
Troitsk Institute for Innovation and Thermonuclear Research, Troitsk, Moscow Region, Russia

2P56 **Simulation of Wire Array Implosions on High-Current Pulsed Power Generators**

N.A. Gondarenko and A.L. Velikovich[1]
GNG Enterprises, Inc., Springfield, VA, USA
[1]Berkeley Research Associates, Springfield, VA, USA

2P57 **Modeling X-ray Data for the Saturn Z-Pinch Machine**

W. Matuska, D.L. Peterson, C. Deeney[1] and M.S. Derzon[1]
Los Alamos National Laboratory, Los Alamos, NM, USA
[1]Sandia National Laboratories, Albuquerque, NM, USA

2P58 **Wire Array Implosion Experiments on the Inductive Storage Generators GIT-4 and GIT-8**

R.B. Baksht, I.M. Datsko, A.A. Kim, V.A. Kokshenev, B.M. Koval'chuk, S.V. Loginov, A.Yu. Labetsky, A.V. Fedunin, A.G. Russkikh, and A.V. Shishlov
High Current Electronics Institute, Tomsk, Russia

2P59 **The Effect of Shell Thickness on Rayleigh-Taylor Mitigation in High Velocity, Annular Z-pinch Implosions**
M.R. Douglas, C. Deeney and N.F. Roderick[1]
Sandia National Laboratories, Albuquerque, NM, USA
[1]University of New Mexico, Albuquerque, NM, USA

2P60 **Computational Modeling of Wall-Supported Dense Z-Pinches**
P.T. Sheehey, R.A. Gerwin, R.C. Kirkpatrick, I.R. Lindemuth and F.J. Wysocki
Los Alamos National Laboratory, Los Alamos, NM, USA

2P61 **Yield Enhancements in and Spectral Measurements of Al-Mg-KC1 Mixture Arrays on the 7-MA Saturn Generator**
P.D. LePell, B. Failor, C. Deeney[1], T.J. Nash[1], J.P. Apruzese[2], E.J. Yadlowsky[3], K.G. Whitney[2], J. Thornhill[2], R.B. Spielman[1], J. Davis[2], C. Coverdale, P. L'Eplantier[1] and J.C. Riordan
Primex Physics International, San Leandro, CA, USA
[1]Sandia National Laboratory, Albuquerque, NM, USA
[2]Naval Research Laboratory, Washington, DC, USA
[3]HYTECH Research Co., Washington, DC, USA

2P62 **Detailed Spectral Simulations in Support of PBFA-Z Dynamic Hohlraum Z-Pinch Experiments**
J.J. MacFarlane, M.S. Derzon[1], T.A. Haill[1], T.J. Nash[1], P. Wang and D.L. Peterson[2]
University of Wisconsin–Madison, Madison, WI, USA
[1]Sandia National Laboratories, Albuquerque, NM, USA
[2]Los Alamos National Laboratory, Los Alamos, NM, USA

2P63 **A Simple Scaling Estimate of Input Powers for X-ray Lasers Excited in Capillary Discharges**
C.B. Collins, W. Rosenfeld[1], R. Dussart[1], C. Cachoncinlle[1], D. Hong[1], C. Fleurier[1] and J.M. Pouvesle[1]
CQE, UTD, Richardson, TX, USA
[1]GREMI, CNRS/Université d'Orléans, France

2P64 **Measurement of the Radial Evolution of a Gas-Puff Z-Pinch by Inverse Bremstrahlung Absorption of HeNe Laser Light**
G.S. Sarkisov[1], A. VanDrie, B. Moosman, Y. Song and F.J. Wessel
University of California at Irvine, Irvine, CA, USA
[1]On leave from P.N. Lebedev Physical Institute, Moscow, Russia

2P65 **Fibres Experiments in the MAGPIE Generator**
R. Aliaga-Rossel, J.P. Chittenden, S. Lebedev, J.H. Mitchell, A.E. Dangor and M.G. Haines
The Blackett Laboratory, Imperial College, London, U.K.

Tuesday Morning – 20 May, 1997
8:30 a.m. – Kon Tiki Ballroom

Plenary Session

Trapped Plasmas with a Single Sign of Charge (An Overview)

Professor Thomas M. O'Neil
University of California at San Diego, La Jolla, CA, USA

Chair: C. R. Ordonez

Tuesday Morning – 20 May, 1997
10:00 a.m. – Kon Tiki Ballroom

Oral Session 3A: 1.4 Computational Plasma Physics I
Chair: J. Huba

3A01 **A Study of Stability and Energy Conservation of a 3-D Electromagnetic PIC Code for Non-Orthogonal Meshes.**
D. Kondrashov, J. Wang[1] and P.C. Liewer[1]
California Institute of Technology, Pasadena, CA, USA
[1]Jet Propulsion Laboratory and California Institute of Technology, Pasadena, CA, USA

3A02 **Massively Parallel 3-Dimensional Particle-in-Cell Plasma Code**
E.E. Wells, S. Al-Sharaeh and N. Singh
University of Alabama in Huntsville, Huntsville, AL, USA

3A03 **Simulation Studies of Optimized Electrode Designs for a Cylindrical IEC**
G.H. Miley, J. DeMora, R.A. Stubbers, R. Zich, J. Sved[1], R. Anderl[2] and J. Hartwell[2]
University of Illinois, Urbana, IL, USA
[1]DASA, Bremmen, Germany
[2]INEL, Idaho Falls, ID, USA

3A04 **Quasineutral Particle Simulation / Monte Carlo Model of Magnetized Plasma Discharges**
M. Lampe, G. Joyce and W.M. Manheimer
Naval Research Laboratory, Washington, DC, USA

3A05 **Long Mean Free Path Kinetic Theory Using Scattering Rates**
W.N.G. Hitchon and G.J. Parker[1]
University of Wisconsin–Madison, Madison, WI, USA
[1]Lawrence Livermore National Laboratory, Livermore, CA, USA

3A06 **Ion Distribution Functions in an ECR Discharge Plasma**
G. Joyce, M. Lampe, W.M. Manheimer and S. Slinker
Naval Research Laboratory, Washington, DC, USA

Tuesday Morning – 20 May, 1997
10:00 a.m. – Board Room

Oral Session 3B: 2.1 Intense Beam Microwaves
Chair: E. Schamiloglu

3B01 **Efficiency Enhanced, Load-Limited MILO**
R.W. Lemke, M.C. Clark and S.E. Calico[1]
Sandia National Laboratories, Alburquerque, NM, USA
[1]Phillips Laboratory, Kirtland AFB, NM, USA

3B02-03 *Invited*—**Success on Elimination of Pulse Shortening of GW-Class, 300 nsec HPM Sources**
K. Hendericks, M. Haworth, R. Lemke[1], M. Sena[2], D. Ralph[2], K. Allen[2], T. Englert, D. Shiffler, T. A.Spencer, M.J. Arman, K. Hackett, S.E. Calico, D. Coleman[1], M.C. Clark[1], and R. Gallegoes[1]
Phillips Laboratory, Kirtland AFB, NM, USA
[1]Sandia National Laboratories, Albuquerque, NM, USA
[2]Maxwell Laboratories, Inc., Albuquerque, NM, USA

3B04 **Recent Results in the Hard-Tube MILO Experiment**
M. Haworth, K. Hendricks, R. Lemke[1], T. Englert, D. Shiffler, K. Hackett, M. Sena[2], K. Allen[2], D. Ralph[2] and D. Henley[2]
Phillips Laboratory, Kirtland AFB, NM, USA
[1]Sandia National Laboratories, Albuquerque, NM, USA
[2]Maxwell Laboratories, Inc., Albuquerque, NM, USA

3B05 **Beam Drift and Diffusion in Linear Beam HPM Sources**
J.N. Benford and G. Benford[1]
Microwave Sciences, Lafayette, CA, USA
[1]University of California at Irvine, Irvine, CA, USA

3B06 **Window and Cavity Breakdown Caused By High Power Microwaves**
A. Neuber, J. Dickens, D. Hemmert, H. Krompholz, L.L. Hatfield and M. Kristiansen
Texas Tech University, Lubbock, TX, USA

3B07 **Performance of a Cathode Mounted Plasma Injection Source on the UNM Long-Pulse BWO**
C. Grabowski, J.M. Gahl and E. Schamiloglu
University of New Mexico, Albuquerque, NM, USA

3B08 **Progress in Implementation of a Frequency Agile, High Power Backward-Wave Oscillator**
C.T. Abdallah, E. Schamiloglu, V.S. Souvalian and G.T. Park
University of New Mexico, Albuquerque, NM, USA

3B09 **Investigation of the Dispersive Properties of Photonic Crystals Using High-Power Microwaves**
K. Agi, M. Mojahedi, K.J. Malloy and E. Schamiloglu
University of New Mexico, Albuquerque, NM, USA

Tuesday Morning – 20 May, 1997
10:00 a.m. – Toucan Room

Oral Session 3C: 3.2 Intense Ion and Electron Beams
Chair: P.R. Menge

3C01 **Development of a High-Brightness, Applied-B Lithium Extraction Ion Diode for Inertial Confinement Fusion**
M.E. Cuneo, R.G. Adams, J. Armijo, J.E. Bailey, C.H. Ching, M.P. Desjarlais, A.B. Filuk, W.E. Fowler, D.L. Hanson, D.J. Johnson, J.S. Lash, T.A. Mehlhorn, P.R. Menge, D. Nielsen, T.D. Pointon, S.A. Slutz, M.A. Stark, R.A. Vesey and D.F. Wenger
Sandia National Laboratories, Albuquerque, NM, USA

3C02-03 *Invited*—**Effects of Electron-Anode Interactions in Applied-B Ion Diodes**
R.A. Vesey, T.D. Pointon, M.E. Cuneo and T.A. Mehlhorn
Sandia National Laboratories, Albuquerque, NM, USA

3C04 **Gas-Breakdown Effects Associated with the Self-Pinched Transport of Intense Light-Ion Beams**
D.V. Rose, B.V. Oliver[1], P.F. Ottinger[2], C.L. Olson[2] and D.R. Welch[2]
JAYCOR, Inc., Vienna, VA, USA
[1]National Research Council Research Associate, Washington, DC, USA
[2]Sandia National Laboratories, Albuquerque, NM, USA

3C05 **Performance of a Shallow-Focus Applied-Magnetic-Field Diode for Ion-Beam-Transport Experiments**
F.C. Young, J.M. Neri, T.G. Jones[1], B.V. Oliver[1], P.F. Ottinger and D.V. Rose[2]
Naval Research Laboratory, Washington, DC, USA
[1]National Research Council Research Associate, Washington, DC, USA
[2]JAYCOR, Inc., Vienna, VA, USA

3C06 **Progress Toward a Microsecond Duration, Repetitive, Intense-Ion Beam Accelerator**
H.A. Davis, D.M. Coates[1], W.A. Reass, J.B. Greenly[3], R.H. Lovberg[4] and H.M. Schleinitz[1]
Los Alamos National Laboratory, Los Alamos, NM, USA
[1]DuPont, Los Alamos, NM, USA
[2]Los Alamos National Laboratory, Los Alamos, NM, USA
[3]Cornell University, Ithaca, NY, USA
[4]University of California at San Diego, La Jolla, CA, USA

3C07 **Oxide Cathodes Produced by Plasma Deposition**
G. Scheitrum, G. Caryotakis, T. Pi[1], R. Umstattd[1], I. Brown[2] and O. Montiero[2]
Stanford Linear Accelerator Center, Menlo Park, CA, USA
[1]University of California at Davis, Davis, CA, USA
[2]Lawrence Berkeley Laboratory, Berkeley, CA, USA

3C08 **Simulation of a Plasma-Focused Electron Gun**
J.P. Verboncoeur
University of California at Berkeley, Berkeley, CA, USA

3C09 **Two Dimensional Child-Langmuir Law**
S. McGee, J.W. Luginsland[1], Y.Y. Lau and R.M. Gilgenbach
University of Michigan, Ann Arbor, MI, USA
[1]Phillips Laboratory, Kirtland AFB, NM, USA

Tuesday Morning – 20 May, 1997
10:00 a.m. – Macaw Room

Oral Session 3D: 2.4 Slow Wave Devices II
Chair: W.L. Menninger

3D01-02 *Invited*—**60% Efficient C-Band TWT for the Microwave Power Module**
D.R. Whaley, C.M. Armstrong, B. Gannon, G. Groshart, E. Hurt, J. Hutchins and M. Roscoe
Northrop Grumman Corporation, Rolling Meadows, IL, USA

3D03 **GATOR: A 3-D Time-Dependent Simulation Code for Helix TWTs**
H.P. Freund[1] and E.G. Zaidman
Science Applications International Corp., McLean, VA, USA
[1]Naval Research Laboratory, Washington, DC, USA

3D04 **Travelling Wave Tube Devices with Non Linear Dielectric Elements**
T.M. Antonsen Jr. and B. Levush[1]
Science Applications International Corp., McLean, VA, USA and University of Maryland, College Park, MD, USA
[1]Naval Research Laboratory, Washington, DC, USA

3D05 **Calculation and Measurement of Intermodulation Products in TWTs**
D.J. Gregoire and W. Menniger[1]
Hughes Research Laboratories, Malibu, CA, USA
[1]Hughes Electron Dynamic Division, Torrance, CA, USA

3D06 **Computational Optimization of RF and Overall Efficiency in TWTs with Simulated Annealing**
J.D. Wilson
NASA Lewis Research Center, Cleveland, OH, USA

3D07 **Three Dimensional Modeling of Multistage Depressed Collectors**
K.R. Vaden, V.O. Heinen and J.A. Dayton Jr.
NASA Lewis Research Center, Cleveland, OH, USA

3D08 **Cold-Test and Interaction Models for Helix TWTs in MMACE**
A.A Mondelli, J.J. Petillo and H.P. Freund
Science Application International Corp., McLean, VA, USA

3D09 **Investigation of the Effect of Support Rod Permittivity on TWT Performance**
C.L. Kory and J.A. Dayton Jr.[1]
Analex Corporation/NASA Lewis Research Center, Cleveland, OH, USA
[1]NASA Lewis Research Center, Cleveland, OH, USA

Tuesday Morning – 20 May, 1997
10:00 a.m. – Cockatoo Room

Oral Session 3E: 4.4 Dense Plasma Focus I
Chair: G.F. Kiuttu

3E01 **Memorial Tribute to Dr. Joseph Mather**
K.D. Ware
Defense Special Weapons Agency, Alexandria, VA, USA

3E02-03 **Present Status of Plasma Focus Research At RRC "Kurchatov Institute"**
N.V. Filippov
RRC Kurchatov Institute, Moscow, Russia

3E04 **Formation of a Closed, Spheromak-Like Magnetic Configuration in Plasma Focus Discharges and the Enhanced Radiation Yield in High-Current Discharges**
A.B. Kukushkin and V.A. Rantsev-Kartinov
RRC Kurchatov Institute, Moscow, Russia

3E05 **X-ray Spectroscopic Diagnostics of High-Temperature Dense Plasmas Created in Different Gaseous Media**
I.Yu. Skobelev, A. Bartnik[1], V.M. Dyakin, A.Ya. Faenov, H. Fiedorowicz[1], R. Jarotcki, J. Kostecki, J. Nilsen[2], A.L. Osterheld[2], M. Szczurek[1]
MISDC of VNIIFTRI, Moscow Region, Russia
[1]Military University of Technology, Warsaw, Poland
[2]Lawrence Livermore National Laboratory, Livermore, CA, USA

3E06-07 **Dense Plasma-Focus Research in Poland**
M. Sadowski
Soltan Institute for Nuclear Studies, Warsaw, Poland

Tuesday Morning – 20 May, 1997
10:00 a.m. – Rousseau Center

Poster Session 3P01-28: 1.1 Basic Processes in Fully and Partially Ionized Plasmas – Waves, Instabilities, Plasma Theory, etc.

3P01 **Modeling of Collisional Effects in RF Plasma Sources**
M.H. Bettenhausen, J.E. Scharer and Y. Mouzouris
University of Wisconsin–Madison, Madison, WI, USA

3P02 **Antenna Coupling and Absorption Mechanisms in a Helicon Source Operation**
Y. Mouzouris, J.E. Scharer and M.H. Bettenhausen
University of Wisconsin–Madison, Madison, WI, USA

3P03 **Helicon Wave Excitation with Bifilar Antennas**
D.G. Miljak and F.F. Chen
University of California at Los Angeles, LosAngeles, CA, USA

3P04 **A Multi-Tube Helicon Source**
J.D. Evans and F.F. Chen and G. Tynan[1]
University of California at Los Angeles, Los Angeles, CA, USA
[1]PMT, Inc., Chatsworth, CA, USA

3P05 **2D Imaging of a Helicon Discharge**
D.D. Blackwell and F.F. Chen
University of California at Los Angeles, Los Angeles, CA, USA

3P06 **Spontaneous Current Disruptions in a Plasma-Driven Double Probe**
A. Svensson and N. Brenning
Alfvén Lab., Stockholm, Sweden

3P07 **Direct Magnetic Field Measurement of Micro-Turbulence Enhanced Electron Collisionality in Magnetized Coaxial Accelerator Channels**
D.C. Black and R.M. Mayo
North Carolina State University, Raleigh, NC, USA

3P08 **Wave Propagation in a Time-Varying and Space-Varying Isotropic Plasma Medium**
D.K. Kalluri
University of Massachusetts at Lowell, Lowell, MA, USA

3P09 **Suprathermal Electron Diagnostics, Based on X-ray Line Radiation Polarization Measurements**
E.O. Baronova
RRC Kurchatov Institute, Moscow, Russia

3P10 **Plasma Species in Methane-Hydrogen and Methane-Hydrogen-Argon Arcjet Plasmas**
M.C. Baker, M. Bartlemass[1], R. Irion, L.L. Hatfield, M. Kristiansen and E. O'Hair
Texas Tech University, Lubbock, TX, USA
[1]No longer at Texas Tech University

3P11 **The Vacuum Arc Discharge in Anode Material Vapour**
V.N. Pavlenko and V.G. Panchenko
Institute for Nuclear Research, Kiev, Ukraine

3P12 **Scattering of Electromagnetic Waves by Density Fluctuations in the Inhomogeneous Plasma with Lower Hybrid Pump**
V.N. Pavlenko and V.G. Panchenko
Institute for Nuclear Research, Kiev, Ukraine

3P13 **Plasmachemical Reactor for Precision Etching of Elements with Submicron Size**
V.N. Pavlenko, V.G. Panchenko, V.V. Ustalov and O.A. Fedorovich
Institute for Nuclear Research, Kiev, Ukraine

3P14 **The Waves Scattering Processes in the Magnetized Plasma with Upper Hybrid Pump**
V.N. Pavlenko, V.G. Panchenko and I.N. Rosum
Institute for Nuclear Research, Kiev, Ukraine

3P15 **Nonstationary Parametric Processes in a Semibounded Plasma**
V.N. Pavlenko and V.G. Panchenko
Institute for Nuclear Research, Kiev, Ukraine

3P16 **Simulations of Modulational and Resistive Instabilities in Cylindrical Crossed-Field Diodes**
P.J. Christenson and V.P. Gopinath
University of California at Berkeley, Berkeley, CA, USA

3P17 **Calculation of the Electric Microfield Distrbution in Plasma Revised**
J. Puerta and C. Cereceda[1]
Universidad Simón Bolívar, Caracas, Venezuela
[1]CEN-Limeil, Orsay, France

3P18 **Wake Potential Due to a Pair of Dust Paticles in a Plasma**
W. Zhang, O. Ishihara and S.V. Vladimirov[1]
Texas Tech University, Lubbock, TX, USA
[1]University of Sydney, New South Wales, Australia

3P19 **The Potential of Particles in Dust Crystal in rf Discharge**
V.A. Schweigert and I.V. Schweigert[1]
Institute of Theoretical and Applied Mechanics, Novosibirsk, Russia
[1]Institute of Semiconductor Physics, Novosibirsk, Russia

3P20 **Propagation of a Wave in a Plasma with Coulomb Collisions**
S.V. Vladimirov and O. Ishihara[1]
University of Sydney, New South Wales, Australia
[1]Texas Tech University, Lubbock, TX, USA

3P21 **Ponderomotive Forces in a Time-Dependent Plasma**
S. Vladimirov
University of Sydney, New South Wales, Australia

3P22 **Alfvén Surface Waves in a Dusty Magnetised Plasma**
N.F. Cramer and S.V. Vladimirov
University of Sydney, New South Wales, Australia

3P23 **Wave Relaxation and Parametric Instability in Partially Ionized Plasma**
M.A. Drofa, L.S. Kuz'menkov and S.G Maximov
Moscow State University, Moscow, Russia

3P24 **Turbulization of Non-Linear Langmuir Oscillations in a Cold Plasma**
A.V. Kovalenko and V.P. Kovalenko
National Academy of Sciences of Ukraine, Kiev, Ukraine

3P25 **"Electron Is Particle" for Scientists**
T. Ohnuma
Tohoku University, Sendai, Japan

3P26 **On Adiabatic Change of State Photon Gas 2**
M. Mészáros
Institute of Physics, Budapest, Hungary

3P27 **Formation of Thermoelectric Field in a Collisionless Non-Equalibrium Plasma**
V.P. Krainov, V.A. Rantsev-Kartinov and E.E. Trofimovich
RRC Kurchatov Institute, Moscow, Russia

3P28 **Experimental Study of Plasma Character Inion Diffusing into Metal Caused by Double Glow Discharge**
Z. Shang
Southwestern Institute of Physics, Chengdu, Sichuan, China

Tuesday Morning – 20 May, 1997
10:00 a.m. – Multipurpose Room

Poster Session 3Q01-15: 5.1 Non-Equilibrium Plasma Processing I (Ion Implantation)

3Q01 **Transport of a Cathodic Arc Plasma Inside a Magnetized Tube**
B.P. Cluggish and B.P. Wood
Los Alamos National Laboratory, Los Alamos, NM, USA

3Q02 **Pulsed-Plasma Deposition of Amorphous Diamond-like Carbon Films on Copper**
S. Chiu, B. Terreault and A. Sarkissian
INRS-Énergie et Matériaux, Varennes QC, Canada

3Q03 **Ultra-Shallow p+/n Junction Formed by Plasma Source Ion Implantation and Solid Boron Source**
H.L. Liu, S.S. Gearhart, J.H. Booske and W. Wang
University of Wisconsin–Madison, Madison, WI, USA

3Q04 **Surface Modification of Cr_{12} MoV Steel by PSII Nitrogen Implantation**
W. Pu
Southwestern Institute of Physics, Chengdu, Sichuan, China

3Q05 **The Application of Ion Beam Implantation for Synthetic Diamond Surface Modification**
W. Pu
Southwestern Institute of Physics, Chengdu, Sichuan, China

3Q06 **Research on Application of Ion Implantation in SWIP**
W. Pu
Southwestern Institute of Physics, Chengdu, Sichuan, China

3Q07 **The PSII-IM Device**
Z. Shang
Southwestern Institute of Physics, Chengdu, Sichuan, China

3Q08 **Ultra-hard Crystalline β-C_3N_4 Films Synthesized Using a Reactive RF Magnetron Plasma Source**
S. Xu, H-S. Li, S. Lee and Y-A. Li[1]
Nanyang Technological University, Singapore
[1]Chinese Academy of Sciences, Beijing, China

3Q09 **Charging of Substrates Irradiated by Particle Beams**
P.N. Guzdar, A.S. Sharma and S.K. Guharay
University of Maryland, College Park, MD, USA

3Q10 **Cathodic Arc Plasma Density and Profile Measurements**
B.P. Wood, M.G. Tuszewski, D. Pesensen[1] and F.J. Wessel[1]
Los Alamos National Laboratory, Los Alamos, NM, USA
[1]University of California at Irvine, Irvine, CA, USA

3Q11 **TiN Prepared by Plasma Source Ion Implantation of Nitrogen into Ti as a Diffusion Barrier for Si/Cu Metallization**
W. Wang, J.H. Booske, H.L. Liu, S.S. Gearhart, S. Bedell[1] and W. Lanford[1]
University of Wisconsin–Madison, Madison, WI, USA
[1]State University of New York–Albany, Albany, NY, USA

3Q12 **Compact High-Voltage Pulse Generator For Plasma Applications**
V.A. Spassov[1], L. Gueorguiev[2], J. Barroso and M. Ueda
National Institute for Space Research, San Jose dos Campos, Brazil
[1]Visiting Scientist, Sofia University, Sofia, Bulgaria
[2]Wayne State University, Detroit, MI, USA

3Q13 **Enhancement of Surface Properties of 45# Steel Using Plasma Immersion Ion Implantation**
S.Y. Wang, P.K. Chu, X.B. Tian, X.F. Wang, A.G. Liu, Q.Z. Lin[1], B.Y. Tang and X.C. Zeng
City University of Hong Kong, Kowloon, Hong Kong
[1]Harbin Institute of Technology, China

3Q14 **Transient Sheath in a Small Cylindrical Bore with an Auxiliary Electrode for Finite-Rise-Time Voltage Pulses**
X.C. Zeng, T.K. Kwok, A.G. Liu, P.K. Chu and B.Y. Tang
City University of Hong Kong, Kowloon, Hong Kong

3Q15 **Effects of the Auxiliary Electrode Radius During Plasma Immersion Ion Implantation of a Small Cylindrical Bore**
X.C. Zeng, A.G. Liu, T.K. Kwok, P.K. Chu and B.Y. Tang
City University of Hong Kong, Kowloon, Hong Kong

Tuesday Afternoon – 20 May, 1997
1:30 p.m. – Kon Tiki Ballroom

Plenary Session

Interaction of Ultra-Intense Lasers with Beams and Plasmas

Dr. Phillip Sprangle
Naval Research Laboratory, Washington, DC, USA

Chair: S. L. Ossakow

Tuesday Afternoon – 20 May, 1997
3:00 p.m. – Kon Tiki Ballroom

Special Panel Session

Changing Career Opportunities in Plasma Science

Dr. Wallace M. Manheimer, Moderator
Naval Research Laboratory, Washington, DC, USA

Panelists:

Dr. Jim Benford
Microwave Science

Dr. Adam Drobot
Science Application International Corp.

Dr. Don Rej
LANL

Professor Georges Zisses
Université Paul Sabatier

Tuesday Afternoon – 20 May, 1997
3:00 p.m. – Rousseau Center

Poster Session 4P29-52: 2.2 Fast Wave Devices

4P29 **Modeling of Wide-Band Gyrotwystron Amplifiers**
B. Levush, M. Blank, B.G. Danly, P.E. Latham[1] and T.M. Antonsen Jr.[2]
Naval Research Laboratory, Washington, DC, USA
[1]Omega-P, Inc., New Haven, CT, USA
[2]University of Maryland, College Park, MD, USA

4P30 **Design of a 80 kW, 700 MHz Bandwidth W-Band Gyroklystron Amplifier Circuit**
M. Blank, B. Levush, B.G. Danly, P.E. Latham[1], J.P. Calame[1], D.E. Pershing[2] and W. Lawson[3]
Naval Research Laboratory, Washington, DC, USA
[1]Omega-P, Inc., New Haven, CT, USA
[2]Mission Research Corporation, Newington, VA, USA
[3]University of Maryland, College Park, MD, USA

4P31 **MAGY: A Self-Consistent Code for Modeling Electron Beam Devices**
M. Botton, T.M. Antonsen Jr. and B. Levush[1]
University of Maryland, College Park, MD, USA
[1]Naval Research Laboratory, Washington, DC, USA

4P32 **Overmoded Abrupt Transition TE_{021} Cavities for a 100 MW Second Harmonic Gyroklystron**
M. Castle, W. Lawson, J.P. Anderson, G.P. Saraph, M. Stattel, B. Hogan, V.L.Granatstein and M. Reiser
University of Maryland, College Park, MD, USA

4P33 **Design of Magnetron Injection Gun and Collector for High Average Power 94 GHZ Gyroamplifiers**
K.T. Nguyen, B. Danly[1], B. Levush[1], M. Blank[1], R.B. True[2], K. Felch[3] and P. Borchard[3]
KN Research, Silver Springs, MD, USA
[1]Naval Research Laboratory, Washington, DC, USA
[2]Litton Systems, Inc., Electron Devices Division, San Carlos, CA, USA
[3]Communications & Power Industries, Inc., Palo Alto, CA, USA

4P34 **Circuit Aspects of the NRL/Industrial 94 Ghz Gyroklystron Amplifier**
D. Pershing, K.T. Nguyen[1], J.J. Petillo[2], J.P. Calame[3], B. Danly[4] and B. Levush[4]
Mission Research Corporation, Newington, VA, USA
[1]KN Research, Silver Springs, MD, USA
[2]Science Application International Corp., McLean, VA, USA
[3]University of Maryland, College Park, MD, USA
[4]Naval Research Laboratory, Washington, DC, USA

4P35 **Calorimeter Analysis and Test for Symmetric Circular Waveguide Mode Output**
A.H. McCurdy, J.J. Choi[1], S.J. Cooke[2], G.S. Park[3], R.H. Kyser[4] and B.G. Danly[5]
University of Southern California, Los Angeles, CA, USA
[1]Science Application International Corp., McLean, VA, USA
[2]University of Maryland, College Park, MD, USA
[3]Seoul National University, Seoul, Korea
[4]Dyncorp, Rockville, MD, USA
[5]Naval Research Laboratory, Washington, DC, USA

4P36 **Theory of the Inverted Gyrotwystron**
G. Nusinovich, M. Walter and V. Granatstein
University of Maryland, College Park, MD, USA

4P37 **Dispersion Characteristics of Spiral-Corrugated Cylindrical Waveguide for a Gyro-TWT Amplifier**
S.J. Cooke and G.G. Denisov[1]
University of Maryland, College Park, MD, USA
[1]Institute of Applied Physics, Nizhny Novgorod, Russia

4P38 **Development of a Thermoionic Magnicon Amplifier at 11.4 GHz**
S.H. Gold, B. Hafizi[1], A.W. Fliflet, A.K. Kinkead[2], O.A. Nezhevenko[3], V.P. Yakovlev[4], J.L. Hirshfield[4] and R.B. True[5]
Naval Research Laboratory, Washington, DC, USA
[1]Icarus Research, Inc., Bethesda, MD, USA
[2]SFA, Landover, MD, USA
[3]On leave from Budker, INP, Novosibirsk, Russia
[4]Omega-P, Inc., New Haven, CT, USA
[5]Litton Systems, Inc., Electron Devices Division, San Carlos, CA, USA

4P39 **Influence of a Nonrandom Gyrophase Distribution on the Cylotron-Resonance Maser Instability**
J.A. Davies and C. Chen[1]
Clark University, Worchester, MA, USA
[1]Massachusetts Institute of Technology, Cambridge, MA, USA

4P40 **Implication of DC Space Charge Induced Velocity Spread on Gyrotron Gun Performance**
C. Liu and T.M. Antonsen Jr.
University of Maryland, College Park, MD, USA

4P41 **Stable Third-Harmonic TE_{41} Gyro-TWT for 2 MW at 35 GHz**
K.X. Liu, B.H. Deng, J.R. VanMeter, L. Dressman, D.B. McDermott and N.C. Luhmann Jr.
University of California at Davis, Davis, CA, USA

4P42 **High Power Ubitron-Klystron**
A.J. Balkcum, D.B McDermott, R.M. Phillips[1] and N.C. Luhmann Jr.
University of California at Davis, Davis, CA, USA
[1]Stanford Linear Accelerator Center, Menlo Park, CA, USA

4P43 **Slotted Third-Harmonic Gyro-TWT**
C.K. Chong, D.B. McDermott[1] and N.C. Luhmann Jr.[1]
CPI, Palo Alto, CA, USA
[1]University of California at Davis, Davis, CA, USA

4P44 **Autororesonant Cavity Acceleration**
D.B. McDermott, V.V. Dinh and N.C. Luhmann Jr.
University of California at Davis, Davis, CA, USA

4P45 **Preliminary Measurements of a Novel 140 GHz Gyro-TWT Amplifier**
W. Hu, K.E. Kreisher, M. Shapiro, and R.J. Temkin
Massachusetts Institute of Technology, Cambridge, MA, USA

4P46 **Fractional Harmonic Raditation from a Prebunched Free Electron Laser**
M.G. Kong and A. Vourdas
University of Liverpool, Liverpool, England

4P47 **FEL Amplification by a Multiharmonically Prebunched Electron Beam**
M.G. Hong
University of Liverpool, Liverpool, England

4P48 **Low Voltage FEL Amplification Based on a Longitudinal Interaction Mechanism**
M.G. Hong
University of Liverpool, Liverpool, England

4P49 **A Frequency-Doubling Millimeter-Wave Amplifer**
J.E. Velazco and P.H. Ceperley[1]
Microwave Technologies, Inc., Burke, VA, USA
[1]George Mason University, Fairfax, VA, USA

4P50 **An Efficient Harmonic Amplifier**
J.E. Velazco and P.H. Ceperley[1]
Microwave Technologies Inc., Burke, VA, USA
[1]George Mason University, Fairfax, VA, USA

4P51 **Operation of a Ka-Band CHI Wiggler Ubitron Amplifier**
J.M. Taccetti, R.H. Jackson[1], H.P. Freund[2], D.E. Pershing[3] and V.L. Granatstein
University of Maryland, College Park, MD, USA
[1]Naval Research Laboratory, Washington, DC, USA
[2]Science Application International Corp., McLean, VA, USA
[3]Mission Research Corporation, McLean, VA, USA

4P52 **A Third Harmonic Magnicon Amplifier at 34 GHz**
O.A. Nezhevenko, V.P. Yakovlev, A.K. Ganguly[1] and J.L. Hirshfield[1]
Budker, INP, Novosibirsk, Russia
[1]Omega-P, Inc., New Haven, CT, USA

Tuesday Afternoon – 20 May, 1997
3:00 p.m. – Multipurpose Room

Poster Session 4Q16-21: 5.1 Non-Equilibrium Plasma Processing II (Atmospheric Discharges)

4Q16 **An Improved Ionizer for Atmosphere Plasmas**
I. Alexeff, M. Rader, L. Wadsworth and P. Tsai
University of Tennessee, Knoxville, TN, USA

4Q17 **Atmospheric Pressure Non-Thermal Plasma**
S.K. Dhali
Southern Illinois University, Carbondale, IL, USA

4Q18 **Experimental Studies on AC Dielectric Barrier Corona Discharge Reactors for NO_x/SO_x Decompositions**
Y.H. Kim and S.H. Hong
Seoul National University, Seoul, Korea

4Q19 **Increasing the Surface Energy of Materials with a One Atmosphere Uniform Glow Discharge Plasma**
J.L. Richardson, A.K. Carr, J.R. Roth
University of Tennessee, Knoxville, TN, USA

4Q20 **The Effect of Active Manipulation of a Plasma Surface Layer on the Aerodynamic Drag of a Flat Plate**
D.M. Sherman, J.R. Roth and S.P. Wilkinson[1]
University of Tennessee, Knoxville, TN, USA
[1]NASA Langley Research Center, Hampton, VA, USA

4Q21 **Killing Microorganisms in a Sealed Sterilization Bag with a One Atmosphere Uniform Glow Discharge**
A.K. Carr, J.R. Roth, C. Brickman, K. Kelly-Wintenberg, T.C. Montie, P. Tsai and L. Wadsworth
University of Tennessee, Knoxville, TN, USA

Tuesday Afternoon – 20 May, 1997
3:00 p.m. – Multipurpose Room

Poster Session 4Q22-28: 5.1 Non-Equilibrium Plasma Processing II (Deposition and Etching)

4Q22 **Monte Carlo Simulation and Experimental Study of an Electron Cyclotron Resonance Plasma for thin Film Deposition**
E. Koretzky, S.P. Kuo and S.C. Kuo[1]
Polytechnic University, Farmingdale, NY, USA
[1]Brookhaven National Laboratory, Upton, NY, USA

4Q23 **Imaging and Spectroscopic Analysis of Channel Spark Electron Beam Ablation Plumes**
S.D. Kovaleski, R.M. Gilgenbach, L.K. Ang, Y.Y. Lau and G.J. Overhiser
University of Michigan, Ann Arbor, MI, USA

4Q24 **Analysis of Surface Structures of a Metal Target from Multi-Pulse KrF Laser Ablation**
L.K. Ang, Y.Y. Lau, R.M. Gilgenbach, H.L. Spindler[1], S.D. Kovaleski and J.S. Lash[2]
University of Michigan, Ann Arbor, MI, USA
[1]Boeing Corporation, Seattle, WA, USA
[2]Sandia National Laboratories, Albuquerque, NM, USA

4Q25 **Poly-Si Etching in Cl_2 Plasma Using Electron-Beam-Excited Plasma Apparatus**
R. Miyano, Y. Mikawa, J-I. Inaguma, Y. Shiraki, M. Fujii, S. Ikezawa, K. Kida, A. Nishiwaki and T. Yoshioka
Chubu University, Kasugai, Japan

4Q26 **An Optical RIE Process Uniformity Control Sensor**
S.C. Shannon, W. Pruka, J.P. Holloway and M. Brake
University of Michigan, Ann Arbor, MI, USA

4Q27 **Characterization and Optimization of Argon Sputter Etching of SiO2 in the GEC Reference Cell**
M.J. Buie, S.C. Shannon[1], J.P. Holloway[1], M. Brake[1], D. Grimard[1] and F. Terry Jr.[1]
Applied Materials, Santa Clara, CA, USA
[1]University of Michigan, Ann Arbor, MI, USA

4Q28 **Experimental Study of Charging Processes on Unpatterned Oxide-Coated Si Wafers in an ECR Etcher**
C. Cismaru, J.L. Shohet, N. Hershkowitz, K. Nauka[1], and J.B. Friedmann[2]
University of Wisconsin-Madison, Madison, WI, USA
[1]Hewlett-Packard Laboratories, Palo Alto, CA, USA
[2]Texas Instruments, Dallas, TX, USA

Tuesday Afternoon – 20 May, 1997
3:00 p.m. – Multipurpose Room

Poster Session 4Q29-32: 5.1 Non-Equilibrium Plasma Processing II (ICP Modeling)

4Q29 **Effect of Plasma Processing Reactor Circuitry on Plasma Characteristics**
S. Rauf and M.J. Kushner
University of Illinois, Urbana, IL, USA

4Q30 **Modeling of the Effects of Die Scale Features on Bulk Plasma Conditions in Plasma Etching Equipment**
M.J. Grapperhaus and M.J. Kushner
University of Illinois, Urbana, IL, USA

4Q31 **Statistical Parametric Study of Non-Parallel Inductive Reactors**
E.R. Keiter and M.J. Kushner
University of Illinois, Urbana, IL, USA

4Q32 **Modeling of 2-Dimensional and 3-Dimensional Etch Profiles in High Density Plasma Reactors**
R.J. Hoekstra, V. Sukharev[1] and M.J. Kushner
University of Illinois, Urbana, IL, USA
[1]LSI Logic Corp., Santa Clara, CA, USA

Wednesday Morning – 21 May, 1997
8:30 a.m. – Kon Tiki Ballroom

Plenary Session

NASA's International Solar Terrestrial Physics Program and the Roadmap Forward

Dr. Robert L. Carovillano
NASA Headquarters, Washington, DC, USA

Chair: E.E. Scime

Wednesday Morning – 21 May, 1997
10:00 a.m. – Kon Tiki Ballroom

Oral Session 5A: 1.3 Basic Phenomena in Partially Ionized Gases – Gaseous Electronics, Electrical Discharges, etc.
Chair: S. Rauf

5A01 **Optical Emission Spectroscopy of High Density Metal Plasma During Magnetron Sputtering**
O.E. Hankins and Z.J. Radzimski
North Carolina State University, Raleigh, NC, USA

5A02 **High Frequency Series Resonance and Surface Wave Sustained Discharges**
D.J. Cooperberg and C.K. Birdsall
University of California at Berkeley, Berkeley, CA, USA

5A03 **Analytical Investigation of Non-Collisional Electron Heating**
S. Rauf and M.J. Kushner
University of Illinois, Urbana, IL, USA

5A04 **Modeling Electro-Negative RF-Discharges in the Low Pressure Regime**
R.P. Brinkmann
Siemens AG, Munich, Germany

5A05 **Approximate, Semi-Implicit Calculation of 3D Electrostatic Potential in a Self-Consistent Plasma Simulation**
E.R. Keiter and M.J. Kushner
University of Illinois, Urbana, IL, USA

5A06 **Double and Triple Layers in Dusty Plasmas**
A. Garscadden, B.N. Ganguly, P. Bletzinger and P.D. Haaland
Wright Laboratory, WPAFB, OH, USA

5A07 **High Pressure Hollow Electrode Discharges**
K.H. Schoenbach, A. El-Habachi, W. Shi and M. Ciocca
Old Dominion University, Norfolk, VA, USA

5A08 **A Plasma Mirror for Electronic Microwave Beam Steering**
R. Meger, J. Mathew, W. Manheimer, R. Fernsler, J. Gregor, D. Murphy, M. Myers and R. Pechacek
Naval Research Laboratory, Washington, DC, USA

Wednesday Morning – 21 May, 1997
10:00 a.m. – Board Room

Oral Session 5B: 2.2 Fast Wave Devices I
Chair: D. Pershing

5B01-02 *Invited*—**High Power W-Band Gyroklystron Amplifier Experiments at NRL**
M. Blank, B.G. Danly, B. Levush and P.E. Latham[1]
Naval Research Laboratory, Washington, DC, USA
[1]Omega-P, Inc., New Haven, CT, USA

5B03 **Study of High Gain Gyrotron Traveling Wave Amplifier**
K.R. Chu, H.Y. Chen, C.L. Hung, C.H. Chang, S.H. Chen[1], T.T. Yang[2] and L.R. Barnett
National Tsing Hua University, Hsinchu, Taiwan
[1]National Center for High-Performance Computing, Hsinchu, Taiwan
[2]Synchrotron Radiation Research Center, Hsinchu, Taiwan

5B04 **Input Coupler for a 35 GHz Gyroklystron**
A.H. McCurdy, J.J. Choi[1], R.H. Kyser[2], B.G. Danly[3] and W.M. Manheimer[3]
University of Southern California, Los Angeles, CA, USA
[1]Science Application International Corp., McLean, VA, USA
[2]Dyncorp, Rockville, MD, USA
[3]Naval Research Laboratory, Washington, DC, USA

5B05 **Simulation Studies of Relativistic Gyroklystron Amplifiers**
G.P. Saraph, J.P. Anderson, W. Lawson and V.L. Granatstein
University of Maryland, College Park, MD, USA

5B06 **35 GHz Gyroklystron Amplifiers**
J.J. Choi, A.H. McCurdy[1], F. Wood[2], R.H. Kyser[2], B.G. Danly[3], B. Levush[3] and R. K. Parker[3]
Science Application International Corp., McLean, VA, USA
[1]University of Southern California, Los Angeles, CA, USA
[2]Dyncorp, Rockville, MD, USA
[3]Naval Research Laboratory, Washington, DC, USA

5B07 **Measured Performance of a Phase-Controlled, Harmonic-Multiplying, Inverted Gyrotwystron**
H. Guo, J. Rodgers, S. Chen, G. Nusinovich, M. Walter and V.L. Granatstein
University of Maryland, College Park, MD, USA

5B08 **Velocity Spread In Gyrobeams Due To Cathode Edge Emission**
R.B. True, G.R. Good, T.A. Hargreaves and K.T. Nguyen[1]
Litton Systems, Inc., Electron Devices Division, San Carlos, CA, USA
[1]KN Research, Silver Springs, MD, USA

Wednesday Morning – 21 May, 1997
10:00 a.m. – Toucan Room

Oral Session 5C: 6 Plasma Diagnostics
Chair: R.J. Leeper

5C01-02 *Invited*—**X-ray Lasers for Plasma Diagnostics**
L.B. Da Silva, T.W. Barbee Jr., R. Cauble, P. Celliers, D.H. Kalantar, R. Snavely, J.E. Trebes, A.S. Wan and F. Weber
Lawrence Livermore National Laboratory, Livermore, CA, USA

5C03 **PROTEX: A Proton-Recoil Detector for ICF Fusion Neutrons**
M.J. Moran
Lawrence Livermore National Laboratory, Livermore, CA, USA

5C04 **Explosively Driven Blast Shutter for Diagnostic Protection**
E.L. Ruden and D.G. Gale[1]
Phillips Laboratory, Kirtland AFB, NM, USA
[1]Maxwell Technologies, Inc., Albuquerque, NM, USA

5C05 **Spectral Analysis in Lithium Ion Beam Transport Experiments**
H.K. Chung, J.J. MacFarlane, P. Wang, G.A. Moses, J.E. Bailey[1], C.L. Olson[1] and D.R. Welch[2]
University of Wisconsin–Madison, Madison, WI, USA
[1]Sandia National Laboratories, Albuquerque, NM, USA
[2]Mission Research Corporation, Newington, VA, USA

5C06 **Infra-Red Absorption Spectroscopy of SiO_x Deposition Plasmas**
P. Fayet, C. Hollenstein[1], C. Courteille[1], A.A. Howling[1] and D. Magni[1]
Tetra Pak (Suisse) SA, Romont, Switzerland
[1]Centre de Recherche en Physique des Plasmas, Romont, Switzerland

5C07 **Low-Z Impurity Visible Line Radiations in the IR-T1 Tokamak**
M. Ghorannevis, M.R. Salami and M. Masnavi
Plasma Physics Research Center of I.A.U., Tehran, Iran

5C08 **Single Channel HCN Laser Interferometer for Electron Density Measurement in the IR-T1 Tokamak**
M. Ghorannevis, M. Monfared and A. Anvari
Plasma Physics Research Center of I.A.U., Tehran, Iran

5CO9 **Design and Fabrication of New Version of Langmuir Double Circuit for the IR-T1 Tokamak**
A. Abbaspour, M. Ghorannevis, R. Z. Khebreh, M.R. Salami and A.M. Bagheri
Plasma Physics Research Center of I.A.U., Tehran, Iran

Wednesday Morning – 21 May, 1997
10:00 a.m. – Macaw Room

Oral Session 5D: 5.3 Plasma For Lighting
Chair: T.J. Sommerer

5D01-02 *Invited*—**FEM-Simulation of High Pressure Discharge Discharge Lamps: Examples for Modeling of Cathode Regions and of 3-D Convective Flow**
M. Neiger and H. Wiesmann
University of Karlsruhe, Karlsruhe, FRG

5D03 **Geometrical Differences of Isotherms In Convective High Intensity Discharge Lamps**
M. Galvez
OSRAM Sylvania Inc., Beverly, MA, USA

5D04 **A Laser-Induced Fluorescence Technique for Measuring Damage to a Fluorescent Lamp Electrode**
R. Davis, Y. Ji and G. Korenowski
Rensselaer Polytechnic Institute, Troy, NY, USA

5D05 **Modeling and Measuring the Rate of Cooling of a Fluorescent Lamp Electrode**
R. Davis, Y. Ji and W.P. Moskowitz[1]
Rensselaer Polytechnic Institute, Troy, NY, USA
[1]OSRAM Sylvania Inc., Beverly, MA, USA

5D06-07 **Radiometric Efficiency of Barium Discharge Plasmas**
H.M. Anderson, J. MacDonagh-Dumler and J.E. Lawler
University of Wisconsin–Madison, Madison, WI, USA

Wednesday Morning – 21 May, 1997
10:00 a.m. – Cockatoo Room

Oral Session 5E: 4.2 Inertial Confinement Fusion
Chair: J. Hammer

5E01 **Plasma Pockels Cell Based Optical Switch for the National Ignition Facility**
M.A. Rhodes, S. Fochs and C.D. Boley
Lawrence Livermore National Laboratory, Livermore, CA, USA

5E02 **Explosion Instability in the Thermal Expansion of a Thin-Walled Cylinder in Ultra-High Magnetic Field**
G.A. Shneerson
State Technical University, St. Petersburg, Russia

5E03 **Progress with Developing a Target for Magnetized Target Fusion**
F.J. Wysocki, B.E. Chrien, G.C. Idzorek, H. Oona, D.O. Whiteson, R.C. Kirkpatrick, I.R. Lindemuth and P.T. Sheehey
Los Alamos National Laboratory, Los Alamos, NM, USA

Wednesday Morning – 21 May, 1997
10:45 a.m. – Cockatoo Room

Oral Session 5E: 4.3 Magnetic Confinement Fusion
Chair: C. Ordonez

5E04-05 *Invited*—**Plasma Confinement within a Solenoidal Magnetic Field Using Nested Electric Potential Wells**
C.A. Ordonez and D.D. Dolliver
University of North Texas, Denton, TX, USA

5E06 **Stability of Transport Barrier in Negative Shear Tokamak Discharge**
A. Hirose, M. Elia, M. Yamagiwa[1] and Y. Kishimoto[1]
University of Saskatchewan, Saskatoon, Canada
[1]Naka Fusion Research Establishment, Naka, Ibaraki, Japan

5E07 **Melt-Layer Erosion Experiments for Electric Launchers and Tokamak Fusion Reactors**
G.E. Dale and M.A. Bourham
North Carolina State University, Raleigh, NC, USA

5E08 **Control of Divertor Heat Flux by Radiative Divertor Operation in DIII-D**
C.J. Lasnier
Lawrence Livermore National Laboratory, Livermore, CA, USA

5E09 **Engineering Aspects and Basic Parameters of the IR-T1 Tokamak**
M. Ghorannevis, M.R. Salami, M. Masnavi, J. Mirzaie, M. Zamani Mehr, A.K. Tafreshi and M. Bakhtiary
Plasma Physics Research Center of I.A.U., Tehran, Iran

5E10 **Beta-Limiting in the IR-T1 Tokamak**
M. Ghorannevis, M. Masnavi and D. Doranian
Plasma Physics Research Center of I.A.U, Tehran, Iran

5E11 **On the Reconstruction of Nonlocal Heat Transport Parameters from Observed Phenomena of the Fast Non-Diffusive Transport in a Tokamak**
A.B. Kukushkin
RRC Kurchatov Institute, Moscow, Russia

Wednesday Morning – 21 May, 1997
10:00 a.m. – Rousseau Center

Poster Session 5P01-15: 2.1 Intense Beam Microwaves

5P01 **Polarization Control in High Power Microwaves from a Rectangular Cross Section Gyrotron**
J.M. Hochman, R.M. Gilgenbach, R.L. Jaynes, J.I. Rintamaki, Y.Y. Lau and T.A. Spencer[1]
University of Michigan, Ann Arbor, MI, USA
[1]Phillips Laboratory, Kirtland AFB, NM, USA

5P02 **Diagnostic Experiments to Measure Frequency and Alpha for Rectangular Cross Section Gyrotrons**
R.L. Jaynes, R.M. Gilgenbach, J.M. Hochman, J.I. Rintamaki, Y.Y. Lau and T.A. Spencer[1]
University of Michigan, Ann Arbor, MI, USA
[1]Phillips Laboratory, Kirtland AFB, NM, USA

5P03 **High Efficiency X-band TWT Amplifiers**
S. Naqvi, G.S. Kerslick, J.A. Nation and Q. Wang
Cornell University, Ithaca, NY, USA

5P04 **Diode Polarity Experiments on a Coaxial Vircator**
K. Woolverton, M. Kristiansen and L.L. Hatfield
Texas Tech University, Lubbock, TX, USA

5P05 **Analytic Investigation of the Transit-Time Instability Including Intense Space Charge Effects**
J.W. Luginsland, M.J. Arman and Y.Y. Lau[1]
Phillips Laboratory, Kirtland AFB, NM, USA
[1]University of Michigan, Ann Arbor, MI, USA

5P06 **Relativistic BWO with Resonant Reflector**
S.D. Korovin, I.K. Kurkan, I.V. Pegel, V.V. Rostov and E.M. Totmeninov
High Current Electronics Institute, Tomsk, Russia

5P07 **PIC Simulations of the Micropulsed Electron Gun (MPG)**
W. Peter and F. Mako
FM Technologies Inc., Fairfax, VA, USA

5P08 **RF Breakdown Experiments at SLAC**
G. Scheitrum, R. Fowkes, X. Xu and L.L. Laurent[1]
Stanford Linear Accelerator Center, Menlo Park, CA, USA
[1]University of California at Davis, Davis, CA, USA

5P09 **Streak Observation of Air Breakdown Triggered by a High-Power Pulsed Microwave**
M. Yatsuzuka, M. Okamoto, M. Tanigawa and S. Nobuhara
Himeji Institute of Technology, Hyogo, Japan

5P10 **Numerical Simulation of 1.5 GHz Vircator**
S.D. Korovin, I.V. Pegel, S.D. Polevin and V.P. Tarakanov[1]
High Current Electronics Insititute, Tomsk, Russia
[1]High Temperatures Institute, Moscow, Russia

5P11 **Study of Microwave Frequency Radiated from a Vircator**
M. Yatsuzuka, M. Tanigawa, S. Nobuhara, D. Young[1] and O. Ishihara[1]
Himeji Institute of Technology, Hyogo, Japan
[1]Texas Tech University, Lubbock, TX, USA

5P12 **Effects of Plasma Filling on Microwave Emission in a BWO with Non-Uniform Slow Wave Structure**
D. Young, O. Ishihara, C. Grabowski[1], J. Gahl[1] and E. Schamiloglu[1]
Texas Tech University, Lubbock, TX, USA
[1]University of New Mexico, Albuquerque, NM, USA

5P13 **X-Band Relativistic BWO with 3 GW Pulse Power**
A.V. Gunin, A.I. Klimov, S.D. Korovin, I.V. Pegel, S.D. Polevin, A.M. Roitmann, V.V. Rostov and A.S. Stepchenko
High Current Electronics Institute, Tomsk, Russia

5P14 **Evaluation of Mode Competition in the Radial Acceletron**
G.E. Sasser, M.J. Arman and J.W. Luginsland
Phillips Laboratory, Kirtland AFB, NM, USA

5P15 **Dynamics of the Space Charge Limiting Current in Gyro-Type Devices**
T.A. Spencer and M.D. Stump
Phillips Laboratory, Kirtland AFB, NM, USA

Wednesday Morning – 21 May, 1997
10:00 a.m. – Rousseau Center

Poster Session 5P16-19: 7.1 MHD and EM/ETH Launchers

5P16 **Numerical and Experimental Research of EMG-720 Flux Compression Generator**
N.F. Popkov, A.S. Pikar, E.A. Ryaslov, V.I. Kargin, G.F. Mackartsev, V.E. Gurin, P.V. Korolev, V.N. Kataev, J.H. Degnan[1], G.F. Kiuttu[1], S.K.Coffey[1], W.J. Summa[2] and K.E. Ware[2]
VNIIEF, Sarov, Russia
[1]Phillips Laboratory, Kirtland AFB, NM, USA
[2]Defense Special Weapons Agency, Alexandria, VA, USA

5P17 **The Experimental Installation for Z-Pinch Pulse Compression**
B.E. Fridman and Ph.G. Rutberg
Russian Academy of Sciences, St. Petersburg, Russia

5P18 **E7-25 Capacitive Energy Store for Power Supplying of Electro-Discharge Loads**
B.E. Fridman and Ph.G. Rutberg
Russian Academy of Sciences, St. Petersburg, Russia

5P19 **On the Mechanism of the Magnetic Field Influence on the Electrical Explosion of a Thin Wire**
Yu.E. Adamyan, A.N. Berezkin, V.M. Vasilevsky, S.N. Kolgatin, S.I. Krivosheyev and G.A. Shneerson
State Technical University, St. Petersburg, Russia

Wednesday Morning – 21 May, 1997
10:00 a.m. – Rousseau Center

Poster Session 5P20-24: 7.2 Plasma Closing Switches

5P20 **High-Repetition-Rate, Short-Pulse Generator Using A Planar Crossatron® Switch**
J. Santoru, D. Goebel and R. Poeschel
Hughes Research Laboratories, Malibu, CA, USA

5P21 **Working Characteristics of the Triggered Three-Electrode Spark Gaps with Different Types of Gas Insulators**
N. Arsic and P. Osmokrovic[1]
Faculty of Electrical Engineering, Pristina, Yugoslavia
[1]Faculty of Electrical Engineering, Belgrade, Yugoslavia

5P22 **Plasma Formation Inside Gap with One-Hole Control Grid**
A.S. Arefjev and B.D. Maloletkov
Ryazan State Radioengineering Academy, Ryazan, Russia

5P23 **Two-Site Marx Switch with Graphite Electrodes**
I.S. Roth, S.K. Lam and P.S. Sincerny
Primex Physics International, San Leandro, CA, USA

5P24 **Functional Model of a Triggered Spark Gap**
D.L. Lockwood
EG&G Optoelectronics Division, Salem, MA, USA

Wednesday Morning – 21 May, 1997
10:00 a.m. – Rousseau Center

Poster Session 5P25-28: 7.3 Fast Opening Switches

5P25 **Measurements of Plasma Density and Magnetic Field in a 100-ns Plasma Opening Switch (POS)**
A. Weingarten, Ya.E. Krasik and Y. Maron
Weizmann Institute of Science, Rehovot, Israel

5P26 **Spectroscopic Investigations of a Planar Microsecond POS**
R. Arad, Ya. E. Krasik, K. Tsigutkin and Y. Maron
Weizmann Institute of Science, Rehovot, Israel

5P27 **Diamond Fast Opening Switches for Inductive Engery Storage Power Modulators**
S.W. Gensler, R.R Prasad, I.V. Tzonev, N. Qi and M. Krishnan
Alameda Applied Sciences Corp, San Leandro, CA, USA

5P28 **An Inverse Pinch Plasma Source for Opening Switches**
J.J. Moschella, E.J. Yadlowsky and R.C. Hazelton
HY-Tech Research Corp, Radford, VA, USA

Wednesday Morning – 21 May, 1997
10:00 a.m. – Multipurpose Room

Poster Session 5Q01-12: 1.2 Space Plasmas

5Q01 **Microwave Plasma Sources for Use in Space Plasma Physics Experimentation**
D.N. Walker, J.H. Bowles and W.E. Amatucci[1]
Naval Research Laboratory, Washington, DC, USA
[1]Sachs Freeman Assoc, Largo, MD, USA

5Q02 **Electromagnetic Interaction of Spacecrafts with the Environment**
V.M. Antonov, A.G. Ponomarenko, V.V. Danilov[1] and O.S. Grafodatsky[2]
Siberian Branch of the Russian Academy of Sciences, Novosibirsk, Russia
[1]Krasnoyarsk State University, Krasnoyarsk, Russia
[2]NPO of Applied Mechanics, Krasnoyarsk, Russia

5Q03 **Helicon Plasmas for Space Relevant Laboratory Experiments**
E. Scime, M. Balkey, P. Keiter and J. Kline
West Virginia University, Morgantown, WV, USA

5Q04 **Three-dimensional Numerical Simulation of Ion and Electron Accelerations by Parametric Decay of Fast Lower Hybrid Waves**
N. Singh, S. Al-Sharaeh, A. Abdelrazek, W.C. Leung and E.E. Wells
University of Alabama in Hunstville, Huntsville, AL, USA

5Q05 **A Laboratory Plasma Source as an MHD Model for Astrophysical Jets**
R.M. Mayo and R.W. Caress
North Carolina State University, Raleigh, NC, USA

5Q06 **A Generation Mechanism for the Frequency Up-Shifted Plasma Lines Observed in the Tromsφ's HF Heating Experiments**
S.P. Kuo, S.C. Kuo[1] and M.C. Lee[2]
Polytechnic University, Farmingdale, NY, USA
[1]Brookhaven National Laboratory, Upton, NY, USA
[2]Massachusetts Institute of Technolgy, Cambridge, MA, USA

5Q07 **Study of ELF/VKLF Wave Generation by HF Heater-Modulated Electrojet**
S.P. Kuo, M.C. Lee[1] and P. Kossey[2]
Polytechnic University, Farmingdale, NY, USA
[1]Massachusetts Institute of Technolgy, Cambridge, MA, USA
[2]Phillips Laboratory, Hanscom AFB, MA, USA

5Q08 **Space Internet from Beam Antenna**
T. Ohnuma and H. Sato
Tohoku University, Sendai, Japan

5Q09 **Automodel Dynamics of Current "Coalescence" in a Thin Current Layer**
B.A. Trubnikov, V.P. Vlasov and S.K. Zhdanov[1]
RRC Kurchatov Institute, Moscow, Russia
[1]Moscow Engineering Physics Institute, Moscow, Russia

5Q10 **Fragmentation of Electron Stream at Propagation Through Plasma**
V. Mel'nik and E. Kontar[1]
National Academy of Sciences, Kharkiv, Ukraine
[1]Kharkiv State University, Kharkiv, Ukraine

5Q11 **Coronal Transient from Drift Electric Field**
H. Jiling
Beijing Normal University, Beijing, China

5Q12 **High Energy Particles from Stochstic Accelerating**
H. Jiling
Beijing Normal University, Beijing, China

Wednesday Afternoon – 21 May, 1997
1:30 p.m. – Kon Tiki Ballroom

Plenary Session

PSAC Prize Address:

Science and Applications of Energy Beam Ablation

Professor Ronald M. Gilgenbach
Director, Intense Energy Beam Interaction Laboratory
University of Michigan, Ann Arbor, MI, USA

Chair: N. Hershkowitz

Wednesday Afternoon – 21 May, 1997
3:00 p.m. – Kon Tiki Ballroom

Oral Session 6A: 2.2 Fast Wave Devices II
Chair: G. Nusinovich

6A01-02 *Invited*—**Cyclotron Wave Amplifiers at Microwave and Millimeter Wave Frequencies**
W.M. Manheimer
Naval Research Laboratory, Washington, DC, USA

6A03 **Theoretical Study of the Gyrotron Backward Wave Oscillator**
S.H. Chen and K.R. Chu[1]
National Center for High-Performance Computing, Hsinchu, Taiwan
[1]National Tsing Hua University, Hsinchu, Taiwan

6A04 **High Power, Low Velocity Spread, Axis Encircling Beam, Electron Gun Development**
D. Gallagher, J. Richards, F. Scafuri and C.M. Armstrong
Northrop Grumman Corporation, Rolling Meadows, IL, USA

6A05 **Theory of Multi-Beam Stagger-Tuned Gyroklystrons**
G.S. Nusinovich, B. Levush[1] and B. Danly[1]
University of Maryland, College Park, MD, USA
[1]Naval Research Laboratory, Washington, DC, USA

6A06 **Single-Stage, Depressed Collector Operation of an 84 GHz Gyrotron**
T.S. Chu, P. Borchard, P. Cahalan, K. Felch, C.M. Loring, T. Shimozuma[1] and M. Sato[1]
Communications & Power Industries (CPI), Palo Alto, CA, USA
[1]National Institute for Fusion Science, Toki, Japan

6A07 **Ultrahigh Intensity Compton Scattering Focused X-ray Source**
F.V. Hartemann, A.L. Troha, G.P. Le Sage, C.V. Bennett, B.H. Kolner and N.C. Luhmann Jr.
University of California at Davis, Davis, CA, USA

6A08 **Compact, High Efficiency Drifting Electron Laser Powered by Slow-Wave Wiggler**
S. Riyopoulos
Science Application International Corporation, McLean, VA, USA

Wednesday Afternoon – 21 May, 1997
3:00 p.m. – Board Room

Oral Session 6B: 4.5 Fast Z-Pinches and X-ray Lasers
Chair: M. Douglas

6B01 **Numerical and Experimental Studies of Magnetic Rayleigh-Taylor Instabilities in Solid Liners**
R.J. Faehl, W.L. Atchinson, R.E. Reinovsky and D.V. Morgan
Los Alamos National Laboratory, Los Alamos, NM, USA

6B02-03 *Invited*—**Optimization of Array Radius, Mass and Wire Number for Tungsten Arrays**
C. Deeney, D.L. Peterson[1], R.B. Spielman, T. Nash, G.A. Chandler, M.R. Douglas, D. Fehl, J.F. Seamen, K.W. Struve, W.A. Stygar, J. McGurn, D. Jobe, T. Gilliland, J.A. Torres, R. Mock, T.W.L. Sanford and M.K. Matzen
Sandia National Laboratories, Albuquerque, NM, USA
[1]Los Alamos National Laboratory, Los Alamos, NM, USA

6B04 **Recent Z-Pinch Experiments on ACE 4**
P.L. Coleman, J. Rauch, W. Rix and J. Thompson
Maxwell Technologies Inc., San Diego, CA, USA

6B05-06 *Invited*—**Modeling Z-Pinch Implosions in Two Dimensions**
D.L. Peterson, R.L. Bowers, J. Brownell, C. Lund, W. Matuska, K. McLenithan, H. Oona, T. Scannapieco, C. Deeney[1], M.S. Derzon[1], R.B. Spielman[1], T. Nash[1], G.A. Chandler[1], R.C. Mock[1], T.W.L. Sanford[1], M.K. Matzen[1] and N.F. Roderick[2]
Los Alamos National Laboratory, Los Alamos, NM, USA
[1]Sandia National Laboratories, Albuquerque, NM, USA
[2]University of New Mexico, Albuquerque, NM, USA

6B07 **Design and Simulation of Stabilized Z-Pinch Loads with Tailored Density Profiles**
A.L. Velikovich, F.L. Cochran and J. Davis[1]
Berkeley Research Associates, Springfield, VA, USA
[1]Naval Research Laboratory, Washington, DC, USA

6B08 **Solid Liner Compression of Working Fluid to Megabar Range**
J.H. Degnan, S.K. Coffey[1], D.G. Gale[2], J.D. Graham[2], T.W. Hussey, G.F. Kiuttu, B.B. Kreh, F.M. Lehr, D. Morgan[3], R.E. Peterkin Jr., D. Platts[3], E.L. Ruden, W. Sommers[2] and P.J. Turchi
Phillips Laboratory, Kirtland AFB, NM, USA
[1]NumerEx, Albuquerque, NM, USA
[2]Maxwell Technologies, Inc., Albuquerque, NM, USA
[3]Los Alamos National Laboratory, Los Alamos, NM, USA

6B09 **Optimization of the Hard X-ray Yield from a Heterogeneous Z-Pinch**

L.I. Rudakov
RRC Kurchatov Institute, Moscow, Russia

6B10 **ZETA - Code for 2-D Complete Simulation of Radiative Z-Pinch and Liner Implosion**

S.V. Zakharov, A.G. Lisitsyn, A.A. Otochin, A.N. Starostin, A.E. Stepanov, V. Roerich, A.F. Nikiforov[1], V.G. Novikov[1], A.D. Solomyannaya[1], V.A. Gasilov[2] and A.Yu. Krukovskii[2]
Troitsk Institute for Innovation and Thermonuclear Research, Troitsk, Moscow Region, Russia
[1]Keldysh Institute for Applied Mathematics, Russia
[2]Institute for Mathematical Modeling, Russia

Wednesday Afternoon – 21 May, 1997
3:00 p.m. – Toucan Room

Oral Session 6C: 1.4 Computational Plasma Physics II
Chair: G.R. Joyce

6C01 **A Beam-RF Simulation Technique Based on Evolutionary Amplification Equations**
R.H. Jackson
Naval Research Laboratory, Washington, DC, USA

6C02 **Simulation of Stratified Nonequilibrium Gas-Plasma Flow in a Strong Masgnetic Field**
V.S. Slavin, K.A. Finnikov and V.V. Danilov[1]
Krasnoyarsk State Technical University, Krasnoyarsk, Russia
[1]Krasnoyarsk State University, Krasnoyarsk, Russia

6C03 **A New 3D MHD Algorithm Using A Boltzmann-Like Distribution Function**
J.D. Huba
Naval Research Laboratory, Washington, DC, USA

6C04 **Numerical Simulation of a Helical, Explosive Flux Compression Generator**
D.E. Lileikis
Phillips Laboratory, Kirtland AFB, NM, USA

6C05 **An Advance Implicit Algorithm for MHD Computations on Parallel Architectures**
U. Shumlak, D.S. Eberhardt, O.S. Jones and B. Udrea
University of Washington, Seattle, WA, USA

6C06 **MAG-Two-Dimensional Radiation Resistive MHD Code, Using Arbitrary Moving Coordinate System**
O.V. Diyankov, I.V. Glazyrin, S.V. Koshelev and N.P. Savina
Russian Federal Nuclear Center, Snezhinsk, Chelyabinsk Region, Russia

Wednesday Afternoon – 21 May, 1997
3:00 p.m. – Macaw Room

Oral Session 6D: 4.4 Dense Plasma Focus II
Chair: D. Lileikis

6D01 **Time Resolved Neutron and Hard X-ray Emission in the Dense Plasma Focus, Revisited**
J.S. Brzosko, V. Nardi, C. Powell and J.R. Brzosko
Compton Research Laboratories, New York, NY, USA

6D02 **Current-Sheath Oscillations and Reactivity in Focused Discharges**
A. Bortolotti, P. DeChiara, P. Desiderio, F. Mezzetti, V. Nardi[1] and C. Powell[1]
University of Ferrara, New York, NY, USA
[1]Compton Research Laboratories, New York, NY, USA

6D03 **Fine Structure of Ion-Cluster Disintegration Modes in PF Discharges**
V. Nardi, C. Powell and C.M. Luo[1]
Compton Research Laboratories, New York, NY, USA
[1]Tsinghua University, Beijing, China

6D04 **Relation Between Filamentary Current Sheath and Ionization Energy in a Plasma Focus**
M-F. Lu
Chinese Academy of Sciences, Beijing, China

6D05 **Effect of Anode End Strucutres on Plasma Pinching in a Plasma Focus**
M-F. Lu
Chinese Academy of Sciences, Beijing, China

6D06 **Spatial Distibution of the High Energy Density Plasma in a Coaxial Gun for Surface Modification**
M-F. Lu, S-Z. Yang and C-Z. Liu
Chinese Academy of Sciences, Beijing, China

Wednesday Afternoon – 21 May, 1997
3:00 p.m. – Cockatoo Room

Oral Session 6E: 7.3 Fast Opening Switches
Chair: W. Rix

6E01-02 *Invited*—**Plasma Opening Switch Scaling Relationships Derived from Operations in the "Switch Limited" Regime**
R. J. Commisso, B.V. Weber, W. Rix[1], P. Coleman[1], J. Thompson[1], D. Kortbawi[2] and J. Goyer[3]
Naval Research Laboratory, Washington, DC, USA
[1]Maxwell Technologies, Inc., San Diego, CA, USA
[2]Primex Physics International, San Leandro, CA, USA
[3]Consultant

6E03 **Improved Output on Decade Module 1**
D. Kortbawi, J. Thompson[1], R.J. Commisso[2], B. Weber[2], P.F. Ottinger[2], M. Babineau[3] and J. Goyer[4]
Primex Physics International, San Leandro, CA, USA
[1]Maxwell Laboratories Inc., Albuquerque, NM, USA
[2]Naval Research Laboratory, Washington, DC, USA
[3]Sverdrup Technologies Inc, Cleveland, OH, USA
[4]Consultant

6E04 **MACH2 Simulations of Some DECADE Plasma Opening Switch Experiments**
D. Keefer and R. Rhodes
University of Tennessee Space Institute, Tullahoma, TN, USA

6E05 **Observation of EMH Effects in a Tri-plate POS**
J.M. Grossman, B.V. Weber, R.A. Riley[1], T.G. Jones[2], R.J. Commisso, D.D. Hinshelwood and S.B. Swanekamp[3]
Naval Research Laboratory, Washington, DC, USA
[1]Logicon/RDA, Arlington, VA, USA
[2]National Research Council Research Associate
[3]JAYCOR, Inc., Vienna, VA, USA

6E06 **2D Magnetic Field Evolution and Electron Energies in Plasma Opening Switches**
R. Arad, A. Fruchtman, K. Gomberoff, Ya.E. Krasik, R. Shpitalnik, K. Tsigutkin, A. Weingarten and Y. Maron
Weizmann Institute of Science, Rehovot, Israel

6E07 **Simulation of a Plasma-Gun Voltage Generator**
D.E. Lileikis, P.J. Turchi, R.E. Peterkin Jr., J.H. Degnan and J.B. Javedani
Phillips Laboratory, Kirtland AFB, NM, USA

6E08 **Inverse-Pinch Flux Compression Generator**
J.B. Javedani, D.E. Lileikis, G.F. Kiuttu, J.H. Degnan, P.J. Turchi and J.D. Graham[1]
Phillips Laboratory, Kirtland AFB, NM, USA
[1]Maxwell Laboratories Inc., Albuquerque, NM, USA

Wednesday Afternoon – 21 May, 1997
3:00 p.m. – Rousseau Center

Poster Session 6P29-32: 2.3 Vacuum Microelectronics

6P29 **Characteristics of Field Emitter Arrays (FEAs) for a Twystrode Amplifier**
M. Garven, M.A. Kodis[1], M.T. Ngo[2], B.J. Sobocinski[3] and F. Calise[3]
University of Maryland, College Park, MD, USA
[1]Naval Research Laboratory, Washington, DC, USA
[2]Mission Research Corporation, Newington, VA, USA
[3]Dyncorp, Rockville, MD, USA

6P30 **Field Emission from HfC or Ni Films Deposited on Single Tip Mo Field Emitters**
W.A. Mackie, T. Xie and P.R. Davis
Linfield Research Institute, McMinnville, OR, USA

6P31 **Field Emission from HfC Films on Mo Field Emitter Arrays and from HfC Arrays**
W.A. Mackie, T. Xie, J.E. Blackwood and P.R. Davis
Linfield Research Institute, McMinniville, OR, USA

6P32 **Computer Simulation of Field Emission Microtriodes with New Volcano-Shaped Emitters**
Y. Hu and Y.C. Lan
National Tsing Hua University, Hsinchu, Taiwan, ROC

Wednesday Afternoon – 21 May, 1997
3:00 p.m. – Rousseau Center

Poster Session 6P33-36: 5.2 Thermal Plasma Processing

6P33 **Generation and Characterization of Atmospheric Plasma Torch Array**
E. Koretzky and S.P. Kuo
Polytechnic University, Farmingdale, NY, USA

6P34 **Numerical Analysis on Plasma Characteristics of High Power Plasma Torch of Hollow Electrode Type for Waste Treatment**
M. Hur, K.D. Kang and S.H. Hong
Seoul National University, Seoul, Korea

6P35 **Magnetic Consequences of an Electrostatic Shield Around an Inductively Coupled Plasma Discharge**
J.L. Giuliani, A.E. Robson[1], V. Shamamian and R. Campbell[2]
Naval Research Laboratory, Washington, DC, USA
[1]Berkeley Scholars, Inc., Springfield, VA, USA
[2]Geo Centers, Inc., Washington, MD, USA

6P36 **Simulations of Flux Uniformity for C12, BC13 and N2 Chemistries in the Sandia Inductively Coupled GEC Reactor**
R. Veerasingam, S.J. Choi[1] and R.B. Campbell[1]
Pennsylvania State University, University Park, PA, USA
[1]Sandia National Laboratories, Albuquerque, NM, USA

Wednesday Afternoon – 21 May, 1997
3:00 p.m. – Rousseau Center

Poster Session 6P37-46: 5.3 Plasma for Lighting

6P37 **Start-up Phase of the High Pressure Mercury Lamp Feeded by an Alternative Current. Application to the Study of a Dynamic Regime for Lighting Micro-Network**
M. Stambouli, K. Charrada and G. Zissis[1]
ESSTT, Tunis, Tunisie
[1]CPAT-University Paul Sabatier, Toulouse, France

6P38 **Cathode Fall Behavior in a Hg-Rare Gas Discharge with a Thermionic Cathode**
R.C. Garner and Y.M. Li
OSRAM Sylvania Inc., Beverly, MA, USA

6P39 **Barium Loss from the Electrode of a Low Pressure Hg-Ar Discharge at Ignition**
P. Moskowitz
OSRAM Sylvania Inc., Beverly, MA, USA

6P40 **Emission and Spectral Characteristics of Electrodeless Indium Halide Lamp**
M. Takeda, A. Hochi, S. Horii and T. Matsuoka
Lighting Research Laboratory, Kyoto, Japan

6P41 **Accurate Atomic Data for Industrial Plasma Applications**
U. Griesmann, J.M. Bridges, J.R. Roberts, W.L. Wiese and J.R. Fuhr
National Institute of Standards and Technology, Gaithersburg, MD, USA

6P42 **Calculations of Acoustic Resonances in Arc Lamp Discharge Vessels**
W.P. Moskowitz
OSRAM Sylvania Inc., Beverly, MA, USA

6P43 **The Low Pressure Sodium Lamp**
J. D. Hooker
GE Lighting, Leicester, United Kingdom

6P44 **Study of The Discrepancy Between Electron Temperature and Gas Temperature in the Vicinity of the Anode of an Electric Arc**
M. Razafinimanana, M. Bouaziz, A. Gleizes and S. Vacquie
CPAT-University Paul Sabatier, Toulouse, France

6P45 **High Voltage Ignition of High Pressure Microwave Powered UV Light Sources**
J.D. Frank, M. Cekic and C.H. Wood
Fusion U.V. Curing Systems, Corp., Gaithersburg, MD, USA

6P46 **Operating Characteristics of a High Pressure "Wire" Hollow Cathode Plasmas**
H. Kirkici
Auburn University, Auburn, AL, USA

Wednesday Afternoon – 21 May, 1997
3:00 p.m. – Rousseau Center

Poster Session 6P47-54: 5.5 Environmental / Energy Issues in Plasma Science

6P47 **Oxidation of Volatile Organic Compounds by Microwave Plasma at Atmospheric Pressure**
D.J. Lee and T.E. Ruden[1]
Aneptek Corporation, Natick, MA, USA
[1]Microwave Consultant, Newton Highlands, MA, USA

6P48 **Strong Current Arc Discharges of Alternating Current**
Ph.G. Rutberg, A.A. Safronov and V.L. Goryachev
Russian Academy of Sciences, St. Petersburg, Russia

6P49 **About Biological and Chemical Effect of Dense Low Temperature Oxygen-Hydrogen Plasma**
V.L. Goryachev, Ph.G. Rutberg, A.A. Ufimtsev and V.N. Pfedyokovich
Russian Academy of Sciences, St. Petersburg, Russia

6P50 **Development of Glow Discharge Plasma-Catalytic Reactors Operated Under Atmospheric Condition**
Y. Hayashi, K. Itoyama[1], S. Tanabe[1] and H. Matsumoto[1]
Fujitsu Laboratories Ltd., Kawasaki, Japan
[1]Nagasaki University, Nagasaki, Japan

6P51 **Development of an Ablation Measurement Technique Using Plasma Armatures**
T.L. King and K. Kim[1]
University of Houston, Houston, TX, USA
[1]University of Illinois, Urbana, IL, USA

6P52 **Intense Electon Beam Application for Flue Gas Treatment**
A.G. Chmielewski, Z. Zimek, E. Iller, B. Tyminski and J. Licki[1]
Institute of Nuclear Chemistry and Technology, Warsaw, Poland
[1]Institute of Atomic Energy, Otwock-Swierk, Poland

6P53 **Flue Gas Treatment by Simultaneous Application of Electron Beam and Microwave Discharge**
Z. Zimek, A.G. Chmielewski, S. Bulka and H. Nichipor[1]
Institute of Nuclear Chemistry and Technology, Warsaw, Poland
[1]Institute of Physical and Chemical Problems, Minsk, Belarus

6P54 **Spectroscopic Investigation of Arc Spot Ignition on Cold Cathodes**
M. Schumann, D. Nandelstadt, J. Schein, B. Michelt and J. Mentel
Ruhr-Universität Bochum, Bochum, Germany

Wednesday Afternoon – 21 May, 1997
3:00 p.m. – Multipurpose Room

Poster Session 6Q13-14: 2.2 Fast Wave Devices

6Q13 **Design of Novel Hybrid Traveling-Wave Amplifiers in X- and Ka-Band**
W. Lawson, M.R. Arjona, A. Fernandez, T. Hutchings, P.E. Latham and G.P. Saraph
University of Maryland, College Park, MD, USA

6Q14 **Initial Operation of the Univiversity of Maryland X-Band Coaxial Gyroklyston Experiment**
W. Lawson, N. Ballew, J.P. Calame, M. Castle, J. Cheng, P. Chin, V.L. Granatstein, B. Hogan, M. Reiser and G.P. Saraph
University of Maryland, College Park, MD, USA

Wednesday Afternoon – 21 May, 1997
3:00 p.m. – Multipurpose Room

Poster Session 6Q15-23: 2.4 Slow Wave Devices

6Q15 **Overmoded Backward-Wave Oscillator: A Comparison of Experimental Results with Non-linear Analysis**
D.K. Abe, S.M. Miller[1], Y. Carmel[2], A. Bromborsky, T.M. Antonsen Jr.[2], B. Levush[3] and W.W. Destler[2]
Army Research Laboratory, Adelphi, MD, USA
[1]ENSCO, Springfield, VA, USA
[2]University of Maryland, College Park, MD, USA
[3]Naval Research Laboratory, Washington, DC, USA

6Q16 **Effect of Random Manufacturing Errors on Slow Wave Circuit Performance**
D. Dialetis and D. Chernin
Science Application International Corp., McLean, VA, USA

6Q17 **Density Profiles and Current Flow in a Crossed-Field, Electron Vacuum Device**
D.J. Kaup and G.E. Thomas[1]
Clarkson University, Potsdam, NY, USA
[1]Communications & Power Industries Inc. (CPI), Beverly, MA, USA

6Q18 **Rectangular Grating Periodic Structure for Low-Voltage Amplifiers**
L.J. Louis, J.E. Scharer, J.H. Booske[1] and M.J. McNeely
University of Wisconsin–Madison, Madison, WI, USA

6Q19 **A New Resonator Design for Smith-Purcell Free Electron Lasers**
C.L. Platt, M.F. Kimmitt, J.H. Brownell and J.E. Walsh
Dartmouth College, Hanover, NH, USA

6Q20 **Numerical Cold Testing for Plasma Loaded Slow-Wave Circuits**
J.M. Oslake, J.P. Verboncoeur and C.K. Birdsall
University of California at Berkeley, Berkeley, CA, USA

6Q21 **Simulation of TWT's and Twystrodes**
D. Smithe, B. Goplen, M.A. Kodis[1], E. Zaidman[1], T.M. Antonsen Jr.[1] and B. Levush[1]
Mission Research Corporation, Newington, VA, USA
[1]Naval Research Laboratory, Washington, DC, USA

6Q22 **Novel Computer Model for Simulation of Backward Wave Oscillators**
G.I. Zaginayklov, Yu.V. Gandel and P.V. Turbin[1]
Kharkiv State University, Kharkiv, Ukraine
[1]Scientific Center of Physical Technologies, Kharkiv, Ukraine

6Q23 **High Power Microwave Generation and Beam Transport in the PASOTRON™ BWO Source**
D.M. Goebel, E.S. Ponti[1], J. Feicht and R. Watkins
Hughes Telecommunications and Space, Torrance, CA, USA
[1]Hughes Research Laboratories, Malibu, CA, USA

Wednesday Afternoon – 21 May, 1997
3:00 p.m. – Multipurpose Room

Poster Session 6Q24-44: 6 Plasma Diagnostics

6Q24 **Silicon Photodiode Soft X-ray Detectors**
G.C. Idzorek and R.J. Bartlett
Los Alamos National Laboratory, Los Alamos, NM, USA

6Q25 **Determination of Copper Concentration in a SF6 Arc Plasma in an Electrical Circuit Breaker**
C. Fleurier, S.S. Ciobanu, D. Hong, F. Gentils and C. Fievet[1]
Université d'Orléans, Orléans, France
[1]Centre de Recherches Schneider Electric, Grenoble, France

6Q26 **Radiation Diagnostics and X-ray Output from 12-13 Mega-Ampere Plasma Implosions**
H. Oona, G.C. Idzorek and J.H. Goforth
Los Alamos National Laboratory, Los Alamos, NM, USA

6Q27 **Plasma Diagnostics on the DIII-D Tokamak**
R.T. Snider and the DIII-D Group
General Atomics, San Diego, CA, USA

6Q28 **A New Design of a Parallel Chord Optical Probe and Its Application to the Plasma Diagnostics**
H.K. Na, N.S. Yoon, B.C. Kim, J.H. Choi, G.S. Lee and S.M. Hwang
Korea Basic Science Institute, Taejeon, Korea

6Q29 **Compact, Rugged, Flexible Fiber Optic Interferometer for Sensitive Gas and Plasma Density Meaurements**
G.G. Peterson, N. Qi, S.W. Gensler, R.R. Prasad, G. Rondeau[1] and M. Krishnan
Alameda Applied Sciences Corp., San Leandro, CA, USA
[1]Consultant, San Leandro, CA, USA

6Q30 **Bremsstrahlung Characterization at PBFA Z**
M.S. Derzon, R. C.Mock, C.L. Ruiz, M.A. Sweeney, S.E. Lazier[1], A. Schmidlapp[1] and G.W. Cooper[2]
Sandia National Laboratories, Abluquerque, NM, USA
[1]Ktech Corporation, Abluquerque, NM, USA
[2]University of New Mexico, Abluquerque, NM, USA

6Q31 **Arc Channel Impedance Estimation According to Voltage and Current Oscillograms with Programmable Discharge of Capacitive Energy Store**
B.E. Fridman and Ph.G. Rutberg
Russian Academy of Sciences, St. Petersburg, Russia

6Q32 **LIF Diagnostic for Measuring Beam-Transport Magnetic Fields**
T.G. Jones, W.A. Noonan[1] and P.F. Ottinger[2]
National Research Council Research Associate
[1]University of Maryland, College Park, MD, USA
[2]Naval Research Laboratory, Washington, DC, USA

6Q33 **Measurement of Energetic (>6 MeV) Particles in Wire Array Pinches on PBFA Z**
C.L. Ruiz, M.S. Derzon, G.W. Cooper[1] and F.A. Schmidlapp[2]
Sandia National Laboratories, Albuquerque, NM, USA
[1]University of New Mexico, Albuquerque, NM, USA
[2]Ktech Corp, Albuquerque, NM, USA

6Q34 **Targets Development at Sandia National Laboratories**
M.L. Smith, D. Hebron, M.S. Derzon, R. Olson and T. Alberts[1]
Sandia National Laboratories, Albuquerque, NM, USA
[1]W.J. Schafer Associates, Inc., Livermore, CA, USA

6Q35 **Plasma Diagnostics**
S.E. Lazier
Ktech Corporation, Albuquerque, NM, USA

6Q36 **Modeling of a Soft X-Ray Diode Using Particle-in-Cell and Monte-Carlo Simulations**
R.K. Keinigs, R.J. Faehl and D. Platts
Los Alamos National Laboratory, Los Alamos, NM, USA

6Q37 **New Method for Negative Ion Diagnostics**
E. Stamate and K. Ohe[1]
Faculty of Physics, Al. I. Cuza University, Iasi, Romania
[1]Nagoya Institute of Technology, Nagoya, Japan

6Q38 **Temperature and Density Measurements in High Intensity Microwave-Excited Excimer Lamps**
S. Popovic and M. Cekic[1]
Old Dominion University, Norfolk, VA, USA
[1]Fusion UV Systems, Gaithersburg, MD, USA

6Q39 **Photoelectron Spectroscopy for Soft X-Ray Measurements in a Small Tokamak**
S-H. Seo and H-Y. Chang
Korea Advanced Institute of Science and Technology, Taejon, Korea

6Q40 **Obtaining Plasma Potential Measurements in Hall Thruster Plumes**
C.M. Marrese, J.E. Foster and A.D. Gallimore
University of Michigan, Ann Arbor, MI, USA

6Q41 **A High Frequency Probe for Absolute Measurements of Electric Fields in Plasmas, II**
N. Brenning, H. Gunell and S. Torvén
Royal Institute of Technology, Stockholm, Sweden

6Q42 **A Pulsed-Laser X-ray Source for X-ray Diagnostic Calibration**
A.R. Moats, F. Camacho, S. Cameron, D.L. Fehl, C. Martinez, J. Porter, L. Ruggles and R.B. Spielman
Sandia National Laboratories, Albuquerque, NM, USA

6Q43 **Spectroscopic Characterization of an ECR Processing Plasma**
D. Lafrance and A. Sarkissian
INRS-Énergie et Matériaux, Varennes, Qc, Canada

6Q44 **Interferometer Measurements In Pulsed Plasma Experiments**
I.V. Lisitsyn, T Kawauchi, S. Kohno, T. Sueda, S. Katsuki and H. Akiyama
Kumamoto University, Kumamoto, Japan

Thursday Morning – 22 May, 1997
8:30 a.m. – Kon Tiki Ballroom

Plenary Session

Tokamak Fusion Science Research on the DIII-D Tokamak

Dr. Thomas C. Simonen
Director , DIII-D Program
General Atomics, La Jolla, CA, USA

Chair: J. Hyman

Thursday Morning – 22 May, 1997
10:00 a.m. – Kon Tiki Ballroom

Special Panel Session 7A: 2.7 Microwave Generation and Microwave Plasma Interactions
Chair: J. W. Luginsland

7A01 **The Impact of CAD in the Computational Design Process on Total System Development**
L. Ives and W.F. Vogler
Calabazas Creek Research, Inc., Saratoga, CA, USA

7A02 **Emission Properties of the Silicon Cathodes Coated with Doped Diamond-Like Carbon Films**
V.G. Litovchenko, A.A. Evtukh, N.I. Klyui, R.I. Marchenko and V.A. Semenovich
Institute of Semiconductor Physics, Kiev, Ukraine

7A03 **Wiggler Enhanced Cyclotron Autoresonance Maser Amplifiers**
A.T. Lin and C-C. Lin
University of California at Los Angeles, Los Angeles, CA, USA

7A04 **Nonlinear Theory of the Interaction Between an Annular Electron Beam and the Azimuthal Surface Waves (ASW)**
V. O. Girka and T. Malykhina
Kharkiv State University, Kharkiv, Ukraine

7A05 **Diode Plasma Effects on the Microwave Pulse Length from Relativistic Magnetrons**
D. Price, J.S. Levine and J.N. Benford[1]
Primex Physics International, San Leandro, CA, USA
[1] Microwave Sciences, Lafayette, CA, USA

7A06 **Laboratory Simulation of Ionospheric Plasma Heating Experiments**
M.C. Lee, R.J. Riddolls, N.E. Dalrymple, K. Vilece, M.J. Rowlands, D.T. Moriarty, K.M. Groves[1], M.P. Sulzer[2] and S.P. Kuo[3]
Massachusetts Institute of Technology, Cambridge, MA, USA
[1]Phillips Laboratory, Hanscom AFB, MA, USA
[2]Arecibo Observatory, Arecibo, Puerto Rico
[3]Polytechnic University, Farmingdale, NY, USA

7A07 **The Influence of Plasma on the Amplification of Traveling Slow Waves**
S. Kobayashi, T.M. Antonsen Jr., G. Nusinovich and Y. Carmel
University of Maryland, College Park, MD, USA

Thursday Morning – 22 May, 1997
10:00 a.m. – Board Room

Oral Session 7B: 5.5 Environmental / Energy Issues in Plasma Science
Chair: L. Christophorou

7B01-02 *Invited*—**UV Photon and Low-Energy (5-150 eV) Electron-Stimulated Processes at Environmental Interfaces**
T.M. Orlando
Pacific Northwest National Laboratory, Richland, WA, USA

7B03 **Plasma-Produced Erbia Coatings For Waste Reduction In Plutonium Casting Operations**
B.P. Wood, D. Soderquist, A. Gurevitch, J. Steele, F. Hampel, K.C. Walter, A.J. Perry[1] and J. Treglio[2]
Los Alamos National Laboratory, Los Alamos, NM, USA
[1]AIMS Consulting, San Diego, CA, USA
[2]ISM Technologies, Inc., San Diego, CA, USA

7B04 **Aerosol Plasma for Aqueous Wastes Treatment**
V.M. Bystritskii, Y. Yankelevich, T. Wood, F.J. Wessel and D. Yee
University of California at Irvine, Irvine, CA, USA

7B05 **Decomposition of Methylene Chloride in Non-Thermal Plasmas**
B.M. Penetrante, M.C. Hsiao, J.N. Bardsley, B.T. Merritt, G.E. Vogtlin, A. Kuthi[1], C.P Burkhart[2] and J.R. Bayless[2]
Lawrence Livermore National Laboratory, Livermore, CA, USA
[1]Plasma & Materials Technologies, Inc., Chatsworth, CA, USA
[2]First Point Scientific, Inc., Agoura Hills, CA, USA

7B06 **Modeling of Plasma Remediation of VOCs in Dielectric Barrier Discharges**
X. Xu and M.J. Kushner
University of Illinois, Urbana, IL, USA

7B07 **Decomposition of Dichloroethane in a Plasma Arjet Reactor: Experiment and Modeling**
H.R. Snyder and C.B. Fleddermann
University of New Mexico, Albuquerque, NM, USA

7B08 **Oxidation of Styrene Using a Silent Discharge Plasma**
G.K. Anderson, J.J. Coogan and H.R. Snyder
Los Alamos National Laboratory, Los Alamos, NM, USA

Thursday Morning – 22 May, 1997
10:00 a.m. – Toucan Room

Oral 7C: 5.4 Flat Panel Displays
Chair: C-M. Tang

7C01-02 *Invited*—**Phosphors for Flat Panel Field Emission and Plasma Displays**
C.J. Summers
Georgia Institute of Technology, Atlanta, GA, USA

7C03 **Development of Low Voltage Field Emitter Cathodes With Enhanced Electron Emission Coatings For Flat Panel Displays**
W.D. Palmer, D. Temple, J. Mancusi, L. Yadon, D. Vellenga and G.E. McGuire
MCNC Electronic Technologies Division, Research Triangle Park, NC, USA

7C04 **Three-Dimensional Simulation of Field Emitter Arrays Using EO-3D**
C-M. Tang
National Institute of Standards & Technology, Gaithersburg, MD, USA

7C05-06 *Invited*—**Dry Etching Trends in Flat Panel Display Processing**
W.W. Yao
dpiX, A Xerox Co., Palo Alto, CA, USA

7C07 **Microhollow Electrode Discharge Flat Panel Displays**
K.H. Schoenbach, T. Tessnow, F.E. Peterkin and W.C. Nunnally[1]
Old Dominion University, Norfolk, VA, USA
[1]University of Missouri–Columbia, Columbia, MS, USA

7C08 **Low-Temperature Deposition Pathways to Silicon Nitride, Amorphous Silicon, Polycrystalline Silicon and n Type Amorphous Silicon Films Using a High Density Plasma System**
S. Bae, D. Farber, A. Kalkan and S. Fonash
Pennsylvania State University, University Park, PA, USA

7C09 **MgO Erosion in Plasma Displays Measured with Microbeam RBS**
R.T. McGrath, H. Schone[1], D. Walsh[1], R. Veerasingam and C. Zarecki[2]
Pennsylvania State University, University Park, PA, USA
[1]Sandia National Laboratories, Albuquerque, NM, USA
[2]Photonics Imaging, Northwood, OH, USA

Thursday Morning – 22 May, 1997
10:00 a.m. – Macaw Room

Oral Session 7D: 7.1 MHD and EM/ETH Launchers
Chair: R.D. Richardson

7D01 **Plasma Parameters in Burn Rates Processes of a Solid Propellant for Electrothermal-Chemical Launch Devices**
M.A. Bourham, J.G. Gilligan and C.J. Boyer
North Carolina State University, Raleigh, NC, USA

7D02 **Progress on TURBFIRE, a Simulation of Plasma-Surface Interactions in Electric Launchers**
E.C. Tucker, N.P. Orton, J.G. Gilligan and M.A. Bourham
North Carolina State University, Raleigh, NC, USA

7D03 **Optical Diagnostics in High Current Pseudospark Discharges**
M. Schlaug, C. Bickes, D.H.H. Hoffmann, P. Felsner, K. Frank, U. Prucker and A. Schwandner
University of Erlangen-Nuremberg, Erlangen, Germany

7D04 **High Voltage Subnanosecond Dielectric Breakdown**
J. Mankowski, L.L. Hatfield, M. Kristiansen, F.J. Agee[1], J.M. Lehr[2] and J. Wells[2]
Texas Tech University, Lubbock, TX, USA
[1]Phillips Laboratory, Kirtland AFB, NM, USA
[2]Fiori Industries, Inc., Albuquerque, NM, USA

7D05 **Hydrogen Heating in the Discharge Chamber of Powerful Electric Discharge Launcher**
Ph.G. Rutberg, A.A. Bogomaz, A.V. Budin, V.A. Kolikov and A.G. Kuprin
Russian Academy of Sciences, St. Petersburg, Russia

Thursday Morning – 22 May, 1997
10:00 a.m. – Cockatoo Room

Oral Session 7E: 4.6 Spherical Configurations / Ball Lightning
Chair: U. Shumlak

7E01-02 *Invited*—**Results from The HIT-II Coaxial Helicity Injection Spherical Tokamak**
B.A. Nelson, T.R. Jarboe, R. Ewig, C. Hoffman, A.K. Martin, K. McCollam, D.J. Orvis, U. Shumlak and B. Udrea
University of Washington, Seattle, WA, USA

7E03 **Internal Magnetic Field Measurements Using the Transient Probe on the Helicity Injected Tokamak**
M.A. Bohnet, T.R. Jarboe and A.T. Mattick
University of Washington, Seattle, WA, USA

7E04 **Inertial Electro-Magnetostatic Plasma Neutron Sources**
D.C. Barnes, R.A. Nebel, M.M. Schauer and M.M. Pickrel
Los Alamos National Laboratory, Los Alamos, NM, USA

7E05 **EHD and MHD Models of Fireballs and their Relevance to Natural and Artificial Ball Lightning**
H. Kikuchi
Nihon University, College of Science & Technology, Tokyo, Japan

7E06 **Radiation Sources for Industrial Applications: The Spherical Pinch and the Vacuum Spark**
A. Ikhleff, L. Zhang and E. Panarella[1]
Advanced Laser and Fusion Technology, Inc., Hull, PQ, Canada
[1]University of Tennessee, Knoxville, TN, USA

7E07 **Three-Dimensional Nonlinear Simulation of the Spheromak Tilt Instability**
B. Udrea and U. Shumlak
University of Washington, Seattle, WA, USA

7E08 **Compact Toroid Properties Compared to Ball Lightning**
C. Seward
Electron Power Systems Inc, Acton, MA, USA

7E09 **The Motion of Wave Energy and the Behavior of Plasma Fireball in the Atmosphere**
Y. Zou
University of Utah, Salt Lake City, Utah, USA

Thursday Morning – 22 May, 1997
10:00 a.m. – Rousseau Center

Poster Session 7P01-10: 1.4 Computational Plasma Physics

7P01 **Hybrid PIC Acceleration Schemes for Discharges**
K.L. Cartwright, J.P. Verboncoeur and C.K. Birdsall
University of California at Berkeley, Berkeley, CA, USA

7P02 **A Hybrid Fluid Model Approach to Plasma Dynamics**
R. Cottam
NYMA Inc./NASA Lewis Research Center, Brook Park, OH, USA

7P03 **Eigenmodes of Microwave Cavities Containing High-Loss Dielectric Materials**
S.J. Cooke and B. Levush[1]
University of Maryland, College Park, MD, USA
[1]Naval Research Laboratory, Washington, DC, USA

7P04 **A Laplace Expansion Solution Technique for 2D Simulation of PPM Fields**
R.H. Jackson
Naval Research Laboratory, Washington, DC, USA

7P05 **A Simple Analytic ICP Model and Comparison to Experiment**
D.R. Juliano, D.B. Hayden and D.N. Ruzic
University of Illinois, Urbana, IL, USA

7P06 **SPICES 1: A New Vlasov-Fokker-Planck Simulation Code**
V. Riccardo, G.G.M. Coppa and G. Lapenta
Politecnico di Torino-Dipartimento di Energetica, Corso Duca degli Abruzzi, Torino, Italy

7P07 **Numerical Studies of Orbits in a 3-D Magnetic Cusp Geometry**
S.K. Wong and A. Walton
City University of Hong Kong, Hong Kong

7P08 **Lagrangian MHD in 2D and 3D**
T.A. Oliphant, J.E. Morel, W.P. Gula and G.W. Pfeufer
Los Alamos National Laboratory, Los Alamos, NM, USA

7P09 **Approximate Modeling of Cylindrical IEC Fusion Device**
B.P. Bromley, L. Chacon and G.H. Miley
University of Illinois, Urbana, IL, USA

7P10 **Human Plasmas**
T. Ohnuma and H. Soda
Tohoku University, Sendai, Japan

Thursday Morning – 22 May, 1997
10:00 a.m. – Rousseau Center

Poster Session 7P11-25: 3.1 Plasma, Ion and Electron Sources

7P11 **Measurement and Control of RF Power in Inductively Coupled Plasma**
B.M. Alexandrovich, V.A. Godyak and R.B. Piejak
OSRAM Sylvania Inc., Beverly, MA, USA

7P12 **Ion Temperature Measurements in Helicon Plasmas**
P. Keiter, M. Balkey, J. Kline, M. Koepke, E. Scime and M. Zintl
West Virginia University, Morgantown, WV, USA

7P13 **Ion Charge State Distribution in the ECR Source with Pumping by Millimeter-Wave Gyrotron Radiation**
S.V. Golubev, S.V. Razin and V.G. Zorin
Russian Academy of Science, Nizhny Novgorod, Russia

7P14 **Boron Doping to Diamond and DLC Using Plasma Immersion Ion Implantation**
T. Ikegami, T.A. Grotjohn[1], D. Reinhard[1] and J. Asmussen Jr.[1]
Visiting from Kumamoto University, Kumamoto, Japan
[1]Michigan State University, East Lansing, MI, USA

7P15 **High Current Plasma Electron Emitter**
G. Fiksel, D.J. Hartog, D. Holly, J. Anderson[1], D. Craig[1], R. Kendrick[1], S. Oliva[1], J. Sarff[1] and M. Thomas[1]
Sterling Scientific, Inc., Madison, WI, USA
[1]University of Wisconsin–Madison, Madison, WI, USA

7P16 **A High Current Vacuum Arc Ion Source for Heavy Ion Fusion**
N. Qi, S.W. Gensler, R.R. Prasad, M. Krishnan, F. Liu[1] and I.G. Brown[1]
Alameda Applied Sciences Corp, San Leandro, CA, USA
[1]University of California at Berkeley, Berkeley, CA, USA

7P17 **Experimental Results of Fluid Flow in Capillary Tubing to Cool Particle and RF Transmission Windows**
R.J. Vidmar
SRI International, Menlo Park, CA, USA

7P18 **Penning Ionization of Cesium by Photexcited Mercury–Radiation Transport Effects**
K.R. Stalder and R.J. Vidmar
SRI International, Menlo Park, CA, USA

7P19 **The Negative Hydrogen Ion Sourse based on Reflecting Discharge with Metal-Hydride Cathode**
I.A. Bitnaya, V.N. Borisko, E.V. Klochko and Yu.V. Sidorenko
Kharkiv State University, Kharkiv, Ukraine

7P20 **Special Features of Gas Discharge Characteristics of Magnetron Diode with Metal-Hydride Cathode**
I.A. Bitnaya, V.N. Borisko and E.V. Klochko
Kharkiv State University, Kharkiv, Ukraine

7P21 **Electron Emitter Pulsed-Type Cylindrical IEC**
G.H. Miley, Y. Gu, R.A. Stubbers, R. Zich, J. Sved[1], R. Anderl[2] and J. Hartwell[2]
University of Illinois, Urbana, IL, USA
[1]DASA, Bremmen, Germany
[2]INEL, Idaho Falls, ID, USA

7P22 **Electron Optics Aspects of X-Ray Tube Design**
B.P. Curry
EM SciTek Consulting Co., Glen Ellyn, IL, USA

7P23 **50 Hz Electron Emission from PZT Ferroelectric Cathodes**
D. Flechtner, Cz. Golkowski, J.D. Ivers, G.S. Kerslick, J.A. Nation and L. Schachter
Cornell University, Ithaca, NY, USA

7P24 **Magnetic Field Topography of the Anode Layer Thruster**
M.T. Domonkos and A.D. Gallimore
University of Michigan, Ann Arbor, MI, USA

7P25 **Plasma Flow in Nonhomogeneous Magnetic Field as a Lens for Focusing of Ion Beams**
V.I. Maslov and I.N. Onishchenko
Kharkiv Institute of Physics & Technology, Kharkiv, Ukraine

Thursday Morning – 22 May, 1997
10:00 a.m. – Rousseau Center

Poster Session7P26-41: 3.2 Intense Ion and Electron Beams

7P26 **Computational and Experimental Studies of the Beam-Target Interaction for High-Dose, Multi-Pulse Radiography**
B.G. DeVolder, T.J.T. Kwan, R.D. Fulton, D.C. Moir, D.M. Oro and D.S. Prono
Los Alamos National Laboratory, Los Alamos, NM, USA

7P27 **Nanostructured Surface Processing by an Intense Pulsed Ion Beam Irradiation**
M. Yatsuzuka, T. Masuda, Y. Hashimoto[1], T. Yamasaki, H. Uchida, S. Nobuhara and Y. Yoshihara[2]
Himeji Institute of Technology, Himeji, Japan
[1]Kobe City College of Technology, Kobe, Japan
[2]Nippon Steel Co., Himeji, Japan

7P28 **Collision of a High Energy Plasma Clot with an Obstruction Including Interpenetration and Generation of Electromagnetic Radiation**
E.L. Stupitsky, A.Yu. Repin and G.F. Kiuttu[1]
Russian Defense Central Institute of Physics and Technology, Sergiev Posad, Russia
[1]Phillips Laboratory, Kirtland AFB, NM, USA

7P29 **Generation of Secondary Electrons from the Interaction of High-Energy Beams with the Upper Atmosphere**
V.V. Kurnosov, E.L. Stupitsky and G.F. Kiuttu[1]
Russian Defense Central Institute of Physics and Technology, Sergiev Posad, Russia
[1]Phillips Laboratory, Kirtland AFB, NM, USA

7P30 **Creation of a Monoenergetic Pulsed Positron Beam**
S.J. Gilbert, C. Kurz, R.G. Greaves and C.M. Surko
University of California at San Diego, La Jolla, CA, USA

7P31 **Inclusion of Non-Ideal Effects in 3-D PIC Simulations of Ion Diodes**
T.D. Pointon, R.A. Vesey, T.A. Mehlhorn and M.E. Cuneo
Sandia National Laboratories, Albuquerque, NM, USA

7P32 **X-Ray Diagnostic Development for Measurement of Electron Deposition to the SABRE Anode**
J.S. Lash, M.S. Derzon, M.E. Cuneo, R.A. Vesey and S.E. Lazier[1]
Sandia National Laboratories, Albuquerque, NM, USA
Ktech Corporation, Albuquerque, NM, USA

7P33 **Multistage Acceleration of Light Ions for Fusion**
S.A. Slutz
Sandia National Laboratories, Albuquerque, NM, USA

7P34 **Bidirectional Pulse Generator System for Linear Induction Accelerators**
T. Kobayashi, J. Ohmura, A. Okino, J-H. Park[1], K-C. Ko[1] and E. Hotta[2]
Tokyo Institute of Technology, Tokyo, Japan
[1]Hanyang University, Seoul, Korea
[2]Tokyo Institute of Technology, Yokohama, Japan

7P35 **Electron Flows in a Low Voltage Gap Exposed to an Oblique External Magnetic Field**
A.L. Garner, Y.Y. Lau and D. Chernin[1]
University of Michigan, Ann Arbor, MI, USA
[1]Science Application International Corporation, McLean, VA, USA

7P36 **Characteristic of RF Plasma Cleaning Protocols for Removal of Contaminants in High Voltage Beam Diodes**
J.I. Rintamaki, R.M. Gilgenbach, W.E. Cohen, J.M. Hochman, R.L. Jaynes, Y.Y. Lau, L.K. Ang, M.E. Cuneo[1] and P.R. Menge[1]
University of Michigan, Ann Arbor, MI, USA
[1]Sandia National Labortories, Albuequerque, NM, USA

7P37 **Modeling Lithium Plasma Formation by Laser Ionization Based on Resonance Saturation (LIBORS) and Implications for Extreme-Current Ion Sources**
P. Wang, J.J. MacFarlane, T.A. Mehlhorn[1], A.B. Filuk[1] and M.E. Cuneo[1]
University of Wisconsin–Madison, Madison, WI, USA
[1]Sandia National Laboratories, Albuquerque, NM, USA

7P38 **Development of a High Brightness, Ohmically Generated Thin Film Lithium Ion Source**
P.R. Menge, M.E. Cuneo, M.A. Bernard and W.E. Fowler
Sandia National Laboratories, Albuquerque, NM, USA

7P39 **Study of the High Energy Diagnostic Neutral Beam Characteristics of TdeV on Its Test Stand**
A.H. Sarkissian and E. Charette
CCFM, Varennes, Québec, Canada

7P40 **Electron Beam Generation in Turbulent Plasma of Z-Pinch Discharges**
V.V. Vikhrev and E.O. Baronova
RRC Kurchatov Institute, Moscow, Russia

7P41 **Photofield Emission from Tip Cathodes**
E. Garate and N. Rostoker
University of California at Irvine, Irvine, CA, USA

Thursday Afternoon – 22 May, 1997
1:30 p.m. – General Atomics

GENERAL ATOMICS

Tour of the DIII-D Tokamak Facility

Busses Leave From the Front of the
Catamaran Hotel Conference Area
Promptly at 1:30 p.m.

All Guests Must Register by Tuesday May 20, 1997
at the Registration Desk on the second floor
of the Catamaran Hotel Meeting Rooms

Thursday Afternoon – 22 May, 1997
3:00 p.m. – Rousseau Center

Poster Session 8P42-45: Unscheduled Papers

8P42 **α-γ Transition Properties of an RF Discharge in Argon**
V.A. Lisovskiy
Kharkiv State University, Kharkiv, Ukraine

8P43 **Electron Temperature Axial Pattern in the RF Discharge**
V.A. Lisovskiy, V.S. Boichuk, V.D. Yegorenkov
Kharkiv State University, Kharkiv, Ukraine

8P44 **Characterization of Radiation Induced Brightness and Darkening in Fiber-Optic Cables at PBFA-Z**
S.E. Lazier, M.S. Derzon[1], J.S. Lash[1]
Ktech Corporation, Albuquerque, NM, USA
[1]Sandia National Laboratories, Albuquerque, NM, USA

8P45 **Dense-Plasma Emission Pumping of Q-Switched Ti:Sapphire Tube-Laser**
J-T. Seo, K.S. Han, J.H. Lee
Hampton University, Hampton, VA 23668

CONFERENCE RECORD—

ABSTRACTS

Monday Morning, 19 May 1997
8:15 a.m. – Kon Tiki Ballroom
Plenary Session 1

Plenary 1

Welcome to Conference Participants

Dr. Jay Hyman, Conference Chair
Hughes Research Laboratories

Monday Morning – 19 May, 1997
8:45 a.m. – Kon Tiki Ballroom

Keynote Address:

Changes in the Nature of Plasma Science in the Post-Cold War Era

Professor Roald Z. Sagdeev
University of Maryland
College Park, MD, USA

Chair: Dr. Jay Hyman

Monday Morning, 19 May 1997
10:00 a.m. – Kon Tiki Ballroom

Oral Session 1A:
1.1 Basic Processes in Fully Ionized Plasmas – Waves, Instabilities, Plasma Theory, etc. I
Chair: O. Ishihara

1A01-02 ***Invited***

Helicon Waves in Theory and Experiment

Francis F. Chen
University of California at Los Angeles, Los Angeles, CA USA

The use of helicon waves to produce high density plasmas for semiconductor chip fabrication tools is by now well known in that industry. Basic research on helicon discharges in the last ten years has greatly improved our understanding of how these plasma sources work. At high magnetic fields, the wave fields have been carefully measured and found to agree well with the classical theory of helicon waves. The theory has been extended to low magnetic fields by including the coupling to cyclotron waves. Experiments in this range have also been done. The transition to zero magnetic field turns out to be nontrivial and rather interesting; this is a region in which many industrial plasma sources operate. As a result of efforts by several groups, numerical computations that include the effects of damping, plasma inhomogeneity and antenna coupling can now be made on a simple computer. Unfortunately, the very nonuniform magnetic fields in production tools still require extensive modeling. We are now in a position to answer several intriguing questions that have puzzled experimentalists for many years: 1) What is the rf absorption mechanism that makes helicon discharges so efficient? 2) Why is the $m = -1$ azimuthal mode so much harder to excite than the $m = +1$ mode? 3) What causes the discontinuous jumps in density as the magnetic field or rf power is increased? 4) What fields are generated under and near the antenna? Experimental and theoretical data that bear on these questions will be shown.

1A03

Velocity-Shear Origin of Broadband Electrostatic Noise*

M. E. Koepke, J. J. Carroll III, M. W. Zintl
Department of Physics, West Virginia University, Morgantown WV 26506-6315

Multiple, independent eigenmodes of an inhomogeneity-driven instability are observed simultaneously with large and comparable amplitude. This is in sharp contrast to the usual case in plasmas in which one eigenmode dominates or, for conditions far above the excitation threshold, a collection of harmonics appears. The significance is that the spectral features are not separated by the ion gyrofrequency ω_{ci}, or any other normal-mode frequency of the plasma. This has implications regarding the spectral width of the fluctuations, which, in some cases, can exceed 50% of center frequency. Furthermore, the spectral features are Doppler downshifted, in some cases to frequencies associated with ion-acoustic modes. For example, ω/ω_{ci} = 0.25 are readily observed (recall that T_i/T_e is of order unity). These facts are particularly unexpected because the plasma conditions correspond to large excitation thresholds for current-driven electrostatic ion-cyclotron (CDEIC) and ion-acoustic (IA) waves. The results have direct relevance to recent SCIFER and AMICIST rocket experiments[1] in the Earth's cleft ion fountain where electrostatic waves ($\omega < \omega_{ci}$) are observed and are strongly correlated with transverse ion heating and reduced plasma densities, but with the unexplained characteristic that the spectral features are not separaed by ω_{ci}.

*Work supported by ONR and NSF.

1Kintner et al., Geophys. Res. Lett. 23 1873, 1996; Bonnell et al., GRL 23, 3297, 1996.

1A04

Experimental Study of Polarization of Lines, Emitted by the Plasma of Z-pinch Devices

E.O. Baronova
NFI, RRC Kurchatov Institute Moscow, 123182, Russia

Polarization of x-ray lines is well known fact in solar plasma. Experimental study of polarization of x-ray line emission from laboratory plasmas (plasma focus device, vacuum spark device) are given in this paper. The investigation of spectra of He-like Ar in the range of 3,5-5 A, emitted from the plasma of Mather type focus device and spectra of He-like Fe in the range of 1,7-2 A from vacuum spark device were carried out by two focusing spectrographs with quarts crystals (2d = 8,5 A; 2d=6, 67 A). The dispersion planes of devices were oriented perpendicular one with respect to another. The main feature of the spectra obtained is the difference between the relative intensities of resonance and intercombination lines, registered in the same experiment with different spectrographs.

Such a feature may be explained by the presence of different degree and direction of polarization of corresponding lines. The reason for this phenomena may be both Stark, Zeeman effects and the unisotropy of electron velocity distribution function. The yield of each mechanisms are discussed.

From the experimental results some practical conclusions on determining the parameters of dense high temperature plasmas were made.

1A05

Gyrobroadening of Fast Ion Energy Spectrum in Magnetized Plasma

K. R. Chen
Department of Physics, National Changhua University of Education Changhua, Taiwan, ROC

A gyrobroadening process causing the perpendicular energy of fast ions to be broadened by cyclotron instabilities due to the weak relativistic mass variation of the fast ions in magnetized plasma is reported. At low cyclotron harmonics, a two-gyro-stream instability can be excited with the involvement of thermal ions if the condition $l_f\,\omega_{cf} < \omega < l_s\,\omega_{cs}$ is satisfied. The fast ions can be anomolously thermalized. Their lost energy goes to bulk ion heating. While the fast proton can satisfy the condition, the fast alphas cannot. The low harmonics are linearly stable for the alphas. Therefore, for low harmonics one has to inject waves to affect the alpha dynamics. However, the alphas can excite high harmonic cyclotron waves in the lower hybrid regime, in which thermal ions respond as cold plasma. The interaction becomes selective. Only alphas with high pitch angle are involved. This is presented as an interesting collective thermal dynamics issue while the implications for application are also assessed.

1A06

Influence of Density Gradient on Absorption of Upper Hybrid Pump Energy in Turbulent Plasma

V. N. Pavlenko, V. G. Panchenko
Institute for Nuclear Research
Kiev, Ukraine

In present report on the base of kinetic fluctuation theory we study the absorption of upper hybrid wave in magnetized inhomogeneous plasma with density gradient. We have calculated the effective collision frequency $V_{eff.}$ in the turbulent state of such plasma when the amplitude of pump wave E_o exceeds the parametric instability threshold E_{th}. As it turns out $V_{eff.} >> V_{ei}$ where V_{ei} is the electron-ion collision frequency.

We have thus deduced the efficiency for the absorption of upper hybrid wave energy in a plasma, as the absorbed power is proportional to $V_{eff.} E_o^2$. Our results can thus be of interest for upper hybrid heating of plasmas.

1A07

Cross Correlation of the Low-Frequency Electromagnetic Excitations and Anomalous Diffusion in a Plasma

M. O. Vakulenko
Institute for Theoretical Physics
Kiev, Ukraine

It is known that the magnetic perturbations in a plasma result in enhanced transport [1-3]. The more interesting and complicated situation when the potential and magnetic fluctuations are correlated, requires further analytical investigation [4-5]. Such correlation may be induced by an external current and electric field or neutral beam injection etc.

The General Renormalized Statistical Approach with Cross-Field Correlations [5] applied to the study of long-wave (wave lengths greater than the ion Larmor radius) low-frequency (frequencies not exceeding the ion Larmor frequency) electro-magnetic plasma fluctuations, yields that the cross correlations produce negative correction to the renormalized damping coefficient of the electro-static perturbations and therefore, attenuate the diffusion.

[1] A. G. Sitenko, P.P. Sosenko, Physica Scripta 47, 250 (1993)

[2] M. Vlad, F. Spineanu, J. H. Misguich, R. Balescu, Phys. Rev. E. 53 (5), 5302 (1996)

[3] M. O. Vakulenko, Physica Scripta 48, 373 (1993)

[4] S. Ghosh, V. H. Matthaeus, D. Montgomery, Phys. Fluids 31, 2171 (1988)

[5] M. O. Vakulenko, Phys. Scr. (1994)

1A08

Boundary Conditions for Use in Plasma Simulations

C.A. Ordonez, K.F. Stephens II
Department of Physics
University of North Texas
and
R.E. Peterkin, Jr.
High Energy Plasma Division
Phillips Laboratory
Kirtland Air Force Base, New Mexico 87117

Boundary conditions are presented for use in magnetohydrodynamic, particle-in-cell, and multi-fluid computer programs. The boundary conditions consist of velocity moments for three plasma species near a plasma-facing surface. The three plasma species are plasma ions, plasma electrons and surface emitted electrons. The boundary conditions are developed using a fully kinetic theoretical description of the plasma sheath which takes into account space-charge saturated electron emission from a plasma-facing surface. [C. A. Ordonez, Phys. Rev. E (to be published).] It is necessary to take into account space-charge saturated electron emission from the plasma-facing surface because of a recent finding which indicates that most of the commonly-used plasma-facing surface materials can reach secondary electron emission coefficients large enough for the emission to be space-charge limited. [C. A. Ordonez and R. E. Peterkin, Jr., J. Appl. Phys. **79**, 2270 (1996).] The boundary conditions are in terms of sheath and presheath potential drops and simple expressions (which are fits to numerical results) are provided for these potential drops.

This work was supported by the Air Force Office of Scientific Research.

1A06

Self-Sustained Oscillations In Spatially Confirmed Beam-Plasma Systems

V.P. Kovalenko and I.M. Parneta
Institute of Physics of the National Academy of Sciences of Ukraine
Prospect Nauki 46 Kiev 252022 Ukraine

There have been two ways the problem of non-linear beam plasma interaction is formulated for theoretical researches in a number of papers. Either time dynamics of small perturbations (i.e. system instability) or spatial increase of beam modulation was considered. As for experiment, only established oscillations are usually studied.

This paper is dedicated to stable oscillations that, in our opinion, result from finite dimensions of the beam-plasma system. Both longitudinal restriction and finite radius of the beam create disrupted feedback and supply initial beam bunching. The task has been solved for self-consistent approach. Neither traveling nor standing wave is postulated.

Non-linear integro-differential equations have been formulated in the basis idea of beam bunching. The equations implicitly include the necessary amplitude and phase relations. The condition of solvability of the equations determines the spectrum of frequencies for possible self-excited oscillations and the solutions give the amplitude of beam bunching wave and its spatial dependence. Also the case of oppositly directly beams in a plasma has been analyzed.

Monday Morning, 19 May 1997
10:00 a.m. – Board Room

Oral Session 1B:
5.1 Non-Equilibrium Plasma Processing (Inductively Coupled Plasmas, Etching Plasmas and Modeling) I
Chair B. P. Wood

1B01-02 Invited

Simulation Tools for the Design and Analysis of Plasma Processing Equipment*

Shahid Rauf, Michael Grapperhaus,
Robert J. Hoekstra and Mark J. Kushner
University of Illinois, Urbana, IL 61801

Plasma processing equipment has become one of the most important tools used for microelectronics fabrication. The increasing complexity of microelectronics devices is making it imperative to develop a thorough understanding of these equipment. In order to accomplish this goal, a hierarchy of simulation tools have been developed at the University of Illinois in the recent years. These tool are centered around the Hybrid Plasma Equipment Model (HPEM), detailed plasma model. This paper gives an overview of the HPEM, its extensions and the variety of problems these tools can address.

The HPEM consists of three sets of coupled modules. The first set of modules computes the inductive electromagnetic fields, the second set addresses the electron dynamics and the third set computes species densities, fluxes and the electrostatic fields. A number of options exist within each set, which allows a user to simulate the plasma with varying degree of detail. To demonstrate the capabilities of the HPEM, results from simulations of an ionized metal deposition system are described.

To investigate problems related to the design and analysis of plasma processing equipment, a number of extensions of HPEM have been developed. These include a sensor and actuator package (VPEM) that makes HPEM convenient for investigating feedback control problems. The VPEM has been used to test controller designs and evaluate control strategies. To examine the effects on the substrate, two off-line Monte Carlo modules have been developed. They examine the energy and angular distribution of plasma species on the substrate and determine the time evolution of etch profiles in two and three dimensions.

*This research has been supported by ARPA/AFOSR (F49620-95-1-0524), NIST, SRC and NSF (ECS94-04133).

1B03

Real Time Characterization of Plasma Etch Selectivity.

M. Harper, M. Sarfaty, C. Baum, and N. Hershkowitz
ERC for Plasma-Aided Manufacturing
University of Wisconsin, Madison

In-situ real-time measurement of thin film etching and deposition is necessary for semiconductor process development as well as monitoring and control. The relatively high process rates in high density plasma tools and the shrinking thickness of the films, call for a fast estimate of the process rates. Two-color laser interferometry operated at two locations is used to determine in real-time, within a second, the etch rate and thickness of two thin transparent films. The advantages of two-color laser interferometry will be described. The selectivity of the process is calculated from the ratio of the instantaneous process rates of the films as a function of the tool state. The experiment is carried out in a magnetically confined ICP tool. The tool state, gas flow, pressure, and RF power to the antenna and the electrostatic chuck, used to bias and cool the wafer, are computer controlled and monitored. The etch selectivity of polysilicon and SiO_2 films using CI_2 ,CF_4 and CHF_3 gases over a large parameter space of tool states will be described. The experimental setup is configured to utilize both single and double laser points. Both schemes are used to determine the etch rate of the two films. In the single point scheme the etch selectivity is determined from sequential etching of stacked films. In the two points scheme the selectivity is determined in real time during the etch process. Both films are etched simultaneously by using a wafer half coated with each film. The dependence of the etch selectivity on various equipment controlled parameters will be described. A comparison between the etch selectivity obtained by the two methods will be discussed. Issues related to patterned wafers will be discussed.

This work is funded by NSF grant No. EEC-8721545.

1B04

Real-Time Control and Modeling of Plasma Etching

M. Sarfaty, C. Baum, M. Harper,
and N. Hershkowitz
ERC for Plasma-Aided Manufacturing
University of Wisconsin–Madison, Madison, WI 53706

To meet the challenge of real-time advanced process control, the instantaneous process state needs to be determined. The relatively high process rates in high density plasma tools as well as the shrinking thickness of the films, require a fast estimate of the process state in order to implement process control. The research objective is to determine within a second the process rates and to implement real-time control of film's etch rate. Several in-situ, non-invasive and non-destructive sensors such as a laser interferometer and a full wafer interferometer are used to monitor the process state in a magnetically confined ICP tool. The gas phase state is monitored by optical emission spectroscopy and a residual gas analyzer. The equipment state, gas flow, pressure and RF power to the antenna and the electrostatic chuck, used to bias and cool the wafer, are computer controlled and monitored. A two-color laser interferometer enable us to determine in real-time, within 1 second, the etch rates and thickness of thin transparent films. The local information obtained by the laser sensor is complemented by a full wafer interferometer, that after processing provides time averaged process rates over a couple of fringes across the entire wafer. The advantages of two-color laser interferometry for real-time process monitoring and control will be described. Langmuir kinetics modeling of the measured etch rates of polysilicon and SiO_2 films using CI_2 ,CF_4 and CHF_3 gases over a large parameter space of antenna and wafer-stage rf power, gas flow, pressure and gas additives will be described. Etch modeling enabled us to develop a real-time control algorithm. The results of real-time etch rate control of unpatterned SiO_2 and polysilicon films will be describe.

This work is funded by NSF grant No. EEC-8721545

1B05

Model Etch Profiles for Argon and Chlorine Ion Energy Distribution Functions in Inductively Coupled Discharge Plasmas

W. Chen, B. Abraham-Shrauner*
Department of Electrical Engineering
Washington University
St. Louis, MO 63130
and J. R. Woodworth
Department 1128, MS 1423
Sandia National Laboratories
Albuquerque, NM 87185

Measured argon[1] and chlorine ion energy and angular distribution functions are fitted to drifted Maxwellian distribution functions by a simulated annealing procedure.[2] The ion energy and angular distribution functions have been measured in inductively coupled radio frequency discharges in argon and chlorine plasmas in a modified GBE reference cell. The ion energy distribution function data for several gas pressures and rf powers are a good fit to one drifted Maxwellian and an excellent fit to two drifted Maxwellians in most cases. Etch rates for trenches are calculated for the fitted ion energy distribution functions from approximate analytical expressions found previously for drifted Maxwellians.[2,3] The etch rate expressions are valid in the ion flux-limited regime where the etch rate is proportional to the ion energy flux for long rectangular trenches. Trench etch profiles on semiconductor wafers are calculated numerically from the trajectory equations of the etch profile equation with the computer program MatLab.

*Research supported by the National Science Foundation under Grants No. ECS-9310408 and ECS-9500251.

1. J.R. Woodworth, M.E. Riley, D.C. Meister and B.P.ÊAragon, J. Appl. Phys. 80, 1304 (1996).

2. W. Chen and B. Abraham-Shrauner, "The effect of ion sheath colliions on trench etch profiles," J. Vac. Sci. Technol.B (in press).

3. B. Abraham-Shrauner and C.D. Wang, J. Appl. Phys.Ê77 3445 (1995).

1B06

Characterization of Stationary and Rotating Magnetic Fields in an MERIE

M.J. Buie and J.T.P.Pender
Applied Materials
Dielectric Etch Division
Santa Clara, CA95054

Magnetically enhanced reactive ion etchers (MERIE) have been shown to be useful for etching half micron feature and below. The benefits of adding magnetic field are two fold: a higher plasma density and low ion energies. Rotation of the magnetic field results in excellent etch uninformities.

The etch rate uniformity across blanket and thermal oxide wafers was studied for stationary and rotating magnetic fields under a variety of typical contact etch processing conditions. The plasma uniformity has been mapped through measurement of the wafer etch pattern under conditions of a stationary B field. Of particular interest is the correlation between the instantaneous plasma uniformity and the resulting (time averaged) uniformity seen by the wafer as the B field is rotated. Process conditions that gave not only the best etch uniformity but also exhibit the best instantaneous plasma uniformity were the goal of this study.

1B07

PLASMA-ION BEAM TREATMENT OF AL FOR ENHANCED CORROSION

V.M.Bystritskii, Y.B. Yankelevich, A.V. Kharlow*,
E. Garate, V. Grigoriev**, E. Labernia, X. Dong
University of Californiat at Irvine, Irvine, CA 92697
**Institute of Electrophysics, Ekaterinburg, Russia*
***Institute of Nuclear Physics, Tomsk, Russia*

The Micro-second Plasma Opening Switch (MPOS) provides an innovative approach for efficient generation (up to 50% and higher) of large area (10^2-10^3 cm^2) intense ion beams with variable and controlled density in the range of 10-10^2 A/cm^2, and energy of 10^{5-6} eV^1. For conventional coaxial configuration of the MPOS the ion energy density input corresponds to 10^{-1}-10 J/cm^2, which is sufficient for fast melting and evaporation of the various materials surface layer. The small ion range (few microns) and fast cooling of the upper melted layer (up to 1010°K/s) could result in formation of nano- and

amorphous structures characterized by improved corrosion and errosion properties.

The paper describes the experimental device and results on the application of low voltage ion beams generated in MPOS for various metals surface modification with focus on Al alloys (Al 2014-24, Al 7075, Al-6061). At a charging voltage of 40 kV, the induced voltage, total MPOS stored current, and ion current amplitudes are 150-200 kV, 100-130 kA and 25 kA, respectively, with the ion current density varying in the range of 10-120 A/cm^2 along the inner cathode surface. Analysis on structural and electro-chemical properties of the MPOS treated Al samples are given, supported by computer simulation results on the solid/ melted/gas phases transition dynamics in the upper layer.

1. V. Bystritskii, E. Garate, Y. Yankelevich, E. Lavernia, Material Surface Modification Using Ion Beams, Generated in a Plasma Opening Switch, Bull. of APS, November 96, v. 41, n.7, p. 1538).

This study was supported under the AFOSR grant #F49620-96-1-0181.

1B08

Ionized Physical Vapor Deposition Characterized for Ionization Fraction and Deposition Rate

D.B. Hayden, D.R. Juliano and D. N. Ruzic
University of Illinois, Urbana, IL 61810

An inductively coupled plasma (ICP) RF antenna is added to a commercial magnetron sputtering machine. The power absorbed by this multi-turn water-cooled coil heats the electrons and raises their density, thereby increasing the ionization cross section for the metal sputtered neutrals. This creates up to 78% ionization of the depositing flux with less than 800 W of RF power at 2.5 kW of magnetron power. By applying a bias to the substrate the majority of the metal can be deposited normally, and at energies controllable by the set bias level. Aluminum and copper targets are used with argon and neon working gases. Operating pressures of 15 to 35 mTorr are investigated. Alternate ionization schemes not requiring an in-situ antenna are also investiaged. The applications of this design to higher aspect-ratio trenches and sub-.5μm features is discussed.

Monday Morning, 19 May 1997
10:00 a.m. – Toucan Room

Oral Session 1A:
3.1 Plasma Ion and Electron Sources
Chair: J. Asmussen, Jr.

1C01-02 *Invited*

Investigation of Diagnostic Sensors and Control Models for a Compact Ion Source

M.-H. Tsai and T. A. Grotjohn
State University, East Lansing, MI 48824

The diagnostic measurement, modeling, and control of a compact ion/radical source operating at 2.45 GHz microwave frequency is investigated for argon and hydrogen discharges. The investigation of the plasma source includes relating the run-time adjustable inputs, plasma source sensor outputs and process control models. The adjustable inputs include input microwave power, chamber pressure, gas flow rate, and resonant cavity tuning. The plasma source sensor outputs include reflected microwave power, electron temperature, ion density, electron/ion energy distribution and plasma potential. In order to determine the neutral and charged species in the hydrogen discharge, actinometry and OES measurements are used. The process model is the relationship between sensor measurements and input settings or the relationship of output parameters to the input and sensor readings. The sensor measurements combined with analytical and numerical models are used to estimate the plasma source output at various positions.

1C03

Laser-Driven Ion Sources for High-Brightness High-Puristy Ion Beams*

A.B. Filuk, C.H. Ching, M.E. Cuneo, J.E. Bailey, M.A. Bernard, B.F. Clark, W.E. Fowler, P. Lake, J.S. Lash, J. McKenney and P.R. Menge
Sandia National Laboratories
Albuquerque, NM 87185-1187

D. Cohen and P. Wang
University of Wisconsin–Madison, Madison, WI 53719

Surface-plasma ion sources are critical to generating high-brightness, high purity ion beams on applied-B ion diodes. The source plasma must meet requirements for species, thickness, purity, degree of ionization, conductivity, formation timescale, and engineering feasibility. Laser ionization schemes have been used on high-power ion diodes with encouraging but inconsistent results in diode impedance and beam purity. We are characterizing two laser-driven Li^+ schemes for 100-200 cm^2 sources: a single 10 ns Nd:YAG pulse at 0.3-1 J/cm^2, or the 2-laser LEVIS scheme.† Recognizing anode surface contamination as a key issue in 10^{-5}-10^{-6} Torr pulsedpower vacuum, we subject well-characterized 0.5 μm LiAg films on stainless substrates to extended 150-400°C heating and plasma discharge sputter cleaning after pumpdown in a test chamber, prior to pulsing the source lasers. A detailed diagnostic set includes absolutely-calibrated, streaked, CCD-imaged spectrographs for plasma properties, 2-color laser deflection for plasma/neutral expansion, ion time-of-flight spectrograph with ionizer for species content, and a tunable narrow-band dye laser for near-resonant absorption. The drive laser uniformity is measured with a CCD. Initial results on uncleaned LiAg show a single laser at >0.3 J/cm^2 can generate thin dense plasma, with acceptable expansion speeds at or below 2 cm/μs.

*Funding has been provided by the U.S. DOE under contract DE-AC04-94-AL85000.

†G.C. Tisone et al, Rev. Sci Instr. 61,562 (1990).

1C04

A Plasma Purification Method for Plasma Source Ion Implantation Doping of Semiconductors

T.G. Snodgrass, D.E. Arnott, J.L. Shohet and J.H. Booske
Engineering Research Center for Plasma-Aided Manufacturing
University of Wisconsin–Madison, Madison, WI
M.J. Kushner
Engineering Research Center for Plasma-Aided Manufacturing
University of Illinois, Urbana, IL

Using Plasma Source Ion Implantation (PSII) to create the shallow source and drain structures required for next generation devices may be a necessity[1]. For example, future devices are predicted to require heavy metal doses be kept less than 3×10^9 atoms per square centimeter.[2]

Plasma purification is done using ion cyclotron resonance to selectively expel unwanted ions from the plasma where they are neutralized upon collision with the chamber wall and no longer an implantation hazard[3]. With a computer simulation we determine the necessary field strengths and uniformity for plasma purification, cleaning efficiency and frequency/mass resolution of the method.

A quadrupole mass spectrometer is used to measure the mass spectrum of the ions exiting the chamber on axis with the magnetic field. By comparing the flux of the contaminant ions with the rf electric field on and off one can determine the cleaning efficiency of the chamber.

Work supported by the National Science Foundation under Grant EEC-8721545.

[1]Semiconductor Industry Association, The National Technology Roadmap for Semiconductors, (1994).

[2]N. Natsuaki, T. Kamata, K. Kondo, Y. Kureishi (1995), Nucl. Inst. Meth. Phys. B, 96, 62.

[3]J.L. Shohet, E.B. Wickesberg, M.J. Kushner (1994), J. Vac. Sci. Technol. A, 12(4), 1380.

1C05

EVALUATION OF THE RESONANT MODE BEHAVIOR OF A COMPACT, END FEED, MICROWAVE PLASMA SOURCE

Mark Perrin and Jes Asmussen
Michigan State University, East Lansing, MI 48824

Investigations of a small end excited microwave ECR plasma source have uncovered cavity resonances in the operational parameter space that are not fully explained by existing theory. One of the resonances involves the TE_{111} cylindrical cavity mode excitation. However, the other resonance involves TM-like or TEM-like excitation.

The plasma source in this investigation consists of: microwave applicator, quartz discharge chamber, and ECR magnet array.[1] The microwave applicator is a cylindrical stainless steel microwave cavity, of 9.8 cm inner diameter. The cavity is internally tuned, by the adjustment of: 1) a sliding short, and 2) an adjustable end feed loop. The cylindrical quartz discharge chamber has an inner diameter of 70 mm and height of 56 mm. An eight pole 45 MGO permanent magnet array is placed around the circumference of the discharge chamber. This ERC source is operable over a range of power from 50 Watts to 300W and a range of pressures from 0.5 mtorr to 100 mtorr.

This source was evaluated with an Argon discharge at pressures from 0.5 mtorr to 20 mtorr. Flow rate was held at a constant 35 sccm for all pressures investigated. Input microwave power, at a constant frequency of 2.45 GHz, was varied from 50 W to 250 W. The cavity length was varied, by moving the sliding short, from 4 cm to 12 cm in length. The adjustable coupling loop was varied in length from 1.5 cm to 5.5 cm.

This investigation: 1) fully investigates the unexplained resonances, 2) makes comparisons of this source to the global plasma model, 3) investigates resistive wall losses and source efficiency, and 4) compares the experimental behavior to other larger but similar ECR discharges.[2]

[1] Perrin, Asmussen, ICOPS-96, Conf. Abstracts, 3IP04 p. 217, Boston

[2] Mak, Asmussen, J. Vac. Science, V15, Jan. 1997.

1C06

Two-Dimensional MHD Simulation of Plasma Closure in High Current-Density Diodes*

P.J. Turchi** and R.E. Peterkin, Jr.
Phillips Laboratory, Kirtland AFB, NM, USA

Operation of charged-particle beam diodes is often limited by closure of the interelectrode gap due to plasmas created at the electrode surfaces. In particular, cold-emission cathodes that depend on the generation of plasmas by external means or by explosion of surface asperities (e.g., whiskers) are immediately subject to the consequences of such plasmas. These consequences include variation of the diode impedance with time during the current pulse, curtailment of the pulsetime, and limitation of the ability to operate the diode repetitively. Plasma closure in diodes has been observed experimentally for many years and found to depend strongly on the cathode material, but relatively weakly on operating current and voltage.

The present paper describes the use of the MACH2 code to simulate the dynamics of a plasma layer adjacent to the cathode of a high current-density diode. MACH2 is a 2-1/2 dimensional MHD code that includes resistive diffusion of magnetic flux, thermal transport by conduction and radiation, separate ion, electron and photon temperature, anomalous resistivity models, and access to properties of partially-ionized gases (e.g., SESAME tables). It does not handle non-neutral, charged-particle beam flows. To study plasma closure, however, the vacuum region is assumed to contain a plasma at very low density, with an electrical resistivity sufficiently high to simulate the impedance of a diode with space-charge limited flow. This resistivity is so high that magnetic diffusion from the diode insulator occurs in a few nanoseconds through the vacuum region. Two-dimensional magnetic diffusion into the thin plasma layer at the cathode surface then provides a nearly uniform current density normal to the cathode. The plasma is heated by this current flow (which is in series with the flow across the interelectrode gap at a nearly constant speed (in the range of 1.5×10^4 m/s); this speed varies less than 40% for a factor of three change in circuit voltage. Calculations have been performed with surface plasmas of hydrogen, carbon, and carbon-phenolic (available in the SESAME tables), indicating significant variations with assumed molecular properties. Simulations have also been conducted to examine the consequences of initial non-uniformities in plasma properties. Simulations have also been conducted to examine the consequences of initial non-uniformities in plasma properties over the surface, with the aim of understanding the importance of uniform plasma

initiation. Gross non-uniformities appear to be sustained during gap closure, rather than filling in due to plasma expansion.

*This work supported by the Air Force Office of Scientific Research, Washington, DC, and the Ohio State University.

**Professor of Aerospace Engineering, The Ohio State University, Columbus, OH, USA. On sabbatical leave (1996-1997).

1C07

Preliminary Design and Experimental Evaluation of Carbide Field Emitters in mTorr Pressure Environments

Colleen M. Marrese, William A. Mackie and Alex C. Gallimore
University of Michigan, Ann Arbor, MI USA

The recent thrust towards developing sub-100 W electric propulsion systems warrants the development of a cathode to operate on a comparable scale. Applications exist that are both ground- and space-based for plasma processing and spacecraft propulsion systems. Propellant requirements include xenon for propulsion systems and oxygen for both propulsion and plasma processing applications. With appropriate field emitter materials to withstand the hostile environment and emitter-gate electrode configurations, a field emitter array cathode is a plausible candidate as a low power and efficient electron supply for micro-propulsion systems.

This report describes an on-going effort to develop field emitter cathodes for mTorr-level discharges. Hafnium carbide and zirconium carbide emitters were used for their hardness, chemical inertness and low work functions. Single HfC emitters were tested in oxygen at mTorr pressures. They showed resistance to damage due to backsputtering even at relatively large extraction voltages. Emitter-gate electrode configurations were then optimized for mTorr pressure environments to prevent catastrophic failure of the arrays from arcing. The results of the design analysis, emission measurements under various gases and pressures, and experimental evaluations of the design are presented in this report.

1C08

Beam Discharge for New Technology

M. Ghorannevis, A. Abbaspour, M. R. Salami, S. Zorriasatin and A. Pouraslan
Plasma Physics Research Center of I.A.U.
Poonak, Hesarak, P.O. Box 14835-159, Tehran, Iran

For new technological developments, here is proposed a high efficiency ionization method—Plasma Beam Discharge In Magnetic Field. This type of the discharge makes possible to obtain a highly ionized plasma in a large volume.

Great varieties of substances can be used for plasma generation (Gases and Metal vapors), for instance air, nitrogen, oxygen, hydrogen, methane, carbon dioxide, feron, argon, and etc.

Very large surfaces can be treated with this method (up to 0.5m in diameter and 2m in length). In this experiment very pure plasma was obtained and the impurity level was low. The shape of the pieces to be treated in plasma can be complex, the electrostatic potential from some volt to few thousands volts can be applied to the pieces in the plasma. This method can be used for surface cleaning, etching, and coating. The operational conditions are: $P = 10^{-4}$ to 10^{-1} torr, B = 500−5000G, Electron beam current = 0.1-4 A, and acceleration voltage = 100-5000V.

Detail will be discussed in full paper.

1C09

Thermal and Mechanical Loading of Particle and RF Transmission Windows Exposed to Atmospheric Pressure

Robert J. Vidmar
SRI International, Menlo Park, CA 94025

The mechanical design of a transmission window that seals a port between a low-pressure side and an atmospheric-pressure side for the purpose of passing a high-energy particle beam or radio-frequency waves has many forms. Thermal loading due to energy loss from the beam or the waves and mechanical loading due to the pressure differential across the window constrain the window design. Techniques to dissipate heat such as radiation, conduction, natural convection, evaporation, and forced convection are discussed in general. Specific details of forced convective cooling with fluids within the

transmission window are also discussed. This cooling consists of a fluid such as water flowing under high pressure in capillary tubing with an inside diameter of ~100 μm. A high-pressure hydraulic system operating at ~20 Mpa (3,000 psi) can generate a fluid flow at 40 m/s in a 6-cm-long capillary tube. For water flowing with a Reynold's number in excess of 10,000, the convective heat transfer coefficient can rise to over 500,000 W/m^2-° K, leading to heat dissipation on the order of 1 kW/cm^2. The use of other fluids such as liquid metals can increase heat dissipation by several orders of magnitude.

This work was supported by the Air Force Office of Scientific Research under Contract F49620-95-C-0009.

Monday Morning, 19 May 1997
10:00 a.m. – Macaw Room

Oral Session 1D:
4.1 Laser Produced Plasmas
Chair: R. E. Peterkin, Jr.

1D01-02 *Invited*

Production of X-rays from Laser-Heated Gas Targets

J. Grun, A. Fisher, R. Burris
Naval Research Laboratory, Washington, DC

C.A. Back, C.D. Decker, O.L. Landen, L.J.Suter and R. Wallace
Lawrence Livermore National Laboratory, Livermore, CA

J.L. Davis
Alme Associates, Alexandria, VA

Debris-free and efficient multi-kilovolt x-ray sources are needed for materials testing and for use as backlighters in future Inertial Confinement Fusion experiments. Laser-plasma x-ray sources are particularly attractive for these uses since their spectrum can be controlled by proper choice of plasma material and laser intensity, and because many laser-plasma sources can be designed to produce little or no particulate debris. We investigate the use of laser-heated gas to produce multi-KeV x-rays. In one experiment 20 kJ of 0.35 μm pulse from the Nova laser heats 1 - 2 atm. of Xe gas confined in a Be can. It is predicted that confinement of the Xe plasma by the Be can will increase the conversion efficiency into 4 KeV x-rays from 2 - 10% observed with solid or gas bag targets to ~15%. In a second experiment 1 kJ of 1.06 μm pulse from the Pharos laser heats different gases injected into vacuum by a high-pressure nozzle. The emission from these sources is diagnosed with time-gated x-ray imagers, time-resolved and time-integrated spectroscopy, and with XRD and PCD detectors. Experimental results will be presented and compared to theoretical calculations.

Supported by Defense Special Weapons Agency and U.S. Department of Energy at LLNL under W-7405-ENG-48.

1D03

Stochastic Theory of Dense Laser Produced Plasma

V.I. Arefyev
Russian Space Agency
Central Research Institute of Machine Building
Korolev, Moscow Region, 141070, Russia

The model of intensive ultra short pulse laser radiation interaction with matter has been built with regard to the effect of the produced plasma atoms and nucleus.

1D04

Collective Effects of Atomic Structures in Super Strong Fields

V.S. Beliaev
Russian Space Agency
Central Research Institute of Machine Building
Korolev, Moscow Region, 141070, Russia

It has been shown that with nowadays laser radiation parameters this radiation effects on atomic and nuclear structures by means of their interaction with electromagnetic fields of laser produced plasma and this interaction is being accompanied by strong action at nucleus.

1D05

Laser Produced Plasma as Accelerator Fast Particles

A.V. Komissarov
Russian Space Agency
Central Research Institute of Machine Building
Korolev, Moscow Region, 141070, Russia

It has been shown that the development of the high frequency potential and vortical instabilities at the leading edge of the laser pulse at the conditions of high ionization frequency leads towards the small electrons group collective acceleration with high tempo which is more than 1 Mev/fsec.

1D06

Potential of Eximer Laser System with Pumping Power g-Pulse Radiation for Studying of Plasma Physics and 0.1-1.0 MJ ICF.

E.C.Bonuishkin, R.I.Il'kaev, A.P.Morovov, A.I.Pavlovski, B.V.Lashintsev
Russian Science-Research Institute of Experimental Physics, Russian Federal Nuclear Center
Arzamas-16, Nizhnii Novgorod Region, 607200, Russia

The results of spatial, temporal and energy characteristics of such lasers are considered. It has shown that laser systems on basis these lasers have characteristic set which is necessary for JCF-high accuracy of laser pulses synchronizing, high laser radiation contrast, possibility of temporal and wavelength radiation forming.

1D07

RF from Two Pulse Laser Plasmas in Atmospheric Pressure Gas

G.K. Chawla and C.W. von Rosenberg, Jr.
Textron Systems Corporation, Wilmington, MA 01887

We have measured the production of rf produced by a mode-locked (M-L) CO_2 laser (100 mJ macro pulse, 3 ns pulselets @ 25 Mhz) focused onto a target of copper in a background of atmospheric pressure N_2 and He. Prior to the arrival of the M-L laser pulse, a small (few mm to cm) "vacuum bubble" is prepared at the focus by a pre-pulse laser (brought to the same focus) which is either another CO_2 laser or a YAG laser. In all cases rf in the 0.1 to 20 GHz region is produced as measured by an encircling, near-field, "band sensor" of ~5 cm diameter. Use of the pre-pulse laser enhances the rf power by a factor of up to 100. We present data showing rf signals vs pre-pulse laser energy and time interval between the pre-pulse laser and the M-L laser. We also present open shutter photographs of plasma plumes generated with the pre-pulse lasers as well as the M-L CO_2 laser. We give calculations of plasma bubble formation mechanisms, as well as bubble volume and time to form. We connect this work to our earlier work in vacuum, and propose that the rf is mainly due to "hot electrons" (~keV) produced by the M-L laser through the mechanism of resonance absorption occurring at a critical surface, near the focus, inside the vacuum bubble formed by the pre-pulse.

1D08

When Air Becomes an Electrical Pathway

Karl R. Umstadter, Don L. Millard, Robert C. Block
Rensselaer Polytechnic Institute
Troy, NY 12180-3590

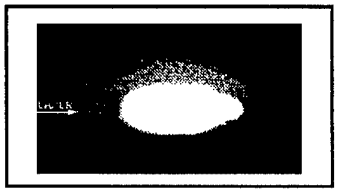
The ongoing decrease in the feature size of new printed wiring assemblies has made it more difficult to test these boards with conventional methods. We have developed a noncontact electrical test method (NCT) to replace the conventional method of potentially damaging physical contact with the desired lead. The NCT method utilizes a small volume of highly-ionized air, commonly referred to as a plasma, as a bi-directional conductive pathway. The pathway is capable of supplying or measuring current with negligible distortion.

At ICOPS'96 we presented some of the research that explored the properties and characteristics of NCT laser plasmas. These include the effects of different gas environments, frequency doubling the Nd:YAG laser, various optical pathway as well as methods of extending the plasma lifetime and normal NCT plasma dimensions.

Building upon this research we have explored laboratory plasma properties which will enhance the possibility of developing a laser NCT plasma method for wafer die features. Generating an NCT plasma is a two step process. The first step, a "multiphoton process" which occurs very quickly, governs the ignition of a

plasma. We have determined the photon fluxes required for plasma generation, important because it measures the threshold of ionization of different gas volumes more accurately than the accepted irradiance calculation. Using studies of the plasma lifetime we have calculated the rate of growth of the plasma volume or probe size. The system properties necessary to generate smaller, denser plasmas have been calculated as well.

Because the plasma is a current carrying path its resistance is of great importance. Extensive research was completed to determine the drop in the load resistance over the plasma with varying geometry. Plasma potential generated in air was also explored to determine the electrical effects on devices to be tested. The culmination of this research may eventually permit an entire wafer to be accessed at once via laser NCT probing, thereby rendering potentially destructive physical contact methodologies obsolete and provide industry a time and cost effective approach.



(Laser-Produced NCT Plasma)

Monday Morning, 19 May 1997
10:00 a.m. – Cockatoo Room

Oral Session 1E:
2.3 Vacuum Microelectronics
Chair: K.L. Jensen

1E01-02 *Invited*

Arcing and Voltage Breakdown in Vacuum Microelectronics Microwave Devices Using Field Emitter Arrays: Causes and Possible Solutions

Francis Charbonnier
Linfield Research Institute, McMinnville, OR 97128

Emission gated microwave amplifiers require electron sources capable of high current, extremely high average beam current density (e.g., 500A/cm^2), high transconductance and low capacitance. Since the mid 1950s Dyke and others investigated the use of field emitter arrays (FEAs) for microwave applications but failed to produce practical devices because microfabrication techniques were as then undeveloped.

Recent fabrication and processing advances create the potential for producing electron beams with the desired characteristics. FEAs manufactured by several organizations, particularly SRI, MIT, MCNC and Varian/GRC, have been tested at CPI to evaluate potential FEA performance. Great progress has been made during the past year, but early failure is still observed at emitted current levels well below those expected based on field emission initiated vacuum arc theory and experience.

We review briefly the differences between conventional and microelectronics devices which impact FEA performance. We then review recent progress and state of the art FEA performance, analyze a number of possible causes of failure and suggest methods, particularly coating FEAs with refractory carbides, in order to stabilize FEAs and achieve prolonged arc free operation at increased current level.

1E03

LASER PRODUCED SILICON FIELD EMISSION ARRAYS

A.A. Evtukh, E.B. Kaganovich, V.G. Litovchenko, R.I. Marchenko, S.V. Svechnikov and E.G. Manoilov
Institute of Semiconductor Physics, 45 prospekt Nauki, Kiev, 252650, Ukraine

Commonly the Si tips of electron emitters are manufactured using the wet or dry etching formation routes. The aim of this work is to create Si field emitters without lithography by using new laser technology. Monocrystalline Si wafers were processed on air by YAG:Nd^{3+} laser irradiation with energy density that overstepped the melting threshold with following stain etch. When the laser beam scanned wafer in continuous regime, we obtained strongly macrorough surface without single tips. Under influence one by one laser pulses, the single conical tips were formed. The distances between tips were 50 μm, their heights were 50 - 100 μm, as SEM micrographs showed. In both cases the surfaces are very developed with many protrudes on them.

Only laser processed regions demonstrated the electron emission. The electron emission is controlled by the sharp asperities with 10 - 100 nm long, and not by tip apex. The measurements of emission current were performed in the diode structure in vacuum chamber. The minimum obtained electric field at emission turn-on was

approximately ~10^5 V cm^{-1}, the maximum current density was ~10^3 A cm^{-2}. Fowler-Nordheim current-voltage characteristics were observed with all samples tested. The structures with relatively high emission parameters: effective emission areas $\alpha = 5 \bullet 10^{11}$ cm^2, local field enhancement factors $\beta = 1 \bullet 10^5$ cm^{-1} have been received. These parameters combined with laser method of fabrication make investigated emitter arrays an attractive alternative to others.

1E04

Fabrication of Field-Emitter Arrays for Inductive-Output Amplifiers

R.A. Murphy, C.T. Harris, R.H. Mathews,
C.A. Graves and M.A. Hollis
MIT Lincoln Laboratory, Lexington, MA 02173
M.A. Kodis, J. Shaw, M. Garven,
M.T. Ngo and K.L. Jensen
NRL Electronic Science and Technology Division, Washington, DC 20357

Field-emitter arrays (FEAs) are being fabricated for X-band inductive-output amplifiers, such as Twystrodes and Klystrodes. The pre-bunched electron beam supplied by a gated FEA cathode provides smaller size, increased efficiency, and faster turn-on compared to a thermionic-cathode tube. For this application, the FEAs must supply beam currents on the order of 80-100 mA and be designed so that the microwave input drive signal can be efficiently coupled to the modulating gate of the FEA.

The Lincoln FEAs are fabricated using laser-interferometric lithography, which has provided high yields of Mo-tip arrays having 0.32-μm tip-to-tip and 0.08-μm gate-to-tip spacings. These small dimensions reduce the gate modulation voltage that is required for suitable beam modulation and improve the high-frequency performance; they represent the smallest dimensions and highest density yet reported for FEAs. Improvements in fabrication technology, testing methods, and conditioning techniques will be presented that have resulted in emission currents as high as 22 mA from one quarter of an FEA cathode. The measured input impedance agrees well with theory and can be matched by appropriate techniques.

Simulations predict an output power of approximately 50 W with a gain of approximately 10 dB at X-band. A multi-organizational team is presently integrating an FEA cathode into a prototype tube to demonstrate such performance.

*The work at Lincoln Laboratory was supported by the Naval Research Laboratory.

1E05

Application of Gated Field Emitter Arrays in Microwave Amplifier Tubes

S.G. Bandy
Varian Associates/GRC, Palo Alto, CA
M.C. Green
CPI MPTP
C.A. Spindt
SRI International, Menlo Park, CA
M.A. Hollis
Massachusetts Institute of Technology, Lincoln Laboratory, Lexington, MA
D. Palmer and B. Goplen
Mission Research Corporation, Newington, VA
E.G. Wintucky
NASA Lewis Research Center, Cleveland, OH

This paper will describe the progress made on the recently completed Phase II of the ARPA/NRL Vacuum Microelectronics Initiative. This program was a team effort between several manufacturers and laboratories, and represents the first major effort to incorporate field emitting cathode arrays into a specifically-designed microwave tube by a manufacturer.

Using gated field emitter arrays as the source of a pre-bunched linear electron beam, the program goal was the delivery of a 50 W 10 Ghz amplifier having at least 10 dB of gain. An efficiency of at least seventy percent was expected. Along with the elimination of the heater power supply, compactness and light weight are other attributes of the approach proposed.

After a brief review of the tube design to meet the performance goals of this program, this paper will describe the results of the dc testing of the emitter arrays by the manufacturer, the problems of interfacing the arrays into the tube structure and, finally, the rf performance of the arrays in the Klystrode tube vehicle.

Supported in part by the ARPA/Tri-Services/NRL Vacuum Electronics Initiative through NASA Contract No. NAS3-27362

1E06

Field-Emitter-Aray Development for Microwave Applications

C.A. Spindt, C.E. Holland, P.R. Schwoebel and I. Brodie
Sri International, Menlo Park, CA 94025, USA

In this paper we report on progress in an ongoing program to develop microfabricated field-emitter arrays to meet the microwave requirements for the ARPA/NRL Vacuum Microelectronics Initiative administered by the NASA Lewis Research Center. The goal of the effort is to demonstrate 50 Watts of output power at 10 GHz with a Klystrode® amplifier tube.

The key for achieving this goal is to fabricate an emitter array with a transconductance to capacitance ratio (g_m/C) of 10^{10} A/V/F or better. Thus we must maximize g_m and minimize C. The capacitance is an area and emitter-array dielectric thickness issue, and the transconductance relies on the field-forming factor, β as in ($E=\beta V$), the emitter tip's effective work function ($\varnothing$), and emitting area (number of tips).

The β depends on cathode size and shape and improves as dimensions increase. The $\varnothing$ is fundamentally a materials property but is also influenced by the operating environment and *in situ* processing of the emitter surface. As a practical matter $\varnothing$ is difficult to manipulate and usually accepted as is. The emitting area is essentially an emitter-tip packing-density issue because of the constraints on total area due to capacitance considerations. Lithography is the key to achieving higher tip packing density, and new and emerging techniques now make it possible to achieve packing densities of up to 10^9 tips/cm^2. Packing densities of this magnitude require gate apertures diameters of about 100 nm, and this required the development of emitter cone fabrication process that produce very high aspect ratio (cone height to base diameter) cones in order to preserve adequate spacing between the base and gate for reasonable capacitance.

The development program has focused on these issues, and experimental results will be shown demonstrating that it is indeed possible to fabricate arrays with the required (g_m/C) of 10^{10} A/V/F or better. A g_m of 10^{-6} Siemens/tip, capacitance of 6 nF/cm^2, tip packing densitie of 10^8 tips/cm^2 and tip loading of 10 μA/tip have been achieved. Based on these results, a ring-shaped emitter array with a 600-μm outer diameter and a 560-μm inner diameter would have a (g_m/C) of 1.7 x 10^{10} A/V/F, and would produce 160 mA of emission with a tip loading of 4.4 μA/tip. These values meet the specifications for the Klystrode® design. Up-to-date results will be presented.

1E07

Analysis of Isotropic and Anisotropic Etch Field Emitter Array Cathodes*

R.B. True, G.R. Good, T.A. Hargreaves
Litton Electron Devices Division, San Carlos, CA 94070

W.D. Palmer
MCNC Electronic Technologies Division
Research Triangle Park, NC 27709

This paper summarizes computer modelling and numerical results on two field emitter array (FEA) cathode designs manufactured by MCNC. DEMEOS, a deformable triangular mesh finite element gun code, which includes a Fowler-Nordheim model of emission as an option, was used to perform the analysis. This code can include curved dielectrics and irregular shaped tips. Further, the variable mesh feature enables a whole tip and gate structure to be analyzed expeditiously in a single computer run.

An isotropically etched tip design was analyzed as well as an anisotropically etched tip design. Experimental and calculated results compare quite well for the isotropic design for which there is much experimental data. It was found and verified experimentally that the isotropic tip has a lower turn-on voltage than the flatter faced anisotropic tip. On the other hand, the beam emerging from the anisotropic tip has significantly lower angular divergence which is important in FEA cathodes contemplated for use in linear beam microwave tubes.

---

*Partial support from NRL Contract Number: N00014-94-C-2241.

1E08

Microgun

Vu Thien Binh, V. Semet, S.R. Purcell and D. Guillot
Laboratoire d'Emission Electronique
DPM-UMR CRNS
Université Claude Bernard Lyon 1
69622, Villeurbanne, France

The microgun is the association of a nanotip with coplanar lenses that have micrometer scale opening. This association will take advantage of the specific properties intrinsic to the nanotips and microlenses for the purpose of field emission extraction of low energy coherent e-beam, with focusing and deflection possibilities.

A systematic study, including computer simulations and experiments, has been done in order to highlight the field emission behaviour within different microlens geometries. Results about the energy distribution and electron trajectories within electron optics approach, for example, are presented for different kind of field emission sources: Spindt-type microtips, regular microtips and nanotips. Applications appropriate to the different sources are proposed.

1E09

Diamond Cold Cathodes

M.W. Geis, J.C. Twichell, T.M. Lyszczarz,
K.E. Krohn and N.N. Efremow
Lincoln Laboratory, Massachusetts Institute of Technology, Lexington, MA 02173-9108

Substantial progress has been made in understanding the physics of diamond cold cathodes. Four distinct regions: the metal contact, bulk diamond, vacuum interface, and free space, exhibit distinct physical processes affecting the behavior of the cathode. The contact region mediates the transfer of electrons and holes between the metal and the diamond. The bulk of the diamond limits the transport of carriers. Any dopants in this region will modify the fields throughout the diamond. The vacuum interface and the diamond termination at this interface control the emission into the vacuum, and impact the field in the diamond. Finally the electrons transit the vacuum region outside the diamond. Here, the electric field is set by the difference in potential between the anode and the diamond surface, which in turn depends on the charge distribution within the diamond. A number of diagnostics have been used to examine the characteristics of each region.

While II-b p-type diamond field emitters are quite robust, their behavior is similar to metals. The back contact is a standard forward biased Schottky diode and electrons are emitted from the valence band. In contrast, type I-b diamonds are semi-insulating. Substitutional nitrogen plays the role of an n-type dopant at the electron injecting back contact. Optical DLTS measurements demonstrate the substantial positive charge resides at this interface. Photocondition experiments confirm the contact character, and provide transport coefficients. While problems remain, much of the initial variability of diamond cold cathodes can now be related to distinct physical processes.

*This work was sponsored by the Defense Advanced Research Projects Agency. Opinions, interpretations, conclusions, and recommendations are those of the author and are not necessarily endorsed by the United States Government.

1E10

A Simplified FEA-based TWT model

K.L. Jensen, E. G. Zaidman, K. Nguyen,
M.A.Kodis and M. Garven
Naval Research Laboratory, Washington, DC 20375

Knowledge of emitter geometry and materials allows prediction of gain, efficiency, power output, and circuit length of an emission gated TWT. The extension of a simple analytical model* examines the basic physics involved, and gives a lower limit to the performance from an FED-based TWT.

Previous approaches to modeling an FEA cathode in an emission gated TWT (Twystrode) treated the FEA and tube physics separately, and joined analyses using the Fowler-Nordheim A and B parameters. These parameters were therefore independent. Here, A and B can be predicted on the basis of the geometry, materials, and uniformity of the array, allowing for a seamless relation of fabrication issues to tube performance.

The emitter parameters are tip and gate radius, tip height, cone angle, work function and the uniformity of the array (i.e., distribution in the B value). The performance of the simple TWT model is characterized by gain, electronic efficiency, rf power, helix length and taper. The input power is given from an analysis of the array, and the emitted current is modulated by sinusoidally varying the gate potential. The beam is accelerated into the helix circuit, where the output (rf) power is extracted. An analytical model is used to determine the portion of the electron kinetic energy converted to rf power.

We present the results of this analysis for obtainable emitters, as well as emitters expected in the near term. An estimation of the actual performance would require particle simulation modeling. Rather, the present study is a complementary study for such simulations, which are essential for the determination of the competitiveness of an emission grated rf amplifier. We will compare the analytical model to numerical simulations of the beam-circuit interaction.

This work supported by the Office of Naval Research.

*K.Nguyen, *et al.*, Monterey Power Tube Conf. 1996

Monday Morning, 19 May 1997
10:00 a.m. – Rousseau Center

Poster Session 1P01-07:
2.5 Microwave Systems

1P01

Parametric Excitement of Surface Waves on Harmonics of Cyclotron Frequencies in External Pumping Electric Field

V.O. Girka, V.I. Lapshin, V. Pavlenko
Kharkiv State University, Svobody sq.4, 310077 Kharkiv, Ukraine

A parametric excitement of the surface waves (SW) on the harmonics of the cyclotron frequencies is investigated. This frequency region is used often for the additional plasma heating by the HF generators. The SW on the harmonics of the cyclotron frequencies can propagate in plasma bounded by dielectric when the external magnetic field is perpendicular to plasma interface. Such orientation of magnetic field can be realized in the divertor region of the fusion devices. The initial equation system consists of the kinetic equation for plasma particles and the Maxwell equation system for the considered wave field. An external alternating electric field $\vec{E_o} \sin(w_o t)$ is directed along plasma interface. The values of the parametric instability increments are obtained both analytically and numerically. It is shown that the increment values are greater for microwave perturbation with wave length $\lambda \approx \rho_e$, where ρ_e is Larmor radius. The obtained results are useful for the interpretation of experimental data concerned the surface waves excitation in divertor layers of the fusion devices. The propagation of such type SW may be cause of the dense plasma producing near the boundary.

1P02

Cold and High-Power Tests of a Multibunch X-Band Photoinjector

G.P. LeSage, C.V. Bennett, L.L. Laurent, J.A. Van Meter, V. Dinh, A.L. Troha, B.H. Kolner, F.V. Hartemann, and N.C. Luhmann, Jr.
Dept. of Applied Science
University of California at Davis, Davis, CA

A high brightness X-band photoinjector, capable of multi-bunch operation at GHz repetition rates, and developed as a collaboration between the UC Davis DAS and SRRC, is reaching the initial phase of high power tests. The photoinjector was designed using SUPERFISH, PARMELA, POISSON, URMEL and HFSS. Cold test showed excellent agreement between the design parameters and the rf characteristics of the prototype. In addition, the phase noise and jitter characteristics of the laser and rf systems of the high gradient X-band photoinjector have been measured experimentally. The laser oscillator is a self-modelocked Titanium:Sapphire system operating at the 108th subharmonic of the rf gun. The X-band signal is produced phase-locking a dielectric resonance oscillator to the laser oscillator, and amplified by a pulsed TWT. A comparison between the TWT phase noise and the fields excited in the rf gun demonstrates the filtering effect of the high Q structure, thus indicating that the rf gun can be used as a master oscillator, and could be energized by either a magnetron or a cross-field amplifier. Finally, high power tests are currently underway, including the 20 MW SLAC klystron, the rf system, and the rf gun. In particular, dark current, spatial, temporal, and momentum beam distributions will be fully characterized.

Work supported by DoD/AFOSR(MURI) F49620-95-1-0253, AFOSR (ATRI) F30602-94-2-001, ARO DAAHO4-95-1-0336, and LLNL/LDRD DoE W-7405-ENG-48 IUT B335885.

1P03

Frequency Response in Multipactor Discharge*

A. Valfells, R.A. Kishek, Y.Y. Lau and R.M. Gilgenbach
University of Michigan, Ann Arbor, MI 48109-2104

There is a resurgence of activities on the analysis of multipactor discharge [1-3], which is a medium to low voltage phenomenon in microwave cavities, windows, satellite rf payloads, and accelerator structures. In this paper, we extend our previous model [1] to examine the frequency response of the multipactor discharge in an rf circuit, with special emphasis on the effects of loading and detuning of the circuit. We have calculated analytically the frequency band in which steady state multipactor could occur. The saturation level is also calculated. These results are found to be in excellent agreement with those obtained from numerical simulations. In general, the frequency band in which multipactor would occur narrows as the quality factor Q increases. We have recently initiated a study of multipactor on insulators, preliminary results will be presented.

1. R. Kishek and Y.Y. Lau, Phys. Rev. Lett. **75**, 1218 (1995); Phys. Plasmas 3, 1481 (1996); ibid., in the press (1997).

2. S. Riyopoulos, D. Chernin, and Dialetis, Phys. Plasmas **2**, 3194 (1995); IEEE Trans. Electron Devices (in the press, 1997).

3 V.P. Gopinath, private communications (1996).

*This work was supported by NRL/ONR, MURI/AFOSR, and by Northrop-Grumman Industrial Affiliates Program.

1P04

Initial Results from the Multi-Megawatt 110 GHz ECH System for the DIII-D Tokamak*

R.W. Callis, J. Lohr, R.C. O'Neill, D. Ponce, R. Prater
General Atomics
Daquing Zhang
Institute of Plasma Physics, Hefei, Anhui, Peoples Republic of China

The first of three MW-level 110 GHz was operated into the DIII-D tokamak in late 1996. Two additional units will be commissioned during 1997. Each gyrotron is connected to the Tokamak by a low-loss-windowless evacuated transmission line using circular corrugated waveguide carrying the HE_{11} mode. The microwave beam spot is well focused with a spot size of approximately 6 cm and can be steered poloidially from the center to the outer edge of the plasma. The initial operation with about 0.5 MW delivered to a low density plasma for 0.5 s showed good central electron heating with peak temperature in excess of 10 keV. The system status will be described and the initial physics results will be presented, including heating efficiencies, power deposition profiles, and overall system performance.

* Work supported by U.S. Department of Energy under Contract DE-AC03-89ER51114.

1P05

Design and Characteristics of a High-T_c Superconducting Magnet for Electron Beam Control

A.C. Day, W.P. Geren, M. Strasik, D. Garrigus and K.E. McCrary
Defense and Space Group, Seattle Washington 98124
arthur.c.day@boeing.com

Flux-trap magnets based on high-temperature superconductors have been proposed for e-beam control elements. Application could include accelerators, klystrons, and mm-wave amplifiers. We have constructed compact magnets using bulk YBCO crystals which exhibit fields of 0.5 - 0.8 Tesla at 77K, and in excess of 1T at 65K. We have also developed techniques of field-charging the superconducting rings in-place. The characteristics of the materials and the assembled magnets will be presented, and application to specific types of mm-wave tubes will be discussed.

1P06

Rep-Rate Modulator & Electron Gun for High Power Microwave Research Using Ferroelectric Cathodes*

J.D. Ivers, D. Flechtner, Cz. Golkowski, J.D. Ivers, G.S. Kerslick and J.A. Nation
Cornell University, Ithaca, NY 14850

A novel pulse modulator, previously described at the 1995 PAC meeting, has been reconfigured to give a better pulse shape at a slightly lower beam energy and with a higher current (500 kV, 1000A). The device has been run at rated voltage and current for pulse durations in excess of 200 ns and at a low ~0.1 Hz power supply limited repetition rate. The modulator, which is designed for use in our high power microwave research program, has been coupled to an electron gun which uses a ferroelectric cathode. We report in this paper on the revised design and performance of the modulator and present data on the electron gun design and characteristics. The recessed ferroelectric cathode is located in the fringing field of a 3 kG solenoidal magnetic field so that the 500 A emitted current is compressed to about a 1 cm diameter pencil beam. The cathode emission is initiated by a 100 ns 2 kV pulse inductively decoupled from the ground by a coaxial cable wound around the transformer core. The pulse transformer, which is driven by three pairs of 10Ω pulse lines in parallel, feeds a fourteen to one step up transformer giving a source impedance of 500Ω. It is switched independently of the ferroelectric trigger to provide maximum flexibility in the design. Results will be reported on all aspects of the system design and operation.

*Work supported by USDOE & AFOSR MURI High Power Microwave Program.

1P07

Construction of a Multi-Cell Resonator for a 94 GHZ Extended Interaction Klystron

K.W. Zieher
Department of Electrical Engineering, Texas Tech University, Lubbock, TX 79409-3102

Microwave generation at 94 GHz allows high resolution radar, using small antennas and taking advantage of the transmission window of air at that frequency. In communications the higher frequency will allow a larger bandwidth. In an extended interaction klystron a theoretical conversion efficiency of electron beam energy into microwave energy of about 50% is indicated. The available microwave power could be about 30% of the beam power. The intermediate goal is to generated 1 kW available microwave power from a 50 keV, 100 mA electron beam in 16 cells. The construction of the resonator is a critical aspect of the klystron. The cavities are built using a silver soldered sandwich of copper and iron layers which are then turned to a cylinder of about 2.5 mm diameter. The cylinder is copper plated and brazed into a copper tube. A central hole is then drilled and the iron removed using sulfuric acid. A 4-cell resonator will have an outer diameter and an overall length of about 3.2 mm. Serveral 4-cell resonators have been built. The surface quality of the resonators has to be improved and the low melting solder has to be replaced with a higher conductivity silver alloy.

Work supported by AFOSR (MURI).

Monday Morning, 19 May 1997
10:00 a.m. – Rousseau Center

Poster Session 1P08-15:
2.6 Microwave Plasma Interactions

1P08

Temporal Evolution of a Beam-Plasma Wave Spectrum

V. Tkachenko, P. Turbin
Scientific Center of Physical Technologies
Kharkiv, 1ovgorodskaya Str., 310145 Ukraine

The interaction of monoenergetic small density electron beam with a plasma has to be essentially depend on a type of wave spectrum in a plasma. If spectrum consists of alone mode and one is in resonance with a beam it takes place one-mode beam instability in a system. [I.N. Onischenko et. al. Pis'ma v JETP, 12, 407, (1970)]. The existence of a broad wave spectrum in plasma is equal to introducing of effective dissipation into a system. In this case a resonance beam instability changes his nature on dissipative one with corresponding losses of beam energy and stationary level of generated waves to it [V.V. Gulenko, V.I. Tkachenko. Pis'ma v JETP, 14, 2179 (1988)]. The temporal dynamics of wave spectrum due to beam-plasma instability was investigated in this paper. Here it was supposed that wave spectrum is equidistant with a fixing phase at the beginning of a beam-plasma interaction. The temporal evolution of linear and non-linear wave spectrum was obtained

$$W_k \sim k^2 In^2(k/k_0)/(k^2-k_0^2)^2 ,$$

where **k**-wave number, $\mathbf{k_0}$-resonance wave number. Destruction of system invariant due to chaos was shown.

1P09

A Plasma of the Positive Column of Cs-Xe DC Gas Discharge as a Fast Highly Nonlinear Volumetric Medium for Microwaves

M.S. Gitlin, N.A. Bogatov, D.A. Dikan
and G.A. Luchinin
Institute of Applied Physics, Russian Academy of Sciences, 46 Ulyanov str., 603600 Nizhny Novgorod, Rusia

Microwave nonlinear quasi-optical devices such as phase-conjugation mirrors, passive self-limiters, power-controlled switches, etc. are of great interest in many fields, for instance, radar, navigation, microwave communications, beamed microwave power transmission. However, the lack of appropriate uniform nonlinear medium for microwaves with high nonlinear high-frequency refractive index and fast response time is considered a bottleneck in achieving potential of the field. A plasma of the positive column of DC gas discharge in a Cs-Xe misture was shown to provide an effective volumetric nonlinear medium for microwaves. In such a gas-discharge plasma under xenon pressure 30 Torr and electron density $N_e > 10^{12}$ cm^{-3}, uniform spatial distribution of electron density with sizes much larger than the wavelength of microwaves was achieved. Using a 35 GHz microwave beam with intensities up to 0.25 W/cm^2, it has been found that the plasma of the positive column Cs-Xe discharge has a very high nonlinear refractive index, n_2 = -0.1 cm^2/W, and a fast response time of about several microseconds.

1P10

Dynamics of a Laser Produced Plasma and its Properties for Microwave Reflection

G. Ding, J.E. Scharer, K.L Kelly, M.H. Bettenhausen, and N.T. Lam
Department of Electrical and Computer Engineering
University of Wisconsin, Madison 53706

A large plasma sheet is created by a 193 nm laser ionizing a low ionization potential molecule-Tetrakis-(dimethylamino)ethylene (TMAE). The plasma density is diagnosed by a fast response single Langmuir probe, and special features of the probe measurements at early times in the laser produced plasma are discussed. On microsecond time scales, the plasma decay is dominated

by a two-body recombination process, and other plasma decay processes, such as plasma diffusion, electron attachment, three-body recombination with either another molecule or an electron as the third body, can be neglected. The initial plasma densities vary for different experimental conditions, but all the density traces at later times approach a same limit, which is only sensitive to the two-body recombination co-efficient. Based on plasma density measurements, a dielectric model is developed to calculate the properties of microwave reflection from the plasma sheet. The critical reflection angles for different plasma densities, as well as the polarization effects on the microwave reflection are discussed. The calculations of microwave reflection from the plasma density measurements agree well with those obtained by direct microwave measurements.

This work is supported in part by AFOSR Grant F49620-94-1-0054 and AFOSR AASERT Award F49620-93-1-0465.

1P11

Microwave Reflections from a VUV Laser Produced Plasma Sheet

K.L. Kelly, J.E. Schrarer, G. Ding, M.H. Bettenhausen and N.T. Lan
Department of Electrical and Computer Engineering
University of Wisconsin–Madison, Madison, WI 53706

A Vacuum Ultra-Violet (VUV) Laser pulse is used to create a plasma sheet in an organic gas.[a] A bi-static antenna system is used for transmitting and receiving X-band microwaves which interact with the plasma. Reflected signals are measured for amplitude and phase analysis. Amplitude and phase shifts are compared to an aluminum conducting sheet placed in the same position as the plasma. The working gas is tetrakis(dimethylamino) ethylene (TMAE) with an ionization energy of 5.36 eV. The ionizing source is an excimer laser (W_{max} = 300 mJ) operating at 193 nanometers (6.4 eV). The laser beam is transformed into a sheet using VUV thin-film matched lenses. A plasma sheet with a peak density of 2.5 x 10^{13} cm^{-3} and T_e = 0.8 eV is formed with dimensions - 2.0 cm x 8.5 cm x 30 cm. Additional measurements of transmitted signals are utilized to determine plasma density and collision frequency. A computer model of the microwave transmission and reflection levels has been developed to optimize reflected signal levels as a function of density and thickness and to interpret experimental results. Comparison between the experimental results and the model show that this system is attractive for use as a microwave reflector.

This was supported in part by AFOSR Grant F49620-94-1-0054 and AFOSR AASERT Award F49620-93-1-0465.

[a]W. Shen, J.E. Sharer, N.T. Lam, B.G. Porter and K.L. Kelly; Journal of applied Physics. 78. 6974. October 1995.

1P12

Numerical Analysis of Microwave Propagation and Interaction with Plasma in Surface-Wave Plasma

Qing Chen, Makoto Katsurai
Department of Electrical Engineering
University of Tokyo, Japan

In surface-wave plasma using a planar (rectangular) configuration (Komachi, 1993) the surface wave is a 2.45 GHz electromagnetic field. Under the proper conditions, this surface wave propagates inside a chamber containing the gas Ar, creating a cold nonmagnetized plasma with a plasma frequency (ω_p) several times higher than that of the surface wave and a high electron density, i.e., about 10^{12} [cm^{-3}]. The surface wave energy is absorbed by the plasma maintaining a continuous plasma discharge. In this work, we use a novel finite-difference time-domain method (FDTD)/kinetic-equation formulation, to simulate the surface wave propagation and electron distribution inside the plasma. The simulation results are found to be in good agreement with experimental results. It is found that provided the electron-neutron collision frequency ν_c is greater than 10 ω_p, an electromagnetic wave can propagate inside the plasma with a small attenuation constant making it unnecessary to put an air gap and glass sheet between the dielectric medium and the plasma to create a uniform field distribution.

1P13

Interaction of an Air Plasma Layer Covering a Conducting Surface with Microwaves*

Mounir Laroussi
Microwave & Plasma Laboratory, Dept. of Electrical Engineering, University of Tennessee Knoxville, TN 37996-2100

Due to their extremely high collision frequency (THz), atmospheric pressure plasmas interact with electromagnetic waves, in a quite different fashion than low pressure plasmas [1]-[3]. In this paper, we study the attenuation, refelection, total scattering, and backscattering of microwaves, by a uniform, steady-state sheet of air plasma, covering a conducting surface. The effect of parameters such as the plasma number density, sheet thickness, wave frequency and polarization, will be investigated.

[1] M. Laroussi, Int. J of Infrared of Millimeter Waves, Vol. 16, No. 12, pp. 2069-2083, 1995.

[2] M. Laroussi, in Proc. 1996 IEEE Int. Conf. on Plasma Sci., p. 294.

[3] M. Laroussi, Int. J. of Infrared & Millimeter Waves, Vol. 17, No. 12, pp. 2215-2232, 1996.

*Supported by Air Force Office of Scientific Research contract AFOSR95-0277

1P14

On Phonomenon of Plasma-loaded High-power Backward Wave Oscillator

G.I. Zaginaylov
Kharkiv State University, Kharkiv, Ukraine
and
P.V. Turbin
Scientific Center of Physical Technologies Kharkiv, Ukraine

Recently it has been demonstrated that presence of a low density background plasma in a slow wave structure (SWS) of a backward wave oscillator (BWO) can lead to the sufficient enhancement in the output power [1]. There exist several treatments of this effect at present, but it appear to be that the full clarity has not been achieved yet. In this message we would like to point out one effect which may be important in this regard but has not been analyzed before. It is well-known that BWO output power is strongly sensitive to the variation of the cavity length [2], i.e. to the mutual placement of synchronous point frequency and nearest eigenfrequency of SWS. Presence of plasma changes the optical length of SWS and shifts its aigenfrequensies. Therefore it can cause increase in the output power. To examine the role of this effect the acurate computer simulation of finite-length plasma-filled BWO has been performed using the singular integral equation method [3] which takes into account "full wave" solution for electromagnetic fields and selfconsistent mode coupling at the output and input ends of the SWS within the scope of the linear beam model. The results obtained indicate the periodic output power dependence on plasma density which is similar to that obtained in experiment at length variation [2]. However, the output power enhancement is not too essential (50-100%) as that obtained in plasma-filled BWO experiment [1]. Possibly non-linear processes (for example, interaction between plasma and electromagnetic waves and others) which do not include in our model are also important for plasma-filled BWO operation. According to [4] the plasma wave instability can be sufficiently strong and can cause a great increase in energy extract from the beam.

[1] J. Carmel et al., Phys. Fluids B, 4, 2286 (1992).

[2] E. Schamiloglu, L.D. Moreland and R.W. Lemke. Conference Record of ICOPS 1995, p. 96; L.D. Moreland, E. Schamiloglu, R.W. Lemke and A.M. Roitman, ibid., p. 227.

[3] Yu. V. Gandel', V.D. Dushkin, G.I. Zaginaylov. Electromagnetic waves and electron systems, 1,38, (1996); G.I. Zaginaylov, P.V. Turbin. Proc. Int. Conf. Math. Meth. in Electromagn. Theory, Lviv, Ukraine, p. 162, 1996.

[4] G.I. Zaginaylov, Phys. Rev. E, submitted

1P15

Electrodynamics of Wide Spectrum Plasma Waveguide Surrounding with a Periodic Succession of Metallic Rings

V.A. Balakirev, Yu.P. Bliokh, A.V. Borodkin, O.F. Kovpik, E.A. Kornilov, I.N. Onishchenko and G.V. Sotnikov
Kharkiv Institute of Physics & Technology, Kharkiv, Ukraine

Hybrid plasma slow-wave structure as a combination of conventional structure and plasma waveguide is promising for wideband HF-devices with enhanced efficiency. In present investigations the periodic succession of metallic rings surrounding plasma waveguide is considered. The dispersion characteristics, fields

topography, HF-power distribution, growth rate and efficiency estimations are represented. The possibility of wide-band high frequency generation in the structures considered is shown.

This work was partially supported by STCU Contract #256.

Monday Morning, 19 May 1997
10:00 a.m. – Multipurpose Room

Poster Session 1Q01-09:
1.3a Basic Phenomena in Partially Ionized Gases – Gaseous Electronics, Electrical Discharges (High Pressure Discharges)

1Q01

Stability Measurements of PPL Atmospheric Pressure Arc.

L. Roquemore, S.J. Zweben
Princeton Plasma Physics Laboratory, Princeton, NJ
G. A. Wurden
Los Alamos National Laboratory, Los Alamos, NM

Experiments on the stability of atmospheric pressure arcs have been started at PPL to understand and improve the performance of arc furnaces used for processing applications in metallurge and hazardous waste treatment. Previous studies have suggested that the violent instabilities in such arcs may be due to kink modes[*,†]. A 30 kW, 500 Amp CW DC experimental arc furnace was constructed with a graphite cathode and a molten steel anode. The arc plasma is diagnosed with 4000 frames/sec digital camera, Hall probes, and voltage and current monitors. Under certain conditions, the arc exhibits an intermittent helical instability, with the helix rotating at ≈600 Hz. The nature of the instability is investigated. A possible instability mechanism is the self-magnetic field of the arc, with saturation occuring due to inhomogeneous heating in a helical arc[‡]. The effect of external DC and AC magnetic fields on the instability is investigated.

Additionally, arc deflection due to external transverse magnetic field is investigated. The deflection angle is found to be proportional to the applied field, and is in good agreement with a simple model of the $\vec{J}\times\vec{B}$ force on the arc jet.

*P.M. Bellan and J.W. Higley. IEEE Trans. Plasma Sci., 20(6):1026-1035, Dec. 1992.

†Ben Bowman. Electric Furnace Conf. Proc., pp 111-120, 1994.

‡H.H. Maecker and H.G. Stablein. IEEE Trans. Plasma Sci., 14(4):291-299.

1Q02

A New DC Electric Gas Breakdown Criterion

V.A. Kisovskiy
Kharkiv State University, pl. Svobody 4, Kharviv, 31077, Ukraine

This report presents the gas breakdown criterion in the constant uniform electric field. It includes the gas ionization by electron impact, electron and ion drift in DC electric field, anisotropic electron diffusion along and across the electric field, ion-electron emission from the cathode surface as well as limited dimensions of the discharge chamber. Our criterion can be put in the form

$$\frac{\nu_i}{D_T}=\left(\frac{2.405}{R}\right)^2+\frac{D_L}{D_T}\bullet a^2+\frac{\nu_e}{D_T}\bullet a \quad (1)$$

where the quantity a satisfies the condition

$$\frac{sin(aL)}{1-cos(aL)}\bullet\frac{a}{\alpha}\bullet\frac{1}{2\bullet\gamma-1}=1 \quad (2)$$

ν_i is the electron impact ionization frequency, ν_e is the electron drift velocity, D_L and D_T are the longitudinal and transverse diffusion coefficients, α and γ are the first and second Townsend coefficients, R is the chamber radius, L is the interelectrode spacing. The DC discharge criterion describes both branches of the Paschen curve as well as the ambiguity region in helium.

1Q03

Generalized Moment Method of an AC Plasma Display Panel Cell

Y.B. Kim, Y.K. Shin, H.J. Lee, J.K. Lee
Pohang University of Science and Technology
Pohang 790-784, KOREA

We present a self-consistent fluid model of the plasma physics in an AC plasma display panel cell. The model is based on a multi-fluid description of electron, ion and neutral particle transport, coupled with Poisson's equation. We employed a generalized Chapman-Enskog method[1] to retain the most dominant kinetic effects on fluid description, similar to reduced Braginskii equations[2] in unmagnetized plasma. Momentum balance equation now includes viscous stress force with kinetic closure. The same moment method has been also utilized to determine rate coefficients and mobilities, hence generalizing customary E/N dependence in these coefficients. A 1D numerical result on the physical, electrical and optical properties of an AC PDP cell will be discussed.

[1] S. Chapman & T.G. Cowling, "The Mathematical Theory of Non-uniform Gases," 2nd ed., Cambridge, London, 1952.

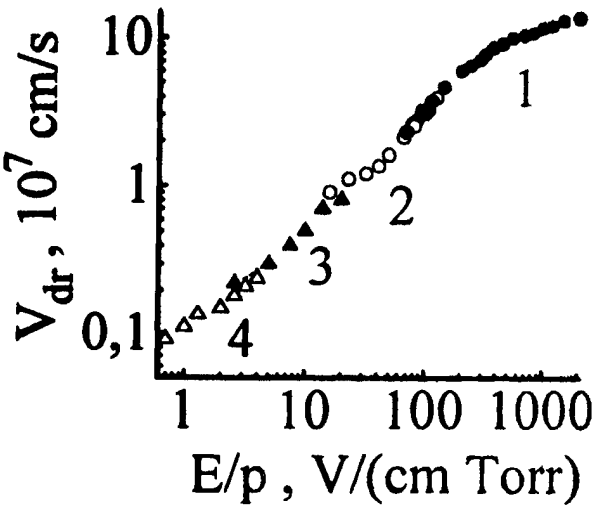
[2] S.I. Braginskii, "Transport Properties in a Plasma," in M.A. Leontovich (ed.), "Reviews of Plasma Physics," Consultants Bureau, NY 1965.

1Q04

Electron Drift Velocity Determination in Air

V.A. Lisovskiy and V.D. Yegorenkov
Kharkiv State University, pl. Svobody 4,
Kharkiv, 310077 Ukraine

We have determined the electron drift velocity v_{dr} from the location of the turning points of the diffusion-drift branch of RF breakdown curves. As is known (Lisovskiy, V.A. et al–J.Phys.D, 1994, V.27, p.2340) at these points the electron displacement amplitude in the RF field $A = eE/(m\upsilon_{en}\omega)$ (ν_{en} is the effective electron-neutral collision frequency, $\omega = 2\pi f$) is equal to one half of the electrode spacing L. At the same time $A = v_{dr}/\omega$, therefore one finds easily the function $v_{dr}(E/p)$ from measured breakdown curves. RF frequency $f = 13.56$ MHz. Figure shows the functon $v_{dr}(E/p)$ in air: 1 is for our data, 2 is for data (Rosnerski, W., Leja, K.–J. Phys. D, 1984, V.17, p. 279), 3 is for data (Nielsen, R.A. et al–Phys. Rev., 1937, V.51, p69), 4 is for data (Rees, J.A.–Austr. J. Phys., 1973, V.26, p.247).



1Q05

Control of Trichel Pulses of Corona by Geometric and Gasdynamic Factors

Yu. S. Akishev, A.P. Napartovich, M.V. Pan'kin and N.I. Trushkin
TRINITI, Troitsk, Moscow region, 142092, Russia

Upon applying of step of high voltage that is over an inception one, the ignition of negative corona is accompanied by a sharp splash of discharge current with duration of a pulse about 10^{-7} s. As a rule, for electropositive gases (N_2, Ar, etc.) the corona current falls after splash and goes to the stationary value that is much smaller than that one for initial pulse. For electronegative gases (air, O_2, etc.) in which electrons are fast turned to negative ions, instead of stationary state the pulsed regime of corona with regular splashes of discharge current is established that named as Trichel pulses. The physical condition for existence of regular Trichel pulses lies in the fact that a displacement current of corona has to approach the conductivity current in this regime. This condition is easy devised for corona in air, O_2 in which the negative ions are main carriers of charge through the interelectrode gap. In the case that electrons are the major carriers of charge (N_2, Ar, etc.) the reduction in the contribution of conductivity current to the total current can be reached

only for corona with the interelectrode gap more than 15-20 cm. We were first to obtain the Trichel pulses for negative corona in N_2, Ar.

We found out for ambient and dry air that amplitude of the Trichel pulses depends strongly on the conditions of current spreading both in the vicinity of corona pin and in the drift region of corona. Change in the geometry of current spreading in the neighborhood of pin we realized by use of different dielectric shields surrounding the pin. Geometry of current spreading in the drift region we modified by means of use of different form of anodes. Gas-dynamic action on pin region of corona was realized by use of a powerful jet stream of air directed through plane meshy anode towards tip of pin. A rise both in amplitude of Trichel pulses and period of its repetition was found out with increase of gas flow velocity.

In general, the results of experimental investigations on active control of Trichel pulses by gas-dynamic and geometric factors will be presented in this report.

1Q06

Study on Factors for the Starting Potential of Short Gap Discharge in N_2+NO Gas

Kagehiro Itoyama and Takafumi Nishimura
Nagasaki University, Nagasaki 852 Japan
Takeshi Yanobe
Hokushin Industries Inc., Yokohama, 230 Japan

Authors had reported the removing for TOx gases by employing short gap discharge under the condition of atmosphere. In this work, we measured the starting potential of short gap discharge with lapse of time with changing pressure in the discharge chamber, electrode gap, source voltage and discharge current.

Effects of Pressure: The starting potential decreases exponentially as a function of time under the pressure of 500 Torr or more. The relation between starting potential, Vs, and time, t, is expressed in the following equation.

$$Vs = V'exp(-kt) + Vss$$
$$= Vso\ exp(-kt) + Vss\ (1-exp(-kt)) \quad (1)$$

Where k is constant. The values of Vso and Vss obtained by the method of least square show the linear relation for pressure. However, the starting potential does not satisfy eq.(1) under the condition of low pressure.

Effect of Electrode Gap: The starting potential becomes high and the drop of voltage becomes small for changing time with extending the electrode gap. Usually, electrode gap has larger influence on the starting potential than pressure in the discharge chamber.

Effect of Source Voltage and Current: The starting potential shows a large drop of voltage with a lapse of time with increasing source voltage, although the starting potential does not differ much in various source voltage at t=0. The change of starting potential for discharge current also shows a similar tendency. The starting potential decreases largely with increasing discharge current. This means that the power consumed in discharge has a great influence on the starting potential in long operation.

1Q07

An Electrostatic MHD Theory for Helical Instabilities of Arc Discharges

Xiaogang Wang
Department of Physics & Astronomy
University of Iowa, Iowa City, IA 52242, USA

Arc discharge plasmas have wide-range applications in many areas. Therefore, research for equilibria and helical magnetic instabilities of arc discharge plasmas is a very important subject in low temperature (in comparison with high temperature fusion plasmas) plasma physics. An arc discharge column can be unstable due to helical perturbations and the rotational symmetry by those modes.

An analytic linear study for "slow" magnetic helical instabilities of arc discharges in a cylindrical plasma is developed in this paper. Based on a set of electrostatic magno-hydro-dynamic (MHD) equations, we investigate "slow" m=1 helical modes with an external axial magnetic field. The stability analysis by the criterion obtained in this paper shows that the "slow" resistive-viscous helical instabilities are linearly stable in both long wave-length and short wave-length limits. These results are in agreement with numerical results. To the most dangerous instabilities with a wave-length of order of the length of a discharge arc, the helical mode are marginally stable. The theory shows that an external axial magnetic field can destabilize those helical modes. This result contradicts to ideal MHD "fast" kink mode theory with a growth rate much faster than the resistive viscous dissipation, such as the ideal MHD kink mode theory for tomamaks where a strong axial field stabilizes the mode, and the previous theory for electric furnace arc discharges. However helical instabilities generated by an axial external field are indeed observed in recent experiments.

1Q08

Simulation of Microdischarges in a Dielectric Barrier Discharge

Jing Li and Shirshak Dhali
Department of Electrical Engineering, Southern Illinois University, Carbondale, Illinois 62901

The results of simulation of a streamer like microdischarge in a dielectric-barrier discharge will be presented. The simulations were done using a two-dimensional fluid model on an adaptive grid.

The discharge voltages and currents have been studied for different values of dielectric capacitance. The dielectric has very little influence on the streamer development and propagation until the very last stage. When the streamer gets very close to the dielectric, sufficient charge is deposited on the dielectric, and subsequently the discharge is quenched.

The radical production efficiency has not been found to depend strongly on the dielectric capacitance. Calculation will be presented for oxygen and air.

1Q09

Stripping Properties of a Free Electron Target Produced in a Pseudospark Discharge

M. Engelbrecht, J. Kolb, R. Kowalewicz, J. Philipps and D.H.H. Hoffmann
University of Erlangen-Nürnberg, Physics Department I, 91058 Erlangen, Germany
Tel. 09131/857118, Fax 09131/858774

To make efficient use of particle accelerators high ion charge states are required to achieve high particle energies. Generally ion sources do not provide these high charge states. Therefore it is necessary to enhance the charge state by additional stripping processes at the beginning of the ion acceleration. Usually gas or foil targets are used as stripping devices. The charge state distribution of ions passing through a stripper target is determined by ionization (collisional ionization by ions and electrons, charge transfer ionization) and recombination processes (bound electron capture, radiative electron capture, dielectronic recombination, 3-body recombination). The equilibrium charge state of the ion depends on the ionization and recombination cross sections. Previous calculations and recent computer simulations predict a much smaller cross section for recombination for free electron capture compared to bound electron capture. Therefore the mean charge state of an ion beam penetrating a fully ionized plasma target or a free electron target is expected to be much higher than for a cold gas target because the recombination processes are strongly reduced. We investigated the interaction of an ion beam with a free electron target. The free electrons are produced in a pseudospark discharge. Through a hole in the anode a high energy electron beam is emitted. By applying different discharge voltages (10-30 kV) the electron beam energy can be varied. The influence of the discharge current and the gas pressure on the interaction properties is investigated. Electron density and temperature of the discharge are conceived from spectroscopy. With these experiments we want to determine the best operational parameters to obtain the highest possible stripping efficiency. The device is tested at the tandem accelerator in Erlangen with different ion species. We used a Monte Carlo simulation to estimate the experimental measurements. First results and comparison with the simulation will be presented.

1Q10

Designing Planar Magnetron Cathodes: Analysis and Experiment

Manuel Garcia
Lawrence Livermore National Laboratory, L-490, PO Box 808, Livermore, CA 94550
garcia22@llnl.gov, (51) 422-6017

Planar magnetron cathodes have arching magnetic field lines which concentrate plasma density to enhance ion bombardment and sputtering. Typical parameters are: helium at 1 to 300 milli-torr, 200 to 2000 gauss at the cathode, 200 to 800 volts, and plasma density decreasing by ten to a thousand times within 2 to 10 cm from the cathode. A 2D, quasineutral, fluid model yields formulas for the plasma density: $n(x,y)$, current densities: $j(x,y)$, $j_e(x,y)$, $j_+(x,y)$, the electric field: $E_y(y)$, and the voltage between the cathode surface and a distant plasma. Experiments shows that $T_e(3\rightarrow 8$ eV) adjusts to ensure that $\alpha_0\tau \approx 2.5$ in helium for ionization rate $\alpha_0(10^4\rightarrow 10^5\ s^{-1})$, and electron transit time to the unmagnetized plasma τ ($10\rightarrow 100$ μs). Helium glow discharge cathode fall $\alpha_0\tau$ is about 2.5, though this occurs at much higher voltage.

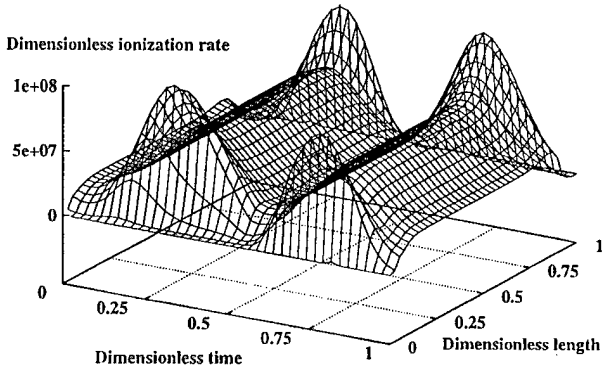
This work was performed under the auspices of the U.S. DOE by LLNL under contract no. W-7505-Eng-48.

1Q11

One-Dimensional Continuum Modeling of Chlorine Radio-Frequency Discharges

Jean-Noël Baléo[†] and Marie-Josèphe Vignes[‡]
[†]*École des Mines de Nantes, 4 rue Alfred Kastler, BP 20722, 44037 Nantes Cedex 3, France*
[‡]*Matra MHS, La Chantrerie, route de Gachet, BP 70602, 44036 Nantes Cedex 3, France*

Theoretical predictions of a one-dimensional model of chlorine radio-frequency low discharge at low pressure are presented. The model consists of continuity equations for electrons, positive and negative ions, and of the electron energy conservation equation, coupled self-consistently with Poisson's equation. The effects of the interelectrode distance, of the rf voltage amplitude and of the neutral gas pressure are investigated. The existence of peaks of electron temperature contributing to the level of electron density is shown to be controlled by the peak rf voltage while the pressure mainly influences the level of electron energy at the sheath-bulk interface and the sheath thickness.



1Q12

Time-Dependent Global Model for Electronegative High-Density Plasma Discharges

H.J. Yoon, T.H. Chung, and J.K. Lee[a)]
Dong-A University, Pusan 604-714, Korea
[a)]*Pohang University of Science and Technology, Pohang 790-784, Korea*

We develop a global model of high-density plasma discharges in molecular gases. The global model consists of the energy and particle balance equations for neutral and ionic species. The energy balance equation includes energy-loss for electron-neutral collisions, and electronic excitation, dissociation, ionization, dissociative attachment, and recombination. Particle balance equations are written for all species of interest. For a specified discharges length and diameter, absorbed power, pressure, reaction rate coefficients and surface recombination constants, we solve these equations to determine all species densities and the election temperature. High-density discharges such as inductively coupled plasma sources typically operate at low pressure of 1-20 mTorr and high input powers of 1-3kW. Pulsed-time modulation of the input power has been used to improve processing rates and etch selectivity in high-density discharges. We investigate plasma characteristics of a pulse-time modulated high-density discharge using volume averaged global model. Also, we calculate the fractional dissociation and the ratio of the negative ion density to the electron density as a function of the wall recombination constant.

1Q13

Negative Ion Densities in Cl_2 and BCl_3 Inductively-Coupled Plasmas*

C.B. Fleddermann[†] and G.A. Hebner
Sandia National Laboratories, Albuquerque, NM 87185-1423

The chlorine negatie ion density and the electron density in Cl_2 and BCl_3 inductively-coupled plasmas have been measured in a GEC reference cell operated in the inductively-coupled mode. The chlorine negative ion density was measured as an excess electron density produced by photo-dissociation of the negative ions by 266 nm radiation from a frequency-quadrupled Nd:YAG laser. Both the excess electron density and the steady-state electron density were measured using a microwave interferometer. Various gas mixtures were investigated including pure Cl_2, pure BCl_3, and combinations of these gases with each other and with N_2 and Ar. Cl^- densities up to 4 x 10^{11} cm^{-3} were measured depending on the gas mixture. The ratio of electron density to Cl^- density was as high as 3 in Cl_2 mixtures, and up to 5 in BCl_3 mixtures. The plasma probed at lower photon energy (355 nm) to photodetach electrons from other negative ions possibly present in the plasma: to within the sensitivity of the measurement (1.3 x 10^8 cm^{-3}), no other negative ions such as BCl_x^- or Cl_2^- ions were detected. The Cl^- density also changed when BCl_3 was added to Cl_2 discharges. Addition of Ar or N_2 to Cl_2 plasmas had little

effect on Cl^- density, but nitrogen addition had very dramatic effects when added to BCl_3, causing a factor of two increase in the Cl^- density.

This work was supported by the United States Department of Energy under Contract DE-AC04-94AL85000. Sandia is a multiprogram laboratory operated by Sandia Corporation, a Lockheed Martin Company, for the United States Department of Energy.

[†]Permanent address: Department of Electrical and Computer Engineering, University of New Mexico, Albuquerque, NM 87131

1Q14

Characterization of Pulse-Modulated Inductively Coupled Discharges in Argon and Chlorine

G.A. Hebner and C.B. Fleddermann[1]
Sandia National Laboratories
Albuquerque NM 87185-1423

The characteristics of pulse modulated inductively coupled plasmas in argon and chlorine have been experimentally investigated. Measurements were performed for peak rf powers between 150 and 400 W, duty cycles between 10 and 90%, pulse repetition frequencies between 3 and 20 kHz, and argon or chlorine gas. Over this parameter space, measurements were performed of the forward and reflected rf power into the matching network, coil voltage, rf variation of the plasma potential using a capacitive probe, electron density using a microwave interferometer, and Cl^- density using laser photodetachment spectroscopy. These measurements indicate that for the firs 50 - 100 rf cycles of each rf pulse, the discharge may be operating in a capacitive discharge mode with rf variations in the plasma potential of several hundreds of volts and relatively low electron density. Measurements of the electron density in pulse modulated chlorine discharges indicate that the steady state electron density is a function of the duty cycle; the steady state electron density is lower for higher duty cycles. This may indicate that the ratio of Cl to Cl_2 is changing with duty cycle. As a result, the dominate ions and neutrals that strike and etch the surface are also changing. In addition, a microwave radiometer was used to provide an indication of the time dependent electron temperature. Large spikes in the microwave radiation temperature were noted at the turn on of the rf power and in some cases at the transition from a capacitively coupled to an inductively coupled plasma.

This work was supported by the United States Department of Energy (DE-AC04-94AL85000).

[1]Permanent address: University of New Mexico, Department of Electrical and Computer Engineering, Albuquerque, NM 87131

1Q15

Operation Characteristics of an ICP Plasma Source

K.C. Leou, T.L. Lin, C.H. Tsai, J.H. Li, S.C. Pan, S.L. Wu and J.L. Tsai
National Tsing Hua University, NEEP Department
Hsinchu, Taiwan, ROC

Operation characteristics of an inductively-coupled plasma source have been measured by several different measurement techniques: Langmuir probe, 36 GHz hetrodyne interferometer, optical emission spectroscopy and plasma impedance probe. The Ar plasma is generated by exciting a planar inductive coil with 13.56 MHz RF power which is coupled into the 400 mm diameter plasma chamber through a quartz window. Measurements have been made for two different size of antenna: 150 mm and 270 mm with window sizes 200 mm and 320 mm, respectively. The tip of the Langmuir probe is isolated from the bias and measurement electronics by an inductor to force the probe tip to follow the AC plasma floating potential. The 36 GHz hetrodyne interferometer employs two free running Gunn oscillators and the phase change was measured by a 70 MHz quadrature mixer. The measurement results have been used to calibrate the Langmuir probe. The RF power absorbed by the plasma was measured by the plasma impedance probe placed between the antenna and matching network. Spatial variations of optical emission from the plasma for different operation conditions have also been measured by a monochrometer/CCD system with an optical fiber head. Detailed measurement results for different values of gas pressure and RF power will be presented.

(Work supported by NSC grant No 86-2112-M-007-045, ROC, and NTHU internal fund.)

1Q16

Damage to Ferroelectic Cathodes from Surface Discharge and Mechanical Strain*

T. Cavazos and C. Fleddermann
Electrical and Computer Engineering Department, University of Mexico, Albuquerque, NM 87131

High power microwave devices require electron sources with high current densities (1-5 kA/cm^2) which have constant emission properties over a long pulse duration (0.5-1.0 μs). Typically explosive emission cathodes are used, however these sources produce plasma along with the electron beam which interferes with the beam shape and contributes to gap closure. Ferroelectric ceramic materials are currently being investigated as an alternate source. To achieve electron emission from these materials it is necessary to create a charge imbalance at the surface rapidly altering the polarization which is usually done with a pulsed electric field. The conditions of the experiment also create a triple point at the metal-vacuum-dielectric interface at which the intensity of the electric field may be several oreders of magnitude higher than the bulk electric field. This enhancement can cause a plasma discharge at the edge of the grid. Damage to the grid from this phenomenon has been documented using a scanning electron microscope. The critical field at which this discharge occurs can be increased by polishing the ceramic surface. The intensity of the drive pulse will also produce intense strains within the ceramic material which can lead to fractures. Thus there are at least two physical limits–the triple point electric field and the mechanical elastic limit–to the excitation pulse applied to ferroelectric ceramics.

The materials studied include 8/65/35 (Pb,La)(Zr,Ti)O_3 (PLZT) ferroelectrics, antiferroelectrics, and Pb(Zr,Ti)O_3 piezoceramic materials. The samples are disk shaped measuring 1 mm thick by 15 mm in diameter and they are metalized with a 1 μm thick gold film.

This work is supported through a High Energy Microwave Devices Consortium funded by an AFOSR/DOD MURI grant and administered through Texas Tech University.

1Q17

A Large Area ECR Plasma Source

T.L. Lin, Y. Hu, K.C. Leou, J.H. Shiau and Y.C. Lan
NEEP Dept., National Tsing Hua University, Hsinchu, Taiwan, ROC

A large area, permanent magnets ECR plasma source employing a buffer cavity and a TE_{01} mode converter has been designed and is being constructed at NTHU. The magnet structure consists of two sets of ring with radially directed magnets along with iron pole-pieces and a shielding envelop. Calculation using the PANDIRA code has been employed to yield the desired magnetic field profile. The 2.45 GHz microwave power is coupled from a rectangular waveguide to the TE_{01} circular waveguide mode through a Flower-Pedal mode converter. The design of converter has been modeled by a finite element electromagnetic simulation code. HFSS, yielding a conversion efficiency of 96%. A buffer cavity developed in our previous work[1] is also employed to increase operation stability by reducing the variation of load impedance seen by the microwave generator. The ECR heating of plasma and wave propagation have been investigated by the PIC-MCC simulation code developed previously.[2] Both the design and simulation results will be presented.

(Work supported by AEC Grant No. 85200/NTD009 & 862001NTD107 and NSC grant No. 86-2112-M-007-045 ROC)

1. F.T. Ning, Y. Hu and T.L. Lin, IEEE Int. Conf. On Plasma Science, Boston, MA, June 1996, p. 217.

2. Y. Hu, et al, IEEE Int. Conf. On Plasma Science, Boston, MA, June 1996, p. 137.

1Q18

STABLE REGIMES, MODE TRANSITIONS AND DISCHARGE DISRUPTIONS IN A HELICON PLASMA SOURCE

K.P. Shamrai
Institute for Nuclear Research 252022 Kiev, Ukraine

Inductively coupled helicon plasma source demonstrates abrupt changes of discharge regimes which may arise at a smooth variation of external parameters such as input rf power, magnetic field, or driving frequency. These changes are displayed as discontinuous

jumps from low to high-density modes, or as discharge disruptions.

Abrupt changes of discharge regimes are treated proceeding from the model which assumes the rf power absorption in a helicon source as originating in a linear conversion of helicon waves into electrostatic waves at a plasma edge. The efficiency of conversion and thus of absorption depends strongly on the amplitude of helicon wave near the plasma boundary. It is low at the anti-resonances of helicon wave excitation, that is provided that the boundary amplitude of helicon wave is reduced. Since a driving antenna excites in plasma a variety of spatial modes, the absorbed power varies with plasma density non-monotonically with peaks arising due to different harmonics. The specific shape of absorption curve depends on the source design, and on the shape of driving antenna, as well as on the strength and profile of external magnetic field.

The power balance arranged with conversion mechanism of absorption permits to explain naturally both the low-to-high density jumps, as mode transitions between different absorption peaks, and discharge disruptions.

Experimental evidences for the model are given, and the possibility for a control of plasma parameters in a helicon source by a driving antenna and by a magnetic field shape is discussed.

1Q19

Basic Experimental Results of MCEBPS

T.Y. Kim, K.H. Chung
Seoul National University, Seoul, Korea
Y.B. Kang
Hanyang University, Seoul, Korea
D.K. Ko, J.K. Jung
Joongang University, Seoul, Korea
and S.J. Noh
Dankook University, Seoul, Korea

The conceptual design and the basic experiments of the Multi-Cathode Electron Beam Plasma Source (MCEBPS) were carried out. The MCEBPS can efficiently produce uniform and dense plasmas through direct interaction of electrons and neutral gases in the wide area with a diameter of 300mm or above. The nonuniformity of the radial plasma density must be within ±3% to be suitable for the process of next generation semiconductor devices.

The MCEBPS has seven LaB_6 cathodes (multi-cathode) whose array is concentric in order to obtain a wide areal and uniform plasma density profile at the target position. The initial electron beam is extracted with an electron energy about 50 - 200 eV. This can be done by changing the voltages of extraction electrodes. The electron beam current can be also controlled to the desired value by adjusting the cathode temperature. The energy and the current of the electron beam can be controlled independently.

In the working chamber plasmas for the process of target material are produced through the direct interaction of the extracted electron beam and the neutral gases which are fed from outside. The adoption of multipole or additional permanent magnets is under consideration to enahnce the plasma confinement and uniformity. The results of basic experiments will be presented in the conference.

This study is supported in part by the Korea Ministry of Trade, Industry and Energy and also inpart by Soosan Precision Co., LTD.

1Q20

Mass-Spectrometrical Study of Neutral Component of Plasma in Gas Discharge with Metal-Hydride Cathode

V.V. Bobkov, V.N. Borisko, E.V. Klochko,
D.L. Ryabchikov, Yu.V. Sidorenko
Kharkiv State University, Svobody sq.4, 310077, Kharkiv, Ukraine
E-mail: azarenkov@pem.kharkov.ua

The composition of neutral component of gas discharge in hydrogen, desorbed from the metal-hydride cathode, was studied. On the basis of mass-spectrometrical measurements it was showed that the use of metal-hydride cathode resulted in the intensification of plasma-chemical reactions with participation of hydrogen in the discharge volume. In this case the anomal change of the neutral component of plasma discharge in range of discharge current magnitude 50-200 mA is viewed. The increase of the discharge current above 200 mA lead to disappearance of the discovered anomalies. The chemical composition of neutral component of plasma changed only when the metal-hydride cathode was used but no change was observed (the discharge parameters were the same) when the cathode was made of steel and the hydrogen from cylinder was used.

Monday Morning, 19 May 1997
10:00 a.m. – Multipurpose Room

Poster Session 1Q21-32:
1.3c Basic Phenomena in Partially Ionized Gases – Gaseous Electronics, Electrical Discharges (Electron and Ion Transport and Fundamental Data)

1Q21

Electron Behavior in Inhomogeneous DC Discharges

T. Kimura and K. Ohe
Department of Systems Engineering, Nagoya Institute of Technology, Showa-ku, Nagoya 466, Japan

The radial dependence of the electron energy distribution function (EEDF) in N_2 and He positive columns is measured by a Langmuir probe. The discharge is produced in a 1.8 cm-ϕ glass chamber, in which the gas pressure is from 0.32 Torr to 1.0 Torr and the discharge current range from 20 mA to 100 mA.

In the He discharge, the EEDF measured at any radial position can be approximated by shifting the EEDF measured at the tube axis by the ambipolar potential from the axis to the wall except for its tail, since the energy relaxation length for electrons with the energy relaxation length for electrons with the energy below 20 eV is much longer than the tube radius. The electron behavior is described by the non-local kinetics based on the potential, while there is ambiguity in applying the non-local kinetics to electrons with the energy higher than 23 eV.

In the N_2 discharge, the bulk of EEDF measured at a radial position is independent of the ambipolar potential, while its tail depends on the potential, since the relaxation length for low energy electrons which may be correlated with the vibrational collision, is much shorter than the tube radius and that for high energy electrons ($\varepsilon \geq 4$ eV) is much longer. Thus, the behavior of electrons with such a low energy can be determined by the local electric field. However, the effective electron temperature, which can be estimated by the measured slope of the bulk {d log[f(r,ε)]/ de: f(r,ε) the local electron energy probability function}, gradually decreases from the axis to the wall. This phenomenon may be caused by the diffusion cooling and the decrease of the superelastic collision towards the wall. Further experimental and theoretical investigations for the variation of effective temperature towards the wall will be necessary.

1Q22

Mode Transition and Nonlinear Dynamics in the Beam-Injected Plasma

H.J. Lee, J.K. Lee, Y. Yang, M.S. Huh, Y.B. Kim, and M. Yoon
Pohang University of Science and Technology Pohang 790-784, Korea
T.H. Chung
Dong-A University, Pusan, Korea

The motions of electron beams in a discharge plasma are simulated using the 1-D particle-in-cell code (XPDP1[1]). With appropriate pressures, beam current, beam velocity, and voltages, there is mode transition from the anode glow mode (AGM) to the temperature limited mode (TLM). The transition happens when the ionized ions which make the potential positive fill the entire space. During transition from AGM to TLM, the dynamics show chaotic motions and the current increases to the injected beam current. After the TLM is established, the dynamics of electron current and potential show self oscillation, periodic doubling, or chaos for various electron to ion number ratios, sheath sizes, and bulk potential levels. The higher bulk potential level is, the larger fluctuation amplitude of current is observed. For higher pressures of neutral gas, the dynamics show more chaotic but small amplitude of fluctuation motions.

[1] C. K. Birdsall, IEEE Trans. Plasma Sci. **19**, 65 (1991)

1Q23

Ion-Energy Distributions in Townsend Discharges of CHF_3 at High *E/N*

M.V.V.S. Rao, R.J. Van Brunt and J.K. Olthoff
National Institute of Standards and Technology Gaithersburg, MD 20899

In this paper we present ion kinetic-energy distributions (IEDs), mean energies, and relative abundances of CF_3^+, CF_2^+, CF^+, CHF_2^+, CHF^+. CH^+, C^+, and H^+ ions produced in dc Townsend discharges in pure CHF_3. The discharges are generated between two circular parallel-plate electrodes at electric field-to-gas density ratios (*E/N*) ranging from 5×10^{-18} Vm^2 to 25×10^{-18} Vm^2 (5 to 25 kTd). A stable discharge could not be attained below 4×10^{-18} Vm^2 due to the electronegative nature of CHF_3. Ions sampled from the discharge through a small orifice in the center of the grounded electrode were

energy and mass analyzed by a 45° electrostatic energy analyzer attached to a quadrupole mass spectrometer. The present apparatus is equipped with ion optics that allow measurements of ion energies up to 1000 eV [1].

In the present experiments, the parent ion CHF_3 was not observed, and CHF_2^+ was determined to be the dominant ion at all *E/N*, followed by CF^+. At 5 kTd, the IEDs of all the ions exhibit Maxwellian behavior. However, at higher *E/N* the role of collisional dissociation processes increases and the IEDs of most of the ions deviate from those predicted by simple collisional charge-transfer models. At 15 kTd and above, the IEDs for CF^+, C^+, and H^+ exhibit maximum ion energies that are equivalent to the applied discharge gap voltage.

[1] M.V.V.S. Rao, R.J. Van Brunt and J.K. Olthoff, Phys. Rev. E**54**, 5641 (1996).

1Q24

Secondary Electron Emission Influence on the RF Gas Breakdown

V.A. Lisovskiy, N.Yu. Kropotov
Kharkiv University, Kharkiv, Ukraine
V.I. Farenik
Scientific Center of Physics and Technology
pl. Svobody 4, Kharkiv 310077, Ukraine

The conditions of the RF discharge studied earlier have revealed the ambiguous link between breakdown voltage and gas pressure (Levitskii S.M.-Zhurn. Tekh. Fiz., 1957, V.27, p.970; Lisovsky V.A. et al-J. Phys. D, 1994, V.27, p.2340). It is of interest to study the influence of the electrode material on the characteristics of the low-pressure gas breakdown in RF fields. The field frequency is f = 13.56 MHz, gas pressure p = 0.01 - 10 Torr, d = 14 - 30mm is the distance between plane electrodes of stainless steel and aluminum of 100 mm in diameter. To decrease the secondary electron emission, the steel electrodes have been covered with soot, and to increase electron emission the aluminum electrodes have been employed. At sufficiently high pressures the right-hand branches of breakdown curves coincide (for identical contents of the gas medium in the chamber). On decreasing pressure, the more the secondary electron emission of electrodes is, the less are the voltage values necessary to break the gas, the breakdown curves pass through the region of lower pressures.

1Q25

Ion Cyclotron Instability in Rotating Plasma

M.V. Sospatrov
Scientific Center of Physical Technologies,
Kharkiv, 1 Novgorodskaya Str., 310145, Ukraine

It's known that in plasma which is immersed in crossed electrical and magnetic fields under certain conditions, the ion cyclotron instability can by occurs [1]. It lead to the spatial redistribution of plasma parameters and increase of ions flow from the discharge.

In the unstable regime the dynamics of ion motion is very complicated. Now the phenomenological model of ion motion in such regime is developed. It is based on experimental results [2]

In given report the possibility of control of the instability is considered by means of ion beam injection in discharge region where unstable oscillations are located. By changing of beam parameters and direction of injection the essential variation of instability level and flow intensity of ions of certain kind from discharge was obtained. The optimal ion beam parameters corresponding to the maximum of ion cyclotron oscillations amplitude was defined. On the basis of results obtained the quantitative astimations for parameters of plasma ions which are employed in the instability were performed, including their energy spectrums and qualitative consistency.

The results are in good agreement with that obtained earlier.

[1] A.M. Rozhkov, K.N. Stepanov et. al. Plasma Phys. 12, 519 (1970).
[2] M. Sosipatrov Records of ICOPS '95, p. 143.

1Q26

Non-Local Electron Kinetics in a Weakly Ionized Plasma*

E. Furkal, A. Smolyakov and A. Hirose
Department of Physics and Engineering Physics
University of Saskatchewan, Saskatoon, SK Canada

Electron kinetics in a weakly ionized plasma is analyzed under the condition such that the electron mean free path is not small compared to the characteristic length scale of electric field inhomogeneity. In this case the standard two-term approximation is not valid and higher order spherical harmonics in the perturbed electron

distribution function have to be taken into account. The electron distribution function is represented by an infinite series of spherical functions. This results in the infinite hierarchy of coupled equations for separate angular harmonics that can be reduced to an infinite continued fraction. This continued fraction is approximated by a simple algebraic function for a case of low frequencies, $\omega < \nu$.. Expression for the perturbed electron distribution function is found. The anomalous penetration of the electric field into a semi-infinite plasma and profiles of the heat deposition are analyzed. Expressions for the surface impedance are obtained, for two cases (a) collision frequency is independent of electron's velocity, and (b) proportional to it.

*Supported by the NSERC and National Fusion Program of Canada.

1Q27

Acoustic Pulse Magnification at Its Propagation Along Structurally-Modified Zone of Radiation-Matter Interaction

V.A.Deryuga, A.I.Kalinichenko, G.F.Popov
Kharkiv State University, Kharkiv, Ukraine
A.G.Ponomarev and V.V.Uvarov
Ukrainian Scientific Center, Institute of Physics and Technology, Kharkiv, Ukraine

The acoustic emission caused by high-current tubular electron beam in rod polycrystalline metal samples was experimentally studied. Two zones of beam-rod interaction emitted in a rod matter equal thermoacoustic pulses, those propagated along rod body to acoustic detectors connected to each of free butt-ends of rod target. In spite of conditions of generation were equal, the second pulse arriving a detector exceeds the first one nearly on 30%. Such phenomenon is possibly connected with incomplete relaxation of residual thermoelastic stress in irradiated metal over time interval between two pulses passing. The first pulse comes to detector passing through nonirradiated material, whereas the second one passes through radiation-modificated zone on its way to detector. Herewith the variable stress breakaways dislocations from stoppers causing coherent acoustic emission from structurally-modified zone that amplifies the propagating pulse. The investigations show clearly presence of nonthermoelastic component in generated stress wave. A deposit of bulk expansion due to phase structural transitions in radiation-acoustic effect may exceed significantly that from thermal expansion. Some modification of radiation-acoustic equations providing account of phase transitions are discussed.

1Q28

The Ion Motion in the Field of Ion-Sound Surface Wave

A.N. Azarenkov, O.A. Bizyukov, A.V. Gapon and I.B. Denisenko
Kharkiv State University, Svobody sq.4, Kharkiv, 310077,Ukraine
E-mail: azarenkov@pem.kharkov.ua

The motion of ions in the field of ion-sound surface wave (ISSW) is considered. The investigation is carried out for two planar structures. In the first case is considered the ISSW propagating at the boundary between plasma and vacuum medium. The process for ISSW propagating between two parallel metal planes is investigated too. In the last case the presence of a vacuum-gap sheath region separating the metal planes from the plasma is assumed. The consideration of problem studied is carried out for different values of the plasma density, electron temperature, field frequency and field amplitude. The process is studied for argon and flour plasmas. The obtained results have shown that by a means of varying of plasma density, electron temperature, field frequency and field amplitude the different velocities of ions and directions of their motion may be reached. The carried out investigation has a technological importance too. On the base of studied process the construction devices for polishing of surfaces is possible. The conditions when number of particles which fall on the polished surface (which is parallel to boundary between a plasma and a vacuum region) under angle smaller when 60 degree (oblique particles) is more when 50% from all particles which takes part in motion in SW field are founded. The dependencies of number of oblique particles from field frequency, amplitude, electron temperature and plasma density are obtained.

1Q29

The Dispersion Properties of Ion-Sound Surface Waves Propagating Between Two Parallel Metal Planes and Some Applications of These Waves.

N.A. Azarenkov, I.B. Denisenko and A.V. Gapon
Kharkiv State University, Svobody sq.4, 310077 Kharkiv, Ukraine
E-mail: azarenkov@pem.kharkov.ua

The dispersion properties and electromagnetic field topography of ion-sound surface waves (ISSW) propagating between two parallel metal planes are investigated. The presence of a vacuum-gap sheath region separating the metal planes from the plasma is assumed. The dependence of the surface-wave dispersion properties on plasma density, electron temperature, sheath thickness and thickness of plasma layer is presented for symmetrical and anti symmetrical surface waves. It is shown that in the case when the sheathes are absent the studied surface waves can not exist. The regions of frequencies where the symmetrical and anti symmetrical waves have a normal dispersion dependence and anti symmetrical ISSW have anomaly dispersion dependence is founded. The comparison of the dispersion curves obtained for the case of the ISSW propagating between a semiinfinitive plasma bounded vacuum medium is carried out. The shifts of wavenumber and frequency ranges compared with the case of a semiinfinitive plasma bounded vacuum region for cases of symmetrical and anti symmetrical waves is found too.

The possibility of application of studied structure for creation of gas discharge produced and sustained by the ISSW is considered. It is shown that the application of the ISSW propagating in the studied structure for polishing of surfaces is possible.

1Q30

Electron Interactions with C_2F_6

L.G. Christophorou* and J.K. Olthoff
National Institute of Standards and Technology Gaithersburg, MD 20899

Perfluoroethane (C_2F_6) is a man-made gas with many important applications in the semiconductor industry, in plasma chemistry and etching technologies, and in pulsed power switching. Knowledge of the interactions of slow electrons (≤100 eV) is fundamental in optimizing the parameters involved in particular applications and in modeling industrial processes. We, therefore, have critically assessed and synthesized existing knowledge on electron interactions with C_2F_6, as done previously for CF_4 [1]. With the exception of electron attachment and electron impact ionization, the existing data on most of the fundamental electron-C_2F_6 interaction processes are limited. Nontheless, the present synthesis has led to a reasonable body of results which will be presented and discussed. These include (I) cross sections for total electron scattering, total and partial ionization, momentum transfer, integral elastic, vibrational inelastic, total dissociation, and electron attachment; and (ii) coefficients for electron attachment, ionization, effective ionization, and electron transport (drift velocity and lateral electron diffusion). Cross sections for electron scattering, momentum transfer, and dissociation of C_2F_6 into neutral fragments are especially needed.

[1] L.G. Christophorou, J.K. Olthoff and M.V.V.S. Rao, J. Phys. Chem. Ref. Data **25**, 1341 (1960.

*Also at the Department of Physics, The University of Tennessee.

Research sponsored in part by the U.S. Air Force Wright Laboratory under Contract No. F3361596-C-2600 with the University of Tennessee.

1Q31

High-Accuracy Expressions for the Rotational-Vibrational Energies of the O_2, N_2, NO and CO Molecules

Francisco J. Gordillo-Vazquez and Joseph A. Kunc
Department of Aerospace Engineering and Physics University of Southern California, Los Angeles, CA

Properties of rotationally and vibrationally excited diatomic molecules are of significant importance in studies of dissociation and rotation-vibration, vibration-vibration and vibration-translation transitions in high-temperature gases in material and plasma processing, light sources and environmental studies.

Application of the Hamilton-Jacoby theory and the Bohr-Sommerferld quantization rule to the rotating Morse oscillator yields analytical expressions for the rotational-vibrational energy levels of the O_2, N_2, NO and CO molecules in electronic ground states. The expressions give more realistic values of the moderately and highly excited rotational-vibrational levels than the corresponding levels obtained from the common truncated expansion solution of the Schrödinger equation for the rotating Morse oscillator.

Spectroscopic Determination of W I and W II Oscillator Strengths

B. Michelt, R. Sielker and J. Mentel
Allgemeine Elektrotechnik und Elektrooptik
Ruhr-Universität Bochum, D-44870 Bochum, Germany

Oscillator strengths of 43 W I and 27 W II lines in the wavelength range 240-560 nm have been measured with a wall-stabilized arc. The arc was operated at 10-80 A in argon at atmospheric pressure with an admixture of tungsten hexafluoride. A set of relative W I and W II f-values was determined by a combination of emission and absorption measurements with a special optical setup. The qualities of these measurements do not require any assumptions concerning the plasma state. The relative set of 43 W I lines has been converted to an absolute scale by means of radiative lifetimes. The overall uncertainties of these oscillator strengths are within 10% for strong up to 36% for weak lines. The relative oscillator strengths of 9 W II lines have also been converted by using the radiative lifetimes of the upper levels. Because of missing lifetime data the absolute oscillator strengths of 18 W II lines had to be determined with the aid of temperature measurement under the assumption of a Boltzmann distribution. The absolute error for these f-values lies between 7% and 17%.

Monday, 19 May 1997
1:30 p.m. – Kon Tiki Ballroom

Plenary Session

Plasma Propulsion for Deep-Space Missions

Professor Roald Z. Saagdeev

University of Maryland, College Park, MD, USA

Chair: S.L. Ossakow

Monday Afternoon, 19 May 1997
3:00 p.m. – Kon Tiki Ballroom

Oral Session 2A:
5.1 Non-Equilibrium Plasma Processing II
Chair: B. Cluggish

2A01-02 *Invited*

Surface Modification of Polyurethane and Silicane Rubber for Biomedical Applications

Zhizhen Jiang, Changqion Zheng and Junguo Ran
Sichuan Union University, (Chengdu University of Science and Technology)
Chengdu, Sichuan 610065, P.R. China

There are many exciting and novel plasma discharge treatments and processes which may be used to modify the surface of biomaterials and make them useful in diagnostic or therapeutic applications.

Radiofrequency, inductively coupled glow-discharge plasmas affect materials only over a range of hundreds to thousands of angstroms in depth, even over long exposure times. This allows surface modification of biomedical polymers without affecting the bulk properties of the materials.

In this paper, we report research on the surface modification of biomedical polyurethane with nitrogen, argon, hydrogen, and methane for enhanced blood compatibility. We also report the surface modification of silicane rubber, used to make contact lenses, with ammonia, argon, methane, and oxygen for hydrophilicity and impermeability to proteins, lipids, and other macromolecules. Such treatment does not affect the oxygen permeability of the contact lens. Optical transmission shows only a slight decrease from 90% to 86.4%. Modified surfaces in both applications were characterized using attenuated total reflectance infrared analysis (ATR-IR) and electron spectroscopy for chemical analysis (ESCA). Surface morphologies were determined using SEM images. The molecular mechanisms of surface modification were probed using thermally stimulated current (TSC) spectroscopy. Results demonstrate that plasma processes can achieve significant improvement in the clinical application of polymeric materials.

2A03

High Power Nitrogen-Incorporating Remote Plasma Oxidation Process for MOS Applications

C.G. Parker, G. Lucovsky and J.R. Hauser
North Carolina State University, Raleigh, NC 27695

A 400W remote plasma oxidation process has been developed in a cluster tool which uses N_2O and O_2 for controlling incorporated amounts of nitrogen within the grown oxide. This technique has been developed for Si/SiO_2 interface formation for addition of nitrogen at the interface. Verification through in-situ Auger electron spectroscopy demonstrates that nitrogen is incorporated within the 15 Å grown oxide and is therefore confined to the Si/SiO_2 interface. Ex-situ SIMS analysis indicates incorporation of ~8 x 10^{14} atoms/cm^2 of nitrogen at the interface for a 30 second oxidation in pure N_2O, and the nitrogen content can be effectively controlled by adding O_2 to the process mixture and varying the N_2O/O_2 percentage. Gate stacks for MOS devices are fabricated by depositing a bulk oxide by remote plasma enhanced CVD (RPECVD) on top of the grown interface and then capping the structure with rapid thermally deposited polysilicon. MOSFET devices demonstrate the usefulness of this oxidation technique for interface formation. Device mobility at high field is increased with no degradation in peak mobility. Also device lifetime in hot electron stress tests is greatly increased with no degradation in peak mobility. Also device lifetime in hot electron stress tests is greatly increased with the addition of nitrogen at the Si/SiO_2 interface. When compared to gate oxides grown by rapid thermal oxidation in N_2O, MOSFETs using this two-step remote plasma oxide process demonstrate equivalent device mobilities.

This work is supported by NSF, SRC, and ONR.

2A04

Reaction Pathways for Nitrided Si-SiO_2 Interfaces by Remote Plasma Assisted Oxidation

H. Niimi, K. Koh and G. Lucovsky
North Carolina State University, Raleigh, NC 27695

Nitrided Si-SiO_2 interfaces have been prepared by a 300°C remote plasma assisted oxidation (RPAO) process. The process uses excited species created by rf plasma excitation of He/N_2O gas mixtures. Flow rates of He and

N_2O through a 1 inch plasma tube are 200 sccm and 20 sccm; rf plasma power at 13.56 Mhz is 15 W. Plasma activated species have been monitored by in-situ optical emission spectroscopy (OES) and mass spectrometry (MS). The active species for nitrogen incorporation at the growth interfaces is NO+ as identified by MS. Interface formation process is a two step microscopic process in which NO+ species react initially with the SI substrate and produce Si surface nitridation. The Si-N surface bond is attacked by O_2* metastable species produced concurrently with NO+ resulting in N-atom removal and oxide growth. This is followed by N-atom reinsertion "underneath" the growing oxide film. Since off-line SIMS and optical second harmonic generation measurements indicate interface nitridation at the monolayer level, the N-atom reinsertion step is the "fast" step, and the N-atom removal-oxide growth step is the rate limiting step. This mechanism has been confirmed by experiments in which (a) O-atom terminated interfaces were prepared by RPAO, and (b) N-atoms have eliminated from interfaces by sequential processing in N_2O and O_2.

This work is supported by NSF, SRC, and ONR.

2A05

Profile of Electric and Magnetic Field Strength in New Plasma Source Using Coaxially Symmetric Surface Wave in VHF Band

Shunjiro Ikezawa, Ryuichi Miyano, Jun-ichi Inaguma, Yasunori Shiraki, Yasuhiro Mikawa, Kiyohide Baba, Keisuke Kida, and Akira Nishiwaki
Chubu University, Kasugai, Japan
Masaaki Nagatsu
Nagoya University, Nagoya, Japan
Yukio Okamoto
Toyo University, Kawagoe, Japan
Shigehiko Nonaka
Toyota Technological Institute, Nagoya, Japan
Masashi Kando
Shizuoka University, Hamamatsu, Japan

For plasma process, a uniform plasma over larger area has been required. As the plasma source satisfying this condition, surface-wave produced plasma (SWP) utilizing rf or microwave has gained attention as new plasma sources. Therefore, a new type of SWP employing coaxial antenna, into which rf (frequency of 149 MHz in VHF band and power of 900 W) is launched, is presented in this report. Its remarkable advantage is that the form of the produced plasma can flexibly vary with bending the antenna. In order to apply it to various processes, it is necessary to understand basic characteristics. Hence, we calculated profiles of electric and magnetic field strength, using finite-element method. As a result, it is found that surface wave propagating in the boundary between dielectric and plasma surfaces produces a plasma, and the plasma diffuses in the radial direction.

2A06

Study of Plasma Chemistry in Plasma Doping Processes

Shu Qin, Yuanzhong Zhou, Chung Chan
Plasma Science and Microelectronics Laboratory
Department of Electrical and Computer Engineering
Northeastern University, Boston, MA 02115
Jiqun Shao and Stuart Denholm
Eaton Corporation, Semiconductor Equipment Operations, 108 Cherry Hill Drive, Beverly, MA 01915

Plasma ion implantation (PII) is a promising method for semiconductor doping. However, due to the lack of a mass separation mechanism, all ions in the chamber will be implanted. The dopant sources for PII doping are compound gases such as B_2H_6, BF_3, PH_3, *etc.*, or the mixtures with H_2 or He gases for safety. The study of plasma chemistry for these multi-species plasma is very important for the precise prediction of the doping results and optimal control of the process. Because the dopant gases such as B_2H_6, PH_3, AsH_3, *etc.* are highly toxic, modeling and simulation of the dopant plasmas and processes are necessary for safety.

An empirical-analytic approach has been used for the plasma chemistry analysis of PII doping experiments. Least square (LS) fittings of SIMS profiles have been performed to find the relationship between gas, plasma, and dose compositions in multi-species plasmas and to optimize gas recipes and process conditions. A dynamic sheath model of the multi-species plasma has been used as a basic function for fitting. Good consistence between modeling and experiments for BF_3 and PH_3 PII doping processes was present. A PDP1 plasma simulation verified the results of the modeling.

2A07

Hydrodynamic and Analytical Models for Plasma Immersion Ion Implantation with Dielectric Substrates

Yuanzhong Zhou, Shu Qin and Chung Chan
Plasma Science and Microelectronics Laboratory
Department of Electrical and Computer Engineering
Northeastern University, Boston, MA 02115

The characteristics of the plasma sheath and ion energy during plasma immersion ion implantation (PIII) process are very important for the optimum configuration design and process control. A hydrodynamic model and a quasistatical model have been established to describe PIII process for dielectric substrates.

The models include the effect on the voltage at the dielectric-plasma interface from both the charges in the sheath and accumulated in the insulating layer. In the analytical model, explicit formulas are found for determining ion-matrix and dynamic expanding sheaths, ion current density to the target surface, the voltage at the dielectric-plasma interface. In the hydrodynamics model, Poisson's equation is applied to the dielectric and plasma region. Upon this model, numerical simulation is carried out to obtain the ion current density, the ion and electron density distributions, the implanted ion energy, the potential and electrical field distribution. The results indicates that previous models using a capacitor to present dielectric layer underestimate the effect of the insulating surface.

2A08

A Theory of the Plasma Torch for Waste-Treatment

Han S. Uhm
Naval Surface Warfare Center
West Bethesda, MD 20817 USA
Sang H. Hong
Seoul National University, Seoul 151-742, Korea

Arc-plasma technology has broad applications to waste treatment processing including the safe disposal of hazardous and low-level radioactive wastes. The plasma torch could be useful to the development of an efficient, compact, lightweight, clean burning incinerator for industrial and municipal waste disposal in an environmentally beneficial way. We therefore develop a simple theoretical model describing physics of the plasma torch plume in connection with its applications to the arc-plasma waste-treatment system. The theoretical analysis is carried out by making use of Bernoulli's pressure-balance equation, which provides a stable equilibrium solution of the gas density in the plume ejected from the torch into a high-pressure reactor chamber with $4\varepsilon < 1$. The pressure depression parameter ε is proportional to the gas temperature and inversely proportional to the square of the chamber pressure. In a low-pressure chamber, characterized by $4\varepsilon > 1$, there is no stable equilibrium solution satisfying Bernoulli's equation. Therefore, it is expected that the observable plasma data may change abruptly as the chamber pressure crosses the borderline defined by $4\varepsilon = 1$. Indeed most of the plasma data measured in an experiment change abruptly at the pressure borderline of $4\varepsilon = 1$.

*Work was supported by the IR fund at NSWC and by the Ministry of Trade, Commerce and Industry in Korea.

Monday Afternoon, 19 May 1997
3:00 p.m. – Board Room

Oral Session 2B:
1.1 Basic Processes in Fully Ionized Plasmas – Waves, Instabilities, Plasma Theory, etc. II
Chair: D.K. Kalluri

2B01-02 *Invited*

Heating and Melting of the Dusty Crystal in rf Discharge

I.V. Schweigert and V.A. Schweigert†
Institute of Semiconductor Physics, Novosibirsk, Russia
†Institute of Theoretical and Applied Mechanics, Novosibirsk, Russia

The non-linear analysis of instability of the dusty crystal in the sheath of radio-frequency discharge is presented. Varying the gas pressure, we revealed the boundaries of stability of the crystal for Coulomb and screened potentials. The analysis have been done on the base of numerical calculations of the system of Newton equations for particle motion. Using the periodical boundary conditions we simulated only the fragment of 448 particles of infinite in the radial direction hexagonal lattice which has two layers in the longitude direction.

The repulsion between particles of the lattice, the attraction between particles and effective positive charges of ion clouds are taken into account. We consider also the changing of kinetic energy of particles due to friction and impacts with neutral atoms. As a result we obtain the temperature of particles as function of time and friction, the critical pressure for phase transition, introducing the modified Lindeman criteria. The calculated mean temperature for the different pressure coincides with experimental one.

2B03

An Analytic Treatment for Radial Density Profiles of a Large ECR Source

K.-S. Chung, S.M. Hwang*, G.H. Kim†, J.I. Kim,
J.S. Chun, T.H. Noh, D.H. Chang
Department of Nuclear Engineering,
Hanyang University, Seoul, Korea
**Joint Research Facility, Korea Basic Science Institute*
Daejeon, Korea
†Department of Physics, Hanyang University,
Ansan, Korea

Radial variations of ion densities are measured by a scanning electric probe in a large electron cyclotron resonance plasma source with diameter 160 cm and height 70 cm. Measured density profiles are explained by an analytic fluid model based upon the classical transport theory assuming the plasma generation along the resonance layer. Dependance of density profiles on the position of resonance layer and magnitude of magnetic flux along the radial direction are analyzed. Improvement of uniformity by changing the resonance position and application to the development of larger plasma sources will be discussed.

2B04

Sawtooth Oscillation in the IR-T1 Tokamak with Tomographic Reconstructions

M. Ghorannevis, M. Bakhtiary, M.R. Salami,
A.K. Tafreshi, M. Zamani Mehr, J. Mirzaei
Plasma Physics Research Centere of I.A.U.
Poonak, Hesarak, P.O. Box 14835-159 Tehran, Iran

The IR-T1 tokamak is an air-core transformer type with major and minor radii of 45.00 cm and 12.50 cm respectively. Other major parameters are as follows:

$$I_p = 25 - 40\ kA$$

$$\eta_e = 1.3 \times 10^{13} \frac{1}{cm^3}$$

$$V_\ell = 2.6 - 8v$$

$$Z_{eff} \leq 2$$

$$T_e = 180 - 250\ eV$$

$$B_t = 0.6 - 0.9 Tesla$$

The major heating system is ohmic. In order to investigate and study the instability we used tomography in conjunction with Cormack's method. Fourier expansion of Cos(mφ) and Sin(mφ) were applied on soft x-ray profiles. The rigid rotation assumption of the plasma column and least-square fit method for derivation of coefficients of Zernicke polynomial were used to find the final dispersion equation.

As a result large m=1 oscillation in soft x-ray signals have been observed in the IR-T1 tokamak and has been found that this phenomenon is caused by rotation of plasma column containing perturbation, the reconstructed images revealed that in the phase before a sawtooth crash, the hot plasma core has moved gradually toward the wall. This is considered as the increasing m=1 kink mode. Detail will be in full paper.

2B05

Narrow, Stationary and Stable Electric Field Spikes Produced by an Electron Beam in an Inhomogeneous Plasma

H. Gunnell, J.P. Verboncoeur, N. Brenning and S. Torvén
Div. of Plasma Physics, Alfvén Laboratory,
Royal Institute of Technology,
SE-100 Stockholm, Sweden

In a laboratory experiment it is found that high frequency waves, which are driven by a strong electron beam propagating along a density gradient, can form stationary, spatially concentrated "HF spikes" which extend typically one wavelength (in our case 1 cm) in the direction along the electron beam. The frequency is of the order of the plasma frequency. Both the experiment and closely matched computer simulations show that the spike is a standing wave with nodes at the boundaries to regions with propagating waves.

Judging from the simulations, this type of standing narrow HF spike only forms in plasma density gradients. The same electron beam in a homogeneous plasma excited propagating waves in the same frequency range, but with an amplitude which varied much more slowly along the beam.

In contrast to cavitons formed by Langmuir collapse (see *e.g* Wong and Cheung, Phys Rev. Lett. 1984, vol 52, no 14, p. 1222) the HF spikes form without trapping of the waves in density cavities, and remain stable after formation, *i.e.*, there is no tendency towards collapse of the structure.

First results are published in Phys. Rev. Lett. 77, 5059 (1996).

2B06

On A Sphere of Applicability of the Vlasov Equation

V. I. Erofeev
Institute of Automation & Electrometry,
Siberian Branch of Russian Academy of Sciences

At the International Conference of Plasma Physics NAGOYA 96 the author reported a new calculation of the collision integral for three-wave interactions [1]. Unlike the traditional calculations based on the Vlasov equation, this one was based on the Klimontovich-Dupree equation. Formally, the latter equation is the same partial differential equation as the former one. The difference is only in assumptions on the solution to this equation. Conceptually, the Klimontovich-Dupree equation operates with a mixture of discrete charged particles, whereas the Vlasov equation eventually with an imaginary continuous liquids of electron and ion components. The former mixture is a more realistic approximation to a real plasma than the latter liquids; the new three-wave collision integral far exceeds its traditional counterpart, therefore the genuine picture of non-linear phenomena in a collisionless plasma cannot be revealed with applying the Vlasov equation.

Here we demonstrate in another way that the sphere of application of the Vlasov equation should be reduced. Consider a plasma with large spatial scales of slow motions. In this plasma a smooth distribution can be defined by averaging of the usual Klimontovich-Dupree's distribution (the microdistribution further on) over small (but voluminous with respect to the particle content) vicinities of points in phase space. The Vlasov's distribution cannot but coincide with this averaged microdistribution. But the time derivative of the latter differs with the Vlasov equation. This derivative is defined by the difference of the particle currents entering the domain of averaging and leaving it. Apart from the terms that correspond to the Vlasov equation, this difference contains some correlative terms that are due to the plasma discreetness. Their contribution is stressed in comparison with the former terms, because of the electron screening of the ion electric fields.

[1] Erofeev V.I., *Derivation of an equation for three-wave interactions based on the Klimontovich-Dupree equation*, J. Plasma Phys., 1997 (in press).

2B07

Surface Waves Parametric Excitation in Planar Plasma Filled Waveguides

N. Azarenkov and V. Girka
Kharkiv State University, Kharkiv, Ukraine
A. Sporov
Scientific & Technological Center of Electrophysics,
National Academy of Sciences of Ukraine,
Kharkiv, Ukraine

The report is devoted to the investigation of parametric excitation of the surface waves on the second harmonic of electron cyclotron frequency (SW) in uniform planar plasma layer bounded by two thick dielectric slabs. External steady magnetic field $\vec{B}_o$ is applied parallel with

respect to plasma-dielectric interface. The studied SW are extraordinary polarized modes and propagate across $\vec{B}_o$. The problem is solved in kinectic approach under the condition of weak plasma spatial dispersion. The amplitude value of the electric pump wave is assumed to be a small one. We consider the case of a dense plasma (plasma frequency is much greater than a cyclotron one). The effect of the pump wave and waveguide parameters on the increment value is studied. Simple analytical expressions of the eigenfrequencies of the SW, their damping rates and increments of parametrical instability are calculated. They are in a good accordance with the results of the carried out numerical investigation. The obtained results can be used in controlled fusion of the carried out numerical investigation. The obtained results can be used in controlled fusion researches in order to avoid undesirable regime of the plasma periphery heating in fusion devices which use the resonance electron cyclotron heating methods.

2B08

Quantization Problems of Electromagnetic Field 2

Milán Mészáros
α Group Laboratories, Inc., Institute of Physics,
11 Rutafa Street, Bldg. H, H-1165 Budapest, Hungary
Phone/Fax: + 36(1) 403 7544
E-mail: alphagr@mail.c3.hu

Present paper shows up that the deforming electromagnetic radiation fields (photon gas) or deforming ionized plasma cannot be quantized, in general. Namely, in deforming systems, the quantum structure of the fields collapses generally because then a magnetic current density appears in the Maxwell equations. But these completed Maxwell equations have a nonsinusoidal solutions in general. Therefore, changing topology of quantum radiation fields or quantum plasmas cannot exist.

In connection with these systems this question is raised: Can the general nature of the behaviour of the deforming electromagnetic radiation systems be investigated without quantum physics with the help of qualitative theory of second-order linear differential equations so that the results are true with respect to classes of fast-changing or singular deformations?

Present paper answers this question and presents some applications, too.

References

(1) Milán Mészaros, *"Adiabatic Change of State of Photon Gas"* accepted for publication in; *The Enigmatic Photon*, Vol, IV, Chap. 7, ed. by M. W. Evans and J. P. Vigier (Kluwer Academic Press, Dordrecht, 1997).

(2) Milán Mészaros and Pál Molnár, Physics Essays **5**, 463 (1992).

(3) Henning Harmuth, *Propagation of Nonsinusoidal Electromagnetic Waves* (Academic Press, New York, 1986), Chapters 1.7 and 1.8, pp. 36-43.

2B09

Lyapunov Stability of MHD-Like Plasmas with Flows

Victor I. Ilgisonis
RRC "Kurchatov Institute", Moscow 123182, Russia

An adequate variational approach allowing for a stability analysis of plasmas with stationary flows is developed. This approach generalizes the method successfully applied to ideal magnetohydrodynamics (MHD) with both isotropic [1] and anisotropic [2] plasma pressure for a case of a nonabelian Hamiltonian plasma dynamics obeying, e.g., the Hall MHD [3] or Electron MHD. The key element of the approach is a use of the Clebsh-like representation of Hamiltonian instead of the adding to the Hamiltonian an arbitrary chosen set of Casimirs (while the whole set is infinite). Such a procedure makes the sufficient stability criterion to be obtained closer to a necessary one than earlier known.

[1] V.I. Ilgisonis, V. P. Pastukhov, Plasma Phys. Rep., **22**(3), 228 (1996).

[2] V.I. Ilgisonis, Physics of Plasmas, **3**(12) (1996).

[3] D.D. Holm, Physics of Fluids 30(5), 1310 (1987).

Monday Afternoon, 19 May 1997
3:00 p.m. – Toucan Room

Oral Session 2C:
2.6 Microwave-Plasma Interactions
Chair: T. Katsouleas

2C01-02 ***Invited***

ATMOSPHERIC PRESSURE COLLISIONAL PLASMA ABSORBER: THEORY, EXPERIMENTS, AND ISSUES RELATING TO EFFICIENT PRODUCTION

Robert J. Vidmar
SRI Intrernational, Menlo Park, CA 94025

The dispersion relation for a cold collisional plasma is known to predict absorption of radio frequency waves due to energy transfer from the wave to plasma electrons, and then to a neutral species in a momentum-transfer collision. For a plasma source that generates a smooth decreasing electron density as a function of decreasing distance from the source, theoretical models predict that the reflection coefficient from such plasma distributions can be very small. Hence, a collisional plasma with smooth density gradients can attenuate radio frequency waves without significant reflection. Calculations for a collisional plasma with a smooth gradient predict broadband absorption of 40 dB or more from 100 MHz to 10 GHz. Experiments using electron-beam impact ionization and photon sources for photoionization have quanitfied laboratory-scale plasma absorbers in waveguides and cubic-meter-size systems operating at atmospheric pressure. Simple but efficient means of plasma production in air are needed, but have been slow in development. Modern approaches will be discussed, as well as fundamental processes in a plasma made of ambient air that affects the power budget for plasma production.

This work was supported by the Air Force Office of Scientific Research under Contract F49620-95-C-0009.

2C03

VUV Laser Plasma Formation and Microwave Agile Mirror/Absorber

J.E. Scharer, K. Kelly, G. Ding and M. Bettenhausen
Dept. of Electrical and Computer Engineering
University of Wisconsin–Madison, Madison, WI 53706

Agile microwave reflectors are of interest as potential replacements for large phased arrays on mobile crafts. Preliminary measurements of microwave reflection from a VUV (λ = 193 nm) excimer laser produced plasma (W = 20 mJ, τ = 17 ns) in an organic gas (TMAE).[a,b] This work investigates the reflection of X-band microwaves at oblique incidence by a planar TMAE sheet of dimensions: 8 cmW × 4-15mm H × 20- cm L, produced by a new (W = 300 mJ) excimer laser. Fast Langmuir probes are used to determine the laser produced plasma density and temperature profiles, at TMAE neutral pressures in the 25-60 m Torr range. Densities and temperatures in the ranges of $n = 5 \times 10^{12} - 2 \times 10^{13}$ cm^{-3} and T_e = 0.5-0.7 eV are obtained. The amplitude and phase of the transmitted and reflected microwave signals are measured using both homodyne and heterodyne systems with hybrid-tee mixers. A time history of the plasma temperature and density is obtained with Langmuir probes and compared with measurement based on microwave transmission through the plasma. Reflected and transmitted signals are compared with those from a calibration aluminum sheet of the same dimensions as the plasma. Future plans for plasma creation in air will be discussed.

Acknowledgments

This research is supported by AFOSR Grant F44620-94-1-0054 and an AFOSR AASERT Award.

[a]Y.S. Zhang and J.E. Scharer, "Plasma Generation in TMAE Vapor by an Ultraviolet Laser Pulse," J. Appl. Phys. **73**, p. 4479 (1993).

[b]W. Shen, J.E. Scharer, N.T. Lam, B.G. Porter and K.L. Kelly, "Properties of a Vacuum Ultraviolet Laser Created Plasma Sheet for a Microwave Reflector," J. of Appl. Phys. **78**, p. 6974 (1995).

2C04

Radiation Generation by an Ionization Front in a Gas-Filled Capacitor Array

P. Muggli, R. Liou, C.H. Lai and T. Katsouleas
University of Southern California, Los Angeles, CA
C. Joshi, W.B. Mori and J. Dawson
University of California at Los Angeles, Los Angeles, CA

A new radiation source, in which the static electric field of an alternatively biased capacitor array is directly converted into coherent radiation by a laser produced ionization front (i.e., a moving vacuum/plasma boundary), is investigated experimentally. The frequency of the radiation is approximately given by $\omega_p^2/2k_oc$, where $k_o=\pi/d$ is the wavenumber defined by the distance d between the capacitors. Its electric field is approximately equal to that of the capacitor field E_o. The device can potentially produce coherent pulses of high power (MW), tunable radiation in different frequency regimes (microwave, Thz, ...). In a proof-of-principle experiment, short (<5 ns) microwave pulses with tunable frequency scaling linearly with the plasma density were generated between 6 and 21 Ghz. These results, as well as results obtained with other structures: Ka-band waveguide and coaxial line in the microwave range, and a μ-structure in the 10 μm range, will be presented.

Work supported by AFOSR grant No. F49620-95-1-0248 and US DoE Grant No. DE-FG03-92ER-40745.

2C05

Time Domain Wave Phenomena in Rapidly Created Periodic Plasmas

S.P. Kuo, James Faith and E. Koretzky
Department of Electrical Engineering
Polytechnic University, Farmingdale, NY 11735

Periodic media are of great interest in the field of solid state physics as the potential formed by a regular lattice of ions is periodic. In this case the dispersion relation of the electron wave has a band diagram which determines the frequencies of all the Floquet modes. Likewise, if the plasma is produced with a periodic spatial distribution, the dispersion relation of the electromagnetic wave is also expected to become an infinite number of discrete branches, where each branch represents a Floquet mode. It is also known that the frequency of a wave in a rapidly created uniform plasma is upshifted in order to satisfy the new dispersion relation.[1] Therefore, the additional periodic feature of the rapidly created plasma will convert the preexisting background wave into many components corresponding to the Floquet modes of both upshifted and downshifted frequencies.[2]

Experimental and numerical results will be presented. It will be shown that under the appropriate condition, i.e., the initial frequency of the wave is less than the maximum plasma frequency, the downshifted modes will be trapped within the periodic plasma structure until the plasma decay away. This trapping has the practical effect of greatly enhancing the efficiency of the interaction process for the generation of frequency downshifted spectral lines. The experiment is simulated numerically and good agreement is demonstrated. A theory based on the impedance distribution of the plasma for each Floquet mode is formulated to explain the wave trapping phenomenon.

1. S.P. Kuo, Phys. Rev. Lett. 65, 1000 (1990).
2. James Faith, S.P. Kuo and Joe Huang, Phs. Rev.E, 55 (1), 1997.

2C06

Tunable Microwaves from Cerenkov Wakes in Magnetized Plasma

J. Yoshii, C.H. Lai and T.C. Katsouleas
University of Southern California,
Los Angeles, CA 90098-0484
W.B. Mori and C. Joshi
University of California at Los Angeles,
Los Angeles, CA 90024

The Cerenkov wake excited by a particle beam or short laser pulse in a perpendicularly magnetized plasma is analyzed. The wake has both electrostatic and electromagnetic components and couples to a vacuum microwave at the plasma/vacuum boundary. The transmission coefficient depends on the boundary scale length and the ratio of ω_c/ω_p. The frequency of the forward going radiation is approximately ω_p, and its amplitude is ω_c/ω_p times the amplitude of the wake excited in the plasma (for a sharp boundary). The possibility of tapering the magnetic field and density profile to optimize the output coupling is then discussed for a continuous boundary. We also use 1-D PIC simulations to verify the scaling laws. Since plasma wakes as high as a few GeV/m are produced in current experiments, the potential for a high power (i.e., Gwatt) coherent microwave to Thz radiation source exists.

2C07

Electromagnetic Wave Propagation Below Cutoff

P. Sprangle and E. Esarey,
Plasma Physics Division,
Naval Reseach Laboratory, Washington, DC
B. Hafizi
ICARUS Research, Inc., Bethesda, MD
S.E. Harris
Stanford University, Stanford, CA

A small amplitude electromagnetic wave can propagate in a plasma below cutoff in the presence of a high frequency large amplitude wave. This is referred to electromagnetically induced transparency (EIT).[1] We extend the analysis of EIT to include relativistic and collisional effects as well as density gradients. We show that the small amplitude wave is unstable in certain parameter regimes. Well above cutoff the instability goes over to the usual backward Raman instability. In addition, the propagation of a large amplitude wave in an inhomogeneous plasma and its penetration beyond the critical surface is analyzed.

Supported by ONR and DOE.

[1]S.E. Harris, Phys. Rev. Lett. 77, 5357 (1996).

2C08

γ-Ray Production in Colliding Laser Pulses

F.V. Hartemann, J.R. VanMeter and N.C. Luhmann, Jr.
Dept. of Applied Science,
University of California at Davis, Davis, CA
A.K. Kerman
Physics Dept., Massachusetts Institute of Technology, Cambridge, MA

The acceleration of charged leptons to a TeV energies is a problem of considerable importance. At these energies, electroweak spontaneous symmetry breaking and the Higgs mechanism are expected to play a dominant role in the interaction physics. Alternatively, short wavelength photons can also be used to probe this energy range, as exemplified by the γ–γ collider project. We show that the combination of vacuum ponderomotive acceleration with Compton backscattering can produce high energy photons with a high intensity laser and an electron beam of relatively modest energy. In this manner, the high energy acquired by the electrons within the drive laser pulse is effectively extracted in the form of short wavelength photons by a colliding probe laser pulse, without requiring complex structures to terminate the interaction. In this process, the photon energy scales as

$$h\nu \cong 4\frac{hc}{\lambda_0}\gamma_0^2 A_\perp^4 \quad ,$$

where λ_0 is the laser wavelength (pump and probe), γ_0 is the electron beam energy, and

$$A_\perp = \frac{e\lambda_0}{\pi m_0 C^{5/2}}\sqrt{\frac{I_0}{2\varepsilon_0}} \quad ,$$

is the normalized vector potential of the drive wave laser wave. For example, 1-TeV photons could be produced with an 8.5 10^{20} W/cm^2 drive pulse at 800 nm, interacting with a 550 MeV beam. By comparison, an FEL using the same laser wavelength for an electromagnetic wiggler would require over 200 GeV of beam energy.

Work supported by DoD/AFOSR (MURI) F49620-95-1-0253, AFOSR (ATRI) F30602-94-2-001, ARO DAAH04-95-1-0336, and LLNL/LDRD DoE W-7405-ENG-48 IUT B335885.

2C09

Wave Propagation in a Transient Anisotropic Plasma Medium—Development of a Green's Function

Dikshitulu K. Kalluri, Tom Huang
Department of Electrical Engineering,
University of Massachusetts at Lowell,
Lowell, MA 01854

Transient plasmas have a time-varying plasma frequency $\omega_p(t)$ with a rise time T_r, If the period t_0 of a source wave existing before the transient effect begins is much larger than the rise time, the ionization change may be idealized as a sudden switching of the medium. The solution to this initial value problem with a step-change in the electron density profile is known and this profile will be considered as a reference profile. The switching action gives rise to new waves whose frequencies are either upshifted or downshifted.

The topic of this paper is the solution of the initial value problem when t_0 is comparable to the rise time T_r. The initial motivation for investigating the problem is given below.

Using the solution for the reference profile, Green's function for a switched anisotropic plasma medium is constructed. Using the Green's function a perturbation

technique is developed and the solution of the initial value problem, when t_0 is comparable to T_r, is obtained.

The power reflection coefficient vs the rise time T_r of an R2 [1] wave for various values of the electron gyrofrequency f_b are calculated.

[1] D.K. Kalluri, *IEEE Trans. Plasma Sci.*, vol. 21, no. 1, pp 77-81.

Monday Morning, 19 May 1997
3:00 p.m. – Macaw Room

Oral Session 2D:
2.5 Microwave Systems and
2.4 Slow Wave Devices I
Chair: G.P. Scheitrum

1D01

Low Cost Infrared Temperature Measurement and Optimal Process Control in Microwave Sintering Systems*

J.P. Calame, Y. Carmel, E. Pert and D. Gershon
Institute for Plasma Research, University of Maryland College Park, MD 20742

Ceramic sintering based on microwave heating has the potential to create final products with unique mechanical and electrical properties. This results from the rapid heating cycles which are made possible by the volumetric heating nature of microwaves. An important issue for industrial systems involves the non-contact measurement of temperature at multiple positions in a cost-effective manner. We have been experimentally investigating the application of direct detecting, commercial infrared thermocouples to this problem. We have designed and implemented a system using a series of these detectors in conjunction with movable gold mirrors and BaF_2 optical components (which operate to wavelengths as long as 20 microns). Experiments comparing the accuracy and reproducibility of this system to conventional thermocouples and optical pyrometers will be described for several materials.

Optimal control of the temperature depends on a detailed knowledge of the electromagnetic and thermal response throughout the object undergoing sintering. However, temperature can only be measured at a limited number of locations in the object; hence simulations must be used to infer what is happening in the rest of the object during the sintering process. Such complex simulations cannot be performed in real-time, but instead must be done prior to the sintering and used to form a processing plan of action for actual production. Real-time, closed loop process control can then be used to compensate for differences between reality and the simulations. This concept will be discussed.

*Work supported by AFOSR/MURI and ARO

2D02

Sintering of Ceramic Compacts in a 35 GHz Gyrotron-Powered Furnace*

A.W. Fliflet, R.W. Bruce† and R.P. Fischer
Plasma Physics Division,
D. Lewis, III, B.A. Bender, G.-M. Chow and R.J. Rayne,
Materials Science and Technology Division,
L.K. Kurihara and P.E. Schoen,
Center for Biomolecular Science and Engineering, Naval Research Laboratory, Washington, DC 20375

The development of powerful gyrotrons has opened up the millimeter-wave regime (≥28 GHz) for processing ceramic materials. Millimeter-waves couple more strongly than pure oxides, eliminating the need for auxiliary heating at low temperatures, and highly uniform fields intensities can be achieved in compact overmoded cavity applicators. A number of low and high frequency microwave sintering studies have generally indicated that sintering proceeds much faster in microwave furnaces than in conventional furnaces, and that densification occurs at lower temperatures. Lower sintering temperatures are desirable for minimizing grain growth which usually has a negative effect on mechanical properties of ceramics. To assess the potential of high frequency microwave sintering, and to investigate the possibility of a specific microwave mechanism, the Naval Research Laboratory (NRL) has recently undertaken a systematic study focused on alumina because of its industrial importance, large data base, and challenging microwave properties. This paper presents 35 GHz sintering data obtained at NRL, using a gyrotron-powered furnace, for fine grain (submicron) alumina compacts and compares our data with results from other high frequency microwave and conventional sintering studies. Our results indicate that the microwave sintering process appears to densify more quickly at a given temperature than in a conventional furnace. However, densification does not appear to occur at much lower temperatures than for conventional sintering. The

faster processing possible in a microwave furnace appears to be helpful in reducing grain growth.

*Work supported by the Office of Naval Research.
†SFA, 1401 McCormick Dr., Landover, MD 20785

2D03

Rapid Waveguide System and Component Design Using Scattering Matrices and Computer Optimization

Lawrence Ives, Jeff Neilson and William Vogler
Calabazas Creek Research, Inc.,
Saratoga, CA 95070

Scattering matrix analysis revolutionized the design of overmoded gyrotron circuits and is now used for designing waveguide components, including pillbox and coaxial windows, mode converters, tapers, and transitions. The addition of computer optimization dramatically reduces design time while significantly increasing performance.

Scattering matrix codes generate the scattering matrix by calculating the coupling coefficients between transitions, including the affects of dielectrics. The input is simple, and the analysis typically takes only a few minutes. The accuracy equals, and often exceeds, that obtained with mesh type codes, such as HFSS and Eminence, and requires a fraction of the time these finite element codes require. The analysis can also find and identify trapped resonances generated by ghost or trapped modes.

Computer optimization maximizes or minimizes a user specified performance function, such as VSWR over a frequency band, by using established routines, such as the Levenberg-Marquardt optimization algorithm. Using this technique, complex ripple wall mode converters with output purities exceeding 99% are routinely obtained in a few hours.

Combining computer optimization with scattering matrix analysis allows users to design entire waveguide systems in a few hours with performance exceeding what usually takes days to obtain with other programs. This presentation will describe the application of scattering matrix and optimization analysis to waveguide system design and provide several examples.

2D04

Computer Analysis Of The Effect Of A Spectrum Anomaly On The RF System For The Cassini Mission

James A. Dayton, Jr. and Jeffrey D. Wilson
NASA Lewis Research Center, Cleveland, OH
Carol L. Kory
Analex Corporation / NASA Lewis Research Center
Cleveland, OH

An anomaly was observed in the output of the flight TWTA (traveling wave tube amplifier) for the 32 GHz experiment scheduled to fly on the Cassini Mission to Saturn which will be launched in October 1997. The anomaly was an apparent intermodulation product in the neighborhood of 35 GHz which was manifest only when the TWTA was driven in a range from 10 to 15 dB below saturated drive. This effect was not observed until 18 months after the production run of the TWT (the Hughes 955H) had been terminated, and the tube and its power supply had been packaged for flight. There was, therefore, opportunity for only very limited testing of the TWTA and no chance of building and qualifying a replacement prior to launch. The effect was observed to occur only outside the expected mission performance profile, however, system engineers had serious concerns that the anomaly might interfere with the 32 GHz experiment if changes in tube performance were to occur during the mission. An analysis of the TWT was conducted using the Detweiler and MAFIA computer codes which produced an explanation of the observed phenomena, a generic defect inadvertently incorporated in the slow wave circuit design, and predicted that the most likely outcome of TWT aging would be to reduce or eliminate the anomaly.

2D05

Gyrotron-Based Millimeter-Wave Beams and their use in Material Processing

T. Hardek, W. Cooke and D. Rees
Los Alamos National Laboratory
P.O. Box 1663, Los Alamos, NM 87545

Researchers at Los Alamos National Laboratory have been utilizing quasi-optical millimeter-wavelength microwave beams for materials processing applications over the past several years. We have recently added a multi-mode-cavity gyrotron-based 30 GHz processing system produced

by the Institute of Applied Science, Nizhny Novgorod, Russia. The new system allows us to process materials in a large-volume uniform 30 GHz microwave field. The system includes a processing chamber which can be evacuated or pressurized to maintain a controlled environment during the processing cycle and is computer controlled to allow experiments to be precisely repeated. The ability to apply uniformly intense microwave fields to large samples or large quantities of small samples under controlled environmental conditions gives our group a unique capability to study materials properties achievable only through microwave processing techniques. An overview of the present status of our gyrotron based facilities is presented along with a detailed description of the new multi-mode gyrotron system.

2D06

MILLIMETER-WAVE FOLDED WAVEGUIDE TWT DEVELOPMENT AT NORTHROP GRUMMAN

D. Gallagher, J. Richards and C. Armstrong
Northrop Grumman Corporation
Electronic & Information Warfare Systems
600 Hicks Road, M/S H6402
Rolling Meadows, IL 60008
Tel (847) 259-9600

A viable manufacturing technology to fabricate rugged, wide band millimeter wave circuits for Traveling Wave Tubes (TWTs) was developed and fully demonstrated. A simple and effective method of obtaining circuit attenuation is inherent to the technology.

Eight devices operating over the instantaneous 40 to 55 GHz frequency band have been fabricated and successfully tested. Test results to be discussed include more than 100 W output power over the 40 to 50 GHz band, with unsaturated power levels of 50 W at 55 GHz, 180 W at mid-band, 135 W average power, 30 dB gain. Reproducibility of device fabrication will also be discussed.

The applicability of the technology in the 80-to-110-GHz frequency range has now been demonstrated by successfully fabricating and testing for the first time ever a full gain circuit with graphite attenuator. The basic design of a PPM focused, 100 W, 30 dB gain device has been nearly completed. The design incorporates the miniaturization technology of the Microwave Power Module (MPM). Therefore the device could be inserted into a W-Band MPM. It is expected that test results will be available by December from this first device.

The application and benefits of high temperature superconducting focusing magnets, as applied to this device, will also be discussed.

Finally, this technology can be easily scaled down in frequency, thereby opening a new array of power amplifiers in Ka-Band or at lower frequency.

2D07

High-Perveance Electron Beams for High-Power, Slow-Wave Microwave Devices*

MA. Basten, J.H. Booske, J.E. Scharer and L.J. Louis
Department of Electrical and Computer Engineering
University of Wisconsin–Madison, Madison, WI

One of the problems in the scaling of high-power vacuum microwave sources to higher frequencies is the need to transport beams with high space charge density, since the rf circuit transverse dimensions tend to decrease with wavelength. Research results establish that novel periodic magnetic focusing optics offer the opportunity to propagate much higher beam currents than previously achievable in slow-wave vacuum microwave devices.

Theory and simulations establish that stable, edge-focused transport of linear sheet electron beams can be realized with periodically-cusped magnetic (PCM) focusing for *very* high current density beams (> 200 A/cm^2) at low beam voltages (10 kV). Edge focusing options include offsetting the poles of the planar PCM array or using periodic permanent quadrupole magnetic (PPQM) edge focusing. Both options provide stable edge focusing with the former method requiring fewer magnet pieces and the latter method providing superior beam matching capability.

Using quadrupole magnetic optics to produce very large aspect ratio elliptical sheet electron beams is well suited for laboratory experiments. Simulation and experimental results with a 10 kV, 2 A electron beam confirm the feasibility of this approach.

Round beam focusing by short period PPQM arrays was also studied. The focusing force from PPQM arrays can be an order of magnitude greater than that of conventional periodic permanent magnet (PPM) arrays for beam voltages from 10-40 kV. Analytic and numerical studies demonstrate the potential of this configuration but also show that beam ripple may be problematic. Experimental measurements are in good qualitative

agreement with the predictions of envelope and PIC code simulations.

*Supported by ONR (DoD Vacuum Electronics Initiative) administrated by NRL, and in part by an NSF Presidential Young Investigator Award.

2D08

Plasma Induced Gain Enhancement in Backward Wave Oscillators Using Pencil Beams

A. T. Lin and Chih-Chien Lin
Department of Physics, University of California Los Angeles, CA 90024-1547

Experiments[1,2] on plasma induced performance enhancement in backward wave oscillators using pencil beams have recently been carried out. In Ref.[1], the enhancement is attributed to the excitation of beam-plasma instability. If this mode is also in resonance with the desired backward wave oscillation, the beam-wave interaction is observed to be substantially enhanced. Ref.[2] observed that the background plasma neutralizes the beam dc space charge force and produces a pinching force which increases the beam current density and facilitates the beam transport. We have carried out computer simulations which show that the device gain can be enhanced just from the response of plasma to the backward wave oscillation without invoking the beam-plasma instability. This is because the direction of plasma response field is always in the same direction as that of the backward wave oscillation.

*This work has been supported by the DoD Muri Program (High Energy Microwave Source) as managed by AFOSR under Grant No. F49620-95-1-0253.

1. Yu.P. Bliokh, et. al., Plasma Phys. Report, 20, 767 (1994).
2. D. M Goebel, et. al., IEEE Trans. on Plasma Science 22, 547 (1994).

Monday Afternoon, 19 May 1997
3:00 p.m. – Cockatoo Room

Oral Session 2E:
1.2 Space Plasmas
Chair: E.E. Scime

2E01-02 *Invited*

Spacecraft Potential Control on the POLAR Satellite by the Plasma Source Instrument

R.H. Comfort
CSPAR, University of Alabama in Huntsville, Huntsville, AL 35899
T.E. Moore and P.D. Craven
Space Sciences Laboratory, NASA/MSFC, Huntsville, AL 35812
C.J. Pollock
SWRI, 6220 Culebra Road, San Antonio, TX 78284
F.S. Mozer
University of California at Berkeey, Space Sciences Laboratory, Berkely, CA 94720
W.S. Williamson
Hughes Research Laboratories, 3011 Malibu Canyon Rd, Malibu, CA 90265

The importance of low energy core plasma to magnetospheric plasma transport has been increasingly recognized in recent years. However, in low density space plasmas, spacecraft charging makes observation of low energy plasma particles difficult. The Plasma Source Instrument (PSI) on the POLAR satellite effectively controls both positive and negative spacecraft charging through the emission of electrons and ions, as needed, to maintain the potential near that of the ambient plasma. This paper provides information on the nature of the instrument, its operation, and the consequences for low energy ion observations. Data from the Electric Field Instrument (EFI) on POLAR is used to demonstrate how well PSI controls the spacecraft potential. High latitude observations from the Thermal Ion Dynamics Experiment (TIDE) provide a clear view of the plasma dynamic environment, which in the past has been obscured by the normally present spacecraft potential.

2E03

Reactive Plasma System for On-Orbit Cleaning of Spacecraft Thermal Radiators

W.S. Williamson
Hughes Research Laboratories, Malibu, California 90265-4799
B.L. Drolen and D.A. Kaufman
Hughes Space and Communications Company, El Segundo, California 90245

Thermal radiators, used to dissipate heat from orbiting spacecraft, lose their effectiveness over time because they become contaminated by a thin polymeric coating that absorbs sunlight several times more strongly than the uncontaminated radiator. The contaminants consist of hydrocarbons and silicones that are outgassed by the spacecraft and polymerized onto sunlit radiators by the action of solar UV. Contaminated radiators are a problem for spacecraft designers because they reduce spacecraft power-handling capability, increase operating temperature range, and must be oversized to offset these effects.

We have developed a reactive plasma system intended for flight application that removes radiator contaminant films, maintaining thermal performance at or near pristine levels. The helicon plasma source operates on water vapor and uses only 1 W of electrical power. It is intended to be mounted on the solar-wing drive so that the diurnal motion of the wing causes the plasma plume to sweep over nearly the entire radiator surface.

2E04

Versatile Toroidal Facility (VTF) for Space Plasma Research

M.C. Lee, R.J. Riddolls, D.T. Moriarty, M.J. Rowlands and N.E. Dalrymple
Massachusetts Institute of Technology, Cambridge, MA 02139

The Versatile Toroidal Facility (VTF) is a student-built large toroidal plasma machine having a helical magnetic field, that guides electrons emitted from heated LaB_6 filaments to flow from the bottom side to the topside of the plasma chamber. These upward flowing electrons serve two purposes: (1) creating a background plasma through electron collisions with neutral gases (e.g., H_2, Ar, O_2) and (2) forming a field-aligned electric current. The VTF plasma machine is ideal for the study of ionospheric plasma heating [Lee et al., 1997 IEEE ICOPS] and space plasma processes, in a plasma environment characterized by: $\omega_{pe}/\omega_{ce} \geq 3$ and $T_e \sim T_i \sim 5$ *ev* where ω_{pe}, ω_{ce}, T_e, and T_i represent the electron plasma frequency, the electron gyrofrequency, the electron temperature, and the ion temperature in the VTF, respectively. The VTF plasma has sharp density gradient in the radical direction and intense magnetic field-aligned electric currents. These VTF plasma conditions can properly simulate auroral plasma condition for the excitation of low-frequency ionospheric density fluctuations. Recent VTF experiments have found that certain low frequency modes can be suppressed by the injected o-mode microwaves. In addition, ducted whistler wave propagation along the helical magnetic field has been studied in the VTF. These ducted whistler waves have cutoff frequencies slightly greater than half of the local electron gyrofrequency in the VTF. The distinct difference between the VTF experiments and space plasma experiments will be discussed.

2E05

A Laboratory Quiescent Plasma Device for Modeling Velocity Shear in Space

M.W. Zintl, M.E. Koepke and J.J. Carroll III
Department of Physics, West Virginia University, Morgantown, WV 26506-6315

A continuing topic of interest among the space physics community is the acceleration of low-altitude ionospheric ions and the underlying mechanisms. One such mechanism, which has gained much attention in the past few years, is ion acceleration due to turbulence generated by a velocity-shear layer transverse to the local magnetic field, in particular, in situations where magnetic-field-aligned currents may be too small to destabilize current-driven electrostatic ion-cyclotron modes. These situations are modeled in a plasma produced by the WVU Q-machine. The plasma is a collisionless, low-temperature ($T_i \approx T_e = 0.2$ *eV*), low-neutral-density alkali metal, typically sodium or barium, confined by a uniform magnetic field (*B=0.5-3.0kG*). The shear layer is created by a segmented-disk electrode placed at the end of the plasma column opposite to the source; the voltage drop across any two groups of segments creates a radially localized electric field, and thus an inhomogeneous azimuthal **ExB** plasma drift. A variety of space-relevant parameters can be adjusted, such as the ratio of gyroradius to inhomogeneity scale length (ρ_i/L), ion-electron temperature ratio (T_i/T_e), ratio of ions to neutrals (to model different altitudes), and ratio of ion densities in the case of multi-ion-species plasma studies. Recent measurements will be presented of

waves whose signatures change dramatically as the shear parameters in the plasma are varied.

Work sponsored by ONR and NSF.

2E06

"SPACE EXPERIMENTS" IN THE LABORATORY

V.M. Antonov, A.G. Ponomarenko and Yu.P. Zakharov
Institute of Laser Physics, Siberian Branch of the Russian Academy of Sciences
630090 Novosibirsk, Russia

The main results of the investigations which have been directed to the development of ideology and justification of the possibility for conducting a "space experiment" under laboratory conditions are presented.

The simulation program has the following items:

1. nonstationary processes in the space and near-Earth plasmas;

2. active space experiments to investigate the background medium and to look for new physical effects;

3. electromagnetic interaction of spacecrafts with the background medium;

4. power sources and technology.

To fulfill the program we have developed an experimental facility .named KI-1 (Space Investigations-1) consisting of a high-vacuum chamber with diameter 1.5m and length 5m , terrella scale models with characteristic dimensions 5 .. 20cm and magnetic moment 1.0E+6 – 2.0E+7 G*cm^3, a background plasma injector (50 kJ) and quasistationary magnetic field 1 kG, high-power sources of laser radiation with energy 0.1 - 1.0 kJ at pulse duration 1.0E-7 .. 1.0E-6 s, wide-aperture electron and ion beams with energy 10 - 300 keV, current 1 - 10 kA and pulse duration 1.0E-6 - 1.0E-4 s, diagnostic complex used for the probe, electromagnetic and optical measurements with high time-space resolution.

2E07

Spacecraft Interactions with Beam Emissions

Shu T. Lai
Phillips Laboratory, Hanscom AFB., MA 01731
Joseph Wang
Jet Propulsion Laboratory, Pasadena, CA 91109

This is an overview on effects of charged beam emissions from spacecraft. In the classical situation, the spacecraft potential increases with the beam current. At high beam currents, new phenomena may ensue. We discuss two such phenomena. (1) A virtual electrode may appear in the beam near the exit point for an unneutralized beam with a high current density. Partial beam return occurs. The phenomenon is more prominent for ion beams than electron beams, and more so for wide ion beams. (2) Supercharging may occur for high beam current emissions with beams diverging under the repulsive force of the beam space charge. Those beam electrons, or ions, with exceedingly high angular momenta cannot return to the spacecraft even if the spacecraft potential reaches, or even exceeds, that of the beam energy. This phenomenon is prominent for narrow unneutralized beams with high current density. These effects affect the spacecraft potential. We present theories and computer simulations, and also provide interpretations to space observations in support of these ideas.

2E08

Ion Bunching as a Source of Field-Aligned Currents in Space Plasmas

N. Brenning
Div. of Plasma Physics, Alfvén Laboratory, Royal Institute of Technology, SE-100 Stockholm, Sweden

A spatially inhomogeneous population of heavy minority ions in a magnetized plasma can be produced *e.g.*, by ionization out of an injected neutral cloud, or by the passage of the plasma through a region with rapidly changing transverse electric field. In both cases, the result can be a periodic bunching of the heavy ions, which can persist far from the source of the inhomogeneity.

The transverse velocity of such ion bunches is locked to the motion of the source of the inhomogeneity, rather than to the plasma's drift velocity $\mathbf{ExB}/B^2$. In the plasma's rest frame (*i.e.*, the frame where $\mathbf{E} = 0$), the ion bunches therefore represent temporal changes in the ion density. Space charge neutrality, however, must be

maintained. For weak injections, field-aligned electron currents can achieve this. For sufficiently strong injections this is not possible, and transverse electric fields have to build built up to counteract the bunching of the ions.

Three separate works on such ion bunching are compared and put into a common frame: (1) Ion phase space bunches which were optically observed from ground in the CRRES releases by Bernhardt *et al*, and interpreted in terms of weak injection, (2) the CRIT I and CRIT II releases which were in the range between weak and strong injection, and where the electric field and the current systems were measured *in situ*, and (3) the model by Rothwell *et al* where oxygen ion bunching in the magnetotail is proposed to be an important generator mechanism in the auroral current system.

2E09

Comparison Between Measured and Simulated Features of Current Collection by the Tethered Satellite

Nagendra Singh and W.C. Leung
Department of Electrical and Computer Engineering, University of Alabama in Huntsville, Huntsville, AL 35899

The reflight of the tethered satellite system has revealed an intriguing set of plasma processes affecting collection of electrons by a conducting body biased at a positive potential. Currents greatly in excess of that predicted from the Parker-Murphy theory have been measured, but the scaling of the current with the bias potential (Φ_0) is found to be approximately the same as predicted by the theory for sufficiently large value of Φ_0. Three-dimensional particle-in-cell simulations of current collection by a conducting spherical body in a magnetized plasma reveals similar behaviors of the current collection. The geometrical aspects of the current flow in the plasma contributing to the collection of electrons by the body and the structure of the sheath will be discussed.

2E10

Propagation of Electron Beam in Inhomogeneous Plasma

E. Kontar and V. Lapshin
Kharkiv State University, Kharkiv, 310077, Ukraine
V. Mel'nik
Institute of Radio Astronomy of Ukrainian Academy of Sciences, Kharkiv, 310002, Ukraine

The propagation of electron beam generating solar type III bursts is considered at the distances much larger than the length of quasilinear relaxation. As it takes place in homogeneous plasma the electron beam being initially monoenergetic propagates as a beam-plasma structure that consists of electrons and Langmuir waves. Beam-plasma structure propagating in uniform plasma loses a part of the fastest and the slowest electrons that leads to its decay. The maximum of electron density and energy density of plasma waves propagates with constant velocity. The numerical simulations fulfilled show that the inhomogeneity with decreasing density at the scales larger than the relaxation length can increase the time of this structure existence in corona.

Monday Afternoon, 19 May 1997
3:00 p.m. – Rousseau Center

Poster Session 2P16-22:
4.1 Laser Produced Plasmas

2P16

Reconstruction of Refraction Angle Topology from Laser Plasma Interferogram

G.S. Sarkisov
P.N. Lebedev Physical Institute, Moscow, Russia

The technique for reconstruction of the radial and axial components of refraction angle as well as it's module from the interferogram with visualization fields are discussed. In this approach the refraction angle is treated like a changing angle of normal vector of the disturbed phase surface of the probing electromagnetic wave in comparison with it's non-disturbed position. It is possible to reconstruct the phase surface of the probing beam from

the interferogram. The expressions for the components of regraction angle are:

$$tg(\beta) = \lambda \cdot |\nabla\delta(x,y)| = \lambda \cdot \sqrt{(\partial\delta/\partial x)^2 + (\partial\delta/\partial y)^2}$$

$$tg(\beta_x) = \frac{\lambda \cdot (\partial\delta/\partial x)}{\sqrt{1+\lambda^2 \cdot (\partial\delta/\partial y)^2}}$$

$$tg(\beta_y) = \frac{\lambda \cdot (\partial\delta/\partial y)}{\sqrt{1+\lambda^2 \cdot (\partial\delta/\partial x)^2}}$$

where: β- is a absolute value of refraction angle in rad; β_x and β_y - radial and axial component of refraction angle in rad; $\delta(x,y)$- 2D phase shift in lines; λ- probing wave-length. This procedure of reconstruction does not require symmetry of the object being investigated. The results of reconstruction of refraction angles structure for laser plasma are presented. The interferogram was created in experiments on interaction of 2ns/25J second harmonic of Nd laser with planar Al target. Probing beam was Raman-shifted second harmonic of Nd laser (~630nm). Moment of probing was ~1.5ns after heating pulse. The 2D analysis of refraction angle topology results in an axial component (-2.12 ÷ +2.22deg) which is ~2 times larger than the radial component, (0 ÷ +4.25 deg). This means that the reason the observed non-transparent region in laser plasma (planar target) is due to axial refraction. This type of analysis of interferogram is especially useful in understanding the origin of non-transparent region of the dense plasma in laser-probing experiments with Z-pinches and for the analysis of plasma inhomogeneous structure.

2P17

Satellite Transitions Near He_α Lines in a Dense Plasma Heated by 120 fsec Laser

F.B. Rosmej
Ruhr-Universitaet Bochum, Institute fuer Experiment/physik Y, Germany
I.Yu. Skobelev, A.Ya. Faenov and T.A. Pikuz
Multicharged Ion Spectra Data Center, VNIIFTRI, Mendeleevo, 141570 Russia
M. Fraenkel and A. Zigler
Racah Institute of Physics, The Hebrew University of Jerusalem, Israel

Experimental X-ray spectra near resonance line of He_α of Mg XI with simultaneously high spectral (up to $\lambda/\Delta\lambda$ = 10000) and spatial (Δx = 10 mkm) resolution was obtained from plasma, heated by laser with duration of pulse 120 fsec and energy about 20 mJ (flux density on the target was more than 10^{16} W/cm^2). We demonstrated the important role of inner-shell excitation mechanism for low confinement parameters and propose new excitation channels from highly populated excited states (Li-like and Be-like satellite levels). The collision excitation cross sections for these processes do not decrease with principal quantum number. These channels can be also subject to electron beam excitation. It was shown also the big role of transient effects for Rydberg-Satellites due to a strong three-body recombination into high n-states in the cooling phase. Total spectra simulations are in rather close agreement with experimental results.

2P18

Characteristics of a YAG Triggered Plasma Shutter for a CO_2 Laser Beam

R.L. Williams and K.M. Chase
Department of Physics, Florida A. and M. University, Tallahassee, Florida 32307

We report the results of studies on the truncation of a CO_2 laser pulse using a plasma shutter. A short pulsed YAG laser is focused (f/3.4) into a low pressure gas (≈200T) along with a longer pulsed CO_2 laser (f/1.25). The plasma produced by the YAG laser rapidly truncates the CO_2 laser pulse. We study the characteristics of the shutter as a function of the intensity of both lasers and their relative timing; and the plasma density and species. The resulting shortened CO_2 laser pulse will be used in plasma wave excitation experiments.

This work is supported by DOE and NASA CeNNAs.

2P19

Numerical Model for Plasma Electron Acceleration in Laser Wakefield Accelerators

R.F. Hubbard, E.Esarey, A. Ting, and P. Sprangle
Plasma Physics Division, Naval Research Laboratory, Washington D.C.

Plasma wakefields produced by a sub-picosecond, high intensity laser pulse in a dense gas jet can accelerate plasma electrons to high energies. The acceleration is believed to be a two stage process in which plasma electrons are accelerated to moderate energies by a low phase

velocity wave and then trapped and accelerated by the high phase velocity (v_p ~ c), large amplitude wakefield. The laser wakefield accelerator (LFWA) experiment at the Naval Research Laboratory has produced up to 30 MeV electrons with no external injector when operating in the self-modulated regime.[1] The low phase velocity wave in this case could arise from the beating of the laser pump pulse with a wave arising from the backward Raman instability. This interpretation is supported by a numerical model which follows the motion of plasma electrons in analytically-prescribed fields corresponding to the laser pump pulse, the forward-going wakefield, and the Raman waves. The accelerated electrons have a large energy spread and are trapped in several bunches. Esarey, *et al.*[2] have proposed a scheme which would operate in the "standard" LWFA regime and employs three collinear laser pulses: the large amplitude pump pulse, a lower amplitude follower pulse at the same frequency, and a counterstreaming colliding pulse at a slightly lower frequency. The interaction between the follower pulse and the colliding pulse produces the first stage of acceleration. The numerical model predicts that if the delay between the pump and follower pulses is optimized, a single short pulse bunch of accelerated plasma electrons with ~20-30% energy spread can be produced. Even if there is no guiding of the laser pulse, the model predicts that the beam energy can be tens of MeV with a bunch length of tens of femtoseconds. Potential applications include high energy physics injectors and ultrafast imaging.

Supported by DOE and ONR.

[1]A. Ting, *et al.*, to appear in Phys. Plasmas

[2]E. Esarey, *et al.*, submitted to Phys. Rev. Lett.

2P20

Evidence for the Electromagnetic Decay Instability Driven by Two Plasmon Decay

K.L. Baker, B.B. Afeyan, K.G. Estabrook and R.P. Drake
Plasma Physics Research Institute, University of California at Davis and Lawrence Livermore National Laboratory, Livermore, CA

This paper examines the electromagnetic decay instability (EDI) and its role in laser-produced plasmas. The electromagnetic decay instability provides another channel through which parametric instabilities involving Langmuir waves can saturate. In the case where EDI is pumped by the Langmuir waves associated with two plasmon decay, EDI is shown to present an explanation for $\omega_0/2$ emission from laser-produced plasmas which is consistent with experimental observations.

2P21

Simulation of Magnetic Field Generation in Laser Plasma Jet

Igor V. Glazyrin, Oleg V. Diyankov, Serge V. Koshelev and Vladimir A. Lykov
Russian Federal Nuclear Center
All-Russian Institute of Technical Physics, P.O. Box 245, Snezhinsk, Chelyabinsk Region, Russia

Plasma expansion due to laser irradiation in a target has been studied, using MAG code[1]. The special attention has been paid to the spontaneously generated magnetic field effect on the laser induced plasma jet dynamics.

2D MAG code was used for this numerical modeling. The magnetized transport coefficients were taken from the Braginskii model. The ideal gas equation of state and the bremsstrahlung radiation losses were taken into account.

Initially Al plate of 5 mkm thickness and 340 mkm length with 2.7 g/cm**3 density was heated by laser beam, focused into 50 mkm. The energy with amplitude of 0.4J with triangle shape of time dependence (0.5ns front duration and 0.5ns its decay) was absorbed in the critical density. The plate was expanding in vacuum or in gas, and in the center of the jet the hot plasma region appeared.

The results of calculations show, that maximum temperature is 1.5 times higher, when the spontaneous magnetic field is taken into account. The main reason of its increasing is the process of heat conductivity coefficient magnetizing.

The work was supported partially by ISTC, project #107, 009, 350.

References:

[1] O.V. Diyankov, I.V. Glazyrin, S.V. Koshelev. MAG-two-dimensional resistive MHD code using arbitrary moving coordinate system. Submitted to Computer Physice Communications

The MAG code for the 2D radiative plasma flows in magnetic field is presented. The algorithm has been formulated for an arbitrary moving coordinate system. The code has some interesting features,which allow to simulate MHD plasma flows with large deformations inside the flow region, conserving the correct description

of its weakly deformated boundaries. The model realized in the code, contains terms for the description of the following phenomena: spontaneous magnetic fields, Hall effect, magnetizing of transport coefficients, kinetics or ionization, radiation transfer. The code has been used for inertial fusion modeling and plasma liners implosion modeling. This work is supported partially by ISTC, projects #107, #009, #350. The authors are grateful to Dr. Vadim Yu. Politov for his work on the ionization kinetics model development, and useful discussions of the received results.

2P22

Threshold of Nonstationary Laser Supported Detonation Wave

Vlad Semak
Center for Laser Applications, University of Tennessee Space Institute, Tullahoma, TN 37388

Threshold laser intensity required to support laser induced detonation wave in air was measured for the different laser pulse shapes. A TEA CO_2 laser used in the experiments generated pulses consisting of a leading high amplitude peak with 300 ns width on the half maximum and a tail with 5μs duration. A cell filled with SF_6 was used to change the amplitude of the leading peak. The separation of the shock wave from the plasma front, indicating the detonation wave decay, was detected using schlieren photography. Higher threshold intensity of laser supported detonation wave decay was measured for higher amplitude of the leading peak in the laser pulse shape. An explanation for the effect is given on the basis of earlier proposed mechanism of nondimensional laser supported detonation wave decay.

Monday Afternoon, 19 May 1997
3:00 p.m. – Rousseau Center

Poster Session 2P23-28:
4.2 Inertial Confinement Fusion

2P23

Analysis of Filtered Silicon Diode Data from MAGO/MTF Experiments

Ronald C. Kirkpatrick and George Idozorek
Los Alamos National Laboratory, Los Alamos, NM 87545

We have acquired filtered silicon diode data from energetic magnetized plasma generation experiments fielded jointly by Los Alamos National Laboratory and the All-Russia Scientific Institute for Experimental Physics (VNIIEF) in Sarov, Russia. The diode responses extend from the visible to the hard X-ray region of the spectrum, and the filters define various spectral ranges. We have attempted to infer time-dependent plasma temperature and density histories from these measurements, with limited success. We see evidence for a plasma initially over 200 eV, decaying quickly to about 200 eV and slowly decaying thereafter, but remaining above 120 eV until about 5 μs, at which time the analysis fails. Some details of the experiment and analysis, as well as our interpretation will be presented.

2P24

Plasma Uniformity Issues in a 2x1 Plasma-Electrode Pockels Cell*

Scott Fochs, Mark A. Rhodes, C. D. Boley
Lawrence Livermore National Laboratory, Livermore, CA

An optical switch based on large-aperture plasma-electrode Pockels cells (PEPC) is an important part of the National Ignition Facility (NIF) laser design.

In a PEPC, low-pressure helium discharges (1-2 kA) are formed on both sides of a thin slab of electro-optic material (typically KDP). These discharges form highly conductive, transparent sheets which allow uniform application of a high-voltage pulse (17 kV) across the

crystal. A 37 cm x 37 cm PEPC has been in routine operation for two years on the 6 kJ Beamlet laser at LLNL. For the NIF, a module four apertures high by one wide (4x1) is required. However, this 4x1 mechanical module will be comprised electrically of a pair of 2x1 submodules.

To achieve uniform electro-optic switching across the entire PEPC aperture, it is important that the plasma density be sufficiently high and sufficiently uniform. We have observed a number of plasma effects which can degrade plasma uniformity. These include magnetic displacement of the plasma by external return currents and nearby sources of magnetic interference, current channel formation due to plasma self-fields, anode and cathode electrode design, and the potential of the insulated metal housing that surrounds the plasma.

We have studied these effects both analytically and experimentally in a 32 cm x 32 cm plastic housing PEPC and more recently in an 80 cm x 40 cm, two-aperture, aluminum-housing PEPC. The results of this work are presented here.

*This work was performed under the auspices of the US Department of Energy by Lawrence Livermore National Laboratory under the contract number W-7405-EN-48.

saturated vapor pressure model, used in wall erosion studies,[2] to compute the rate atoms leave a liquid/solid surface as a vapor is questionable. An improved model is developed which treats the heated layers for $T > T_c$ as a Van der Waals fluid with variable compressibility, $Z=P/\rho RT$. The ablation rate is thus determined by the rapidity of the outward hydrodynamic expansion. Since the X-ray pulse is very short (~3 ns), the ablation layer covering the solid surface will be extremely thin, allowing us to use BUCKY1 in the 1-D planar mode for all surfaces. To handle off-normal incidence, the X-ray deposition within the spatial zones of BUCKY1 can be solved using an equivalent model in which the incident directional flux and X-ray absorption coefficient transform like:

$$I_{||} \rightarrow I_{||} \cos\theta(z) \ , \quad \sigma(E) \rightarrow \quad \sigma(E)/\cos\theta(z)$$

The code calculates the areal mass erosion ΔM (g/cm^2) and other quantities. The total mass eroded from the TI is 0.108 g, with 40% (60%) from the side section (blunt nose).

[1]H.R. Leider, et al., Carbon 11, 555 (1973).

[2]A.T. Anderson, et al., "Modeling and Experiments of X-ray Ablation of NIF First Wall Materials," 12th Topical Meeting on the Technology of Fusion Power, Reno, Nevada (1996).

*Work supported by General Atomics IR&D funds.

2P25

Target Inserter Ablation Studies for ICF Reactors*

P.B. Parks and R.B. Stephens
General Atomics, San Diego, CA
R.R. Peterson and R.B. Stephens
University of Wisconsin–Madison, Madison, WI

BUCKY1 is a flexible 1-D Lagrangian radiation-hydrodynamics code that can simulate a variety of high-density ICF plasma conditions in planar, cylindrical, or spherical geometries. At GA we are using BUCKY1 to simulate the response of the conically-shaped target inserter (TI) located inside the target chamber of the National Ignition Facility (NIF) to the time- and energy-dependent X-ray spectrum from a 20 MJ hohlraum target. The TI configuration we have studied consists of a blunt nose cone with two conically shaped sections tilted at different angles, and the entire surface is coated with carbon. For NIF the maximum X-ray fluence on the target is ~800 J/cm^2, which is over 600 times the fluence received by the first wall. At these intensities the surface layer can be heated above the critical temperature of carbon $T_c \approx 6900$ K.[1] Under these conditions, application of the

2P26

Laser Plasma Interaction at High Intensities

Meenu Asthana
Laser Program Center for Advanced Technology, Indore (M.P.) India

For ultra fast laser pulses lasting the order of a picosecond or less, the drift velocity of electrons in a plasma can be comparable to the velocity of light, causing a significant increase in the mass of the electron and consequently in the effect dielectric constant of the plasma. This leads to self-focusing of laser beam. The fact that the relativistic mechanism is the only mechanism of self-focusing that can manifest itself for subpicosecond pulses makes the understanding of this mechanism very important. The steady state nonlinear refraction of ontense linearly polarized, gaussian electromagnetic beams in an inhomogeneous plasma taking relativistic effects into account is studied. The mass variation of the electron in the field of the pump wave are shown to have a major

effect on the nonlinear dynamics of propagation of intense electromagnetic waves. It promotes the self-focusing of the beam. This paper presents the problem of anomalous penetration of laser radiation in an inhomogeneous plasma. To organize the work the Nonlinear dielectric constant is obtained. The self-focusing equation relating the variation of beamwidth parameter with distance of propagation, self-trapping condition and critical power are evaluation followed by numerical calculations. The present theory has a much wider range of applications compared to earlier theories, and is therefore applicable at all intensities, high and low.

2P27

Scattering of Laser Radiation At The Heating Of Low Density Foam Targets

S.Yu. Guskov, Yu. S. Kas'anov*, M.O. Koshevoi, V.B. Rozanov, A.A. Rupasov, A.S. Shikanov
P.N. Lebedev Physical Institute, Moscow, Russia
**General Physics Institute, Moscow, Russia*

Experimental study of the radiation scattered at the laser heating of low density foam targets is presented. The Experiments were carried out on laser facility with wavelength 0.53 μm, pulse duration 2.5 ns, focal spot diameter 15 μm, flax density on target surface ~5 10^{14} W/cm^2. The targets have been prepared from porous polypropylene $(CH)_x$ with average density ~0.02 g/cm^3 and cell size ~50 μm. Both forward-, side- and back-scattered radiations including one created by the stimulated Brillouin scattering have been registered, that enabled to study the dynamics of the process of burning-through of the thick foam targets, the velocities of the plasma critical density motion as well as mass velocity of the plasma. The intensities of stimulated Brillouin scattering for the porous targets had the same value as for the solid ones (3-4 % from laser density) but the spectral-temporal characteristics were quite different for these kinds of targets that confirms the different scattering properties and different ablation dynamics for the solid and the foam matter.

2P28

Plasma Formation Dynamics For Laser Interaction With Near Critical Foam Matter

S.Yu. Guskov, Yu.S. Kas'anov*, M.O. Koshevoi, V.B. Rozanov, A.A. Rupasov, A.S. Shikanov
P.N. Lebedev Physical Institute, Moscow, Russia
**General Physics Institute, Moscow, Russia*

Experimental study of the laser pulse interaction with low density porous matter is presented. The experiments were carried out on laser facility with wavelength 0.53 μm, pulse duration 2.5 ns, focal spot diameter 15 μm, flux density on target surface ~5 10^{14}W/cm^2. Targets were prepared from porous polypropylene $(CH)_x$ with average density ~0.02 g/cm^3 and cell size ~50 μm. The dynamics of plasma formation was investigated by means of registration of scattered laser radiation and selfluminosity of the plasma with spatial and temporal resolution. The experimental data show an essential difference of plasma processes occurring in the porous targets and solid ones with the same chemical composition. The general features of the porous targets are a volume distributed absorption, when a laser beam forms a low density "channel" inside a porous matter, and larger spatial scales of transverse energy transport.

Monday Afternoon, 19 May 1997
3:00 p.m. – Rousseau Center

Poster Session 2P29-35:
4.3 Magnetic Confinement Fusion

2P29

Poloidal Current Drive By Rotting Magnetic Field

Y. Maeda, A. Okino[1], M. Maeyama[2] and E. Hotta
Department of Energy Sciences, Tokyo Institute of Technology, Midori-ku, Yokohama 226, Japan
[1]Department of Electrical and Electronic Engineering, Tokyo Institute of Technology, Meguro-ku, Tokyo 152, Japan
[2]Department of Electrical and Electronic Systems, Saitama University, Urawa 338, Japan

The non-inductive current drive is a key issue in the fusion oriented research. In order to control or sustain the magnetic field configuration of reversed field pinch (RFP) plasmas, the poloidal current drive by rotating magnetic fields (RMF) is one of the promising means. This method also can be used to generate and maintain the field reversed configuration (FRC) steadily.

For the RMF to penetrate into plasma columns, the skin depth plays an essential role. It is well known that there are two kind of skin depths, the resistive one and that dominated by electron inertia. For high temperature plasmas, the latter overcomes the resistive one and becomes very important.

While the current drive by the RMF in the case of resistive plasmas is analyzed by many authors, but that in the case of high temperature plasmas is not. Therefore, the poloidal current drive by the RMF was simulated and the effect of electron inertia on the rise time of the driven current was analyzed.

Simulation results show that for high temperature plasmas, taking into account of the electron inertia, the rise time of driven current is much shorter than that in the case of neglecting the electron inertia. Thus, it is shown that in high temperature plasmas the electron inertia plays a crucial role in the current drive by the RMF.

2P30

A Novel Technique for Disruption Simulation and Accident Analysis Using an ET Plasma Source*

J.P. Sharpe, M.A. Bourham, J.G. Gilligan
Department of Nuclear Engineering, North Carolina State University, Raleigh, NC 27695

Disruption events in future tokamak reactors are expected to be severely intense due to high energy inventory within the confined plasma. For example, the proposed International Thermonuclear Experimental Reactor (ITER) has the potential for disruption heat loads up to 100 MJ/m^2 incident upon the divertor area. Obviously destructive to any exposed material by vaporization and/or melting, hard disruptions are generally included in severe accident scenarios and contribute significantly in reactor safety analyses. Of particular concern regarding reactor safety following a hard disruption is aerosol generation from activated plasma-facing materials.

In order to generate defensible safety analyses for future tokamak reactors, disruption effects on plasma-facing materials and subsequent aerosol formation mechanisms must be well understood and benchmarked with a relevant database. One technique for disruption simulation involves the use of an electrothermal (ET) plasma source. The ET facility SIRENS at North Carolina State University has been modified to study disruption-induced aerosol mobilization for ITER relevant materials. Particle transport properties obtained from experiments will contribute to a materials database for use in ITER safety analysis.

Electrothermal plasma sources have been used to simulate disruptions because magnitudes and physical mechanisms of heat transfer in the ET source are very similar to those in a disruption. However, to study vaporization and subsequent condensation of plasma-exposed surfaces requires modifications to the ET source. This paper describes the necessary modifications to SIRENS and provides a physical and parametric comparison of the experiment and its relevance to disruption mobilization in ITER.

*Work supported by The U.S. Department of Energy, Office of Energy Research, under NCSU Contract DE-FG02-96ER54363.

2P31

Measurement of Edge Plasma Parameters in KT-1 Tokamak by Single/Mach Probes

D.H. Chang, K.S. Chung, B.H. Oh[1], K.W. Lee[1] and S.K. Kim[1]
Department of Nuclear Engineering, Hanyang University, Seoul, Korea
[1]Nuclear Fusion Laboratory, Korea Atomic Energy Research Institute, Seoul, Korea

Combined system of a single probe and a Mach probe is used for the simultaneous measurement of electron temperature, plasma density, floating potential and flow velocity from edge plasma in KT-1 small tokamak (R:27cm a:5cm) during Ohmic discharges. Typical values of electron temperature, plasma density, and floating potential by a single probe are 19~22eV, ~3 × 10^{11}cm^{-3}, and -14 ~ -22 volts, respectively, for the most discharges. Mach probe has been used for the measurement of toroidal flow velocity, plasma density, and directional electron temperatures. Big difference of parallel and antiparallel electron temperatures indicates the asymmetry of electron behavior around the plasma facing components (PFC).

2P32

Fast Adiabatic Compression of a Toroidal Plasma to Thermonuclear Ignition

C.A. Ordonez
Department of Physics, University of North Texas, Denton, TX 6203-0368
and
R.E. Peterkin, Jr.
High Energy Plasma Division, Phillips Laboratory, Kirtland AFB, NM 87117

Fast adiabatic compression of a magnetically confined toroidal plasma is proposed as a means to achieve plasma ignition. The approach relies on producing and compressing a compact toroid. (A compact toroid is essentially a spheromak with an aspect ratio larger than unity.) The basic method of compressing a compact toroid has been described. [R.E. Peterkin, Jr., Phys. Rev. Lett., **74**, 3165 (1995); J.H. Degnan, et al., Phys. Fluids B, **5**, 2938 (1993)]. In the analysis presented, the ignition approach is optimized by minimizing the energy required to create and compress the compact toroid. The parameters obtained for a compressed DT compact toroid plasma at the point of ignition include: a very high plasma density (7.2×10^{22} m^{-3}), very small major and minor radii (5.8 cm and 2.2 cm), a moderate beta (0.1), a high magnetic field (60 T), and low ion and electron temperatures (10 and 2.5 keV). The total energy (including plasma and magnetic contributions) of the compressed compact toroid at ignition is slightly less than 1 MJ. The concept is a straightforward extension of existing research. For example, nine time radial adiabatic compression of an argon compact toroid plasma has been achieved at the 10 MJ Shiva-Star facility at Phillips Laboratory.

This work was supported in part by the Air Force Office of Scientific Research.

2P33

Steady-State Plasma Current Production in a Discharge Device with Magnetic Field Confinement

Weiyi Luo, Hansi Li, S. Xu and S. Lee
Nanyang Technological University, Division of Physics, School of Science, NIE
469 Bukit Timah Road. 259756, Singapore

Theoretical analysis and experimental Investigation have been shown that a steady-state plasma current can be driven using an uniform transverse oscillating magnetic field (OME). In this paper, the production of a steady-state toroidal driven current is experimentally investigated by a highly reproducible 7ms pulse duration discharge in an inductively coupled plasma device, which is consisted of spherical Pyrex vessel of 28 cm inner diameter applied with a transverse oscillating magnetic field (OMF) and a perpendicularly oriented vertical magnetic field. There is an apparent linear relationship between the toroidal driven current and the strength of the applied vertical equilibrium field, and the driven current is zero in the absence of the vertical field. The reversal vertical field generated by the driven current is clearly demonstrated. The scaling of the total driven current with the vertical field has been undertaken using a Rogowski belt at 490 kHz frequency, 640 W RF input power and 2 mTorr filling argon pressure. The generation of the rotating magnetic field, the bi-directional toroidal magnetic field and the strong frequency double term of the time varying magnetic field were observed and measured in detail. These experimental measurements were compared with the existing theoretical analysis. In addition, the electron number density n_e and temperature T_e were also measured using a floating Langmuir double probe.

2P34

On the Possibility of the ITER Machine to Reach Ignition

E. Panarella*
Department of Electrical Engineering,
University of Tennessee, Knoxville, TN 37996 USA

The present analysis of ITER is based on the known parameters for its operation, i.e., temperature 20 kV decreasing linearly from the center towards the plasma periphery; magnetic field profile: 5 Tesla decreasing towards the plasma periphery with a known relation; particle density: 10^{14} cm^{-3}; major radius: 8m; minor radius: 4m. It is assumed that 400 MW of power input are required to bring it toward ignition, and that the reactor works with an efficiency of 30% of conversion of thermal energy into electricity.

At regime, the alpha particle heating and that part of the power input that goes into the plasma, as determined by an energy transfer efficiency a, has necessarily to be transferred to the liquid blanket of the reactor in the form of heat and bremsstrahlung. For simplicity, the blanket is assumed to be water at 300° C, for which the thermal conductivity is well known.

On the basis of the above data and assumptions, it is found that the heat loss from the entire plasma is ~5 x 10^8 watts. Moreover, it is found that the temperature of the first wall is 40 eV for an energy transfer efficiency a = 13.1%, or 60 eV for a = 37.5%. When one integrates over the entire volume of the plasma the energy balance, i.e., energy produced by neutrons and alpha particles, and losses by bremsstrahlung and heat, one finds that the machine cannot reach ignition.

---

* Also with Advanced Laser and Fusion Technology, Inc., 189/7 Deveault St., Hull, P.Q. J8Z 1S7 Canada

2P35

A Heavy Ion Beam Probe for the Madison Symmetric Torus

K. A. Connor, U. Shah, Y Dong, P. M. Schoch,
T.P. Crowley, J. Lei
Rensselaer Polytechnic Institute, Troy, NY 12180
and
S.C. Aceto
InterScience Inc., Troy, NY

A design study of a heavy ion beam probe has been completed for application on the Madison Symmetric Torus. We expect to begin installation of this system within the next year. The MST-HIBP system will use a 200 kV accelerator such as the one used on the Advanced Toroidal Facility (ATF) at ORNL. The ions used for primary beam injection will include Potassium and Sodium. However, ions may be used in some experiments.

Planned HIBP measurements on MST include the steady state potential profile, fluctuations in electron density and electrostatic potential, the equilibrium magnetic field and magnetic field fluctuation measurements. None of these quantities have yet been measured in a core of a hot RFP. The ability of HIBP to measure the magnetic field on this device has not been demonstrated yet, but if possible, it can provide enhanced understanding of the macroscopic behavior of RFP's, discrete dynamo events, current profile and core transport. In addition, measurement of the radial electric field can provide pivotal information on transport and mode locking and can also test shear flow theories during improved confinement.

Due to the size limitations of the diagnostic ports the system will require a different beam sweep system than is traditionally used. We will probably use sweep systems on both the primary and secondary beamlines. A detailed study of this cross over sweep systems will be presented. This serves to overcome restrictions in injection angles that would otherwise limit accessibility within the plasma. Detailed trajectory calculations show that a complete radial profile of the plasma cross section can be achieved by varying the primary beam energy. Detailed energy scan lines showing plasma accessibility will also be presented. The ion trajectories for MST are strongly three dimensional. In this aspect, the MST-HIBP more closely resembles the AFT beam probe than those on previous Tokamaks.

Work supported by U.S. Doe.

Monday Afternoon, 19 May 1997
3:00 p.m. – Rousseau Center

Poster Session 2P36-44:
4.4 Dense Plasma Focus

2P36

On the Plasma Focus-Produced Spheromak-Like Magnetic Configuration for Jet Propulsion

A.B.Kukushkin and V.A. Rantsev-Kartinov
INF RRC "Kurchatov Institute," Moscow 123182 Russia

Conceptual design of a Filippov-type plasma focus-based thruster is presented. The propulsion mechanism is based on the phenomenon [1] experimentally observed in certain Filippov-type plasma focus discharges and characterized by the following features, namely:: (i) cyclical self-production of the high energy density plasma confined by the large-scale (several cm) closed, spheromak-like magnetic configuration (SLMC); (ii) further compression of the SLMC-trapped plasmas by the residual (i.e. not incorporated in the closed magnetic configuration) magnetic field of the plasma focus discharge; (iii) strong repulsion of the SLMC away from the anode thanks to regular accumulation of magnetic field at the anode, due to the Hall effect in plasmas.

Experimental results presented in [1] suggest the possibility of achieving the fusion ignition in the central part of the SLMC along with reasonable confinement of the fusion-born charged particles by the SLMC that could make such a system a sound candidate for e.g. the D-^{3} He fusion-based thruster. The energy flow in fusion propulsion system is outlined and the technological advantages of the concept are discussed.

References

[1] Kukushkin, A.B., Rantsev-Kartinov, V.A., Terentiev, A.R., Fusion Technology, 1997 (to be published); Transactions of Fusion Technology, **27** (1995) 325.

2P37

HEAVY ION BEAM GENERATION IN PF-SYSTEMS

N.V.Filippov and T.I.Filippova
RRC "Kurchatov Institute," sq. Kurchatov, 1., Moscow, 123182, Russia

Experimental studies of the processes of generating the accelerated multicharged heavy ions - occurring in the contact zone (CZ) of PF-discharge with an anode, as a result of electric fields emerging in it and having the accelerating voltage of a few MeV - are represented.

An X-ray image of CZ, together with the image of a track, where an "ion image" shift due to the accelerated heavy ion drift in an azimuthal magnetic field of the pinch is seen, has been produced with the combined pinhole camera. Implementation of the additional longitudinal (axial) magnetic field which is captured and compressed by a plasma sheath moving along the anode surface has allowed us to explain a spiral-like nature of CZ-translation along the anode surface. This phenomenon is related with the emergence of radial "metallic" near-anode plasma jets under destruction of the pinch.

For finding the energy of accelerated ions the TOF-technique with the control by deviation in a magnetic field and the technique of absorption in metallic foils have been used.

The conclusion has been done that the accelerating electric fields emerging in a "metallic" plasma at the places of destruction in the azimuthal pinch current Cz-structure symmetry under formation of radial jets and under magnetic configuration reconnection have the common genesis with the similar fields in a gaseous pinch.

2P38

Studies of a Plasma Focus Operated at Higher D_2 Filling Pressure

Ming-fang Lu
Institute of Physics, Chinese Academy of Sciences, Beijing 100080, Peoples Republic of China

Investigations on the plasma motion of a small Mather-type plasma focus device (20 kV, 18 kJ) operated at a higher D_2 filling pressure (4.0 Torr) than the optimum one (2.5 Torr) for neutron emission by using laser differential interferometer show that the current

sheath (CS) structure and pinching dynamics are of two factors which are responsible to the low and largely deviated neutron yield at this pressure. For a solid anode (copper, 64 mm in diameter), the larger gas resistance in front of the imploding CS causes an instability to occur at the CS front near the anode surface just prior to the pinching. This part of the CS forms a pinch (first pinch, radius r=2 mm) rapidly in front the upper part of the CS which is still in implosion. Later on, the upper part CS implodes on the first pinch and forms a "complex" pinch. It has a larger radius (r=6 mm) and an extraordinarily long time duration (τ ~ 140 ns, for ordinary pinch, τ ~ 30 ns) and a rather lower density (one order lower than ordinary pinch). It produces a neutron yield of $Y_n=(0.9 \pm 0.6) \times 10^8$ per shot which is about 60% lower than the ordinary pinch. For a hollow anode (the hollow is 44 mm in diameter), the discharges in succession can be clearly distinguished into two distinct groups according to their neutron yields: the "good" shots that always have the higher neutron yield of $Y_n=(4.5 \pm 1.3) \times 10^8$ per shot (44 percent), and the "bad" shots that always have the lower neutron yield of $Y_n=(0.9 \pm 0.5) \times 10^8$ per shot (56 percent). It is shown that for the "good" shots, the imploding CS has a uniform, dense and thinner sheath structure (sheath thickness δ=1.6 mm), while for the "bad" shots, the CS is non-uniform and has a thicker and less dense structure (δ=3.9 to 5.4 mm). The time duration for the "good" pinch is about 30 ns, while for the "bad" pinch is about 70 ns.

2P39

Modification of Polyester Film By High Energy Density Plasmas

Ming-fang Lu, Si-ze Yang and Chi-zi Liu
Institute of Physics, Chinese Academy of Sciences, Beijing 100080, Peoples Republic of China

The high specific surface resistivity of most polymers (usually $>10^{16}$ Ω) is a key factor that causes electrostatic hazards in many industrial fields. Various methods have been tested to decrease the surface resistivity of polymers, including chemical treatment, humid environment, ion wind and ion implantation, etc. The first three methods are sometimes limited by the application conditons, while the last one is usually costly. In this article, the high energy density plasma (HEDP) generated by a simple gas-puff coaxial plasma gun is introduced to treat the polymer surface. The operation parameters of the gun include: charging voltage V=1 to 3.5 kV (capacitance C=6 x 185 μF), aluminum electrodes, N_2 gas (tank pressure p_{N2}=1.0 atm). The typical plasma parameters include: T_e=10-20 eV, $n_e=(5.70) \times 10^{13}$ cm^{-3}, directed velocity v=10-50 km/s, pulse duration τ=10-100 μs, energy deposition $P_d=10^4$-10^5 W/cm^2 and E_d=1-10 J/cm^2. The polyester film with a surface resistivity of 10^{16} Ω was selected as the sample. It was put to face the gun muzzle with a distance of 3 cm. For V=2.5 kV, the results show that for only one shot, the surface resistivity of the modified area drastically decreased to 10^7 Ω. After three shots, the surface resistivity further decreased to 10^4 Ω and in the center part 40 to 100 Ω. Also, the modified area is transparent and without deformation, and appears in slightly silver-gray color which is a thin aluminum layer of about 1 μm deposited on the film. The polyester film, after modified by the HEDP, is fairly safe to static electricity. Friction tests show that the modification layer has good adhesive to the substrate. Further analyses of the modified layer by infrared absorption spectra etc. are now undertaking.

2P40

Modified Thomson Spectrometer for the Detection of Low Energy (1 keV) High Power Ion Beams

Ming-fang Lu, Si-ze Yang and Chi-zi Liu
Institute of Physics, Chinese Academy of Sciences, Beijing, 100080, Peoples Republic of China

The Thomson parabola spectrometer with the CR-39 nuclear track detector as detection plate has been widely used in the detection of mass and energy spectra of pulsed high power ion beams in a wide energy range from 30 keV to more than MeV[1]. However, its application to even low energy ion beams detection, say 1 to several keV, is limited by the threshold energy for the particle track formation of the detection plate which is usually higher than 30 keV. The pulsed high power and low energy ion beams, such as N^+, C^+ and B^+ and so on, with energy of about 1 keV in the high energy density plasma streams generated by the coaxial plasma gun are of special interest in materials surface modification and film deposition[2]. To solve the detection problem, we designed an after-acceleration electric field near and cross the detection plate to accelerate the ions, after deflected by the electric and magnetic fields of the spectrometer, to enough higher energy for effectively registered by the detection plate. The acceleration field is formed by a front grounded planar metal mesh electrode 3 mm in front of the detection plate and a back electrode applied to a pulse voltage of 50 kV behind the plate. Primary experimental results

show that the ion spectra can be effectively registered with this modified spectrometer. Since the ratio of the accelerated energy to the original ion energy (for single charged ions) is larger than 50, the acceleration field does not influence the spectra distribution of the ion beams notably.

References

[1] M.S. Opecunov, G.E. Remnev, A.N. Grishin and I.V. Ivonin, Radiation Measurements, 25 (1995) 739-740

[2] M.F. Lu, S.Z. Yang and C.Z Liu, Spatial distribution of the high energy density plasma in a coaxial gun for surface modification, also presented to this Conference.

2P41

X-ray Emission from PF-1000 Plasma-Focus Device Admixtured with Argon

M. Scholz, M. Borowiecki, L. Karpinski, R. Miklaszewski, W. Stepniewski, M. Sadowski, A. Szydlowski[1], V.M. Romanova[2], S.A.Pikuz[2] and T.Ya Faenov[3]

Institute of Plasma Physics and Laser Microfusion, Warsaw, Poland

[1]Soltan Institute for Nuclear Studies, Swierk, Poland

[2]P.N. Lebedev Physical Institute, Moscow, Russia

[3]MISDC of VNIIFTRI, Mendeleevo, Russia

A new PF 1000 Mather-type plasma focus device with a 1.2MJ capacitor bank, charging voltage U=45kV, short circuit current I=15MA, is now operated at IPPLM. The series of experiments with a hydrogen-argon mixture was performed within the energy range 250-450kJ. The partial argon pressure was up to 20%. The hard and soft X-ray radiation was registered by means of scintillation probes, pinhole cameras and spectrometer equipped with a spherical crystal. The plasma current sheath dynamics was studied with streak cameras. To measure a discharge current a Rogowski coil and miniature magnetic probes were used.

In some shots there was observed the second current increase after a standard singularity. In those cases two hard X-ray pulses were registered. The first one was synchronized with the peculiarity and the second one appeared a few microseconds later. Two possible explanations of this phenomenon were proposed. One hypothesis relates the delayed hard x-ray pulse with the secondary current sheath formation, which was registered in some shots by means of the streak camera. The second one explains this phenomenon the magnetic field relaxation during the stagnation phase. The X-ray pinhole camera (pinhole diameter of 100 micrometer covered with Be foil 10 and 25 micrometer thick) showed a few hot spot regions especially intensive in the shots performed with argon admixture. The helium-like lines of argon were registered with the crystal spectrometer. From the spectral lines the electron temperature was estimated to be of 500-700 eV.

2P42

Influence of Electrode Structure on Neutron Emission in PF-40*

M. Han, M.F. Lu, T.C. Yang, X.X. Wang

Gas Discharge and Plasma Laboratory, Dept. of Electrical Engineering, Tsinghua University, Beijing, China

The Mather type PF-40 Plasma Focus Device consists of 27x3 μF capacitors in parallel arranged in nine units. Neutron emission was investigated in two ways. The neutron yield and it's jetter of different end shapes and structures of the inner and outer electrodes were measured using a silver activation counter. At the same time, the propagation and structure of plasma sheath in pinch phase were recorded by a laser differential interferometer in every case, respectively. A uniform and symmetric configuration of the pinch plasma is essential for obtaining higher neutron. The anode end structure effect the neutron yield through influencing the configuration and status of motion of the plasma sheath. By improving the electrode structure, we have obtained the average neutron yield of ~10^9 per shot at operating voltage 20kV(18kJ) which is close to the value predicted by the scaling law. The jetter of neutron yield related average value is about (20~80)%.

The time dependent neutron emission from PF-40 was recorded with a measure system of plastic scintillator coupled a photomultiplier. The picture show that there are two peaks. The first is related to hard X-ray and the second to neutron signals. The duration time (FWHM) of neutron emission is (40~60)nS and hard X-ray is 30nS.

*This work is supported by the National Natural Science Foundation of China.

2P43

Electron Beam and Neutron Yields in Dependence on Initial Parameters I of Plasma Focus

V.V. Vikhrev and E.O. Baronova
NFI, RRC Kurchatov Institute, Moscow 123182, Russia

Current and energy of electron beam as well as the neutron yield in dependence of inductance, radius of camera, gas pressure, storage energy and voltage are analyzed. Numerical analysis was made in the frame of the simple model of z-pinch plasma formation, described in [1]. The energy radiation losses and thermonuclear heat release were not considered. The simple model provides one with parameters of z-pinch neck (temperature, density, radius) depending on time and may be successfully used for determination of integral parameters of plasma such as soft and hard x-ray emissions, neutron and electron beam yields.

The theory of electron beam generation [2], based on runaway mechanism within the turbulent z-pinch plasma conditions and the model of neutron generation [1] were accounted.

It has been shown the existence of optimum for gas pressure and inductance when the neutron and electron beam yields appears to be maximized. It may be stated that the experimental data obtained on the fruitful plasma focus devices are in good agreement with theoretical predictions.

References

[1] V.V. Vikhrev, C.A. Ananin, Preprint KIAE-3514/4, 1981

[2] V.V. Vikhrev and E.O. Baronova, In: Proc ICPP 96 Nagoya, 12C12, 1996

2P44

Preliminary Estimations of a Possibility of Creation of Inductive Current Source with Power 10^{12} W for a Large Plasma Focus Device with Energy ~ 100MJ

A.P. Lototsky, E.A. Azizov and M.K.Krylov
TRINITI, Moscow Region, Troitsk, Russia
N.V.Filippov
RRC Kurchatov Institute, Moscow, Russia

One of the problems of creation of a high-power impulse neutrons source on multi-megajoule plasma focus facility base consists of development of an pulse supply system with currents in tens MA and digit potency 10^{12} W. We have offered new the concept of a magnetic accumulator with the inductive cascade for power amplification and for solution of this problem.

The conducted analysis of probable schematics of such amplifier took into account the following moments:

1. Optimization of efficiency of transmission of a magnetic energy between inductive coils of the cascade.
2. Working condition of commutators_circuit breakers of a current and power performance of an pulsed system.
3. Matching of a current supply with plasma focus device.

Technique of optimization of the power supply system is offered. The possibility of using of inductive storage TIN-900, included in installation TSP (TRINITI, Russia), for feed of plasma focus device with energy in a plasma sheet up to 100 M_{TDK} is shown. Separate problems of a construction of similar inductive current source with output power $>10^{12}$ W are considered which are connected to effective transmission of a magnetic configurations of large storage coils

Monday Afternoon, 19 May 1997
3:00 p.m. – Rousseau Center

Poster Session 2P45-65:
4.5 Fast Z-Pinches and X-Ray Lasers

2P45

Laser Probing Experiments with X-Pinches

G.S. Sarkisov, S. Pikuz, T. Shelkovenko, V. Romanova
P.N. Lebedev Physical Institute, Moscow, Russia

For investigating the internal structure of the neck, the position of the neck in the relation to the cross-point of the X-inch wires, the neck structure during pinching, plasma parameters in the vicinity of the neck and in the plasma around of the wire's core were studying using pulsed lasers. For solving this problem we used shadowgraphy and interferometry. For the plasma probing we used a second harmonic of Nd laser with ~7nsec pulse duration and ~50mJ energy. Accuracy of synchronization

wrrent was ±5ns. Spatial resolution was ~15μm. An X-pinch is formed by placing two fine (20-50μm) wires between the output electrodes of a high current pulser so that the wires cross and touch in mid-gap. The parameters of installation were: maximum current ~300kA, voltage ~50kV, pulse duration ~100ns. The axial displacement of the position of the neck from cross-point of the wire on value ~50μm was recorded. Reconstruction of the electron density in the transparent region of the neck gives value ~1.6×10^{20} cm^{-3} at a distance of ~50μm from axis. Behavior of the interference lines shows that two different regions in X-pinches exist. In the external region of X-pinch plasma the parameters change slowly. In the internal region- we observed fast motion of plasma from the exploding wire to axis of Z-pinches. Laser pulse duration is not short enough for resolving the interference lines in the internal region of X-pinch. The interference line position was observed in the high absorption region in the vicinity of the neck. Maximum electron density in this region equals 4×10^{19} cm^{-3}. Maximum refraction angle ~1.7deg. In the region of the neck refraction angle up to ~3.2deg. Estimation of the electron temperature (from inverse bremsstrahlung of laser light) in vicinity of the neck gives value ~1.5eV. For the neck, the maximum electron temperature (from x-ray spectroscopy) gives ~100eV. Double exposed shadow pictures (20ns between pulses) gives information about development of m=1 instability.

2P46

Expectations For Hohlraum Environment Driven By Spatially Compressed Flying Radiation Case At Intermediate Currents

R.L. Bowers, J.H. Brownell and H. H. Rogers
Los Alamos National Laboratory, Los Alamos, NM

The radiation environment produced by the magnetic implosion of a hot, low density plasma and its stagnation on an axial cushion (a Flying Radiation Case) is modeled using a two-dimensional radiation magnetohydrodynamic code and drive parameters for the PFZA-Z machine pulsed power machine. We consider the effects of instability growth in the plasma during the implosion, its reassembly on the cushion, and plasma interactions with shaped electrodes. The radiation environment within the pinch and in an axial side hohlraum are modeled. We also consider effects of the pinch on the side hohlraum. The computational approach has been successful in modeling the implosion and radiation output of Z-pinches on the Pegasus facility at Los Alamos National Laboratory, and on the Saturn and PFZA-Z machines at Sandia National Laboratories.

2P47

Measurements of Z-Pinch Plasma Parameters with Crystal Spectroscopy on PBFAZ and SATURN

T. Nash, C. Deeney, T.W.L. Sanford, G.A. Chandler, R.B. Spielman, D. Jobe, J. Seaman, T.K. Gilliland and J. McGurn
Sandia National Laboratories, Albuquerque, NM
J. MacFarlane
University of Wisconsin-Madison, Madison, WI
J.P. Apruzese, K.G. Whitney, P.E. Pulsifier and J. Davis
Naval Research Laboratory, Washington, DC
B. Failor, P.D. LePell, B. Whitton and J.C. Riordan
Primex Physics International, San Leandro, CA
Ed Yadlowsky
HYTECH Research Co., Washington, DC

We have used a spatially-resolved time-integrated convex crystal spectrometer to measure spectra above 1 keV on the pulsed power machines PBFAZ and SATURN. We observe a tungsten M absorption edge from tungsten z-pinches on PBFAZ. From the energy shift and depth of the edge we infer the z-pinch halo plasma electron temperature and rho*r to be 150 eV and 0.00018 g/sq cm. The slope of the tungsten spectrum indicates a 700 eV core electron temperature on PBFAZ, up from a 350 eV slope measured on the smaller accelerator SATURN. In contrast to tungsten pinches on SATURN, for an array consisting of aluminum wires coated with potassium chloride, we have measured the core electron temperature by three independent techniques to be 1200 eV. These three techniques are the aluminum K-shell free-bound continuum slope, the ratio of isoelectronic helium-alpha lines in potassium and chlorine, and the ratio or Lyman to helium alpha in chlorine.

2P48

Determining the Effects of Wire Diameter in Tungsten Wire Array Implosions

C. Deeney, M.R. Douglas, D.L. Peterson, R.B.Spielman, T. Nash, G.A. Chandler, D. Fehl, J. Seaman, K. Struve, W.A. Stygar, J. McGurn, D. Jobe, T. Gilliland, J. Torres, R. Mock, T.W.L. Sanford and M.K. Matzen
Sandia National Laboratories, MS-1194, Albuquerque, NM 87185-1194

Initial experiments with 40-mm, 120 and 240 wire arrays on the 18-MA PBFAZ generator [1,2] have produced 1.85 MJ, 160TW of x-ray power in a 8.5 ns pulse. These experiments and experiments on Saturn [3] indicated that the pulsewidth was primarily being determined by the diameter of the individual wires. Two dimensional rad-MHD calculations suggest that the thinner the wire, the lower the initial perturbation levels which may seed Rayleigh-Taylor instabilities.[4] In this paper, we present results from a wire array scan where the wire number, array diameter and implosion times are held constant. The wire diameter is changed and the charge voltage on the PBFAZ generator is adjusted to keep the implosion time constant. We then measure the pulsewidth as the wire size varies. 2D MHD calculations of the initial wire expansion will also be compared with the level of random density perturbations needed to simulate the implosion in 2D.

[1] C. Deeney et al, to be submitted to P.R.L. (1997).
[2] R.B. Spielman, Proc. of the 1996 BEAMS Conf, (1996)
[3] C. Deeney et al, Submitted to PRE, (1996).
[4] D. Peterson et al, Phys. Plasmas , 368, (1996).

*Los Alamos National Laboratory, MS B-259, Los Alamos, NM 87545

2P49

Method to Unfold the Density Distribution of Any Axially Symmetric Liner from Radiographic Data

Huan Lee
Los Alamos National Laboratory,Los Alamos, NM 87545

In many applications experiments using pulsed power, x-ray radiography is an essential diagnostic tool to provide valuable information about the configuration of the imploding liner. When the driving current is sufficiently high, such as in the recent experiment carried out at Los Alamos to achieve multi-megabar shock pressures, the outer layer of the liner will melt or even ionized while the inner portion remains solid. In such case, the liner cylindricity will deteriorate as the magnetically driven Rayleigh-Taylor instabilities develop during the implosion. From the 2-D magnetohydro-dynamic simulations we expect that the liner will become more like a bellow as the instabilities grow, but its inner surface remain cylindrical if the solid layer has the sufficient shear strength to desist the instabilities. This is verified by our subsequent experimental observation from the radiographic pictures.

Since the outer liner layer where the instabilities develop consists of liquid and high density plasma phases, it is of great diagnostic interest to be able to unfold the radial density distribution of the bellows-like liner from the radiographic data. In this paper we propose a numerical method, coupled with a set of straight forward experimental calibrations, which will enable us to do so. This method is applicable in general provided that the liner has a good axial symmetry. The spatial resolution of the radiography are limited by the finite size of the x-ray source and also complicated by the scattered radiation. Detailed formulation of our method will be discussed together with these experimental complications.

This work was supported by the U.S. Department of Energy.

2P50

Compression and Heating History of an Imploding Z-Pinch Plasma

G. Davara, L. Gregorian, E. Kroupp, V. Fisher and Y. Maron
Physics Deptartment, Weizmann Institute of Science, Rehovot, Israel

We present a complete set of time and radius dependent parameters of the plasma measured during the implosion phase of a gas-puff, 1μs, 300 kA z-pinch. We determined the ion radial velocity distribution from measurements of Doppler shifts of line emission in the UV-visible spectral range, and the radial distribution of charge-state from axial (head on) observations. From measurements of the Stark line widths, the particle ionization times, and the continuum light intensity we determine the electron density. The electron temperature was obtained from measurements of line intensity ratios

of different charge-state ions. The magnetic field and current density distributions were obtained from high-resolution measurements of Zeeman splitting of spectral lines, yielding the plasma conductivity. The ion temperature is shown to be similar to the electron temperature. These results allow to follow trajectories of various Lagrangian mass cells and to observe plasma compression and heating, magnetic field evolution, and plasma-composition history in the cells. Experimental data are used to analyze the balance of plasma heating and cooling mechanisms, namely the Joule effect, heating due to thermal conduction, compressional heating, and cooling caused by ionization and radiation. The analysis is based on 1-D single-fluid hydrodynamics equations and time dependent collisional-radiative codes for carbon and oxygen plasmas.

2P51

Wire-Array Initiation and Interwire-Plasma Merger Concerns in PBFA-Z Tungsten Z-Pinch Implosions*

T. W. L. Sanford, R. B. Spielman, G. O. Allshouse, B. M. Marder, K. W. Struve, G. A. Chandler, C. Deeney, D. L. Fehl, T. J. Nash, W. A. Stygar, R. C. Mock, J. F. Seaman, J. S. McGurn, D. O. Jobe, T. L. Gilliland, A. R. Moats, J. A. Torres, M. Vargas and M. K. Matzen
Sandia National Laboratories, Albuquerque, NM
D.L. Peterson
Los Alamos National Laboratory, Los Alamos, NM

Experiments with annular wire-array loads to generate high quality, high-power, z-pinch implosions on Saturn have shown the importance of maintaining azimuthal symmetry and how the individual wire plasmas merge to form a plasma shell [1,2]. Here we discuss the impact of current symmetry, current prepulse, interwire spacing, and wire size on generating high-quality, high-power, z-pinch implosions on PBFA-Z [3], with annular tungsten-wire loads.

B-dot monitors measured the current as a function of azimuth in the MITLs and 4.5 cm upstream of the load. Bolometers and filtered XRDs and PCDs, spanning the energy range ~0 eV to 6 keV, monitored the temporal characteristics of the radiation. Time-integrated and time-resolved, filtered, fast-framing, x-ray pinhole cameras, and a crystal spectrometer monitored the spatial and spectral structure of the radiation.

The radial dynamics of single-wire plasmas from the solid-state, using the measured current, was calculated by 1D radiation magnetohydrodynamics code (RMHC) and used as input to an xy RMHC. These calculations together with 2D RMHC simulations [4] in the rz plane are discussed and correlated with the measurements.

[1] T. W. L. Sanford et al., *Rev. Lett.* **77**, 5063 (1996).
[2] C. Deeney et al., submitted *Phys. Rev. E (1996).*
[3] R. B. Spielman et al., this conference.
[4] D. L. Peterson et al., *Phys. Plasmas* **3**, 368 (1996)

*Sandia is a multiprogram laboratory operated by Sandia Corp. a Lockheed Martin Co., for the US Department of Energy under Contract No. DE-ACO4-94AL85000.

2P52

Monochromatic X-ray Backlighting of Dense Z-pinch Plasmas Using an X-pinch X-ray Source

S.A. Pikuz and T.A. Shelkovenko
P.N. Lebedev Physical Institute, Russian Academy of Sciences, Leninsky Prospect 53, Moscow, Russia
D.A. Hammer and D.F. Acton
Laboratory of Plasma Studies, Cornell University, Ithaca, NY 14853 USA

X-ray backlighting of high density plasmas such as the z-inches being produced on PBFA-Z can be extremely effective diagnostic tool. Monochromatic X-ray backlighting using imaging x-ray optical elements offers a way to use the backlighting technique with a backlighter x-ray source that is a many-orders-of-magnitude less powerful x-ray source than the plasma being probed. X-pinch plasmas, produced by using 2 or more fine wires as the load of 250-350 kA pulsed power generators, and spherically bent mica crystal x-ray optical elements, have been used to backlight test objects and exploding wire plasmas using monochromatic x-rays ranging from 1.8 keV to 7.8 keV. The field of view can be as large as a few cm by a few mm, and spatial resolution as fine as 4μm has been demonstrated. For example, the He-like Ni line at 1.588Å has been used to image test objects with spatial resolution of about 10μm. In this case, the backlight source size is about 0.1 mm and the pulse width is ~1 ns. We estimate that this Ni line powered by a 350 kA pulser could be used as a backlighter of a z-pinch such as that produced by PBFA-Z having an intensity up to (1-10)kJ/Å in the bandwidth of the backlighter line. This backlighting method could prove to be much less expensive to implement than a laser-based x-ray source with similar capability.

2P53

Shear Flow Stabilization of the Hydromagnetic Rayleigh-Taylor Instability

N.F. Roderick
University of New Mexico, Albuquerque, NM
U. Shumlak
University of Washington, Seattle, WA
M. Douglas
Sandia National Laboratories, Albuquerque, NM
R.E. Peterkin, Jr. and E. Ruden
Phillips Laboratory, Kirtland AFB, NM

Numerical simulations have indicated that shear flow may help stabilize the hydromagnetic Rayleigh-Taylor instability in imploding plasma z-pinches. A simple extension to a model presented in Chandrasekhar[1] has been developed to study the linear stability of incompressible plasma subjected to both a shear flow and acceleration. The model has been used to investigate the stability plasma implosion schemes using externally imposed velocity shear which develops from the plasma flow itself. Specific parameters were chosen to represent plasma implosions driven by the Saturn and PBFA-Z, pulsed power generators at Sandia National Laboratories. Results indicate a high shear is necessary to stabilize the z-pinch implosions studied.

1. S. Chandrasekhar, Hydrodynamic and Hydromagnetic Stability (Oxford University Press: 1961)

2P54

"Two-dimensional MHD Numerical Simulation of Radiating Exploding Wire Plasma Dynamics"

W.Stepniewski, R.Miklaszewski and M.Scholz
Institute of Plasma and Laser Microfusion, Warsaw, Poland

A two-dimensional MHD code, as developed at the IPPLM, was used to model the dynamics of plasma column created in the radiating exploding wire experiment [1,2]. The physical model is based on the nonideal MHD equations. Ionization kinetics was included using an average-charge approximation. The radiation transport was treated with the diffusion 3T approximation. The numerical algorithm was based on the modified Free Point Method (FPM). We started our computation from an initially ionized tungsten plasma column with a parabolic density profile. An initial distribution of plasma parameters was randomly disturbed an amplitude below 1%. Realistic dimensions of the wire were considered (length-4mm, radius-250 μm) together with a sinusoidal current rising from 10 to 300 kA in 100ns time. Transport coefficients and the equation of state were taken from wide range formulas.

Numerical results show that a growth of m=0 instability starts after the compression phase. Its wavelength is shorter than that in the optically thick model [2]. In a nonlinear stage of sausage instability intense plasma streams out-flowing from two adjacent necks collide. As a result the maximum temperature (30 eV) was observed not at the m=0 instability necks but in these adjacent regions.

1. W. Stepniewski, A. Galkowski and M. Scholz, in: Proceedings of the Japan-Central Europe Workshop on Advanced Computing in Engineering, Warsaw, 1994, p. 345-348.
2. G.V. Ivanenkov and W. Stepniewski, Sov. J. Plas. Phys., Vol.22, No.6, 1996, p.528-540

2P55

Stepping-Up of a Generation of High Intensity X Radiation in Liner Systems

S.V. Zakharov
Troitsk Institute for Innovation & Thermonuclear Investigations, TRINITI 142092 Troitsk, Moscow Oblast, Russia

The problem of intense hard x radiation producing based on the use of strongly radiating Z-pinches or liners as the loads of electrical generators is connected with the problem of a high Z > 10 dense plasma heating. The x radiation is emitted as a result of the heating of a multicharge plasma during the randomization of the kinetic energy of the liner compressed by a magnetic field and the Joule heating of the plasma in its compressed state- in a pinch. The duration of the radiation pulse and thus the power are determined by the liner thickness. A lower limit is set on the characteristic thickness of the shell by the size of the skin layer Ref. 1, this thickness may increase as the result of macro- and microscopic plasma instabilities. In addition, during the compression of a liner of a heavy-ion plasma, with a large atomic number, it is difficult for the energy acquired in the shock wave to be transferred from the ions to the electrons. The duration of the ion-electron exchange, which is proportional to the ratio of the ion and electron masses

and inversely proportional to the plasma density, may thus also determine the duration of the radiation pulse [2].

In this report a liner system which is capable of generating a high intensity radiation pulse is proposed. The system consists of a strongly radiating liner and a central solid foil cylinder. The diameter of this foil is roughly a tenth that of the liner. The difference of this scheme with respect to well known Double-Liner [3,4] been used for high intensity thermal radiation producing inside the cavity is in mach higher mass and density of the inner cylinder and plasma compound too.

The liner, accelerated by the magnetic pressure to a velocity V > 50 cm/μs, and compressed by a factor of about ten limited by the liner instability, collides with the sublimated foil plasma. As it is decelerated, its kinetic energy converts into radiation. Outer layers of the foil cylinder during the liner implosion are exposed to heat and radiation of a liner plasma, sublimate (ablate) and form plasma corona with high density gradient around the foil cylinder. The compression of the radiating liner in the interaction of the liner shell with the plasma corona of leads to the high increase in the density of the liner plasma and a reduction of its local thickness [5]. As a result, the thermal energy specific input, rate of the ion-electron energy exchange and local electron temperature impetuously rise, the intensity of the radiation increases. Optimization of foil and liner parameters permits to rich the maximum of radiation at the foil plasma density peak and to get intense radiation yield up to the hard x-ray range.

References

[1] S.F. Grigor'ev, S.V. Zakharov, Sov. Tech. Phys. Lett. Vol. 13, 254 (1987).

[2] V.D. Vikharev, G.S. Volkov, S.V. Zakharov, et. al, Sov. J. Pl. Phys. 16,388 (1990).

[3] S.V. Zakharov, V.P. Smirnov, et. al, Collision of Current Driven Cylindrical Liners. Kurchatov Institute of Atomic Energy, Moscow. Preprint 4587/6, 1988.

[4] S.V. Zakharov, V.P. Smirnov, E.V. Grabovskii, et. al., Imploding Liner as a Driver for Indirect Driven Target Physics Studies. Proc. of IAEA Tech. Com. Met. on Drivers for ICF, Paris, France, Nov 14-18, 1994.

[5] V.A. Gasilov, S.V. Zakharov, V.P. Smirnov, JETP Lett., Vol. 53, No. 2, 85 (1991).

2P56

Simulation of Wire Array Implosions on High-Current Pulsed Power Generators

N.A. Gondarenko
GNG Enterprises, Inc., Springfield, VA
and A.L. Velikovich
Berkeley Research Associates, Springfield, VA

We have developed a dynamic model for wire array implosions that fully accounts for the inductive coupling between the individual wires and the current return structure [1]. The model simulates implosions of complex loads, which might include separation (tearing) and interpenetration of the straight current-carrying elements on the plane normal to the pinch axis. We show the model's capability to simulate fast commutation of multi-MA current in double wire array loads (with 120 to 240 and more wires) imploded on PBFA II-Z, which is likely to increase the output radiation power, see [1,2], formation of the plasma and current precursor near the pinch axis, coalescence of individual wires into a plasma shell, production of sheared rotation in an imploded load and generation of debris particles in the current return structure.

1. J.Davis *et al.*, Appl. Phys. Lett. **70**, 170 (1997).
2. Baksht *et al.*, Plasma Phys. Rep. **23** (1997).

2P57

Modeling X-Ray Data for the Saturn Z-Pinch Machine

Walter Matuska and Darrell Peterson
Los Alamos National Laboratory, Los Alamos, NM 87545
Christopher Deeney and Mark Derzon
Sandia National Laboratories, Albuquerque, NM

A wealth of XRD and time dependent x-ray imaging data exist for the Saturn z-pinch machine, where the load is either a tungsten wire array or a tungsten wire array which implodes onto a $Si0_2$ foam. Also, these pinches have been modeled with a 2-D RMHD Eulerian computer code. In this paper we start with the 2-D Eulerian results to calculate time and spatially dependent spectra using both LTE and NLTE models. Then using response functions, these spectra are converted to XRD currents and camera images, which are quantitatively compared with the data. Through these comparisons, areas of good and lesser quality agreement are determined, and areas are

identified where the 2-D Eulerian code should be improved.

This work was supported by the U.S. Department of Energy.

2P58

Wire Array Implosion Experiments on the Inductive Storage Generators GIT-4 and GIT-8

R.B. Baksht, I.M. Datsko, A.A. Kim, V.A. Kokshenev, B.M. Koval'chuk, S.V. Loginov, A.Yu. Labetsky, A.V. Fedunin, A.G. Russkikh and A.V. Shishlov
High Current Electronics Institute
634055, Tomsk, Russia

All wire array implosion experiments have been carried out on the inductive storage generators GIT-4 (0.6MJ, 1.5 MA) and GIT-8 (1.2MJ, 1.9MA). The maximum radiation power in the region of 1.5÷2 keV observed in the experiments were 70 GW/cm and 150 GW/cm respectively for the GIT-4 and GIT-8 generators. The increase in the radiation power is primarily related to the increase in the current derivative (5.10^{13} A/s for the GIT-8, and 2.10^{13} A/s for the GIT-4). The measurements of the K-shell radiation power and the K-shell radiation yield as a function of liner mass and diameter have been performed. The results of the recent gas-puff on wire array experiments will be also presented.

This work was supported by US Defense Nuclear Agency, contract number DNA001-94-C-0047.

2P59

The Effect of Shell Thickness on Rayleigh-Taylor Mitigation in High Velocity, Annular Z-pinch Implosions

M. Douglas and C. Deeney
Sandia National Laboratories, Albuquerque, NM 87185
N. Roderick
University of New Mexico, Albuquerque, NM 87131

The magnetic implosion of thin annular shells is often accompanied by the Rayleigh-Taylor (RT) instability. At large diameters and high velocities characteristic of PBFA Z, this can lead to severe deformation of the plasma shell and poor pinch performance. Many techniques have been suggested to decrease the RT growth in such cases. In particular, previous computational and experimental investigations of uniform fill loads have proven to be quite promising in mitigating RT development. However, such loads are known to be less efficient in coupling to the electrical energy of the machine. To capitalize on the stabilizing properties of uniform fill loads while maintaining the efficiencies observed with annular implosions, the transition between these two configurations has been numerically investigated. Using parameters indicative of PBFA Z, two dimensional magnetohydrodynamic simulations have been carried out for a range of shell thicknesses for both aluminum and tungsten loads. Simulations show that RT growth is reduced with increasing shell thickness while the peak implosion velocity appears to be strongly dependent on the severity of the RT instability. These factors combined provide a measure of optimal performance for a given application.

2P60

COMPUTATIONAL MODELING OF WALL-SUPPORTED DENSE Z-PINCHES

P.T. Sheehey, R.A. Gerwin, R.C. Kirkpatrick, I.R. Lindemuth and F.J. Wysocki
Los Alamos National Laboratory, Los Alamos, NM 57545

In our previous computational modeling of deuterium-fiber-initiated Z-pinches intended for ohmic self-heating to fusion conditions, instability-driven expansion cause densities to drop far below those desired for fusion applications; such behavior has been observed on experiments such as Los Alamos' HDZP-II. A new application for deuterium-fiber-initiated Z-pinches is Magnetized Target Fusion (MTF), in which a preheated and magnetized target plasma is hydrodynamically compressed, by a separately driven liner, to fusion conditions. Although the conditions necessary for a suitable target plasma–density O(10^{18} cm^{-3}), temperature O(100 eV), magnetic field O(100 kG)_are less extreme than those required for the previous ohmically heated fusion scheme, the plasma must remain magnetically insulated and clean long enough to be compressed by the imploding liner to fusion conditions, e.g., several microseconds. A fiber-initiated Z-pinch in a 2-cm-radius, 2-cm long conducting liner has been built at Los Alamos to investigate its suitability as an

MTF target plasma. Two-dimensional magnetohydrodynamic modeling of this experiment shows early instability similar to that seen on HDZP-II; however, when plasma finds support and stabilization at the outer radial wall, a relatively stable profile forms and persists. Comparison of experimental results and computations, and computational inclusion of additional experimental detiails is being done. Analytic and computational investigation is also being done on possible instability-driven cooling of the plasma by Benârd-like convective cells adjacent to the cold wall.

2P61

Yield Enhancements in and Spectral Measurements of Al-Mg-KCl Mixture Arrays on the 7-MA Saturn Generator

P.LePell, B. Failor, C. Coverdale, and J. Riordan
Primex Physics International Company, San Leandro, CA 94577
C. Deeney, T. Nash, R. Spielman and P. L'Eplantier
Sandia National Laboratories, Albuquerque, NM
J. Apruzese, K. Whitney, J. Thornhill and J. Davis\
Naval Research Laboratory, Washington, DC
E. Yadlowsky
HYTECH Research Co., Washington, DC

Based on previous near-Z mixture calculations and experiments, a set of experiments have been performed on the 7-MA Saturn generator. Arrays of 30 wires on a 24mm diameter were imploded in 55ns. These arrays were composed of Al-Mg alloys (1% and 6%), Al-Mg coatings (19 or 36% Mg) and Al-Mg 1% alloy with 19 or 36% KCl coating. The 6% Mg alloys and the Mg-coatings gave more kilovolt yield than the 1% alloy as has been seen in other experiments. The addition of KCl did not enhance the yield significantly but this appears to be due to the presence of a significant aluminum free-bound continuum that already produces tens of kilojoules of x-rays. We will also report on the spectral analyses of temperature from seven different line ratios and the slope of the free-bound continuum plus density estimates based on Stark broadening of hydrogen-like aluminum lines and by matching the observed radiated powers.

Work supported by DSWA and DOE.

2P62

Detailed Spectral Simulations in Support of PBFA-Z Dynamic Hohlraum Z-pinch Experiments

J.J. MacFarlane and P. Wang
University of Wisconsin-Madison, Madison, WI
M.S. Derzon, A. Haill and T.J. Nash
Sandia National Laboratories, Albuquerque, NM
D.L. Peterson
Los Alamos National Laboratory, Los Alamos, NM

In PBFA-Z dynamic hohlraum Z-pinch experiments, 16-18 MA of current is delivered to a load comprised of a tungsten wire array surrounding a low-density cylindrical CH foam. The magnetic field accelerates the W plasma radially inward at velocities ~40-60 cm/μs. The W plasma impacts into the foam, generating a high T_R radiation field which diffuses into the foam. We are investigating several types of spectral diagnostics which can be used to characterize the time-dependent conditions in the foam. In addition, we are examining the potential ramifications of axial jetting on the interpretation of axial x-ray diagnostics. In our analysis, results from 2-D radiation-magnetohydrodynamics simulations are post-processed using a hybrid spectral analysis code in which low-Z material is treated using a detailed collisional-radiative atomic model, while high-Z material is modeled using LTE UTA (unresolved transition array) opacities. We will present results from recent simulations and discuss ramifications for x-ray diagnostics.

2P63

A SIMPLE SCALING ESTIMATE OF INPUT POWERS FOR X-RAY LASERS EXCITED IN CAPILLARY DISCHARGES

C.B. Collins
CQE, UTD P.O. Box 830688, Richardson, TX
W. Rosenfeld, R. Dussart, C. Cachoncinlle, D. Hong, C. Fleurier and J.M. Pouvesle
GREMI, CNRS/Université d'Orléans, BP 6759, 45069 Orléans cedex, France

Since the first demonstration of a real discharge pumped table-top x-ray laser by Rocca et al [1], an important emphasis of experimental activity has continued to be the search of new discharge devices and new laser transitions. This is highly motivated not only by system

compactness, but also by the very high wall-plug efficiencies, obtained with these systems, that are orders of magnitude greater than in the case of laser-pumped soft x-ray lasers. This is of crucial importance when considering the dramatic increase in the pump energy required to obtain lasing at shorter wavelength. Beside a well adapted discharge geometry, the development of new devices must carefully consider the energy transfered to the amplifying medium in order to reduce energy cost while maintaining input powers (Pt) at a sufficient level to obtain substantial gain over threshold. In this work, we present the development of scaling approximations that may be used in systems analysis and which can help to guide experimental design. Example is given for the Ne-like series of ions. At the simplest level of approximations, the derived expression of Pt is found to scale with material as $Pt(Z)=0.16\ (Z/10)^6\ GW/cm^3$. In the case of Neon-like Argon, this leads to input powers of the order of 5.5 GW/cm^3 in rather good agreement with the excitation levels reported by Rocca et al, suggesting the utility of this form of scaling estimate in the evaluation of proposed schemes of excitation of Ne-like x-ray lasers directly excited in capillary discharges.

[1] J.J. Rocca, V. Shlyaptsev, F.G. Tomasel, O.D. Cortazar, D. Hartshorn, and J.L.A. Chilla, Phys. Rev. Lett. 73, 2192 (1994).

2P64

Measurement of the Radial Evolution of a Gas-Puff Z-Pinch by Inverse Bremstrahlung Absorption of He-Ne Laser Light

G.S. Sarkisov*, A. VanDrie, B. Moosman, Y. Song and F.J. Wessel
University of California at Irvine, Irvine, CA

Streak measurement of the inverse Brumstrahlung absorption of the laser light in a Z-pinch provides information about the stability and temperature evolution of a high density pinch with high time and spatial resolutions. Our experiment uses the UCI Staged Pinch with peak parameters: 50 kV, 63 kJ, 1.7 msec rise time, and 2 MA maximum current. A 20 mW He-Ne laser (633nm, single mode) backlights the plasma and a Hamammatsu 1370 streak-camera records the image. A double cylindrical lens collimator before the plasma increases the probe light intensity which is focused to a 1mm line in the midplane of the pinch. A 10mm filter and narrow slit placed at the light focus reduces the influence of plasma self-luminosity. These shots were accompanied by a two frame nitrogen laser shadow pictures, (λ=337nm). These images were separated in time by ~15ns, with ~1ns exposure.

This work was supported by US DoE OFES.

*On leave from the P.N. Lebedev Physical Institute, Moscow, Russia.

2P65

Fibres Experiments in the MAGPIE Generator

R. Aliaga-Rossel, J.P. Chittenden, S. Lebedev, I. H. Mitchell, A. E. Dangor and M. G. Haines
The Blackett Laboratory, Imperial College, London SW7 2BZ, U. K.

A result of a series of experiments that are being carried out on the MAGPIE generator with carbon, CD2 and D2 fiber loads will be presented. Fibers 2 cm long and diameters between 10-200 μm are used to study the dynamics of the pinch as well as the initial behaviour of the plasma. Two frames of visible schlieren and interferometry are used to investigate the evolution of the coronal plasma and the growth rate instabilities. In carbon fibers was detected the presence of instabilities as early as 10ns. Comparison with CD2 and D2 fibers will be presented. The dynamics of the hot spot is also studied with both a 4-frame camera and an x-ray streak camera. Movement or bifurcation of hot spots was detected and spatial correlation with optical bright spot was found. The hot spot behaviour in fibers with different diameters will be discussed. Hard x-ray emission and high energy electron beams are detected with a combination of plastics scintillator-photo multipliers. A disruption mechanism responsible of such high energy emission will be discussed. Time resolved neutron emission is detected with plastics scintillators and total neutron yield is measured with silver activated counter. Measurements in D2 fibers will be presented.

Tuesday, 20 May 1997
8:00 a.m. – Kon Tiki Ballroom

Plenary Session

Trapped Plasmas with a Single Sign of Charge (An Overview)

Professor Thomas M. O'Neil

University of California at San Diego,
La Jolla, CA, USA

Chair: C. R. Ordonez

Tuesday Morning, 20 May 1997
10:00 a.m. – Kon Tiki Ballroom

Oral Session 3A:
1.4 Computational Plasma Physics I
Chair: J. Huba

3A01

A Study of Stability and Energy Conservation of a 3-D Electromagnetic PIC Code for Non-Orthogonal Meshes

Dmitri Kondrashov
California Institute of Technology, Pasadena, CA
Joseph Wang and Paulett C. Liewer
JPL/California Institute of Technology, Pasadena, CA

A 3-D electromagnetic particle-in-cell code (EMPIC) was developed for large-scale plasma simulation on parallel computers. To simulate plasma problems with complex geometries such as high-power microwave generation devices, curvilinear coordinates were used. A logically connected cartesian grid consisted of hexahedral cells that could be deformed to body-fit complex shapes. A finite-volume method for a non-orthogonal grid was used to calculate the electromagnetic field. This method is based on Gedney-Lansing [1] and Madsen [2] algorithms, and is reduced to a standard FDTD algorithm for an orthogonal grid. Particle updates use current deposit formulation of Villasenor and Buneman [3] generalized to non-orthogonal meshes, preserving charge and current.

The stability of the entire code and of the electromagnetic algorithm in particular was analyzed on non-orthogonal meshes. Questions of how the code stability and energy conservation are influenced by numerical mesh distortion, are addressed. Ways of improving the code stability and accuracy are discussed.

[1] S. Gedney and F. Lansing, "A Generalized Yee-Algorithm for the Analysis of Microwave Circuit Devices", submitted to *IEEE Trans. Microwave Theory and Techniques* (1995).

[2] N.K. Madsen, "Divergence Preserving Discrete Surface Integral Methods for Mawell's Curl Equations Using Non-Orthogonal Unstructured Grid", *J. Comp. Phys.*, 119: 34-35 (1995).

[3] J. Villasenor and O. Buneman, "Rigorous Charge Conservation for Local Electromagnetic Field Solvers", *Comp. Phys. Comm.*, 69: 306-316 (1992).

3A02

Massively Parallel 3-Dimensional Particle-in-Cell Plasma Code

E. Earl Wells, S. Al-Sharaeh and Nagendra Singh
Deaprtment of Electrical and Computer Engineering, University of Alabama at Huntsville, Huntsville, Alabama 35899

This paper describes ongoing research to apply Single Program Multiple Data, SPMD, domain decomposition techniques to the three-dimensional simulation of plasma phenomena using a particle-in-cell (PIC) code. In this work, techniques are presented which perform static allocation of particle computation to the set of processing elements based upon each particle's initial position within the simulation's physical geometric domain. Dynamic load balancing strategies are then applied as necessary to maintain the desired level of efficiency. A major focus has been to develop augmented techniques which are scaleable and can be easily applied across a wide range of parallel and distributed computing environments. The effectiveness of the techniques are evaluated empirically by applying them to a study on nonlinear evolution of lower hybrid waves. This was done using multiple interprocessor communication paradigms on a 256 node Cray T-3D massively parallel processor.

3A03

Simulation Studies of Optimized Electrode Designs for a Cylindrical IEC

G.H. Miley, J. DeMora, R.A. Stubbers and R. Zich
Fusion Studies Lab, University of Illinois, Urbana, IL
J. Sved
DASA, Bremmen, Germany
R. Anderl and J. Hartwell
INEL, Idaho Falls, Idaho

The cylindrical version (c-device) of the single grid inertial electrostatic confinement (IEC) device is of strong interest for various neutron activation analysis (NAA) applications[1,2]. The present version produces ~10^6 D-D fusion neutron/s steady-state, and a higher yield pulsed version is under development[3]. In both designs the grid configuration must be optimized for maximum neutron yield. An ion tracking code, SIMION[4], has been adapted for this purpose. While it includes several key approximations (e.g., neglects self-fields and collisions),

it still predicts trends well for the present regime of operation, and provides improved physical insight.

Recent simulations have examined variations of the reference electrode design, covering a wide range of diameters and lengths. Thus, for example, with a 10-cm long cathode and 3-cm long anodes the optimum diameter is predicted to be 60-80 mm. As the diameter is reduced further, the ion beam focus is lost. Further, the plasma sheath at the inside cathode wall begins to distort the beam path. These simulations will be described along with results for several novel designs, including a modular cathode and multiple "segmented" electrode concept will be presented.

Supported under DOE Contract DE-AC07-941D13223

[1]Y. Gu. et al, "A Portable Cylindrical Electrostatic-fusion Device for Neutronic Tomography," *Fusion Technol, 26 3,* Part 2, 929-232 (1994).

[2]G.H. Miley, et al, 3rd Int. Conf. On Dense Z-pinches, AIP Conf. Proc. 299, 675-689 (1994).

[3]G.H. Miley, Electron Emitter Pulsed-type Cylindrical IEC, paper submitted to ICOPS, 1997.

[4]J.M. DeMora, et al, Proc. SOFE '95, 1486-1489, (1996).

3A04

Quasineutral Particle Simulation / Monte Carlo Model of Magnetized Plasma Discharges*

Martin Lampe, Glenn Joyce, W.M. Manheimer
Plasma Physics Division, Naval Research Laboratory, Washington, DC 20375-5346

In quasineutral plasmas it is difficult and inefficient, indeed unnatural, to calculate the electrostatic field from Poisson's equation. We have developed a particle-in-cell/Monte Carlo (PIC/MC) simulation method in which the electric fields within the bulk plasma are determined directly from the requirement of quasineutrality. In the case of a discharge in contact with material walls, the sheaths are treated as thin potential barriers, and the sheath potentials are also calculated self-consistently from the requirement of quasineutrality. The Bohm criterion for ion flux into the sheath is imposed as a boundary condition. Thus the entire discharge can be modeled without the use of Poisson's equation. Electron plasma oscillations do not appear in the model, and the Debye length is essentially set to zero, so short temporal and spatial scales are excluded. This focuses the model on the macroscopic time and space scales of interest, and affords great efficiency in numerical simulation. Kinetic features of quasineutral modes, e.g. Landau damping of ion sound modes, are represented correctly. We present some results from a two-dimensional (rz) simulation of an electron cyclotron resonance (ECR) processing discharge, in which the electrons but not the ions are strongly magnetized, and both species are subject to Coulomb collisions and elastic and inelastic collisions with neutral particles. The simulations afford new insights into such matters as the effect of insulating vs. conducting walls on a discharge, and the way in which cross-field diffusion is regulated by sheath potentials. We believe the simulation technique is applicable generally to a wide variety of phenomena in plasmas that may be magnetized or unmagnetized, bounded or unbounded, collisional or collisionless.

* Supported by Office of Naval Research

3A05

Long Mean Free Path Kinetic Theory Using Scattering Rates

W.N.G. Hitchon*
Department of Electrical and Computer Engineering and Engineering Research Center for Plasma-Aided Manufacturing, University of Wisconsin-Madison, Madison WI 53706-1691
and G.J. Parker
Lawrence Livermore National Laboratory, Plasma Physics Research Institute, Livermore, CA 94550

Numerical computation of the scattering rates of particles can provide information equivalent to the full distribution function, but can be much less computationally expensive to obtain. The calculation involves iterating a (discretized) integral equation. The difficulty lies in finding an accurate, realistic and sufficiently compact form for the 'kernel' in the integral equation. Different representations of the kernel will be discussed. Applications have been made to long-mean-free path plasma chemistry,[1,2] transport of sputtered particles[3] and kinetics of injected ions inside a crystal[4]. These will be outlined with emphasis on neutral transport in a plasma environment.

[1] R.E.P Harvey, W.N.G. Hitchon and G.J. Parker, *J. Appl. Phys.*, **75**, 1940 (1994); *IEEE Trans. Plas. Sci*, **23**, 436 (1995).
[2] W. Tan, R.J. Hoekstra and M.J. Kushner, *J. Appl. Phys.*, **79**, 3423 (1996).
[3] G.J. Parker, W.N. G. Hitchon and D.J. Koch, *Phys. Rev. E*, **51**, 3694 (1995).
[4] G.J. Parker, W.N.G. Hitchon and E.R. Keiter, *Phys. Rev. E*, **54**, 938 (1996).

*Supported in part by NSF contract EEC-8721545

3A06

Ion Distribution Functions in an ECR Discharge Plasma*

Glenn Joyce, Martin Lampe, W.M. Manheimer
and Steve Slinker
Plasma Physics Division. Naval Research Laboratory, Washington DC 20375

We have recently developed an axisymmetric quasi-neutral particle simulation code to study hearing and transport of plasma in an ECR reactor configuration. All species are treated as particles with the electrons always strongly magnetized, and the degree of magnetization of the ions varying spatially. The code contains a formulation for ECR heating. For this system with pressures on the order of a few milliTorr, the plasma can be high density and weakly collisional, with mean free paths on the order of a few centimeters. Particles may collide with the neutral gas in various states. The ion velocity distribution is primarily determined from the particle dynamics in the quasi-neutral fields, and sheaths, and by collisions with the neutral gas. The neutral collisions include momentum transfer and charge exchange. Ion collisions in the pre-sheath are particularly important, since they may determine the anisotropy of the ions after they traverse the sheath. We will present ion distribution functions at various locations in the plasma and near the sheaths.

*Supported by Office of Naval Research

Tuesday Morning, 20 May 1997
10:00 a.m. – Board Rooom

Oral Session 3B:
2.1 Intense Beam Microwaves
Chair:E. Schamiloglu

3B01

Efficiency Enhanced, Load-Limited MILO

R. W. Lemke and M.C. Clark
Sandia National Laboratories, Albuquerque, NM 87185
and S.E. Calico
USAF Phillips Laboratory, Kirtland AFB, NM 87117

The self-insulating property of a magnetically insulated line oscillator[1] (MILO) obviates the need for an external circuit to supply the magnetic field, but restricts the efficiency of power production to values far below (factor of 4) what is achievable with a conventional magnetron (80%). Nevertheless, this corresponds to gigawatts of power output at modest voltage (500 kV) and impedance (5 ohms).

Experience has shown that, while it is straightforward to guild a MILO that oscillates at a specific frequency, maximum efficiency (power) cannot be achieved without careful consideration of the design. We have accomplished this using a load-limited MILO which uses an rf choke (Bragg reflector) at the upstream end to provide maximum feedback and, thereby, maximum power. We discuss various aspects of the design of this efficiency enhanced, multi-gigawatt, load-limited MILO, and present results of simulations and experiments. An upper limit on power efficiency is also discussed.

1. R.W. Lemke, S.E. Calico and M.C. Clark, "Investigation of a load-limited magnetically insulated transmission line oscillator (MILO)", IEEE Trans. Plasma Sci., to be published April 1997.

This work was supported in part by the USAF Phillips Laboratory, and the US Department of Energy under contract DE-ACO4-AL85000. Sandia is a multi-program Corporation, a Lockheed Martin Company, for the United States Department of Energy.

3B02-03 Invited

Success on Elimination of Pulse Shortening of GW-Class, 300 nsec HPM Sources

Kyle Hendricks, Mike Haworth, Ray Lemke†,
Mike Sena*, Dale Ralph*, Ken Allen*, Thad Englert,
Don Shiffler, Tom Spencer, Moe Arman, Kirk Hackett,
Steve Calico, Dale Coleman†, Collins Clark†
and Roque Gallegoes†
Phillips Laboratory, Kirtland AFB, NM
†Sandia National Laboratories, Albuquerque, NM
Maxwell Laboratories, Inc., Albuquerque, NM

We have demonstrated two different HPM sources which radiate Rf power in excess of 1 GW: the MILO and RKO. The pulse lengths are limited only by the duration of the prime power. Both sources have been operated on the Sandia IMP pulser (500 kV, 5 Ω, 300 nsec) pulse power driver. While the physics of these sources are different, both have shown Rf pulses shorter than the applied electron beam pulse. Following careful investigations both sources now generate Rf pulse to the end of the electron beam pulse. This success has been achieved by closely comparing experimental performance and optimized computer simulation. Our results suggest that designing a long pulse HPM source and then being able to make the source operate as desired is usually limited by overlooking subtleties of the actual source operation. While it most certainly is true that stray plasma production may limit pulse length. Stray plasma production in these two sources is a symptom of design errors. We are preparing longer pulse experiments to investigate the next source of pulse shortening.

3B04

Recent Results in the Hard-Tube MILO Experiment

M. Haworth, K. Hendricks, T, Englert D. Shiffler
and K. Hackett
Phillips Laboratory, WSQ Division,
Kirtland AFB, NM 87117
R. Lemke
Sandia National Laboratories, Albuquerque, NM 87185
M. Sena, K. Allen, D. Ralph, and D. Henley
Maxwell Laboratories, Inc., Albuquerque, NM 87119

The Hard-Tube MILO (**M**agnetically **I**nsulated transmission **L**ine **O**scillator) is an all stainless steel, brazed version of the gigawatt-class, L-band tube reported by Calico *et al.*[1]. The Calico MILO generated a 1.5-GW, 60-ns FWHM microwave pulse using a 500-kV, 60-kA, 500-ns electron beam, while the Hard-Tube MILO generates a 1.8-GW, 170-ns FWHM microwave pulse using a 500-kV, 60-kA, 300-ns electron beam. We show that this improved performance is due to suppression of unwanted electron emission from the cathode in the region of the first two tube cavities. We also report on experiments to identify the breakdown mechanism in the vacuum radome for the Vlasov antenna which is used as a high-power microwave load for both MILO experiments. Finally, experimental results are presented for an optimized version of the Hard-Tube MILO that computer simulations have shown should generate over 3.0 GW.

[1] S. Calico *et al.*, "Experimental and theoretical investigations of a magnetically insulated line oscillator (MILO)," *Proc. SPIE*, vol. 2557, pp. 50-59, 1995.

3B05

Beam Drift and Diffusion in Linear Beam HPM

James Benford*
Microwave Sciences, 1041 Los Arabis Lane,
Lafayette, CA 94549
and Gregory Benford
Department of Physics and Astronomy, University of California at Irvine, Irvine, CA 92717

Observations show that the ubiquitous pulse shortening in HPM devices arises from formation of plasma, electron streaming, high-E-field breakdown and beam disruption. Linear beam devices exhibit all these mechanisms; in particular, beam disruption by ExB drifts in the strong microwave fields and diffusion in turbulent electric field appears common. We present models for both drift and diffusion. We argue that since drift velocity is proportional to microwave power, microwave energy is fixed for a given device. Since source geometry is usually determined by resonance conditions, energy is fixed for each class of source. Thus drift due to microwave power leads to microwave destruction and high power microwaves are essentially self-limited in energy. We present theory that predicts that beam diffusion due to strong Langmuir turbulence in the background plasma may be the cause of microwave cutoff. Even 10 kV/cm microwave electric fields may cause high rates of beam spreading. We compare theory predictions with experimental measurements of both drift and diffusion.

*Work supported by the AFOSR MURI HPM Source Program

3B06

Window and Cavity Breakdown Caused by High Power Microwaves.

A. Neuber, J. Dickens, D. Hemmert, H, Krompholz, L.L. Hatfield and M. Kristiansen
Departments of El;ectrical Engineering and Physics, Texas Tech University, Lubbock, TX 79409-3102

Physical mechanisms leading to microwave breakdown on windows and in cavities are investigated for power levels on the order of 100 MW at 2.85 GHz. A 3 MW magnetron coupled to a traveling wave resonator is used. Various configurations of dielectric windows are investigated. In a standard pillbox geometry with a pressure of less than 10^{-8} Torr, surface discharges on an alumina window and multipactor-like discharges starting at the waveguide edges occur simultaneously. Window breakdown with purely tangential electrical microwave fields is investigated for special geometries. To access geometries relevant for vacuum-air interfaces, an air-filled two-window setup is integrated into the resonator as well. Diagnostics include the measurement of reflected/ transmitted power, discharge luminosity, x-ray emission, and the measurement of local microwave electric fields. All quantities are recorded with 0.2 to 1 ns resolution. Based on the experimental results, methods to increase the power density which can be transmitted through windows will be investigated as well. In addition, parametric studies are conducted, in which window materials, profiles, and surface coatings are varied.

Work supported by AFOSR (MURI).

3B07

Performance of A Cathode Mounted Plasma Injection Source on the UNM Long-Pulse BWO*

C. Grabowski, J.M. Gahl and E. Schamiloglu
Electrical and Computer Engineering Department University of New Mexico, Albuquerque, NM 87131

Several studies conducted with high power backward wave oscillators (BWO's) have shown that significant increases in output power and generation efficiency can be obtained when a plasma is injected into the slow-wave structure (SWS) of the device prior to operation. Optimally, the injected plasma should be confined closely to the axis of the device, while the electron beam driving it should be as close to the walls as possible. Previous schemes for injecting the plasma have utilized sources mounted downstream of the SWS and relied upon the converging field lines of the electron beam's guiding magnetic field to compress the plasma close to the axis as it entered the SWS. This paper presents data on a plasma source mounted internal to the cathode structure of a high power BWO, thus providing injection of the plasma directly on axis in the strong, unform field region of the BWO. Such a scheme eliminates the obstruction to microwave extraction caused by downstream source hardware, as well as the presence of the plasma itself in this region.

The studies conducted with the cathode mounted plasma source have been performed at the University of New Mexico (UNM) on the UNM Long-Pulse BWO Experiment. The BWO is driven by a modified Physics International Pulserad 110A electron beam accelerator, which can provide intense relativistic beams for the BWO having energies of 200 ~ 500 kV at currents of 1.5 ~ 4.0 kA with pulse durations of 500 ~ 600 ns.

Data describing plasma prefill density at different axial positions within the BWO prior to operation will be presented. A comparison will then be made of BWO performance with and without the prefill plasma. Details of the novel plasma injection system will also be presented.

**Research supported thru a high energy microwave devices consortium funded by an AFOSR/DOD MURI grant and administered through Texas Tech University.*

3B08

Progress on Implementation of a Frequency Agile, High Power Backward-Wave Oscillator*

C.T. Abdallah, E. Schamiloglu, V.S. Souvalian and G.T. Park
Electrical & Computer Engineering Department University of New Mexico, Albuquerque, NM 87131

Recent work at the University of New Mexico has demonstrated that finite length effects in a high power *vacuum* backward wave oscillator (BWO) can be exploited to achieve frequency agility for constant beam and magnetic field parameters [1]. Specifically, the axial displacement of the slow wave structure with respect to the cutoff neck "inlet" to the electrodynamic system results in a periodic variation of both radiated power and frequency. In this presentation we discuss progress in automating this axial "shifting" on a shot-to-shot basis

using compact precision motors. This capability will then facilitate the use of a robust controller to achieve various control objectives. In particular, the preliminary design of a controller to i) maximize the frequency bandwidth for a given constant power output, ii) maximize the power radiated at a given frequency in the bandwidth, and iii) maximize the beam-to-peak microwave power conversion efficiency will be presented.

[1] L.D. Moreland, E. Schamiloglu, R.W. Lemke, A.M. Roitman, S.D. Korovin, and V.V. Rostov, "Enhanced Frequency Agility of High Power Relativistic Backward Wave Oscillators," IEEE Trans. Plasma Sci. **24**, 852 (1996).

**This Work is supported through a High Energy Microwave Devices Consortium funded by an AFOSR/DOD MURI grant and administered through Texas Tech University.*

3B09

*Investigation of the Dispersive Properties of Photonic Crystals Using High-Power Microwaves

K. Agi[1], M. Mojahedi[1],K.J. Malloy[1] and E. Schamiloglu[2]
[1]*Center for High Technology Materials*
[2]*Pulsed Power and Plasma Science Laboratory*
Electrical and Computer Engineering Department
University of New Mexico, EECE Bldg./Rm. 125,
Albuquerque, NM 8713

Photonic crystals (PCs) are three-dimensional, metallic or dielectric periodic structures that exhibit pass and stop bands in their frequency response. They are potentially useful components for a wide variety of applications. We present the characterization of the dispersive properties of PCs using high-power microwaves (HPMs). The advantage of high power characterization is the ability to measure decaying waves in the attenuating stop bands of the PCs. It is anticipated that the HPM characterization will provide higher signal-to-noise ratio than conventional low-power characterization schemes. A Sinus-6 driven backward-wave oscillator (BWO) is used to generate a 10 nsec microwave pulse at 9.65 GHz. Two dielectric PCs were fabricated for these experiments. The first crystal had a stop band centered about the excitation frequency of the BWO. The second crystal had a pass band at the source frequency. Using the two crystals, the temporal evolution of the dispersive properties of the PC is investigated leading to advanced concepts in the design of PCs for use in pulsed applications.

* This material is based on work supported by, or in part by, the U.S. Army Research Office under contract/grant number DAAH04-96-1-0439 and by an AFOSR/DoD MURI Grant.

Tuesday Morning, 20 May 1997
10:00 a.m. – Toucan Room

Oral Session 3C:
3.2 Intense Ion and Electron Beams
Chair: P.R. Menge

3C01

Development of a High-Brightness, Applied-B Lithium Extraction Ion Diode for Inertial Confinement Fusion*

M.E. Cuneo, R.G. Adams, J. Armijo, J.E. Bailey, C.H. Ching, M.P. Desjarlais, A.B. Filuk, W.E. Fowler, D.L. Hanson, D.J. Johnson, J.S. Lash, T.A. Mehlhorn, P.R. Menge, D. Nielsen, T.D. Pointon, S.A. Slutz, M.A. Stark, R.A. Vesey and D.F. Wenger
Sandia National Laboratories, P.O. Box 5800-1193, Albuquerque, NM 87185

The light ion fusion program is pursuing the development of a high brightness lithium ion beam on the SABRE accelerator at Sandia (6 MV, 0.25 MA). This will require the integration of at least three conditions: 1) an active, pre-formed, uniform lithium plasma ion source, 2) modification of the electron sheath distribution in the AK gap, and 3) mitigation of undesired electrode plasmas. These experiments represent the first attempt to combine these three conditions in a lithium ion diode. Our primary goal is the production of a lithium beam with a micro-divergence at peak ion power of ≤ 20 mrad, about half the previous value achieved on SABRE. A secondary goal is reduction of the impedance collapse rate. Our primary approach is a laser-produced lithium plasma generated with 10 ns YAG laser illumination of LiAg films. Laser fluences of 0.5 - 1.0 J/cm^2 appear to be satisfactory to generate a dense, highly ionized, low temperature plasma. An ohmically-generated, thin-film ion source is also being developed as a backup, longer term approach. Small-scale experiments are performed to study each ion source in detail, prior to fielding on the accelerator. Pre-formed anode plasmas allow the use of high magnetic fields (Vcrit/V ≥ 2) and limiters which slow the onset of a high

beam divergence electromagnetic instability and slow impedance collapse. High magnetic fields will be achieved with 1.8 MJ capacitor banks. An extensive array of in-situ electrode cleaning techniques have been developed to limit parasitic ion loads and impedance collapse from electrode contaminant plasma formation. Advanced ion beam, electron sheath and spectroscopic AK gap diagnostics have also been developed.

*This work was supported by the US DOE under Contract DE-AC04-94AL85000. Sandia is a multiprogram laboratory operated by Sandia Corporation, a Lockheed Martin Company, for the US DOE.

3C02-3C03 *Invited*

Effects of Electron-Anode Interactions in Applied-B Ion Diodes*

R.A. Vesey, T.D. Pointon, M.E. Cuneo, T.A. Mehlhorn
Sandia National Laboratories, Albuquerque, NM 87185-1187

The transverse magnetic field in an applied-B ion diode is designed to minimize electron loss to the anode. However, 3-D particle-in-cell (PIC) simulations show that electron loss escalates once the ion current is sufficiently enhanced such that the ion mode instability dominates. Thus the transition from the diocotron mode to the ion mode is accompanied not only by an increase in ion beam divergence, but also by an increased flux of high-energy electrons striking the anode surface. Coupled electron-photon Monte Carlo simulations have been used in conjunction with PIC diode simulations to assess electron reflection, energy deposition leading to anode heating and thermal desorption of contaminants, enhanced ionization of desorbates due to secondary electron emission, and photon production. Electron reflection is included in the 3-D PIC simulations, and although no macroscopic diode effect is seen in the present model, the anode heating profile is affected by high-energy reflected electrons, and low-energy secondary electrons may enhance the effective electron-impact ionization cross-section by factors of 7-10 for desorbed contaminants. The high spatial non-uniformity in the predicted electron loss profile leads to local hot spots on the anode surface which exceed 300-400°C soon after the ion mode transition. Thermal and stimulated desorption results in complete desorption of contaminants with 15-20 kcal/mole binding energies during the power pulse in high-dose regions of the anode surface. Predicted time-dependent photon distributions from electron-anode collisions are available for comparison with X-ray detector measurements.

*Funding has been provided by the US DOE under contract DE-AC04-94-AL85000.

3C04

Gas-Breakdown Effects Associated with the Self-Pinched Transport of Intense Light-Ion Beams*

P.F. Ottinger
Plasma Physics Division, Naval Research Laboratory, Washington, DC 20375-5346
D.V. Rose
JAYCOR, Vienna, VA
B.V. Oliver
National Research Council Research Associate
C.L. Olson
Sandia National Laboratories, Albuquerque, NM
D.R. Welch
Mission Research Corp., Albuquerque, NM 87106

Self-pinched transport (SPT) of intense light-ion beams is being considered for delivering energy to a high-gain, high-yield inertial confinement fusion target. Proton beam SPT experiments are underway on the Gamble II generator at the Naval Research Laboratory. The physics of SPT in low-pressure gas is being analyzed with analytic theory and numerical simulations.

A 1-D theory[1] estimates the net current fraction necessary for stable transport as a function of gas density for a given beam profile. SPT simulations using the 3-D hybrid particle-in-cell (PIC) code IPROP[2] determine the beam profile. Important to both theory and simulations is the inclusion of gas-breakdown physics. A comparison between the theory and the self-consistent simulations using IPROP is made.

Additional SPT simulations have been carried out using the 2-D hybrid PIC code SOLENZ[3] which assumes a pre-ionized plasma. this simulation model enables the investigation of long time scale beam propagation issues. A comparison between IPROP and SOLENZ will be presented. SOLENZ simulations with the Gamble II beam parameters demonstrate SPT but point to the need to study the injection conditions to improve beam confinement. Simulations examining beam-to-wall distance and injection conditions will be presented.

[1]D.R. Welch, et al., Fusion Eng. and Design, *to be published* (1997).
[2]D.R. Welch, et al., Phys. Plasmas **1**, 764 (1994).
[3]B.V. Oliver, et al., Phys. Plasmas **3**, 4725 (1996).

*Work supported by DOE through Sandia National Labs.

3C05

Performance of a Shallow-Focus Applied-Magnetic-Field Diode for Ion-Beam-Transport Experiments*

F.C. Young, J.M. Neri, P.F. Ottinger
Plasma Physics Division, Naval Research Laboratory, Washington, DC 20375-5346
T.G. Jones and B.V. Oliver
National Research Council Research Associates
D.V. Rose
JAYCOR, Vienna, VA

An applied-magnetic-field ion diode to study the transport of intense ion beams for light-ion inertial confinement fusion is being operated on the Gamble II generator at NRL. A Large-area (145-cm^2), shallow-focusing diode is used to provide the ion beam required for self-pinched transport (SPT) experiments.

Protons from a wax-grooved annular aluminum anode of 10.5-cm outer radius are directed to a focus as 70 cm by shaping the anode surface. The nagnitude and ration of the currents in the inner and outer cathode coils are adjusted to produce the diode insulating B-field and to provide a radially uniform anode current density. An initial counter-pulse current in these coils is used to place the B-field separatrix on the ion emission surface in the diode gap at peak power. The separatrix location minimizes off-axis ion-beam mis-direction at the focus due to angular momentum.

Experiments have demonstrated focusing at 70 cm for 1.2-MV, 40-kA protons. Beyond the focus, the beam hollows out consistent with 20-30 mrad microdivergence. The effect of the counter-pulse B-field on altering the ion-beam trajectories and improving the focus has been diagnosed with a multiple-pinhole-camera using radiachromic film. This diagnostic is also used to determind the radial and azimuthal uniformity of ion emission at the anode for different B-field conditions.

Increasing the diode voltage to 1.5 MV and optimizing the ion current are planned before initiating SPT experiments. Experiments to measure the spatial beam profile at focus, i.e., the SPT channel entrance, are in progress. Results will be presented .

Work supported by DOE through SNL.

3C06

Progress Toward a Microsecond Duration, Repetitive, Intense-Ion Beam Accelerator*

H.A. Davis and W.A. Reass
Los Alamos National Laboratory, Los Alamos, NM 87545
D.M. Coates and H.M. Schleinitz
DuPont, Los Alamos, NM
J.B. Greenly
Cornell University, Ithaca, NY
R.H. Lovberg
University of California at San Diego, San Diego, CA

A number of intense ion beam applications are emerging requiring repetitive high-average-power beams. These applications include ablative deposition of thin films, rapid melt and resolidification for surface property enhancement, advanced diagnostic neutral beams for the next generation of Tokamaks, and intense pulsed-neutron sources. We are developing a 250 keV, 15 kA, 1μs duration, 1-30 Hz intense-ion beam accelerator called CHAMP (Continuous High Average-Power Microsecond Pulser).

The accelerator will use a magnetically insulated extraction diode in ballistically focused gemoetry. The 450 cm^2 active plasma anode (MAP diode) can utilize any gaseous species. Gas is supplied from a puff valve located on the system axis and is ducted through a radial flow channel. The anode plasma is formed by currents induced in the gas by a fast-rising two-turn, flat, spiral wound coil with four parallel sets of windings. The insulating transverse magnetic field will be generated by two magnetic field coils on the grounded cathode focusing cones. We will use a set of parallel lumped-element Blumlein circuits and a step-up pulse transformer to supply the diode acceleration voltage.

Hardware for first anode plasma generation tests is being assembled and results from characterization of the anode plasma source will be presented.

*Sponsored by DOE contract W-7405-ENG-36

3C07

Oxide Cathodes Produced by Plasma Deposition

G. Scheitrum and G. Caryotakis
Stanford Linear Accelerator Center, Menlo Park, CA
T. Pi and R. Umstattd
University of California at Davis, Davis, CA
I. Brown and O. Montiero
Lawrence Berkeley Laboratory, Berkeley, CA

These are two distinct applications for high-current-density, long-life thermionic cathodes. The first application is as a substitute for explosive emission cathodes used in high-power microwave (HPM) devices being developed for Air Force programs. In order to provide kiloamps, current densities up to 100 A/cm^2 are required. The second application is in SLAC's X-band klystrons for the Next Linear Collider (NLC). SLAC requires inexpensive cathodes with 50,000+ hours life for the NLC.

The best oxide cathodes have been capable of long life and high-current-density. The problem has been the ability to consistently reach maximum performance. The complex chemistry of the deposition and activation process have made consistent performance unrealizable.

SLAC, UCD, and LBL are developing a plasma deposition process that eliminates the problems with binders, carbonate reduction, peeling, and porosity. The emission layer is deposited using plasma deposition of metallic barium in vacuum with an oxygen background gas. An applied bias voltage drives the oxide plasma into the nickel surface. Since the oxide is deposited directly, it does not have problems with poisoning from a hydrocarbon binder. The density of the oxide layer is increased from the 40% to 50% for standard oxide cathodes to nearly 100% for plasma deposition. It is expected that the repeatable process, increased density, and elimination of poisoning agents will provide a long-life, high-current-density cathode for a variety of applications.

Major funding for this program is provided by the AFOSR MURI program, the facilities, equipment and additional funding are provided by DOE.

3C08

Simulation of a Plasma-Focused Electron Gun*

J.P. Verboncoeur
Dept. EECS, University of California at Berkeley, Berkeley, CA 94720-1770
johnv@eecs.berkeley.edu

Plasma can play an important role in the physics of an electron gun. It can provide an important focusing mechanism, and plasmas are often present in varying densities in many devices designed for vacuum operation. Plasma can also be a source of noise and instability for a microwave beam device. A plasma-focused electron gun is modeled using the PIC code XOOPIC.[1] The plasma is formed via electron impact ionization with an argon background gas at 10^{-4} Torr. Electron-neutral interactions are included using a Monte-Carlo model.[2] The gun operates close to the space charge limit, with V=30 kV, I=9A for a 7 mm AK gap. A solenoidal coil with an iron core provides a peak field on axis of B_{max} = 180 G. Argon ions streaming back toward the cathode cause erosion of the surface. Most of the ion flux passes through a 1 mm hole in the center of the cathode. The flux at the cathode surface is characterized, including energy and angle of incidence. In addition, the beam emittance is examined as the plasma builds up to steady state over a microsecond timescale.

*This work is supported in part by U.S. Energy Corp. and Air Force Office of Scientific Research MURI grant F49620-95-1-0253.

[1] J.P. Verboncoeur, A.B. Langdon and N.T. Gladd, *Comp. Phys. Comm.* **87**, 199 (1995).

[2] V. Vahedi and M. Surendra, *Comp. Phys. Comm.* **87**, 179 (1995).

3C09

Two Dimensional Child-Langmuir Law*

Sarah McGee, Y.Y. Lau and R.M. Gilgenbach
University of Michigan, Ann Arbor, MI 48109-2104
J.W. Luginsland
Phillips Laboratory, Kirtland AFB, NM 87117-5776

By considering unform emission of electrons over a finite strip of width W in a planar gap of gap separation D, we extend the classical 1-dimensional Child-Langmuir law to 2 dimensions. The analysis is done with two simulation codes, MAGIC[1] and OOPIC[2]; which yield

similar results. These numerical results have been synthesized into a scaling law[3], which expresses the non-relativistic 2-dimensional limiting current density, $J_{CL}(2)$, in units of the classical 1-dimentional Child-Langmuir value, $J_{CL}(1)$:

$$J_{CL}(2)/J_{CL}(1) = 1 + 0.3145/(W/D). \qquad (A)$$

Equation (A) is found to fit the numerical data to within 5% over the range simulated: $0.1 < WD < 8$. More surprisingly, this expression is found to be also valid, regardless of the magnitude of the external magnetic field that is imposed along the mean flow[3]. We have extended our analysis to include th erelativistic effects and self magnetic field effects. We found that they strongly affect the critical current for laminar flows, resulting in a limiting current density below that predicted by the 1-dimenstional relativistic Child-Langmuir value.

[1] Goplen, Ludeking, Smithe, and Warren, Comput. Phys. Commun. **87**, 54, (1995)

[2] Verboncoeur, Langdon, and Gladd, Comput. Phys. Commun. **87**, 199 (1995).

[3] Luginsland, Lau, and Gilgenbach, Phys. Rev. Lett. **77**, 4668 (1996).

*Supported by NRL/ONR, MURI/AFOSR, DoD/ AASERT, and NRC Research Associateship.

Tuesday Morning, 20 May 1997
10:00 a.m. – Macaw Room

Oral Session 3D:
2.4 Slow Wave Devices II
Chair: W. L. Menninger

3D01-02 *Invited*

60% Efficient C-Band TWT for the Microwave Power Module

D.R. Whaley, C.M. Armstrong, B. Gannon, G. Groshart, E. Hurt, J. Hutchins and M. Roscoe
Northrop Grumman Corporation, Electronic & Information Warfare Systems, 600 Hicks Rd., M/S H6402, Rolling Meadows, IL 60008
Tel (847) 259 9600

Northrop Grumman's ongoing development of microwave power modules (MPMs) provides microwave power at various power levels, frequencies, and bandwidths for a variety of applications including communications, radar, and ECM. The MPM combines an integrated power conditioner (IPC), solid state amplifier (SSA), and traveling wave tube (TWT) within a single module resulting in a small, lightweight package for efficient DC/RF energy conversion. Recent advances in the C-Bank TWT have resulted in a module efficiency greater than 50% at power levels in excess of 170W.

The MPM TWT operates at a circuit efficiency of 31% and uses a four-stage depressed collector to increase the total power-added efficiency to 61%. The output circuit profile design of the TWT provides the good phase bunching and synchronism throughout the length of the tube necessary for high efficiency operation. Careful magnetic field design and fabrication has resulted in excellent body current characteristics over all ranges of operation and uses a shimless PPM stack and a field immersed cathode to provide the confined flow conditions for the electron beam. A second development program for TWTs operating at lower perveance and higher power has also been pursued using the same methods as for the C-Band MPM TWT and has resulted in nearly identical performance of 32% circuit efficiency and 63% total efficiency at power levels in excess of 240W. Performance characteristics of the C-Band MPM and both TWT programs will be presented.

Work supported in part by the Naval Research Laboratory under contract No. N00014-94-C-2242.

3D03

GATOR: A 3-D Time-Dependent Simulation Code for Helix TWTs*

H. P. Freund† and E. G. Zaidman
Naval Research Laboratory,
Washington, D.C. 20357-5347 USA

A time-dependent collective nonlinear analysis of a helix traveling wave tube (TWT) including space-charge effects is presented for a configuration where an electron beam propagates through a sheath helix surrounded by a conducting wall. The effects of dielectric- and vane-loading of the helix are included as is efficiency enhancement by tapering the helix pitch and external focusing by means of either a uniform solenoidal magnetic field or a periodic field produced by a periodic permanent magnet (PPM) stack. Dielectric-loading is described under the assumption that the gap between the helix and the wall is uniformly filled by a dielectric material. Vane-loading describes the insertion of an arbitrary number of vanes running the length of the helix. The electromagnetic field is represented as a superposition of azimuthally symmetric waves in a vacuum sheath helix. The propagation of each wave *in vacuo* as well as the interaction of each wave with the electron beam is included by allowing the amplitudes of the waves to vary in z and t. The dynamical equation for the field is solved in conjunction with the three-dimensional Lorentz force equations for an ensemble of electrons. Collective effects from the fluctuating (RF) beam space-charge waves and the DC self-fields. The simulation is compared with a linear theory of the interaction, and an example is described corresponding to a tube built at Northrop-Grumman Corp.

This work supported by the Office of Naval Research.
†Permanent Address: Science Applications International Corp., McLean, VA 22102

3D04

Travelling Wave Tube Devices with Non Linear Dielectric Elements

T.M. Antonsen Jr.† and B. Levush
Vacuum Electronic Branch, Naval Research Laboratory
Washington D.C. 20375

The performance of travelling wave tube amplifiers incorporating nonlinear dielectric elements is studied via computer simulation. Two different situations are investigated: a) the use of voltage controlled dielectrics to provide rapid modification of the dispersion characteristics of the slow wave structure, and b) the use of nonlinear dielectric elements to reduce intermodulation distortion. In the first case the goal is to design an amplifying structure whose gain as a function of frequency can be varied electrically. Preliminary design studies show that relatively large changes in the center frequency of the amplification band can be achieved with relatively modest changes in the dielectric constant of helix support structure. In the second case, the use of dielectrics with negative second order susceptibilities is studies as a means of reducing phase and intermodulation distortion. Use of these dielectrics along with dynamic velocity taper to reduce amplitude modulation distortion results in marked reduction of predicted intermodulation distortion.

†Also Science Application International Corporation and University of Maryland

3D05

Calculation and Measurement of Intermodulation Products in TWTs

Daniel J. Gregoire
Hughes Research Laboratories, Malibu, CA 90265
email: dgregoire@msmail4.hac.com
William Menninger
Hughes Electron Dynamic Division, Torrance, CA
email: will@gatling.to.hac.com

Dependable tools for physically modeling the effects of multiple tones in traveling-wave tubes (TWT) are required in order to modify TWT designs to increase linearity and reduce the significance of intermodulation distortion (IMD). Ideally, the calculation tools are capable of running in short time intervals on desktop workstations. We will present the results of a study aimed at predicting the performance of a tube under development at Hughes Electron Dynamics Division (HEDD). The analysis consists of two distinct parts. In the first part, we use *Qhelix*, a proprietary TWT design code developed at HEDD which predicts IMD by post-processing the TWT amplitude and phase transfer curves using a Fast Fourier Transform (FFT) method. In the second part of this study, we model the TWT with *Christine*[1], a true multi-tone TWT code developed by researchers at the Naval Research Laboratory (NRL), that tracks the interaction of multiple RF signals with the electron beam in the TWT structure. This is a physically more direct method of calculating the

IMD products. Comparisons of these two techniques will be presented along with the results from tube measurements.

This work was funded by Hughes Electronics IR&D.

[1] Thomas M. Antonsen and Baruch Levush, *CHRISTINE, A Multifrequency Simulation Code for Traveling Wave Tube Amplifiers*, NRL Report, 1996.

3D06

COMPUTATIONAL OPTIMIZATION OF RF AND OVERALL EFFICIENCY IN TWTS WITH SIMULATED ANNEALING

Jeffrey D. Wilson
NASA Lewis Research Center, Cleveland, OH

An RF phase velocity taper in the output section of a TWT slow-wave circuit is commonly used to increase RF power efficiency. In order to determine the optimal phase velocity profile, a simulated annealing algorithm has been developed and coded into the NASA 2.5-Dimensional TWT Computer Model[1]. The advantage of simulated annealing over most other optimization techniques is that it allows a solution to escape from a local extremum towards the ultimate global optimum.

With the incorporation of this algorithm, the model can now be used to optimize any calculated output characteristic in terms of any combination of input parameters. The algorithm was first tested on a paper design for a 60-GHz coupled-cavity TWT. The lengths of the cavities at the end of the output section were optimized for center-frequency RF efficiency. The resulting nonlinear taper showed a computed increase in efficiency form 7.2% to 13.5%.

For space TWTs, overall efficiency, which depends on spent beam energy recovered by a multi-stage depressed collector (MDC), is generally more critical than RF efficiency. Presently, the model is being used to optimize the phase velocity profile and collector stage voltages in a helix TWT design for overall efficiency.

[1] J.D. Wilson, NASA TP-2675, 1987.

3D07

Three Dimensional Modeling of Multistage Depressed Collectors

K.R. Vaden, V.O. Heinen and J.A. Dayton, Jr.
NASA Lewis Research Center, Cleveland, OH

The computer modeling of instantaneous currents within three dimensional multistage depressed collectors (MDC) will be discussed. MAFIA, a three dimensional particle-in-cell (PIC) code available from AET associates, is used for these computations. For several years, the method of modeling MDCs at NASA Lewis Research Center employed two dimensional computer codes. The Detweiler code was used for the large signal analysis of the slow wave circuit that produces the spent beam model and the Hermannsfeldt code was used for the actual collector analysis. While this computational procedure has been successfully applied to the analysis of circularly symmetric collectors, it can only be applied to asymmetric collectors as an approximation. In addition, the Hermannsfeldt code is a steady state solver and cannot utilize any phase space information associated with the spent beam model. The MAFIA code can analyze the time dependency of collector currents, and compute the energy dissipated by the incident beam on the collector electrodes. The computational procedure to be reported will again use the Detweiler code to produce a spent beam model that will be converted to a PIC model for use by MAFIA. The collector current distribution produced will be compared to that obtained using Hermannsfeldt and with experimental measurements for the 10 Watt, 32 GHz TWT developed for the Cassini Mission.

3D08

Cold-Tested and Interaction Models for Helix TWTs in MMACE*

A.A. Mondelli, J.J. Petillo and H.P. Freund
Science Applications International Corporation, McLean, Virginia 22102

The tri-service MMACE program has developed a numerical framework for the design of microwave power tubes, with particular attention to the design of helix TWTs. This paper will describe a new model for the cold-test, small-signal and large-signal behavior of microwave power tubes that is under development as part of the MMACE tools initiative. Its architecture and projected

capabilities will be described, and first results will be presented.

Two simulation tools are already integrated into the MMACE environment. One of these, the ARGUS/ESP[1] code, is a three-dimensional electromagnetic cold-test code. The second code, Gator[2], is a TWT interaction model that solves the dynamical equations for the evolution of the field amplitudes of a collection of modes in conjunction with the Lorentz force equations for an ensemble of electrons. The application of these tools in MMACE will be described through examples of actual helix TWT designs.

*This work had been supported by NRL Vacuum Electronics Branch. H. Freund's work was funded by NRL as an on-site activity. Portions of the effort were monitored by R. Worley, WL/ELM (Contract No. F33615-94-C-1578) under the MMACE program.

[1] J.J. Petillo, A. Mankofsky, A. Drobot, A. Mondelli, W. Krueger, and M. Kress, Proc. 14th Intl. Conf. on the Numerical Simulation of Plasmas, (Annapolis, MD, 3-6 September 1991)

[2] H.P. Freund, E.G. Zaidman, and T.M. Antonsen Jr., Phys. Plasmas **3**, 3145 (1996).

3D09

Investigation of the Effect of Support Rod Permittivity on TWT Performance

Carol L. Kory
Analex Corporation/NASA Lewis Research Center, Cleveland, OH
James A. Dayton, Jr.
NASA Lewis Research Center, Cleveland, OH

The results of some in-house research on dielectric material commonly used as support rods in traveling-wave tube (TWT) slow-wave circuits, show that the permittivity can vary within the same plate of material by as much as +/- 10%. This indicates that the support rod dielectric constant may vary by this amount from tube to tube, from rod to rod, or axially along the length of a single support rod. Recent advances in the state of the art of computer modeling[1] offer the possibility for the first time to evaluate the effect of slow-wave structure support rod dielectric constant variations, on the performance of helical TWT's.

The cold-test parameters including dispersion and on-axis interaction impedance, have been calculated for a Northrop-Grumman helical TWT slow-wave circuit using MAFIA, the three-dimensional electromagnetic finite-integration computer code. The helix model includes tape thickness, dielectric support geometry and material properties consistent with the actual circuit. Measured and simulated cold-test data for the helical circuit will be presented, showing excellent agreement. These parameters will also be compared for several variations on the dielectric constant of the rods, including axially and azimuthally asymmetric configurations, consistent with likely variations occurring in actual manufactured TWTs. The large deviation in TWT performance due to these variations suggest a need for more accurate dielectric data and improved control of material fabrication processes.

[1] C.L. Kory, "Three-Dimensional Simulation of Helix Traveling-Wave Tube Cold Test Characteristics Using MAFIA, IEEE Trans. ED-43, no. 8, pp. 1317-1319, Aug. 1996.

Tuesday Morning, 20 May 1997
10:00 a.m. – Cockatoo Room

Oral Session 3E:
4.4 Dense Plasma Focus I
Chair: G. F. Kiuttu

3E01

MEMORIAL TRIBUTE TO DR. JOSEPH MATHER

K.D. Ware
Defense Special Weapons Agency, Alexandria, VA

Joe Mather, one of the originators of the dense plasma focus, died recently. We review some of his pioneering work on plasma focus devices.

3E02-03 *Invited*

Present Status of Plasma Focus Research at RRC "Kurchatov Institute"*

N.V. Filippov and PF-team
RRC "Kurachatov Institute", 1 Kurchatov Sq., Moscow, 1123182 Russia

The experiments at RRC were carried on two identical machines ISPF and PFE ($W \leq 100$ kJ) as well as on PF-3 ($W = 1$ MJ). PF chambers were filled with D_2, Ne and Ar mixtures; the central part of the anodes have Cu, Mo, W and/or Ta inserts. X-ray spectral (HXR: 20-100 keV and SXR: ~1 keV) were measured with sub-nanosecond time resolution. The pinch dynamic was diagnosed by the use of the speedy multi-frame photography and X-ray chronography allowing to relate the volumetric and temporal characteristics of a SXR-radiation with the plasma current sheath dynamics at a compression stage. The conversion of a quasi-static accelerating electric field into a ring-like expanding CZ was identified. It was found that the current break process is damped due to a self-regulating current flow around the area with a reduced electric conductivity emerging under explosive anode surface evaporation. CZ-expansion limits the voltage drop across a ring-like transition layer (plasma diode) and explains observed quasi-stationary conditions of electron and ion acceleration. For flux density $\geq 10^{13}$ W/cm^2 an explosive evaporation of the anode material is accompanied by the chipping destruction of a rear electrode surface and provides the ion flux injection into the acceleration zone. Observed ion acceleration in the ring-like diode and generation of multi-MeV-beams of heavy ions is related to: (I) violation of azimuthal homogeneity in the ring-like layer, and (ii) acceleration processes due to magnetic field reconnection in the pinch current.

Plasma focus machine of the MINIK program is based on experiences gathered during ISPF, PFE and PF-3 experiments and utilize existing inductive storage at TRINITY. A new PF will have chamber with anode of ϕ=2.5m filled with Ar. It is expected that from 100 MJ of energy stored as much as W=20MJ will be transferred into plasma. The relevant experience with PF-3 and feasibility of MINIK (PF aspects) will be discussed.

The work was supported in part by the Int. Science Foundation, #M53S300 and the Russian Foundation of Basic Res., #95-02-04-422.

PF-team: A.N. Filippov, T.I. Filippova, M.A. Karakin, V.I. Krauz, A.N. Mokeev, V.V. Mialton, S.A. Nikulin, V.P. Tykshaev and V.P. Vinogradov.

3E04

Formation of a Closed, Spheromak-Like Magnetic Configuration in Plasma Focus Discharges and the Enhanced Radiation Yield in High-Current Discharges

A.B. Kukushkin, V.A. Rantsev-Kartinov
INF RRC "Kurchatov Institute", Moscow 123182 Russia

The enhanced SXR radiation yield observed in recent pulsed power Z-pinch experiments and the relatively high efficiency of input energy conversion into SXR radiation in certain Filippov-type plasma focus discharges are analyzed in the frame of the concep[1] of self-consistent formation of a closed, spheromak-like magnetic configuration (SLMC) in plasma focus discharges. The relationship is analyzed between the major characteristic features of the 3D resistive two-fluid helicity-rich radiation magnetohydrodynamics of strongly inhomogeneous plasmas, verified by numerous experimental data (see [2]) on the formation of the large-scale (several cm) SLMC with complicated short-scale structure, and the enhanced efficiency of the input energy conversion into SXR radiation.

The diagnostics strategy is formulated which is needed for the identification of the role of the effects outlined. Both the diagnostic array requirements and diagnostic space-time scales are discussed.

References

[1] Kukushkin A.B., Rantsev-Kartinov V.A., Preprint of RRC "Kurchatov Institute", IAE 5646/6, Moscow, June 1993.

[2] Kukushkin A.B., Rantsev-Kartinov V.A., Terentiev A.R., Fusion Technology, 1997 (to be published); Transactions of Fusion Technology, **27** (1995) 325.

3E05

X-Ray Spectroscopic Diagnostics of High-Temperature Dense Plasmas Created in Different Gaseous Media

I.Yu. Skobelev, V.M. Dyakin, A.Ya. Faenov, R. Jarotcki and J. Kostecki
Multicharged Ion Spectra Data Center, VNIIFTRI, Mendeleevo, 141570 Russia
A. Bartnik, H. Fiedorowicz
Institute of Optoelectronics, Military University of Technology, 01-489 Warsaw, Poland
J. Nilsen, A.L. Osterheld and M. Szczurek
Lawrence Livermore National Laboratory, Livermore, CA 94551 USA

The investigations of emission X-ray spectra of multicharged ions of some chemical elements (S, F, Ar, Fr, O) have been carried out. These atoms are contained in a gases and consequently can be used as diagnostic elements in a dense plasma focus experiments.

Our investigations were done in the dense high-temperature plasma ($N_e \approx 10^{21}$ cm^{-3}, $T_e \approx 500$ eV) created by laser heating of high-pressure gas puff targets, and X-ray spectrographs with a spherically bent mica crystals were used for spectra observations. Some new spectroscopic results (line identifications, high-precision wavelength measurements) have been obtained and have been applied to determine a spatial distribution of plasma parameters. It is shown that spectroscopic techniques used is a very suitable tool for studies of a plasma with complicated spatial structure.

3E06-07 *Invited*

DENSE PLASMA-FOCUS RESEARCH IN POLAND

M. Sadowski
Soltan Institute for Nuclear Studies, 05-400 Otwock-Swierk n. Warsaw, Poland

Recent PF experiments, as performed with different PF facilities of energy from 2 kJ to 440 kJ, are compared. The MAJA machine[1], operated up to 60 kJ/35 kV, is used for X-ray and fast e-beams studies. X-rays are measured with pinhole cameras and scintillation detectors with foil filters. It was shown that hot-spots are formed along the pinch axis in a given sequence, starting from the front plane of the anode and moving toward the maximum compression region[2]. To determine plasma parameters within hot-spots the use was made of two X-ray spectrographs equipped with concave quartz crystals. For deuterium-argon shots there were registered H- and He-like Ar-lines within a spectral range of 3.5-5Å. The electron concentration, as estimated from relative intensities of the intercombination and resonance lines, was about 10^20 cm^{-3}. The electron temperature, as calculated from the dielectronic satellite and resonance lines, was above 1 keV[2]. Recently, there have been studied polarization effects of selected X-ray lines[3].

The PF-360 machine[4] operated up to 240 kJ/35kV, is used for the optimization tests and fast ion emission studies. Recently, deuterium pressure limits for the DPF operation have been determined and compared with results obtained in small-scale PF devices[4]. Time-resolved measurements of charged particles, neutrons, and X-rays[5] have been continued supplying new data about their correlation.

Other small-scale PF experiments were performed within the Argentinean-Polish joint project[6]. For the first time there were registered ion energy spectra for pure nitrogen shots. They have been used for a comparison of NTDs calibration diagrams and for application-oriented research.

The SINS team participated also in a mega-joule PF experiment carried out at the IPPLM in Warsaw. Preliminary tests have been performed up to 440 kJ/28kV. Measurements of X-rays, neutrons (from deuterium shots), and ions, are compared with results of other large-scale PF experiments.

Prospects of DPF research in Poland are also discussed.

[1] L.Jakubowski, M.Sadowski:22nd EPSConf. (1995) **2**, 161.
[2] L.Jakubowski, et al.; Proc. ICPP (Nagoya 1996)-in print.
[3] L Jakubowski, et al.; submitted for 4th ICDZP (1997).
[4] M.Sadowski, et al.; 21st EPS Conf. (1994) **3**, 1320.
[5] M.Milanese, et al.; Proc. 81st Meet. APS (Tandil 1996).
[6] M.Sadowski, et al.; Radiation Measurements-in print.

Tuesday Morning, 20 May 1997
10:00 a.m. – Rousseau Center

Poster Session 3P01-28:
1.1 Basic Processes in Fully and Partially Ionized Plasmas – Waves, Instabilities, Plasma Theory, etc.

3P01

Modeling of Collisional Effects in RF Plasma Sources

M.H. Bettenhausen, J.E. Scharer and Y. Mouzouris
Dept. of Electrical and Computer Engr.
University of Wisconsin-Madison, Madison 53706

Collisions are an important factor for power absorption in most radio-frequency (RF) plasma sources. Our chief interest in this work is the effect of collisional damping in helicon-type plasma sources. We consider sources with the frequency of operation on the order of 10 Mhz and neutral background pressures ranging from a few mTorr to atmospheric. The characteristic collision frequency varies greatly over this pressure range. We consider three different regimes: $\nu << \omega$, $\nu \approx \omega$ and $\nu >> \omega$ where ν is the characteristic collision frequency and ω is the frequency of the RF source. We present results which show the differences of the radial power deposition for these three regimes using the ANTENA2 code,[a] which employs a Krook-type model to calculate collisional damping. We discuss limitations of and possible improvements to this collision model. We also discuss the use of these results for improving the design of sources which will operate at neutral pressures.

This research is supported by AFOSR Grant F44620-94-1-0054 and NSF grant No. ECS-9632377.

[a] Y. Mouzouris and J. Scharer, IEEE Trans. on Plasma Science, **24**(1), (1996).

3P02

Antenna Coupling and Absorption Mechanisms in a Helicon Source Operation

Y. Mouzouris, J.E. Scharer, and M.H. Bettenhausen
Dept. of Electrical and Computer Engr.
University of Wisconsin-Madison, Madison 53706

The MAX_EB computer code[a] was used to study and model helicon sources. MAX_EB, a two-dimensional (r, z) simulation code, calculates the electromagnetic wave fields and power absorption in an inhomogeneous cold plasma immersed in a non-uniform magnetic field. A phenomenological collision frequency is used to simulate power dissipation. The current distribution of the launching antenna which provides the full antenna spectra is included in the model. We are in the process of improving the code to include thermal effects. A local k_z value will be estimated from the calculated 3-D (r, θ, z) electromagnetic wave fields. This k_z value will be used to approximate the hot plasma dielectric tensor. Preliminary studies of the power absorption profile that includes the Landau damping term are presented. We will benchmark the modified MAX_EB code with our ANTENA2 code[b] for an axially uniform plasma in a uniform axial magnetic field. 2-D profile on the wave properties and power absorption is investigated. Detailed studies of the wave fields and electron heating profile due to collisional and collisionless wave absorption mechanisms in a non-uniform plasma for the dominant azimuthal mode numbers are presented.

Work supported by NSF grant No. ECS-9632377.

[a] L.A. Berry and J.C. Whitson, private communication (1996)

[b] Y. Mouzouris and J. Scharer, IEEE Trans. on Plasma Science, **24**(1), (1996)

3P03

Helicon Wave Excitation with Bifilar Antennas

David G. Miljak and Francis F. Chen
University of California at Los Angeles,
Los Angeles, CA

A bifilar, helical antenna has been used to produce an RF field that rotates in time as well as space. A special match box was constructed to tune the two helices with adjustable phase and amplitude. In this way, one hoped to excite the left-hand polarized $(m = -1)$ mode of the helicon

wave, which is usually not seen. We find that the strongest coupling is achieved when both the spatial and temporal rotations match those of the $m = +1$ mode, with the temporal rotation being more important. When both the time and space variations are set to excite the $m = -1$ mode, it can indeed be seen, but only close to the antenna. It damps rapidly, and downstream from the antenna only the weakly excited $m = +1$ mode remains. These observations are in agreement with computations by D. Arnush, which show that the antenna coupling to the $m = -1$ mode is much weaker than to the $m = +1$ mode.

said to be operating predominantly in a "wave-mode", or at least primarily inductively coupled, capacitive coupling from the antenna can still have a significant effect on the plasma profile. Transverse images also show that with all other conditions being the same a helical antenna produces brighter plasmas than a straight Nagoya Type III antenna, and with the helical antenna a configuration corresponding to excitation of the $m = +1$ helicon mode produces a longer brighter plasma than the $m = -1$ configuration. A connection between these results and simplified helicon wave theory with the calculated power spectra of the antennas is discussed.

3P04

A multi-Tube Helicon Source

John D. Evans, Francis F. Chen
University of Californiat at Los Angeles, Los Angeles, CA
George Tynan
PMT, Inc.

A seven-tube array of helicon sources is used to create a large-area plasma for semiconductor processing. Each source is 5 cm in diam with a helical antenna and a magnetic field of 0-100 G. Above a certain threshold power, the RF match circuit distributes the power equally to all the tubes. The plasma is injected into a 50-cm diam magnetic bucket, and the density uniformity is measured at various distances downstream from the source. Experiments were done in A and Cl and at frequencies of 13.56 and 27.12 MHz. Initial trials gave fairly uniform plasmas over a 30 cm diameter, and continuing work will optimize the tube diameter and spacing, the antenna configuration, and the magnetic field shape.

3P05

2D Imaging of a Helicon Discharge

David D. Blackwell and Francis F. Chen
University of California at Los Angeles, Los Angeles, CA

Two dimensional images from the ionized argon light of a helicon discharge are made both along and across the magnetic field with various antenna configurations. It is shown that even at high densities where the discharge is

3P06

Spontaneous Current Disruptions in a Plasma-Driven Double Probe

A. Svensson and N. Brenning
Div. of Plasma Physics, Alfvén Lab., Royal Institute of Technology, SE-100 Stockholm, Sweden

Measurements are made to investigate the nature of fast current disruptions appearing in one of the experimental devices in the Alfvén Laboratory. The disruptions appear when we, in a transversely magnetized plasma flow, let the induced electric field ($\mathbf{E} = -\mathbf{vxB}$) drive a current between two externally short-circuited, floating, probes. In this configuration, the effective probe bias is $\mathbf{E}\cdot d$, where $.d$ is the distance across the magnetic field between the probes.

One of the two probes collects ions (the ICP), and the other collects electrons (the CP). Simultaneous current and plasma density measurements show that the current during a disruption typically drops from a value 1 - 2 times larger than, and down to, the local ion saturation current at the ICP. We believe that cathode spots are repeatedly ignited at the surface of the ICP, and that the observed disruptions reflect that these cathode spots are extinguished 10-100 ns after ignition, during a phase when the current is still rising.

The roles of the external circuit, the shapes of the probes, the probe bias, and the plasma stream parameters are investigated in detail.

The investigated mechanism is interesting for three reasons (1) it presents an opportunity to study cathode spots in the ignition phase, (2) it shows that probe measurements with too poor time resolution could contain undetected disruptions resulting in serious errors in probe evaluation (in our case the limit is typically 100 ns), and

(3) it gives an opportunity to study the penetration of fast-changing current pulses into a plasma.

3P07

Direct Magnetic Field Measurement of Micro-Turbulence Enhanced Electron Collisionality in Magnetized Coaxial Accelerator Channels

D.C. Black and R.M. Mayo
Department of Nuclear Engineering
North Carolina State University, Raleigh, NC 27695

A movable 10 coil magnetic probe array is used to map out in detail the time varying axial and azimuthal magnetic fields within the annular flow channel of the Coaxial Plasma Source (CPS-1) facility at the North Carolina State University. The time dependent current distribution, and magnetic field and flux profiles within the coaxial flow channel are constructed from these magnetic field measurements. The dynamic displacement of contrours of constant magnetic flux provides a quantitative measure of field line distortion, which is compared against expected field line deformation for classical, resistive MHD flow and miro-turbulence dominated flow. Employing a resistive, Hall MHD applied field distortion model, the ratio of axel to azimuthal magnetic field strengths is sued to estimate the electron magnetization parameter, $\Omega = \omega_{ce}/\nu_e$, thereby providing a direct measure of the electron collision frequency (ν_e) from field measurements alone. This technique yields estimates of the anomaly parameter $\left(\nu_{e_{an}}/\nu_{e_{cl}}\right)$ in the range of 20 to 50, thus indicating a significant contribution from magnetofluid micro-turbulence to the electron collisionality in these devices. Comparison with results from the Los Alamos Coaxial Thruster eXperiment (CTX) indicates that the level of anomalous dissipation scales inversely with the ratio of classical collision frequency to lower hybrid frequency. This suggests lower hybrid modes may be responsible for the observed micro-turbulence, and that collisions are important in the saturation of these instabilities.

3P08

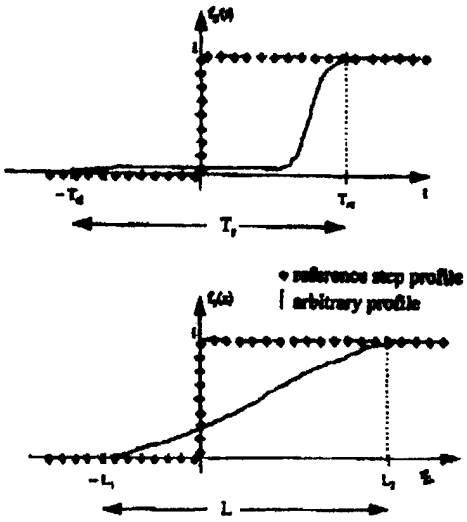
Wave Propagation in a Time-Varying and Space-Varying Isotropic Plasma Medium

Dikshitulu K. Kalluri
Department of Electrical Engineering
University of Massachusetts at Lowell,
Lowell, MA 01854

A sudden creation of a plasma half space considered in [1] is a mathematical idealization of a rapid creation of a plasma medium with a sharp boundary. The steady state reflected field in free space is comprised of A and B waves. A waves have the same frequency as the source wave and the B waves have shifted frequencies. A more realistic dynamic plasma medium problem should model the $\omega_p^2(z,t)$ profile by

$$\omega_p^2(z,t) = \omega_{p1}^2 + \left(\omega_{p2}^2 - \omega_{p1}^2\right) f_1(z) f_2(t)_{(I)}$$

where ω_{p1} is the plasma frequency of the medium 1 as $z \rightarrow -\infty$ and $t \rightarrow -\infty$ and ω_{p2} is the plasma frequency of the medium 2 as $z \rightarrow -\infty$ and $f_1(z)$ and $F_2(t)$ functions describe the transition of the plasma frequency from its asymptotic values (Figure). The effects of non zero values for L (range length) and T_r (rise time) on the reflection coefficients R_A and R_B of A and B waves will be discussed.



[1] D.K. Kalluri, IEEE Trans. Plasma Sci. vol. 16, no. 1, pp. 11-16.

3P09

Suprathermal Electron Diagnostics, Based on X-ray Line Radiation Polarization Measurements

E.O. Baronova
NFI, RRC Kurchatov Institute, Moscow, 123182, Russia

Suprathermal electrons play an important role in energy transfer and in formation of emission spectra in plasma. An opportunity of electron beam energy estimation on the basis of polarization measurements of x-ray lines are presented in this paper.

Experiments were carried out on PF Mather type facility. The investigation of specta of He-like Ar in the range of 3,5-5A was made by two focusing crystal spectrographs, oriented perpendicular one with respect to another and to discharge axis. Such arrangement makes it possible to measure the dependence of relative intensities of x-ray lines on crystal orientation. The remarkable peculiarity of spectra obtained was the difference in relative intensities of resonance and intercombination lines registered in the same experiment with different spectrographs. As the degree and the direction of polarization of various lines are different and depend on the electron beam energy by different way, this peculiarity may be explained with polarization phenomena of corresponding lines. The reflection coefficients for polarized and unpolarized emission were quantitatively compared after the analysis of spectra obtained. Such comparison permits one to evaluate the degree of polarization and also the electron beam energy.

Results were interpreted under the assumption of the suprathermal electrons determined to be the main reason for the polarization. The validity of such assumption is analyzed at a qualitative level.

3P10

Plasma Species in Methane-Hydrogen and Methane-Hydrogen-Argon Arcjet Plasmas

Mary C. Baker, Martin Bartlemass*, Reed Irion*,
Lynn Hatfield, M. Kristiansen, and Edgar O'Hair
Texas Tech University, Lubbock, TX 79409

An arcjet engine plume was used to generate methane-hydrogen plasma for the growth of diamond films. The plasma species were determined through emission spectroscopy. Of particular interest were those species present that are known to play a role in diamond. The measurements were done to produce of profile both longitudinally and vertically in the plasma plume to determine the distribution of species throughout the plume as a function of several parameters, including gas mixture, pressure, and arcjet power. In addition, Argon was added to the arcjet to determine its effects on the plasma species present. It was found that a small amount of Argon had a significant effect on the species present.

*No longer at Texax Tech.

3P11

The Vacuum Arc Discharge in Anode Material Vapour

V.N. Pavlenko and V.G. Panchenko
Institute for Nuclear Research, prosp. Nauki 47, Kiev, 252028, Ukraine

In our experiments the discharge gas lighted up between the thermionic cathode and water-cooled anode. A1, Cu, Ni, Cr, Ti, Ta, Mo, B, C, W are embedded on the anode as a working substance. Using the cylindrical electrode and electromagnetic system we have the possibility for creation the transverse electric and magnetic fields.

It is shown that plasma-flow ionization coefficient may reach the value up to 80%. Thus the data presented in this paper (high ionization coefficient, charge-compensated plasma flow) demonstrate the perspective of wide practical utilization of such type of discharge for creation of thin high-adhesive films.

3P12

Scattering of Electromagnetic Waves by Density Fluctuations in the Inhomogenous Plasma with Lower Hybrid Pump.

V.N. Pavlenko and V.G. Panchenko
Institute for Nuclear Research, prosp. Nauki 47, Kiev 252028, Ukraine

In the present report scattering of a transverse electromagnetic wave by density fluctuations in a magnetized inhomogeneous plasma in the presence of

parametric decay instability of a lower hybrid pump wave are investigated.

It is shown that for typical parameters of hot plasma the differential scattering cross section can exceed the one due to the scattering by thermal fluctuations by several orders of magnitude and depends on pump wave amplitude and density gradient.

3P13

Plasma Chemical Reactor for Precision Etching of Elements with Submicron Size

V.N. Pavlenko and V.G. Panchenko
Institute for Nuclear Research, prosp. Nauki 47, Kiev, 252028, Ukraine

We have created plasma chemical reactor with the possibility of ion energy control from 50 W up to 500 W and more. In the main working regime the ion energy is regulated in the range 50-150 W. It is shown the etching velocity of Al films is $v_{et} \leq 0.5$ μm/min at the anisotropy coefficient $q > 7$ and the etching selection relatively Si ~ 20 and the size of elements are nearly: 0.3 - 0.5 μm.

3P14

The Waves Scattering Processes in the Magnetized Plasma with Upper Hybrid Pump

V.N.Pavlenko and V.G.Panchenko
Institute for Nuclear Research, prosp. Nauki 47, Kiev, 252028, Ukraine

We investigate the scattering of electromagnetic wave by density fluctuations when the frequency of the pump wave is close to the upper hybrid frequency.

It is shown that the differential scattering cross section in the region above the instability threshold region is greater than usual thermal noise term by 2-3 orders of value for typical ionospheric and hot plasma parameters.

3P15

Nonstationary Parametric Process ing in a Semibounded Plasma

V.N. Pavlenko and V.G. Panchenko
Institute for Nuclear Research, prosp. Nauki 47, Kiev, 252028, Ukraine

We consider the interaction of two transverse waves and one longitudinal surface wave in a relativistic electron beam plasma system with sharp boundary. The space-time evolution of this three wave interaction process leads to a diffusion broadening in space of the electromagnetic wave packets. The diffusion length is determined.

These investigations are very important for plasma electronics and free-electron lasers because the nonlinear wave interaction processes may lead to up conversion of the frequency of the scattered wave as compared to the frequency of the incident electromagnetic wave.

3P16

Simulations of Modulational and Resistive Instabilities in Cylindrical Crossed-Field Diodes*

P.J. Christenson and V.P. Gopinath
EECS Department, University of California at Berkeley, Berkeley, CA 94720

Modulational[1] and resistive[2] instabilities in planar crossed-field diodes has been discovered and analyzed. It was noticed that in planar anode-cathode gaps in which the applied magnetic field was above cutoff (i.e. $B > B_H$), steady cycloidal electron flow in the gap was violently unstable to the application of a small AC voltage perturbation. This phenomenon occurs over a wide band of frequencies and is caused by the formation of virtual cathode immediately in front of the cathode. A resistive instability in the crossed-field cycloidal electron equilibria was also found wherein energy dissipation in an external resistor triggered an instability in the flow which leads, again to the formation of a virtual cathode.

While these studies were done on planar cross field diodes, most devices are coaxial. However, the solutions to equations in cylindrical coordinates are not always easily available. It has been shown that[3] coaxial crossed field devices follow planar theory, both for $B < B_H$ *and* $B > B_H$ for radius ratios up to 5, and over a range of bias voltages.

This work explores the presence of these instabilities using 1D3V PIC simulations in cylindrical geometries and compares the results to those of planar simulations and theory. In addition, the effects of thermal, as opposed to cold, electron emission is examined. The work also explores the instabilities over a range of radius ratios to locate limits of agreement.

*This work was supported by the Miller Institute for Basic Research in Science and by ONR under Grant FD N00014-90-J-1198.

[1] P.J. Christenson and Y.Y. Lau, *Phys, Rev. Lett.* Vol 76, **18**, p. 3324

[2] P.J. Christenson, D. Chernin, A.L. Garner and Y.Y.ÊLau, "Resistive destabilization of cycloidal electron flow and universality of (near) Brillouin flow in a crossed-field gap," to appear in Phys. Plas., (1997).

[3] V.P. Gopinath, J.P. Verboncoeur and C.K. Birdsall, *Phys. Plasmas* **3** (7), p. 2766 (1996).

3P17

Calculation of the Electric Microfield Distribution in Plasma Revised

J. Puerta and C. Cereceda*
Dept. de Fisica, Univ. Simón Bolívar Apdo. 89000, Caracas-Venezuela
**CEN-Limeil, Orsay, France*

Recently new calculations for the probability field distribution in plasma generating a new expression for the Debye screening fields was proposed by P. Martin and R. Perez[1]. The method that we here present is based mainly on the introduction of this adequate field in the calculus of the distribution. We find the spectral function $F(\mathbf{k})$ carrying out the Fourier transform of the field which is numerically calculated for each representative value of the variable in **k** space and then fitting these data in order to get $F(\mathbf{k})$. Thus, after the usual numerical integration on the wave number space, the field strength distribution is achieved. These approximation recovers the Holtsmark[2] distribution in the limit of high temperature and/or small densities. This method is an improvement of previous procedures and simple to obtain.

[1] P. Martin and R. Perez (1996), Tesis

[2] K.H. Spatschek. Theoretische Plasma-physik. Teubner Studienbuecher (1990), **3.4**.

3P18

Wake Potential Due to a Pair of Dust Particles in a Plasma*

Wu Zhang and Osamu Ishihara
Department of Electrical Engineering, Texas Tech University, Lubbock, TX 79409
and Sergey V. Vladimirov
School of Physics, University of Sydney New South Wales 2006, Australia

A wake potential due to a test dust particle in a plasma with ion flow was studied[1,2] based on the interaction of the dust particle with ion acoustic oscillations. The wake structure by the dust particle was found to be characterized by the periodic potential. We extend the wake potential study to the system of two dust particles interacting with the ion acoustic oscillations in a plasma with ion flow. Our approach to the wake potential is based on the semiclassical interaction Hamiltonian in which virtual quasiparticles are exchanged between two dust particles. The explicit form of the resulting wake potential is obtained by carrying out the canonical transformation.

*Supported by the AFOSR Grant No.F49620-97-1-0007 and the Australian Research Council.

[1] S.V. Vladimirov and O. Ishihara, Phys. Plasmas **3**, 444 (1996).

[2] O. Ishihara and S. V. Vladimirov, Phys. Plasmas **4**, January Issue (1997).

3P19

The Potential of Particles in Dust Crystal in rf Discharge

V.A. Schweigert and I.V. Schweigert†
Institute of Theoretical and Applied Mechanics, Novosibirsk, Russia
†Institute of Semiconductor Physics, Novosibirsk, Russia

The 3D-numerical calculation of radio frequency discharge containing the two-layer dusty crystal in the sheath have been done. We solve self-consistently the kinetic equations for electrons and ions by Monte-Carlo technique and Poisson equation for the potential distribution. The electron and ion losses on the dusty grains are included in our model. We obtain charge of particles and the rate of particle charging as function from gas pressure. The characteristics of rf discharge and parameters of dusty crystal such as the interlayer distance

and the charge of particles agree with the experimental data. The potential distribution around the particles is essentially asymmetrical in vertical direction and explain the vertical alignment observed in the experiments.

3P20

Propagation of a Wave in a Plasma with Coulomb Collisions

S.V. Vladimirov
Research Centre for Theoretical Astrophysics, School of Physics, The University of Sydney, N.S.W. 2006, Sydney, Australia
and O. Ishihara
Department of Electrical Engineering and Department of Physics, Texas Tech University, Lubbock, Texas 79409-3102

Influence of Coulomb collisions on the wave propagation in plasmas is considered. It is demonstrated that the nonlinear coupling of the nonresonant wave with electric field fluctuations resonant with the plasma particles as well as contribution of the system nonstationarity induced by the collisions is crucial to obtain the correct conservation equation for the wave occupation number. In contrast to the occupation number, the canonical wave energy changes because of the nonstationarity of the system. Since the definition of the wave energy is not necessarily unique and depends on separation into background and wave subsystems, the result for the change of the canonical wave energy is not universal. Alternative way of separation into background and wave subsystems is discussed.

3P21

Ponderomotive Forces in a Time-Dependent Plasma

S.V. Vladimirov
Research Centre for Theoretical Astrophysics, School of Physics, The University of Sydney, N.S.W. 2006, Sydney, Australia

Forces acting on a plasma due to the presence of electric and magnetic fields are closely connected with energy and momentum densities of the fields. Although the corresponding expressions in the stationary case are well known, the problem for a time-dependent plasma is less trivial. The main point is that in a (weakly) time-dependent transparent medium an imaginary part of the dielectric function appears which depends on the slow time scale.

The high-frequency electrostatic field in a non-stationary plasma creates three types of forces: the ponderomotive force, dissipative force (which necessarily includes terms because of the nonstationarity), and, finally, the force due to change of momentum of the field. We find that for normal plasma modes, the general macroscopic consideration is sufficient to establish that only the pondermotive forces acts on the medium regardless of whether the system is open or closed.

3P22

Alfvén Surface Waves in a Dusty Magnetized Plasma

N.F. Cramer and S.V. Vladimirov
Department of Theoretical Physics and Research Centre for Theoretical Astrophysics, School of Physics, The University of Sydney, N.S.W. 2006, Sydney, Australia

Surface wave propagation in a magnetized plasma containing high-Z impurities is considered at frequencies below and of the order of the ion-cyclotron frequency, but well above the dust cyclotron frequency. The dust grains are assumed to be stationary, but to carry a proportion of the negative charge of the plasma. The dispersion relation for surface waves propagating on an interface between a dusty plasma and a vacuum is derived and discussed. The damping of the waves due to Alfvén resonance absorption in a narrow but non-zero width interface is derived.

3P23

Wave Relaxation and Parametric Instability in Partially Ionized Plasma

M.A. Drofa, L.S. Kuz'menkov, S.G. Maximov
Moscow State University, named after M.V. Lomonosov, Faculty of Physics, Division of Theoretical Physics 119899, Moscow, Russia

In our work we theoretically consider the influence of the photo ionization in the partially ionized plasma on the collective electromagnetic processes. To do this we derive from basic principles equations describing the dynamics of collective processes in the system with non constant number of particles and obtain the asymptotic formulae for the dynamics of collective electromagnetic perturbations near the state of ionization equilibrium in the cases of weak and strong ionization.

It was found that if the ionization radiation is constant then the process of momentum exchange between particle flows at the moments of particle birth and death results in strong absorption of electromagnetic radiation. This was observed experimentally [1]. The dependence of absorption of electromagnetic radiation on the frequency of this radiation is determined by velocities of elementary processes in the partially ionized plasma and can be used for its diagnostic.

For alternating intensity of ionization as it was shown parametric Langmuir oscillation instability arrives if the frequency of modulation is about of two plasma frequencies. Value of the instability threshold and the maximum increment are calculated. For the case of weak ionization the instability due to alternating intensity of ionization is suppressed by the absorption but if the ionization is strong then the instability is dominant.

[1] K.R. Stalder, R.J. Vidmar, D.J. Eckstrom, J. Appl. Phys. 72 (1992) 5089-5094

3P24

Turbulization of Non-Linear Langmuir Oscillations in a Cold Plasma

A.V. Kovalenko and V.P. Kovalenko
Institute of Physics of the National Academy of Sciences of Ukraine, Prospect Nauki 46 Kiev 252022 Ukraine

It is shown that the electric field of Langmuir oscillations of cold plasma contains a component which is independent of time. This electric field component appears at the very first period of oscillation since it is not caused by the ponderomotive drift of electrons or an instability. This field sets ions into motion. Using Langrange variables, one-dimensional dynamics of plasma in respect of the interaction between electron oscillations and ion movement is investigated. As a consequence of this interaction the crossing of electron trajectories occurs even at small amplitudes at time Tc, i.e. one-dimensional turbulence appears in the system. The expression for Tc has been found. It is shown that in time Tc ion displacements as well as ion energy, representing only an insignificant part of oscillation energy, depend only on the electron-ion mass relationship. Thus, it can be expected that in such a scenario of turbulence the main part of the oscillation energy will be transferred to chaotic movement of electrons.

3P25

"Electron Is Particle" For Scientists

Toshiro Ohnuma
Department of Electrical Engineering, Tohoku University, Sendai 980 Japan

"ELECTRON IS PARTICLE" is very simple and normal sentence for many scientists. However, when one use the phrase for quantum fields, it has very important meaning. Some plasma scientists have used the quantum effects for their studies. All of them cannot (maybe) understand the essential fundamentals, i.e. the uncertainty principle and the fact that electrons become waves.

For this problem, the author proposes a drastic new model "Electron is always Particle", and quantum waves can be constructed by Many (Times) Electrons.[1)] Many times electrons are named for an electron which passes many times the same area, for example, an electron around a proton.

For this new model, the author proposes also that the relations for energy E and momentum p in quantum waves, $E = h'\omega$, $p = h'k$, $(h'=h/2\pi)$, are for many (times) electrons, and not for one electron. The applications of the relations for one electron have made many ambiguities up to present.

The new electron model will open many new scientific pages.

1) T.Ohnuma, "Lecture: Advanced Electromagnetics" (Corona Pub.,in 1997)

3P26

On Adiabatic Change of State of Photon Gas 2

Milán Mészáros
α Group Laboratories, Inc., Institute of Phsyics
11 Rutafa Street, Bldg, H, H-1165 Budapest, Hungary
Phone/Fax: + 36 (1) 403 7544
Email: alphagr@mail.e3.hu

Present paper shows up that the equations of state $PV^{4/3}$ = const, $TV^{-4/3}P^{1/3}$ = const and PV = E/3 cannot be valid simultaneously for the adiabatic change of state of photon gas. Furthermore, the Planck's distriubtion – and so the Wien's law and the Raylaeigh-Jeans connection as well – cannot be invariant in case of adiabatic change of state of photon gas. Namely, in case of adiabatic change of state of photon gas, a new type fo ultraviolet catastrophe appears. The cause of these contradictions can be the lack of longitudinal magnetic flux density $\mathbf{B}^{(3)}$ in the usual description.

These results possess a fundamental importance in case of arbitrary deformation of electromagnetic radiation fields or quantum plasmas, too.

(1) Milán Mészáros and Pál Molnár, Annalen der Physik **46**, 153 and 381 (1989)

(2) Milán Mészáros and Pál Molnár, Physics Essays **5**, 463 (1992)

(3) Myron W. Evans, Foundations of Physics **25**, 175 and 383 (1995).

3P27

Formation of Thermoelectric Field in a Collisionless Non-Equilibrium Plasma

V.P. Krainov, V.A. Rantsev-Kartinov, E.E. Trofimovich
RRC "Kurchatov Institute", Moscow 123182 Russia

Microscopic approach to calculating the macroscopic electric field in a weakly inhomogeneous, collisionless plasma is formulated, and the explanation of the mechanism of field formation is given. The thermoelectric field is shown to be caused by the difference in dynamical screening of electrons and ions in an inhomogeneous plasma. A universal analytic expression for the thermoelectric potential in a non-isothermal plasma is derived, which takes into account the quasineutrality and weak temperature inhomogeneity.

The influence of this thermoelectric field upon local plasma macroscopic parameters and the competition of the electron and ion contributions to the thermoelectric coefficient are investigated. Numerical results for various spatial profiles of plasma temperature and density in tokamak plasmas appear to be in good agreement with the corresponding experimental data on electric potential profiles, including the change of potential's sign at plasma periphery.

3P28

Experimental Study of Plasma Character in Ion Diffusing into Metal Caused by Double Glow discharge

Zhangkui Shang
Southwestern Institute of Physics, P.O. Box 432, Chengdu, Sichuan, 610041, P.R. China

Ion diffusing into metal by means of double glow discharge is a new plasma surface metallurgic technique. In a vacuum chamber, the source pole and the cathode are put in parallel each other. The wall of vacuum chamber is served as a common anode. The cross-interaction between plasma of the cathode and the source pole is a kinetic process in dynamic equilibrium. The experimental results show that the distribution of plasma density (n_i) in vacuum chamber is not uniform and the strong edge-effect exists in double glow discharge. The cross-interaction mechanism of two plasmas in double glow discharge is studied both in experiment and theory. The preliminary results are given.

Tuesday Afternoon, 20 May 1997
10:00 a.m. – Multipurpose Room

Poster Session 3Q01-15:
5.1 Non-Equilibrium Plasma Processing I (Ion Implantation)

3Q01

Transport of a Cathodic Arc Plasma Inside a Magnetized Tube*

B. P. Cluggish and B. P. Wood
Los Alamos National Laboratory, Los Alamos, NM

We are investigating the implantation and deposition of material on the inside of a steel tube using a cathodic arc plasma source which is located at one end of the tube. To achieve uniform deposition, losses to the walls of the tube must be minimized by an axial magnetic field, allowing the tube to fill uniformly with plasma. However, the losses must also be periodically maximized (by biasing the tube and/or plasma) to implant and deposit the ions on the walls. To this end, we are performing experiments on the transport of cathodic arc plasmas inside magnetized tubes. Previous experiments[1] have shown wall losses much greater than would be predicted by classical, collisional transport theory, but the cause of the anomalous losses is still unknown. In our experiments, we will attempt to reduce these anomalous losses by using a magnetic field strong enough to magnetize the ions; previous work has focused on the regime where the field is only strong enough to magnetize the electrons. The effect of biasing the tube will be compared to the effect of biasing the plasma. Measurements of the ion flux, plasma potential, and plasma velocity as functions of position and experimental parameters will be presented.

* Supported by US Department of Energy

[1] J. Storer, J.E. Galvin, and I.G. Brown, *J. Appl. Phys.* **66**, 5245 (1989)

3Q02

Pulsed-Plasma Deposition of Amorphous Diamond-like Carbon Films on Copper

C. Chiu, B. Terreault and A. Sarkissian
INRS-Énergie & Matériaux, Varennes, Qc, Canada J3X 1S2

Single-crystal diamond film growth upon some practical nondiamond substrate is highly desirable. Specially, it will open up the possibility of making diamond-based semiconductors. The resulting devices would be able to operate many times faster than their silicon counterparts and at temperatures up to 700 degree Celsius. Furthermore, the high thermal conductivity makes diamond films an ideal heat diffuser material for high temperature, high power semiconductor devices, thus allowing a high degree of circuit integration and denser packaging of the devices without thermal problems. To realize this potential, however, the true diamond heteroepitaxy must first be achieved. Recent results of pulsed-laser melting on room temperature carbon-ion-implanted copper, reported by Narayan et al [1], showed the diamond film produced to be defect-free single crystal over large areas of several square microns with no grain boundaries. Subsequently, Hoff et al [2] also claimed to have produced untwined single crystal diamond films over a micron in size using the so-called "Carbon-Implantation-Out-Diffusion" (CIOD) method. This technique essentially involves implanting carbon into copper lattice at high temperatures (800-1000°C). As such, the implanted carbon atoms should diffuse to a nearby surface or buried carbon cluster and arrange themselves, under the influence of the host materials, to form diamond. Copper was chosen as the substrate because it has a lattice constant near that of diamond and does not dissolve or react chemically with carbon atoms under any implantation conditions below its melting point. Even though the first reported results appear successful, the reproducibility of these processes was not demonstrated by other groups [3,4]. Using the new pulsed-Plasma Source Ion Implantation (PSII) as an alternate implantation technique for diamond growth by CIOD method allows us to investigate the effect of a higher C ion flux, which is suspected to be the main factor leading to diamond formation in copper [5]. Single crystal and polycrystalline copper disk samples were dc-biased at negative voltages ranging from 0-30 V and exposed to a pulsed or dc methane (pure or 1% CH_4 in H_2) plasma. The copper substrate temperature is kept at either 800-1000°C or at ambient temperature during plasma exposure. The resulting films are examined by Raman Spectroscopy, XPS, and SEM. Preliminary results show only growth of graphitic and diamondlike carbon films on copper

substrates negatively dc-biased at 0-10 kV and kept at 800-950°C during exposure to 1% CH_4/H_2 dc plasma.

[1] J. Narayan et al, SCIENCE 252 (1991) 416
[2] H.A. Hoff et al, APPL. PHYS. LETT. 62 (1993)
[3] S.T. Lee et al, APPL. PHYS. LETT. 60 (1992) 2213
[4] T. Cabioc'h et al, THIN SOLID FILMS 263 (1995) 162.

3Q03

Ultra-Shallow p+/n Junction Formed by Plasma Source Ion Implantation and Solid Boron Source*

Henley L. Liu**, Steven S. Gearhart,
John H. Booske and Wei Wang
Engineering Research Center for Plasma-Aided Manufacturing, University of Wisconsin–Madison, Madison, WI 53706

Using Plasma Source Ion implantation (PSII), a novel technique has been developed to fabricate ultra-shallow p^+/n junctions for the application of sub-micron CMOS source/drain formation. This process avoids the hazards and costs of handling highly toxic and reactive gases. In this method, a thin boron layer is first sputter deposited onto the wafer from a solid boron target. Then PSII with Ar plasma is used to knock boron atoms into the Si substrate by means of ion beam mixing. Ultra-shallow p^+/n junctions with junction depths ranging from 27 to 85nm have been fabricated with this technique.

In addition to Ar PSII, Ne PSII has been investigated for forming shallow p^+/n junctions with the same technique, because Ar implantation was reported to form defects which are difficult to remove during the annealing steps. Preliminary results show that neon PSII results in more shallow boron profile, lower boron dose and higher sheet resistance.

In order to avoid a possible contamination and dopant loss during the transportation step between the boron sputter deposition step and the PSII process, the sputtering gun has been incorporated into the PSII chamber to make the "in-situ" boron sputter deposition possible. Preliminary results show that this in-situ technique avoids the dopant loss and significantly reduces the sheet resistance.

Currently, p^+/n diodes are being fabricated by using the novel boron implantation method to characterize junciton leakage current.

*Supported by the NSF under grant EEC-8721545

**email address: henley@cae.wisc.edu

3Q04

Surface Modification of Cr_{12} MoV Steel by PSII Nitrogen Implantation

Wei Pu
Southwestern Institute of Physics, P.O. Box 432, Chengdu, Sichuan 610041, P.R. China

The PSII nitrogen implantation for Cr_{12} MoV steel modification is performed in the PSII-IM facility. The implantation is carried out at different implantation doses but keep the same other conditions. After implantation the samples are analyzed by using Micro-Hardness Tester, Ball-on-disc Multifunctional Tribometer. X-ray Diffraction Spectrometer and XPS. The results show that after PSII nitrogen implantation, the surface mechanical properties are improved greatly. The X-ray analysis demonstrates that in the Cr_{12} MoV steel, PSII implantation results hard carbide Fe_7C_3 and Cr_7C_3 growth because of high concentration of carbon and fast diffusion speed at elevated temperature implantation. The XPS analysis shows that from the surface to the deep layer, the binding energy of N atoms shift from high energy to low energy. The high energetic ion bombardment, thermal diffusion, fined hard carbide growth and formation of new phrase during nitrogen implantation are the main reasons to improve the surface mechanical properties of Cr_{12}MoV steel at elevated temperature.

3Q05

The Application of Ion Beam Implantation for Synthetic Diamond Surface Modification

Wei Pu
Southwestern Institute of Physics, P.O. Box 432, Chengdu Sichuan, 610041, P.R. China

The ion beam implantation for surface modification of synthetic diamond tools and nature diamond have been widely investigated in the previous work. In this article, the ion beam implantation for surface modification of synthetic diamond powder in Southwestern Institute of physics is described. The nitrogen ion and titanium ion with energies of 20-70 kev have been chosen as the implantation ions, the experiment performed in the multi-function implanter which developed by ourself. The ion depth distribution and microstructure have been tested by XRD (X-ray Diffraction). It shows that the implanted ion have a good chemical combination with the surface saturationless bond carbon atom. The high temperature

DTA experimental result shows that the oxidation start temperature of the post implanted synthetic diamond with either nitrogen ion or metal ion implantation have been improved from 730°C to 800-850°C and the improve extent is increasing with the ion does increasing, but there also exists an optimum implantation doses. Furthermore, the property of diamond transfer to graphite at high temperature have been also greatly improved, the metalation property for Ti implanted diamond have been tested by mill machine and tension testing after the sintering process, the result shows that the adhesive force of the ion implanted synthetic diamond with matrix have been increased by a factor of 2. The Ion Beam Enhanced Deposition (IBED) and double elemental ion implantation have been also applied with preliminary results being given in this paper.

3Q06

Research on Application of Ion Implantation in SWIP

Wei Pu
Southwestern Institute of Physics, P.O. Box 432, Chengdu, Sichuan, 610041, P.R. China

In the last ten years, the research on application of ion implantation modification in SWIP of China has encompassed work in the areas of ion implantation equipment manufacture, material surface modification and its industrial applications including plasma source ion implantation (PSII) and ion beam ion implantation (IBII) technologies. Implantation equipments with the function of implantation and enhanced-deposition have been constructed. MEVVA ion source for metal ion implantation and vacuum arc plasma source for metal plasma ion implantation and deposition have been employed successfully in IBII and PSII equipments respectively. Material surface modification have been carried out in different modes. The modified workpieces have been tested in some industrial field. In this paper the highlights of the above efforts on ion implantation research have been presented.

3Q07

The PSII-IM Device

Zhengkui Shang
Southwestern Institute of Physics, P.O. Box 432, Chengdu, 610041, P.R. China

A new PSII device (PSII–IM) has been set up for development of industrial application in Southwestern Institute of Physics (SWIP). The vacuum chamber is made of stainless steel with 1000mm diameter and 1070mm height surrounded by multicusp permanent magnets. The device is equipped with a cryogenic, a diffusion and a mechanical pump. The background pressure is less than 8×10^{-5} Pa. The plasma can be generated by multifilament discharge or RF discharge in gas. In addition, there are four metal plasma sources, six sputtering targets, cold and hot target supports. The PSII-IBED experiments are carried out on the device. The pulsed negative high voltage is 10-90 kV, the repeated frequency is 10-500 Hz. Generally, plasma density (gas) is 10^8 - 10^{10} cm^{-3}, metal plasma density is 10^8 - 10^{10} cm^{-3}, deposition rate is 0.1 ~1.0 nm/s.

3Q08

Ultra-Hard Crystalline β-C_3N_4 Films Synthesized Using a Reactive RF Magnetron Plasma Source

S. Xu, Han-shi Ki and S. Lee
School of Science, National Institute of Education, Nanyang Technological University, 469 Bukit Timah Road, Singapore, 2509756
Yin-an Li
Institute of Physics, Chinese Academy of Sciences, Beijing, China

Crystalline β-C_3N_4 was successfully synthesized on Kbr(100), KCI(100), Si(100) and stainless steel substrates using a purpose-designed, high density, low temperature, RF Magnetron plasma source. The substrates were held at ambient temperature during deposition. The films were characterized using various analytical means. XRD, TEM and SEM analyses indicated that the films were of polychrystalline β-C_3N_4 with the biggest crystal grain of over 20 μm. XPS and EDX results showed that the films were composed primarily of carbon and nitrogen. The measured interplanar spacings were in good agreement with the theoretical predictions. To out knowledge, this is the first time crystalline β-C_3N_4 was successfully

synthesized by means of reactive RF Magnetron sputtering technique.

3Q09

Charging of Substrates Irradiated by Particle Beams

P.N. Guzdar, A.S. Sharma, and S.K. Guharay
Institute for Plasma Research, University of Maryland, College Park, MD 20742

Charging of a substrate due to irradiation of charged particle beams is a major problem in many applications of current interest, namely, ion implantation, etching, lithography, etc. In order to understand the underlying physical processes and identify the control parameters, a new approach is developed, both analytically and numerically, when the charged particle motion from the source is followed self-consistently and some simple considerations for beam-solid interactions are invoked. The problem is studied for three distinct irradiating species - positive ions, negative ions and neutrals. The time history of the charging potential with the variation of the beam parameters, namely, beam current and beam voltage, is examined. It has been noted that the charging potential of an isolated substrate is minimum for the negative ions, for example, a few volts for beam voltage of several tens of kV. The charging of the substrate reaches a steady state in a time scale of ~ few microsec in the case of negative ions. The situation is rather serious for positive ions when the substrate is noted to be charged to the beam potential and a steady state does not occur. In the case of irradiation by neutrals, the substrate is charged less than the case of the positive ions, but it is higher than the negative ion case. Thus, the negative ions seem more attractive for the aforementioned applications. Although the present study is done essentially in 1-D case, the results explain the observations by Ishikawa [Rev. Sci. Instrum **67**, 1410, 1995]. Details of the work will be discussed.

3Q10

Cathodic Arc Plasma Density and Profile Measurements*

B.P. Wood and M.G. Tuszewski
Los Alamos National Laboratory, Los Alamos NM 87545
D. Pesensen and F. Wessel
University of California at Irvine, Irvine, CA 92697

We report a series of measurements of ion current density (with a Faraday cup) and integrated electron line density (with a microwave interferometer) for a cathodic arc derived plasma. The ion current measurements were made at various radii from the center of the plasma plume. We compare the differences in electron density and plasma radial profile between cathode materials (erbium and titanium), arc current (100 A to 400 A), pressure (10^{-6} torr to 10^{-3} torr), and the presence or absence of a series magnetic solenoid around the coaxial anode and cathode. We find that:

1. Higher pressure reduces the peak current density.
2. Ti yields a higher peak current density than Er.
3. Er yields a wider FWHM plasma profile than Ti.
4. Presence of a solenoid yields a higher peak current density and higher integrated line density.
5. Higher arc current yields a higher peak current density and higher integrated line density.

*Work supported by U.S. Department of Energy

3Q11

TiN Prepared by Plasma Source Ion Implantation of Nitrogen into Ti as a Diffusion Barrier for Si/Cu Metallization

W. Wang, J. Booske, H.L. Liu and S.S. Gearhart
ERC for Plasma Aided Manufacturing, University of Wisconsin-Madison, Madison, WI
S. Bedell and W. Lanford
Dept. of Physics, State University of New York-Albany, Albany, NY 12222

TiN films prepared by plasma source ion implantation (PSII) of nitrogen into sputtered Ti films as adhesion promoter and diffusion barriers for Si/Cu metallization in ultra large scale integrated circuits (ULSIs) were investigated. The nitrogen-PSII process utilized a dose of $1x10^{17}$ ions/cm^2 and peak voltages of

-10, –15 and –20 kV, respectively. The microstructures and phase identification of the nitrogen-PSII treated TiN films were performed by using scanning electron microscope (SEM), transmission electron microscope (TEM) and x-ray diffraction (XRD). The properties of such TiN films as diffusion barriers between Cu and Si were investigated by annealing Cu (2000A)/TiN/Si stack films in vacuum from 500°C to 700°C, and by analyzing with four-point probe sheet resistance measurements, Rutherford backscattering spectrometry (RBS) and Auger electron spectroscopy (AES).

The XRD and RBS analysis showed that δ-TiN About 350A and 450A formed after nitrogen-PSII treatment at peak voltages of –15 and –20 kV. These TiN films were stable barriers against Cu diffusion after annealing at temperatures as high as 700°C.

3Q12

A Compact High-Voltage Pulse Generator For Plasma Applications

V.A. Spassov[1,2], J. Barroso[1], M. Ueda[1] and L. Gueorguiev[3]
[1]*National Institute for Space Research (INPE), Associated Plasma Laboratory (LAP), P.O. Box 515, 12201-970, San Jose dos Campos, S.P., Brazil*
[2]*Visiting Scientist, Sofia University, Faculty of Physics, 5 J. Bourchier Blvd., Sofia-1126, Bulgaria*
[3]*Wayne State University, 3832 Eldridge, Detroit, MI 48212*

The design and construction of a compact high-voltage pulse generator for providing input electron beam power for the LAP/INPE 32 GHz Gyrotron and for treatment of metal and polymer materials by plasma ion immersion implantation (PIII) are described. The generator was built on a circuit category of Pulse Forming Network (PFN), consisting of nine LC sections with L = 270 μH and C = 2.5 nF. The instrument was designed to produce a flat 30 kV, several Amps pulse in 15 μs pulse length with pulse repetition frequency (PRF) of 8 to 100 Hz. By means of a resonant charging inductance it is possible to gain an output voltage with a factor of 1.8 higher than the voltage supplied by the pulse generator. The generator is fed with sine-wave, constant current source, and a 60 kV, 15 mA switching power supply.

3Q13

Enhancement of Surface Properties of 45# Steel Using Plasma Immersion Ion Implantation

S.Y. Wang[a,b], P.K. Chu[a*], X.B. Tian[a,b], X.F. Wang[a], A.G. Liu[a], Q.Z. Lin[b], B.Y. Tang[a] and X.C. Zeng[a]
[a]*Department of Physics & Materials Science, City University of Hong Kong, Kowloon, Hong Kong*
[b]*Harbin Institute of Technology, China*

45# steel, which has good mechanical strength and is relatively cheap, is a common constituent in industrial components, such as precision gears, piston columns of oil pumps, and so on. However, since the working environment of these industrial parts is sometimes quite harsh and unforgiving, they are vulnerable to wear and corrosion. Replacing 45# steel with stainless or alloy steel increases the cost significantly, and a better alternative is to improve its surface properties and lifetime using plasma immersion ion implantation (PIII). We have devised a variety of treatment processes using PIII, including radio-frequency (RF) plasma nitriding, RF plasma nitriding and nitrogen PIII, Ti deposition in conjunction with nitrogen PIII (IBED), as well as Cr deposition followed by nitrogen PIII (IBED). To assess the efficacy of the processes, the microhardness and mass loss due to wear were measured for both the untreated and treated 45# samples. A salt fog test was also conducted to evaluate the resistance against rusting. Our experimental results show that the microhardness and resistance against rusting of the treated 45# steel samples are much improved, and the mass loss due to wear is reduced substantially. In this paper, we will compare the effectiveness of each treatment technique in addition to showing supporting data.

3Q14

Transient Sheath in a Small Cylindrical Bore with an Auxiliary Electrode for Finite-Rise-Time Voltage Pulses

X.C. Zeng, T.K. Kwok, A.G. Liu, P.K. Chu and B.Y. Tang
Department of Physics & Materials Science, City University of Hong Kong, Kowloon, Hong Kong

Because of its ability to implant non line-of-sight surfaces, plasma immersion ion implantation (PIII) can be used to process the interior surfaces of odd-shapes

specimens such as a cylindrical bore. However, the impact energy tends to be drastically reduced and we suggested the use of a grounded auxiliary electrode positioned along the axis of the cylindrical bore sample to improve the impact energy. Our previous work concentrates on the determination of the ion-matrix sheath and the temporal evolution of the plasma sheath in a small cylindrical bore for zero-rise-time voltage pulses. Because realistic voltage pulses have a finite rise time, this paper addresses the temporal evolution of the plasma sheath in a small cylindrical bore with an auxiliary electrode for different rise times by solving Poisson's Equation and the equations of ion continuity and motion numerically using the appropriate boundary conditions. The ion density, flux, dose, energy, energy distribution, and average impact energy on the surface of the target for different rise times are determined and compared to the case when the auxiliary electrode is absent. Our results predict a substantial improvement of the impact energy during PIII of a cylindrical bore when an auxiliary electrode is employed even for finite-rise-time voltage pulses.

3Q15

Effects of the Auxiliary Electrode Radius During Plasma Immersion Ion Implantation of a Small Cylindrical Bore

X.C. Zeng, A.G. Liu, T.K. Kwok,
P.K Chu and B.Y Tang
Department of Physics & Materials Science, City University of Hong Kong, Kowloon, Hong Kong

Plasma immersion ion implantation (PIII) has a number of advantages over conventional beam-line ion implantation techniques. One of them is the ability to implant "interior" surfaces that are not line-of-sight accessible. The inner surfaces of many industrial components, such as dies, bushings, pipes, and so on are difficult to process and inner surface modification using PIII is both interesting scientifically and commercially. We have proposed a method to improve the impact energy of ions implanted into the interior sidewalls of cylindrical specimens by using an auxiliary electrode having a zero potential. The ion-matrix sheath and the temporal evolution of the plasma sheath is a small cylindrical bore with an auxiliary electrode have been calculated for an auxiliary electrode of a regular radius. In this paper, the effects of the auxiliary electrode radius are discussed. We compute the critical radius of the cylindrical bore when the ion-matrix sheath just overlaps as well as the number of implanted ions. The ion density, flux, dose, energy, energy distribution, and average impact energy are also determined for different radii of the auxiliary electrode by solving Poisson's equation and the equations of ion continuity and motion numerically. Our results provide the theoretical background for the implementation of an auxiliary electrode in a PIII instrument.

Tuesday Afternoon, 20 May 1997
1:30 p.m. – Kon Tiki Ballroom

Plenary Session

Interaction of Ultra-Intense Lasers with Beams and Plasmas

Dr. Phillip Sprangle

Naval Research Laboratory, Washington, DC, USA

Chair: S.L. Ossakow

Tuesday Afternoon, 20 May 1997
3:00 p.m. – Kon Tiki Ballroom

Special Panel Session

Changing Career Opportunities in Plasma Science

Dr. Wallace M. Manheimer, Moderator
Naval Research Laboratory, Washington, DC, USA

Panelists:

Dr. Jim Benford
Microwave Science

Dr. Adam Drobot
Science Application International Corp.

Dr. Don Rej
LANL

Professor Georges Zisses
Université Paul Sabatier

Tuesday Afternoon, 20 May 1997
3:00 p.m. – Rousseau Center

Poster Session 4P29-52:
2.2 Fast Wave Devices

4P29

Modeling of Wide-Band Gyrotwystron Amplifiers

B. Levush, M. Blank, B.G. Danly, P.E. Latham[†]
and T.M Antonsen, Jr.[‡]
Naval Research Laboratory, Washington, DC 20375

The Naval Research Laboratory is currently investigating wide-band gyro-amplifiers as high power sources for millimeter wave radars. A theoretical model was developed to analyze the cyclotron maser interaction in the gyrotwystron configuration [1]. Recently, the simple bunching model described in ref. 1 has been improved, and the theory now includes explicit modeling of the buncher cavities. A numerical code, based upon the improved model, was written and a W-band gyrotwystron design with one buncher cavity is presented as an example. Studies show that careful design of the traveling wave section is necessary to minimize the backward wave interaction over a wide bandwidth. In addition, the time-dependent, self-consistent code MAGY [2] has been modified to study gyrotwystons with multiple buncher cavities. Preliminary results will be presented.

This work was supported by the Office of Naval Research. The computational work was supported in part by a grant of HPC time from the DoD HPC Center NAVO.

[1] P.E. Latham, and G.S. Nusinovich, Phys. Plasma, Vol. 2 No. 9, 1995, pp. 3494-3510.

[2] S.Y Cai, T. Antonsen, G. Saraph, B. Levush, Int. J. Electron., Vol. 72, 1992, p. 759.

[†] Omega P, Inc., New Haven, CT

[‡] University of Maryland, College Park, MD

4P30

Design of a 80 kW, 700 MHz Bandwidth W-Band Gyroklystron Amplifier Circuit

M. Blank, B. Levush, B.G. Danly, P.E. Latham[†],
J.P. Calame[†], D.E. Pershing[‡], W. Lawson*

Naval Research Laboratory, Washington, D.C. 20375

A four cavity TE_{01} mode gyroklystron amplifier has been designed as the driver for a W-band radar currently under development at NRL. The performance goals for the amplifier are 80-100 kW peak output power, 10 kW average power, and 600 MHz -3 dB bandwidth. A time dependent version of the non-linear code MAGYKL [1] was developed to design the interaction circuit. The stagger tuning and cavity Q's were optimized through extensive theoretical studies to determine the tradeoffs between peak output power and bandwidth. A mechanical tolerance study was performed. Stability of the cavities and cutoff drift regions was also examined. The resulting circuit is predicted to achieve 80 kW peak output power and 20% efficiency with a 65 kV, 6 A electron beam with a velocity ration of 1.5 and a perpendicular rms velocity spread of 4.5%. Simulations indicate that the -3 dB bandwidth will be 700 MHz. Details of the circuit and design studies will be presented.

This work was supported by the Office of Naval Research. The computational work was supported in part by a grant of HPC time from the DoD HPC Center NAVO.

[1] P.E. Latham, W. Lawson, V. Lawson, V. Irwin, IEEE Trans. Plasma Sci., Vol 22, No. 5, pp. 804-817, 1994.

[†] Omega P, Inc., New Haven, CT

[‡] Mission Research Corp., Newington, VA

* University of Maryland, College Park, MD

4P31

MAGY: A Self-Consistent Code for Modeling Electron Beam Devices

M. Botton* and T.M. Antonsen
Institute for Plasma Research, University of Maryland, College Park, MD 20742
and B. Levush
Naval Research Laboratory, Washington D.C. 20375

MAGY is a quasi three dimensional self consistent time dependent code for modeling of electron beam

systems. We assume that the system consists of a cylindrically symmetric waveguide with an arbitrarily varying wall radius (including jump discontinuities) and represent the electromagnetic fields as a set of transverse electric and transverse magnetic modes which are defined by the local value of the wall radius. We thus obtain a set of coupled transmission line equations for the voltage and current amplitudes of the various modes. The coupling of among the modes originates in the variations of the wall radius, finite conductivity of the walls and the electron beam. We describe the electron dynamics using the guiding center formulation of the equations of motion with an arbitrary profile of the guiding magnetic field. A significant simplification of these equations is obtained when all the particles traverse the cavity in a time shorter than the cavity fill time. The combined set of equations for the electromagnetic amplitudes and the electron trajectories form the reduced description we are employing in the MAGY code. In this work we present first results obtained with the new MAGY code for a generic Gyro-devices and a Backward Wave Oscillator.

Work supported by AFOSR and ONR.

* On leave from Rafael, Haifa, Israel.

4P32

Overmoded Abrupt Transition TE_{021} Cavities for a 100 MW Second Harmonic Gyroklystron

M. Castle, W. Lawson, J.P. Anderson, G.P. Saraph, M. Stattel, B. Hogan, V.L. Granatstein and M. Reiser
Electrical Engineering Department, Institute for Plasma Research, University of Maryland, College Park, MD 20742

Two overmoded, coaxial, abrupt transition cavities have been designed and are being built and experimentally cold tested at the University of Maryland. They are both designed to operate in the TE_{021} mode at 17.136 GHz. They are to be installed in the microwave circuit of a 3-cavity, 100 MW, 1 μs pulse length, coaxial gyro-klystron amplifier in the near future.

The first cavity will serve as a bunching cavity. It is located near the center of the dielectrically loaded drift region of the gyroklystron. The cavity was designed with a scattering matrix code. After the geometry was selected, simulations with a linear stability code outlined criteria for the cavity's stable operation. Finally, a finite element code that can include lossy dielectric media (HFSS) was used to verify the findings of our scattering matrix code. Experimental cold testing will be completed at the time of presentation, and these results along with the theoretical work will be detailed.

The second cavity is an output cavity whose microwave energy is extracted axially from a radial lip. This cavity was designed with our scattering matrix code to have a Q of 320. Further numerical analysis shows this to be stable within experimental current values (up to 800A). Along with these results, simulations of the circuit operation and current status of the second harmonic experiment will be reported.

This work was supported by the US Department of Energy.

4P33

Design of Magnetron Injection Gun and Collector for High Average Power 95 Ghz Gyro-Amplifiers

K. Nguyen*, B. Danly, B. Levush and M. Blank
Naval Research Laboratory, Washington, D.C.
R.True
Litton Electron Devices, San Carlos, CA
K. Felch and P. Borchard
Communications & Power Industries, Inc., Palo Alto, CA

The electrical design of a magnetron injection gun and collector for high average power TE_{01} gyro-amplifiers has recently been completed using the EGUN[1] and DEMEOS[2] codes. The gun employs an optimized double-anode geometry and a radical cathode cone angle of 50° to achieve superior beam optics that are relatively insensitive to electrode misalignments and field errors. Perpendicular velocity spread of 1.6% at an perpendicular to axial velocity ratio of 1.52 is obtained for a 6 A, 65 kV beam. The 1.28" diameter collector, which also serves as the output waveguide, has an average power density of <350 W/cm^2 for a 59 kW average power beam. Further details on the gun and collector, and results from the design sensitivity studies will be presented and discussed at the conference.

This work is supported by ONR, DARPA, and in part by grants of HPC time from the DOD HPC centers, NAVO and CWES.

[1] W.B. Hermannsfeldt, AIP Conf. Proc. 177, pp. 45–58, 1988.

[2] R. True, AIP Conf. Proc. 297, pp. 493–499, 1993.

*KN Research, Silver Spring, MD 20906.

4P34

Circuit Aspects of the NRL/Industrial 94 GHz Gyroklystron Amplifier[1]

D. Pershing*, K. Nguyen[#], J. Petillo[%], J. Calame[&], B. Danly and B. Levush
Naval Research Laboratory, Washington, DC 20375

A wide bandwidth, high average power W-band gyroklystron amplifier is currently under development at NRL. The amplifier circuit is comprised of 4 stagger-tuned cavities operating in the fundamental TE_{011} circular cavity mode. The input coupler is the first cavity of the circuit and must exhibit reasonable coupling strength between the TE_{10} mode in rectangular waveguide and the desired TE_{011} circular cavity mode over a better than 600 MHz bandwidth centered at 93.4 GHz, with high TE_{01} mode purity. A single WR-8 rectangular waveguide drives a combined coaxial/cylindrical cavity system. The coaxial cavity, resonating in the TE_{411} mode is tightly coupled to the cylindrical cavity, excited to resonate in the TE_{011} mode via rf magnetic field coupling through 4 apertures. Design of the penultimate cavity is especially challenging. Due to the high average power that must be dissipated to achieve the desired cavity Q of 175, resistive wall loading is impractical. A novel scheme has been developed for loading of the desired mode as well as parasitic modes, employing 6 aperture coupled radial vanes azimuthally separated by 60° at each end of the cavity. The cavity frequency and Q requirements are met by appropriate choices of aperture and waveguide dimensions. Dielectric blocks on the broadwall of each vane absorb the out-coupled power. Input coupler and penultimate cavity design details will be presented, as well as comparisons between the predicted and measured performance.

[1] Work supported by the Office of Naval Research

* Mission Research Corp., Newington, VA 22122
# KN Research, Silver Spring, MD 20906
% Science Applications Int. Corp., McLean, VA 22102
& University of Maryland, College Park, MD 20742

4P35

Calorimeter Analysis and Test for Symmetric Circular Waveguide Mode Output*

A.H. McCurdy[§], J.J. Choi[†], S.J. Cooke[‡], G.S. Park[@], R. H. Kyser[&], and B.G. Danly

To measure the radiated power from a high power millimeter wave device it is preferable to perform calorimetry. A calorimeter has been designed and tested for measurements on a 35 GHz gyroklystron amplifier experiment at NRL. The output radiation is in the form of a TE_{01} circular waveguide mode in a highly overmoded guide (operating frequency is more than three times cutoff). The final calorimeter design is an inverted cone structure with power absorption by octyl alcohol. Low radiation reflection, mode conversion, and extraneous heat dissipation are obtained. Three levels of analysis are performed. A simple ray tracing theory allows reflection coefficient and mode conversion to be found by replacing the symmetric circular mode with an equivalent rectangular one. A finite difference code based on a planar circuit analysis provides the same information with a more rigorous treatment of the rectangular boundary conditions. Finally, HFSS simulations are carried out for a restricted number of candidate designs using the actual circular structure. Cold test results will be described in additions to details of the calorimeter construction and calibration.

*Work supported by the Office of Naval Research.

[§] Permanent Address: University of Southern California, Los Angeles, CA 90089
[†] Science Applications International Corp., McLean, VA 22102
[‡] Permanent Address: University of Maryland, College Park, MD 20740
[@] Seoul National University, Seoul, ROK
[&] Dyncorp, Rockville, MD 20850

4P36

Theory of the Inverted Gyrotwystron

G. Nusinovich, M. Walter, and V. Granatstein
IPR, University of Maryland, College Park, MD 20742
e-mail: mwalter@glue.umd.edu

The inverted gyrotwystron is a device consisting of the input waveguide, drift section, and output cavity. The

traveling signal wave in the waveguide may induce a high harmonic content in the electron current density. Then the prebunched electron beam can excite phase-locked oscillations in the cavity at an arbitrary harmonic of the signal frequency.

We have developed the formalism describing the operation of the inverted gyrotwystron at arbitrary harmonics. The operation of the input waveguide at the fundamental and the output cavity at the second harmonic was studied. It was shown that the electron prebunching in the input waveguide provides a better harmonic content than the ballistic prebunching in gyroklystrons. It was also shown that the dependence of the locking bandwidth on the input power is in qualitative agreement with the Adler's relation while quantitatively the bandwidth in our device is much larger due to prebunching. The electron velocity spread causes a shrinkage of the bandwidth even when the efficiency changes only slightly.

This work was supported by the DoD MURI program under grant F49620-92-J-0152 and by the Vacuum Electronics Initiative under grant N0014941G036.

4P37

Dispersion Characteristics of Spiral-Corrugated Cylindrical Waveguide for a Gyro-TWT Amplifier

S.J. Cooke†
Institute for Plasma Research, University of Maryland, College Park, MD 20742-3511
Email: sjcooke@glue.umd.edu

G.G. Denisov
Institute of Applied Physics, Nizhny Novgorod, Russia

The electromagnetic wave dispersion characteristics of a cylindrical waveguide can be modified by a wall perturbation in the form of a spiral corrugation, to create a periodic structure which resonantly couples modes of differing azimuthal order. Due to asymmetry of the coupling with respect to left- and right-handed modes, and to forward and backward waves, a propagating eigenmode may exist having infinite phase velocity ($k_z = 0$) but non-zero group velocity. For a traveling wave amplifier, such a dispersion characteristic may permit operation with increased bandwidth and reduced sensitivity to beam velocity spread by operating close to the point $k_z = 0$. Numerical calculations will be presented to show the beam-coupled dispersion characteristics, stability and gain profiles of such an amplifier based upon a simple, coupled wave theory.

We would like to thank Dr. S.N. Spark, DRA Malvern, UK. Research performed at the University of Strathclyde, was supported by DRA Malvern, UK.

†Supported in part by the Office of Naval Research.

4P38

Development of a Thermionic Magnicon Amplifier at 11.4 Ghz*

S.H. Gold, B. Hafizi,† A.W. Fliflet, and A.K. Kinkead‡
Plasma Physics Division, Naval Research Laboratory, Washington, DC 20375

O.A. Nexhevonko§, V.P. Yakovlev§ and J.L. Hirschfield
Omega-P, Inc., New Haven CT 06520
R. True
Litton systems, Inc., Electron Devices Division, San Carlos CA 94070

The magnicon is a scanning-beam microwave amplifier tube that is being developed as an rf source for the proposed TeV Next Linear Collider. In it, a solid electron beam is spun up to high transverse momentum in a series of deflection cavities containing synchronously rotating TM modes, and then spun down again in an output cavity whose mode is synchronous with that of the deflection cavities. A recent magnicon experiment at NRL, using a ~650 kV, 225 A, 5.5-mm-diam. electron beam produced from a cold cathode driven by a single-shot Marx generator, demonstrated 14 MW (±3 dB) at 11.12 GHz with 10% efficiency in the synchronous magnicon mode, but was limited by plasma loading in the deflection cavities to a regime in which the last cavity of the deflection system (the penultimate cavity) was unstable.[1] This plasma problem was attributed to inadequate vacuum conditions, and to the inability to condition the rf circuit, since the experiment operated on a single-shot basis. As a result, amplifier operation could not be demonstrated.

A new 11.4 GHz rep-rated thermionic magnicon experiment is being assembled, using an advanced ultra-high-convergence electron gun driven by a 10 Hz, 1.5 microsecond modulator top produce a 500 kV, 210 A, 2-mm diameter electron beam. The magnicon circuit has been optimized for minimum surface rf fields and maximum efficiency, and will be engineered for high temperature bakeout and high vacuum operation. This

experiment should begin operation in the Summer of 1997. The predicted power is 60 MW at ~60% efficiency.[2]

*This work was supported by DoE, ONR, and a DoE Phase II SBIR grant to Omega-P Inc.

†Icarus Research, P.O. Box 30780, Bethesda, MD 20824.

‡SFA, 1401 McCormick Dr., Landover, MD 20785

§On leave from Budker INP, Novosibirsk, Russia.

[1] S.H. Gold, et al., *IEEE Trans. Plasma Sci.* **24**, 947 (1996).

[2] S.H. Gold, *et al., Proc. 7th Workshop on Advanced Accelerator Concepts*, in press.

4P39

Influence of a Nonrandom Gyrophase Distribution on the Cyclotron-Resonance Maser Instability*

J.A. Davies** and C. Chen
Plasma Science and Fusion Center,
Massachusetts Institute of Technology,
Cambridge, Massachusetts 02139

An analysis is made of the effect of a nonrandom equilibrium distribution in ϕ on the cyclotron-resonance maser instability of a relativistic electron beam propagating along a uniform magnetic field B_0e_z. Here ϕ is the phase angle of the transverse component of the electron momentum $p_\perp$. Equilibrium distributions are assumed to be either of the form $f_0(p_\perp, p_z, \zeta)$ where $\zeta = \phi - \Omega_c t/\gamma$ or $f_0(p_\perp, p_z, \zeta)$ where $\zeta = \phi - m\Omega_c z/p_z$. The quantity Ω_c is the nonrelativistic cyclotron frequency. A Fourier analysis of the Vlasov-Maxwell equations leads in general to integral equations relating the components of the perturbed electric field. Only for special cases are the usual algebraic relations obtained. Effects of nonrandom distriubtions in ϕ on radiation growth rates are determined for a variety of equilibrium distributions.

* Work supported in part by AFOSR.

**Permanent address : Clark University, Worcester, Massachusetts 01610

4P40

Implication of DC Space Charge Induced Velocity Spread on Gyrotron Gun Performance

C. Liu and T.M. Antonsen Jr.
Institute for Plasma Research, University of Maryland,
College Park, MD 20742

The confinement of mirror trapped electrons under the influence of DC space charge and their effect on the velocity distribution in a configuration corresponding to a double-anode 170 GHz magnetron injection gun is investigated. Most trapped electrons escape from the gun due to pitch angle scattering by the spatially periodic electrostatic potential created by the forward propagating beam. However, a small portion scatter into orbits which are more deeply trapped and can escape only by striking modulation anode. A loss rate due to interception with the modulation anode is obtained by assuming a small azimuthal inhomogeneity of current emission. As particles diffuse in velocity, the velocity distribution in the gun region extends towards increasing perpendicular velocity. On the other hand, the accumulation of trapped electrons near the cathode induces an additional velocity spread in the main beam. Consequently, the main beam exhibits an increased velocity spread and a reduced transverse momentum when it enters the cavity.

4P41

Stable Third-Harmonic TE_{41} Gyro-TWT for 2 MW at 35 Ghz

K.X. Liu, B.H. Deng, J. Van Meter, L. Dressman,
D.B. McDermott and N.C. Luhmann, Jr.
Department of Applied Science,
University of California at Davis, Davis, CA 95616

Harmonic gyro-TWT amplifiers can stably generate much higher power than at the fundamental because the start-oscillation current for the absolute instability is significantly increased due to the relatively weaker harmonic interaction. The concept has recently been successfully demonstrated by a 207 kW second-harmonic TE_{21} gyro-TWT amplifier [1]. Here, the concept is extended to a higher power third-harmonic gyro-TWT. The TE_{41} cylindrical circuit is sliced to suppress modes without an *m=4* azimuthal symmetry by interrupting their wall currents, a technique employed in the second-harmonic gyro-TWT, where the round-trip loss was

measured to be 40 dB for the odd-order azimuthal modes and negligible for the operating mode. The guiding center of the 100 kV MIG electron beam is placed on the null of the strongest remaining gyro-BWO modes. The peak power predicted by the self-consistent large-signal code is 2 MW with an efficiency of 20%, 30 dB saturated gain, and 6% saturated bandwidth.

This work has been supported by ONR under Grant USN N00014-94-1-GO35 (Tri-Services), ARO under Contract DAAH04-95-1-0336, and AFOSR under contract F30602-94-2-0001 (ATR1) and Grant F49620-95-1-0253 (MURI).

[1] Q.S. Wang, D.B. McDermott and N.C. Luhmann, Jr., *Phys. Rev. Lett.* 75, pp. 4322-4325, 1995.

4P42

High Power Ubitron-Klystron

A.J. Balkcum, D.B. McDermott, R.M. Phillips[†] and N.C. Luhmann, Jr.
Department of Applied Science, University of California at Davis, Davis, CA 95616
[†]Stanford Linear Accelerator Center, Menlo Park, CA

A coaxial ubitron is being considered as the rf driver for the Next Linear Collider (NLC). Prior simulation[1] of a traveling-wave ubitron using a self-consistent code found that 200 MW of power and 53 dB of gain could be achieved with 37% efficiency. In a ubitron-klystron, a series of cavities are used to obtain an even tighter electron bunch for higher efficiency. A small-signal theory of the ubitron-klystron shows that gain scales with the square of the cavity separation distance. A linear stability theory has also been developed. Verification of the stability theory has been achieved using the 2-1/2-D PIC code, MAGIC, and our particle-tracing code[2]. Saturation characteristics of the amplifier will be presented using both MAGIC and a simpler self-consistent slow-timescale code currently under development.

The ubitron can also operate as a compact, highly efficient oscillator. Cavities only two wiggler periods in length have yielded up to 40% rf conversion efficiency in simulation. An initial oscillator design for directed energy applications will also be presented.

This work has been supported by AFOSR under Grant F49620-95-1-0253 (MURI) and Contract F30602-94-2-0001 (ATRI).

[1] A.J. Balcum, D.B. McDermott, R.M. Phillips, A.T. Lin and N.C. Luhmann, Jr., *IEEE Trans. Plasma Sci.* 24, 802, 1996.

[2] K.R. Chu, M.E. Read and A.K. Ganguly, *IEEE Trans. Micro. Theory Tech.* MTT-28, 318 1980.

4P43

Slotted Third-Harmonic Gyro-TWT

C.K. Chong[†], D.B. McDermott, N.C. Luhmann, Jr.
Department of Applied Science,
University of California at Davis, Davis, CA 95616
[†]Present Address: CPI, Palo Alto, CA 94303

A low magnetic field, low voltage gyro-TWT has been designed in collaboration with CPI/Varian for operation at 95 GHz and tested in a scaled experiment at 10 GHz. A slotted interaction circuit is utilized to achieve strong interaction at the third harmonic. Analytical theory was used to check for oscillation from gyro-BWO and the absolute instability. A self-consistent slow-timescale simulation code predicts the three-section, slotted third-harmonic gyro-TWT, which utilizes an 11.6 kG magnet and a 50 kV, 3 A, $v_\perp/v_z$ = 1.4, axis-encircling electron beam with an axial velocity spread of 6%, will yield an output power of 30 kW with an efficiency of 20%, a saturated gain of 40 dB and a constant-drive bandwidth of 2%.

This design has been tested in a scaled X-band experiment. A gyroresonant rf accelerator is used to produce the required axis-encircling electron beam. An input coupler with excellent selectivity into the π-mode over a 20% bandwidth was designed with the HFSS code. To ensure the amplifier's stability, the circuit has been sliced to suppress the competing modes by interrupting their wall currents. By driving the two-section amplifier with a 1 kW helix TWT, the stable slotted third-harmonic gyro-TWT yielded an output power of 6 kW with 7% efficiency and 12 dB saturated gain over a bandwidth of 3%.

This work has been supported by ONR under Grant USN N00014-94-1-G035 (Tri-Services), AFOSR Contract F30602-94-2-0001 (ATRI), and Varian Subcontract 109BAR05943.

4P44

Autoresonant Cavity Acceleration

D.B. McDermott, V.V. Dinh and N.C. Luhmann, Jr.
Department of Applied Science,
University of California at Davis, Davis, CA 95616

The autoresonance effect is of considerable interest for efficiently accelerating electron beams to multi-MeV energies. Under an ideal autoresonant interaction, the resonance condition of the electrons with the wave, $\omega=\Omega_{co}/\gamma+k_z v_z$, is completely maintained because the two terms on the RHS change to compensate one another. It is

incorrectly believed that autoresonance cannot occur in a cavity. However, an autoresonant TE_{111} cavity accelerator has been employed [1] to produce MeV-level electron beams in a distance of only one wavelength with a modest RF power of ~1 MW. An advantage to operating with a cavity accelerator over a traveling-wave accelerator [2] is the enhancement of the fields by a factor $\sqrt{Q}$ which yields much stronger acceleration. In addition, one can choose to be in resonance with either the forward or backward wave. The most attractive case is where the electrons switch from being in resonance with the backward-wave to resonance with the forward-wave as the axial velocity slows. This leads to an energy gain one order of magnitude higher than in the more conventional case of strictly forward-wave resonance.

This work has been supported by ARO under contract DAAH04-95-1-0336 and AFOSR under Contract F30602-94-2-001 (ATRI) and Grant F49620-95-1-0253 (MURI).

[1] D.B. McDermott, D.S. Furuno, and N.C. Luhmann, Jr., *J. of Appl. Physics*, 58, 4501 (1985)

[2] M.A. LaPointe, R.B. Yoder, C.B. Wang, A.K. Ganguy and J.L. Hirschfield, *PRL* 76, 1718 (1996).

4P45

Preliminary Measurement of a Novel 140 GHz Gyro-TWT Amplifier

W. Hu, K.E. Kreischer, M. Shapiro and R.J. Temkin
Plasma Fusion Center, Massachusetts Institute of Technology, Cambridge, MA 02139

We have designed and are currently building a novel gyro-twt amplifier to operate at 100 kW and a frequency of 95 GHz. However, due to equipment availability in our laboratory, the amplifier will actually be operated at a frequency of 140 GHz. The electron beam will be provided by an existing MIG electron gun which has been previously used in gyrotron oscillator research at 100 kW power level at 140 Ghz. The gun operates at 65 kV and up to 8A with a velocity ratio of 1.5. The novel wave circuit consists of two facing mirrors with confocal profiles in the transverse direction and flat profiles in the longitudinal direction. The mode is Gaussian-like in the transverse direction. This design effectively reduces the mode competition problem in conventional amplifiers from two dimensional to one dimensional. Another advantage of this curcuit is the relatively large cavity size, which improves power capacity. Calculations indicate that the linear gain is about 2.7 dB/cm with an efficiency exceeding 20%. An experiment using an oscillator configuration has also been designed. Preliminary experimental results including cold tests will be presented at the conference.

4P46

Fractional Harmonic Radiation from a Prebunched Free Electron Laser

M.G. Kong and A. Vourdas
Dept of EEE, University of Liverpool, Liverpool, England

Free electron laser (FEL) devices driven by prebunched electron beams have been a subject of intensive research. One common feature of these prebunched FEL systems is that the electron beam receives a sinusoidal modulation. However if the electron beam is not modulated at one sinusoidal frequency, unconventional interaction mechanisms may be uncovered and this can lead to an improved system performance.

In this contribution, we consider the usage of two sinusoidal modulation signals at different frequencies, instead of one sinusoidal modulation signal. The electron modulation is thus not periodic but quasi-periodic. This quasi-periodicity may be realized either from a substantially nonlinear beam-wave interaction, or from an external modulation induced by a quasi-periodic device for instance a double-period wiggler magnet structure. This approach is motivated by recent studies of quasi-periodic systems in very different context, for instance quasi-crystals in crystallography.

A prebunched FEL with two modulation frequencies is studied in the small signal regime and its gain formulation is developed with the aid of number theory. It is found that the electron beam may radiate strongly at a frequency that is not an integral multiple of either modulation frequency when the two modulation frequencies are of irrational ratio. The new radiation frequency is shown to be a fractional multiple of both modulation frequencies and thus its radiation is referred to as fractional harmonic generation. Other unusual radiation characteristics are also revealed, some of which are shown to have implications to the system performance improvement of free electron laser devices.

4P47

FEL Amplification by a Multiharmonically Prebunched Electron Beam

M.G. Kong
Dept. of Electrical Engineering & Electronics, University of Liverpool, Liverpool, England

It is well known that improved FEL amplification may be achieved with a prebunched electron beam. In all published theoretical and experimental studies of prebunched FELs, it appears that a single sinusoidal signal at the laser frequency is invariably adopted for electron bunching. Whilst elegant and easy for implementation, this approach is intrinsically inefficient in optimizing the electron bunching and hence fails to achieve the maximum possible laser amplification.

In this paper, we consider a multiharmonic bunching technique in which the electron beam is prebunched at both the fundamental laser frequency and its harmonics. To demonstrate its principle, the new technique is applied to a waveguide free electron laser. It is shown that by optimizing the electron bunching, this multiharmonic bunching technique is capable of producing a greater enhancement of laser amplification than what is achievable with the fundamental frequency bunching technique. This comparison is further explored by considering the energy spread effect in prebunched waveguide FEL devices. An analytical formulation of the energy spread effect suggests that the beam quality requirement is essentially the same no matter whether a waveguide FEL is prebunched at the fundamental frequency or at multiharmonic frequencies. Therefore the projected enhancement of the laser amplification can be achieved without imposing a more stringent requirement for electron beam quality. With some straightforward modifications to an existing prebunched FEL experiment apparatus, for instance adding harmonic bunched cavities, the beam-wave interaction should be enhanced using the same waveguide and magnet system.

4P48

Low Voltage FEL Amplification Based on a Longitudinal Interaction Mechanism

M.G. Kong
Dept. of Electrical Engineering & Electronics, University of Liverpool, Liverpool, England

Compact free electron lasers (FELs) operatng in the spectrum from millimetre to the far infrared have recently received much attention largely because of their many realistic applications in medicine and industry. These FELs employ low current electron beams to reduce the size and cost of the required electron beam source, and hence their output power is usually moderate. As a result, many gain and efficiency enhancement techniques have been suggested such as the usage of the energy recovery technique and prebunched electron beams.

A parallel approach to reduce the size of suitable FEL drivers is to minimize the electron voltage necessary for a strong FEL radiation of a given frequency. The main thrusts are at present to employ either slow-wave waveguiding structures or microwiggler magnets. In this contribution, we consider an alternative approach based on the interaction between the longitudinal component of the electrons' undulating motion and the longitudinal electric field of TM modes of the waveguide electromagnetic wave.

A small signal analysis is presented to study the longitudinal interaction mechanism in a FEL amplifier consisting of a circular waveguide and a planar wiggler magnet. It is shown that as the longitudinal component of the electron undulating motion varies at a period half as long as the wiggler period, λ_w, the electron beam involved in the longitudinal interaction experiences an effective wiggler magnet of 0.5 λ_w. Therefore for a FEL based on the longitudinal interaction mechanism, the required electron voltage for a FEL radiation at a given frequency is less than that for a FEL based on the usual transverse interaction mechanism. Detailed characteristics of the longitudinal FEL interaction mechanism is illustrated with system designs.

4P49

A Frequency-Doubling Millimeter-Wave Amplifier*

Jose E. Velazco
Microwave Technologies Incorporated, Burke, VA 22015
Peter H. Ceperley
George Mason University Fairfax, VA 22030-4444

We report on the design of a novel frequency-doubling millimeter-wave amplifier (MWA). The MWA is a very compact, lightweight, fixed-frequency source capable of producing several kilowatts of microwave radiation in a frequency range between 1—50 GHz with an efficiency >60% and 20–30 dB gain. The MWA makes use of very narrow electron bunches to efficiently produce microwaves in a TM output cavity at the output frequency ω. Bunching of a small diameter electron beam is produced in a deflection "chopper" cavity operating at the drive frequency $\omega/2$. This mechanism does not require a focusing system. We will present a MWA design, including 2-1/2D and 3D particle-in-cell simulations performed on MAGIC[1] and SOS[2], respectively. MWA design, ~1 kW of 20 GHz radiation is obtained with an efficiency of ~70% and 20 dB gain. Potential applications of the MWA are airborne systems, satellite communications, wireless systems, and the Microwave Power Module.

*Research funded by the Ballistic Missile Defense Organization under contract F19628-96-C-0100 and by the Virginia's Center for Innovative Technology.

[1, 2]MAGIC/SOS User's Manual, Mission Research Corporation, Newington, VA 22122

4P50

An Efficient Harmonic Amplifier*

Jose E. Velazco
Microwave Technologies Incorporated, Burke, VA 22015
Peter H. Ceperley
George Mason Univesity, Farifax, VA 22030-4444

We present the design considerations, computer simulations and initial experimental results of a new high-efficiency microwave harmonic amplifier (HARA). The HARA is a very compact, lightweight amplifier that can deliver multi-kilowatt radiation with very high efficiency and gain. The HARA system employs a rotating helical beam to excite circularly polarized radiation in an output Tm_{max} cavity that operates at a frequency that is an m multiple harmonic number of the rotating frequency of the beam. We will present a 35 GHz HARA design including three-dimensional particle-in-cell simulations performed in SOS[1]. The design is aimed at the generation of 150 kW of 35 GHz radiation using the 6th harmonic with an efficiency of 65%. We will also present initial experimental results of the prototype under development. An important feature of this novel device is that it does not require a beam focusing system which makes the HARA very appealing for a large number of applications where size, weight and efficiency are critical.

*This work is supported by the Ballistic Missile Defense Organization under contract DASG60-96-C-0172 and by the Virginia's Center for Innovative Technology.

[1] SOS User's Manual, Mission Research Corporation, Newington, VA 22122.

4P51

Operation of a Ka-Band CHI Wiggler Ubitron Amplifier

J.M. Taccetti†, R.H. Jackson, H.P. Freund§, D.E. Pershing‡ and V.L. Granatstein†
Naval Research Laboratory, Washington, DC 20375-5347
taccetti@mmace.nrl.navy.mil
Phone (202) 767-9202

The status of a 35 GHz CHI (Coaxial Hybrid Iron) wiggler [1] ubitron amplifier experiment being performed at the Naval Research Laboratory will be presented. The purpose of the experiment is to study the CHI wiggler's potential of generating high wiggler fields at short wiggler periods as well as its excellent beam focusing and transport properties. The wiggler is immersed in an applied axial field which acts to both create the wiggler field and enhance the interaction. This enhancement near autoresonance will also be investigated, for both Group I and II orbits. The wiggler period is 6.4 mm. The operation point is chosen at grazing incidence (at 35 GHz) of beam and rf uncoupled dispersion curves, resulting in a wide instantaneous bandwidth. A SLAC klystron gun has been modified to produce an annular 100 kV, 10 A beam. Focusing of the beam from the gun into the CHI structure is provided by a system of three DC magnet coils. Broadband (≈20%) rf input and output couplers have been designed to couple from a rectangular TE_{10} to the coaxial TE_{01} interaction mode. Simulations using the above

parameters have shown an intrinsic untapered efficiency of 6.75% when operating at an applied field of 7.7 kG. The instantaneous bandwidth was ≈25%, with a gain of 28.3 dB, saturating at a distance of 63 cm for 100 W drive power. Results to date will be reported, along with measurements of the performance of the separate components.

[1] R.H. Jackson, H.P. Freund, D.E. Pershing and J.M. Taccetti, Nucl. Instr. and Meth. A341 (1994) 454.

† Permanent Address: University of Maryland, College Park, MD 20742

§ Permanent Address: SAIC, McLean, VA 22102

‡ Permanent Address: MRC, Newington, VA 22122

4P52

A Third Harmonic Magnicon Amplifier at 34 Ghz\

O.A. Nezhevenko†, V.P. Yakovlev†, A.K. Ganguly and J.L. Hirschfield
Omega-P Inc., New Haven, CT

Magnicon[1] is a high power, high efficiency microwave device. The magnicon has been successfully operated at the fundamental (1 GHz, 2.5 MW) and the second harmonic (7 GHz, 42 MW). The efficiencies are 73% and 45%, respectively. In the present paper we examine the feasibility of a third harmonic magnicon amplifier at 34 GHz with 1 μs pulse width as a possible high power, high efficiency RF source. Preliminary calculations show that such a magnicon can operate at an efficiency of about 40% with power exceeding 40 MW. The surface RF field in the cavities is in the range of 700–900 kV/cm which is below the breakdown level at 34 GHz for 1 μs pulse length. The newly proposed active RF pulse compressors[2] would make it possible to generate hundreds of MW power with 40 ns pulse suitable for multi=TeV e^-e^+ linear colliders. The maximal cathode loading does not exceed 15 A/cm^2. Details of numerical simulations and optimum design parameters will be presented.

[1] O.A. Nezhevenko, IEEE Trans. on Plasma Science, vol. 22, 756 (1994)

[2] M.I. Petelin, A.L. Vikharev and J.L. Hirschfield, Proc. 7th Workshop on Advanced Accelerator Concepts, Lake Tahoe, CA (1996).

†Permanent Address: Budker INP, 630090, Novosibirisk, Russia.

Tuesday Afternoon, 20 May 1997
3:00 p.m. – Multipurpose Room

Poster Session 4Q16-21:
5.1 Non-Equilibrium Plasma Processing II (Atmospheric Discharges)

4Q-16

An Improved Ionizer for Atmospheric Plasmas

Igor Alexeff, Mark Rader, Larry Wadsworth and Peter Tsai
University of Tenessee, Knoxville, TN

We have just received a United States Patent, #5592357, "Electrostatic charging apparatus and method", for creating dense atmospheric ion plasmas. The idea is to create positive and negative ions by means of dc or ac corona points, and to combine them into an atmospheric plasma. The new idea is to surround each corona point with a localized cloud of non-electron absorbing gas, such as nitrogen or argon. The ions then migrate from the formation region to form a large volume of air plasma. The use of the localized gas flow results in a plasma density increase of ten. We have created up to 10 exp 16 ions per cubic meter. We also have developed new diagnostic methods for use in these plasmas. The original objective of this work was to electrostatically charge plastic cloth to form electrets that last for several years. These act as excellent dust filters. However, other possible applications include surface and volume sterilization by the ions (free radicals), and removal of atmospheric pollutants.

Work supported in part by the Air Force Office of Scientific Research.

4Q17

Atmospheric Pressure Non-thermal Plasma

Shirshak Dhali
Department od Electrical Engineering, Southern Illinois University, Carbondale, IL 62901

We discuss several configurations of dielectric-barrier discharges to produce stable and uniform plasma in air. The discharges have potential applications in manufacturing, pollution cleanup and sterilization.

A dual pressure discharge will be discussed. Here the UV produced by low pressure discharge is coupled to a high pressure discharge to create a uniform discharge. The electrical characteristics of the discharge will be discussed. It has been found that UV irradiation increases the number of microdischarges. Therefore the discharge is more uniform and efficient in producing radicals

4Q18

Experimental Studies on AC Dielectric Barrier Corona Discharge Reactors for NO_x/SO_x Decompositions

Y.H. Kim and S.H. Hong
Department of Nuclear Engineering, Seoul National University, Seoul 151-742, Korea

Recently the interest in the AC dielectric barrier corona discharge (DBCD) is rapidly growing because of their successful application to the decomposition of air pollutants such as NO_x/SO_x. DBCD has a configuration of inserted dielectric barrier between highly non-uniform metal electrodes in the form of either cylinder-wire or pins-plate arrangement. Geometrical configuration of DBCD is of great importance for optimal design of flue gas purification reactors.

In this work, two types of DBCD reactors, cylinder-wire and pins-plate, are designed and experimented, and their decomposition efficiencies of No_x and So_x are compared. The powered electrodes of either tungsten wire or pins having a radius of curvature of 1 mm are fixed at 20 mm away from dielectric barriers of pyrex tube or acryl plate with a thickness of 2 mm. Stainless steel tube and plate of 100 mm in length are used as a grounded electrode of both type reactors, respectively. The gas treatment time is about 1 sec at a flow rate of 8 l/min in a discharge volume of about 120 cm^3. An AC high-voltage transformer, simulating pollutant gases containing 500-ppm NO or SO_2, and a gas analyzer are employed in the decomposition experiments for finding out an optimal reactor type and operating parameters. Decomposition efficiencies are measured by varying the amplitudes and frequencies of applied voltage and the flow rates and compositions of simulating pollutant gases.

The experimental results show that the cylinder-wire type is more efficient in decomposing NO and SO_2 than pins-plate one. For example, decomposition efficiencies of the cylinder-wire type reach 72% for NO and 16% for SO_2 at an operation condition of 30 kV and 7.5 l/min, while 35% for NO and 6% for SO_2 in case of pins-plate type. As a result of experiments, it is concluded that decomposition efficiencies depend almost linearly on the maximum electric field strength near the powered electrode and the power density per flow rate supplied to the reactor. For enhancing decomposition efficiency, a DBCD reactor of knife-plate types together, is also designed and its experimental results are presented in this work.

4Q19

Increasing the Surface Energy of Materials with a One Atmosphere Uniform Glow Discharge Plasma

Jerry L. Richardson, Anna K. Carr, J. Reece Roth
UTK Plasma Science Laboratory, Department of Electrical Engineering, University of Tennessee, Knoxville, TN 37996-2100

A surface suitable for printing with water-based inks has been obtained using a One-Atmosphere Uniform Glow Discharge Plasma (OAUGDP). Surface energies above 70 dynes per centimeter were obtained immediately after exposure. These values remained above 50 for the plastic substrate, and decayed to pre-exposure values for the metal. The surfaces were exposed to an ambient air plasma at atmospheric pressure. The samples were left in a normal laboratory environment after exposure, without special precautions for isolation or protection. Plastic (polyethylene Terephthalate–PET, obtained from the Textiles and Nonwovens Development Center–TANDEC) and metal (shiny side of Reynolds Wrap domestic heavy duty aluminum foil #109243) were exposed to a plasma with a RF electrode voltage of 11.6 kV rms at 5,000 Hertz across 14 centimeter diameter electrodes. A 2 millimeter thickness of Pyrex covers each of two electrodes, which are parallel plates with a 3mm air gap. Exposure times of 0, 3. 5, 10, 30,60 seconds were used for the plastic, and 0, 15, 30, 60, 90 and 120 seconds for the metal. The surface

energy was tested at increasing intervals after exposure. Exposure to the OAUGDP caused an increase in surface energy. The increase correlated positively to duration exposure. The metal returned to its original state about one day after exposure. The surface energy of the exposed plastic samples decayed to a value above 50 dynes/cm after about 24 hours. These results are similar to those obtained ref. 3, but are obtained in a normal atmosphere instead of a vacuum.

*This work was supported in part by a research agreement with March Instruments, Inc., Concord, CA.

[1] Roth J.R. (1995), Industrial Plasma Engineering, ISBN 0-7503-0318-2, Chap. 12, Sect. 12.5.2

[2] Roth, J.R. & Ku, Y., "Surface Cleaning of Metals in Air with a One Atmosphere Uniform Glow Discharge Plasma" Proc. 1995 ICOPS #95CH35796, p251

[3] D. Korzek, J. Papp, D. Theirich, & J. Engmann: "Cleaning of Metal Parts in an Oxygen Radio Frequency Plasma" J. Vac. Sci. Tech. A, Vol. 12, No. 2, (1994) pp369-78

4Q20

The Effect of Active Manipulation of a Plasma Surface Layer on the Aerodynamic Drag of a Flat Plate*

D.M. Sherman and J.R. Roth
University of Tennessee at Knoxville, Knoxville, TN
S. P. Wilkinson
NASA Langley Research Center, Hampton, VA

We will report further experimental results on the aerodynamic drag of a flat panel covered with a layer of One Atmosphere Uniform Glow Discharge Plasma (OAUGDP)[1] which has been operated in the NASA-Langley Research Center's 7 x 11 Inch Low Speed Wind Tunnel. In particular, we hope to present results on the effects of electrode geometry, including whether there exists an optimum electrode spacing, both parallel and perpendicular to the airflow; and the first test of a OAUGDP flat panel in a DC accelerator configuration in which the plasma is accelerated with, against, and at right angles to the airflow.

Prior testing showed that with the plasma present the aerodynamic drag increased as the electrode spacing increased up to a spacing of 6mm.[2] These results suggest that biasing the plasma with an additional set of electrodes which imposes a DC electrical field, (a DC accelerator OAUGDP panel) may lead to electrical control of the aerodynamic boundary flow and thus drag reduction.

*Supported in part by the NASA Langley Research Center, Grant MCC1-223.

[1]Roth, J.R. (1995): *Industrial Plasma Engineering: Vol. 1. - Principles.* Institute of Physics Press, Bristol, UK ISBN 0-7503-0318-2.

[2] Sherman, D.M., Roth, J.R., Wilkinson, S.P., Influencing an Aerodynamic Boundary Layer using a Surface Layer of One Atmosphere Uniform Glow Discharge Plasma, APS Bulletin, Vol. 41, No.7, page 1539, Nov. 1996.

4Q21

Killing Microorganisms in a Sealed Sterilization Bag with a One Atmosphere Uniform Glow Discharge*

Anna K. Carr and J. Reece Roth
UTK Plasma Science Laboratory, Department of Electrical Engineering
C.Brickman, K. Kelly-Wintenberg and T.C. Montie
Department of Microbiology
Peter Tsai and Larry Wadsworth
Textile and Nonwovens Development Center
University of Tennessee, Knoxville, TN 37996

With the proprietary technology of a One Atmosphere Uniform Glow Discharge, we have been able to sterilize surfaces contaminated with various microorganisms and bacteria.[1] To sterilize the material, typical plasma reactor operating conditions of 4 to 6 kVrms and 5 to 6 kHz can be used. So far, we are able to achieve the complete killing of Stephylococcus Aureus, E-coli, and Candida Albicans in minutes. These samples were seeded on nonwoven fabrics and then exposed in the One Atmosphere Uniform Glow Discharge Plasma Reactor at the UTK Plasma Science Laboratory.[2] We expect to report data on killing bacterial spores inside the medical sterilization bag as well as in other media.[3] This

application can be useful to the medical industry, the food packaging industry and others.

*Supported in part by the UTK Center for Materials Processing.

1 Y. Ku, C. Brickman, K. Wintenberg, T.C. Montie, P. Tsai, L. Wadsworth and J.R. Roth, "Sterilization of Materials Using a One Atmosphere Uniform Glow Discharge Plasma," 1996 ICOPS#96CH35939, p175.

[2] J.R. Roth, Industrial Plasma Engineering, IoP Publishers, Bristol, UK, ISBN 0-7503-0318-2 (1995) pp.453-461.

[3] The authors thank Helen M. Roth, R.N. for providing sterilization bags for this research.

Tuesday Afternoon, 20 May 1997
3:00 p.m. – Multipurpose Room

Poster Session 4Q22-28:
5.1 Non-Equilibrium Plasma Processing II (Deposition and Etching)

4Q22

Monte Carlo Simulation and Experimental Study of an Electron Cyclotron Resonance Plasma for Thin Film Deposition*

E. Koretzky and S.P. Kuo† and S.C. Kuo‡
Polytechnic University, Farmingdale, NY 11735

Plasma generated by electron cyclotron resonance (ECR) can have a nonequilibrium electron energy distribution (EED). ECR plasma has been shown to be particularly suitable for the synthesis of hard diamond-like carbon (DLC) films. In a low background gas pressure (10^{-5} to 10^{-2} torr at 298°K) its EED consists of two temperature components, where the temperature of the tail portion of electronics can exceed 30eV. Thus, the ECR plasma is also being considered for the deposition of polycrystalline diamond films, however, success has been limited.

Monte Carlo simulation of electron behavior in an ECR microwave discharge, maintained by the TM_{11} mode of a cylindrical waveguide, has been performed. The results[1] show that at low pressures (~0.5 mtorr) the temperature of the tail portion of the EED exceeds 40eV and the sheath potential is about -200V. These results are about twice as high as the previous[2] using the TM_{01} mode.

An ECR plasma source has been designed accordingly. A Langmuir probe is used to measure the characteristics of the plasma. Hydrogen mixed with 1% methane at a pressure of 0.5 mtorr is used as the background gas. The simulation and experimental results will be presented.

*Work supported by the AFOSR

† Department of Electrical Engineering, Polytechnic University, Route 110, Farmingdale, NY 11735

‡ Department of Applied Science, Brookhaven National Laboratory, Upton, NY 11973

[1] S.C. Kuo and S.P. Kuo, *J. Appl. Phys.*, **80(4),** 2512, 1996.

[2] S.C. Kuo, E.E. Kunhardt, and S.P. Kuo, *J. Appl. Phys.*, **73,** 4197, 1993.

4Q23

Imaging and Spectroscopic Analysis of Channel Spark Electron Beam Ablation Plumes*

S.D. Kovaleski, R.M. Gilgenbach, L.K. Ang, Y.Y. Lau and G.J. Overhiser
Intense Energy Beam Interaction Laboratory, Nuclear Engineering and Radiological Sciences, The University of Michigan, Ann Arbor, MI 48109-2104

Ablation of metals by a channel spark electron beam has been studied with several optical diagnostics. The channel spark is a high current (~1500A) low energy (<15-20keV) electron beam source developed by KFK [1] in Karlsruhe, Germany. The channel spark electron beam propagates in a low pressure (5-20mTorr) background of Ar, providing ion focusing. The channel spark electron beam is intended as a pulsed energy source for material ablation and redeposition as a thin film. The metals studied in this work are Fe and Ti. Ablation dynamics have been studied via various photographic imaging diagnostics. Plume composition and ionization have been studied through optical emission spectroscopy. Ionization of the background gas has also been examined through these methods. In addition, current diagnostics have provided information on beam transport and correlation of beam properties with ablation dynamics. Computational models of energy deposition and beam reflection at the

target have also been performed using the ITS-TIGER code [2] developed at Sandia National Laboratory.

*Supported by the National Science Foundation

[1] G. Muller and C. Schultheiss, Proc. of Beams '94, Vol. II, p833.

[2] Sandia Report No. SAND 91-1634.

4Q24

Analysis of Surface Structures of a Metal Target from Multi-pulse KrF Laser Ablation

L.K. Ang, Y.Y. Lau, R.M. Gilgenbach, H.L. Spindler*, S.D. Kovaleski and J.S. Lash†
The University of Michigan
Ann Arbor, Michigan 48109-2104

Aluminum targets were ablated by focusing a KrF excimer laser (248 nm, 40 ns, <1.2 J) down to a spot size of 0.05 cm^2 with a fluence of approximately 4.9 J/cm^2 [1]. After a few tens of pulses, surface irregularities (corrugations and pits) progressively emerge, with size 1-100 μm which is much larger than the laser wavelength. Such large scale surface roughness causes multiple reflections of the laser light, and may increase the absorption coefficient over a pristine, flat surface by an order of magnitude. Thus, as much as 16% (at room temperature) of the power of the KrF laser may be absorbed by the aluminum target. Scaling laws on the enhanced absorption due to surface roughness are derived [2]. We have also examined various physical mechanisms that lead to these large scale surface structures. The most promising candidate appears to be hydrodynamic instabilities of intense plasma formation near to the surface. A model is developed which yields the growth rate as a function of wave number, thickness of molten layer, energy density and spatial extent of the surface plasma, and the thermophysical properties of the irradiated material. We found that there is a threshold of plasma energy density for the occurrence of the instability.

This work was supported by NSF Grant No. CTS-9522282 and HLS by an NSF Graduate Fellowship.

[1] H.L. Spindler, R.M. Gilgenbach, and J.S. Lash, Appl. Phys. Lett. **68**, 3245 (1996).

[2] L.K. Ang, Y.Y. Lau, R.M. Gilgenbach, H.L. Spindler Appl. Phys. Lett. (Feb. 10, 1997 issue)

*Boeing Corp., Seattle, WA

†Sandia National Laboratories, Albuquerque, NM

4Q25

Poly-Si Etching in Cl_2 Plasma Using Electron-Beam–Excited Plasma Apparatus

Ryuichi Miyani, Yasuhiro Mikawa, Jun-ichi Inaguma, Yasunori Shiraki, Motoyuki Fujii, Shunjiro Ikezawa, Keisuke Kida, Akira Nishiwaki and Toshitaro Yoshioka
Chubu University, 1200 Matsumoto, Kasugai, Japan

An electron-beam–excited plasma (EBEP) apparatus is able to produce high density plasma (i.e., high ion-current) under low pressure on the order of 0.1 Pa. In addition, energy and density of electron beam for plasma generation can independently be controlled by accelerating voltage V_A and discharge current I_D, respectively. As one of its applications, poly-Si etching is tried in a pure Cl_2 plasma by means of reactive ion etching. A typical experimental results is shown in Fig. 1. An under cut on etched wafer tends to decrease as V_A increases, since sheath potential increases as V_A increases.

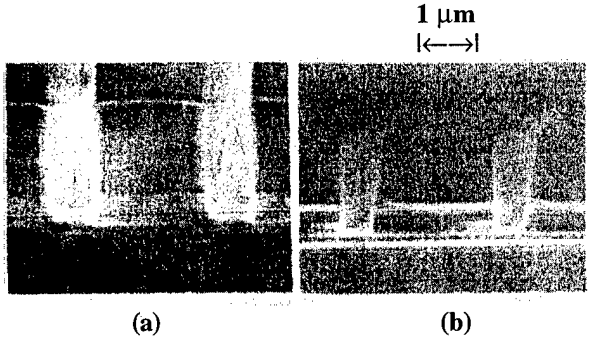


Fig. 1. Cross section of etched Poly-Si wafer (pressure of 0.1 Pa, I_D = 5 A). (a) V_A = 70 V; (b) V_A = 100 V.

4Q26

An Optical RIE Process Uniformity Control Sensor

Steven C. Shannon, William Pruka,
James Paul Holloway and Mary Brake
Depatment of Nuclear Engineering and Radiological Sciences, University of Michigan, Ann Arbor, MI

Radial etch process measurement techniques have been compared using a GEC reference cell for Argon sputter etching of silicon oxide. Post process reflectometry measurements. Langmuir probe studies, and optical tomography results were used to study the process uniformity at various set points. The purpose of this experiment is to demonstrate the ability of a small window plasma tomography sensor to function as a process diagnostic, allowing in situ process monitoring and an alternative uniformity measurement to post process wafer measurements.

The small window plasma tomography sensor is based on a rotating point sensor at the surface of a window and reconstructs emissivity from a thin, pie shaped field of view. This design not only allows for use in small window geometries, but also provides a stronger, more accurate signal, essential for accuracy in the ill posed reconstruction process. The reconstruction of the radial emissivity profile is a regularized inversion algorithm. Continuous and descretized profile algorithms, both utilizing Tikonov regularization are compared. This analysis is conducted for both argon neutral and ion lines.

An overview of the sensor geometry, signal reconstruction, and comparison to Langmuir probe and reflectometry measurements will be presented. Future work will include similar optical analysis for more complex plasma chemistries and industrial reactors.

Supported by SRC contract 96-FC-085, NSF grant ECS-9358344 and SEMITECH project ETCH001.

4Q27

Characterization and Optimization of Argon Sputter Etching of SiO2 in the GEC Reference Cell

Melissa Buie
Applied Materials, Santa Clara, CA
Steven C. Shannon, James Paul Holloway, Mary Brake,
Dennis Grimard and Fred Terry Jr.
University of Michigan, Ann Arbor, MI

In these experiments, the GEC reference cell is used to etch SiO2 off 4" wafers. Etch rate and uniformity data are measured using a reflectormeter, for wafers etched in a range of system operating conditions (power, pressure, and gas flow rate). These measurements are then used in a statistically designed orthogonal screening experiment. The goal of these experiments is two fold:

- To understand the major trends of each of the control parameters on the etch rate and uniformity
- To use this data to determine the optimum etch conditions in the GEC reference cell.

Both graphical and analysis of variance (ANOVA) techniques are performed on the etch rate and uniformity data to accomplish these goals.

Supported by SRC contract 96-FC-085, NSF grant ECS-9358344.

4Q28

Experimental Study of Charging Processes on Unpatterned Oxide-Coated Si Wafers in an ECR Etcher

C. Cismaru, J.L. Shohet, N. Hershkowitz
Engineeering Research Center for Plasma-Aided Manufacturing, University of Wisconsin-Madison, Madison, WI
K. Nauka
Hewlett-Packard Laboratories, Palo Alto, CA
and J.B. Friedmann
Semiconductor Group, Texas Instruments, Dallas, TX 75265

During plasma processing, used in the fabrication of integrated circuits, oxide surface charging is becoming more of a concern due to its increased damage potential.

In this work, plasma induced charging mechanisms onto the surface of oxide-covered unpatterned 4" Si wafers

exposed to non-uniform O_2 and Ar electron-cyclotron-resonance (ECR) plasma are investigated. Wafers covered with a 1000Å oxide layer were exposed to the ECR plasma under non-uniform etching conditions, and the induced surface charge was mapped on the wafers using the Contact Potential Difference [1] (CPD) technique. During processing, plasma parameters (floating potential, plasma potential, electron temperature, and ion density) were monitored in the bulk of the plasma using Langmuir probes as well as on the surface of the wafers (i.e. surface potential) along with the same magnetic field lines using special wafer probes. With the use of these parameters, along with other processing factors (e.g. RF power and voltage applied to the wafer stage), a surface charging model is developed. These results are compared with the CPD wafer maps of the induced surface charge.

This work was supported in part by the National Science Foundation under Grant No. EEC 8721545.

[1] K. Nauka, "Application of Surface Photovoltage and Contact Potential Difference for In-line Monitoring of IC Processes", International Symposium on Semiconductor Characterization, Nat. Inst. Stand. Tech. NIST, January, 1995.

Tuesday Afternoon, 20 May 1997
3:00 p.m. – Multipurpose Room

Poster Session 4Q29-32:
5.1 Non-Equilibrium Plasma Processing II (ICP Modeling)

4Q29

Effect of Plasma Processing Reactor Circuitry on Plasma Characteristics*

Shahid Rauf and Mark J. Kushner
Dept. of Electrical and Computer Engineering, University of Illinois, 1406 W. Green Street, Urbana, IL 61801

It is well know that external circuitry greatly influences the performance of plasma processing reactors. Simulation of external circuits difficult since the time in which the external circuit attains the steady-state is several orders of magnitude longer than typical plasma simulation time scales. In this paper, we present a technique to simulate the external circuit concurrently with the plasma, and implement it into the Hybrid Plasma Equipment Model (HPEM). The resulting model is used to investigate the influence of external circuitry on plasma behavior.

The technique assumes that plasma is being simulated in an iterative manner. At the end of each iteration, the resulting plasma parameters are used to construct a simple circuit model of the plasma. The sheaths are replaced with nonlinear circuit elements and inductive coils with transformers. All other components are explicitly included. In our studies, we have used Riley's[1] model for the nonlinear sheath element. The resulting nonlinear plasma-circuit model is simulated until steady-state conditions are obtained. The external circuit quantities (e.g. blocking capacitor voltage) serve as the starting point for the next plasma simulation iteration. This procedure is repeated until the plasma and external circuit attain the steady-state.

We implemented this technique in the HPEM. The resulting model was used to investigate the influence of blocking capacitor, stray capacitances and matching network on the performance of inductively coupled and reactive ion etching reactors. The role of external circuitry in exciting and controlling nonlinear behavior in the sheathes was also studied.

*This research has been supported by ARPA/AFOSR (F49620-95-1-0524). NIST, SRC and NSF (ECS94-04133).

[1] M. Riley, Sandia Report SAN95-0775 (1995).

4Q30

Modeling of the Effects of Die Scale Features on Bulk Plasma Conditions in Plasma Etching Equipment*

Michael J. Grapperhaus and Mark J. Kushner
University of Illinois, 1406 W. Green Street, Urbana, IL 61801

The patterning of the wafer during microelectronics fabrication can have a significant effect on bulk plasma properties as well as producing local pattern dependent etch rates. Sputtering of photoresist, loading effects, and other surface interactions couple the chemistry at the wafer surface to the bulk plasma chemistry. A model has been developed which uses a Monte Carlo simulation to model quasi-steady state die scale surface chemistry in plasma etching reactors. This model is integrated within the Hybrid Plasma Equipment Model (HPEM)[1] which resolves two-dimensional reactor scale plasma conditions.

The HPEM consists of an electromagnetics, electron Monte Carlo simulation, and a fluid plasma modules. The surface Monte Carlo simulation is used to modify the flux boundary condition at the wafer surface within the HPEM. Species which react on the surface, or which are created at the surface are tracked on and near the wafer surface. This gives a quasi-steady state surface chemistry reaction mechanism resolved in two dimensions on the die scale. An inductively coupled etching reactor is used to demonstrate the effect of surface chemistry on bulk plasma conditions over a range of pressures from 10 to 100 mtorr, 100's W of inductively coupled power and 10's to 100's V rf applied substrate voltage. Under high etch rate conditions, macroloading effects are shown. As pressure is varied from 10 to 100 mtorr and the effect of local photoresist sputter and redeposit on nearby exposed etch area is shown to increase which leads to different etch rates near the boundaries of etching regions versus unexposed regions.

*Work supported by SRC, NSF, (ECS 94-04133) and the University of Wisconsin ERC for Plasma Aided Manufacturing.

[1] M.J. Grapperhaus and M.J. Kushner, J. Appl. Phys., **81**, no. 2, (1997).

4Q31

Statistical Parametric Study of Non-Parallel Inductive Reactors

Eric R. Keiter and Mark. J. Kushner
Dept. of Electrical and Computer Engineering, University of Illinois, 1406 W. Green St., Urbana, IL 61801

Parametrization of new plasma processing very time consuming process. By combining statistical techniques with computer simulation, one can construct a "numerical design of experiment" (NDOE), which minimizes the time required for the investigation. Here we present the results of such an NDOE, applied to a generic non-parallel inductively coupled reactor, as there has recently been interest in inductive reactors with a dome shaped quartz top. We use a statistical design of experiment software too, Echip©, to construct the experiment and then perform the experiment with the Hybrid Plasma Equipment Model (HPEM)[1]. Echip© is also used in the post-experiment analysis. The goal is to determine functional relationships between ion and neutral flux uniformity to the wafer and geometrical parameters such as focus ring height, reactor height, and reactor radius. Additionally, we consider several non-geometrical variables such as substrate bias and pressure. By combining numerical modeling with statistics software we have been able to determine optimal parameters sets for different gas systems. Of the geometric parameters, focus ring height appears to have the strongest correlation with the ion and neutral flux uniformity. Correlation becomes worse at higher pressures for most parameters.

*This research has been supported by AFOSR/ARPA, Applied Materials Inc., SRC and NSF (ECS94-04133)

[1] M.J. Grapperhaus and M.J. Kushner, J. Appl. Phys. **81,** no. 2, (1997)

4Q32

Modeling of 2-Dimensional and 3-Dimensional Etch Profiles in High Density Plasma Reactors*

Robert J. Hoekstra and Mark J. Kushner
Dept. of Electrical and Computer Engineering, University of Illinois, 1406 W. Green St., Urbana, IL 61801
Valeriy Sukharev
LSI Logic Corp., Santa Clara, CA 95054

In order to model the plasma etching process from plasma generation to etch profile evolution, processes from the macroscopic reactor scale to the microscopic feature scale must be simulated. An integrated Monte Carlo feature Profile Model (MCFPM) has been developed to examine the time evolution of etch profiles in high density plasma systems. By integrating the MCFPM with the Hybrid Plasma Equipment Model (HPEM)[1],we are able to self-consistently determine the etch profiles for specific regions on the wafer in specific reactor geometry with specified parameters for power, chemistry, gas flow, etc.

The latest improvements of the model include the effects of incoming particle angle and energy on reaction and reflection based on the results of molecular dynamics simulations. Increase in specular reflection of high energy particles leads to more vertical sidewalls and corner clearing but can also cause deformation of the bottom of the profile surface. For Chlorine etching of 2D and 3D profiles in polysilicon, the model results will be compared to experimental results in an inductively couple etching reactor. The changes due to radial location as well as sub wafer and superwafer topography be examined.

*Work supported by SRC, NSF, and University of Wisconsin ERC.

[1] M. J. Grapperhaus and M. J. Kushner, J. Appl. Phys. **81**, no. 2 (1997)

Wednesday, 21 May 1997
8:30 a.m. – Kon Tiki Ballroom

Plenary Session

NASA's International Solar Terrestrial Physics Program and the Roadmap Forward

Dr. Robert L. Carovillano

NASA Headquarters, Washington, DC, USA

Chair: E. E. Scime

Wednesday Morning, 21 May 1997
10:00 a.m. – Kon Tiki Ballroom

Oral Session 5A:
1.3 Basic Phenomena in Partially Ionized Gases–Gaseous Electronics, Electrical Discharges, etc.
Chair: S. Rauf

5A01

Optical Emission Spectroscopy of High Density Metal Plasma During Magnetron Sputtering

O.E. Hankins[1] and Z.J. Radzimski[2]
[1]*Department of Nuclear Engineering*
[2]*Department of Materials Science and Engineering*
North Carolina University, Raleigh, NC 27695

During conventional magnetron sputtering with an inert gas, the target material is sputtered in the form of neutrals and ions. The majority of sputtered species are neutrals which while traveling through the plasma region above the magnetron source may become ionized. With an electric potential across the dark space field above the target in the order of a few hundred eV, target ions extracted from the plasma have enough energy to sputter target material. If a self-sputtering yield (ratio of sputtered secondary target species to number of incident target ions) is high enough, the process can transition without an inert gas into a self-sustained mode. This mode of sputter deposition has been achieved in the ETERNA magnetron sources for a variety of materials which were sputtered without argon at a chamber background pressure in the 10^{-6} Torr range.

The ability to sputter deposit in the self-sustained mode without an inert gas indicates that a high ionization efficiency of the neutral target species has been achieved and that a purely metal ion plasma can be formed using magnetron source. In this paper, the mechanisms responsible for such effective ionization of copper sputtered from the target are investigated using optical emission spectroscopy. Light emission spectra were taken for various conditions of magnetron operation to understand the transition from standard to self-sputtering mode. We offer explanations on the factors which may be responsible for effective self-sputtering and ionization of the target species.

5A02

High Frequency Series Resonance and Surface Wave Sustained Discharges

D.J. Cooperberg and C.K. Birdsall
Electronics Research Laboratory, University of California at Berkeley, Berkeley, CA 94720-1774

The typical parallel plate RF discharge relies on capacitive coupling in sustaining discharges. At HF the natural resonances and normal modes in an unmagnetized plasma slab can be used to resonantly sustain plasma discharges.[1] These resonantly sustained plasmas have many features which distinguish them from the conventional capacitive discharge.

These distinguishing features including scaling laws, plasma impedance, minimum operating voltages, and wave structure will be discussed. In addition, the stability of these discharges will be verified and an observed transition in the heating mechanism and EEDG's which is brought on by varying the neutral gas pressure will be demonstrated. Experimental results are based on PIC-MCC simulation in one and two dimensions and will be compared with theory where possible.

This work supported by Office of Naval Research contract N00014-90-J-1198.

[1] D.J. Cooperberg and C.K. Birdsall, IEEE Conference Record - Abstracts, **1996 IEEE ICOPS**, 162

5A03

Analytical Investigation of Non-Collisional Electron Heating*

Shahid Rauf and Mark J. Kushner
University of Illinois, 1406 W. Green St., Urbana, IL 61801

Non-collisional heating is an important phenomenon in low pressure inductively coupled plasmas. In this paper, a self-consistent analytical model for non-collisional heating is developed. The model is used to investigate the physical mechanism of non-collisional heating, and quantify the effect of plasma density, electron temperature and excitation frequency. It is also demonstrated that this model can adequately take account of non-collisional heating effects in plasma simulations.

The model considers a one-dimensional plasma-vacuum interface upon which a plane electromagnetic (EM) wave impinges from the vacuum side. EM fields

within the plasma are computed by self-consistently solving the Maxwell-Boltzmann equations. Electrons are assumed to have a Maxwellian energy distribution and constant density. Analysis yields an expression for warm plasma conductivity (σ_w). The model reduces to the correct limits in the cold plasma and collisionless situations.

Non-collisional heating in this context can be explained by a resonant interaction of the EM wave with electrons whose velocities are comparable to the effective wave phase speed. Electrons gain net directed energy during the resonant interaction process, which is converted to random thermal energy through collisions. We also show that warm plasma non-collisional heating effects become more pronounced if the electron temperature increases, electron density increases, wave frequency decreases or electron collision frequency decreases.

The analytical expression for σ_w can be used to include in non-collisional heating effects in plasma simulations. We demonstrate the feasibility of this approach by integrating σ_w in the Hybrid Plasma Equipment Model and comparing simulation results with those of a more general plasma model.

*This research has been supported by ARPA/AFOSR (F49620-95-1-0524), NIST, SRC and NSF (ECS94-04133).

5A04

Modeling Electro-Negative RF-Discharges in the Low Pressure Regime

R.P. Brinkmann
Siemens AG, Corporate Technology

A new fluid dynamics/Monte-Carlo hybrid approach to the self-consistent simulation of electro-negative RF-discharges in the low pressure regime is described. The model is an extension of a previously presented formalism for electropositive discharges [1] and is intended to capture the essential physics of micro-electronic manufacturing processes like plasma etching (PE), reactive ion etching (RIE), and plasma enhanced chemical vapor deposition (PECVD).

The fluid part of the model consists of an equation of continuity and a balance of momentum for the positive ions, a drift-diffusion-equation for the negative ions, and assumes local Boltzmann equilibrium for the electrons. In the sheath regions, the electrical field is calculated by means of Poisson's equation; in the bulk, it is determined via the quasi-neutrality condition. Regularization with respect to nonlinear Langmuir oscillations is provided.

Coupled to the fluid-dynamical equations is a one-particle Monte-Carlo model, which is used to calculate the electron and ion energy distribution without recurring to the assumption of shifted Maxwellians. This enables a realistic determination of reaction rates and transport coefficients, and allows to incorporate the phenomenon of non-local heating.

The model is applied to calculating the energy and the angular distribution of the ions incident on the surface of a semiconductor wafer. The resulting information can be used to determine the evolution of the wafer topography during plasma etch and deposition processes (feature scale simulation) [2].

[1] R.P. Brinkmann et al., JES, 143(6), 1996.
[2] J.S. Han et al., J. Vac. Sci. & Tech., 13(4) 1995.

5A05

Approximate, Semi-Implicit Calculation of 3D Electrostatic Potential in a Self-Consistent Plasma Simulation

Eric R. Keiter and Mark J. Kushner
Department of Electrical and Computer Engineering, University of Illinois, 1406 West Green Street, Urbana, IL 61801

Numerical Modeling of low pressure plasma reactors is subject to numerous time step constraints, and among the most restrictive of these is the dielectric relaxation time. In recent years, semi-implicit flux-correction techniques have allowed plasma modelers to loosen the dielectric relaxation time step restriction [1]. However, since these simulations do solve a form of Poisson's equation, they still have a restriction on time step based on a modified, albeit less restrictive, dielectric relaxation time. For some parameter spaces this is acceptable, but for very large scale simulations (for example in three dimensions) and for simulations of systems having long time scales, obtaining a longer time step is crucial.

Using a generalization of a technique presented in [2], we present a method for obtaining an approximate electrostatic potential which has no dielectric relaxation time restriction. Implementation is of comparable difficulty to that of a conventional Poisson's equation, and is no more computationally intensive. The module is implemented within a large, self-consistent hybrid plasma equipment model (HPEM) [3]. A rearranged continuity

equation is solved, and charge neutrality is assumed. A comparison to the HPEM running with Poisson's equation is presented, for both two and three dimensions, and for electropositive and electronegative gases.

*This research has been supported by AFOSR/ARPA, Applied Materials Inc., SRC and NSF(ECS94-04133).

[1] Peter L.G. Ventzek et al J. Vac. Sci. Technol. B **12**(1) Jan/Feb 1994

[2] U. Kortshagen, et al Phys. Rev. E **51**, 6 June 1995.

[3] M.J. Grapperhaus and M.J. Kushner, J. Appl. Phys. **81**, no. 2, (1997).

5A06

Double and Triple Layers in Dusty Plasmas

A. Garscadden, B.N. Ganguly, P. Bletzinger and P.D. Haaland
Wright Laboratory, WPAFB, Ohio 45433

The results of experiments on dusty plasmas in rf excited discharges are reported. These discharges use graphite electrodes and helium gas fills around 1 Torr. Laser scattering data was recorded on a system with 4:1 area ratio graphite electrodes, mounted vertically. This configuration eventually produces a thin dust layer at the edge of the larger electrode sheath. As the dust density of this disk increased, the electrode sheath expanded (indicating a higher sheath potential drop) and a similar thick sheath appeared on the side of the dusty layer facing the large electrode. The thickness of the dust sheath on the plasma side was much smaller. The results indicate that the dust increases the impedance of the plasma locally. This causes an increase in the electrode sheath voltage and a corresponding increase in the dust sheath voltage. The disk of dust acts like a suspended insulator that is charged to different potentials on its two sides, thus creating two double layers. In the early stages, the disk sides can be at equal potential, resulting in a triple space charge layer. It should be noted that the resulting electrode sheath voltage drops are in the opposite direction to those expected in a non-dusty plasma in this asymmetric configuration. Other results show the mapping of the potential distributions by the dust layers.

5A07

High Pressure Hollow Electrode Discharges

K.H. Schoenbach, A. El-Habachi, W. Shi and M. Ciocca
Physical Electronics Research Institute
Old Dominion University, Norfolk, VA 23529

Reduction of the cathode hole diameter into the submillimeter range has allowed us to extend the pressure range for hollow electrode discharge operation to values on the order of 50 Torr [1]. In recent experiments with cathode holes of 0.2 mm diameter we obtained stable glow discharge operation up to approximately 900 Torr in argon. The current-voltage (I-V) characteristics of these discharges (with currents ranging from the ten's of μA to ten mA) show three distinct discharge modes: at low current, a discharge with positive differential resistivity, followed by a range with strong increase in current and reduction in voltage, and, at high current, again a resistive discharge mode. For low pressure (<100 Torr) these modes correspond to the predischarge, hollow cathode discharge (sustained by "pendulum" electrons), and abnormal glow discharge, respectively [1,2]. At higher pressure the discharge in our short gap system (anode-cathode distance: 0.25 mm) changes from a hollow cathode discharge to, what seems to be a "pulseless" partial glow discharge [3]. In hollow cathode discharges operated in the Torr range the electron energy distribution is known to be strongly non-maxwellian with a large concentration of electrons at energies greater than 30 eV [4]. This holds also for hollow cathode discharge at high pressure and for partial discharges as indicated by the presence of strong excimer lines in the VUV spectrum of Ar-discharges at 128 nm and Xe-discharges at 172 nm. The resistive characteristic of high pressure hollow electrode discharges over a large range of current allows us to generate arrays of these discharges for use as flat panel, direct current, excimer lamps.

Supported by DOE, Advanced Energy Projects Division.

[1] K. Schoenbach et al., Appl. Phys. Lett. **68,** 13 (1996).

[2] A. Fiala, L.C. Pitchford, and J.P. Boeuf, XXII ICPIG, Hoboken, NJ, July 1996, Contr. Papers 4, p. 191.

[3] R. Bartnikas, and J.P. Novak, IEEE Trans. Electrical Insulation **27**, 3 (1992).

[4] K. Fujii, Jpn. J. Appl. Phys. **16,** 1081 (1977).

5A08

A Plasma Mirror for Electronic Microwave Beam Steering*

R. Meger, J. Mathew, W. Manheimer, R. Fernsler, J. Gregor[a], D. Murphy, M. Myers and R. Pechacek[b]
Plasma Physics Division, Naval Research Laboratory Washington DC 20375

A planar plasma may be used as a reflector for microwaves if the plasma frequency (at the angle of incidence) is greater than the microwave frequency. If this plasma mirror can be repositioned electronically, it could have the capability of redirecting microwave beams on a very fast time scale, and as such it could have important applications to radar and communication systems. The goal is the generation of planar plasmas which have the potential of reflecting microwave beams [1-4]. The plasma is formed with a unique hollow cathode glow discharge. It produces a sheet plasma, square and about 60 cm on a side. This plasma has been studied mostly in air, although other gases have been used also with similar results. The background pressure is about 100 mtorr, and a uniform magnetic field of about 100 G is in the plane of the plasma. Microwave experiments show that as far as flatness and noise temperature are concerned, the plasma acts like a metal plate. Furthermore, the velocity of the reflecting surface can be as low as a few centimeters per second.

*This work is supported by the Office of Naval Research.

[1] W. Manheimer, IEEE Trans. Plasma Sci, PS-19, 1228, (1991)

[2] A. Robson, R. Morgan, and R. Meger, IEEE Trans. Plasma Sci. PS-20, 1036 (1992)

[3] R. Meger, J. Mathew, J. Gregor, R. Pechacek, R. Fernsler, W. Manheimer, and A. Robson, Phys. Plasmas 2, 1532, (1995)

[4] J. Mathew, R. Fernsler, R. Meger, J. Gregor, D. Murphy, R. Pechacek, W. Manheimer, Phys. Rev. Let. 77, 1982 (1996)

Wednesday Morning, 21 May 1997
10:00 a.m. – Board Room

Oral Session 5B:
2.2 Fast Wave Devices I
Chair: D. Pershing

5B01-02 *Invited*

High Power W-Band Gyroklystron Amplifier Experiments at NRL

M. Blank, B.G. Danly, B.Levush, P. E.Latham[†]
Naval Research Laboratory, Washington, DC 20375

The Naval Research Laboratory is currently investigating gyroklystron amplifiers as high power, moderate bandwidth sources for millimeter wave radars. A four cavity W-band gyroklystron amplifier experiment is now underway at NRL. The gyroklystron has produced 55.5 kW peak output power and 23.5% electronic efficiency in the TE_{01} mode for a 56 kV, 4.2 A electron beam. The -3 dB bandwidth is greater than 400 MHz. The small signal and saturated gains are 36 dB and 28 dB, respectively.

A time dependent version of the non-linear code MAGYKL [1] was developed to design the interaction circuit. Theoretical performance predictions are in good agreement with experimental results. Extensive stagger tuning and output cavity Q studies have led to a wider bandwidth design, which will be built and tested in the near future.

This work was supported by the Office of Naval Research. The computational work was supported in part by a grant of HPC time from the DoD HPC Center NAVO.

[1] P.E. Latham, W. Lawson, V. Irwin, IEEE Trans. Plasma Sci., Vol 22, No. 5, pp 804-817, 1994.

[†] Omega P, Inc., New Haven, CT

5B03

Study of High Gain Gyrotron Traveling Wave Amplifier

K.R. Chu[1], H.Y. Chen[1], C.L. Hung[1], C.H. Chang[1], S.H. Chen[2], T.T. Yang[3] and L.R. Barnett[1]
[1] *Dept. of Physics, National Tsing Hua University*
[2] *National Center for High-Performance Computing*
[3] *Synchrotron Radiation Research Center*
Hsinchu, Taiwan, Republic of China

High gain operation of a millimeter wave gyro-TWT enhances the possibility of spurious oscillations caused by various internal and external feedback mechanisms. Three types of oscillations have been analyzed theoretically with realistic modeling of the interaction structure. It is shown that each type of oscillation exhibits different characteristics. Experiments have been conducted to investigate properties of these oscillations and their stabilization by proper distribution of wall losses. Experimental observations are in reasonable agreement with theoretical predictions. Based on these results, a Ka-band gyro-TWT with 50 dB saturated gain has been designed and is being put together for test.

5B04

Input Coupler for a 35 GHz Gyroklystron*

A.H. McCurdy[§], J.J. Choi[†], R.H. Kyser[&], B.G. Danly and W. M. Manheimer[‡]
Naval Research Laboratory, Code 6840,
Washington, DC 20375

Gyroklystron amplifiers at 35 GHz are currently being designed and operated at the Naval Research Laboratory. To couple the input signal, in a relatively broadband way, into the desired TE_{011} circular cavity mode, a coaxial cavity is constructed around the right circular input cavity. The two cavities are coupled by slots cut in the shared wall. Significant analysis and cold test has been done on this device. Theoretical analysis includes a circuit model, a combined mode-matching/dipole aperture theory, and HFSS simulations. The design goals are for a resonant frequency of 35 GHz, Ohmic quality factor of over 1000, total quality factor of near 175 with over 99% mode purity. Cold test results indicate the success of the design work. Sensitivity of the cavity resonance to slot orientation, cavity length, and aperture alignment is studied. A particular problem is encountered in attempting to match in the input drive signal to the cavity. Limits on attainable match are found using conventional filter theory. The final design for the cavity will be described as well as initial tests with an injected electron beaM.[1]

Work supported by the Office of Naval Research.
[§] Permanent Address: University of Southern California, Los Angeles, CA 90089
[†] Science Applications International Corp., McLean, VA 22102
[‡] Dyncorp, Rockville, MD 20850
[&] Code 6707, Naval Research Laboratory
[1] J. J. Choi, et. al., in this conference.

5B05

Simulation Studies of Relativistic Gyroklystron Amplifiers*

G.P. Saraph, J.P. Anderson, W. Lawson and V.L. Granatstein
Institute for Plasma Research
University of Maryland, College Park, MD 20742

High power, pulsed gyroklystrons operating in the X, Ku, and Ka bands are being developed for driving future linear colliders. Various design aspects of two and three cavity, coaxial, relativistic gyroklystron systems are studied. Nonlinear simulations predict that over 40% efficiency, 45-50 dB gain, and 100-160 MW power levels are possible for the fundamental and second harmonic designs operating at 8.6, 17.1, and 35.0 GHz frequencies

Gyroklystron designs should also satisfy phase and frequency synchronization criteria for driving large accelerators. Small manufacturing tolerances can lead to 10-20 MHz changes in cold cavity frequencies. It is desirable to have some frequency tunability to compensate for this effect. It is shown that the desired frequency tunability can be achieved by making small adjustments in the axial magnetic field level. Effect of voltage pulse on the device efficiency and output phase is studied using time-dependent simulations. The pulse-shape plays an important role in determining phase stability.

Advance design features such as radial coupling slots in the input and output cavities and dielectric loading are studied using HFSS simulations. An improved three cavity, Ku band design will be presented based on these features. In addition, a possible implementation scheme for energy recovery using a single-stage depressed collector will be presented. It is shown that the energy recovery could boost the net device efficiency above 50%.

*This work is supported by a research grant from the U. S. Department of Energy.

5B06

35 GHz GYROKLYSTRON AMPLIFIERS*

J.J. Choi†, A.H. McCurdy§, F. Wood&, R.H. Kyser&, B.G. Danly, B. Levush and R.K. Parker
Naval Research Laboratory, Code 6840, Washington, D.C. 20375

Experiments on two-cavity and three-cavity gyroklystron amplifiers are underway to demonstrate a 140kW, 35GHz coherent radiation amplification for radar applications. High power, high duty (10%) relevant gyroklystrons require a TE_{011} cylindrical cavity mode, operating at a fundamental beam cyclotron mode. An electron beam of 70kV, 6A produced from a magnetron-injection–gun is injected into the cavities through a high compression magnetic field powered by a 13kG superconducting magnet. Drift tubes consisting of lossy ceramic rings are designed to suppress undesired oscillations. A drive signal is injected into the first cavity through a mode selective coaxial coupler [1]. A capacitive probe is placed directly before the input cavity to measure the beam velocity ratio. Large signal non-linear calculations [2] predict that the two-cavity gyroklystron produce a peak power of 140kW, corresponding to efficiency of 33% and a saturated gain of 23dB over a 0.35% bandwidth at $\alpha = 1.5$, $\Delta v_z/v_z = 15\%$, 13.3kG, $Q_1 = 150$, and $Q_2 = 200$. In order to increase an amplifier bandwidth, a stagger tuned three cavity circuit is designed. Calculations show a bandwidth of 0.7% (increased by a factor of two compared with the two-cavity circuit), gain of 33dB and efficiency of 28%. Experimental results of the amplifier will be presented and compared with the non-linear theory.

*Work supported by the Office of Naval Research.

†Science Applications International Corp., McLean, VA 22102

§USC, Los Angeles, CA 90089

+Dyncorp, Rockville, MD 20850

[1] A.H. McCurdy, et al., in this conference.

[2] P. Latham, W. Lawson, and V. Irwin, IEEE Trans. Plasma Sc. 22, p. 804, 1994.

5B07

Measured Performance of a Phase-Controlled Harmonic-Multiplying, Inverted Gyrotwystron

H. Guo, J. Rodgers, S. Chen, G. Nusinovich, M. Walter and V.L. Granatstein
Institute for Plasma Research, University of Maryland, College Park, MD

This is a preliminary report on operation of the phase-controlled, harmonic-multiplying, inverted gyro-twystron (phigtron) which uses a magnetron injection gun (MIG) (60kV/10A), a combined TE_{0n} mode-launcher/ input-coupler, a Ku-band fundamental gyro-TWT pre-bunching section, a radiation-free drift section, and a Ka-band complex output cavity. Depending on preset operating parameters, the phigtron can be operated either as an efficient, phase-locked oscillator or as a frequency-multiplying amplifier with medium bandwidth. For the oscillator, we obtained 180 kW output, 33% efficiency, 30 dB phase-locking gain, and ~1 MHz locking bandwidth around 34.4 Ghz; widest bandwidth operation gave 100 kW output, 25% efficiency, 30 dB phase-locking gain and 8 MHz locking bandwidth around 34.6 GHz. For the amplifier, 150 kW output, ~20% efficiency, and ~35 dB saturated gain were measured. Amplification was observed in a band of 1.5% around 31.8 GHz. Amplification range is improved, compared to a gyro-klystron, by replacing the input cavity with a traveling wave interaction structure. The second harmonic content of the beam may develop within both the gyro-TWT section and the drift space, resulting in high gain. Finally, stable operation of the phigtron is attributed in part to employing a TE_{0n} mode selective circuit as an input coupler and at each interaction stage to suppress competing modes.

This work was supported by the DoD MURI program under grant F49620-92-J-0152 and by the DoD Vacuum Electronics Initiative under grant N0014941G036. The authors thank D.S. Wu, Y.H. Miao, D. Cohen and J. Pyle for technical support.

5B08

VELOCITY SPREAD IN GYROBEAMS DUE TO CATHODE EDGE EMISSION*

R.B. True, G.R. Good and T.A. Hargreaves
Litton Electron Devices Division,
San Carlos, California 94070
K.T. Nguyen
KN Research, Silver Spring, MD 20906

In analyzing the design of the magnetron injection gun and beam optical system to be used in the 94 GHz NRL/CPI/Litton gyroklyston, a major source of velocity spread in gyrobreams was discovered. Basically, when we set up a detailed model of the region between the emitter strip and the focus electrodes in DEMEOS (used for the simulations), we observed a large amount of current pouring from the edges of the cathode strip due to the level of field penetrating the gaps. This edge emission caused a major increase in velocity spread (both parallel and perpendicular) over the idealized case and by including it, computed and typical observed results are now in line.

In the paper, we will show quantitatively how velocity spread is affected by the gap geometry (cathode and focus electrode edges perpendicular to the axis, perpendicular to the cathode, or parallel to the axis). Also, we will show how edge emission affects α, and explain why α cannot be increased beyond a certain level (lower than theory predicts) without mirroring. We will show the difference in results due to use of a thermal beam model, and the inclusion of self-magnetic field. Finally, we will present means of reducing or eliminating edge emission in order to bring velocity spreads down. We think that the control of edge emission in magnetron injection guns and the subsequent reduction in velocity spread may be the key to unlocking the full efficiency potential of various cyclotron resonance devices.

* This work was performed under NRL Contract Number N00014-94-C-2136.

Wednesday Morning, 21 May 1997
10:00 a.m. – Toucan Room

Oral Session 5C:
6 Plasma Diagnostics
Chair: R. J. Leeper

5C01-02 *Invited*

X-ray Lasers for Plasma Diagnostics*

L.B. Da Silva, T.W. Barbee, Jr., R. Cauble, P. Celliers, D.H. Kalantar, R. Snavely, J.E. Trebes, A.S. Wan and F. Weber
Lawrence Livermore National Laboratory,
Livermore, CA 94550

Soft x-ray lasers have evolved from the early demonstration phase to becoming reliable xuv sources. They operate over a wide wavelength range extending from 35 to 400 Å and have output energies as high as 10 mJ in 150 ns pulses. The beam divergence of these lasers is less than 15 mrad and they have a typical linewidth of $\Delta\lambda/\lambda \sim 10^{-4}$ making them the brightest xuv sources available. In this talk I'll describe our use of x-ray lasers to probe high density plasmas using a variety of diagnostic techniques. Taking advantage of recently developed multilayer beamsplitters we have constructed and used a Mach-Zehnder interferometer operating at 155 Å to probe 1-3 mm size laser produced plasmas. We have also used x-ray lasers and a multilayer mirror imaging system to study hydrodynamic imprinting of laser speckle pattern on directly driven thin foils with 1-2 μm spatial resolution. We are now planning a moiré deflectometry to measure the electron density profile in ICF hohlraums. The results of these experiments and the limitations of these techniques will be presented. The prospects for short wavelength (10 Å) x-ray lasers which are better suited to higher density probing will also be discussed.

*Work performed under the auspices of the U.S. Department of Energy by LLNL under contract number W-7405-ENG-48.

5C03

PROTEX: A Proton-Recoil Detector for ICF Fusion Neutrons

Michael J. Moran
Lawrence Livermore National Laboratory
Livermore, CA 94550

Fusion neutron diagnostics are important to Inertial Confinement Fusion (ICF) because they characterize the fusion performance and help to provide the understanding that is needed to develop higher-yield sources. Present yields in excess of 10^{13} (D,T) neutrons can be measured with a proton-recoil detector. This technique, which has not been practical with lower yields, is desirable because it provides prompt, accurate, and unambiguous results. The design that is described in this paper features a compact coaxial cylindrical geometry that optimizes sensitivity and provides in-situ independent recording of background signals. The design also allows for simple adjustments that will make possible consistent measurement of ICF sources as their yields increase to National Ignition Facility levels. At these levels, the proton-recoil technique also will serve as the basis of more detailed studies such as spectral measurements, or perhaps even energy-resolved imaging.

This work was performed under the auspices of the U.S. Department of Energy by the Lawrence Livermore National Laboratory under Contract number W-7405-ENG-48.

5C04

Explosively Driven Blast Shutter for Diagnostic Protection

E.L. Ruden
Phillips Laboratory, High Energy Sources Division, Phillips Laboratory, Kirtland AFB, NM
and D.G. Gale
Maxwell Technologies, Inc., Albuquerque, NM

Phillips Laboratory has developed a fast closing shutter designed to protect diagnostics or other devices from damage due to plasma and solid debris subsequent to exposure to high energy transient events such as PL's solid liner working fluid compression geometry (J.H. Degnan, et al., this conference). The device uses a cartridge brass (alloy C26000) tube with a 0.8 cm diameter biconic orifice which is crimped shut in 15 μs after a 60 μs delay. The crimping is accomplished by the simultaneous impact of two opposing 3 g Titanium slugs each propelled by a Reynolds, Inc. RP1 Electronic Bridge Wire detonator. The crimp forms a high vacuum seal with a leak rate with an established upper bound of 10^{-9} l/s STP air. The assembly is contained by a reusable 14 cm by 14 cm by 5 cm heat treated chrome molybdenum steel casing. The only expendables are the tube, the RP1's, and two 2 g steel disks which buffer the Ti slugs from the RP1's with a total cost of about $400. The slugs themselves appear to be reusable for an, as yet, undetermined number of firings. Refurbishment time is approximately 1 hour. Given the initial tube wall thickness of 1.75 mm, the design should prove useful for applications which require considerable stopping power. Design and performance details, including optical measurements of device's orifice area vs. time during closure, will be presented.

5C05

Spectral Analysis in Lithium Ion Beam Transport Experiments

H.K. Chung, J.J. MacFarlane, P. Wang, G.A. Moses, J.E. Bailey[1], C.L. Olson[1] and D.R. Welch[2]
University of Wisconsin–Madison, Madison, WI

An analysis of visible emission from an argon plasma generated during Li ion beam transport experiments is summarized. High-energy, high current Li ion beams generated in a barrel-type diode have been transported in an argon gas cell and focused towards a target in the center. In the transport region, an argon plasma is formed which provides current and charge neutralization for the ion beam. The argon plasma can be generated by collisions with energetic Li beam ions and plasma electrons. According to PIC code simulations, plasma electrons has Maxwellian energy distribution and energetic component, which is produced by beam ion collisions or by strong local electric fields. Since the ion beam pulse length is on ~20 ns, plasma conditions rapidly change accordingly during beam pulse time. The goal of investigation is to understand the gas ionization dynamics and determine plasma conditions. To characterize the highly transient plasma, visible spectra have been recorded from the gas cell in 3 ns intervals. The line intensities and widths from singly ionized argon (AR II) have been analyzed using a time-dependent collisional-radiative mode. The atomic processes considered are collisional processes by thermal and energetic electrons, and beam ions, and radiative processes. Synthetic spectra calculated from the population densities are compared with the

measured line intensities and widths. The spectral implications for determining the properties of plasma conditions for energetic particles as well as thermal electrons are discussed.

[1]Sandia National Laboratories
[2]Mission Research Corporation

5C06

Infra-Red Absorption Spectroscopy of SiO_x Deposition Plasmas

P. Fayet[a], Ch. Hollenstein[b], C. Courteille[b], A.A. Howling[b], D. Magni[b]
[a] *Tetra Pak (Suisse) SA, Tetra Pak Materials R&D, CH-1680 Romont, Switzerland*
[b] *Centre de Recherche en Physique des Plasmas, EPFL, PPH-Ecublens, 1015 Lausanne, CH-Switzerland*

Plasma deposition of SiO_x is widely used in semi-conductor device technology as an interlayer insulator and is today an emerging technology in the packaging industry to generate new gas and aroma barrier materials. Recently it has been shown that Fourier Transform Infra-Red spectroscopy (FTIR) is a powerful diagnostic for the understanding of deposition plasmas. We applied this technique to SiO_x deposition processes which allowed us to obtain new aspects of the gas behaviour and the powder usually produced in these plasmas. For this purpose we used commercial FTIR equipment to investigate hexa-methyldisiloxane (HMDSO) plasmas in rf capacitively-coupled reactor and for *ex-situ* analysis of the deposited layer on industrial plastic substrates such as Low Density Polyethylene (LDPE). Our results show the influence of various plasma parameters (gas mix, pressure, power, excitation frequency, temperature...) on the gas phase behaviour and the powder created in the plasma. In addition the correlation between spectra obtained in the plasma and spectra from the deposited SiO_x films shall be discussed. These FTIR results are complemented by extensive mass spectrometry, light scattering on the powder and electrical measurements of the reactor.

5C07

Low-Z Impurity Visible Line Radiations in the IR-T1 Tokamak

M. Ghorannevis, M.R. Salami and M. Masnavi
Plasma Physics Research Center of I.A.U.
Poonak, Hesarak, P.O. Box 14835-159, Tehran, Iran

Impurities emitted from the limiter and/or wall by the bombardment of plasma and hot neutral particles play an important role in tokamak discharges. The Spectroscopic measurements of line emission are commonly used to evaluate the concentration, influx rate and power radiated by low-Z impurities. During the ohmic heating discharge, the quasi-stationary profiles of the Carbon (CIII) and Oxygen (OII, OIII) impurity ionization stages in IR-T1 Tokamak (R=45 cm, a=12.4 cm, I_p=20–40. KA, B_t=0.6–0.9 tesla, τ_d=20–25 ms) were determined by monitoring visible line emissions with a single-channel visible (or near ultraviolet) monochromator with 0.6 cm space resolution, in which there is a two-lens image system in front of the spectrometer entrance slit and a multichannel optical fiber attached to its exit slit. The numerical analysis was done by set of coupled continuity equations in cylindrical coordinates with ionization and recombination coefficients given by Lotz semi-emperical formula and by Kramer formula, respectively.

The solar corona model was used to relate the stage densities and line emissivities. We found that the majority of the Oxygen and Carbon ions are He-like ones.

5C08

Singlechannel HCN Laser Interferometer for Electron Density Measurement in the IR-T1 Tokamak

M. Ghorannevis, M. Monfared and A. Anvari
Plasma Physics Research Center of I.A.U.
Poonak, Hesarak, P.O. Box 14835-159, Tehran, Iran

The IR-T1 tokamak is an air-core transformer type with major and minor radii of 45.00 cm and 12.50 cm, respectively. Other major parameters are as follows:

$$I_P = 25 - 40kA,\ n_e = 1.3 \times 10^{13}\ \frac{1}{cm^3},\ V_l = 2.6 - 8v$$
$$Z_{eff} \leq 2,\ T_e = 180 - 250ev,\ B_t = 0.6 - 0.9Tesla$$

Interferometry is a standard technique for measuring the line integrated electron density of magnetically confined plasma. It is based on the fact that an electromagnetic

wave, on its passage through a plasma, experiences a phase change with respect to the reference beam.

A single channel far-infrared (FIR) hydrogen cyanide (HCN) laser interferometer was developed to measure plasma electron density on the IR-T1 tokamak. The structure of the single channel FIR laser interferometer is described. The laser source used in the interferometer was a continuous-wave glow discharge HCN laser with a cavity length of 2 m and power output of about 50 mW at 377 μm. This system we used from a heterodyne laser interferometer.

The heterodyne frequency is 10 kHz produced by a rotating grating the optical signal are received by pyroelectric detectors, and the detection sensitivity is 1/15 fringe with a temporal resolution of 100 μs.

Details will be in the full paper.

5C09

Design and Fabrication of New Version of Langmuir Double Circuit for the IR-T1 Tokamak

A. Abbaspour, M. Ghorannevis, R. Zakeri Khebreh, M.R. Salami and A.M. Bagheri
Plasma Physics Research Center of I.A.U., Poonak, Hesarak, P.O. Box 14835-159, Tehran, Iran

The IR-T1 is an air core transformer type tokamak with no diverter and conducting shell on it. The major parameters are: R=45.00 cm, a=12.50 cm, I_p=20–40 kA, τ_d=20–25 ms, B_t=6.1–9.0 kG, V_{loop}=2.6–8V, n_e=0.7–3.0 x 10^{13} cm^3, T_e=150–250ev, Z_{eff}<2. The relative measurement of electron temperature and density, was done by a set of asymmetric Langmuir double probe. This probe can be operated in a relatively small voltage region, provides sufficient information about the plasma edge parameters, and therefore there is no need for a direct measurement of the ion saturation current which is about a few milliampere. The reduction of applied voltage should greatly simplify the operation of the double probe and will eliminate unwanted induced electric fields in small tokamak devices. For this reason we had to design a set of collectors so that the sheath surface area be large enough to consider it as a plasma. The probe power supply was designed and completed at this research institute.

Details will be discussed in full paper.

Wednesday Morning, 21 May 1997
10:00 a.m. – Macaw Room

Oral Session 5D:
5.3 Plasma for Lighting
Chair: T. J. Sommerer

5D01-02 *Invited*

FEM-Simulation of High Pressure Discharge Lamps: Examples for Modelling of Cathode Regions and of 3-D Convective Flow

M. Neiger and H. Wiesmann
Lighting Technology Institute, University of Karlsruhe/FRG

Lamps with high radiance or high luminance are getting increasing importance for projection applications, fiber based light distribution, or photolithographic applications. Such lamps must have short arcs of a few millimeters only and very high operating pressure of the lamp filling (mostly Xe, Hg, p ≅ 5 bar, without or with dopants). Such lamps are usually operated with d.c. current, even if dopants are present. Because of the short electrode distance, electrode regions and arc column can no longer be clearly distinguished. The high operating pressures lead to strong convective flow within the lamp bulb, which creates strong local thermal loading of the quartz wall. Because of these problems, design and construction of such lamps require a good understanding of plasma regions close to the electrodes and of 3-dimensional convective flow patterns. The paper will address both topics. A new approach for modelling both the LTE-plasma between the electrodes and the non-LTE–region very close to the cathode with a single set of equations will be presented and FEM-results for 2-D, non-cylindrical lamp geometries will be discussed. 3-D convective plasma flow modelling results for different lamp pressures and lamp operating positions will also be presented.

5D03

GEOMETRICAL DIFFERENCES OF ISOTHERMS IN CONVECTIVE HIGH INTENSITY DISCHARGE LAMPS

Miguel Galvez
OSRAM Sylvania Inc, Lighting Research Center
Beverly, MA 01915

It is known that convective effects in High Intensity Discharge (HID) Lamps play a significant role by transporting heat from the arc plasma core towards the arc tube walls. The effects of convection in a vertically operated HID lamp are studied via computer simulations and the results are presented.

The governing equations, in the simulations, are the Navier-Stokes equations and Poisson's equation; the latter allows for a volumetric Joule heating that is included in the energy equation. The transport coefficients of the gas are assumed to be those of a Hg and Ar mixture in an isobaric system. Radiation transport was not included in the simulations.

The effects of convection on isothermal and isospeed surfaces at different locations within the gas are presented. The behavior of such isosurfaces with increasing arc tube diameter is also included.

5D04

Laser-Induced Fluorescence Technique for Measuring Damage to a Fluorescent Lamp Electrode

Yunfen Ji, Gerald Korenowski and Robert Davis
Rensselaer Polytechnic Institute, Troy, NY 12180

The proliferation of solid-state electronic ballasts for fluorescent lamps has led to many different starting and operating scenarios for these lamps. Because these scenarios often differ from those described in relevant ANSI standards, the effects on the operating lives of lamps is not known. This paper describes a pilot study that used a laser-induced fluorescence (LIF) technique to directly measure the rate of barium loss from a fluorescent lamp electrode under a variety of starting and operating parameters. The experimental results are provided and the potential applications of the technique for commercial lighting products are discussed.

5D05

Modeling and Measuring the Rate of Cooling of a Fluorescent Lamp Electrode

Robert Davis, Yunfen Ji
Rensselaer Polytechnic Institute, Troy, NY 12180
Philip Moskowitz
OSRAM Sylvania Inc., Beverly, MA

Rapid-cycle testing of fluorescent lamps has become a common practice as a way to accelerate the collection of lamp life data. However, the relationship of rapid-cycle data to standard life data is unknown, due to the dynamic thermal properties of the lamp electrodes immediately after the lamp is extinguished. This paper describes both a simple theoretical model of the electrode cooling process and empirical results of a experiment that measured electrode resistance during the cool-down period. Agreement between the model and the measured data was good. Results can inform recommendations for suitable cycle times for rapid-cycle testing.

5D06-07 *Invited*

Radiometric Efficiency of Barium Discharge Plasmas*

Heidi M. Anderson, J. MacDonagh-Dumler
and J.E. Lawler
University of Wisconsin-Madison, Madison, WI

Barium has a number of characteristics that indicate it may be a good atomic radiator in a glow discharge. 1) At practical operating temperatures Barium has a vapor pressure in the mTorr range (3 mT at 840 K). 2) The excitation energy of the primary radiating level in Barium is less than half of the ionization energy. 3) The wavelength of the resonance transition is suitable for direct use as a visible light source. At 553 nm, this radiation lies at the peak of the eye sensitivity curve. For these reasons, a Barium glow discharge may prove to be of interest to the Lighting Industry for use in a novel, efficient white light source. Progress in experimental determination of the radiometric efficiency of a dc glow discharge in Barium and progress in a modeling study of the radiometric efficiency of a Barium glow discharge will be reported.

*Supported by the NSF.

Wednesday Morning, 19 May 1997
10:00 a.m. – Cockatoo Room

Oral Session 5E:
4.2 Inertial Confinement Fusion
Chair: J. Hammer

5E01

Plasma Pockels Cell Based Optical Switch for the National Ignition Facility*

Mark A. Rhodes, Scott Fochs, C. D. Boley
Lawrence Livermore National Laboratory, Livermore, CA 94550

The National Ignition Facility (NIF), now under construction at Lawrence Livermore National Laboratory, is based on a multi-pass power amplifier. A key component in this laser design is an optical switch that closes to trap the optical pulse in the cavity for four gain passes and then opens to divert the optical pulse out of the amplifier cavity. The switch is comprised of a Pockels cell and a polarizer and is unique because it handles a beam that is 40 cm x 40 cm square and allows close beam packing in four 4x12 clusters for a total of 192 beams. Conventional Pockels cells do not scale to such large apertures or the square shape required for close packing. Our switch is based on a Plasma-Electrode Pockels Cell (PEPC).

In a PEPC, low-pressure helium discharges (1-2 kA) are formed on both sides of a thin slab of electro-optic material (typically KDP). These discharges form highly conductive, transparent sheets which allow uniform application of a high-voltage pulse (17 kV) across the crystal. A 37 cm x 37 cm PEPC has been in routine operation for two years on the 6 kJ Beamlet laser at LLNL. For the NIF, a module four apertures high by one wide (4x1) is required. However, this 4x1 mechanical module will be comprised electrically of a pair of 2x1 sub-modules.

Recently, we demonstrated full operation of a prototype 2x1 PEPC. In this PEPC, the plasma spans two KDP crystals. A major advance in the 2x1 PEPC over the Beamlet PEPEC is the use of anodized aluminum construction which provides sufficient insulation to allow formation of the planar plasmas.

In this paper, we present here many interesting design details and experimental results which include observation of plasma and discharge effects which can degrade plasma uniformity including MHD plasma displacement from external return currents, current channel formation, and the effect of housing bias potential.

*This work was performed under the auspices of the US Department of Energy by Lawrence Livermore National Laboratory under the contract number W-7405-EN-48.

5E02

Explosion Instability in the Thermal Expansion of a Thin-Walled Cylinder in Ultra-High Magnetic Field

G.A. Shneerson
State Technical University, St. Petersburg, Russia

Thermal expansion of a thin-walled cylinder in fast Joule heating enables to obtain high wall velocity (up to 10000 m/s) without its evaporation. In strong longitudinal magnetic field the heating by azimuthal current has the decisive role. The process then follows the succeeding line: with the wall velocity increase the induced in it azimuthal current and Joule heating power grow. This, in its turn, results in the wall acceleration due to its thermal expansion. So, the self-excitation process of the azimuthal current and sharp acceleration of the wall are possible. The calculations described in the report are made in the assumption of constant induction B_o at the outer cylinder wall. They show that the process has the character of explosion instability: azimuthal current sharply increases in finite time near certain time instant t_1:

$$I_\varphi = [(6h\gamma R_0)/(\Gamma_0 B_0)](t_1 - t)^{-2}.$$

The wall velocity follows the same law. This effect is observed for the liquid metal shell in spite of the action of electromagnetic braking forces. It is characteristic that the heating and acceleration of the shell consume the energy of the external field. The wall acceleration is possible also for a solid wall, if induction has the order of 100 T or more.

5E03

Progress with Developing a Target for Magnetized Target Fusion

F.J. Wysocki, B.E. Chrien, G. Idzorek, H. Oona, D.O. Whiteson, R.C. Kirkpatrick, I.R. Lindemuth and P.T. Sheehey
Los Alamos National Laboratory, Los Alamos, NM 87545

Magnetized Target Fusion (MTF) is an approach to fusion where a preheated and magnetized plasma is adiabatically compressed to fusion conditions.[1,2] Successful MTF requires a suitable initial target plasma with an embedded magnetic field of at least 5 T in a **closed-field-line** topology, a density of roughly 10^{18} cm^{-3}, a temperature of at least 50 eV, and must be free of impurities which would raise radiation losses. Target plasma generation experiments are underway at Los Alamos National Laboratory using the Colt facility; a 0.25 MJ, 2-3μs rise-time capacitor bank. In the first experiments, a Z-pinch is produced in a 2 cm radius by 2 cm high conducting wall using a static gas-fill of hydrogen or deuterium gas in the range of 0.5 to 2 torr. Follow-on experiments will use a frozen deuterium fiber along the axis[3] (without a gas-fill). The diagnostics include B-dot probes, framing camera, gated OMA visible spectrometer, time-resolved monochrometer, silicon photodiodes, neutron yield, and plasma-density interferometer. Operation to date has been with drive currents ranging from 0.8 MA to 1.9 MA. Optical diagnostics show that the plasma produced in the containment region lasts roughly 20 to 30μs, and the B-dot probes show a broad current-profile in the containment region. The experimental design and data will be presented.

[1] I.R. Lindemuth and R.C.Kirkpatrick, *Nuclear Fusion* **23**, 263 (1983).

[2] R.C. Kirkpatrick, I.R. Lindemuth, and M.S. Ward, *Fusion Technology* **27**, 201 (1995).

[3] P.T. Sheehey *et al., Physics of Fluids B* **4**, 3698 (1992).

Wednesday Morning, 21 May 1997
10:00 a.m. – Cockatoo Room

Oral Session 5E:
4.3 Magnetic Confinement Fusion
Chair: C. Ordonez

5E04-05 *Invited*

Plasma Confinement Within a Solenoidal Magnetic Field Using Nested Electric Potential Wells

C.A. Ordonez and D.D. Dolliver
Department of Physics, University of North Texas, Denton, Texas 76203-0368

Confinement of ions and electrons in two regions of space which overlap has recently been achieved using a solenoidal magnetic field for radial confinement and externally produced electric fields for axial confinement. Two methods were used. One method relied on using time-dependent (Paul- type) fields for axial confinement of electrons and static (Penning-type) fields for axial confinement of ions. [J. Walz, S.B. Ross, C. Zimmermann, L. Ricci, M. Prevedelli, and T.W. Hansch, Phys. Rev. Lett. **75**, 3257 (1995).] The other method relied on using a Penning/Malmberg type plasma trap to produce a nested pair of oppositely-signed electric potential wells. [D.S. Hall and G. Gabrielse, Phys. Rev. Lett. **77**, 1962 (1996).] A third method is presented which relies on a time dependent nested-well potential profile. This third method is predicted to be suitable for confining a neutral region of plasma comprised of electrons and equal-temperature, singly-charge ions with the ion density exceeding the Brillouin ion-density limit. [C.A. Ordonez, IEEE Trans. on Plasma Sci. **24** 1378 (1996).] This is an intriguing possibility because of the excellent plasma confinement properties such an approach represents. With good plasma confinement, the approach should be suitable for use in semiconductor processing, for basic plasma studies, and as a new magnetic confinement approach to fusion energy production.

This work was supported by the National Science Foundation under Grant No. ECS-9627612.

5E06

Stability of Transport Barrier in Negative Shear Tokamak Discharge

A. Hirose and M. Elia
Plasma Physics Laboratory, University of Saskatchewan Saskatoon, Saskatchewan S7N 5E2, Canada
M. Yamagiwa and Y. Kishimoto
Naka Fusion Research Establishment, JAERI Naka, Ibaraki, Japan

The inner transport barrier (ITB) in tokamaks is characterized by steep density and temperature gradients and thus large ballooning parameter α. In the JT-60U tokamak operated in negative shear [1], improved confinement has been achieved with clear formation of ITB having $\alpha \simeq 3$. The ideal ballooning mode is known to be stable if shear is negative. However, as shown recently [2], an ion temperature gradient driven kinetic ballooning mode, which has characteristics similar to the mode identified in the MHD second stability regime with positive shear [3], may still persist. Also, the well known finite β stabilization of the predominantly electrostatic ion temperature gradient (ITG) mode found for positive shear may not be operative when shear is negative. The analysis is based on a kinetic shooting code [3] in which ions and trapped electrons are treated fully kinetically and ion transit effects perturbatively. For ITB parameters similar to those in JT-60U, long wavelength kinetic ballooning and ITG modes have been found to be stable. Large ballooning parameter and steep density gradient are effective stabilizing factors. However, a trapped electron driven drift type mode exists in relatively short wavelength region. Since ions do not resonate with a drift type mode, the mode is not expected to enhance the ion thermal diffusivity. The electron thermal diffusivity should be at the Ohmic level since the drift type mode prevails commonly in various tokamak discharge modes.

*Sponsored in part by NSERC, Canada.

[1] H. Kimura and JT-60 Team, Phys. Plasmas **3,** 1943 (1996).

[2] A. Hirose and M. Elia, Phys. Rev. Lett. **76,** 628 (1996).

[3] A. Hirose, L. Zhang, and M. Elia, Phys. Rev. Lett. **72,** 3559 (1994); Phys. Plasmas **2,** 859 (1995).

5E07

Melt-Layer Erosion Experiments for Electric Launchers and Tokamak Fusion Reactors

G.E. Dale and M.A. Bourham
Department of Nuclear Engineering, North Carolina State University, Raleigh, NC 27695-7909

Melt-layer erosion is a major concern in electric launchers and fusion reactors, where components are exposed to high heat fluxes produced during transient plasma events. Melt-layer erosion is currently under investigation at NCSU. Samples are exposed to plasma formed by the electrothermal plasma generator PIPE.[1,2]. Sample materials currently under consideration are 306SS, OFHC Cu, and Al. The cylindrical samples are 4.8 mm in diameter and 25.4 mm long. The samples are exposed at one end, 6.35 mm from the barrel of the source. Following exposure, the samples are bisected along the axial direction, polished, and etched for electron microscopy. Scanning Electron Microscopy (SEM) is used to determine the thickness of the re-solidified material retained on the surface, as well as micro-structural changes with the sample. Results are compared to current computer models of the phenomena [3]. Current results are discussed.

Work supported by the US Army Research Office Contract DAAH04-95-1-0214 and the US Office of Naval Research Contract N00014-95-1-1221.

[1] M.A. Bourham and J.G. Gilligan, "Erosion of Plasma-Facing Components Under Simulated Disruption-Like Conditions Using an Electrothermal Plasma Gun", Fusion Technol., **26**, 517, November 1994.

[2] M.A. Bourham, J.G. Gilligan, M.L. Huebschman, D. Lanos and P.D. Aalto, "review of Component Erosion in Electric Launcher Technology", IEEE Trans. Magnetics, **31**, 678, January 1995.

[3] A. Hassanein, "Erosion of Melt Layer Developed During a Plasma Disruption", 18th Symposium on Fusion Technology, Karlsruhe, Germany, 22-26 August 1994.

5E08

Control of Divertor Heat Flux by Radiative Divertor Operation in DIII-D

C.J. Lasnier
Lawrence Livermore National Laboratory, Livermore, CA 94550

The DIII-D tokamak divertor program is focused on obtaining the physics understanding of the divertor and scrape-off layer plasma required for leaning how to control divertor energy and particle flux in future large tokamaks such as ITER. We have made significant progress, reducing peak divertor heat flux by a factor of 5. This is done using deuterium or impurity gas puffing, which increases divertor density and radiative loss. Thomson Scattering measurements in 2-D have shown that the electron temperature is reduced from more than 100 eV at the upstream separatrix to less the 1 eV near the divertor plate. We are now correlating this and simultaneous data from an extensive diagnostic set including fixed and fast-plunging Langmuir probes, VUV spectrometers, bolometers, visible-light TV cameras, and infrared cameras, with predictions from a 2D fluid code. In this low-temperature regime, atomic and molecular physics must now be added to improve our understanding, In addition, we are working toward independent control of core and divertor plasma.

5E09

Engineering Aspects and Basic Parameters of the IR-T1 Tokamak

M. Ghorennevis, M.R. Salami, M. Masnavi, J. Mirzaie, M. Zamani Mehr, A.K. Tafreshi, and M. Bakhtiari
Plasma Physics Research Center of I.A.U. Poonak, Hesarak, P.O. Box 14835-159, Tehran, Iran

The IR-T1 tokamak is an air core transfer type, with no divertor and conductive shell on it. Its area, height, and weight are 1.6 m^2, 2.5 m, and 2.7 tons, respectively. IR-T1 tokamak (R=45.00 cm, a=12.50 cm, I_p=20–40 kA, τ_d=20–25 ms, B_t=6.1–9.0 kG, V_{loop}=2.6–8V, n_e=0.7–3.0 x 10^{13} cm^3, T_e=150–250ev, Z_{eff}<2) consists of four major systems (1. Vacuum chamber, 2. Toroidal, 3. Ohmic Heating, and 4. Vertical Magnetic Field coils). This tokamak was established to concentrate mainly on plasma confinement, MHD behavior and control of instabilities. Fundamental diagnostic systems such as ECE, visible spectrometer, soft X-ray, and electromagnetic measurement system are used. The magnetic measurement system which include; 10 Rogowsky coils, 8 loop lines, 2 sine saddle coils, 2 cos coils, 2 circuit units, 1 diamagnetic flux coil, 1 concentric coil, and 1 circuit unit, are used to measure the plasma current, loop voltage, horizontal and vertical displacement, and diamagnetic respectively. To measure the magnetic fluctuation of plasma column and to investigate the different aspects of MHD modes and high frequency fluctuations, two sets of Mirnov coils and ℓ=2/n-1 and ℓ=3/n-1 helical magnetic windings have been installed.

5E10

Beta-Limiting in the IR-T1 Tokamak

M. Ghorannevis, M. Masnavi and D. Doranian
Plasma Physics Research Center of I.A.U., P.O. Box 14835-159, Tehran, Iran

An experimental investigation has been carried out on the β-limiting phenomena in the IR-T1 plasma during ohmic heating discharges. The IR-T1 is a small air-core transformer tokamak without conducting shell and divertor: (R=0.45m; a=0.125m; Bϕ<1T; I_p≈35kA; Te(0)= 230ev; Z_{eff}<2.2; q(a)>2). One goal was the determination of the maximum achievable value of β_m (Troyon limit) as a function of q(a), in steady state operation. Another goal of this paper is a detailed study of the MHD phenomena giving rise to the observed β_m-limit. In particular, we studied the hard disruptive instability occurring in the IR-T1 plasma under a range of reproducible conditions, for 3>q(a)>2. We use Soft x-ray, ECE, a Visible Spectrometer and Mirnov diagnostic systems to infer the structure of the MHD modes at the $\beta_m \approx 1.8\%$. It is found that the maximum β_m is limited by the occurrence of a coupled (m/n=3/2) and (m/n=2/1) modes.

5E11

On the Reconstruction of Nonlocal Heat Transport Parameters from Observed Phenomena of the Fast Non-Diffusive Transport in a Tokamak

A.B. Kukushkin
INF RRC "Kurchatov Institute", Moscow 123182 Russia

A physics model[1] for the nonlocal heat transport by a long mean-free-path plasma waves – of the order and much larger than plasma characteristic size – and the respective formalism[2] of an integral equation, in space variables, are shown to provide universal explanation of major features of recently observed phenomena of the fast non-diffusive heat transport in a tokamak, which being interpreted in formalisms of diffusion-like, differential equations give instant jumps of thermal diffusivities in a large part of plasma volume.

The inverse problem is formulated for reconstructing the parameters of nonlocal component of anomalous cross-field energy transport, and the results of numerical modeling are presented for initial stage of the following phenomena: (i) net inward flux of energy during off-axis heating; (ii) prompt rise/drop of electron temperature in the core in experiments on fast cooling/heating of the periphery; (iii) fast "volumetric" response of energy transport to plasma edge behavior during L-H transitions.

[1] Kukushkin A.B., Proc. 14th IAEA Conf. on Plasma Phys. Contr. Fusion, Wuerzburg, 1992, v.2, p.35; JETP Lett. **56** (1992)487; Proc. 20th EPS Conf., Lisbon, 1993, p.IV-1391.

[2] Kukushkin A.B., Mat. 4th ITER Database and Modell. Expert Group Workshop, Moscow, April 1996; 38th Ann. Meeting APS-DPP96, Bull.Am. Phys.Soc., Nov.1996, **41**, No.7, 6F11.

Wednesday Morning, 21 May 1997
10:00 a.m. – Rousseau Center

Poster Session 5P01-15:
2.1 Intense Beam Microwaves

5P01

Polarization Control in High Power Microwaves from a Rectangular Cross Section Gyrotron*

J.M. Hochman[#], R.M. Gilgenbach, R.J. Jaynes, J.I. Rintamaki[a], Y.Y. Lau and T.A. Spencer[+]
Intense Energy Beam Interaction Laboratory, Nuclear Engineering and Radiological Sciences Dept., University of Michigan, Ann Arbor, MI 48109-2104

We summarize the results of experiments on a gyrotron utilizing rectangular-cross–section (RCS) interaction cavities. Current issues under investigation include polarization control as a function of magnetic field, power versus pulselength of microwave emission, and mode competition. The electron beam driver producing an annular beam is the Michigan Electron Long Beam Accelerator (MELBA) at parameters: V=-0.7 to -1.0 MV, I_{diode}=1–10 kA, I_{tube}=0.1–3 kA, and $\tau_{e\text{-}beam}$=0.4–1.0 μs. The annular e-beam is spun up into an axis-encircling beam by passing it through a magnetic cusp prior to entering the RCS interaction cavity. Initial experimental results show a high degree of polarization [$P(TE_{10})/P(TE_{01})$=30 or 1/30] as a function of cavity fields. Megawatt microwave output shifts from the fundamental mode, which dominates the next order mode by an order of magnitude, to the next order mode as the field is raised from 1.4 to 1.7 kGauss. Frequency measurements using microstrip bandpass filters and a superheterodyne mixer support this result as well as MAGIC simulations. MAGIC code simulations using various magnetic fields will be presented as well as results utilizing the E-gun code.

*Research supported by the Air Force Office of Scientific Research, Multidisciplinary University Research Initiative (MURI) through Texas Tech University contract, Phillips Lab, Northrop Grumman Corp., and the AFOSR-sponsored MAGIC Code User's Group, administered by Mission Research Corp.

[#] AFOSR Augmentation Award for Science and Eng Research Training

[a] DoE MFET Graduate Fellowship

[+] Permanent Address: Air Force Phillips Lab, PL/WSR, Kirtland AFB, NM 87117-5776

5P02

Diagnostic Experiments to Measure Frequency and Alpha for Rectangular Cross Section Gyrotrons*

R.L. Jaynes, R.M. Gilgenbach, J. M. Hochman+, J.J. Rintamaki#, Y.Y. Lau and T.A. Spencer**
Intense Energy Beam Interaction Laboratory Depart,emt of Nuclear Engineering and Radiological Sciences, University of Michigan, Ann Arbor, MI 48109-2104

Comparisons of microwave frequency and electron beam alpha (Vperp/Vparallel) measurements to gyrotron dispersion relations are investigated. Alpha measurements are obtained by measuring radiation darkening patterns of glass plates. Frequencies are determined to within 500 MHz using microstrip microwave frequency filters. More accurate frequency measurements are taken using heterodyne detection. Frequency and alpha measurements are essential for determining the mode of operation of the rectangular cross section (RCS) gyrotron. The RCS gyrotron can be operated from 2-4 GHz in either the TE10 and TE01 modes. The relativistic electron beam is generated by MELBA (Michigan Electron Long Beam Accelerator) with the following operating parameters: -800kV, 1-10kA diode current, 0.2-0.5 kA tube current, 0.5-1.0 μs pulselength.

*Research supported by the Air Force Office of Scientific Research Multidisciplinary University Research Initiative (MURI) through Texas Tech University, Phillips Lab, and the AFOSR-sponsored MAGIC Code User's Group, administered by Mission Research Corp. Support from Northrop Grumman Corp. is also acknowledged.

+ AASERT support from AFOSR

DoE MFET Graduate Fellow

**Permanent Address: Phillips Lab, Kirtland AFB, NM

5P03

High Efficiency X-band TWT Amplifiers*

S. Naqvi, G.S. Kerslick, J.A. Nation and Q. Wang
Cornell University, Ithaca, NY 14850

We report on a research program to increase the efficiency of relativistic traveling wave amplifiers to >50%. The two stage amplifier consists of a bunching periodic structure with phase velocity and a decelerating section with phase velocity significantly lower than the beam velocity. The position of the decelerating stage with respect to the bunching stage is chosen such that the narrowest bunches are sustained in the decelerating field for the longest possible time before significant debunching occurs. Two schemes are under investigation. In the first scheme, a resistive sever is placed between the two stages to suppress temporal phenomena. In the second scheme, the bunching and decelerating stages merge into each other by a gradual change in the iris radius over a wavelength. An absorbing section in this case is placed before the start of the bunching stage. A Coaxial extraction [1] geometry is used in both schemes. Efficiencies obtained form MAGIC simulations are comparable to those obtained in high efficiency klystrons (50-50%) but carry the important advantage of broad-bandwidth, low sensitivity on dimensions, low surface fields, and simplicity of design.

*Work supported by USDOE & AFOSR MURI High Power Microwave Program.

[1] *Appl. Phys. Lett.* **69**, 1550 (1996).

5P04

Diode Polarity Experiments on a Coaxial Vircator*

Kevin Woolverton, M. Kristiansen and L.L. Hatfield
Pulsed Power Laboratory, Departments of Electrical Engineering and Physics, Texas Tech University, P.O. Box 43102, Lubbock, TX 79409-3102

A study on the interaction dynamics of a positively and negatively pulsed coaxial vircator is being performed at Texas Tech University. MAGIC, a 2.5D particle-in-cell code, is used to simulate the different geometries. The simulations performed indicate an increase in efficiency by approximately a factor of 2 for the negatively pulsed system compared to the positively pulsed system. Simulations are also performed to better understand the influencing factors of the systems.

This paper describes the experimental results which are performed on a coaxial vircator with diode voltages ranging from 400-500 kV at diode currents of 40-50 kA with pulse durations of~50 nsec. Results that are given include microwave power, efficiency, spectral content and a possible explanation for the results.

This work is supported by AFOSR (MURI).

5P05

Analytic Investigation of the Transit-Time Instability Including Intense Space Charge Effects

J.W. Luginsland[1], M.J. Arman and Y.Y. Lau[2]
USAF Phillips Laboratory
High Energy Sources Division
Kirtland AFB, NM 87117-5776

A circuit model is used to investigate the Transit-Time Instability (TTI). Although it has been known since the 1930's, recent efforts to develop a High-Power Microwave (HPM) source using the TTI have focused on using modern pulsed-power technology to create high current (10's of kAmp) beams to drive the source. It is well known that the space charge associated with intense beams can severely complicate the analysis of HPM devices. This circuit model clarifies the role of space charge in the transit-time instability. Application of the model to the Radial Acceletron, currently being investigated at Phillips Laboratory, yields an analytic expression of the starting condition for microwave oscillations. Numerical solution of the governing equations gives growth rates, saturation levels, and elucidates the saturation mechanism in the presence of space charge. These results are consistent with full Particle-in-Cell simulations of the device.[3].

---

1. Work supported as a National Research Council Research Associate.

2. With the University of Michigan, Dept. of Nuclear Engineering and Radiological Sciences, Ann Arbor, MI 48109-2104

3. M. J. Arman, IEEE Trans-PS, **24**, 964 (1996).

5P06

Relativistic BWO With Resonant Reflector

S.D. Korovin, I.K. Kurkan, I.V. Pegel, V.V. Rostov and E. M. Totmeninov
High Current Electronics Institute, Tomsk, Russia

The paper presents the theoretical and experimental studies of an X-band BWO having the electrodynamic system with a resonant reflector which serves for reflection of backward wave and output of microwave power towards the collector edge of the tube. As in the majority of relativistic BWO's, the lowest axisymmetric TM-wave of circular waveguide is used as the operating wave. However, instead of the traditional beyond cutoff-neck (having the diameter ~0.7λ), a short resonant cavity - a circular slot - is used as a reflector. The low-Q oscillation is formed by the <<locked>> wave TM_{02} and therefore the minimum diameter of the system can rise up to ~1.5 λ. The diffractive losses due to transformation into running wave TM_{01} exceed significantly (by several orders) the conductive losses in the cavity. Thus, the reflection of TM_{01} wave at resonance frequency is closed to unit. The value of Q-factor is chosen from the requirement that the band of reflector sufficiently overlaps the generation spectrum of BWO. The longitudinal electric field in the reflector region even for a low value of cavity Q-factor significantly exceeds the amplitude of the synchronous spatial harmonic of the corrugated slow wave structure. Therefore, the reflector serves simultaneously as a short modulating gap which facilitates the selection of waves by their transversal structure. Appropriate location of reflector provides the decrease of start current and the favorable phase of electron beam modulation.

The results of 2.5D time-dependent PIC-simulation using KARAT [1] code indicated that the efficiency of generation ~26% is available. Experiments are planned to conduct within a pulse-repetitive regime of electron accelerator, with the use of a DC magnetic system. We expect that the increase of SWS cross-section makes it possible to raise the power and duration of generated microwave pulses.

[1] V.P. Tarakanov User's Manual for Code KARAT. - Springfield, VA: BRA. - 1992.

5P07

PIC SIMULATIONS OF THE MICROPULSED ELECTRON GUN (MPG)

W. Peter and F. Mako
FM Technologies, Inc., Fairfax, VA 22032

We have developed a surface physics package which has been introduced into the 2-1/2D particle-in-cell code OOPIC [1] in order to model the MPG, a novel electron gun based on electron multipacting [2]. The simulations are in cylindrical geometry, and can include electromagnetic effects such as cavity loading. The object-oriented nature of OOPIC was particularly suitable for the code development and computational modeling of the device. Scaling of current density vs. frequency, and other characteristic parameters of the gun, will be presented. Comparisons of the numerical results with a 2-1/2D Cartesian code FMTSEC, and with experimental data

showing the device performance, will be presented. The MPG can provide up to 10 kA/cm^2 of current with pulse lengths of 1-100 ps. It has been demonstrated to operate for at least 2.5 x 10^{13} pulses, or approximately 25,000 Coulombs, and is still continuing to operate. Applications include microwave generation and accelerator injection.

[1] J.P. Verboncoeur, A.B. Langdon, and N.T. Gladd, J. Comp. Phys. **87**, 199 (1995).

[2] F. Mako and W. Peter, "A high-current micro-pulse electron gun", in *Proc. of the 1993 Particle Accelerator Conference,* Washington, D.C., (IEEE, New York, 1993), p. 2702 (patent pending).

5P08

RF Breakdown Experiments at SLAC

G. Scheitrum, R. Fowkes and X. Xu
Stanford Linear Accelerator Center, Menlo Park, CA
L. Laurent
University of California at Davis, Davis, CA

The Next Linear Collider (NLC) design that is currently being developed at Stanford Linear Accelerator Center (SLAC) requires the X-band RF structures to support significant RF electric fields. The klystron RF sources for the NLC require lower E fields but also have lower breakdown thresholds.

The goals of the program are to improve RF breakdown thresholds, to identify the cause of the lower breakdown thresholds in klystron cavities vs accelerator cavities, and to develop a set of protocols for manufacturing that will yield the highest breakdown levels for all NLC components.

SLAC's X-band resonant ring is being used to test a series of RF breakdown cavities. Early tests were performed on a series of TM_{010} cavities. A new TM_{020} cavity has been designed with demountable noses that will allow accurate, pre and post breakdown evaluation of the high field surfaces. A gated CCD camera and X-ray scintillator will image the breakdown surfaces through a tungsten pinhole in the outer wall of the cavity. The removable noses will allow SLAC to evaluate a variety of materials, processes, and coatings to determine both the best breakdown threshold and the relative amount of damage due to a breakdown event.

In parallel with the breakdown tests, the RF component manufacturing processes are being examined to determine their effects on the potential emission sites that trigger RF breakdown.

Major funding for this program is provided by the AFOSR MURI program, the facilities, equipment and additional funding are provided by DOE.

5P09

Streak Observation of Air Breakdown Triggered by a High-Power Pulsed Microwave

M. Yatsuzuka, M. Okamoto, M. Tanigawa
and S. Nobuhara
Himeji Institute of Technology,
Himeji, Hyogo 671-22, Japan

The high-power microwave with the peak power of 20 MW, frequency of 12 GHz and pulse duration of 14 ns, which is produced by a virtual cathode oscillation, is irradiated to a discharge electrode in a stainless steel vacuum vessel. A DC voltage less than a gap-breakdown voltage is applied to the discharge electrode consisted of a pair of needle and plane electrodes. The gap separation is 1.7 cm. Time and spatial evolutions of breakdown luminosity are observed by a high-speed image converter camera.

Microwave induced breakdowns occur at the pressure range less than 760 Torr for negative polarity and less than 600 Torr for positive polarity. An injection of microwave at first leads to local luminescence at several spots between the gap. Each luminescence grows mainly toward the positive electrode. When these luminescences link together, the air breakdown occurs to grow suddenly the discharge current between the gaps.

5P10

Numerical Simulation of 1.5 GHz Vircator

S.D. Korovin, I.V. Pegel, S.D. Polevin
and V. P. Tarakanov*
High Current Electronics Institute, Tomsk, Russia
**High Temperatures Institute, Moscow, Russia*

On the base of fully electromagnetic 3D computer simulation using KARAT code, an oscillator was designed

to operate at 1.5 GHz. The device possesses the features of both the vircator and the split-cavity oscillator. The construction uses rectangular waveguides and includes the main running-wave cavity, the modulating cavity, a feedback loop, and the coaxial diode with explosive emission. No external magnetic field is used. The operating wave is TE_{10}, with possible further conversion into a Gaussian beam. The simulated efficiency of the vircator is ~10%. The device is resonant, the time of generation establishment is 15-18 ns. The microwave power is ~500 MW at a beam current of ~9 kA and diode voltage of ~600 kV. The oscillator is efficient in a relatively wide range of beam powers. Optimizations of various parameters of the generator were made in the simulation.

Experimental studies of the vircator are planned to conduct using the high current repetitively-pulsed electron accelerator SINUS-7 built at HCEI. The maximum parameters of the accelerator are: electron energy 2 MeV and beam current 20 kA in single-pulse regime and 1.5 MeV and 15 kA at 100 p.p.s. repetition rate. The beam pulse duration is 45 ns.

5P11

Study of Microwave Frequency Radiated from a Vircator

M. Yatsuzuka, M. Tanigawa, S. Nobuhara, D. Young[a] and O. Ishihara[a]
Department of Electrical Engineering, Himeji Institute of Technology, Hyogo 671-22, Japan
[a]Department of Electrical Engineering, Texas Tech University, Lubbock, Texas 79409-3102

Microwave frequency radiated from a virtual cathode oscillator (vircator) is studied experimentally. The vircator diode consists of an annular cathode of diameter of 2.0 – 3.5 cm and 1 mm in thickness and an aluminum foil anode of 15 μm in thickness. The emitted microwaves were extracted axially through a circular waveguide with a diameter of 4.5 cm and a length of 1 m, and radiated outward through a circular horn attached to the waveguide. The radiated microwave signals were picked up by an open-end rectangular waveguide antenna (WRJ-10) at the position of 1 m from the circular horn. The microwave frequency was then determined from the propagation time of the signals in a line of 105-m waveguide.

The cross-section of a pinched electron beam on the anode was measured by an X-ray pinhole camera. The beam plasma frequency was determined by the measured cross-section and the beam current at the downstream of 1 mm from the anode. The observed frequency is slightly higher than the beam plasma frequency and in good agreement with the oscillation frequency driven by reflecting electrons between real and virtual cathodes.

5P12

Effects of Plasma Filling on Microwave Emission in a BWO with Non-Uniform Slow Wave Structure*

Douglas Young and Osamu Ishihara
Texas Tech University, Lubbock, TX 79409-41051
C. Grabowski, J. Gahl and E. Schamiloglu
University of New Mexico, Albuquerque, NM

In a Backward Wave Oscillator (BWO), an electron beam flowing in a waveguide interacts with a ripple in the waveguide wall, known as a slow wave structure (SWS), to produce high power microwaves. The introduction of either a non-uniform ripple or plasma filling in the waveguide has been shown to increase the output power of the BWO. The effect of a non-uniform ripple and plasma filling is studied using the computer code MAGIC. For a BWO with a non-uniform SWS geometry similar to that used in experiments at UNM, the effects of plasma density, plasma radius, and the amount of plasma filling on microwave emission are being simulated. Preliminary results suggest that higher power is produced only with a plasma density less than the electron beam density. In addition, our MAGIC simulations are testing the prediction made by an analytical study[1] which suggests that higher output power will be generated with a plasma concentrated within a small radius and an annular electron beam flowing at a larger radius close to the SWS ripples. The effects of the amount of plasma filling are also studied to determine if the presence of plasma beyond the SWS inhibits the production of high power microwaves in a plasma filled BWO.

*Supported by the AFOSR/DOD MURI Grant for High Power Microwave Sources.

[1]M. Ali et al., J. Phys. Soc. Jpn. **60**, 2655 (1991).

5P13

X-Band Relativistic BWO With 3 GW Pulse Power

A.V. Gunin, A.I. Klimov, S.D. Korovin, I.V. Pegel, S.D. Polevin, A.M. Roitman, V.V. Rostov and A.S. Stepchenko
High Current Electronics Institute, Tomsk, Russia

At high powers of generation, as the electric field strength on the surface of electrodynamic structure rises, limitation of pulse duration is observed in microwave sources. One of the reasons of this phenomenon [1] is that the generation is affected by explosive electron emission excited on the surface of electrodynamic structure by intense high frequency electric fields.

In this paper, the results of study of a 3-cm relativistic BWO with lowest electric wave TM_{01} of circular waveguide are presented. The experiments have been conducted using the high current repetitively-pulsed electron accelerator SINUS-7 constructed at HCEI. The maximum parameters of the accelerator are as follows: electron energy up to 2.0 MeV and the beam current up to 20 kA in single-shot regime and 1.5 MeV and 15 kA at a repetition rate of 100 p.p.s. The pulse duration is 45 ns. In experiments, the maximum microwave power 3 GW was obtained, with the efficiency of generation about 20% and the pulse duration about 6 ns. It was observed that the duration of microwave pulse depends on the power, rising at lower powers. Typically, it is closed in order to the estimated time of appearance of explosive emission centers [2] on the surface of BWO slow wave structure.

[1] El'chaninov A.S., Zagulov F. Ya., Korovin S.D. // Lett. J. Tich. Phys. (Sov.) - 1981. - V. 7. - N. 19. - P. 1168 - 1171.

[2] Mesyats G.A., Proskurovskii D.I., Pulsed Electric Discharge in Vacuum. - Novosibirsk, <<Nauka>>, 1984. - 255 p.

5P14

Evaluation of Mode Competition in the Radial Acceletron

G.E. Sasser, M.J. Arman and J.W. Luginsland
Phillips Laboratory, Kirtland AFB, NM 897117

Simulations of the radial acceletron are presented. The radial acceletron is a low-impedance high power microwave (HPM) source which is compact, relatively low voltage (250 kV), and requires no external magnetic field. Microwave radiation is produced through bunching of emitted electrons caused by the radial transit-time effect and interaction with cavity modes in the diode region of the device. Simulations are performed using the parallel 3D particle-in-cell (PIC) code, ICEPIC. The time required to reach saturation is very long in this device (>100 nsec). The existence of competing non-axisymmetric modes could prevent efficient operation. The purpose of these simulations is to determine whether such modes are likely to exist.

5P15

Dynamics of the Space Charge Limiting Current in Gyro-type Devices*

Thomas A. Spencer and Mark D. Stump
The Air Force Phillips Laboratory, Electromagnetics Sources Division, Bldg. 66071, 3550 Aberdeen Ave SE, Kirtland AFB, NM 87117-5776

The Air Force Phillips Lab is investigating the dynamic change interactions which occur between the growing electromagnetic waves generated in a gyro-type device, and an electron beam with non-zero perpendicular velocity operating near the space-charge limiting current. The 2-1/2D code MAGIC is being used to perform simulations of the TE_{01} mode, and results will be presented. Initial results show that beams of this nature can suffer from a different kind of pulse shortening than typically found in other devices, thus placing an upper limit on the power and pulse length of gyro-type devices.

This work is supported in part by AFOSR

Wednesday Morning, 21 May 1997
10:00 a.m. – Rousseau Center

Poster Session 5P16-19:
7.1 MHD and EM/ETH Launchers

5P16

Numerical and Experimental Research of EMG-720 Flux Compression Generator

N.F. Popkov, A.S. Pikar, E.A. Ryaslov, V.I. Kargin, G.F. Mackartsev, V.E. Gurin, P.V. Korolev and V.N. Kataev
VNIIEF, Sarov, Russia
J.H. Degnan, G.F. Kiuttu and S.K. Coffey
Phillips Laboratory, Kirtland AFB, NM
W.J. Summa and K.E. Ware
Defense Special Weapons Agency, Alexandria, VA

As the result of international cooperation, we previously developed and tested a 30 MJ generator which can be used to drive high-power stationary plasma radiation sources. For further improvement of the generator design and increase in output energy it is necessary to study in more detail the physical processes and to minimize the main loss mechanisms. In this paper we present experimental results and compare them with numerical simulations. It is shown that the main losses of magnetic flux are associated with nonlinear diffusion of the field in conductors and flux disruption at section joints. Expected performance parameters for an updated design with decreased flux losses are given.

5P17

The Experimental Installation for Z-Pinch Pulse Compression

B.E. Fridman and Ph.G. Rutberg
Institute of Problems of Electrophysics of the Russian Academy of Sciences, 18, Dvortsovaya nab., St. Petersburg, 191184, Russia
Phone No. (812) 315-1757, Fax No. (812) 311-5056

The installation is intended for experimental studying of the substances phase conversions with super-high pulse pressure. The pressure is created at passage of the large pulse current through the cylindrical heavy liner (z-pinch scheme). The installation is connected to the terminal of the E7-25 type Capacitive Energy Store and its designs on 10 MA current pulse with 20 kV voltage, 100 μs.

The regimes of dynamic compression are presented, in which there are not over-heating of studying substances. Estimations of the electrodynamical forces, acting on the installation's elements, are made.

The work on creation of the installation is being done under support of Russian Fund for Basic Researches (project No 96-02-16009a).

5P18

E7-25 CAPACITIVE ENERGY STORE FOR POWER SUPPLYING LOADS OF ELECTRO-DISCHARGE LOADS

B.E. Fridman and Ph.G. Rutberg
Institute of Problems of Electrophysics of the Russian Academy of Sciences, 18, Dvortsovaya nab., St. Petersburg, 191184, Russia
Phone No. (812) 315-1757, Fax No. (812) 311-5056

Capactitive energy store is intended for supplying the experiments with electro-discharge launchers and other loads. Designed stored energy is 17.2 MJ, maximum voltage is 25 kV, discharge current range is 10 MA, frequency of the discharge current oscillations in short circuit is 8 kHz. The store was built on the module principle. It contains 23 modules, all modules consist of 8 cells. Every cell has capacitors on 94 kJ stored energy and vacuum triggered vacuum switch. Control and synchronization systems of the storage provide remotely operating by every module and non-simultaneous programmed discharge, where triggered switches in cells are switched-on in definite time. The first phase of the store was put in operation with 9 MJ of stored energy (12 modules) and was tested with 10 MA discharge current.

5P19

On the Mechanism of the Magnetic Field Influence on the Electrical Explosion of a Thin Wire

Yu.E. Adamyan, A.N. Berezkin, V.M. Vasilevsky, S.N. Kolgatin, S.I. Krivosheyev and G. A. Shneerson
State Technical University, St. Petersburg, Russia

The radial plasma flow in its electrical explosion in longitudinal magnetic field originates azimuthal current, which in the interaction with the axial field generates an additional component of the radial Ampere force. If its value is large enough, the compression of the wire and the stabilization of two-dimensional instabilities are possible. On the other hand, the considerable azimuthal current results in additional Joule heating of those conductor layers where the current flows. At large values of azimuthal current j the process of thermal expansion in heating may be competitive to retention, and the longitudial field will not hamper, but accelerate plasma flying apart.

The calculations, as well as the analytical estimates, allowed to assess approximately the boundary of the transition of conditions when very large field or considerable velocity of flying apart caused by the high rate of the current increase result in the "self-excitation" of azimuthal current that becomes the key factor of plasma heating in its flying apart. The threshold conditions correspond to very strong field (induction about 100T at current density $j = 1$ MA/sm^2).

The experiments on the wire explosion of diameter 0.2 mm in a vacuum at currents up to 30 kA with induction up to 60 T have shown that the excitation of azimuthal current begins in more a weak field that it follows from the calculations by single-liquid hydrodynamic model. The generation of the diamagnetic signal has been registered (flux displaced by plasma) exceeding the calculated value. This suggests the possible influence of unbalanced ionization processes in the plasma external region and may indicate the fact that the self-excitation threshold of azimuthal current is lower than the calculated one.

Wednesda Morning, 21 May 1997
10:00 a.m. – Rousseau Center

Poster Session 5P20-24:
7.2 Plasma Closing Switches

5P20

High-Repetition-Rate, Short-Pulse Generator Using a Planar Crossatron®* Switch**

Joseph Santoru, Dan Goebel and Robert Poeschel
Hughes Research Laboratories, Malibu, CA 90265

We have developed a high-repetition-rate, high-voltage short-pulse generator that employs a new planar CROSSATRON® switch to discharge a low-inductance capacitor array into a load. Typical pulse parameters are 20-kV capacitor-charge voltage, 50-ns pulse width, 20-40-ns pulse risetime, and up to 120-kHz pulse-repetition rate in bursts of ten pulses. The burst length is limited by the capacitor charging power supply, not the intrinsic characteristics of the tube.

High-repetition rate operation is enabled by a new planar CROSSATRON switch that uses a flat cathode, anode and grids, rather than the cylindrical electrode geometry used in other CROSSATRONs. CROSSATRON switches are plasma-discharge devices that conduct high current with low forward-voltage drop at high speeds. CROSSATRON switches also feature rapid recovery times that permit operation at high pulse-repetition frequencies. In fact, when configured in closing-only applications, as in the short-pulse generator, a maximum closing rate of di/dt = 10^{11} A/s can be obtained with voltage recovery times of <100 μs.

*CROSSATRON® switch is a registered trademark of Hughes Electronics.

**This work was supported by Hughes Aircraft Company IR&D funds.

5P21

WORKING CHARACTERISTICS OF THE TRIGGERED THREE-ELECTRODE SPARK GAPS WITH DIFFERENT TYPES OF GAS INSULATORS

N. Arsic[1] and P. Osmokrovic[2]
[1]*Faculty of Electrical Engineering, Suncani breg bb, 38000 Pristina, Yugoslavia*
[2]*Faculty of Electrical Engineering, Bulevar Revolucije 73, P.O. Box 816, 11000 Belgrade, Yugoslavia*

Comparative analysis of the working characteristics for the gas and vacuum insulated three-electrode spark gaps is presented in this paper. The influence of the different gas insulation parameters on the triggered three-electrode spark gap functioning is considered. Two types of three-electrode vacuum and gas insulated spark gaps have been tested: a spark gap with a third electrode being inside the main electrode, and a spark gap with a separate third electrode. Both types of spark gaps were theoretically sized in the optimal way by computers prediction. In order to investigate the influence of insulation parameters on the spark gap functioning, type of gas and electrode material have been tested. Besides vacuum applied gases were: SF_6, N_2 and a mixture of $0{,}6SF_6 + 0{,}4N_2$. The electrode materials were copper tungsten and steel. The investigation was done by determining the points switching time-working voltage under constant values of the other parameters. The working voltage value was taken as a changeable parameter during measurements. During each test, 60 values of flashover voltage of both polarities were measured. After that, the spark gap delay time or switching time was measured. In order to obtain of the single point delay time-working voltage or switching time-working voltage, the series of 50 measurements was accomplished. Also, 1000 triggering have been accomplished without a change of gas and electrodes. The statistical analyses of results is also presented. In order to test the reversibility characteristics of spark gaps the spark gap switching time and delay time are measured.

5P22

Plasma Formation Inside Gap with One-Hole Control Grid

Alexander S. Arefjev and Boris D. Maloletkov
Ryazan State Radioengineering Academy, 59/1 Gagarin, Ryazan, 390005, Russia

Consider three-electrodes gap, provided there is a perforated one-hole electrode inside the gap. If a positive impulse voltage of the sufficient magnitude is applied to the hole-electrode relative to the cathode, then a nonstationary plasma is formed with increasing concentration of charged particles in the cathode-electrode region. Appearance of particles due to the diffusion and drift in the electrode-anode region makes change of the potential distribution.

5P23

Two-Site Marx Switch With Graphite Electrodes*

I.S. Roth, S.K. Lam and P.S. Sincerny
Primex Physics International, 2700 Merced Street San Leandro, CA 94577-0599

We are developing a Marx switch which will have an extended lifetime. The switch uses graphite electrodes, and has two sites to prevent the graphite from spalling. To ensure that both sites carry current, the switch uses a mixture of 80% Ar and 20% SF_6, and is illuminated with UV. We are presently testing a prototype.

*Work supported by DSWA.

5P24

Functional Model of a Triggered Spark Gap

David L. Lockwood
EG&G Optoelectronics Division, 35 Congress Street, Salem, MA 01970

Gas filled triggered spark gaps exhibit performance characteristics that depend on the gas species, gas pressure, and electrode spacing, as well as the mode of operation. The characteristics of interest are dielectric withstanding voltage turn-on delay time, and cut-off voltage. Dielectric withstanding voltage is described in terms of the gas species, pressure, and electrode spacing by Paschen's equation.

An expression for cut-off voltage is developed using the assumption that the average electron energy is less than the effective ionization potential of the gas. The cut-off voltage and the Townsend gas breakdown criterion are used in the Langevin equation to develop an expression for the turn-on delay time.

The model is shown to agree well with experimental data from a large number of triggered spark gaps.

Wednesday Morning, 21 May 1997
10:00 a.m. – Rousseau Center

Poster Session 5P25-28:
7.3 Fast Opening Switches

5P25

Measurements of Plasma Density and Magnetic Field in a 100-ns Plasma Opening Switch (POS)

A. Weingarten, Ya.E. Krasik and Y. Maron
Weizmann Institute of Science, Rehovot 76100, Israel

Spectroscopic techniques are used to investigate a coaxial POS driven by a 270 kV, 200 kA, 90 ns half-period negative current pulse applied to the inner electrode. The plasma is produced by a flashboard characterized using spectroscopy and biased Faraday cups. The plasma density determined from hydrogen line Stark broadening is $2x10^{14}$ cm^{-3}, an order of magnitude higher than the value obtained by Faraday Cups and Langmuir probes. Thus it is possible that the density in previous POS experiments was higher than inferred from electrical measurements. It was also observed that a similar POS operation is obtained for various flashboard configurations when the same density is reached, regardless of the injection velocity. Thus, previously made scaling considerations may have to be re-examined. The plasma is doped by various elements using laser evaporation techniques to obtain good spatial resolution in the axial direction. All emission lines show fast decrease in the excited level population that is time-correlated with the POS opening. Comparisons of various line intensities and atomic physics calculations show that this sharp decrease results from local evacuation of the electrons. The drop in density propagates from the generator towards the load, and from the cathode to the middle of the POS gap. Local Zeeman splitting measurements of PbII lines are used to determine the magnetic field and current distribution in the plasma. The opening mechanism is investigated by correlating the time dependent data on magnetic field and the local density.

5P26

Spectroscopic Investigations of a Planar Microsecond POS

R. Arad, Y. Krasik, K. Tsigutkin and Y. Maron
Physics Dept., Weizmann Institute of Science, Rehovot 76100, Israel

We study the operation of a planar microsecond plasma opening switch in which a current of 180 kA is generated by a low inductance generator and is conducted by the plasma during 400–600 ns before opening into an inductive load within ≈80 ns. The POS region is prefilled with a flashboard plasma of an electron density of 8 ±2 x 10^{14} cm^{-3}. Local spectroscopic measurements are obtained by doping the plasma with various species using molecular beam injection through holes in the cathode. Spatial resolution in three dimensions is obtained by observing the characteristic emission of the doped particles perpendicular to the beam. The doped column was seen to have a FWHM of ≈1 cm and a density around $1x10^{14}$ cm^{-3}. Using this method we obtained a 3-D map of the local velocity distributions of helium, neon, and argon doped in the plasma from Doppler broadenings and shifts of their spectral lines. The velocities were seen to scale as z/m and were all much lower than the Alfven velocity. The magnetic field spatial distribution was obtained from Zeeman splitting of helium lines and the magnetic field

was seen to penetrate into the plasma at a velocity of $3x10^7$ cm/s. The electron temperature, studied from comparison of the measured intensities of spectral lines from highly excited states of various ions with collisional-radiative calculations, was seen to increase sharply in the 2.5-cm wide current channel. This will be further investigated for studying the energy dissipation associated with the magnetic field penetration into the plasma.

5P27

Diamond Fast Opening Switches for Inductive Energy Storage Power Modulators*

S.W. Gensler, R.R. Prasad. I.V. Tzonev, N. Qi and M. Krishnan
Alameda Applied Sciences Corp.
2235 Polvorosa Ave., #230, San Leandro, CA 94577

A fast opening switch is the key component of an Inductive Energy Storage (IES) power modulator. An IES modulator can take energy at low power levels across a vacuum insulator and produce high peak powers at the load inside the vacuum. Such a power amplifier is far more compact than equivalent capacitive pulse lines. If the switch can be cycled repetitively, high peak power and high average power can be produced. Applications include all-solid–state, compact, portable multi-gigawatt power modulators for electron and ion beam diodes and high power microwave and x-ray sources.

This paper presents experimental results from natural and CVD diamonds used as fast opening switches in prototype IES circuits. The physical and electrical properties of diamond combine to offer a superb electronic material. Diamond has the highest electrical breakdown strength, highest thermal conductivity, highest operating temperature, and best mechanical strength of any solid state switch material (e.g. Si or GaAs). Diamond switches are capable of ~1kHz operation at ~0.1–1MV amplified voltages. Early results with natural Type IIa diamonds indicate ~0.2–0.5μs conduction times followed by rapid opening with dR/dt values $\sim 5x10^{10}\Omega/s$. Results of experiments at charge voltages up to 10kV and conduction times up to ~1μs will be presented. The power amplification and efficiency of these opening switches will be evaluated in light of several applications such as a 150kA / 150kV / 40ns compact flash x-ray source, high average power microwave sources, and particle-beam drivers.

*Work supported by DSWA under a Phase I SBIR, Contract # DSWA01-96-C-0127.

5P28

An Inverse Pinch Plasma Source for Opening Switches

J.J. Moschella, E.J. Yadlowsky, R.C. Hazelton
HY-Tech Research Corporation, Radford, VA

An inverse pinch plasma device is being developed for plasma opening switch applications. The physical principles behind its operation are essentially the same as the coaxial plasma gun except the inverse pinch utilizes an axial current sheet that expands and ejects plasma radially. It is therefore ideally suited for placement inside the center conductor of a cylindrically symmetric opening switch and has the potential of filling the switch region uniformly with plasma from a single source. Our source has been designed to operate inside a vacuum where a fast puff valve coupled with an annular nozzle injects a suitable amount of gas between two, concentric, disc shaped electrodes supported by a 1 inch diameter insulating quartz sleeve. Upon application of a high voltage pulse (20 kV), a cylindrical current sheet is formed near the insulator that expands radially due to magnetic pressure creating a snowplow front. Plasma is ejected from the device when the front reaches the end of the disc.

This device can produce a range of plasma mass densities that extends over two orders of magnitude. Mass density control is exercised by varying the type of gas and the magnitude of the gas puff. We will present time resolved radial and axial plasma density profiles in a POS gap for H, Ne, and Ar plasmas as well as measurements of the average ionization state in the Ne and Ar plasmas.

Wednesday Morning, 21 May 1997
10:00 a.m. – Multipurpose Room

Poster Session 5Q01-12:
1.2 Space Plasmas

5Q01

Microwave Plasma Sources for Use in Space Plasma Physics Experimentation*

D.N. Walker, J.H. Bowles and W.E. Amatucci[a]
Plasma Physics Division, Naval Research Laboratory, Washington, DC
[a]Sachs Freeman Assoc., Largo, MD

We have developed two microwave plasma sources[1,2] most useful in approximating ionospheric space plasma environments because of the low electron temperatures (<2 eV) and adjustable densities (10^4 - 10^8 cm^{-3}). Both of these sources employ conventional microwave oven magnetrons and are easy to construct and exhibit stable operation over a wide range of neutral gas flow rates and electron densities. Although the production mechanism of the plasma is the same in both cases (microwave cavity resonance), the designs of the two sources are quite different. We report on the use of these types of sources in space plasma experimentation in the Space Physics Simulation Chamber (SPSC) at the Naval Research Laboratory. We will describe construction of these sources and improvements to the design, including an increased surface area to provide a more uniform plasma across the available experimental area.

*Work supported by the Office of Naval Research.

[1] D.N. Walker, et al., Rev Sci Instrum, **65,** 164 (1994).
[2] J.H. Bowles, et al., Rev Sci Instrum, **67,** 455 (1996).

5Q02

ELECTROMAGNETIC INTERACTION OF SPACECRAFTS WITH THE ENVIRONMENT

V.M. Antonov and A.G. Ponomarenko
Institute of Laser Physics, Siberian Branch of the Russian Academy of Sciences
630090 Novosibirsk, Russia
V.V. Danilov
Kransnoyarsk State University
660041 Krasnoyarsk, Russia
O.S. Grafodatsky
NPO of Applied Mechanics, Krasnoyarsk, Russia

The technique of laboratory simulation of spacecraft charging processes at the geostationary orbit has been developed. The dynamics of high-voltage charging, electrical discharges formation, electromagnetic pulse excitation and solar batteries degradation with the effects of such space factors as hot and cold plasmas, external atmosphere, ultraviolet radiation of the Sun with allowance for electrophysical properties and design peculiarities of the surface materials, plasma and gas jets of the engine setups scattering centers and grid screens have been investigated. The problems of background plasma interaction with the man-made magnetosphere which may arise at launching of powerful inductive energy storage into space are examined.

5Q03

Helicon Plasmas for Space Relevant Laboratory Experiments

Earl Scime, Matthew Balkey, Paul Keiter and John Kline
West Virginia University, Morgantown, WV 26506

Helicon sources are regarded as potential candidates for the next generation of plasma etching sources. The high efficiencies, steady-state operation, and high densities also make them attractive plasma sources for basic plasma physics experiments. The use of the West Virginia University (WVU) hot helicon source as part of an experiment designed to investigate ion temperature anisotropy driven instabilities under space-relevant conditions will be discussed. The WVU helicon source is "hot" because the ion temperature has been raised by the addition of ion cyclotron resonant heating. The physics objectives of the experiment, the required plasma parameters, and necessary source parameters will be reviewed.

5Q04

Three-Dimensional Numerical Simulation of Ion and Electron Accelerations by Parametric Decay of Fast Lower Hybrid Waves

Nagendra Singh, S. Al-Sharaeh, A. Abdelrazek,
W.C. Leung and B. Earl Wells
Department of Electrical and Computer Engineering,
University of Alabama in Huntsville
Huntsville, Alabama 35899

The transverse acceleration of ions by fast lower hybrid waves in the topside auroral ionosphere has remained elusive. The linear and nonlinear propagation and evolution of lower hybrid waves are essentially a three-dimensional problem. Analytical treatment of this problem, including the essential kinetic effects for particle acceleration, is a formidable task if not impossible. We have treated this problem by a fully three-dimensional particle-in-cell simulation. It is found that a fast lower hybrid pump wave undergoes a parametric decay generating secondary waves over a broad frequency range from the ion cyclotron frequency Ω_i to just above the lower hybrid frequency $\omega_{\ell h}$. These secondary waves are instrumental in the accelerations of both cold ions and electrons. The ion acceleration is predominantly perpendicular to the ambient magnetic field ($\underline{B}$), and it is accompanied by a relatively weak parallel acceleration in the direction of the phase velocity of the pump wave V_{pllo}. The ion acceleration is also accompanied by a bidirectional electron acceleration along $\underline{B}$, but the acceleration in the direction of V_{pllo} is preferentially enhanced forming an elongated plateau in electron velocity distribution function. These features of particle accelerations seen from the simulations appear analogous to those seen from rocket experiments in which lower hybrid waves and bursts of transversely accelerated ions and downgoing parallel accelerated electrons were simultaneously observed.

5Q05

A Laboratory Plasma Source as an MHD Model for Astrophysical Jets

R.M. Mayo and R.W. Caress
Department of Nuclear Engineering,
North Carolina State University, Raleigh, NC 27695

Astrophysical plasma jets are observed to emanate from a wide variety of sources on extremely diverse spatial scales from YSO to AGN. Various mechanisms have been employed in an attempt to explain their formation, acceleration, collimation, and stability. Many favor Magneto-hydrodynamic (MHD) mechanisms for reasons including the observance of strong magnetic fields in the flows, the recognized ability of the MHD pinch effect to collimate plasma, and the efficiency with which accretion disk rotational energy can be extracted by magnetic fields. MHD models have been developed by others to explain the acceleration and collimation of jets, yet no laboratory model of such flows has been investigated.

The CPS-1 (Coaxial Plasma Source) facility at NCSU is capable of producing high conductivity, high enthalpy magneto-flows in widely varied applied magnetization. Investigation of these laboratory flows has suggested flow regime and morphological similarity with astro-jets through an MHG interpretation. Recent results show that the magneto-plasma flows from CPS-1 remain well collimated beyond seven gun radii downstream from the gun muzzle. We further observe the propagation of strong interaction layers during discharge initiation resembling working surfaces. As well, evidence suggests the formation of detached plasmoid propagation. We will present experimental results from an extensive investigation of the collimation and stability, and initiation flow dynamics of magnetized and unmagnetized CPS-1 flows, the latter showing great morphological similarity to optical and AGN jets.

5Q06

A Generation Mechanism for the Frequency Up-Shifted Plasma Lines Observed in the Tromsq's HF Heating Experiments

S.P. Kuo
Department of Electrical Engineering
Polytechnic University, Farmingdale, NY 11735
S.C. Kuo
Department of Applied Science,
Brookhaven National Lab, Upton, NY
M.C. Lee
Plasma Fusion Center, Massachusetts Institute of Technology, Cambridge, MA 02138

A new spectral feature in the backscattering spectrum of EIS CAT 933 MHz radar was observed throughout most of the observing period of the heating experiments performed with 0-mode heater transmitting near Tromsq, Norway on August 16-18, 1986. The radar returns were enhanced at frequencies offset from the radar frequency by a frequency a few hundred KHz more than the heater frequency of 4.04 MHz [Isham et al, 1990]. Moreover, running alternately with the radar in the chirped and in the unchirped mode it was shown that the enhanced plasma lines seemed to emanate from very local regions [Birkmayer et al, 1986]. It is noted that a similar phenomenon recording frequency upshifted HF-enhanced plasma lines (HFPLs) has also been observed in the Arecibo heating experiments, except the amount of frequency upshift is in the range of a few tens of KHz [Sulzer and Fejer, 1984]. A physical mechanism [Kuo and Lee, 1992] based on a nonlinear scattering process by which the parallelly propagating Langmuir waves generated by the parametric decay instability of the HF pump scatter off the background lower hybrid density fluctuations to produce the observed frequency upshifted plasma lines has successfully explained the Arecibo's observations and has even been verified recently by a laboratory experiment [Lee et al, 1987]. However, the amount of frequency shift observed in the Tromsq's experiments well exceeds the lower hybrid wave frequency. Thus, a different physical mechanism is considered in the present work for explaining the Tromsq's observations. It is the parametric decay of a right handed circularly polarized pump wave (0-mode) into a Whistler wave (decay mode) and a frequency upshifted Langmuir wave (sideband). Since the frequency of Whistler wave extends to the range of a few hundred kHz, the frequency of the excited Langmuir wave agrees with that of the experimental observation.

Work supported by NSF.

W. Birkmayer, T. Hagfors, and W. Kofman, Phys. Rev. Lett., 57, 1008, 1986; B. Isham, et al., Radio Sci., 25, 257 1990; S.P. Kuo and M.C. Lee, Geophys. Res. Lett., 19, 248, 1992; M.C. Lee, et al., Geophys. Res. Lett., 24, Jan 15 issues, 1997; M.P. Sulzer and J.A. Fejer, J. Geophys. Res., 88, 15035, 1994.

5Q07

Study of ELF/VLF Wave Generation by HF Heater-Modulated Electrojet

S.P. Kuo
Department of Electrical Engineering
Polytechnic University, Farmingdale, NY 11735
M.C. Lee
Plasma Fusion Center, Massachusetts Institute of Technology, Cambridge, MA 02138
Paul Kossey
Phillips Laboratory, Hanscom AFB, MA 01731

Generation of ELF/VLF waves by the modulation of the electrojet by the powerful HF heater is of current interest. It is done by applying an amplitude modulated HF heater to modify the electron temperature of the electrojet in time. This in turn causes the modulation of the conductivity and thus, the electrojet current. Emissions are then produced at the modulation frequency and its harmonics. The present work extends the previous one[1,2] of thermal instability to the nonlinear saturation regime. Two heater-modulation schemes are considered. One, corresponding to the one adopted in the Tromsq heating experiments[3], modulated the heater by a rectangular periodic pulse. The other one needs two overlapping heater waves (beat wave) having a frequency difference equal to the desired modulation frequency. It is essentially a sinusoidal amplitude modulation and is the approach adopted in the Arecibo heating experiments. The nonlinear evolutions of the generated ELF/VLF waves are determined numerically. Their spectra are also evaluated. The results show that the signal quality of the beat wave scheme is better (i.e., harmonic components have relatively lower intensities than that of the fundamental

line). The field intensity of the emission at the fundamental modulation frequency is found to increase with the modulation frequency, consistent with the Tromsq results.

Work supported by NSF.

1. S.P. Kuo and M.C. Lee, Generation of ELF and VLF Waves by HF Heater-Modulated Polar Electrojet Via a Thermal Instability Process, Geophys. Res. Lett., 20, 189, 1993.

2. S.P. Kuo, Generation of ELF and VLF Waves by a Thermal Instability Excited in the HF Heated-Modulated Polar Electrojet, Radio Sci. 28, 1019, 1993.

3. P. Stubbe, H. Kopka, and R.L. Dowen, Generation of ELF and VLF Waves by Polar Electrojet Modulation: Experimental Results, J. Geophys. Res., 86, 9073, 1981.

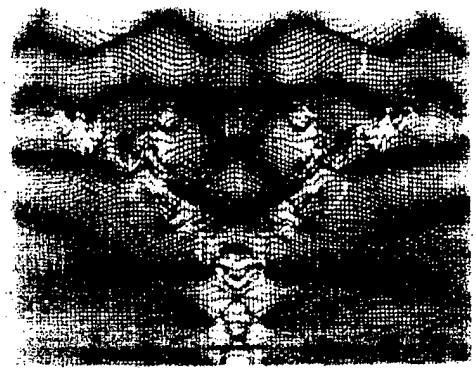
5Q08

Space Internet from Beam Antenna

Toshiro Ohnuma and Hiroyasu Sato
Department of Electrical Engineering
Tohoku University, Sendai 980 Japan

"Space Internet" is investigated by developing beam antennas, experiments of which were performed on Space Shuttle[1]. Space Internet, i.e., Space international network via Satellites[2], is a prospering project for international communications around the Earth.

Fundamental electromagnetic fields for the space internet are obtained by developing electromagnetic fields of beam antennas in space. Typical fields for satellites-network of tree type are shown as follow;



1. T. Ohnuma, Radiation Phenomena in Plasmas (World Scientific, 1994)

2. T. Ohnuma, Proc. 25th URSI (1996)

5Q09

Automodel Dynamics of Current "Coalescence" in a Thin Current Layer

B.A. Trubnikov, V.P. Vlasov and S.K. Zhdanov*
Nuclear Fusion Institute, RRC "Kurchatov Institute," Moscow, Russia.
**Moscow Engineering Physics Institute Moscow, Russia*

The current filamentation dynamics in a thin current layer is being discussed with a dynamic model in a given study:

$$\rho'_t + (\rho v)'_x = 0.\ v'_t + v v'_x = g H \rho,$$

where H is the Gilbert operator, g = const. This model has been first proposed by B.A. Trubnikov in connection with the problem of pinch emergence under interaction of the magnetized plasma clouds [1]. Under disruption of pinch the accelerated electron/ion beams emerge. It is assumed that the bremsstrahling of electrons gives birth to gamma-bursts, and the ions (protons, mainly) feed the galactical cosmic rays.

It has been shown that this dynamic system is a Hamiltonian one. Automodel solutions representing the collapse of the isolated current filaments—in case of selfcompression and under an effect of all other filaments into which the current layer is splitted—have been built.

[1] B.A. Trubnikov, Uspekhi Phys. Nauk, 1990, v. 160, N. 12, pp. 167-186.

5Q10

Fragmentation of Electron Stream at Propagation Through Plasma

V. Mel'nik
Institute of Radio Astronomy of National Academy of Sciences, Kharkiv, 310002, Ukraine
E. Kontar
Kharkiv State University, Kharkiv, 310077, Ukraine

The propagation of electron stream is considered in the limit of weak turbulence when the quasilinear time is much smaller than the time of electron stream flying-off. It is found out that the initial electron distribution function of the electron stream propagating in plasma is unstable to decay into separate beams. Langmuir waves

excited by the fast beams accelerate electrons of slow beams that leads to interaction between them: the number of particles in the fast beams increases and their phases change. Electron distribution function and spectral energy density of plasma oscillation are found in gas-dynamic approximation.

5Q11

Coronal Transient from Drift Electric Field

Han Jiling
Physics Dept., Beijing Normal University
Beijing 100875, China

Without flare in company with, in region of plasma turbulence the coronal transient can be also create by electric field which arises from transient magnetic field.

In solar active region, the transient magnetic field B with time can induct a vortex electric field E_c. The E_c may create a drift electric field E_v of the $E_c \times B$. That the E_c and the E_v interact will cause unlimited growth of drift instability and lead to strong turbulence of ion-acoustic waves.

When plasma turbulence is fully developed and "run-away" electron beam is formed, in turbulent region the Coulomb collision damping and Landau collisionless damping can all be neglected. Under this case, the accelerating of electric field becomes into most effective under a certain conditions, the transient magnetic energy is most effectively transformed into transient kinetic energy by plasma turbulence and electric field accelerating.

5Q12

High Energy Particles From Stochastic Accelerating

Han Jiling
Beijing Normal University, Physics Dept.
Beijing, 100875, China

The ion-acoustic waves were observed by OGO-5 satellite and Vela-3 satellite, etc. in precursor region of earth's bow shock and magnetosphere.

In space plasma, the ion-acoustic waves turbulence can be excited by strong current, great gradient of magnetic field or Langmuir wave turbulence. The stochastic accelerating is effective when charged particles are in a plasma turbulence region for a sufficiently long time. The turbulent stochastic accelerating may transform and distribute the energy from turbulent sources to a few fast particles. When velocity of fast particles increase, they can absorb a larger number of plasmons and thus particle energy will further rapidly be increased and create high energy particles from k(ev) to M(ev).

Wednesday Afternoon, 21 May 1997
1:30 p.m. – Kon Tiki Ballroom

Plenary Session

PSAC Prize Address:

Science and Applications of Energy Beam Ablation

Professor Ronald M. Gilgenbach

Director , Intense Energy Beam Interaction Laboratory
University of Michigan, Ann Arbor, MI, USA

Chair: N. Hershkowitz

Wednesday Afternoon, 21 May 1997
3:00 p.m. – Kon Tiki Ballroom

Oral Session 6A:
2.2 Fast Wave Devices II
Chair: G. Nusinovich

6A01-02 *Invited*

Cyclotron Wave Amplifiers at Microwave and Millimeter Wave Frequencies*

Wallace M. Manheimer
Plasma Physics Division, Naval Research Laboratory, Code 6707, Washington DC 20375

Cyclotron wave parametric, and cyclotron wave electrostatic amplifiers were developed in Russia and the United States in the late 50's and early 50's. The application was for input amplifiers in the receivers of radar and communication systems. While work in the west was abandoned in favor of solid state, it continued in Russia; these are important components of many Russian military and civilian systems. Advantages include low noise temperature, high degree of linearity, receiver protection and very fast recovery time after a microwave overload. The basis of the device is the parametric amplification of the fast cyclotron wave on an electron beam. The beam is cooled in one of two ways to achieve low noise temperature. Recently, a summary of the theory and behavior of these devices have appeared in the United States.[1] They have been developed only at microwave frequencies as high as 35 GHz. To go to higher frequencies means still higher magnetic fields, which is difficult to do with permanent magnets. An alternative is to operate at harmonics of the cyclotron frequency. The theory of cyclotron wave amplifiers at harmonics of the cyclotron frequency has recently been worked out.[2]

*This work is supported by the Office of Naval Research.

[1] V. Vanke, V. Savvin, U. Budzinsky, W. Manheimer, and G. Ewell, *Cyclotron Wave Electrostatic and Parametric Amplifiers,* submitted to IEEE Trans. Plasma Sci, also NRL Memo #7910

[2] W. Manheimer, *On the Possibility of Harmonic Operation of Cyclotron Wave Parametric Amplifiers,* submitted to IEEE Trans. Plasma Sci. also NRL Memo #7911

6A03

Theoretical Study of the Gyrotron Backward Wave Oscillator

S.H. Chen
National Center for High-Performance Computing, Hsinchu, Taiwan, ROC
K.R. Chu
Dept. of Physics, National Tsing Hua University Hsinchu, Taiwan, ROC

Saturated behavior of the gyrotron backward wave oscillator (gyro-BWO) is studied with a particle tracing code which calculates the self-consistent field profile in a weakly non-uniform interaction structure. Characteristics of interest to gyro-BWO operations, such as phase control by injection locking, locking bandwidth, voltage tunability, and effect of end reflections on the efficiency, are examined and compared with experimental observations.[1]

1. C.S. Kou, S.H. Chen, L.R. Barnett, H.Y. Chen, and K.R. Chu, "Experimental Study of an Injection Locked Gyrotron Backward-Wave Oscillator", Phys. Rev. Lett. **70**, 924 (1993).

6A04

High Power, Low Velocity Spread, Axis Encircling Beam, Electron Gun Development[1]

D. Gallagher, J. Richards, F. Scafuri and C. Armstrong
Northrop Grumman Corporation, Electronic & Information Warfare Systems, 600 Hicks Road, M/S H6402, Rolling Meadows, IL 60008
Tel (847) 259 9600

Presented is the status of the development of a low velocity spread, 70 kV electron gun for gyro-device research. The design retains the simplicity of the Northrop Grumman (NG) novel gun concept where possible. The main design goals are: beam current = 3.5 A, magnetic focusing field = 6.5 kG, beam alpha = 1.5, beam ripple $<\pm 10\%$, and axial velocity spread less than 5%. Preliminary design candidates were obtained by the code NOVGUN developed at NG. This code calculates the single electron trajectories in the electric and magnetic fields calculated by solving LaPlace's equation for the electric and magnetic scalar potentials. The gun electrodes and magnetic pole piece electrodes were varied systematically and automatically through hundreds of

iterations until the beam ripple (guiding center spread) and axial velocity spread were minimized. To achieve both low ripple and low velocity spread, it was necessary to incorporate a magnetic ring (floating pole piece) around the cathode to deflect the magnetic field lines away from the cathode. After a preliminary design candidate was found through NOVGUN, the gun was modeled by the Hermannsfeldt code with the magnetics accurately simulated by the MAXWELL code. Cathode surface roughness and the temperature of the cathode ring were taken into account, and the cathode was recessed to reduce edge emission. After fine tuning the design, particularly the shape of the cathode ring, the final simulations indicate all the goal specifications being met. The mechanical design of the gun was completed and all parts and fixtures were ordered and received. Fabrication of the gun will begin in January 1997. To test the gun, a beam tester using a cerium glass scintillator witnes plate, capacitive probes, and a retarded field analyzer (to measure the average axial and transverse beam velocities as well as the velocity spreads) has been designed, and its fabrication is nearly complete. The gun will be tested at reduced voltage, 24 kV, with the magnetic field and frequency scaled accordingly. Peniotron circuits have been designed for RF tasting after beam testing is complete.

[1] Work supported in part by NRL and MURI.

6A05

Theory of Multi-Beam Stagger-Tuned Gyroklystrons

G. S. Nusinovich
Institute for Plasma Research
University of Maryland, College Park, MD 20742
B. Levush and B. Danly
Naval Research Laboratory, Washington, DC

Multi-beam configurations have long been used in linear beam klystrons. The use of a large number of beamlets propagating through individual channels allows one to significantly reduce the space charge effect leading to voltage depression. Therefore the total perveance of multi-beam klystrons is much larger than in single-beam klystrons. Correspondingly, these devices can produce a required power level at a much lower voltage and in a wider bandwitdth.

Recently, NRL has started the development of wide-band high-power millimeter-wave gyroklystrons (GKL's) for radar applications. The present work is done within the frame of this program. In our paper we apply the multi-beam concept to GKL's and analyze the possibilities of further increasing the bandwidth by stagger-tuning the eigenfrequencies of individual input cavities with respect to the signal frequency. The formalism describing the multi-beam stagger-tuned GKL is developed and the small-signal gain in two-stage, two-, three- and four-beam GKLs is analyzed.

This work has been supported by the U.S. Office of Naval Research.

6A06

Single-Stage, Depressed Collector Operation of an 84 GHz Gyrotron

T.S. Chu, P. Borchard, P. Cahalan, K. Felch
and C.M. Loring
Communications Power Industries (CPI)
Palo Alto, CA 94304
T. Shimozuma and M. Sato
Natioanl Institute for Fusion Science, Toki, Japan

Efficient, high-power millimeter-wave sources are needed in electron cyclotron heating (ECH) for many present and futer fusion experiments. CPI, in collaboration with the National Institute of Fusion Sciences, Japan, is developing high-power, CW gyrotrons with an internal converter at 84 GHz for ECH in the Large Helical Device (LHD) Heliotron. The first prototype of this kind of tube has been tested to long pulse [1] and 200 kW, CW [2]. The second prototype has been fabricated and is currently being tested at CPI. In addition to the improved cooling and vacuum pumping capability of the present tube, it is designed to operate with a single stage depressed collector.

With a depressed collector, the overall efficiency of a gyrotron can be increased. In addition, the cooling requirement and X-ray generation of the collector at a given output power is reduced. Furthermore, for 1 MW gyrotron operation, tight voltage regulation would only be required for an 80 kV, 10-50ma power supply instead of an 80kV, 50A supply. This represents a possible saving in power supply cost. Recent gyrotron experiments with a depressed collector have yielded promising results [3,4]. In this paper, we will summariz the design of the new tube and present inital test data. In particular, we will present results of single-stage, depressed collector operation.

[1] M. Sato, T. Shimozuma, Y. Takita, S. Kubo, H. Idei, K. Ohkubo, T. Kuroda, T. Watari, "Development of A High Power 84 GHz CW Gyrotron," in 20th Int.

Conf. Infrared and Millimeter Waves, Conference Digest, 1995, pp.195-6.

[2] Private Communication with T. Shimozuma

[3] K. Sakamoto, M. Tsuneoka, A. Kasugai, T. Imai, Kariya, K. Hayashi, and Y. Mitsunaka, "Major Improvement of Gyrotron Efficiency with Beam Energy Recovery", Phys. Rev. Lett. Vol. 73, No. 26 pp.3532-3535, Dec. 1994

[4] B. Piosczyk, C.T. Iatrou, G. Dammertz, and M. Thumm, "Single Staged Depressed Collectors for Gyrotrons", IEEE Trans. on Plasma Sci. Vol. 24, No. 3., pp. 579-585, June 1996

6A07

Ultrahigh Intensity Compton Scattering Focused X-Ray Source

F.V. Hartemann*, A.L. Troha, G.P. LeSage, C.V. Bennett, B.H. Kolner and N.C. Luhmann, Jr.
University of California at Davis, Davis CA

At ultrahigh intensities, where the normalized vector potential associated with the laser wave exceeds unity, the electron axial velocity modulation due to radiation pressure yields nonlinear Compton backscattered spectra. For applications requiring a narrow Doppler upshifted linewidth, such as the future γ-γ collider or focused X-ray generation, this can pose a serious problem. It is shown that temporal laser pulse shaping using spectral filtering at the Fourier plane of a chirped pulse laser amplifier, or similar approaches, can alleviate this problem, and that this technique can be scaled to the required multi-TW range. Compton backscattered spectra are derived in three cases: hyperbolic secant, hybrid pulses (hyperbolic secant transient and flat-top), and square optical pulses similar to those experimentally obtained by Weiner et al. It is found that the optimum laser pulse shapes correspond to square pulses, yielding a high contrast ratio between the main spectral line and the transient lines. The corresponding spectral filter function is also determined, and its practical implementation in a CPA laser is addressed.

Work supported by DoD/AFOSR(MURI) F49620-95-1-0253, AFOSR (ATRI) F30602-94-2-001, ARO DAAHO4-95-1-0336, and LLNL/DRD DoE W-7405-ENG-48 IUT B335885.

*Also with Nonlinear Technologies, Oakland, CA

6A08

Compact, High Efficiency Drifting Electron Laser Powered by Slow-Wave Wiggler

S. Riyopoulos
Science Applications International Corporation McLean, VA 22102

A tabletop Drifting Electron Laser in a partitioned cavity is proposed. (Sub)mm electrostatic magnetron-type waves are excited in the lower portion of the cavity powered by an emitter cathode. These waves serve as a high power short wavelength wiggler in the upper partition, where relativistically upshifted radiation is produced by the passing of an $\mathbf{E} \times \mathbf{B}$ drifting beam. The device combines, (a) higher wiggler strength α_ω under given power relative to fast wave EM wigglers [1], (b) lower sensitivity to thermal spreads and higher electronic efficiency than the $1/2N_\omega$ FEL limit, due to the DEL principle [2], (c) a compact size comparable to Smith-Purcel FELs [3].

[1] S. Riyopoulos, Phys. of Plasmas **2,** 3526, 1995.

[2] S. Riyopoulos, Phys. of Plasmas **3**, 3528, 1996.

[3] S. Riyopoulos, Submitted Phys. of Plasmas, 1997.

Wednesday Afternoon, 21 May 1997
3:00 p.m. – Board Room

Oral Session 6B:
4.5 Fast Z-Pinches and X-Ray Lasers
Chair: M. Douglas

6B01

Numerical and Experimental Studies of Magnetic Rayleigh-Taylor Instabilities in Sold Liners*

R.J. Faehl, W.L Atchison, R.E. Reinovsky and D.V. Morgan
Los Alamos National Laboratory, Los Alamos, NM 87545

We have studied the nonlinear evolution of Magnetic Rayleigh-Taylor (MRT) instability in solid aluminum liners. Two-dimensional MHD modeling of the configuration have been performed using the measured current pulseform of the PEGASUS II capacitor bank as a magnetic field source. The liner configuration consisted of

a solid aluminum annulus 20 mm long and 0.4 mm thick. The outer surface of the liner was machined with a sinusoidal ripple. Half of the liner was scribed with one wavelength, the other half with another wavelength. A series of experiments was conducted with a smooth surface and ripple wavelengths of 0.5, 0.75, and 2.0 mm. The peak-to-peak ripple amplitude was varied between 0.025 and 0.10 mm, but the ration of the initial amplitude to wavelength never exceeded 7%. Diagnostics consisted of radiography, a center-conductor B-dot probe, and transmission line pulsed power diagnostics. The inner surfaces of the liners were coated with a thin film of gold (Au) to permit measurement of material deformation at various stages of the instability growth. Three radiographs, at different times, were taken for each experiment. The center-conductor magnetic probe was used to measure the magnetic field penetration through the liner. Initial comparisons between the data and the MHD calculations showed excellent agreement with respect to nonlinear instability growth and with the time of field rupture of the liner.

*This work performed under the auspices of the U.S.D.O.E.

6B02-03 *Invited*

Optimization of Array Radius, Mass and Wire Number for Tungsten Arrays

C. Deeney, D. L. Peterson*, R. B. Spielman, T. Nash, G. Chandler, M. R. Douglas, D. Fehl, J. Seaman, K. Struve, W. A. Stygar, J. McGurn, D. Jobe, T. Gilliland, J. Torres, R. Mock, T. W. L. Sanford and M. K. Matzen
Sandia National Laboratories, MS-1194, Albuquerque, NM 87185-1194

On the 7-MA Saturn generator, we produced 4-ns duration, 75 TW x-ray power pulses using tungsten wire arrays.[1] The radiated power increased as the wire number increased, as the velocity increased and/or as the wire size decreased.[1,2] 2-D, 3-T radiation MHD calculations[3] indicated that the wire size decrease could be represented by a decrease in the initial seeding of R-T instabilities. These calculations also showed that the increased collapse velocities result in higher electron temperatures. Initial experiments with 40-mm, 120 and 240 wire arrays on the 18-MA PBFAZ generator[4] have produced 1.85 MJ, 160 TW of x-ray power in a 8.5 ns pulse. In this paper, we will present the scalings from Saturn to PBFAZ and results from and calculations of a radius scan that will optimize the output power by varying the implosion velocity (hence electron temperature and density) and the electrical coupling to the load.

Work supported by DOE.

[1] C. Deeney et al, submitted to P.R.E. (1996)
[2] T. Sanford et al, P.R.L. **77**, 5063 (1996)
[3] D. Peterson et al, Phys. Plasmas **3**, 368, (1996)
[4] R. B. Spielman et al, BEAMS 96

* Los Alamos National Laboratory, MS B-259, Los Alamos, NM 87545

6B04

Recent Z-Pinch Experiments on ACE 4*

P.L. Coleman, J. Rauch, W. Rix and J. Thompson
Maxwell Technologies Inc., San Diego, CA 92123

ACE 4 is a 4 MJ, 2 microsecond risetime, inductive-energy storage (IES) generator equipped with typical diagnostics including calorimeters, time-resolved sensors (PCDs, XRDs, and silicon PIN diodes), and imagers (pinhole and spectra). ACE 4 uses a plasma opening switch (POS) to drive a close-coupled z-pinch at currents of well over 3 MA. Current flows in the annular-plasma column of the POS for up to a microsecond and is then commutated to the central gas puff.

Previously reported experiments[1,2,3] discussed initial experiments using neon. This paper will present recent results using argon and argon-chlorine gas mixtures, emphasizing long implosion times (>200 ns), large initial radii (>3cm), and non-shell (solid fill) gas distribution.

*Work supported by the Defense Special Weapons Agency

[1] J. Thompson, P. Davis, H. Murphy, N. Loter, J. Rauch, E. Waisman, and K. Ware, Bull. of the Amer. Phys. Soc. 34, 1943 (1989).
[2] Thompson, et al, ICOPS 95, Paper 5A08, 1995.
[3] Coleman, et al, ICOPS 95, Paper 5A09, 1995.

6B05-06 *Invited*

Modeling Z-Pinch Implosions in Two Dimensions

D. Peterson, R. Bowers, J. Brownell, C. Lund,
W. Matuska, K. McLenithan, H. Oona, T.Scannapieco
Los Alamos National Laboratory, MS-B259
Los Alamos NM 87545
C. Deeney, M. Derzon, R.B. Spielman, T. Nash,
G. Chandler, R. Mock, T.W.L. Sanford, M.K. Matzen
Sanida National Laboratories, MS-1194
Albuquerque NM 87185-1194
N.F. Roderick
University of New Mexico, Alburquerque, NM 87131

Ideally, simulations of Z-Pinch implosions should provide useful information about important physics processes underlying observed experimental results and provide design capabilities for future experiments. With this goal we have developed a methodology for simulating hollow Z-Pinches in two dimensions and applied it to experiments conducted on the Pegasus I and Pegasus II capacitor banks, the Procyon explosive generator system, and the Saturn and PBFA-Z accelerators. In comparisons with experimental results the simulations have reproduced important features of the current drive, spectrum, radiation pulse shape, peak power and total radiated energy. Comparison of the instability development in the simulations with visible light framing camera photos has shown a close correlation with the observed instability wavelengths and amplitudes. Using this methodology we are analyzing recent Saturn and PBFA-Z experiments and applying the 2-D modeling in developing applications such as the "dynamic hohlraum".

Work supported by DOE.

6B07

Design and Simulation of Stabilized Z-pinch Loads with Tailored Density Profiles

A.L. Velikovich and F.L. Cochran
Berkeley Research Associates, Springfield, VA
J. Davis
Naval Research Laboratory, Washington, DC

We discuss the design of structured Z-pinch loads capable of mitigating the detrimental effect of Rayleigh-Taylor (RT) instability on the performance of fast Z-pinch devices used as plasma radiation sources. We demonstrate that using a structured gaseous load with a radial density profile specifically tailored for a given current wave form, it is possible to delay the onset of the RT instability development for as long as it takes for a shock wave to propagate through the load. Suppression of the RT instability is due to inverted acceleration of the interface between magnetic field and the plasma [1]. Once the acceleration is inverted, perturbations are shown to oscillate rather than to grow exponentially. Our simulation results indicate the possibility of high-quality implosions producing significant Ar K-shell yield from initial radii in the range between 4 and 8 cm, with current pulse duration of 250 ns and longer. The stabilizing effects of current pulse shape (the higher the current rise rate, the better), of the axial (the hourglass effect [2]) and the azimuthal (current switching [3]) density tailoring will be also discussed.

[1] A.L. Velikovich *et al.*, Phys. Rev. Lett. 77, 853 (1996).

[2] M.R. Douglas *et al.*, Bull. Am. Phys. Soc. **41**, 1469 (1996).

[3] J. Davis *et al.*,Appl. Phys. Lett. **70,** 170 (1997).

6B08

Solid Liner Compression of Working Fluid to Megabar Range

J.H. Degnan, S.K. Coffey[1], D.G. Gale[2], J.D. Graham[2],
T.W. Hussey, G.G. Kiuttu, B.B Kreh, F.M. Lehr,
D. Morgan, R.E. Peterkin, D. Platts[3], E.L. Ruden,
W. Sommers[2] and P.J. Turchi
High Energy Sources Division,
Phillips Laboratory, Kirtland AFB, NM

We have used 12 megamp, 5 megajoule axial discharges to electromagnetically implode tapered thickness spherical Aluminum shells, achieving peak implosion velocities above 20 km/sec inner surface, 10 km/sec thickness averaged. The shell thickness was proportional to the inverse of the square of the cylindrical radius. This causes the ratio of magnetic pressure to shell areal mass density (and spherical acceleration) to be independent of polar angle, so that the spherical shape is nominally maintained during the implosion. We have used these implosions to compress hot hydrogen plasmas with initial pressure about 100 atm and initial temperature above 1 eV. The hot hydrogen plasmas were injected beforehand using 1 megamp, 100 kilojoule range co-axial gun discharges through a circular array of vanes to strip away magnetic field. The imploding shell and the compressed hot hydrogen working fluid's effect on a diagnostic compression target were observed with

radiography. Interior magnetic probes and auxilliary shots without working fluid injection were used to confirm that there is no magnetic field interior to the imploding Aluminum shell. Thus, diagnostic target compression, which was observed in working fluid compression experiments, was presumably due to the compressed hot hydrogen pressure. We obtained radiographs at 7 different times during the implosion discharge, from 3 shots with the same operating parameters. 3 of these radiographs were from the same shot. From these, it is possible to obtain average compressed working fluid pressure over time intervals observed by 3 radiographs. This data suggests that the compressed fluid pressure exceeds a megabar approximately 0.1 microseconds prior to contact of the imploding liner inner surface with the diagnostic target outer surface.

[1]NumerEx, Albuquerque, NM
[2]Maxwell Technologies, Inc., Albuquerque, NM
[3]Los Alamos National Laboratory, Los Alamos, NM

6B09

Optimization of the Hard X-Ray Yield from a Heterogeneous Z-Pinch

L.I. Rudakov
RRC Kurchatov Institute, 123182 Moscow, Russia

Conventional Z-pinches are known to be an effective source of soft X-rays [1,2]. However, this approach has limited control in redistributing the radiation spectrum, specifically toward the hard X-Ray regime where photon energies are >10 keV. The generation of such energetic photons requires both high densities and temperatures in the plasma. Due to the Rayleigh-Taylor instability and current (mass) limitations, these plasma conditions are difficult to achieve simultaneously. To produce a harder emitted X-ray spectrum, the "Liner-Converter" scheme was proposed at the Kurchatov Institute [3]. This technique uses the thermal flux from the end of a low-Z pinch to rapidly heat a thin, high-Z converter linked to the edge of the pinch. A temperature of 10 keV can be achieved in the converter by fast and efficient heat transfer from the low Z-pinch liner; this results from the strong dependence of thermal flux on electron temperature. Using a low-Z pinch liner minimizes radiation losses and instability growth, while maximizing end-losses to the converter. By employing a separate converter, there is flexibility in choice of materials and radiator geometry. Computer simulations of this concept and experiments on the 3 MA, S-300 generator will be presented.

[1] Quintenz, J.P. et al. In Proc. 11th Int. Conf. High Power Particle Beams ("Beams-96"), Prague: Czech Rep. Acad. Sci., Vol. 1 p.1 (1996)
[2] J. Davis et al. Ibid., Vol. 2 p. 709
[3] L.I. Rudakov et al. Phys. Fluids B, 3, 2414 (1991)

6B10

ZETA-Code for 2-D Complete Simulation of Radiative Z-pinch and Liner Implosion

S.V. Zakharov, A.G. Lisitsyn, A.A. Otochin,
A.N. Starostin, A.E. Stepanov, V. Roerich
Troitsk Institute for Innovation and Thermonuclear Investigations, Troitsk, Moscow Regio, Russia
A.F. Nikiforov, V.G. Novikov, A.D. Solomyannaya
Keldysh Institute for Applied Mathematics, Russia
V.A. Gasilov, A.Yu. Krukovskii
Institute for Mathematical Modeling, Russia

The ZETA-code is developed for the complete simulation of 2-D multicharged ion plasma magneto-hydrodynamics and radiation. The code consists of three main parts: preprocessor, core processor, and postprocessor.

The code ZRMHD is a core processor of the ZETA-code. It is designed to perform simulations of 2-D axially symmetrical magnetohydrodynamic flows of radiative plasma. The module AERG is introduced into ZRMHD for multigroup radiation transport calculations in the semi-analytical self consistent model. The ZRMHD uses as a rule tables for EOS, opacities, emissivities and plasma electron transport coefficients prepared by THERMOS pre-processor of the ZETA-code.

The ZRMHD involves mathematical model, physical model and control visual system. The mathematical model is based on implicit Newton-type iterative algorithms in the fully conservative difference scheme, in Euler-Lagrange variables with automatic values recalculation to the grid changed and algorithms of a grid reconstruction. The energy balance calculation is carried out for the convergence control during the solution of discrete MHD equations. The physical model includes the quasi neutral plasma magnetohydrodynamics with 3-D magnetic field, energy exchange between "electron" plasma component and the "heavy" one (i.e., ions and neutrals), finite conductivity, heat transport, Hall effect, multigroup radiation transport, LTE to non-LTE approximation.

The THERMOS code is used as a preprocessor of the ZETA-code to calculate opacities, emissivities and

equation of state for LTE and non-LTE high-temperature plasmas. The code gives the possibility to obtain Tables of radiative and thermodynamic properties in a wide range of temperatures and densities for arbitrary materials and mixtures. The Hartree-Fock-Slater quantum-statistical model of self-consistent field for the matter is most widely used in the code with Dirac equation for atomic shells. The exchange effects are included in local density approximation. Bloch-type periodical conditions are used in the average sphere approximation. For electron states with energy more than effective boundary of continuum chosen to fulfill thermodynamical consistency the semiclassical approximation is used. For opacity calculations the ion states probabilities are obtained from a renormalized Gibbs-type distribution.

The postprocessor code ERAYZETA for the 2-D MHD code ZETA was designed for fast simulation of X-ray radiation detailed spectra from high-Z plasma. It allows to trace arbitrary straight observation ray in 3-D geometry with cylindrical symmetry; to calculate populations of ion levels within the framework of collisional-radiative model, atomic model, atomic models for for H-, He-, Li-, Be-, B-, C-, N- and Ne-like ions are supplied; to solve radiation transfer along the observation ray both in continuum and spectral lines with simulation of Doppler effect in a moving plasma. Simulation results for Double Liner and radiative Z-pinch are presented.

Wednesday Afternoon, 21 May 1997
3:00 p.m. – Toucan Room

Oral Session 6C:
1.4 Computational Plasma Physics II
Chair: G.R. Joyce

6C-01

A Beam-RF Simulation Technique Based on Evolutionary Amplification Equations*

Robert H. Jackson
Naval Reseach Laboratory, Washington D.C. 20375
jackson@mmace.nrl.navy.mil
Phone (202) 767-3936

Present TWTA beam-RF simulation techniques fall into roughly two categories, particle-in-cell (PIC) and "envelope." The PIC methods tend toward "full-physics/ geometry" and usually require considerable computational resources. The "envelope" methods are usually parametric physics/geometry and assume *a priori* knowledge of the solution, *e.g.* harmonic time and/or space dependence, in conjunction with an amplitude/phase function which depends solely on z or t. The gulf between these two approaches can sometimes be considerable and unacceptable. This paper will present a computational methodology which bridges the simulation cost/accuracy gap.

One problem which occurs with envelope-type methods is the requirement to treat certain particle fields (i.e. ac and dc space charge) and RF fields either incompletely or differently from the main RF fields. This is caused by the evanescent nature of some of the ODEs resulting from the "envelope" assumptions. This paper will present a stable numerical algorithm for integrating the simplest canonical form of the driven evanescent equation (DEE). This algorithm permits treatment of all fields, purely RF as well as space charge related, on a similar footing and with similar (selectable) degrees of fidelity. The overall simulation strategy is based on orthonormal eigenfuction (of the transverse Laplacian operator) expansion of all fields and self-consistent numerical solution of the resulting system of beam/field ODEs. Amplifier problems are addressed in an axial-evolutionary format in which all fields are self-consistently solved in a transverse plane as the plane is shifted axially. Thus storage requirements are more in line with 2D rather than typical 3D codes. At present, only geometries having boundaries which do not vary axially have been addressed. The DEE algorithm will be presented along with results to date on extension of the method to more complex boundary dependencies.

*Work supported by the Office of Naval Research.

6C02

Simulation of Stratified Nonequilibrium Gas-Plasma Flow in a Strong Magnetic Field

V.S. Slavin, K.A. Finnikov
Krasnoyarsk State Technical University
Krasnoyarsk, Russia
V.V. Danilov
Krasnoyarsk State University,
79 Svobodny,Krasnoyarsk 660041, Russia

The task of simulation of the magnetohydrodynamic process in the nonuniform gas-plasma flow driving recombinated plasma clots is solved. The different types of

diffusive discharge present in the noble gas flow simultaneously. The glow discharge exists in the driving low-ionized gas and the nonequilibrium arc discharge—in the high-ionized plasma clot. For the process simulation the universal kinetic model of the nonequilibrium plasma of noble gases is created, describing the multilevel ionization and recombination kinetics in the framework of the modified diffusional approach. The model takes into account the most important processes for the dense low temperature plasma: collision excitation and de-excitation and the processes with the participation of the molecular ions. The deviation of the electron energy distribution function from the maxwellian one was taken into account also. The kinetics equation included the ambipolar diffusion and the wall losses of electrons. This model allowed to describe the both types of discharge uniformly.

Testing of the model by comparing of the experimental data with the calculated ones has shown, that it works correctly in the case of the glow discharge as well as in the case of the arc one and also gives the satisfactory result in the intermediate field of the contracted discharge. The results of simulation of the MHD processes has shown high efficiency of the energy transformation in the nonuniform flow and the plasma clots stability in respect of the ionizing-overheating instability.

6C03

A New 3D MHD Algorithm Using a Boltzmann-Like Distribution Function

J.D. Huba
Plasama Physics Division, Naval Research Laboratory
Washington, DC 20375

A new three-dimensional magnetohydrodynamic code has been developed. The 3D MHD equations are solved in conservative form. The code is finite-volume and the hydrodynamic variables are updated in a cell by calculating fluxes across the cell interfaces. The novel feature of the code is that the fluxes of mass, momentum, and energy across cell interfaces are calculated by integrating in velocity space using an appropriate Boltzmann-like distribution function. The electric field along cell edges, which is used to update the magnetic field, is also computed using the Boltzmann-like distribution function. A nonlinear switch between an eighth-order spatial scheme and a low order scheme is used based upon the partial donor cell method (*Hain,* 1987). The temporal scheme is accurate to second order. Results will be presented for the Brio-Wu shock problem (*Brio and Wu*, 1988) and compared to other schemes (e.g., FCT). An important aspect of the method is that it can be generalized to incorporate modifications of the 3D MHD equations (e.g., anisotropic ion stress tensor, the Hall term).

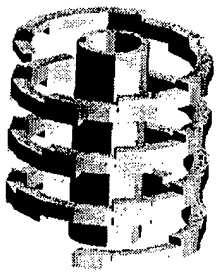
Hain, K., *J. Comput. Phys. 73*, 131 (1987).
Brio, M. and C.C. Wu, *J. Comput. Phys 75*, 400 (1988).

6C04

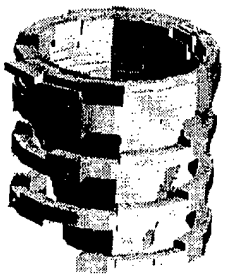
Numerical Simulation of a Helical, Explosive Flux Compression Generator

D.E. Lileikis
Phillips Laboratory, Kirtland AFB, NM

Explosive generators can be used to produce current and voltage waveforms that can be used for a variety of applications including acceleration of a plasma and solid projectiles. In this study, the Phillips Laboratory's parallel, 3D MHD code, **MACH3** was used to simulate an explosive flux compression generator with a helical, outer stator. The code uses an interface tracking capability to follow the movements of the armature and stator. An integrated circuit solver predicts the voltage and current increase during the detonation. These initial simulations will ultimately lead to the simulation of an actual device used by the Phillips Laboratory.



Pre-Detonation



Mid-Detonation

6C05

An Advance Implicit Algorithm for MHD Computations of Parallel Architectures*

U. Shumlak, D.S. Eberhardt, O.S. Jones and B. Udrea
University of Washington
Department of Areonautics and Astronautics
Box 352250, Seattle, Washington 98195-2250

This paper will describe an advanced implicit algorithm for parallel supercomputers to model time-dependent magnetohydrodynamics (MHD) in all three dimensions. The algorithm is a finite volume implementation of a Roe-type approximate Riemann solver with central differenced diffusive terms combined with a lower-upper symmetric Gauss-Seidel iterative method. The ideal MHD equations are hyperbolic, but the addition of non-ideal effects such as resistiveity and viscosity changes the equation's mathematical form to mixed hyperbolic-parabolic. The approximate Riemann solver is well suited for tracking discontinuities in the plasma that arise due to the hyperbolic nature of the MHD equations, and a nested finite volume method is used to track the diffusive nature of the parabolic terms. An iterative solver provides the freedom to choose large time steps. The algorithm also works well for steady-state solutions. In addition to describing the algorithm and its parallel implementation, applications will be presented.

*This work was supported by the U.S. Air Force Office of Scientific Research under grant AFOSR-F49620-96-1-0160.

6C06

MAG—Two-Dimensional Radiation Resistive MHD Code, Using Arbitrary Moving Coordinate System

Oleg V. Diyankov, Igor V. Glazyrin, Serge V. Koshelev, Natali P. Savina
Russian Federal Nuclear Center,
All-Russian Institute of Technical Physics
P.O. Box 245, Snezhinsk, Chelyabinsk Region, Russia

The MAG code for the 2D radiative plasma flows in magnetic field is presented. The algorithm has been formulated for an arbitrary moving coordinate system. The code has some interesting features, which allow to simulate MHD plasma flows with large deformations inside the flow region, conserving the correct description of its weakly deformated boundaries.

The model, realized in the code, contains terms for the description of the following phenomena: spontaneous magnetic fields, Hall effect, magnetizing of transport coefficients, kinetics of ionization, radiation transfer.

The code has been used for inertial fusion modeling and plasma liners implosion modeling.

The work is supported partially by ISTC, projects #107, #009, #350. The authors are grateful to Dr. Vadim Yu. Politov for his work on the ionization kinetics model development, and useful discussions of the received results.

Wednesday Afternoon, 21 May 1997
3:00 p.m. – Macaw Room

Oral Session 6D:
4.4 Dense Plasma Focus II
Chair: D. Lileikis

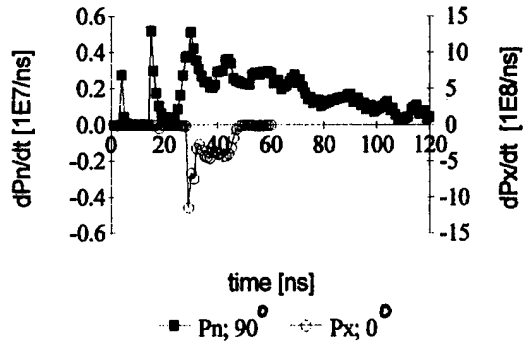
6D01

Time Resolved Neutron and Hard X-Ray Emission in the Dense Plasma Focus, Revisited (*)

J.S. Brzosko, V. Nardi, C. Powedll and J.R. Brzosko
Compton Research Laboratories, New York, NY

The time dependence of the MeV ion abundance can provide critical information on acceleration mechanisms in the dense plasma of focused discharges. Time resolved measurements of neutrons and hard X-rays are used to gauge the time evolution of ion population. The plasma focus (7 kJ; 17 kV) chamber was filled with O_2 (10%) and D_2 (90%) mixture. Time resolved measurements were done at different distances from the pinch (L) and at different angles (θ) from the electrode axis by NE102 (L = 0.15 m; $\theta = 0°$) and NE111 (L = 3.8 m; $\theta = 0° \& 90°$) plastic scintillators. Time integrated absolute measurements of total yield of $D(d,n)^3$ He and $^{16}O(d,n)^{17}F$ nuclear reactions were used to establish population of low ($E_i < 0.5$ MeV) and high ($E_i > 2$ MeV) energy ions. Measured neutron and HXR signals ($E_x \geq 100$ keV) were unfolded to recover the real time resolved emission signals P_n & P_x, respectively [1]. Figure shows a typical example of emission pattern identifying: (i) precursor of neutron emission, (ii) pronounced spike of neutron emission coincident with the

HXR emission spike, and (iii) following emission of bulk neutrons with strong intensity structure. Interpretation of the results in frame of the PDER model [2] will be presented.



* Work was supported in part by AFOSR, grant F49620-95-1-027.

[1] J.S. Brzosko et al., ICOPS '96, p. 238 (4D07);

[2] J.S. Brzosko and V. Nardi, Phys. Lett. A155(1991) 162

6D02

Current-Sheath Oscillations and Reactivity in Focused Discharges*

A. Bortolotti, P. De Chiara, P. Desiderio and F. Mezzetti
University of Ferrara, 44100 Ferrara, Italy
V. Nardi and C. Powell
Compton Laboratories, New York, NY 10301

Oscillations of the current sheath driving force $\underline{J} \times \underline{B}_\theta$ and of its propagation velocity v strongly bear on the maximum energy E_M of the accelerated ions and on the D + D neutron yield Y in the PF pinch. Magnetic probe (MP) signals $|dB_\theta/dt|$ provide the amplitude Δv of the velocity oscillations during the radial implosion phase of the current sheath. The relative amplitude $\Delta v/v \simeq \Delta|dB_\theta/dt| / [|dB_\theta/dt|] \simeq 25\% \pm 15\%$ of the oscillations and their period $T \simeq 35$ ns $\pm$ 17 ns, determined via MP with greater accuracy than ever before, agree with previous measurements via (i) long-exposure–time schlieren imaging and (ii) secondary peaks of the electrode current (I) signal $|dI/dt|$ from a Rogowsky coil between the electrode back plates. If the oscillation of v has an amplitude minimum at $t = t_0 - T$, where t_0 is the time of the sharply defined peak in the $|dI/dt|$ signal, Y is usually higher by a factor $\simeq 4$ than the typical value Y_{av} from discharges where this phase condition is not satisfied. One probe, MP1, is outside the electrode gap, at a radial distance r = 17 mm from the electrode axis, and at $z_1 = +14$ mm from the electrode muzzle end. A second probe, MP2, is located inside, between the electrodes, at $z_2 = -11$ mm. Different values of the filling pressure and three configurations of the electrodes [coaxial cylinders, and two funnel profiles with angular aperture 16° and 30°] were used to assess the generality of the results. Maximum of Y (and of E_M) are achieved when a two stage reduction of I occurs, characterized by maximum drop at t_0 of the MP2 signal (maximum negative peak), with a smaller amplitude peak at $t_0 + T + \Delta T$, and maximum drop at $t_0 + T + \Delta T$ ($\Delta T < 10$ ns) of the MP1 signal, with a smaller peak at t_0. The data lead to discrimination of amperian from displacement current.

* Work supported in part by ENEA, INFM, MURST at Ferrara Un. and by AF-OSR under Grant F49620-95-1-0271 at Compton Labs.

6D03

Fine Structure of Ion-Cluster Disintegration Modes in PF Discharges*

V. Nardi, C. Powell
Compton Laboratories, New York, NY 10301
C.M. Luo
Electrical Engineering Deptartment, Tsinghua University, Beijing, P.R. China

A characteristic of the disintegration mode of ion clusters and superclusters is the pairing of the D_2+ ions, which form the bulk of the ion population emission at 67° from the axis of a plasma focus discharge. A Tohmson (parabola) spectrometer is used for the determination of ion and ion cluster species and of their energy spectrum. The parabolic pattern of each ion species is recorded on a CR-39 target, with ion track etching in NaOH solution.

A second characteristic of the cluster disintegration mode is that each D_2+ ion pair, or each linear sequence of ion pairs, is aligned in the direction orthogonal to the parabolic pattern, at the point where the tracks are located. The D_2+ pairing is directly related to the cluster disintegration mode and not to D_4++ disintegrations because the di-cations D_4++ are not stable and cannot exist outside a heavy cluster or a supercluster. Consistently with this finding, a necessary condition to be satisfied by one of the leading forces, F_d, involved in the cluster disintegration process is $|F_d| \simeq E^2/vB$, where v is the velocity of the cluster entering the spectrometer fringe field, and E, B are the spectrometer electric and magnetic

fields (E // B is applied on the spectrometer magnet poles). Details of the disintegration mechanism are established by the comparison of the D_2+ distribution on the target, with the typical supercluster deformations established in the magnetic-field fringe region, as recorded by earlier measurements.

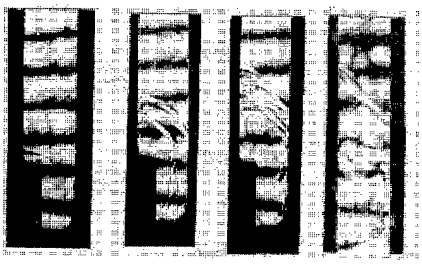
* Work supported in part by AF-OSR, DC, under Grant F49620-95-1-0271

6D04

Relation Between Filamentary Current Sheath and Ionization Energy in a Plasma Focus

Ming-fang Lu
Institute of Physics, Chinese Academy of Sciences, Beijing 100080, P.R. China

Since the discharge current I growths in a sinusoidal form in a plasma focus, one can predict, according to Ref. [1], the formation of filamentary current sheath (CS) in the breakdown and early rundown phases when I is small and the specific plasma energy $\varepsilon < 1$ MJ/g, the energy required to ionize the whole swept gas. This has been verified by the experimental results obtained on a small Mather-type plasma focus device (20 kV, 18 kJ) with use of a laser differential interferometer, Figs. (a) to (d), I = 23-270 kA (I_{max} = 350 kA), p_{D2} = 2.5 torr for neutron emission. The uniform initial CS (a) formed along the insulator surface soon develops into filaments (b) during moving towards the outer electrode driven by the Lorentz force. It then develops into muddled filaments (c) after crosses the coaxial electrodes. Later the filaments re-join to form a uniform CS ((d), I > 200 kA) which accelerates towards the open end of the coaxial gun and forms the pinch there.



(a) t=0.2 μs (b) 0.5 μs (c) 1 μs (d) 1.6 μs

Fig. Interference images, exposure time 10 ns

[1] M. Milanses, R. Moroso, and J. Pouzo, IEEE Trans. Plasma Sci., 21 (1993) 606

6D05

Effect of Anode End Structures on Plasma Pinching in a Plasma Focus

Ming-fang Lu
Institute of Physics, Chinese Academy of Sciences, Beijing 100080, P.R. China

It is known that in the plasma focus the anode (CE) end structure influences the current sheath (CS) implosion and pinching, which then influences the neutron yield. However, the correlation among them is not very clear. This problem is investigated on a small Mather-type plasma focus device (20 kV, 18 kJ) with use of a laser differential interferometer. The results show that the usually used anodes can be roughly grouped into three interrelated series derived from a basic flat-ended solid one according to their effects on the plasma motion: 1) the hollow series for the anode hole; 2) the stub series for the stub and 3) the hemispherical series for the anode edge geometry. The hollow series (the solid anode is of zero hole diameter) affects the CS implosion by the stagnation of the hole edge on the radial movement of its sliding front. A hollow anode with a proper hole diameter forms a uniform pinch which contacts with the anode through an extended CS and is in a purely magnetically confined state, and produces higher neutron yield (Y_n=(2.8 ± 0.6) × 10^8 per shot). The stub series negatively affects the pinching dynamics by seriously deteriorating the CS status just before pinching. The neutron yield is lower and largely deviated (Y_n=(0.93 ± 0.65) x 10^8 per shot). For the hemispherical series, a larger transition radius R at the anode edge helps to avoid sudden change of the CS motion from the axial acceleration to the radial implosion and helps to form a better pinch. For R=40 mm the neutron yield is highest (Y_n =4.9 x 10^8 per shot, $Y_{n,max}$=10^9 per shot). In addition, the magnetic field introduced in front of the CS by an anode end discharge initiated by the "needlepoint"-like erosion structure is also found to have stabilized the imploding CS, which is advantageous to the pinching dynamics and the neutron yield.

6D06

Spatial Distribution of the High Energy Density Plasma in a Coaxial Gun for Surface Modification

Ming-fang Lu, Si-ze Yang and Chi-zi Liu
Institute of Physics, Chinese Academy of Sciences, Beijing 100080, P.R. China

The coaxial plasma gun, by generating the pulsed High Energy Density Plasma (HEDP) with a simple method, is an effective method for materials surface modification. It incorporates fast quenching, ion implantation and film deposition into one process, and produces a modification layer of strongly adhesive to the substrate. The spatial distribution of the plasma stream ejected from the coaxial gun determines the surface modification. In this paper, this problem was investigated on a 40 kV gas-puff coaxial plasma gun by using thermal sensitive (Fax) paper and dosimeter. The operation parameters of the gun include: charging voltage from 25 to 30 kV (capacitance C=4 x 4.5 μF), graphite electrodes. Nitrogen gas (p=1.0 atm) is puffed into the bottom of the electrode gap by a fast electromagnetic valve. The typical plasma parameters include: T_e=10–20 eV, n_e=(5–70) × 10^{13} cm^{-3}, directed velocity v=10–50 km/s, pulse duration τ=10–100 μs, power of energy deposition P_d=10^4-10^5 W/cm^2, deposited energy E_d=1–10 J/cm^2. The results show that for the 25 kV charging voltage, the plasma is uniform with a diameter of larger than 8 cm in the cross section perpendicular to the beam direction within a distance of d=7 cm from the gun muzzle. Beyond this distance, the plasma appears non-uniform. For the 30 kV charging voltage, the distance for the uniform plasma distribution extended to beyond d=17 cm. The results also show that to produce a uniform modification surface and C-N film, the substrate should be put within the uniform plasma region.

Wednesday Afternoon, 21 May 1997
3:00 p.m. – Cockatoo Room

Oral Session 6E:
7.3 Fast Opening Switches
Chair: W. Rix

6E01-02 *Invited*

Plasma Opening Switch Scaling Relationships Derived from Operations in the "Switch Limited" Regime*

R.J. Commisso and B.V. Weber
Plasma Physics Division, Naval Research Laboratory, Washington, DC 20375, USA
W. Rix, P. Coleman, and J. Thompson
Maxwell Technologies Federal Division, 9244 Balboa Avenue, San Diego, CA 92123, USA
D. Kortbawi
Physics International Company, 2700 Merced Street, San Leandro, CA 94577, USA
J. Goyer
Consultant

The Defense Special Weapons Agency has accumulated data on plasma opening switch (POS) operations on a number of different pulse power drivers including HAWK at NRL, DM at Physics International, and ACE 4 at Maxwell resulting in a large data base spanning a wide range of conduction times (200 to 1500 ns) and conduction currents (400 to 5000 kA). In this paper the data is examined to draw conclusions on how POS performance scales over this range when the POS is operating in the "switch limited" regime, i.e. where the POS output voltage is below the voltage which would be generated if all the available current from the POS flowed to the load. By examining the entire data base scaling relationships can be established. Dependent variables such as POS voltage, Flow Impedance, and Gap are examined as functions of Conduction Time, Conduction Current, Plasma Density, and Magnetic Field. The analysis indicates where simple pictures of POS operations appear adequate and where additional independent variables (such as electrode surface conditioning) are required.

*Work supported by the Defense Special Weapons Agency

6E03

Improved Output on Decade Module 1

David Kortbawi
PRIMEX Physics International, San Leandro, CA
John Thompson
Maxwell Labs Inc., Albuquerque, NM
Bob Commisso, Bruce Weber, Paul Ottinger
Naval Research Laboratory, Washington, DC
Mark Babineau
Sverdrup Technologies Inc., Cleveland, OH
John Goyer
Consultant

DECADE Module 1 (DM1) is an engineering development module for the DECADE nuclear weapons effects simulator. It uses a Plasma Opening Switch (POS) with an inductive energy store for the final stage of pulse compression. This paper will report on recent successes in demonstrating the design goals of 20 kRad(Si) over 2500 cm^2 with a 45 ns pulse. This performance is projected for a four module DECADE Quad.

The primary limitations in performance were losses in the switch/load system reducing the current delivered to the load. There also have been indications of significant ion current at the load reducing the efficiency of the energy delivered to the load for making bremstrahlung.

The configuration that was arrived at yielded individual shots in excess of the DECADE requirements. It had a transparent cathode with an extremely hollow tip to minimize ion currents. The converter package/debris shield is also somewhat different from the norm in that there is a 32 mil aluminum sheet as the first layer beam stop. This was put in to minimize contamination of the electrode surfaces from vaporization of organic material in other beam stop materials. It was also found to be important to glean the vacuum chamber using a mixture of 90% argon and 10% oxygen in a glow discharge.

6E04

MACH2 Simulations of Some DECADE Plasma Opening Switch Experiments

Dennis Keefer and Robert Rhodes
University of Tennessee Space Institute, Tullahoma, TN

The DECADE Facility at the Arnold Engineering Development Center (AEDC) is a short pulse high power x-ray generator used for nuclear effects simulation. It uses a plasma opening switch (POS) to produce the high voltage pulse required by the x-ray source. Over the past several years, we at the University of Tennessee Space Institute have used the MACH2 computer code to simulate several experimental POS configurations proposed for the DECADE Facility. It was found that the Hall effect must be included in an MHD code in order to simulate the opening physics. When the Hall effect is correctly implemented in the code, the simulations predict time-delay and voltage characteristics which compare favorably with the experimental results. Cableguns are used for initial plasma injection into the DECADE POS. The current MACH2 simulations use an empirical model based on experimental measurements of cablegun velocity and density to simulate this injection process. Our current efforts to model the cablegun plasma source are described. The methodology and limitations of the newly developed Hall algorithm are described and the simulation results are compared with experimental measurements for several POS configurations.

6E05

Observation of EMH Effects in a Tri-plate POS*

J.M. Gossmann, B.V. Weber, R.A. Riley[a], T.G. Jones[b], and S.B. Swanekamp[c]
Plasma Physics Division, Naval Research Laboratory
Washington, DC, 20375-5346

Experiments on the Hawk generator using a tri-plate plasma opening switch (POS) and an 8-channel interferometer have shown that for the same initial plasma distribution the POS behaves differently depending on whether the center plate of the triplate is pulsed at positive high voltage (positive polarity) or negative high voltage (negative polarity)[1]. In positive polarity, the conduction time is 50% longer compared with negative polarity operation. Gap formation always occurs near the negative electrode and the evolution of the plasma distribution associated with the JxB forces acting on the plasma during the POS conduction phase is markedly polarity dependent.[1] These observations cannot be explained by MHD only.

In the POS region, the outer plates are slotted to allow the POS plasma into the switch region, while the center plate is solid. One explanation for the different POS behavior might be the fact that the opening occurs near a differently shaped surface for each polarity. However, recent experiments performed with slots in the center plate to replicate the electrode structure of the outer plates give equivalent results to the solid centerplate case.

Fluid simulations carried out with a Hall/MHD code, which accounts for electron magnetohydrodynamics (EMH), suggest that the difference in the POS plasma density evolution during conduction is associated with EMH effects. Local field penetration predicted by EMH can evolve into macroscopic current flow paths and associated **JxB** plasma distortion that are very different depending on the direction of the electron current relative to the density gradient.

*Work supported by DSWA

[1] R.A.Riley, B.V. Weber, R.J. Commisso, and J.M. Grossmann, Bull. Am. Phys. Soc. 40, 1688 (1995).

[a]Present address: LOGICON/RDA, Arlington, VA

[b]National Research Council Research Associate

[c]JAYCOR, Inc., Vienna, VA

6E06

2D Magnetic Field Evolution and Electron Energies in Plasma Opening Switches

R. Arad, A. Fruchtman, K. Gomberoff, Ya.E. Krasik, R. Shpitalnik, K. Tsigutkin, A. Weingarten and Y. Maron
Faculty of Physics, Weizmann Institute of Science, Rehovot, Israel

We present measured time dependent 2-D structures of the magnetic field in two Plasma Opening Switches (on 100 ns and 0.5 μs time scales), together with an analytical model based on EMHD used to explain the data for the short time switch. The magnetic field, local in 3-D, is obtained by doping the plasma with various species and observing the Zeeman splitting of their spectral lines, using polarization spectroscopy. In the coaxial 100-ns switch, fast (~10^8 cm/s) field penetration with a relatively sharp field front is observed, together with a non-monotonic axial distribution later in the pulse. The model developed, that utilizes the measured 2D plasma density distribution and assumes fast field penetration along both POS electrodes, provides quantitative explanation for the observed field evolution. In the planar 0.5 μs switch, a 3-D mapping of the field is obtained. The current channel, 2.5 cm wide, is found to propagate downstream at a velocity ~3×10^7 cm/s. The electron energy in the current channel is studied spectroscopically. The replacement of electrons and the energy dissipation due to the field penetration will be discussed. A comparison of the result for the two time-scale switches and for opposite charging polarities in the coaxial switch will be presented.

6E07

Simulation of a Plasma-Gun Voltage Generator

D.E. Lileikis, P.J. Turchi, R.E. Peterkin, J.H. Degnan, and J.B. Javedani,
Phillips Laboratory / WSQ, 3550 Aberdeen S.E. Kirtland AFB, NM 87117-5776

The Phillips Laboratory's 2 1/2 dimensional magnetohydrodynamics code MACH2 was successfully used to simulate a fast rise time, high voltage generator to drive high impedance loads. The generator operates based on a flux compression scheme using a plasma armature. In this scheme the magnetic flux in the inner region of a solenoid, the seed field, is compressed by the discharge of a high current in a hydrogen prefill.[1]

In simulating the experiment an in-house, time-dependent magnetostatics code, DDcode, was used to generate the seed field. This field was then used to set the initial conditions for the field in the MACH2 simulation. Compression of the field yielded high voltage pulses that were in good agreement with the experiment in the open circuit voltage mode. An external RLC circuit was also added to the code in order to study the load line behavior of the generator.

[1] J.B. Javedani et. al., "A Non-Explosive Pulse Generator," ICOPS 96.

6E08

Inverse-Pinch Flux Compression Generator

J.B. Javedani, D.E. Lileikis, G.F. Kiuttu, J.H. Degnan, and P.J. Turchi
Phillips Laboratory / WSQ, 3550 Aberdeen S.E. Kirtland AFB, NM 87117-5776
J. D. Graham
Maxwell Laboratories Inc., 2501 Yale S.E. Suite 300 Albuquerque, NM 87119

In this work, a non-explosive flux compression generator was designed, built and tested. The device is based on an inverse-z-pinch plasma discharge which is used as the piston field in compressing the seed poloidal magnetic field. The feasibility of non-explosive flux compression generators in driving high impedance loads was demonstrated in an earlier experiment where a coaxial plasma discharge was used in compressing a poloidal seed field.[1] Experimental results are compared to a 0-D slug model and, based on a similar approach described in

reference 2. The Phillips Laboratory's 2-1/2 MHD code MACH2 and the time dependent magnetostatic code DDcode were used to simulate the experiment.

[1] Javedani, J.B., et al., "A Non-Explosive Pulse Generator," ICOPS 96.

[2] Lileikis, D.E., et al, "Simulation of a Non-Explosive Pulse Generator," ICOPS 97.

Wednesday Afternoon, 21 May 1997
3:00 p.m. – Rousseau Center

Poster Session 6P29-32:
2.3 Vacuum Microelectronics

6P29

Characterization of Field Emitter Arrays (FEAs) for a Twystrode Amplifier

M. Garven
IPR, University of Maryland, College Park, MD
M.T. Ngo
Mission Research Corporation, Newington, VA
B.J. Sobocinski and F. Calise
Dyn-corp, Rockville, MD
M.A. Kodis
Code 6843, Naval Research Laboratory
Washington, DC 20375-5347
Tel: 1-202-404-4492 Fax:1-202-767-1280

The Naval Research Laboratory is currently investigating a new class of microwave power amplifiers based on vacuum microelectronic, field emitter array (FEA) technology. Advantages of using FEAs in microwave amplifiers include instant activation, higher transconductance and higher current densities than thermionic cathodes resulting in higher performance gridded microwave power tubes. A twystrode employing an FEA cathode is being designed to operate at 10GHz with 50W output power and 10dB gain. FEAs will be used to generate an electron beam of up to 40mA at 2.5kV with a magnetic field of 5 to 6kG.

Prior to the operation of the FEA cathode in the twystrode, a series of experiments has been undertaken to maximize the beam power and beam transport from the FEA cathode. In these experiments both silicon and metal FEA cathodes are operated under high electric fields of up to 17kV/cm as required to draw average emission current densities ~100A/cm^2. The beam transport experiment, in which a solenoidal magnetic field will focus the electron beam from the FEA cathode through a conducting cylinder substituted for the twystrode circuit, will be discussed. Recent results from FEA experiments along with the status of the future twystrode experiment will be presented.

*Work supported by Office of Naval Research

6P30

Field Emission from HfC or Ni Films Deposited on Single Tip Mo Field Emitters

W.A. Mackie, Tianbao Xie and P.R. Davis
Linfield Research Institute
McMinnville, OR 97128-6894

Field emission from Ni films and from HfC films deposited on single molybdenum field emitter tips made from polycrystalline wire have been investigated. *I-V* data and Fowler-Nordheim analysis show that the work function as well as the tip radius have changed in both cases. The emission turn on voltage was lower by as much a 69 percent for HfC films, but only 5 percent for Ni films. Initially, similar field emission current stability was obtained for both films, however after heating the substrate to 400° C the stability increased for the HfC coated emitters. These tips were next exposed to the air. Emission turn on voltages for HfC films increased after air exposure but they were still lower than those observed for Ni dosed tips. Furthermore, emission stability was better for the HfC coated emitter substrate.

Work partially supported by the Vacuum Microelectronics Initiative under AFOSR Grant No. F49620-95-1-0299.

6P31

Field Emission from HfC Films on Mo Field Emitter Arrays and from HfC Arrays

W.A. Mackie, Tianbao Xie, J.E. Blackwood
and P.R. Davis
Linfield Research Institute
McMinnville, OR 97128-6894

Mo FEAs as well as individually fabricated Mo field emitters were dosed via PVD from a high-purity HfC source. The deposited film was subjected to a variety of heating treatments, followed by FEM examination and determination of *I-V* characteristics. The results of these experiments indicate that work function reductions of the order of 1 eV can be achieved. The observed FEM patterns indicate that the lowest film work functions occur on and around the (100) planes of the underlying Mo emitter.

We also report on our continued experiments with HfC film deposition onto Mo field emitter arrays. In the case of HfC on a Spindt array of Mo cathodes we observed a typical decrease of operating voltage from 121V to 74V for 1000 μA emission current following HfC deposition. These results seem consistent and very promising for the use of HfC films on field emitters and field emitter arrays.

Preliminary work is also reported on the formation of emitting cones by deposition of HfC directly into array blanks. This procedure may be able to provide increased emission stability compared with HfC films on Mo cones.

Work supported by ARPA High Definition Systems Initiative under ONR Grant No. N00014-96-1-1011.

6P32

Computer Simulation of Field Emission Microtriodes with New Volcano-Shaped Emitters

Y. Hu and Y.C. Lan
Department of Nuclear Engineering and Engineering Physics,
National Tsing Hua University
Hsinchu 30043, Taiwan, ROC

A modified volcano-shaped field emitter has been proposed [1] and is being studied using MAGIC particle-in-cell simulation code [2]. This new structure consists of a volcano-shaped field emitter tip, a volcano-shaped gate, and a planar anode. The electric field enhancement at the emitter apex is reportedly due to both the sharp-edged rim of the emitter and the shorter distance between the gate and the rim of the emitter. In addition, electrons emitted from a volcano-shaped emitter form a hollow beam instead of a solid beam, resulting in less beam spread.

In this paper, the dependence of the emission current density distribution upon geometrical factors, for example, rim sharpness of the emitter, rim radii of the gate and the emitter, and the distance between the gate and the rim of the emitter, will be presented. The emission characteristics of this modified volcano-shaped field emitter will be compared with the conventional volcano-shaped field emission microtriodes with con-shaped emitters.

[1] S. H. Yang and M. Yokoyama, 1996 International Electron Devices and Materials Symposia, Hsinchu, Taiwan, December 16-20, 1996.

[2] B. Goplen, L. Ludeking, D. Smithe, and G. Warren, MAGIC User's Manual, Mission Research Corp., MRC/WDC-R-282, 1991.

6P33

Generation and Characterization of Atmospheric Plasma Torch Array

E. Koretzky and S.P. Kuo
Polytechnic University, Farmingdale, NY 11735

Using a capacitively coupled electrical discharge, an array of plasma torches can be produced simultaneously by using a common 60 cycle power source (i.e. a simple wall plug) at atmospheric pressure. The size of each torch depends on the geometry of the electrode pair and the streaming speed of the air flow. Such a flat panel plasma torch array can be made into the desired volume and plasma density.

A laser beam is used to measure the dimensions of the torch. It is found that each torch has a radius of about 1 cm and a height of about 6.5 cm. Surprisingly, it is shown that the torch can cause up to 80% modulation of the laser beam intensity. From the voltage and current measurements, the average power consumption of each torch is estimated to be 0.6 kW. The electron density can also be estimated and is found to exceed 10^{13} cm^{-3}.

The discharge may be represented by a lump circuit. Thus, a computer simulation of the discharge is performed. The results are found to be in good agreement with experimental measurements. Simulations have also been performed to study the dependence of average power consumption of the torch array on its average electron density, with the electron-ion recombination coefficient as a parameter. The study is aimed at developing an efficient large volume dense plasma for industrial applications.

6P34

Numerical Analysis on Plasma Characteristics of High Power Plasma Torch of Hollow Electrode Type for Waste Treatment.

M. Hur, K.D. Kang and S.H. Hong
Department of Nuclear Engineering
Seoul National University, Seoul 151-742, Korea

Waste treatment is certainly one of the most promising areas of thermal plasma application, which aims either at the reclamation of waste materials for recovering higher valued products or at the destruction of toxic wastes and the generation of environmentally safe by-products. The high power plasma torches have been widely used for the incineration of waste materials to pyrolyze organic toxins and the vitrify the solid materials through their volume reduction in a not-leacheable compact state.

In this study, the plasma characteristics of a high power nontransferred plasma torch with hollow electrodes are investigated in the atmospheric condition by analyzing the distributions of plasma temperature, velocity and current density. Typical assumptions of steady state, axisymmetry, local thermodynamic equilibrium (LTE) and optically thin plasma are adopted in a two-dimensional magnetohydrodynamic (MHD) modeling of thermal plasma with a special treatment of arc spot positions. A control volume method and the modified SIMPLER algorithm are used for solving the governing equations numerically, i.e., conservation equations of mass, momentum, and energy along with the equations describing the K-ε model for turbulence and the current continuity for arc discharge.

The distributions of plasma temperature, velocity, and current density are calculated in various operation conditions such as gas species, gas flowrate, input currant, and electrode geometry. The calculated results of plasma characteristics in various operations can be useful to determine the design parameters of the high power plasma torch of hollow electrode type for incinerating the hospital and municipal solid wastes.

6P35

Magnetic Consequences of an Electrostatic Shield Around an Inductively Coupled Plasma Discharge*

J. L. Giuliani and A. E. Robson[1]
Plasma Physics Division
Naval Research Laboratory, Washington, DC
V. Shamamian and R. Campbell[2]
Chemistry Division
Naval Research Laboratory, Washington, DC 20375

An electrostatic shield in the form of a hollow metal cylinder is often placed between the exciting coil and the discharge tube of an inductively coupled plasma system in order to screen the plasma from the electric field of the coil. Such fields can, under some circumstances, have a deleterious effect on the process for which the plasma is being used. It is not generally realized that the electrostatic shield can also lead to a significant reduction of the r.f. magnetic field inside the tube as well as altering its axial distribution. This effect needs to be considered in detailed modeling of inductively coupled plasma system and is of practical importance in determining the impedance the plasma presents to the r.f. generator. We have studied the effect by measuring the r.f. magnetic field inside and outside metal cylinders with different slot configurations and have developed electromagnetic models for both thin and thick shields which give good agreement with the observations. In one of the models the shield can be treated as an axisymmetric diamagnetic medium thereby allowing a 2D treatment of an intrinsically 3D problem. The thick shield is relevant to high power systems in which the discharge tube itself is a thick-walled, water cooled, slotted metal cylinder (i.e., a cold crucible). Plasma coupling in such a system has been compared with coupling in a system with dielectric tube and the predictions of the model have been verified.

---

*Work supported by IST/BMDO and ARPA

[1] Berkeley Scholars, Inc., Springfield, VA 22150-0852

[2] Geo Centers, Inc., 10903 Indian Head Hwy., Ft. Washington, MD 20744

6P36

Simulations of Flux Uniformity for C12, BC13, and N2 Chemistries in the Sandia Inductively Coupled GEC Reactor*

R. Veerasingam[1], S.J. Choi, R.B. Campbell
Sandia National Laboratories, NM 87185

Numerical simulations are performed to estimate the flux uniformity at the wafer surface for various mixtures of Cl2, BCl3 and N2, in the Sandia laboratory ICP reactor. To improve metal etch uniformity, it is desireable that the ion and neutral fluxes have uniform profiles across the wafer surface. We also investigate the effect of a ceramic focus ring on the flux uniformity reactor. The focus ring plays an important role in influencing the boundary conditions for the particle fluxes at the wafer edge thereby effecting the flux uniformity across the wafer surface. Numerical simulations will provide insight into the various conditions that may affect flux uniformity. In addition, we will also perform parametric studies of C12, BCL3 and N2 mixtures for the bulk plasma and compare with experimental data. These simulations will include variations in pressure, mixture ratio and power. The calculations will be performed using the HPEM and MPRES reactor simulation models.

*This work was supported by the United States Department of Energy under contract DE-AC04-94AL85000.

[1] The Pennsylvania State University

Wednesday Afternoon, 21 May 1997
3:00 p.m. – Rousseau Center

Poster Session 6P37-46:
5.3 Plasma for Lighting

6P37

Start-up Phase of the High Pressure Mercury Lamp Feeded by an Alternative Current. Application to the Study of a Dynamic Regime for Lighting Micro-network.

M. Stambouli, K. Charrada and G. Zissis*
ESSTT.5 Av. Taha Husseine 1008 Tunis - Tunisie

The lamps electrical characteristics evolution during their warm-up phases generates variable harmonic currents circulation. These harmonic currents induce, in some cases, constraints that cause ominous effects on the supply network (regime of the neutral, unnecessary losses in ballasts and the transformer of feeding, etc.). To understand and analyze the electrical phenomenon evolution in a lighting network, it is desirable to simulate the lamps-circuit system.

It has been shown that the behavior description of the discharge, in the course of the transitory phase, can be obtained by assimilating this phase to three "phases" successive describe by appropriate models (Phase A corresponding to a non LTE regime, Phase B corresponding to an intermediate regime, Phase C corresponding to a regime close to LTE). From the point of view of the network behavior description, these three phases do not present the same importance. It will be shown, in this work, that the phase C accounts for the essential electrical phenomenon linked to lamps. While during phases A and B the behavior of the system differs few that the one observed when lamps are in short circuit. So, in this work, we have studied the interaction lamp-circuit supplied by alternative current with a variable pressure LTE model that describes the most important phase of the dynamic regime. This phase covers the most interesting electrical phenomenon (variation of the arc voltage of 40 to 150V).

Our simulation allows us to put in obviousness and to evaluate overloads and deformations that appear in the network in the course of its dynamic regime. It allows equally to evaluate ominous deformation effects on the system functioning during this phase (overheating of the transformer, harmonic pollution), constraints whose it is

necessary to take account in the study of a lighting installation. However, the evolution of the neutral current constitutes a good indicator of quality of the network. Finally, it seems to us reasonable to hope that the use of such a model in a supervisions system could allow a best estimate of the network behavior and to improve some management.

*CPAT-UPS 118, rte de Narbonne 31062 TLS-FR

6P38

Cathode Fall Behavior in a Hg-Rare Gas Discharge with a Thermionic Cathode

R.C. Garner and Y.M. Li
OSRAM SYLVANIA INC.
71 Cherry Hill Drive, Beverly, MA 01915

Using a Langmuir probe, we have made cathode fall measurements, over a wide range of discharge parameters, for a barium oxide coated, thermionic emitting cathode in a Hg- Ar discharge. These measurements agree well with the results of a recently developed model.

Cathode fall (plasma potential near the cathode), as well as electron density and temperature were derived from the second derivative of the probe *i-v* characteristic. The experimental configuration allowed for axial and radial mapping of the plasma parameters in the entire negative glow of the discharge. As such, we present an extensive parameter study of the negative glow of a Hg-Ar discharge.

The model consists of several interconnected components which describe the negative glow, the collisionless sheath, and the emission and power balance at the cathode. The negative glow model is based on J. Ingold's analytic model.[1] The combined negative glow/sheath/cathode model calculates self-consistently cathode fall, cathode hot spot temperature, and negative glow discharge characteristics.

Agreement between measurements and model provides an improved understanding of the dependence of cathode fall on various discharge parameters. For example, measurements in a dc discharge indicate that cathode fall decreases with increasing discharge current. In the model's scenario an increase in total current causes an increase in ion current impinging on the cathode. This leads to a decrease in cathode fall because the cathode hot spot temperature, and thus the power delivered to the cathode by the impinging ions, remains approximately constant.

[1]J.H. Ingold, *Phys. Rev. A*, 43, 3093-3099 (1991).

6P39

Barium Loss from the Electrode of a Low Pressure Hg-Ar Discharge at Ignition

Phil Moskowitz
OSRAM SYLVANIA, INC.
71 Cherry Hill Dr., Beverly, MA 01915

Using laser absorption, we have continued our measurements of the spatial and time dependent barium ion density in the vicinity of a thermionic cathode for a low pressure mercury-argon discharge.[1] Barium is a constituent of the emissive coil coating in lamps and other discharge devices. Measurements were performed during ignition of the discharge, and can be used to determine the flux of barium from the coil during starting.

Results were obtained for both d.c. and high frequency (~40 kHz) excitation. The experimental method utilizes multiple parallel laser beams traversing chords of the cylindrical 25mm diameter glass discharge chamber in the electrode region. The dye laser is tuned to a resonance line of the singly ionized barium ion. Hence, the attenuation of the beams is a measure of the chord averaged barium ion density. The data is Abel inverted to obtain radially dependent density information. Data are acquired from the moment of ignition until stable thermionic operation of the electrode is attained.

[1]Y.M. Li and P. Moskowitz, 1994 IEEE Int'l Conference on Plasma Science, Santa Fe, NM, June 6-8, 1994.

6P40

Emission and Spectral Characteristics of Electrodeless Indium Halide Lamp

M. Takeda, A. Hochi, S. Horii, T. Matsuoka
Lighting Research Laboratory
Matsushita Electric Industrial Co., Ltd.
3-4 Hikaridai, Seika, Soraku, Kyoto, 619-02, Japan

The electrodeless HID lamp excited by microwave has been intensively investigated because of its long life, high efficacy and environmental aspect.[1,2,3]

This study reports excellent emission and spectral characteristics of electrodeless HID lamp containing indium halides.[4]

We investigate InI and InBr as ingredients, and measure the microwave excited spectra and luminous intensities of lamps which are made from spherical silica

glass in 10 - 40 mm outer diameter and with various amounts of halides.

It is well known that such indium halides in the usual metal-halide lamps have strong blue line emission at 410 and 451nm. But, in our microwave excited lamps, continuous spectrum can be observed in addition in the visible region.

Increasing input of power of microwave makes this continuous spectrum stronger. Below 1kW microwave input power, the spectrum of InBr lamp was almost resemble to the CIE standard illuminant D65. As a consequence of the spectrum, we found that the color rendering and the duv of InBr lamp were excellent as high as 95 and smaller than 0.002, respectively, in the region of 400-800W input power. The efficacy higher than 100 lm/W was further achieved at 400W.

We confirm that the microwave excited indium halides lamps can be applicable to many fields of the lighting.

1) B. P. Turner et al; LS7 Kyoto 35P(1995)p125
2) G. W. Doll et al; ICOPS96 Boston 2A03(1996)p134
3) M. Takeda et al; ICOPS96 Boston 1HP24(1996)p120
4) A. Hochi et al; IDW96 Kobe vol.2(1996)p435

6P41

Accurate Atomic Data for Industrial Plasma Applications

U. Griesmann, J.M. Bridges, J.R. Roberts, W.L. Wiese and J.R. Fuhr
National Institute of Standards and Technology
Gaithersburg, MD 20899

Reliable branching fraction, transition probability and transition wavelength data for radiative dipole transitions of atoms and ions in plasma are important in many industrial applications. Optical plasma diagnostics and modeling of the radiation transport in electrical discharge plasmas (e.g. in electrical lighting) depend on accurate basic atomic data.

NIST has an ongoing experimental research program to provide accurate atomic data for radiative transitions. The new NIST UV-vis-IR high resolution Fourier transform spectrometer has become an excellent tool for accurate and efficient measurements of numerous transition wavelengths and branching fractions in a wide wavelength range. Recently, we have also begun to employ photon counting techniques for very accurate measurements of branching fractions of weaker spectral lines with the intent to improve the overall accuracy for experimental branching fractions to better than 5%.

We have now completed our studies of transition probabilites of Ne I and Ne II. The results agree will with recent calculations and for the first time provide reliable transition probabilities for many weak intercombination lines. Our recent measurements of transition probabilities in NII an OI with wall-stabilized arc emission sources were aimed specifically at transitions where significant disagreements among advanced calculations exist. Our experiments thus provide benchmark data for new critical data compilations at NIST (http://aeldata.phy.nist.gov/nist_atomic_spectra.html) which are largely based on comprehensive atomic structure calculations.

6P42

Calculations of Acoustic Resonances in Arch Lamp Discharge Vessels

Warren P. Moskowitz
OSRAM SYLVANIA INC.
71 Cherry Hill Drive, Beverly, MA 01915

Improvements in switched-mode power electronics have increased the use of electronic power supplies for lighting discharges. An issue of concern for the designers of supplies for high-pressure discharge lamps is the excitation of acoustic resonances by the electrical ripple generated by the switching electronics. These resonances of the gas in the arc discharge vessel have been well known[1,2,3] since the 1960's, with detrimental effects ranging from minor perturbations in the shape or position of the arc, to severe instability and extinguishing the arc.

This paper presents calculations of the frequencies and wavefunctions of the acoustic modes in discharge vessels, complete with the distortion of the modes caused by the thermal distribution in the gas. It also shows the techniques used to make these calculations, which allow for vessel walls which are arbitrarily shaped surfaces of rotation.

[1] J. M. Davenport and R.J. Petti, Acoustic resonance phenomena in low wattage metal halide lamps, J. of IES/April 1985, pp. 253-255

[2] H.L Witting, Acoustic resonances in cylindrical high-pressure arc discharges, J. Appl. Phys. 49(5), May 1978.

[3] R. Schafer and H.P. Stormberg, Investigations on the fundamental longitudinal acoustic resonance of high pressure discharge lamps, J. Appl. Phys. 53(5), May 1962

6P43

The Low-Pressure Sodium Lamp

James D. Hooker
GE Lighting
Melton Road, Leicester, United Kingdom

For many years before the introduction of the sodium vapour lamp, scientists had been aware of the remarkably high luminous efficacy of the sodium discharge. However, many technical problems had to be overcome before these lamps could be marketed. The first commercial low pressure sodium lamps were introduced in the early 1930's and to this day they remain the most efficient light sources available. The high efficacy is due partly to the fact that these lamps emit nearly monochromatic yellow light, which is very close to the peak sensitivity of the human eye. Sodium lamps have come a long way since their introduction, and efficacies are now approaching 200 lumens per watt.

Despite increasing competition from other types of discharge lamp, low pressure sodium lamps of the 'SOX' type find widespread use in road and security lighting, particularly in Great Britain and many other parts of Europe. This paper will review the operation and development of the low pressure sodium lamp, and show what makes it different from the many other types of discharge lamp available.

6P44

Study of the Discrepancy Between Electron Temperature and Gas Temperature in the Vicinity of the Anode of an Electric Arc

M. Razafinimanana, M. Bouaziz, A. Gleizes
and S. Vacquié
CPAT-ESA 5002-UPS, 118 Route de Narbonne 31062 Toulouse (France)

Several studies of arc plasma in the vicinity of the electrodes revealed inconsistencies due to departure of local thermodynamic equilibrium. To analyze this phenomenon we studied the plasma near the copper anode of a wall-stabilized arc and of a transferred arc, running in argon and in nitrogen at atmospheric pressure. We measured the difference between electron temperature and gas temperature, using a relaxation method based on their different rates of decrease.

With a spectroscope we observed the intensities of the line 510.5nm of copper and of the line 696.5nm of argon at a distance of 2mm from the anode. Arc interruption was produced by using a fast thyristor connected to the electrodes which short-circuits the discharge with a turn on time close to 1μs. The signal is stored with a transient recorder.

The intensity of the 696.5nm line exhibits a very sharp increase at the time of switch-off. Inversely, the intensity of the copper line 510.5nm exhibits a very sharp decrease at the time of switch-off. In case of argon, the levels involved in the transition are close to the ionization limit and they are in equilibrium with the free electrons through Saha equation. After the sudden interruption of the current, the electron temperature T_e (initially $T_e > T_g$) decreases up to the gas temperature in less than 10^{-7}s, without modification of the electron density. In this case, Saha equation shows that the number density of atoms excited on the observed level increases. The intensity of the jump increases with the difference T_e-T_g. In the case of copper, the observed levels are close to the fundamental level and they are in equilibrium with this latter through Boltzmann equation. The decrease of T_e leads to a decrease in the number density of atoms excited on the observed level. The intensity of the jump allows us to calculate the difference between Te and Tg. The results obtained with argon and nitrogen are in good agreement. Depending on the current intensity, this difference varies between 300K and 1200K.

6P45

High Voltage Ignition of High Pressure Microwave Powered UV Light Sources

J.D. Frank, M. Cekic, C.H. Wood
Fusion U.V. Curing Systems, Corp., Gaithersburg, MD

Industrial microwave powered ("electrodeless") light sources have been limited to quiescent pressures of ~300 Torr of buffer gas and metal-halide fills. The predominant reason for such restrictions has been the inability to microwave ignite the plasma due to the collisionality of higher pressure fills and/or the electronegativity of halide bulb chemistries. Commercially interesting bulb fills require electric fields for ionization that are often large multiples of the breakdown voltage for air. Many auxiliary ignition methods are evaluated for efficiency and practicality before the choice of a high-voltage system with a retractable external electrode. The scheme utilizes a high voltage pulse power supply and a novel field emission source. Acting together they create localized

condiotn of pressure reduction and high free electron density. This allows the normal microwave fields to drive this small region into avalanche, ignite the bulb, and heat the plasma to it's operating point ($T_e \approx 0.5$ eV). This process is currently being used in a new generation of lamps, which are using multi-atmospheric excimer laser chemistries and pressure and constituent enhanced metal-halide systems. At the present time, production prototypes produce over 900 W of radiation in a 30 nm band, centered at 308 nm. Similarly, these prototypes when loaded with metal-halide bulb fills produce over 1 kW of radiation in 30 nm wide bands, centered about the wavelength of interest.

6P46

Operating Characteristics of a High Pressure "Wire" Hollow Cathode Plasmas

Hulya Kirkici
Electrical Engineering, 200 Broun Hall
Auburn University, AL 36849

Hollow cathode discharges are known to possess high ion and electron concentrations as well as high metastable densities. Additionally, the electron energy distribution function has a definite non-Maxwellian form with a very high density of low-energy electrons (≈2 eV) and a significant population of high energy electrons (≈18 eV). Therefore, energy and charge transfer collision processes which are desirable mainly in the generation of excimer species can be utilized efficiently in hollow cathode discharges to produce UV radiation.

In this work, a "wire" hollow cathode device was designed using the "pd" constraints, where p is the pressure, d is the gap distance between the electrodes, and was operated in a wide pressure range from 10 mbar to several 100s of mbar. The plasma is generated in this device by a set of thin tungsten wires forming the hollow cathode geometry. The design allows to generate plasma between the individual wires at high pressures, and in the volume enclosed by the wires at lower pressures. The two anodes are located axially at the end of the dielectric cylindrical disk holding the cathode electrodes. The enclosure of the electrode assembly is a cylindrical quartz tube allowing the transmission of the UV radiation from the device. The two end-windows are used for optical diagnosis to investigate the radial distribution of the species by radial mapping of the excitation region in the device.

In a gas discharge excimers are produced through either neutral channel (dominant in low pressure) or ionic channel (dominant in high pressure). In this paper we present the operating characteristics of the "wire" hollow cathode device using rare-gas and halogen gas mixtures as the feed gas. These results are displayed as a function of operating parameters such as current and voltage of the discharge and gas pressure in the device.

Wednesday Afternoon, 21 May 1997
3:00 p.m. – Rousseau Center

Oral Session 6P47-54:
5.5 Environmental / Energy Issues in Plasma Science

6P47

Oxidation of Volatile Organic Compounds by Microwave Plasma at Atmospheric Pressure*

D. John Lee
Aneptek Corporation, Natick, MA
Thomas E. Ruden
Newton Highlands, MA

The theory of microwave excited, non-thermal plasma destruction of VOCs at atmospheric pressure is described in U.S. Navy Patents 5,468,356 and 5,478,532. Advantages of the microwave approach as compared to DC or AC corona discharge, AC barrier dielectric discharge, and DC glow pulsed discharge have been discussed [1].

Destruction efficiency of 96% for toluene (C_7H_8) in air was obtained by the Navy using a TM_{010} cavity. Power was 6 kW with 600 W coupled to the plasma. Aneptek Corporation, under a license with the U.S. Navy, has continued this research. Improvements have been made in the cavity arc stability, Q, and coupling iris. Stable operation of the plasma has been achieved at atmospheric pressure at a power of 1 kW and improved coupling of about 70%. Measured flow rates are up to 10 liter/minute with an upper limit not yet established.

Tests on the destruction of isobutylene (C_4H_8) are in progress. Oxidation via the metastable oxygen molecule results in the production of CO_2 and water. We observe a high level of CO_2 generation consistent with the

stoichiometric relationship; CO and No_x are not generated. Monochromator analysis shows that ionization of nitrogen does not occur. In addition, we observe minimal bulk heating of the air. This is consistent with the theory prediction that the electron energy is well below that necessary to excite nitrogen molecules in the air.

We shall report on VOC destruction efficiency, results of various diagnostic tests, and new cavity design concepts.

* Work supported by Aneptek Corporation.

[1] H.S. Uhm, Conference Record, IEEE International Conference on Plasma Science, Paper 4P20, pg. 101, 1991.

6P48

Strong Current Arc Discharges of Alternating Current

F.G. Rutberg, A.A. Safronov, V.L. Goryachev
Institute of Problem of Electrophysics
18, Dvortsovaya nab, 191186 St. Petersburg, Russia

The review of experimental investigations results of strong current ($I=10\text{-}10^4A$) quasistationary alternating current discharges in high pressure gases ($P\geq10^5Pa$). Structural and alternating current arc properties in vortex, turbulent flows of air, argon, nitrogen and hydrogen were investigated. It was determined experimentally the existence of two arc discharge column regimes—contracted and diffusional. Processes of arc heat exchange with surrounding gas for these regimes were studied. Together with the volume processes were investigated mechanisms of discharge shorting on the electrodes surface and their erosion in the spot and without spot regimes in dependence of current quantity, gas pressure and electrodes material. Constructions of powerful ($N=10\text{-}10^3kW$) alternating current plasma generators were designed and created on the base of these investigations.

6P49

About Biological and Chemical Effect of Dense Low Temperature Oxygen-Hydrogen Plasma

V.L. Goryachev, Pf. G. Rutberg, A.A. Ufimtsev and V.N. Pfedyokovich
Institute of Problems of Electrophysics
Dvortsovaya nab. 18, St. Petersburg, 191186, Russia

Plasma is created by pulse-periodical discharge in water ($U_0 = 30\text{–}40kV$, $I_0 = 20\text{–}30A$, $\tau = 20\text{–}30\ \mu s$, $f = 50\text{–}100Hz$). Specific discharge energy $E = 200\ J/sm^3$, specific discharge power $W = 10MW/sm^3$, density of atoms: 10^{21} - $10^{22}sm^{-3}$, $15\text{–}20x10^3K$, pressure: 10–60Mpa. Dynamic of plasma canal development is investigated theoretically and experimentally (speed shooting). Pressure and temperature are measured. Data on bactericidal effect of the discharge (bacterium survival) and hydrogen peroxide generation are represented. Calculation model of H_2O_2 generation by ultra-violet radiation is built upon the basis of the data on water absorption of plasma ultra-violet spectrum radiation and dissolved H_2O_2 in it. The results of calculations are satisfactory conform with the experiment. Obtained data are used for explanation of biological and chemical effects of pulse discharges in water.

6P50

Development of Glow Discharge Plasma-Catalytic Reactors Operated Under Atmospheric Condition

Y. Hayashi*, K. Itoyama, S. Tanabe and H. Matsumoto
**Fujitsu Laboratories, Ltd., Kawasaki, Japan*
Nagasaki University, Nagasaki, Japan

Two kinds of glow discharge plasma-catalytic reactors, zone discharge tube plasma reactor and rotating electrode ring plasma reactor, have been developed and evaluated in various chemical reactions under atmospheric condition. In the former glow discharge occurs between two electrodes through a dielectric materials (Pyrex or quartz tube) and in the latter between a rotating (rotor) and a fixed electrode (stator) to make large volumes of the plasma zone under atmospheric pressure. Each electrode is, furthermore, coated with catalytically active metals, such as Pt, Pd, Rh, Cu or Ni.

Various kinds of decomposition reactions of chemically stable compounds have been examined in order to evaluate the performance of these reactors, such as decompositions

of CO_2, H_2O, NO, CH_4 and Freon into simple molecules. Different characteristic capabilities were observed between these reactors. The conversions of various reactants depend on the input power (voltage, current and frequency), the catalytic metal employed, carrier gas with different meta-stable level and the flow rate of reactant. In most of the reactions investigated, generally speaking, both of reactors showed excellent results in comparison with conventional catalytic reactors.

6P51

Development of an Ablation Measurement Technique Using Plasma Armatures

T.L. King
University of Houston, Houston, TX
K. Kim
University of Illinois, Urbana, IL

A novel technique is being developed to measure the ablation threshold and ablation rate of electrical insulators. Ablation is the loss of material due to incident thermal energy. Ablation thresholds and rates are important parameters for evaluating a material's suitability for a variety of high temperature applications, from high-current switches to fusion reactor inner walls. These measurements are accomplished using a plasma armature railgun containing gun walls fabricated from the test material. Ablation parameters may be determined by measuring the arc's velocity as a function of armature current and background gas pressure. Preliminary experiments have been performed on Lexan and Mullite. The data identified the onset of ablation in Mullite and provided a relative comparison of their ablation rates. This technique may provide an important tool for assessing the suitability of electrically insulating materials for variety of high temperature applications.

6P52

Intense Electron Beam Application for Flue Gas Treatment

A.G. Chmielewski, Z. Zimek, E. Iller, B. Tyminski
Institute of Nuclear Chemistry and Technology, Warsaw, Poland
J. Licki
Institute of Atomic Energy, Otwock-Swierk, Poland

Systematic work concerning electron beam flue gas treatment process upscaling has been performed at Institute of Nuclear Chemistry and Technology since 1986. Laboratory unit with gas flow 400 Nm^3/h has been constructed (accelerator beam power 20 kW, energy 0, 7-2MeV). Than industrial plant with gas flow 20000 Nm^3/h (two accelerators 50 kW, 0,8 MeV) has been build at EPS Kaweczyn. Finally design of 270000 Nm^3/h industrial plant (four accelerators 300 kW, 0,8 MeV) to be build at EPS Pomorzany has been prepared.

Several new solutions mostly leading to power consumption reduction were introduced. The longitudinal, double gas irradiation was applied among them. The technical-economical analysis proved that process is very competitive with conventional technologies widely used for flue gas purification.

6P53

Flue Gas Treatment by Simultaneous Application of Electron Beam and Microwave Discharge

Z. Zimek, A.G. Chmielewski and S. Bulka
Institute of Nuclear Chemistry and Technology, Warsaw, Poland
H. Nichipor
Institute of Physical and Chemical Problems, Minsk, Belarus

The experimental set up for investigation gaseous pollutants removal from flue gases under influence of electron beam and microwave energy discharge has been build. That allows to investigate a combined removal concept based on simultaneous use the electron beam and microwave energy. The energy consumption of the removal process was estimated under such conditions. The simultaneous use the electron beam and microwave energy may creates conditions where the total efficiency of removal process is higher to compare with separate ones.

6P54

Spectroscopic Investigation of Arc Spot Ignition on Cold Cathodes

M. Schumann, D. Nandelstädt, J. Schein,
B. Michelt and J. Mentel
Ruhr-Universität Bochum, D-44780 Bochum, Germany

To investigate the ignition of arc spots on cold cathodes under defined conditions a special experimental set-up was developed. An arc ignited between two horn electrodes in a pure argon gas atmosphere is blown magnetically against a third so called commutation electrode which is negatively biased against the arc plasma. The ignition of arc spots on this cathode was investigated as well by emission spectroscopy and high speed photography as by electrical measurements. The arc traces of short current pulses were examined by in situ optical microscopy of the cathode surface.

Two different modes of arc spot ignition were observed: an initiation by diffuse glow discharge which may pass into a constricted arc spot and an immediate formation of a constricted arc spot. Characteristic spectra of the filling gas and the commutation electrode could be related to the different modes.

The two modes of arc spot ignition at atmospheric pressure were attributed to different surface structures, which can be characterized by the field enhancement factor. Field enhancement by microprotusions may raise the local electron emission more than any known depression of the work function. A sufficiently high density of small emission sites produces by field emission locally such a high average current density that a plasma channel and an arc spot on the cathode surface is formed.

With lower pressure the influence of the surface structure is reduced and pushed back by TOWNSEND-γ emission.

Wednesday Afternoon, 21 May 1997
3:00 p.m. – Multipurpose Room

Poster Session 6Q13-14:
2.2 Fast Wave Devices

6Q13

Design of Novel Hybrid Traveling-Wave Amplifiers in X- and Ka-Band

W. Lawson, M.R. Arjona, A. Fernandez, T. Hutchings,
P.E. Latham and G.P. Saraph
Electrical Engineering Department, Institute for Plasma Research, University of Maryland
College Park, MD 20742

We present the design of two broadband microwave circuits which contain elements of both linear and gyrotron microwave tubes [1]. These tubes utilize a helix slow-wave structure to bunch a linearly-streaming annular electron beam. Linear momentum is converted to rotational momentum via a non-adiabatic magnetic transition which is placed at the location where the beam bunching is maximized. The beam then travels through a tapered right-circular waveguide, where microwave energy is extracted via the gyrotron interaction.

The X-band design considers a first-harmonic interaction between a 45 kV, 8A beam and a microwave signal near 10 Hz. The output is generated in the TE_{01} mode and the drive and output frequencies are identical. The total circuit length is about 33 cm and includes a 12 long helix, an 8 cm drift section, and a 13 cm output waveguide. The predicted peak efficiency and gain are 43% and 22 dB, respectively. The nominal 3 dB band width is nearly 8%

The Ka-band design involves a second-harmonic interaction between a 65 kV, 6A beam and a microwave signal near 35 GHz. The output is generated in the TE_{02} mode. Drive signals at the output frequency and at half the output frequency are considered.

This work is supported by the DOD Tri-Services Program.

[1] W. Lawson and W.W. Destler, "The Axially Modulated, Cup-Injected, Large-Orbil Gyrotron Amplifier," *IEEE Trans. Plasma Sci.* **22** (1994) 895.

6Q14

Initial Operation of the University of Maryland X-Band Coaxial Gyroklystron Experiment

W. Lawson, N. Ballew, J.P. Calame, M. Castle, J. Cheng, P. Chin, V.L. Granatstein, B. Hogan, M. Reiser and G.P. Saraph
Electrical Engineering Department, Institute of Plasma Research, University of Maryland College Park, MD 20742

In this paper we detail the result from the initial operation of the University of Maryland's coaxial gyroklystron experiment, which is being evaluated as a potential driver for future colliders. The interaction is designed to occur between 500 kV, 500 - 700 A beam and a series of coaxial TE_{011} microwave cavities. Output powers in excess of 100 MW at 8.568 GHz are expected with an efficiency of about 40% [1].

The beam is generated via a single-anode magnetron injection gun and is predicted to have an average velocity ratio of 1.5 with an axial velocity spread below 7%. The perveance of the gun has been measured to be about 5.5 μK and is in good agreement with theory.

The initial microwave circuit was a two-cavity system. Both cavities were resonant at 8.568 GHz. The input quality factor (Q) was ~70 and the output cavity Q was ~130. The signal from 150 kW magnetron was injected into the drive cavity via two coupling ports which were separated by 180°. The downtaper which connected the gun to the microwave circuit and the drift region between the two cavities were loaded with lossy dielectrics. Microwaves were coupled into the output waveguide via an axial aperture and traveled through 2 nonlinear uptapers to an anechoic chamber.

We present results of the electron gun performance, the stability of the tube, and the amplification properties of the microwave circuit.

This work was supported by the Department of Energy.

[1] G.P. Saraph, W. Lawson, M. Castle, J. Cheng, J.P. Calame, and G.S. Nusinovich, *IEEE Trans. Plasma Sci.* 24 (1996) 671.

Wednesday Afternoon, 21 May 1997
3:00 p.m. – Multipurpose Room

Poster Session 6Q15-23:
2.4 Slow Wave Devices

6Q15

Overmoded Backward-Wave Oscillator: A Comparison of Experimental Results with Non-linear Analysis

D.K. Abe, S.M. Miller*, Y. Carmel†, A. Bromborsky, T.M. Antonsen, Jr.†, B. Levush‡ and W.W. Destler†
Army Research Laboratory, Adelphi, MD 20783-1197

Overmoded structures have the potential for increasing the power handling capability of linear beam, high power microwave (HPM) devices, reducing internal rf electric fields to below field-emission breakdown levels. However, potential detrimental effects include multi-mode generation and a reduction in efficiency and power.

To study the feasibility of using overmoded structures in HPM generation, we conducted a series of experiments with an overmoded ($D/\lambda \sim 3$), relativistic backward-wave oscillator (BWO) in the 5.4 to 5.6 GHz frequency range. The experiment, which was designed to operate near the edge of the passband of the TM_{01} mode, produced highly coherent radiation ($\Delta f/f \leq 0.5\%$) with a maximum power of 320 MW. Power, efficiency, and frequency were measured as a function of both electron beam parameters and electrodynamic structure length. In parallel, we developed theoretical models of BWOs operating near cut-off, which included end-reflections and finite magnetic field effects.[1,2] For most of the experiment, the measured frequencies were within 5% of the model, which correctly tracked the trend of efficiency with structure length. We present a comparison of the theoretical and experimental results and an interpretation of the physical processes.

*ENSCO, Springfield, VA 22151

†Institute for Plasma Research, University of Maryland, College Park, MD 20742.

‡Vacuum Electronics Branch, Naval Research Laboratory, Washington, D.C. 20375-5347.

[1] S.M. Miller, et al., *Phys. Plasmas*, vol. 5, no. 5, pp. 1625-1638, May 1993.

[2] S.M. Miller, et al., *IEEE Trans. on Plasma Sci.*, vol. 24, no. 3, June 1996.

6Q16

Effect of Random Manufacturing Errors on Slow Wave Circuit Performance*

Demos Dialetis and David Chernin
Science Applications International Corp.
McLean, VA 22102

Manufactured, nominally periodic slow wave circuits inevitably have small errors in their construction, that is, every unit cell is slightly different from every other one. The usual mathematical treatment invokes Floquet's theorem for the perfectly periodic circuit. This formulation is the basis of several computational treatments in which phase shift boundary conditions are applied to a single unit cell in order to compute the resonant frequency(ies) as a function of the phase shift per section. If, however, an actual circuit departs from perfect periodicity, the usual treatment must be modified. In the present paper, we present a method by which this can be done. We apply our formulation to the practical problem of predicting the reflection coefficient (s_{11}) as a function of the rms construction errors in a particular case, namely a pi-section bandpass filter circuit that is used in computer models of crossed-field vacuum tubes. The formula we obtain may therefore be used to specify manufacturing tolerances in circuit construction. Results from computer simulations of the operation of a crossed-field amplifier in which random circuit errors have been introduced will be presented, and compared to simulations using perfectly periodic circuits.

*Work supported by the US Naval Research Laboratory contract N00014-96-C-2107 through DCS Corp., Alexandria, VA.

6Q17

Density Profiles and Current Flow in a Crossed-Field, Electron Vacuum Devices*

D.J. Kaup
Clarkson University, Potsdam, NY 13699-5815
G.E. Thomas
Communications & Power Industries Inc.
Beverly, MA 01915-5595

When a strong RF electric field (with a frequency, ω, and a wavevector, k) is propagating in a cross-field, electron vacuum device, and k and ω are such that a wave-particle resonance ($\omega = v_d k$) can occur at the edge of a Brillouin sheath, then the Brillouin sheath becomes strongly unstable to a Rayleigh instability[1], with the instability being driven by the strong negative density gradient at the edge of the Brillouin sheath. As a consequence of this instability, the average DC density profile, $n_o(y)$, becomes strongly modified and is driven away from the classical Brillouin flow by the RF field, and is driven toward the stationary solutions of a nonlinear diffusion equation

$$\partial_t n_0 + C_2 \partial_y n_0 = \partial_y (D \partial_y n_0) \quad ,$$

where $C_2\Omega^2$ (Ω is the electron cyclotron frequency) is the DC current and D is a nonlinear diffusion coefficient, given simply by

$$D = 2\gamma |\, \xi_y \,|^2,$$

with γ being the linear growth rate of the RF wave that propagates on this stationary density profile, and ξ_y being the y-component of its Lagrangian displacement. We will show that one can find consistent solutions to these equations, wherein the RF fields will satisfy the appropriate linearized equations for the stationary density profile. Examples of stationary solutions for these density profiles will be given, along with plots of DC current vs. tube voltage and magnetic field. The theoretical results will be compared with experiment and the relation between the stationary solutions of the nonlinear diffusion equation and the phenomena of ultra-low noise will be suggested.

* Research supported in part by the AFOSR, ONR and the Naval Surface Warfare Center, Crane Div.

[1] D.J. Kaup and Gary E. Thomas, Phys. Plasmas **3**, 771, (1996).

6Q18

Rectangular Grating Periodic Structure for Low-Voltage Amplifiers*

L.J. Louis, J.E. Scharer, J.H. Booske and M.J. NcNeely
Department of Electrical Engineering
University of Wisconsin-Madison, Madison, WI 53706

The rectangular grating periodic structure is a slow wave device which offers higher power, low voltage, compact Ku band amplifiers. The amplifier measurements are done using a round probe beam of 1 mm diameter from a 10 kV, 0.25 A, electron gun, confined by a 1 kG focusing solenoidal magnetic field. The axial velocity spread of the electron beam is measured using a Faraday cup energy analyzer. The beam spread depends on various factors associated with magnetic beam optics including a sensitivity to alignment of the gun magnetic flux field.

The position of the gun flux shield is optimized to get the best possible beam spread. The gain measurements are obtained with the collector replaced by the energy analyzer and are carried out with both loop and waveguide input couplers. A waveguide Tee section is used for launching the microwave power without affecting the beam launching. This enhances the power coupled into the TE_{Z10} waveguide mode which is converted to the TE_{X10} hybrid mode in the grating periodic amplifier structure. The linear gain measurements for a shallow groove backward wave amplifier are presented and related to the degree of beam energy spread.

*Research sponsored by ONR, DOD Vacuum Electronics Initiative as managed by NSF Presidential Investigator Award.

J. Joe, L. Louis, J. Scharer, J. Booske, M. Basten, "Experimental and Theoretical Investigations of a Rectangular Grating Structure for Low-Voltage Traveling Wave Tube Amplifiers," (submitted for publication to Phys. Plasmas, Dec. 1996).

6Q19

A New Resonator Design for Smith-Purcell Free Electron Lasers

C.L. Platt, M.F. Kimmitt, J.H. Brownell, J.E. Walsh
Dartmouth College, Hanover, NH

A Smith-Purcell Free Electron Laser test-facility has been developed. The structure is used to conduct detailed explorations of effects of resonator design on tunability, start current and other performance criteria.

Initial emphasis is on sources which operate at millimeter wavelengths and utilize moderate energy electron beams. The Smith-Purcell radiation is produced by passing a 3-15 kV, submillimeter diameter electron beam over a metal grating with a rectangular profile. Radiation is produced at 35-40 GHz, 75 GHz and 95-100 GHz using different gratings.

To date three resonator configurations have been investigated. Two are classic planar orotron[1] designs with different quality factors. Starting currents as slow as 1 to 10 mA have been observed in the 35-40 GHz range.

A third configuration is a bare grating without an external feedback elements. Performance was equal or superior to the original planar orotron designs. Radiation from this structure is observed by looking for bound modes launched in the backward direction. Starting currents of 15 mA are observed and the wavelength is continuously tunable. This design is simpler and more robust and allows a better understanding of the operation of the device.

We would like acknowledge support from ARO grant DAAH04-95-1-0640.

[1] E.M. Marshall, P.M. Phillips and J.E. Walsh, "Planar orotron experiments in the millimeter wavelength band", IEEE Trans. Plasma Sci., vol. 16, no. 2, pp 199-205, April 1988.

6Q20

Numerical Cold Testing for Plasma Loaded Slow-Wave Circuits

J.M. Oslake, J.P. Verboncoeur and C.K. Birdsall
Electronics Research Laboratory, University of California at Berkeley, Berkeley, CA 94720-1774

A computer model is developed which numerically calculates the electromagnetic eigenfields and dispersion relation for periodically loaded slow-wave circuits in vacuum and in the presence of a plasma. The presence of a plasma is captured by admitting a space dependent dielectric constant into the circuit. A wave equation in finite difference form is first numerically solved which produces a sequence of eigenfrequencies and eigenfields beginning with cut-off. Fourier decomposition of each eigenfield along selected mesh lines coincident with the location of the electron beam is then performed to establish a correspondence between eigenfrequency and wave number. From this data the dispersion relation for the slow-wave structure can then be formed. This numerical procedure has been demonstrated to require only a few minutes of simulation time on typical workstations. Quantities important in cold circuit testing are calculated for various waveguide structures and plasma density distributions. A vector potential formulation is compared with a numerical approach based on the direct calculation of electromagnetic fields.

This work was supported by the Air Force Office of Scientific Research under MURI contracts F49620-95-1-0253 and F49620-96-1-0154.

6Q21

Simulation of TWTs and Twystrodes

David Smithe and Bruce Goplen
Mission Research Corporation, Newington, VA
Mary A. Kodis, Earnest Zaidman,
Thomas M. Antonsen, Jr.* and Baruch Levush,
Naval Research Laboratory, Washington, DC

Results from simulations of the FEA twystrode using both 2-D PIC[1] and 1-D mode-analysis[2] methods will be presented. Efficiency, bandwidth, and gain performance are charted for varying helix pitch taper, helix length, beam current and beam voltage. FEA twystrode performance, especially harmonic content, is also charted for variations of input modulation amplitude. Efficiency enhancement for various collector configurations is also investigated. The simulations are based upon state-of the-art FEA parameters, and realistic PPM magnetic fields.

Several advances in the simulation state-of-the-art are also reported. A successful approach to the treatment of vanes in helix TWTs has been developed. Precise modeling of attenuators is now commonplace. A new "splitter" diagnostic for the 2-D PIC code MAGIC[1] has been developed, which can separate the Poynting power flow into forward and backward directional flow, and also into the various frequency components. The latter capability has been demonstrated as a powerful tool for the investigation of intermodulation in multi-tone helix TWT amplifiers.

Work supported by Office of Naval Research.

[1]B. Goplen et al., CPC 87 (1995) 54.

[2]Antonsen and Levush, NRL memo, to be published.

*SAIC, permanent address University of Mayland.

6Q22

Novel Computer Model for Simulation of Backward Wave Oscillators

G.I. Zaginaylov and Yu.V. Gandel'
Kharkov State University
Kharkov, 4 Svobody sq., 310077, Ukraine
P.V. Turbin
Scientific Center of Physical Technologies
Kharkov, 1 Novgorodskaya Str., 310145, Ukraine

In recent years, the remarkable advance in the experimental studying and understanding of operation of relativistic backward wave oscillators (BWO) has been made[1,2]. For adequate theoretical treatment of experiments and further BWO optimization the rigorous computer model is required, which is capable to account ac and dc space charge effects, "full wave" representation of fields and selfconsistent mode coupling at the ends and within the resonator. All foregoing theoretical models, as far as we know, account abovementioned effects nonself-consistently, so that some disparities originate in predicted and measured data[2]. The novel theoretical model being free from such lacks has been developed using the singular integral equation method[3]. The first results obtained for the simplified (linear) model of the beam allow us to accurately describe the phenomenon of operating frequency locking (which was observed over wide range of diode voltage[2]) and to understand its physical sense. It appears to be caused by diffractional broadening of spatial harmonics, which also is taken into account in our model. In other words, for each axial eigenmode with given eigenfrequency there is an uncertainty in wavenumber $\Delta k_z \sim \lambda/L$, where L is an effective length of the resonator, λ is wavelength of dominant space harmonic. As in experiments[1,2] λ/L is comparably large (~0.25) the somewhat part of the wave packet of axial eigenmode can be amplified by the beam over wider range of voltage. Due to end coupling the energy, can be redistributed within the wave packet including k_z for which the direct Cherenkov excitation is not possible but the condition of constructive interference holds so that the high level of the radiated power is provided. Thus, the efficient experimental operation at the voltage lower than 400 kV[2] can be explained. The nonlinear timedependent variant of our model will be developed in the nearest future.

[1] E. Schamiloglu, L.D. Moreland and R.W. Lemke. Conference Record of ICOPS 1995, p. 96;
L.D. Moreland, E. Schamiloglu, R.W. Lemke and A.M. Roitman, ibid., p. 227.

[2] S.M. Miller, et al., Phys. Plasmas, 1, 730 (1994).

[3] Yu.V. Gandel', V.D. Dushkin, G.I. Zaginaylov. Electromagnetic wave and electron systems, 1, 38 (1996); Yu.V. Gandel', G.I. Zaginaylov. Conference Record of ICOPS, 1995, p. 280.

6Q23

High Power Microwave Generation and Beam Transport in the PASOTRON™ BWO Source[1]

Dan M. Goebel and Jon Feicht
Hughes Telecommunications and Space, EDD,
3100 W. Lomita Blvd., Torrance, CA
Elmira S. Ponti and Ron Watkins
Hughes Research Laboratories
3011 Malibu Canyon Rd., Malibu, CA 90265

The PASOTRON high-power microwave source utilizes a unique plasma-cathode electron gun and self-generated plasma channel to inject a long-pulse electron beam into a slow-wave structure for microwave generation. The plasma-channel beam transport eliminates the need for an externally-applied axial magnetic field to confine the beam, which results in a very compact low weight HPM source compared to conventional technologies. The PASOTRON is normally configured as a backward-wave oscillator (BWO), and has produced over 10-MW of peak power and ≥500 Joules per pulse. In this talk, we will present the operation of the PASOTRON device for a variety of rippled-wall and helix slow-wave structures. The physics of the plasma channel formation and beam focusing has been studied and a computer model of this process has evolved. A diagnostic tube with two rows of probes extending down the length of the tube at 90° to each other has been used to examine the radial profile of the beam as it propagates as a function of time and axial distance. The dynamics of the plasma channel formation and the plasma density over time will be presented and compared to the model.

[1] This work supported by Hughes Electronics IR&D.

Wednesday Afternoon, 21 May 1997
3:00 p.m. – Multipurpose Room

Poster Session 6Q24-44:
6 Plasma Diagnostics

6Q24

Silicon Photodiode Soft X-Ray Detectors

G. C. Idzorek and R. J. Bartlett
Los Alamos National Laboratory, Los Alamos, NM

Advanced fabrication techniques have produced UV/ soft x-ray silicon photodiodes of uniform quality with thin (60 Angstrom) entrance windows and response times on the order of 100 picoseconds. We have assembled these advanced diodes into small individual detectors and detector arrays used on our plasma diagnostic experiments. Synchrotron x-ray and visible light calibration measurements show an essentially flat response from 10 eV to 600 eV as theoretically expected. Above 600 eV detector response increases above the theoretical calculation due to transmission through an approximately 8000 Angstrom thick SiO_2 protective layer surrounding the central 'active' area of the diode. Measurements on a number of diodes verify the manufacturer's claim of diode to diode response variation of about 5%. Pulsed soft x-ray calibrations show an increase in time response as a function of increased signal level and reduced bias voltage. Silicon photodiodes are the ideal detectors for soft x-ray measurements as they are much more stable and less variable in response than photoemissive detectors and much less costly than photoconductive diamond sensors. These characteristics coupled with the fast time response of the advanced silicon diodes make them excellent sensors for the soft x-ray diagnostics required on plasma experiments.

6Q25

Determination of Copper Concentration in a SF6 Arc Plasma in an Electrical Circuit Breaker

C. Fleurier, S.S. Ciobanu, D. Hong and F. Gentils
GREMI, CNRS, Université d'Orléans, BP 6759, 45067 Orléans, Cedex 2, France
C. Fiévet
Centre de Recherches Schneider Electric, 38050 Grenoble Cedex, France

Measurements of particle temperatures and concentrations were performed for a transient and unstable plasma arc in an industrial circuit breaker operated in a 3 atm SF_6 gas. The large current intensity caused an important vaporization of the electrodes so that the plasma developed in a mixture of SF_6 and Cu. Time resolved photographs of the arc obtained with interference filters showed a compact and homogeneous zone dominated by a S^+-F plasma, and an inhomogeneous zone close to the electrodes dominated by Cu. Average electron densities and temperatures and also the total number of the different emitting atoms or ions were determined in the two zones by spectroscopy using simultaneous time resolved measurements at high and low spectral resolution. Particle concentrations were obtained after an estimate of the volumes of the different plasma zones by spectroscopical methods. Copper density was also inferred from absorption measurements on copper resonance lines by means of a bright flash produced by a Z-pinch discharge. This method allowed to overcome the problem of light beam random deviation by the strong gas turbulence in the plasma chamber.

6Q26

Radiation Diagnostics and X-ray Output from 1213 Mega-Ampere Plasma Implosions

H. Oona, G.C. Idzorek and J.H. Goforth
Los Alamos National Laboratory, Los Alamos, NM

The Procyon explosive pulsed power system has been used to drive 12–13 MA, 2 μ second plasma implosions. These experiments have produced more than 1.5 MJ of soft x-rays in a 250 ns FWHM pulse. Data from bolometers, x-ray photodiodes, and curved crystal x-ray spectrometers are compared and analyzed for the fluence and the plasma temperature. Fitting of the x-ray continuum to a Planckian has suggested temperatures in the 90ev range. Images from high speed electronic cameras show a time sequence of instability growth that indicate effects on the x-ray output. X-ray images taken with filtered pinhole cameras show the location, shape, and size of the pinch. In this report we will present details of this data from several Procyon experiments, point out methods for minimizing instability growth and discuss the diagnostics that are used in the harsh, explosive environment.

6Q27

Plasma Diagnostics on the DIII-D Tokamak*

R.T. Snider and the DIII-D Group
General Atomics, San Diego, CA

Recent advances in our understanding and performance of tokamak plasmas have been made possible largely by the implementation of new plasma diagnostics and improvements in older diagnostic techniques. Very detailed, spatially and temporally resolved measurements of a wide range of plasma parameters have allowed good coupling between the experiments and theories that has spurred broad advances in both areas. The DIII-D tokamak has been in the forefront of much of this work, partly because of its extensive, state of the art diagnostic set. An overview of the measurement capabilities on the DIII-D tokamak and the implications of that capability with an emphasis on recent advances will be presented.

*Work supported by US Department of Energy under Contract DE-AC03-89ER51114.

6Q28

A New Design of a Parallel Chord Optical Probe and Its Application to the Plasma Diagnostics

H.K. Na, N.S. Yoon, B.C. Kim, J.H. Choi, G.S. Lee, and S.M. Hwang
Korea Basic Science Institute
52 Yeoeun-Dong, Yusung-Ku, Taejeon, 305-333, Korea

A new optical probe system which as a dual function of linear and rotating motion is developed. It consists of an optical fiber, a small achromatic bi-convex lens and an optical vacuum feedthrough. The optical configuration of the system is carefully designed to have a parallel chord along the viewing direction. The optical line emission intensity from an ICP (inductively coupled plasma) is measured in axial and radial directions. The probe is moving along the axial direction, but it also can observe the radial direction because a 45 degree inclined mirror assembly can be attached to the probe head. The spatial intensity distribution in axial direction is obtained by a direct differentiation of the line integrated intensity, and the Abel inversion method is used to get the radial intensity distribution. The results are compared with those of Langmuir probe experiment to confirm the utilization of this probe system.

6Q29

Compact, Rugged, Flexible Fiber Optic Interferometer for Sensitive Gas and Plasma Density Measurements*

G.G. Peterson, N. Qi, S.W. Gensler, R.R. Prasad, G. Rondeau† and M. Krishnan
Alameda Applied Sciences Corporation, San Leandro, CA 94577

A prototype fractional fringe Mach-Zehnder fiber optic interferometer (FOI) to measure gas and plasma densities has been built. The interferometer components are secured to a compact 18-cm wide x 22-cm high rigid aluminum frame which makes the system easily portable. A 1550-nm IR beam from a cw diode laser is launched into the fiber system. Evanescent fiber wave couplers are used to split and later recombine the laser beam into equal length probe and reference paths. For the test region a 0.4-mm diameter, 12-cm long free space beam is launched and re-captured with a pair of fiber collimators. Relative phase between the interferometer legs is controlled by stretching and compressing a section of the reference leg fiber with a piezo wafer assembly. This is necessary for "zeroing" the phase difference between the legs prior to a measurement and for calibrating the signal-to-phase gain. The second fiber coupler recombines the paths of the interferometer providing complementary signals on its two outputs. The output signals are detected with photo diodes which are differentially amplified to produce an "ac coupled" interference signal that is proportional to the sine of the phase shift. Gas density measurements as a function of time from a super sonic nozzle are being performed to test and document the sensitivity and utility of this compact system. A complete description of the FOI, a report on the gas density measurements, and an analysis of the system's potential sensitivity limits will be presented.

* Work supported by DSWA under a Phase I SBIR, Contract #DSWA 01-96-C-0137.
† Consultant

6Q30

Bremsstrahlung Characterization at PBFA Z*

M.S Derzon, R. Mock, C.L. Ruiz, M.A. Sweeney
Sandia National Laboratories, Albuquerque NM 87185
S. Lazier and A. Schmidlapp,
Ktech Corporation, Albuquerque, NM
G.W. Cooper
University of New Mexico, Albuquerque, NM

Sandia National Laboratories has developed a >1 MJ soft x-ray source using z-pinch implosions. The machine generates a high energy (>2 MeV) bremsstrahlung background that affects diagnostic development and may preheat the fuel in proposed inertial confinement fusion experiments. In this presentation we will show calculations of the bremsstrahlung spectrum and the estimated heating of the fuel. Measurements of the bremsstrahlung as a background noise source will also be discussed.

*This work is supported by the U.S. Department of Energy under Contract DE-AC04-94AL85000. Sandia is a multiprogram laboratory operated by Sandia Corporation, a Lockheed-Martin Company, for the U.S. Department of Energy.

6Q31

Arc Chanel Impedance Estimation According to Voltage and Current Oscillograms with Programmable Discharge of Capacitive Energy Store

B.E. Fridman and Ph.G. Rutberg
Institute of Problems of Electrophysics of the Russian Academy of Sciences, 18 Dvortsovaya nab., St Petersburg, 191184, Russia
Phone #: (812)-315-1757, Fax#: (812)-311-5056

Programmable discharge of capacitive energy stores allows to obtain optimum regimes of energy emission in the load. Characteristic peculiarities of programmable discharge regime are the voltage step change on the load at the moment of regular capacitance module switching on and the existence of several maximums on the current curve in the load in the time gap between modules switching on. Magnitude of the step on the voltage curve gives possibility to define existing inductance of the load. Voltage at the moment of current peak allows to estimate ohmic resistance of the load. Working out results of oscillogram records of the E7-25 capacitive store programmable discharge on electric arc in the air at atmospheric pressure are presented. High-speed photography of electric arc in the air has demonstrated correlation between measured arc inductance and its form evolution.

6Q32

LIF Diagnostic for Measuring Beam-Transport Magnetic Fields*

T.G. Jones,[a] W.A. Noonan,[b] and P.F. Ottinger
Plasma Physics Division, Naval Research Laboratory, Washington, DC 20375-5346

A novel, spatially-resolved, non-intrusive diagnostic is being developed to measure magnetic fields associated with intense ion beam propagation through a low-pressure gas, as is envisioned for light ion-driven ICF. The diagnostic uses laser-induced fluorescence (LIF), and is varied to measured either small or large fields.

Small fields (B<200 G), as expected in ballistic transport with solenoidal lens focusing using 1 Torr gas, produce Zeeman shifts, $\Delta\lambda_z$, smaller than the transition linewidth, $\Delta\lambda$. High sensitivity for the low-B measurement is achieved by a variation on the Babcock technique using LIF spectroscopy.[1] LIF from a J=1→0 transition in a probe species is viewed parallel to **B**. In this case $\Delta M=0$ fluorescence is not visible, and $\Delta M=\pm 1$ fluorescence is right- and left-circularly polarized, and can be measured separately using polarization filters. If a narrow-bandwidth pump laser is tuned to a half-maximum point of the unsplit transition line, the B-field shifts one of the $\Delta M=\pm 1$ absorption transitions into resonance with the laser and shifts the other further out of resonance. For small fields, the difference in the fluorescence signals of the two polarization is proportional to $\Delta\lambda_z$ and B.

Large fields (B>200 G), as expected in self-pinched transport using 10 to 100 mTorr gas, produce $\Delta\lambda_z$ larger than $\Delta\lambda$. The small-B technique can be adapted to measure large B by adding an etalon to act as a narrow-band optical filter of LIF. The etalon transmission curve then transduces $\Delta\lambda_z$ to a change in detected intensity, analogously to the absorption line profile in the small-B technique. Results of proof-of-principle experiments using calibrated B-fields, and plans for fielding the diagnostic on Gamble-II will be presented.

---

* Work supported by DOE through SNL.

[a] National Research Council Research Associate.

[b] Present address: Univ. Maryland, College Park, MD.

[1] W.A. Noonan, et al., to appear in Rev. Sci. Instrum. **68** (1997).

6Q33

Measurement of Energetic (> 6 MeV) Particles in Wire Array Pinches on PBFA Z

C.L. Ruiz and M.S. Derzon
Sandia National Laboratories, Albuquerque, NM
G.W. Cooper
University of New Mexico, Albuquerque, NM
F.A. Schmidlapp
Ktech Corp., Albuquerque, NM

Sandia National Laboratories has modified the PBFA II accelerator into a z-pinch configuration. To date, PBFA Z has generated x-ray yields exceeding 1 MJ and 100 TW. The loads consist of cylindrical, tungsten wire arrays. Nuclear activation and shielded scintillator measurements indicate that particles are being produced in the pinch that have energies that greatly exceed the nominal applied voltage of 2.5 to 3 MV. In particular, we have observed Co-56 and Mn-52m activation on the stainless steel cathodes. The only credible production mechanisms for these nuclides in PBFA Z are (p,n) reactions on Fe-56 and Cr-52. Since the thresholds for

these reactions are 5.44 and 5.98 MeV, respectively, we argue that protons having energies greater than about 6 MeV are produced in the pinch. In addition, we have observed significant photon signals on a plastic scintillator that was shielded by 6 cm of lead. Simple gamma-ray attenuation arguments suggest that there is a considerable fluence of photons having energies greater than 1 MeV. These photons could be gamma rays produced in prompt (p,γ) reactions and/or bremsstrahlung x-rays produced by energetic electrons. We plan experiments to better characterize these energetic protons with respect to energy spectrum and total energy. This information may lead to a better understanding of the pinch physics and allow us to assess whether these protons may lead to preheat problems in proposed inertial confinement fusion experiments.

*This work is supported by U.S. Department of Energy under contract DE-AC04-94AL85000. Sandia is a multiprogram laboratory operated by Sandia Corporation, a Lockheed Martin Company, for the U.S. Department of Energy.

6Q34

Targets Development at Sandia National Laboratories

Michael L. Smith, David Hebron, Mark Derzon and Rick Olson
Sandia National Laboratories, Albuquerque, NM
Thomas Alberts
W.J. Schafer Associates, Inc., Livermore, California

For many years, Sandia National Laboratories under contract to the Department of Energy has produced targets designed to understand complex ion beam and z-pinch plasma physics. This poster focuses on the features of target designs that make them suitable for Z-pinch plasma physics applications. Precision diagnostic targets will prove critical in understanding the plasma physics model needed for future ion beam and z-pinch design.

Targets are designed to meet specific physics needs; in this case we have fabricated targets to maximize information about the end-on versus side-on x-ray emission and z-pinch hohlraum development. In this poster we describe the fabrication and characterization techniques. We will include discussion of current targets under development as well as target fabrication capabilities.

Advanced Target designs are fabricated by Sandia National Laboratories in cooperation with General Atomics of San Diego, CA and W.J. Schafer Associates, Inc. of Livermore, CA.

This work was supported by the United States Department of Energy under contract DE-AC04-94AL85000. Sandia is a multiprogram laboratory operated by Sandia Corporation, A Lockheed Martin Company, for the United States Department of Energy.

6Q35

Analog fiber-Optic Data

Steve Lazier
Ktech Corp., Albuquerque, NM

Analog fiber-optic data transmission is required for many diagnostics at the Pulsed Based Fusion Accelerator (PBFA-Z). Radiation-induced brightness and darkening has been characterized in fiber optic cables located at distances ranging from 5 cm to several meters from the target. Spectral measurements of this noise signal have been made to determine which combination of bandpass filtering and shielding is adequate for the diagnostics.

6Q36

Modeling of a Soft X-ray Diode Using Particle-in-Cell and Monte-Carlo Simulations

R.K. Keinigs, R.J. Faehl and D. Platts
Los Alamos National Laboratory, Los Alamos, NM

A soft x-ray tube built and developed by one of the authors (DP) is a standard radiographic diagnostic for imploding liner experiments conducted at Los Alamos. For particular experiments one would like to increase the X-ray dose and simultaneously decrease the X-ray spot size generated by this tube. We are using both particle-in-cell and Monte Carlo models to determine those design changes to the diode and/or driving voltage that can produce the desired characteristics. To evaluate the x-ray dose, the spectral features of the radiation, and spot size that are generated from electrons striking a cone-shaped tungsten anode target, we are using the Monte-Carlo transport code, MCNPE. A range of electron energies and incident angles is modeled to try to optimize the x-ray

characteristics. The diode is modeled using the 2-1/2 particle-in-cell code, MERLIN. From the PIC simulations we are able to determine where electrons are striking the anode surface, and at what angle. MERLIN is also employed to calculate the diode impedance. In these simulations the anode and cathode geometries are varied to explore means for controlling the electron current and deposition profiles. Results of both the particle-in-cell and Monte Carlo calculations will be presented.

This work was supported by the U.S. Department of Energy.

6Q37

New Method for Negative ion Diagnostics

E. Stamate* and K Ohe
Nagoya Institute of Technology
Showa-ku, Nagoya 466, Japan

Recently a "test function" for measurements by Langmuir probes[1] was introduced. This function is very sensitive to the body of electron distribution function (EDF), and useful for a plasma whose EDF is Maxwellian or bi-Maxwellian The ion density can be also obtained from the test function values around the plasma potential. The test function method is an improved one, which was proposed to obtain the two electron group parameters in the bi-Maxwellian plasma. The method[2] can distinguish the high electron energy group from the low one, even if the former is less than 2% that of the later[3].

In this work we present how to use the test function for the negative ion diagnostics. The numerical procedures for processing a Langmuir probe characteristic in negative ion plasmas is established and errors included in this procedure is estimated.

The experiments are performed in a multipolar magnetic-confined plasma. To improve the negative ion production, a magnetic filter is used, obtaining a plasma with not so energetic electrons. The plasma parameters were detected by a cylindrical probe in an Ar plasma and then in a Ar-SF_6 one. The results obtained by this new method are compared with those for negative ion detection which takes account of a reduction of electron saturation current due to the presence of negative ions.

[1] E. Stamate and G. Popa, 1996 Int. Conf. On Plasma Phys., 9-13 Sept., Nagoya 1996

[2] D. Ruscanu, G. Popa and E. Stamate, 1992 Int. Conf. On Plasma Phys., Innsbruck, vol .II, 1179 (1992)

[3] E.Stamate, K.Inagaki and K.Ohe, 1997 Int.Conf. on Reactive Plasmas, 21-24 Jan. Nara

*Permanent address: Faculty of Physics, "Al.I.Cuza" University, Iasi-6600, Romania

6Q38

Temperature and Density Measurements in High Intensity Microwave-Excited Excimer Lamps

Svetozar Popovic
Old Dominion University, Norfolk, VA 23529
Miodrag Cekic
Fusion UV Systems, Gaithersburg, MD 20878

Electrodeless microwave-excited rare-gas halide lamps are presently among the most powerful ultraviolet light sources, capable of emitting cw radiation power of several kilowatts in the spectral range between 200 and 350 nm. Development and optimization of high-pressure microwave-excited excimer lamps depends on the knowledge of the excimer plasma parameters, particularly electron temperature and density. Non-coherent excimer light sources are relatively new devices and the information on their plasma parameters is still incomplete. Standard diagnostic techniques of high density discharges are inapplicable in this case, because of the molecular excited state structure and absence of self-absorption. We will present description of two techniques for determination of plasma temperature and electron density. Temperature measurement is based on the equilibrium population of certain vibrational levels of excimer excited states. Electron density was determined from the measurements of Stark profiles of H_β radiation from a small amount of hydrogen mixed with rare-gas halides. Lamps were specially designed and constructed to meet the basic diagnostic requirements, to permit axial radiation detection preserving microwave coupling characteristics of the commercial microwave cavity. Description of lamps, diagnostic apparatus and the method will be presented. Variation of plasma parameters depending on the initial partial pressures of gas components will be shown.

6Q39

Photoelectron Spectroscopy for Soft X-Ray Measurements in a Small Tokamak

Seong-Heon Seo and Hong-Young Chang
Dept. of Physics, Korea Advanced Institute of Science and Technology, Taejon 305-701, Korea

A new x-ray spectroscopy system using the principle of a photoelectron spectroscopy method is developed for the observations of soft x-ray radiations in the KAIST tokamak (R = 53 cm, a = 15 cm). The system uses a high voltage triangular wave generator to analyze photoelectron energy with a retarding potential grid and a current mode preamplifier to measure the signals from a microchannel plate (MCP). We measure the spatial distributions and time evaluations of some impurity line radiations from the plasma in the temperature range of a hundred of eV. The electron temperature is also measured from the continuous spectrum profile. The design of the spectrometer and the experimental results will be presented.

6Q40

Obtaining Plasma Potential Measurements in Hall Thruster Plumes

Colleen M. Marrese, John E. Foster
and Alex C. Gallimore
University of Michigan, Ann Arbor, MI 48109

Plasma potential measurements in electric propulsion systems are necessary for complete performance evaluations. There have been several measurement methods proposed in the past without a clear indication of which method is the most accurate[1,2,3]. An investigation was performed to compare a number of these methods. The techniques employed here include two different emissive probe methods and a procedure that involves the analysis of the electron energy distribution function (EEDF). Near- and far-field measurements were taken in the plumes of a stationary plasma thruster (SPT) and an anode layer thruster (TAL). The techniques employed are explained, and an analysis of the measurements are discussed.

1. R.F. Kemp and J.M. Sellen Jr., "Plasma Potential Measurements by Electrons and Emissive Probes," Rev. of Sci. Instru. 37(4):455-461, April 1966.

2. I. Langmuir, "The Interaction of Electron and Positive Ion Space Charges in Cathode Sheaths," Physical Review, 33(6), June 1929.

3. *Plasma Diagnostics,* O. Auciello and D.L. Flamm, ed., Academic Press, 1989.

6Q41

A High Frequency Probe for Absolute Measurements of Electric Fields in Plasmas, II

N. Brenning, H. Gunell, and S. Torvén
Div. of Plasma Physics, Alfvén Lab, Royal Institute of Technology, SE-100 Stockholm, Sweden

In a previous publication, here called paper I (Torvén *et al*, J. Phys. D: Appl. Phys. 28 (1995), 595), a new technique to measure high frequency electric fields in a plasma was proposed and tested. Instead of maintaining a high probe impedance and measuring the difference in probe potential, the two electrodes of a double probe were externally connected by a low impedance (50 Ω) and the current in this external circuit was measured. This current gives, after proper evaluation, a measure of the electric field within the plasma. The technique is useful for frequencies that are so high that it is difficult to maintain a high probe impedance. We have used it up to about 1 GHz.

In paper I the theory for the operation of such probes in vacuum was presented and tested experimentally. A discussion, and some experimental results, were also given concerning under what conditions the vacuum solution can be used in a plasma.

Here this work is continued with the emphasis on the operation of the probe in a plasma. Important parameters are the following ratios: between the probe wire thickness and the Debye length, between the probe pair separation and the Debye Length, between the wave frequency and the plasma frequency, and between the probe bias and the electron thermal energy.

6Q42

A Pulsed-Laser X-ray Source for X-ray Diagnostic Calibration

A.R. Moats, F. Camacho, S. Cameron, D.L. Fehl, C. Martinez, J. Porter, L. Ruggles and R. Spielman
Sandia National Laboratories, Albuquerque, NM

We are now performing imploding annular wire-array experiments on the PBFA-Z accelerator. The experimental diagnostics include X-ray Diode detectors (XRDs), photo-conducting diode detectors (PCDs), and x-ray pinhole cameras both time-integrating and time-dependent.

We have set up a pulsed-laser x-ray source for calibration of these diagnostics. A pulsed 10-joule Nd:YAG laser is shot onto a low-Z target, and a combination of filters then provides a large-area, mono-energetic source with a one-nanosecond pulse width. Measurements of the diagnostic's sensitivity between 160 eV and 3 keV can be determined with this source with the appropriate combination of target and filter. The reference standard is a 1024x1024 pixel x-ray CCD that measures the source intensity and is calibrated at 100 eV to 2500 eV.

The utility of this calibration facility is the ability to monitor diagnostic sensitivities in a timely fashion as these detectors are exposed to the harsh Z-pinch environment in PBFA-Z.

For this paper, we show the calibration facility setup and sample calibrations of PCDs and XRDs. We also present data on a PCD detector sensitivity vs. bias voltage study.

Sandia is a multiprogram laboratory operated by Sandia Corporation, a Lockheed Martin Company, for the US DOE under Contract DE-AC04-94AL85000.

6Q43

Spectroscopic Characterization of an ECR Processing Plasma

D. Lafrance, A. Sarkissian
INRS-Energie et Matériaux
Varennes, Qc, Canada J3X 1S2

We have developed an electron cyclotron resonance (ECR) plasma source [1] for plasma processing applications. The source has been used for plasma assisted nitriding [1], diamond-like film deposition [2] and for sputter-deposition and ion-mixing of metallic films [3]. The plasma characteristics can influence the properties of the processed surfaces. Therefore, the measurements of plasma parameters, preferably using a non perturbing technique, is essential.

We have used visible spectroscopy to measure the electron temperature of these processing plasmas. The technique relies on the measurement of the ratio of two line intensities [4]. In nitrogen plasma, the ratio of two molecular band heads intensities is used, whereas in other plasmas the ratio of Ar-He line intensities, injected as trace elements, is used.

A 1-m Czerny-Turner spectrometer with a 1200 lines/mm grating is coupled to an optical multi-channel analyzer (ISIT CCD) to give a spectral resolution of 0.02 nm/pixel in the visible region.

We have compared the results of spectroscopic measurements with those obtained from Langmuir probe measurements. The details will be presented at the meeting.

Sponsored by NSERC Canada

[1] Sarkissian et al., Proc. 5th Int. Conf. On Plasma Surface Engineering, Garmish, Germany, Sept. 1996.

[2] S. Chiu et al., ICOPS 1997 in this preceding.

[3] A. Sarkissian et al., accepted for publication in *Surf. Coat. Technol.*, 1997.

[4] K. Berhringer, *Plasma Phys. Contr. Fusion*, **33**, 997.

6Q44

Interferometer Measurements In Pulsed Plasma Experiments

I.V. Lisitsyn, T. Kawauchi, S. Kohno, T. Sueda, S. Katsuki and H. Akiyama
Department of Electrical and Computer Engineering, Kumamoto University
Kurokami 2-39-1, Kumamoto 860, Japan

Short time scale plasma plays key role in most pulsed power systems like plasma opening switch, z-pinch, electromagnetic launchers and in pulsed laser beam-target interaction study. All mentioned plasmas have different densities and temperatures, but these parameters lie inside the operational density range of He-Ne laser interferometer and can be measured. Plasma pulse duration is usually between 100 ns and 1 ms that makes possible to use the interferometer without precise arm length stabilization, because vibration of the optical elements of

the interferometer has characteristic time of several to several tens milliseconds.

A simple He-Ne laser interferometer of Michelson scheme is used to measure the line-integrated plasma density in various plasma experiments. Time- and spatially resolved measurements were performed for plasmas covering the line-integrated electron plasma density range between 10^{14} and 10^{19} cm^{-2}.

In our experiments we used the interferometer based on low average power (5mW) He-Ne laser without complicated and costly stabilization or deduction environments. Nevertheless, using high quality optics and electrical noise reduction system we achieved the phase shift resolution as high as $\pm 0.5^{\circ}$ for low density plasma measurements. The upper density level of measured plasma is limited by laser beam refraction and attenuation. The optical scheme provides low refraction influence which can be neglected in actual experiments. The description of interferometry method and hardware as well as experimental results for plasma opening switch, laser produced plasma, streamer discharge, electrothermal launcher and railgun are given.

Thursday, 22 May 1997
8:30 a.m. – Kon Tiki Ballroom

Plenary Session

Tokamak Fusion Science Research on the DIII-D Tokamak

Dr. Thomas C. Simonen

Director, DIII-D Program
General Atomics, La Jolla, CA, USA

Chair: J. Hyman

Thursday Morning, 22 May 1997
10:00 a.m. – Kon Tiki Ballroom

Special Oral Session 7A:
2.7 Microwave Generation and Microwave Plasma Interactions

Chair: J. W. Luginsland

7A01

The Impact of CAD in the Computational Design Process on Total System Development

Lawrence Ives and William F. Vogler
Calabazas Creek Research, Inc.
Saratoga, CA 95070

The obvious advantage of computer aided design (CAD) software in computational design is instant feedback and visualization of device geometry. CAD can also dramatically reduce the learning curve for new codes and allow rapid turnaround during iterative design.

This is only a fraction of the impact CAD can have, however. Full implementation can reduce mechanical design, drafting, parts procurement, and assembly, while increasing quality and yield. By beginning the computational design process with CAD layouts of existing designs, the user can take full advantage of previous sub-assembly and piecepart mechanical design and development and eliminate redrafting of these peripheral parts and subassemblies. This process facilitates and encourages reuse of existing designs and promotes piecepart and subassembly standardization. The assembly process is simplified because common processes and procedures are possible.

This presentation will demonstrate how the use of CAD for geometrical input in computational design codes, using customized windows and scripts, can simplify the initial setup for new designs. It will demonstrate how a new design, obtained from an existing layout drawing, can eliminate drafting and mechanical design tasks. It will also describe the potential impact on parts procurement, inventory, and assembly.

7A02

Emission Properties of the Silicon Cathodes Coated with Doped Diamond-Like Carbon Films

V.G. Litovchenko, A.A. Evtukh, N.I. Klyui, R.I. Marchenko and V.A. Semenovich
Institute of Semiconductor Physics, 45 Prospekt Nauki, Kiev, 252650, Ukraine

To enhance the filed emission of electrons from cathodes, coated by diamond-like carbon (DLC) films the emission properties of the DLC-films, deposited on the plane silicon wafers and silicon tip arrays have been investigated. The silicon tip arrays were formed by wet chemical etching on n-type Si and sharpened using method of surface oxidation. The DLC films were deposited at low temperature from CH_4:H_2:N_2 mixture using PE CVD. Nitrogen content in gas mixture was varied in wide range. As a result, the DLC films with different content of nitrogen have been obtained. For characterization of these DLC films on silicon, the different methods (namely, ellipsometry, current-voltage dependenses, IR spectrometry) have been used. The optical absorption spectra indicate on the creation the C-N bonds in N-doped DLC, and increasing of sp^3 bond contents have been observed. So, it is reasonable to wait increasing of the stability of such cathodes.

For comparison of the emission properties of the structure with DLC films deposited in different conditions the threshold (onset) voltages, and field enhancement factors, effective emission areas, calculated from Fowler-Nordheim plots analysis, have been used. It was obtained that for the structures with nitrogen doped DLC films the emission appear at remarkable lower voltage and the calculated work function is on ~0.5 eV less than for case of undoped DLC (at the same-values of sp^3 bond contents and refractive index).

The model for explanation of the experimental results will be presented and role of nitrogen will be discussed.

7A03

Wiggler Enhanced Cyclotron Autoresonance Maser Amplifiers*

A.T. Lin and Chih-Chien Lin
Department of Physics, University of California at Los Angeles, Los Angeles, CA 90024-1547

The performance of cyclotron autoresonance maser amplifiers can be significantly improved by using a properly spatially profiled helical wiggler. The enhancement process derives from the unique property of electron orbit in a combined solenoidal and wiggler field. A properly imposed wiggler gives rise to an electron orbit which acts to selectively inhibit autoresonance acceleration of electrons by the electromagnetic wave. The proposed configuration is able to alleviate the severe problem of performance degradation by beam velocity spread. Simulation results show that, by using a 500kV and 200A pencil beam, more than 20% output efficiency can still be attained at 94GHz, even with 5% beam velocity spread. If higher output power is desired, both beam voltage and current could be increased. We will address the effects of beam AC space charge on the amplifier performance.

This work has been supported by DoD Muri program (High Energy Microwave Source) as managed by AFOSR under Grant No. F49620-95-1-0253

7A04

Nonlinear Theory of the Interaction Between an Annular Electron Beam and the Azimuthal Surface Waves (ASW)

V. Girka and T. Malykhina
Kharkiv State University, 310077 Kharkiv, Ukraine

The article is devoted to the investigation of nonlinear interaction between extraordinary polarized electromagnetic eigenmodes of a cylindrical metal waveguide, which is partially filled by cold magnetoactive plasma, and electron beam, which is rotated around plasma column. The ASW propagate with azimuthal wavenumber across external steady axial magnetic field. The problem is solved using method of macro particles. The set of differential equation is calculated numerically. Dependences of the ASW's amplitude and phase on time are obtained. Distribution of the beam particles in the waveguide and phase space is examined. The regime of nonlinear saturation of the beam-plasma instability is accompanied by formation of electron bunches in a shape of "electron needles in a magnetrons". The investigation fulfilled can be applied in the branch of plasma electronics.

7A05

Diode Plasma Effects on the Microwave Pulse Length from Relativistic Magnetrons

D. Price and J.S. Levine
Primex Physics International, San Leandro, CA
J. Benford
Microwave Sciences, Lafayette, CA

A model to account for the relativistic magnetron microwave pulse length based on radial cathode plasma motion is put forth. If the dense plasma front represents one part of the microwave boundary condition, its motion influences the magnetron resonance conditions. Both time varying pulse amplitudes and frequencies are expected. The main plasma ion constituent is believed to be Hydrogen and its source is adsorbed water. Corroboration with measurements in various L-band magnetron configurations is demonstrated. Results of an experiment to defeat the pulse-shortening mechanism are presented and compared to similar experiments conducted by other researchers.

7A06

Laboratory Simulation of Ionospheric Plasma Heating Experiments

M.C. Lee, R.J. Riddolls, N.E. Dalrymple, K. Vilece, M.J. Rowlands, and D. Moriarty
Massachusetts Institute of Technology Cambridge, MA 02139
K.M. Groves
Phillips Laboratory, Hanscom AFB MA 01731
M.P. Sulzer
Arecibo Observatory, Arecibo, Puerto Rico 00613
S.P. Kuo
Polytechnic University, Farmingdale, NY 11735

Laboratory experiments, carried out at MIT Plasma Science and Fusion Center with the Versatile Toroidal Facility, have been conducted to simulate ionospheric plasma heating caused by High Frequency (HF) radio waves. Recent VTF laboratory experiments have

successfully reproduced "cascading" and "Frequency-upshifted" spectra of HF wave-enhanced Langmuir waves resembling the spectra observed in Arecibo experiments. The VTF experimental results are well-explained using the source mechanism proposed by Kuo and Lee [Geophys. Res. Lett, 19, 249, 1992] to interpret observed Langmuir wave spectra at Arecibo, Puerto Rico. This mechanism is referred to as a nonlinear scattering of parametric decay instability (PDI)-excited Langmuir waves by pre-existing lower hybrid waves to preferentially produce anti-Stokes (i.e., frequency-upshifted) Langmuir waves. Recent radar spectral observations of anti-Stokes Langmuir waves at Arecibo with improved range and time resolution [Sulzer and Fejer, J. Geophys. Res., 99, 15,035, 1994] can be reasonably understood in terms of this nonlinear scattering process.

7A07

The Influence of Plasma on the Amplification of Traveling Slow Waves

S. Kobayashi, T.M. Antonsen, Jr., G. Nusinovich and Y. Carmel
University of Maryland, College Park, MD 20742-3511

The performance of traveling wave tube amplifiers is limited by the need to keep the electron beam close to the wall of the slow wave structure. We investigate the possibility of relaxing this constraint by propagating the beam through a magnetized plasma channel. This approach has already found success in the case of a coupled cavity TWT.[1] The role of the plasma is to modify the transverse structure of the amplified wave so that the axial electric field of the wave peaks on the axis of the device. This effect is most dramatic when a so called 'hybrid mode' representing a coupled electromagnetic slow wave and Trivelpiece-Gould mode is formed. The theory addresses the linear gain of a sheath helix TWT driven by a solid beam and filled with a plasma of the same radius as the beam. Numerical results of gain and bandwidth for a variety of parameters will be presented.

This work has been supported by the U.S. Air Force Office of Scientific Research.

[1] L.A. Mitin, et al., Plasma Physics Reports, vol. 20, 662 (1994).

Thursday Morning, 22 May 1997
10:00 a.m. – Board Room

Oral Session 7B:
5.5 Environmental / Energy Issues in Plasma Science
Chair: L. Christophorou

7B01-02 *Invited*

UV Photon and Low-Energy (5–150 eV) Electron-Stimulated Processes at Environmental Interfaces

Thomas M. Orlando
Environmental Molecular Sciences Laboratory
*Pacific Northwest National Laboratory**
Richland, WA 99352

Irradiation of surfaces and interfaces with low-energy (5–150 eV) electrons and ultraviolet photons occurs during the storage of "mixed" (chemical/radioactive) waste forms and during processing steps which involve the use of low temperature plasmas. It is well known that electron- and photon-stimulated desorption (ESD and PSD) from wide band-gap materials and interfaces can be initiated by Auger decay of deep valence and shallow core holes. This process consists of hole production, Auger decay, reversal of the Madelung potential, and ion expulsion due to the Coulomb repulsion. ESD and PSD of neutrals also occurs and involves production of electron-hole pairs and excitons. Generally, neutral yields dominate ESD and PSD cross sections, which typically vary between ~10^{-16} and 10^{-22} cm^2.

We present results on the ESD and PSD of environmentally relevant substrates such as ZrO_2(100), soda-glass, and $NaNO_3$. The major cation thresholds and yields indicate that ESD and PSD from these complex materials involves Auger stimulated events. In particular, desorption thresholds correlate with ionization of the O(2s), Zr(4p), Si(2p) and Na(2s) levels. The near band-gap threshold energy (~5–7 eV) for the desorption of neutrals (i.e., atomic oxygen, NO, etc.) demonstrate the overall importance of self-trapped and localized excitons in both ESD and PSD of typical ceramics and oxides.

*PNNL is operated for the U.S. Dept. of Energy by Battelle Memorial Institute under Contract: DE-AC06-76RLO 1830

7B03

Plasma-Produced Erbia Coatings for Waste Reduction in Plutonium Casting Operations*

B.P. Wood, D. Soderquist, A. Gurevitch, J. Steele, F. Hampel, and K.C. Walter
Los Alamos National Laboratory
Los Alamos, NM 87545
A.J. Perry
AIMS Consulting, San Diego, CA 92127
J. Treglio
ISM Technologies, Inc., San Diego, CA 92131

Disposal of molds used in plutonium casting operations creates a significant waste stream, since such molds are typically only used once or twice, due to the highly corrosive nature of molten plutonium. Erbia (erbium oxide) is inert to molten plutonium, but being a brittle ceramic material, is difficult to make adhere to mold surfaces under severe conditions of thermal expansion mismatch. We report on efforts to utilize an ion implantation process to improve the adhesion of erbia coatings deposited from a cathodic arc derived erbium plasma. Coatings were created using both dc and pulsed cathodic arc sources in a low pressure oxygen background. Ion implantation was achieved by pulse biasing the target to several 10's of kilovolts during some steps in the process. This high energy ion bombardment was found to produce superior coating adhesion, and treated samples successfully resisted attack from molten plutonium in a casting test. The effect of variations in ion implantation parameters, coating parameters, and coating stoichiometry will be discussed.

*Work supported by Advanced Manufacturing Industrial Partnerships, U.S. Department of Energy

7B04

Aerosol Plasma for Aqueous Wastes Treatment

V.M. Bystritskii, Y. Yankelevich, T. Wood, F. Wessel and D. Yee
University of California at Irvine, Irvine, CA 92697-4575

We describe 2-stage technology for degradation of aqueous wastes (containing organic pollutants), based on Aerosol Plasma Treatment combined with bio-treatment stage. Short pulsed corona/streamer discharge in aerosol with controlled applied voltage amplitude of 50–90 kV, pulse duration of 100–150 ns, and reprate of 10^{2-3} Hz is organized inside a 40 liter reactor. The aerosol with drops diameter of 10–100 μm is provided with a commercial atomizer. 2–3 fold pulsed E-field enhancement near the drops surface combined with large specific water/air surface (10^{2-3} cm^2/g) result in copious generation of energetic and hydrated electrons, active free radicals (O, H, OH), providing efficient degradation and partial dechlorination of the primary organic molecules of the pollutants[1].

Estimation of total specific energy cost per degraded molecule of pollutants based on the wall voltage utilization is in the range of 0.1–0.2 keV for Paranitrophenol, and 0.2–1.5 keV for Di-Chlorophenol (DCP) and Per-chloroethylene (PCE) respectively, and depends on the operational parameters of the discharge, and the pollutants concentration. These values are many times lower when compared with other aqueous pollution treatment technologies (Sono-hydraulic, Electro-hydraulic, High energy electron beam, etc.). In the second stage an inoculation of the aerosol-processed DCP water samples (having residual chlorination degree of 65–70%) with bacteria *Pseudomonas mendocina* KR1 demonstrated as high as 90% degree of dechlorination in the first 40 hours after inoculation. The control sample (i.e., not aerosol-processed) inoculated with the same type of bacteria demonstrated no chloride released and no bacterial growth. Main features and advantages of the novel two stage technology are presented and analyzed.

This research was partly supported by LACOR program, grant # 4514U0015-3A

[1] V. Bystritskii, Y. Yankelevich, F. Wessel, Gonzales, T. Olson, T. Wood, V. Puchkarev, D. Yee, L. Rosocha, 2-nd Intern Conf. on Advanced Oxidation Technologies, Cincinnati, 25-29 October, 1996

7B05

Decomposition of Methylene Chloride in Non-Thermal Plasmas

B.M. Penetrante, M.C. Hsiao, J.N. Bardsley, B.T. Merritt and G.E. Vogtlin
Lawrence Livermore National Laboratory
Livermore, CA 94550
A. Kuthi
Plasma & Materials Technologies, Inc.,
Chatsworth, CA 91311
C.P. Burkhart and J.R. Bayless
First Point Scientific, Inc., Agoura Hills, CA 91301

Identification of the mechanism and plasma species responsible for methylene chloride decomposition is important for choosing the most energy efficient type of non-thermal plasma reactor. This paper presents the first experimental evidence showing that the decomposition of methylene chloride in a non-thermal plasma at ambient gas temperature proceeds via reaction with nitrogen atoms. The data is also the first comparison of the energy efficiency of electron beam and pulsed corona processing of methylene chloride under identical gas conditions. We observe that electron beam processing is more energy efficient because of its higher rate for electron-impact dissociation of N_2. In dry air mixtures, the decomposition of methylene chloride is degraded substantially because the nitrogen atoms are consumed in the production of nitrogen oxides. At higher gas temperatures (300°C), the decomposition of methylene chloride in dry air is shown to proceed via reaction with oxygen atoms. The main products of methylene chloride decomposition in dry air mixtures are CO, CO_2, HCl, and Cl_2.

Work performed in part at LLNL under the auspices of the U.S. DOE under Contract # W-7405-ENG-48, with support from the Chemical Sciences Division of the Office of Energy Research.

7B06

Modeling of Plasma Remediation of VOCs in Dielectric Barrier Discharges*

Xudong "Peter" Xu and Mark J. Kushner
Department of Electrical and Computer Engineering,
University of Illinois, 1406 W. Green Street,
Urbana, IL 61801

Since each year significant quantities of toxic wastes containing volatile organic compounds (VOCs) are produced by chemical and allied industries, destruction of these VOCs has become a major environmental concerns. Dielectric barrier discharges (DBDs) are promising low cost plasma sources for destruction of the VOCs. The efficiency of plasma remediation depends on gas mixture, the dielectric constant and format of the voltage pulse.

We have developed 1-d and 2-d plasma chemistry and hydrodynamic models to focus on the energy efficiency and optimum conditions for destruction of chlorinated hydrocarbons including CCl_4 and $CHCl_3$ which are widely used as industrial solvents. The plasma remediation model consists of circuit models, solution of Boltzmann's equation for the electron energy distribution, plasma chemistry modules, and solution of the compressible Navier Stokes equations. CCl_4 and $CHCl_3$ can be initially destroyed by dissociative-electron-attachment which requires different discharge conditions than for generation of radicals for chemical remediation. These different operating regions will be discussed. We will present a detailed description of the major plasma chemical pathways and discuss the effects of varying parameters, such as applied voltage, dielectric constant, gas mixture content in the gas stream, and temperature on the amount and energy efficiency of remediation.

*Work supported by the National Science Foundation and Office of Naval Research.

7B07

Decomposition of Dichloroethane in a Plasma Arcjet Reactor: Experiment and Modeling

H.R. Snyder and C.B. Fleddermann
Department of Electrical and Computer Engineering
University of New Mexico, Albuquerque, NM 87131

A plasma arcjet reactor has been constructed to study the fundamental reaction kinetics for decomposition of hazardous liquids. The arcjet was operated at a power level of 1.5 kW and an argon flow rate of 17.5 LPM. The temperature profile of the plasma jet was measured using an enthalpy probe and the maximum temperature measured in the plasma jet was 1850°C. A surrogate liquid waste, 1,2 dichloroethane, was injected into the plasma jet and the decomposition byproducts were monitored using a residual gas analyzer. A removal efficiency greater than 99% was obtained. The temperature profile was used to model the arcjet as a non-isothermal tubular flow reactor. The experimental results were compared to the predicted byproducts from the tubular reactor model and indicated that a photochemical dissociation process accounted for

some of the decomposition of dichloroethane. The photochemical dissociation processes were attributed to the large amount of UV emitted from the plasma. This research also provided a more comprehensive understanding of the critical parameters associated with thermal plasma chemistry and the destruction of liquid waster.

*This work is supported by the U.S. Department of Energy through the Waste Education and Research Consortium (WERC) administered by New Mexico State University.

7B08

Oxidation of Styrene Using a Silent Discharge Plasma

G.K. Anderson, J.J. Coogan, H.R. Snyder
Los Alamos National Laboratories
Chemical Science and Technology Division
Los Alamos, NM 87545

A cylindrically symmetrical dielectric barrier discharge was constructed to study the oxidation of styrene in the gas phase. Several operating parameters were varied to find the optimum conditions for styrene destruction. An argon/oxygen mix was used to generate the non-thermal plasma with oxygen concentrations ranging from 2–8%. The styrene concentrations ranged from 1000ppm to 6000ppm and energy densities of the SDP cell ranged from .5–3 kJ/liter. The temperature of the SDP cell was varied from 200°C to 450°C. The concentrations of styrene and its partial oxidation products were monitored by a GC-MS and the concentrations of CO_2 and CO were measured by FTIR. Destruction efficiencies of styrene up to 99.9% were measured.

Thursday Morning, 22 May 1997
10:00 a.m. – Toucan Room

Oral Session 7C:
5.4 Flat Panel Displays
Chair: C. M. Tang

7C01-02 ***Invited***

Phosphors for Flat Panel Field Emission and Plasma Displays

Christopher J. Summers, Director
Phosphor Technology Center of Excellence
Georgia Institute of Technology, Atlanta, GA

Truly emissive flat panel displays have long been sought, and have faced many technological challenges, but are now very close to becoming a commercial reality. A review is given of the recent developments of phosphors for low to medium voltage applications in field emission displays (FED) and in new plasma display panels (PDP). For FED's the drive to operate at lower voltage and power, is frustrated by the rapid decrease in phosphor luminous efficiency. This is due to the smaller volume of luminescent activators that are sampled at low electron beam voltages and by the presence of non-radiative surface recombination effects. The higher drive currents possible from a field emission device can be used to compensate for this loss in brightness and efficiency, but for many current phosphors, saturation and coulombic degradation limit the advantage of high current sources. The use of fast activators and a more complete understanding of electron-solid interactions at low voltages is shown to be necessary to characterize and develop solutions to this problem.

In PDP the switch to Xenon plasma excitation sources requires further phosphor optimization to achieve the same efficiencies when pumped by 150–180nm radiation, than the 254nm Hg discharge used in lighting, but many existing phosphors have acceptable properties for current applications. There is, however, a need to increase phosphor lifetimes in a display by developing coating techniques. Additionally, an improved red chromaticity and a faster green phosphor to prevent smearing, are desired as well as a more efficient blue phosphor. Recent progress in this area and the search for more power efficient plasma phosphors will be discussed.

7C03

Development of Low Voltage Field Emitter Cathodes with Enhanced Electron Emission Coatings for Flat Panel Displays

D. Palmer, D. Temple, J. Mancusi, L. Yadon,
D. Vellenga and G.E. McGuire
MCNC/Electronic Technologies Division
Research Triangle Park, NC
(919) 248-1837 dpalmer@mcnc.org

Field emission cathodes are being developed for use in commercial and military applications such as microwave power tubes, sensors, high brightness electron beam sources for analytical instrumentation, and flat panel displays. For all of these applications, lower voltage operation is highly desirable. In flat panel displays, low voltage operation allows the use of inexpensive, off-the-shelf driver electronics and decreases the drive power requirements.

The proposed approach is to decrease the operating voltage of field emission cathodes by using diamond films to lower the work function of the emitting surface as compared to conventional tip materials such as Si or Mo. Under certain conditions, diamond films have been shown to exhibit negative electron affinity, which is expected to result in greatly enhanced electron emission. The diamond films will also improve reliability of the cathodes through decreased probability of vacuum arcs due to the lower operating voltages, and increase stability of the emission current due to the high chemical and mechanical stability of the diamond firm surface.

By producing emission from diamond film on a sharp silicon tip rather than a planar surface, interception of the electron stream by the gate electrode is reduced. Due to the field enhancement of the sharp tip, electron emission takes place only from the tip apex area into a narrow cone which does not normally intercept the gate electrode, as demonstrated by negligible gate current measured from MCNC's uncoated Si cathodes.

An overview of this development program will be presented along with emission data from uncoated Si arrays. These data will compared to those collected from diamond-coated arrays as they are fabricated and tested.

This work was performed under the DARPA/ETO High Definition Systems program, contract number N00014-96-C-0283

7C04

Three-Dimensional Simulation of Field Emitter Arrays Using EO-3D

Cha-Mei Tang
Creatv MicroTech, Inc. and National Institute of Standards and Technology
Gaithersburg, MD 20899

Electron trajectories from the field emitters in the field emitter displays are very important. The trajectories effect the design of pixel size, the phosphor voltage, the gap between the field emitter arrays and the phosphor, color purity, etc. The electron trajectories are effected not only by the local potentials around each emitter, but the global field of each pixel. Two dimensional simulations would not be adequate. We are using a three-dimensional computer code EO-3D by Munro's Electron Beam Software, Ltd. to find the electric potential and the electron trajectories. First, the results of this code will be bench marked with experimental data of simplified field emitter array geometry not that of a display. Later, it will be applied to hypothetical display pixel geometry. We will discuss the properties of this software for these applications as well as the simulation results.

This work is supported DARPA.

7C05-06 *Invited*

Dry Etching Trends in Flat Panel Display Processing

William W. Yao
dpiX, A Xerox Company, Palo Alto, CA

Active Matrix Liquid Crystal Display (AMLCD) market is projected to quadruple in size by the next millennium. Within the last year, the flat panel display (FPD) marketplace has been very dynamic and the product requirements are evolving rapidly towards larger size, higher resolution, lower power consumption and at ever lower price targets. These market forces are driving FPD process technology innovations at a breathtaking pace. For FPD processing, dry etching is in an analogous position to that in IC processing back in the early 80s when the industry was posed to make the transition from wet to dry etch. Up to now, dry etching has only seen widespread manufacturing applications in Si and SiN processing. Within the last year, both Applied Komatsu Technology (AKT) and Lam Research (LRC) have introduced next generation FPD dry etch cluster tools.

These tools offer improved process characteristics and enhanced capability that present many new opportunities to apply dry etching to FPD processing. In the next couple of years, dry etching will be a key enabler for architectural innovation. In this paper, these new dry etch processes and their applications in FPD display will be reviewed.

7C07

Microhollow Electrode Discharge Flat Panel Displays

K.H. Schoenbach, T. Tessnow and F.E. Peterkin
Physical Electronics Research Institute, Norfolk, VA
W.C. Nunnally
College of Engineering,
University of Missouri-Columbia, Columbia, MS

Microhollow electrode discharges, discharges between thin metal foils with submillimeter gap and submillimeter holes in cathode and anode, show three distinct modes of operation; a) at low currents the predischarge mode, a glow discharge between the outer faces of the hollow electrodes, b) at higher current a phase with increased ionization due to "pendulum" electrons in the cathode hole, and c) at even higher current an abnormal glow discharge between the edges of cathode and anode hole. A fourth discharge mode, the so-called partial discharge seems to occur at high gas pressure at pressure times hole diameter values exceeding 10 Torr cm. Experiments in a 0.2 mm diameter hollow electrode geometry with Xe and Ar at atmospheric pressure have shown that the discharges emit excimer radiation[1]. Control of these discharges which have a sustaining voltage of several hundred volts allows their use in flat panel displays. A second mode of operation which allows us to form addressable flat panel displays is the predischarge mode. It could be shown that with a third electrode close to the cathode, but outside the anode-cathode gap, the intensity of the discharge could be linearly varied by varying the voltage at the third electrode in a range below 100 V[2]. The predischarges have a resistive behavior (positive slope of current-voltage characteristics) which allows us to place them in parallel without individual ballast and without segmentation of anode and cathode. This has been demonstrated in a small device with nine addressable microhollow cathode discharges.

Supported in part by DOE, Advanced Energy Projects Division.

[1] K.H. Schoenbach at al., these Proceedings.

[2] K.H. Schoenbach and W.C. Nunnally, US Patent No. 5,561,348.

7C08

Low-Temperature Deposition Pathways to Silicon Nitride, Amorphous Silicon, Polycrystalline Silicon, and n Type Amorphous Silicon Films Using a High Density Plasma System

Sanghoon Bae, David Farber, Ali Kalkan
and Stephen Fonash
Electronic Materials and Processing Research Laboratory, The Pennsylvania State University, University Park, PA 16802

We report on our low temperature deposition approach to silicon nitride, amorphous silicon (a-Si) and polycrystalline silicon (poly-Si), and doped a-Si films using an electron Cyclotron Resonance PECVD system. We find that silicon nitride films, deposited at temperatures as low as 30°C, can be obtained with ~$7x10^{-9}$ A/cm^2 leakage currents, flat band voltages of ~0.6 V, and breakdown field strengths of ~6 MV/cm. In the case of the a-Si and poly-Si films, we employ X-ray diffraction, UV reflectance, photoluminescense, and electrical conductivity for evaluation. We find that a-Si films, deposited in the 30~120°C temperature range, can be obtained with a photo-sensitivity (I_{photo}/I_{dark}) of ~10^4 under AM1 light and that we can also produce polycrystalline films at temperatures as low as 120°C on glass and polyethersulfone substrates. In the case of doped materials, conductivities of 10^{-3}~10^{-2} S/cm can be obtained for the as-deposited layers grown at temperatures as low as 40°C.

7C09

MgO Erosion in Plasma Displays Measured with Microbeam RBS

R.T. McGrath and R. Veerasingam
The Pennsylvania State University, 227 Hammond Bldg., University Park, PA 16802
H. Schone and D. Walsh
Sandia National Laboratories, Albuquerque, NM
C. Zarecki
Photonics Imaging, Northwood, OH

Spatially resolved Rutherford Backscattering (RBS) measurements have been made on interior thin film surfaces of plasma driven flat panel displays. Panels, provided by Photonics Imaging, were manufactured with films of MgO, typically 1000nm thick, on interior surfaces adjacent to the discharge working gas. MgO has

good secondary electron emission properties and its presence enhances the pixel discharge intensity per volt applied. In these experiments, pixels were operated at excessively high voltages for long periods of time in order to accelerate the pixel aging processes. The nuclear microprobe at Sandia National Labs was then used to measure the erosion of the MgO that had occurred. A He microprobe beam at 2.8 MeV and with an average beam spot diameter of ~8 μm was used to examine the MgO film over areas (250 μm x 250 μm) spanning several pixels. The thickness of MgO at each spot was deduced by measuring the shift in the energies of He ions backscattered from the PbO substrate, upon which the MgO had been deposited, and correlating the observed energy losses with the known stopping power of MgO. This allowed measurement of MgO film thickness to an accuracy of ±1.5nm. In previous work, we have measured and modeled the discharge current density during pixel firing. We use these descriptions of ion flux incident upon the pixel interior surface, along with sputtering yields for MgO, to estimate the overall erosion expected, and correlate this to the integrated erosion observed.

Thursday Morning, 22 May 1997
10:00 a.m. – Macaw Room

Oral Session 7D:
7.1 MHD and EM/ETH Launchers
Chair: R. D. Richardson

7D01

Plasma Parameters in Burn Rates Processes of a Solid Propellant for Electrothermal-Chemical Launch Devices

M.A. Bourham, J.G. Gilligan and C.J. Boyer
North Carolina State University
Department of Nuclear Engineering
Raleigh, NC 27695-7909

A plasma source for an electrothermal-chemical (ETC) device produces a high-density, low-temperature plasma, which has a near-blackbody spectrum. Burn rates of solid propellants may be limited by absorption of a large fraction of the source fluence in the developed vapor cloud. The electrothermal-chemical experimental facility PIPE at NC State University is used to characterize the burn rates of single grain monolithic JA2 propellant. It has been shown that burn rates are much higher than that of conventional ignition, especially when the plasma is injected normal to the grain. The plasma core temperature at the source exit is higher than that of the plasma boundary layer, and is evaluated from the measured discharge parameters, then compared to predictions of the 1-D, time dependent code SODIN [1] and analytical scaling laws [2]. Boundary layer temperature and density are evaluated from optical emission spectroscopy [3]. It appears that plasma kinetic pressure has a stronger effect on the burn rate than the plasma radiative heat flux. Results on the effect of source parameters on measured burn rates will be presented.

Work supported by the US Army Research Office Contract DAAH04-95-1-0214, and the US Office of Naval Research Contract N00014-95-1-1221.

[1] J.D. Hurley, M.A. Bourham and J.G. Gilligan, "Numerical Simulation and Experiment of Plasma Flow in the Electrothermal Launcher SIRENS," IEEE Trans. Magnetics, **31**, 616, January 1995.

[2] A. Loeb and Z. Kaplan, "A Theoretical Model for the Physical Processes in the Confined High Pressure Discharges of Electrothermal Launchers," IEEE Trans. Magnetics., **25**, 342, 1989.

[3] O.E. Hankins, M.A. Bourham and D. Mann, "Observation of Visible Light Emission from Interactions Between an Electrothermal Plasma and a Propellant," IEEE Trans. Magnetics, **33**, January 1996.

7D02

Progress on TURBFIRE, a Simulation of Plasma-Surface Interactions in Electric Launchers

E.C. Tucker, N.P. Orton, J.G. Gilligan and M.A. Bourham
Department of Nuclear Engineering
North Carolina State University
Raleigh, NC 27695-7909

Plasma-surface interaction is of great interest for the design and modeling of electric launchers. We are developing a 2-D boundary layer code which includes turbulence and radiation transport, to predict mass evolution rates at plasma-surface interfaces. This code, TURBFIRE, will aid in the understanding of vapor shielding and the effects of turbulence on energy transport to the surface. It has been previously shown that radiation transport is the dominant mechanism of heating and ablating plasma-facing components, and that conduction is

small [1]. Experimental result suggest that turbulence enhances radiation transport through the turbulent mixing of hot outer fluid with the cooler fluid near the surface [2]. Previous models [1,3] have not combined radiant energy transport with turbulent convection in a self-consistent manner. Currently, TURBFIRE allows the determination of energy transport to the surface via both radiation and conduction. The system has been modeled using fluid boundary layer equations, including a two equation (k-ω) model for turbulence, coupled with multigroup thermal radiation transport. Results show that radiation transport to the surface is much greater for turbulent flow than for laminar flow. At present the TURBFIRE code is unstable for cases in which normal pressure gradients are present, including most cases involving ablation of surface material. We have reformulated our equations in terms of the stream-function in an attempt to stabilize the code, and will present preliminary results of this modification.

This work is supported by the U.S. Army Research Office Contract DAAH04-95-1-0214, and the U.S. Office of Naval Research Contract N00014-95-1-1121.

[1] D. Hahn, "Energy transport through the Plasma Boundary Layer," Ph.D. Thesis, NC State University (1989).

[2] C.M. Edwards, M.A. Bourham and J.G. Gilligan, "Experimental Studies of the Plasma-Propellant Interface for Electrothermal Chemical Launchers," IEEE Trans. Magnetics, **31**, 404, January 1995.

[3] N.P. Orton and J.G. Gilligan, "Simulation of the Plasma - Surface Interaction in Electric Launcher," IEEE Trans. Magnetics, **31**, 640, January 1995.

7D03

Optical Diagnostics in High Current Pseudospark Discharges

M. Schlaug, C. Bickes, D.H.H. Hoffmann, P. Felsner, K. Frank, U. Prucker and A. Schwandner
University of Erlangen-Nuremberg, Physics Department I, 91058 Erlangen, Germany

The pseudospark is a low-pressure gas discharge, in which breakdown is at the left branch of the paschen curve. It has meanwhile found world-wide interest as a device for fundamental research and many applications such as high power switches and pulsed electron beam devices. The basic design consists of two electrodes with central apertures which are separated by an insulator. The discharge starts in the hollow cathode and can be triggered by injection of electrons into this region. By the hollow cathode geometry discharge initiation is controlled. Later on electrode phenomena like the "superdense glow" and successive explosive electron emission processes describe the transition to an arc-like high current phase. The paper shortly presents measurements of plasma parameters as a function of gas type and electrode material. The experimental methods used are Laser Induced Fluorescence (LIF), laser absorption spectroscopy, tomographic two-wave interferometry and fast shutter and streak photography. At moderate discharge currents the LIF-method was applied to determine neutral particle density of evaporated electrode material. Typical gas densities are of 10^{19} m^{-3}. Cathode spot formation was investigated with help of laser absorption spectroscopy. Maximum electron densities of about 10^{27} m^{-3} could be detected, spatially correlated to cathode spots. For high peak currents (>40 kA) tomographic two-wave interferometry was used to detect electron density for different electrode materials (e.g. Mo, SiC). The maximum densities are between 10^{24} - 10^{25} m^{-3} the higher values corresponding to metal electrodes. The discharge with metal electrodes was an arc discharge of a few millimetres in diameter compared with semiconductor electrodes, where the discharge is distributed over a significantly larger electrode area.

7D04

High Voltage Subnanosecond Dielectric Breakdown

J. Mankowski, L. Hatfield and M. Kristiansen
Pulsed Power Laboratory, Departments of Electrical Engineering and Physics, Texas Tech University Lubbock, TX 79409-3102
F.J. Agee
Phillips Laboratory, Kirtland AFB, NM 87117
J.M. Lehr and J. Wells
Fiori Industries, Inc., Albuquerque, NM

Present day Ultra Wideband radiation sources produce Megavolt pulses at 100's of picosecond pulsewidths. Empirical data on the breakdown characteristics for dielectric media at these short time lengths and high voltages are either extremely limited or non-existent. In support of the design of these Ultra Wideband sources, we are investigating the breakdown characteristics, at these voltages and time lengths, of several liquids and gases. These include air, N_2, H_2, He, SF_6, transformer oil, and freon-12.

The voltage source used in the experiments will be capable of delivering 700 kV with a 300 picosecond risetime into an open load. The source is charged with a

500 kV Marx bank. The output of the Marx bank is applied to an oil filled, coaxial, charging line. The pulse is then shortened to 300 picoseconds with the use of several peaking gaps. This pulse is applied to the test gap area, capable of housing various gases and liquids at pressures from less than 1 atm to 150 atm.

This work was supported by AFOSR/DOD MURI.
Submitted to ICOPS 97.

7D05

Hydrogen Heating in the Discharge Chamber of Powerful Electric Discharge Launcher

Ph.G. Rutberg, A.A. Bogomaz, A.V. Budin, V.A., Kolikov and A.G. Kuprin
Institute of Problems of Electrophysics of the Russian Academy of Sciences (IPE RAS)
18, Dvortsovaya nab., St. Petersburg, 191186, Russia
Phone #: (812) 315-1757; Fax #: (812) 311-5056

Results of the discharge chamber of electric discharge launcher testing, aiming at heat transfer study is presented. Tests conditions are: initial H2 pressure - 5÷40 MPa, discharge chamber volume - 1400 cm^3, current ≤1.5 MA, energy stored - 1.3 MJ, circuit own frequency - 1 kHz. To simulate gas heating in the EDL discharge chamber and to use high speed camera, diagnostic discharge chamber was made. Basing on the arc dynamics study in the diagnostic discharge chamber, temperature and conductivity estimations of the arc channel were carried out for the EDL chamber. Measured pressure 200 MPa and conductivity 230 $(\Omega xcm)^{-1}$ correspond to temperatures of (3.3–3.5) x 10^4K and of (2.3–2.4) x 10^4K for the arcs, burning respectively in copper vapor and in H_2.

Real temperature seems to lie between these two values. Since the pressure equilibrium in the volume was reached, acoustic oscillations may be used to evaluate gas temperature. Moving arc causes shock waves registered by pressure transducers, placed along discharge length, and by high speed camera. Arc-to-gas energy transfer efficiency rises along with initial H_2 pressure increase and reaches 90% for 40 MPa. Both shock waves propagation and arc radiation absorption contribute to this rise.

Thursday Morning, 22 May 1997
10:00 a.m. – Cockatoo Room

Oral Session 7E:
4.6 Spherical Configurations / Ball Lightning
Chair: U. Shumlak

7E01-02 *Invited*

Results from the HIT-II Coaxial Helicity Injection Spherical Tokamak

B.A. Nelson, T.R. Jarboe, R. Ewig, C. Hoffman, A.K. Martin, K. McCollam, D.J. Orvis, U. Shumlak and B. Udrea
University of Washington, Seattle. WA 98195

The Helicity Injection Tokamak (HIT) has been upgraded to the "HIT-II" configuration. HIT-II extends coaxial helicity injection (CHI) to time scales longer than the wall resistive diffusion time. Previous results on HIT include production and sustainment of up to 250 kA of toroidal plasma current by CHI, *without* a transformer. HIT-II has approximately the same shape as HIT; major radius R = 0.3 m, minor radius a = 0.2 m, with an on-axis toroidal field of up to 0.67 T. The 1 cm copper shell of HIT is replaced in HIT-II by a 6 mm stainless steel shell. Equilibrium fields are provided by 28 feedback controlled poloidal field coils. These coils also provide programmable control of the magnetic flux boundary conditions for CHI current drive and are capable of 100 mWb of transformer flux swing. HIT-II has a graphite inner electrode and uses boronization and helium discharge cleaning for wall conditioning.

Analysis of HIT data has resulted in an equilibrium model for CHI that provides an extremely good fit to data using plasma resistivity as the only fitting parameter. Stability studies are developing a picture of the mechanism for CHI current drive.

7E03

Internal Magnetic Field Measurements Using the Transient Internal Probe on the Helicity Injected Tokamak

M.A. Bohnet, T.R. Jarboe and A.T. Mattick
University of Washington, Seattle, WA 98195

The Transient Internal Probe (TIP) uses a high velocity (2 km/s) magneto-optic probe to measure internal magnetic fields in hot plasmas[1]. TIP has both accurately (2%) measured the internal toroidal field profile and directly measured internal magnetic fluctuation levels of the Helicity Injected Tokamak (HIT). HIT is a low-aspect-ratio (A=1.5) spherical tokamak designed to investigate steady state current drive using coaxial helicity injection[2]. Operating parameters are $T_e \cong 100$ eV, $n_e \cong 5 \times 10^{13}$ cm^{-3} and $I_p = 250$ kA. These tokamaks are characterized by a 30–70 kHz rotating n=1 magnetic distortion. Measurements using TIP confirm that this n=1 mode is present only on the outer edge of the plasma in the bad-curvature region. Fluctuation levels of 150 G in the vicinity of the separatrix dramatically decrease in the core of the plasma.

[1] J.P. Galambos, *et al.*, Rev. Sci. Instrum. **67,** 469 (1996)
[2] B.A. Nelson, *et al.*, Phys. of Plas. **2**, 2337 (1995)

7E04

Inertial Electro-Magnetostatic Plasma Neutron Sources

D.C. Barnes, R.A. Nebel, M.M. Schauer
and M.M. Pickrel
Los Alamos National Laboratory, Los Alamos, NM

Two types of systems are being studied experimentally as D-T plasma neutron sources. In both concepts, spherical convergence of either electrons or ions or both is used to produce a dense central focus within which D-T fusion reactions produce 14 MeV neutrons. One concept uses nonneutral plasma confinement principles in a Penning type trap. In this approach, combined electrostatic and magnetic fields provide a vacuum potential well within which electrons are confined and focused. A small (6 mm radius) spherical machine has demonstrated a focus of 30 μm radius, with a central density of up to 35 times the Brillouin density limit of a static trap. The resulting electron plasma of up to several 10^{13} cm^{-3} provides a multi-kV electrostatic well for confining thermonuclear ions as a neutron source. The second concept (Inertial Electrostatic Confinement, or IEC) uses a high-transparency grid to form a global well for acceleration and confinement of ions. Such a system has demonstrated steady neutron output of 2×10^{10} s^{-1}. The present experiment will scale this to $>10^{11}$ s^{-1}. Advanced designs based on each concept have been developed recently. In these proposed approaches, a uniform-density electron sphere forms an electrostatic well for ions. Ions so trapped may be focused by spherical convergence to produce a dense core. An alternative approach produces large amplitude spherical oscillations of a confined ion cloud by a small, resonant modulation of the background electrons. In both the advanced Penning trap approach and the advanced IEC approach, the electrons are magnetically insulated from a large (up to 100 kV) applied electrostatic field. The physics of these devices is discussed, experimental design details are given, present observations are analyzed theoretically, and the performance of future advanced systems are predicted.

7E05

EHD and MHD Models of Fireballs and Their Relevance to Natural and Artificial Ball Lightning

Hiroshi Kikuchi
Nihon University, College of Science & Technology
1-8, Kanda Surugadai, Chiyoda-ku, Tokyo 101 Japan

Apart from chemical model, main energy of **natural ball lightning** is thought to be plasma energy, since electric energy is limited to an air breakdown threshold, virtually being converted to plasma energy, and magnetic energy comparable seems to be unavailable in nature unless localized high vortex currents are available [1]. However, this leads to a great possibility of producing **artificial high-energy ball lightning,** since such high vortex currents could be produced in the laboratory as proposed by Koloc [2] and described by Roth with particular reference to fusion [3]. Along this line, it is suggested that artificial ball lightning could be produced by rocket-triggered lightning with a trailing inductive coil grounded, thus realizing Koloc's plasmak in the atmosphere. Most favorable conditions are to launch a rocket in an electric cusp formed by near-horizontal cloud and charge configurations, and a coil inductance required for magnetic energy localization can be estimated, for instance, to be more than 5 Henry, using cloud-to-ground capacitance C = 13.9 μF and resistance R = 1.3 kΩ for a

rocket-triggered lightning event on December 12, 1981 in Japan [4].

[1] H. Kikuchi, Ball Lightning, in H. Volland (ed.), Handbook of Atmospheric Electrodynamics, CRC, Boca Raton, Vol. I, Chap. 7 (1995), pp. 167–187.

[2] P.M. Koloc, Method and Apparatus for Generating and Utilizing a Compound Plasma Configuration, U.S. Patent 4,023,065 (May 10, 1977).

[3] J.R. Roth, Ball Lightning: What Nature is Trying to Tell the Plasma Research Community, Fusion Technology, 27, 255-270 (1995).

[4] H. Kikuchi, Electric Reconnection, Critical Velocity, and Triggered Lightning, in H. Kikuchi (ed.), Laboratory and Space Plasmas, Springer-Verlag, New York (1989), pp. 331–344.

7E06

Radiation Sources for Industrial Applications: The Spherical Pinch and the Vacuum Spark

A. Ikhleff and L. Zhang
Advanced Laser and Fusion Technology, Inc. 189/7 Deveault St., Hull, P.Q. J8Z 1S7 Canada
E. Panarella
Department of Electrical Engineering, University of Tennessee, Knoxville, TN 37996

Various plasma-based schemes have been pursued in recent years as radiation sources for industrial applications. ALFT has been engaged for some time now on research and development of the spherical pinch and the vacuum spark as candidates for strong radiation sources.

In the spherical pinch a small and dense plasma can be generated by converging shock waves, whose temperature is high enough for broadband radiation to be emitted from the UV to the soft X-ray region of the spectrum. The source size is smaller than 1 mm. Further improvements on the strength of the source for industrial applications are being carried out.

In the vacuum spark hot plasma spots are formed by the discharge of a capacitor across two properly shaped electrodes in a vacuum, generating radiation around the characteristic lines of the electrode material. Pinhole X-ray photography has shown that the source is less than 0.5 mm. Current research on such a device is concentrated on overcoming the intrinsic difficulties in strengthening its output: debris deposition on the beryllium window, overheating of the electrode material, and limited operating lifetime.

Both kinds of radiation sources will be presented.

7E07

Three-Dimensional Nonlinear Simulation of the Spheromak Tilt Instability

Bogdan Udrea and Uri Shumlak
Department of Aeronautics and Astronautics, University of Washington, Seattle, WA 98195

A spheromak is a force-free spherical plasma configuration that uses only internally generated magnetic fields to contain the plasma. It is known from linear theory that slightly prolate spheromaks are unstable to an m=1 mode tilt. Experimentally oblate sphermomaks have also demonstrated a tilt instability. We are using our non-linear 3D code to investigate this unstable mode as a function of the geometry (of the cylindrical flux conserver). The code is a parallel Riemann solver for the resistive and viscous MHD. We compare the results with those of linear codes and with experimental data.

7E08

Compact Toroidal Properties Compared to Ball Lightning

Clint Seward
EPS, Inc., Acton, MA 01720

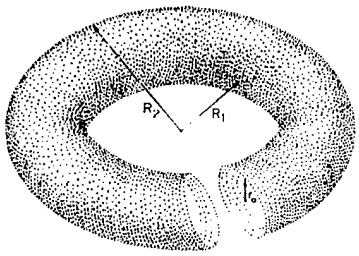
Long duration higher power pulses have been used to create compact toroids. Pulses of 4800 amperes and up to 200 volts have been generated for 150 milliseconds duration. Pressure is held to .01 to .001 atmosphere. Compact toroids are observed to last for more than 200 milliseconds in atmosphere after all fields are removed. Their diameter is measured to be >1 cm. Increasing the current appears to increase the diameter.

An explanation is proposed that the compact toroids are electron spiral toroids (ESTs). The EST is a hollow toroid of electrons where all electrons travel in parallel paths orthogonal to the toroid circumference, and reside in the thin outer shell of the toroid.

The proposed EST explanation quantitatively describes the compact toroids. It explains how the EST can be a stable current ring in high atmosphere with no external magnetic fields, and how the EST can contain many electrons with high energy.

Ball lightning (BL) is often reported (15% of sightings) as a ring, and since a spinning ring appears as a sphere or ball, the EST is a candidate for the BL explanation.

This paper applies the formulas of the EST to the compact toroids and to ball lightning using reported observations.



7E09

The Motion of Wave Energy and the Behavior of Plasma Fireball in the Atmosphere

Yousuo Zou
Department of Meteorology, University of Utah
Salt Lake City, UT 84112

The interactions of wave and plasma in the atmosphere can produce some stable plasma entities. These entities with vortical structure in microscopic scale are called vortons or solitons. Many of such entities macroscopically are plasma vortices, sometimes look like glowing fireballs, whose behavior are similar to those of so called UFOs (Unidentified Flying Objects). As waves are one of required conditions to form plasma fireballs, the motion and properties of wave energy in the atmosphere are closely related to the behavior of UFOs or, atmospheric plasma fireballs. The wave theory for atmospheric plasma fireball can be used to explain many strange UFO phenomena in the atmosphere.

Thursday Morning, 22 May 1997
10:00 a.m. – Rousseau Center

Poster Session 7P01-10:
1.4 Computational Plasma Physics

7P01

Hybrid PIC Acceleration Schemes for Discharges

K.L. Cartwright[1], J. P. Verboncouer[2] and C.K. Birdsall[3]
Electronics Research Laboratory, University of California at Berkeley, Berkeley, CA 94720

Kinetic simulation of plasmas in which equilibrium occurs over ion timescales poses a computational challenge due to the disparate timescales of the electron plasma frequency (~10^9), the ion plasma frequency (~10^7), and the ionization frequency (~10^7). Hybrid electrostatic PIC algorithms are presented in which the electrons reach thermodynamic equilibrium with the ions each time step. There are three different approximations for the electrons. First, the nonlinear Boltzmann relationship for the electrons can be applied to the bulk of a plasma. Second there is a truncated Maxwellian which is used in undriven sheaths; this approximation truncates the electron distribution at the wall potential. The last method used the steady-state electron distribution function in a DC electric field, with elastic collisions between electrons and neutral gas atoms. The collision frequency, $\nu_m(\upsilon)$, can be a tabulated or fitted function; the method is implemented using Argon cross-sections. These approximations neglect effects faster than the ion time-scales, decreasing the computer time used by over an order of magnitude; however, they increase the complexity of the boundary conditions, and the simulation is no longer self-consistent. Theoretical ramifications of these approximations are examined, and results are compared with full PIC simulations of undriven sheaths, ion acoustic waves and DC discharges (PDP).

[1] Supported by ONR-AASERT N100014-94-1-1033.
[2] Supported by the Air Force Office of Scientific Research-MURI under grant F49620-95-1-0253
[3] Supported by the Air Force Office of Scientific Research-under grant FDF49620-96-1-0154

7P02

A Hybrid Fluid Model Approach to Plasma Dynamics

Russell Cottam
NYMA Inc./NASA-Lewis Research Center, Brook Park, OH

The connection between fluid dynamics and kinetic theory is made through the calculation of the moments of the kinetic theory distribution function. This removes the unobserved velocity components of phase space which reduces the number of degrees of freedom of the dynamics calculation. There is unfortunately no rigorous method of truncating the set of moment equations. This paper presents a technique for calculating these moments which is both reversible so that the distribution function itself may be found at any time, and has a natural limit in the number of terms which must be calculated. The technique is based on the use of a modification of the Collocation Method with low order Chebyshev polynomials. It is applied to the two dimensional Vlasov equation, and two sets of calculations are displayed. In one the evolution in time of the electric field and plasma currents and densities near a collecting surface is presented, and in the other the occurrence of the strictly kinetic effect of Landau damping is demonstrated.

Work supported by NASA Contract NAS3-27186.

7P03

Eigenmodes of Microwave Cavities Containing High-loss Dielectric Materials

S.J. Cooke* and B. Levush
Code 6841, Naval Research Laboratory
Washington, DC 20375-5347
Tel: 1-202-404-4491 Fax: 1-202-767-1280
Email: sjcooke@glue.umd.edu

Numerical determination of the electromagnetic field eigenmodes of a microwave cavity containing regions of high-loss dielectric material is of technological importance to many areas, including high power microwave generation or amplification, particle accelerator design and microwave sintering of ceramic materials. This problem has proved problematic to numerical techniques[1], causing poor convergence and long computation times when highly lossy materials are present. The Jacobi-Davidson algorithm[2] applied to this complex eigenvalue problem is shown to be capable of extracting a set of eigenmodes having eigen-frequencies in a specified locality. Convergence is obtained even for the cases of multiply-degenerate eigenvalues and low ohmic-Q cavity modes. Details of the theory and numerical solution using 2-dimensional (planar circuit) and 3-dimensional electromagnetic operators will be presented. The issue of spurious solutions will be addressed.

This work supported by Office of Naval Research. Computational work was supported in part by a grant of HPC time from the DoD HPC Center NAVO.

1. D. Schmitt, R. Schuhmann, T. Weiland, Int. J. Numerical Modeling: Electronic Networks, Devices and Fields, Vol. 8 pp 385-398, 1995.

2. A. Booten, H. van der Vorst, Computers in Physics, Vol. 10, No. 3, pp 239-242, 1996.

*Institute for Plasma Research, University of Maryland, College Park, MD 20742-3511.

7P04

A Laplace Expansion Solution Technique for 2D Simulation of PPM Fields*

Robert H. Jackson
Naval Research Laboratory, Washingto,n D.C. 20375
jackson@mmace.nrl.navy.mil
Phone (202) 767-3936

The magnetic fields generated by periodic permanent magnet (PPM) stacks can be approximated at 2-dimensional with axial symmetry. For such systems with Laplacian fields, it is possible to obtain field solutions in the source-free region around the symmetry axis from a knowledge of the on-axis magnetic potential (or field) by application of the Laplace expansion solution method. This technique employs an incomplete power series expansion of a scalar potential function in the transverse variable where the series coefficients are axial derivatives of the on-axis potential (or field). By approximating a PPM stack with an equivalent system of magnetic coils, the Laplace expansion solution technique can be applied to accurately calculate the 2D off-axis magnetic field of the stack. This solution technique has been implemented in a compact, flexible, and extremely fast numerical code, **lesPPM**. The PPM stack geometry is used to construct an equivalent coil system, which can include key design elements such as end-effects and variation of PPM parameters (period, radius, magnet strength, number of periods, etc.)

This paper will present the general off-axis expansion solution algorithm and specific details concerning its

application to PPM problems. **lesPPM** performance parameters and results for "typical" PPM parameters will be presented and compared with calculations from more general finite-difference/finite-element non-linear codes. The utility of the expansion technique is general (and **lesPPM** in particular) is not as a replacement for more general codes, but as a rapid, flexible, and *reasonably* accurate design adjunct. The compactness of the method makes it ideal for direct incorporation into other programs.

*Work supported by the Office of Naval Research

7P05

A Simple Analytic ICP Model and Comparison to Experiment

D.R. Juliano, D.B. Hayden and D.M. Ruzic
University of Illinois, Urbana, IL 61801

An analytic model is developed for a cylindrically symmetric inductively coupled plasma system in order to find the electron temperature and density distribution. Boltzmann's equations solved by a computer code using a 2-term spherical harmonic expansion. Analytic results are compared to experimental measurements made with a Langmuir probe. The apparatus is a commercial magnetron system donated by Materials Research Corporation with an RF coil inserted between the target and substrate. The RF coil deposits additional power into the system, increasing the electron temperature and density. This increases the amount of metal ionization in the plasma. Far from the target, the resulting plasma is dominated by this ionization source, so the plasma at the magnetron target is not accounted for in the analytic model. In the model, electric and magnetic fields from the RF coil are found as a function of position and the power deposition profile is calculated. Insights gained from this model are used to guide research efforts in ionizing the sputter flux in the magnetron.

7P06

SPICES1: A New Vlasov-Fokker-Planck Simulation Code

V. Riccardo, G.G.M. Coppa, and G. Lapenta
Politecnico di Torino, Dipartmento di Energetica
Corso Duca degli Abruzzi, 24 - 10129 Torino, Italy

The SPICES1 (Smart Particle In Cell ElectroStatic 1D) code is described and tested. Free copies of the program will be available for PCs and UNIX workstations. SPICES1 is based on a multispecies Boltzmann-Poisson description of the plasma in 1D plane geometry with periodic or open boundary conditions. A linear collision operator is included to describe Fokker-Planck interactions. The code uses an optimized implementation of the blob technique for particle simulation.

The blob method belongs to a new class of simulation techniques using smart particles with internal degrees of freedom.[1-3] In the present work, some key problems of the blob method, previously not completely solved, are addressed in detail. First, the initial loading of particles with internal degrees of freedom is optimized carefully. Second, the blob method leads to a growth of the particle size and consequently splitting and coalescing are required. The new code uses an efficient technique to split large particles and reunite smaller particles,[2,3] without increasing their total number.

The code uses the same input structure of the well known ES1 code[4] and produces plots of all the significant quantities. Test runs will be presented for purely collisionless plasmas and for plasmas where Fokker-Planck collisions are present.

1. G.G.M. Coppa, G. Lapenta, V. Riccardo, Phys. Plasma, **3**, 2229 (1996).

2. G.G.M. Coppa, G. Dellapiana, F. Donato, G. Lapenta, V. Riccardo, J. Comput. Phys., **127**, 268 (1996).

3. W.B. Bateson, D.W. Hewett, J. DeGroot, *GaPH-A New Smart Particle Algorithm for Economical Kinetic Modeling,* ICOPS '95 Madison (1995)

4. C.K. Birdsall, A.B. Langdon, *Plasma Physics Via Computer Simulation*, McGraw-Hill, New York (1985).

7P07

Numerical Studies of Orbits in a 3-D Magnetic Cusp Geometry

Seung Kai Wong and Andrew Walton
Department of Physics and Materials Science
City University of Hong Kong, Hong Kong

The magnetic confinement concept known as the Polywell™ [1] makes use of the field created by three pairs of Helmholtz coils situated on the opposing faces of a cube. Near the origin, the rectangular components of the vector potential is given by $A_x \sim y^3 z \sim z^3 y$, plus cyclic permutations. The field configuration has six face cusps and eight corner cusps through which charged particles preferentially escape. Confinement properties of the configuration can be studied by numerical solution of the equation of motion. However, the orbits have to be followed for very long times, and this presents difficulties as the system exhibits chaos in the sense of sensitive dependence on initial conditions.

We have studied a number of numerical methods for solving the equations of motion and found that the simplectic algorithms[2], which apply to Hamiltonian systems, allow the orbits to be followed for the longest time when the same time-steps are used. The Lyapounov exponents are computed as an attempt to understand the origin of the chaotic dynamics.

Statistical studies involving a large number of particles with random initial conditions are also performed. It is found that the average confinement time, defined as the time for the particle to become separated from the origin where it begins its motion by a characteristic distance, becomes insensitive to the step-size when it is sufficiently small, although not small enough to follow the orbit of the individual particles. Based on this observation, the confinement properties of the field configuration are studied. The results of the investigation are understood in terms of simple models of the magnetic trap.

1. R. W. Bussard, *Fusion Technology* **19** 273 (1991); N. A. Krall, *Fusion Technology* **22** 42 (1992)

2. Feng Kang, *Proc. Venice 1989 Symp.*, Ed. R. Spiegler et al, pp17-35 (1990); J. M. Sanchez-Serna, *Physica D* **60** 293 (1992)

7P08

Lagrangian MHD in 2D and 3D

T. A. Oliphant, J.E. Morel, W.P. Gula and G.W. Pfeufer
Los Alamos National Laboratory,
Los Alamos, NM 87545

The cell-centered diffusion differencing scheme presented by Morel *et al.*[1] Has been applied to magnetic diffusion associated with Lagrangian hydrodynamic codes. Thus, the method applies to non-orthogonal meshes. Although the present application involves structured meshes, the method applies equally well to unstructured meshes. Morel's example of application is to 2D diffusion using Ficke's law. Thus, a volume integral approach is applied to the divergence operator. In 2D magnetic diffusion symmetry allows the use of an area integral approach involving the field components normal to the area, e.g. A-theta and B-theta. Instead of a divergence of a term proportional to the field gradient a curl of a term proportional to the curl of the field is used. An essential fact that allows this procedure is that the variable theta is ignorable. A benefit of this approach is that the solenoidal property of the magnetic field is automatic. In the case of 3D it is necessary to return to the volumetric integral approach and to use rectangular components of the vector potential. Successful benchmarks have been run in comparison with the 1D code RAVEN. A typical example is that of a metal cylinder being compressed by a magnetic field applied at the outer boundary. So far, the 3D diffusion model has been tested in the orthogonal case and found to preserve the linear, homogeneous solution. Results of these and further tests will be presented.

[1] Morel, J.E., Dendy, Jr., J.E., Hall, M.L, and White, Jr., S.W., *J. Comput. Phys.* **103**, 286 (1992).

7P09

Approximate Modeling Cylindrical IEC Fusion Device*

Blair P. Bromley, Luis Chacon, George H. Miley
Fusion Studies Laboratory
100 NEL, 103 South Goodwin Avenue
Urbana, IL, 61801-2984

The C-Fusion code has been developed to model the plasma physics of the Inertial Electrostatic Confinement[1] Cylindrical (IEC-C) fusion device and to predict the local volumetric and total neutron generation rates. C-Fusion predictions are used to help support the design and testing

of experimental IEC-C devices for potential scientific and commercial applications as a neutron source.

C-Fusion is a semi-analytical model that employs several simplifying approximations. The plasma is assumed to be locally quasi-neutral; there is a spatially one-dimensional variation of plasma properties; the plasma potential profile is linear. Electrons and ions are assumed to have a monoenergetic distribution, originating at the cathode and anodes respectively. The plasma current is axial and constant throughout the device and assumed equal to the electrode current. Local ion and electron velocities are evaluated based upon the local plasma potential. The effects of collisions are ignored, although the contribution of fast neutrals to the total neutron generation rate is evaluated by computing the local charge exchange rate, and allowing the fast neutrals to react over the rest of the length of the device since they are not impeded by the potential profile.

C-Fusion calculations have been performed and compared against experimental results. Input parameters included deuterium gas pressure (0.5 - 10 mTorr), neutral gas temperature (300-500 K), electrode current (20 - 40 mA), anode voltage (20 - 40 kV), reflector to anode length (23 cm), anode to cathode length (36 cm), anode length (5 cm), cathode length (15 cm), and plasma diameter (10) cm).

C-Fusion predicts that the total neutron generation rate for steady-state operation (10^4 - 10^6 n/s) has a linear variation with anode voltage over a range of currents, with a 10% accuracy. C-Fusion also predicts that for the test parameters used, the majority of fusion neutrons are created within the region of the cathode by beam-background reactions.

Further parametric studies to predict future device operation (including pulsing) show a linear variation of the neutron generation rate (up to 10^8 D-D n/s) for voltages and currents up to 100 kV and 1 A respectively. These studies show that currents greater than 10 A are needed to enter the important beam-beam fusion reaction regime.

The computer code will be described in more detail along with results from further parametric studies.

*Work party supported under Contract CC-S-622904-003-C

[1] Y.Gu, J.B. Javedani, and G.H. Miley. "A Portable Cylindrical Electrostatic-Fusion Device for Neutron Tomography," Fusion Technol., 26, **3** Part 2, 929-932 (1994).

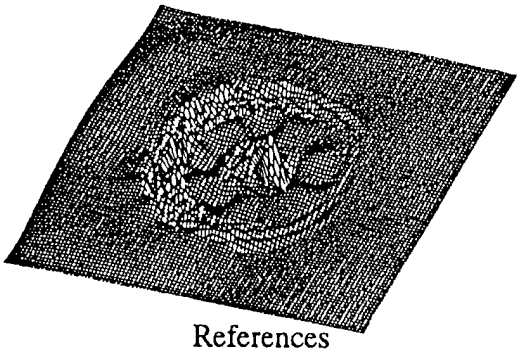
7P10

Human Plasmas

Toshiro Ohnuma and Haruyuki Soda
Department of Electrical Engineering, Tohoku University, Sendai 980 Japan

Interactions of electromagnetic fields with human are becoming very important problem because of many artificial electromagnetic fields. For these studies, new fields of "human plasmas" are proposed and investigated. The proposed new model is ion semiconductors for human, which consist of ions (plus and minus) and neutral particles.

Electromagnetic interactions of radiated EM waves with human plasmas (ion semiconductors) are obtained for several structure models. Typical electromagnetic fields for human plasmas with three layers are shown as follows;



References

1. T. Ohnuma, Human Electromagnetics (Tohoku University Press, 1997).
2. T. Ohnuma, Radiation Phenomena in Plasmas (World Scientific, 1994).

Thursday Morning, 22 May 1997
10:00 a.m. – Rousseau Center

Poster Session 7P11-25:
3.1 Plasma, Ion and Electron Sources

7P11

Measurement and Control of RF Power in Inductively Coupled Plasma

B.M. Alexandrovich, V.A. Godyak and R.B. Pejak
OSRAM SYLVANIA INC.
71 Cherry Hill Drive, Beverly, MA 01915

Inductively coupled plasma (ICP) sources are of growing importance for industrial applications in plasma aided manufacturing and lighting technology. To generate an experimental data base over the wide range of external discharge conditions needed to carefully study such discharges (power, gas pressure and frequency), accurate measurement techniques together with discharge stability are essential. A low-loss, multi-frequency matcher operating at 3.39, 6,78 and 13.56 Mhz, with tuning and matching functions that are practically independent, has been designed to drive a cylindrical ICP maintained with a planar (pancake) induction coil. The matcher has built-in current transformers and voltage dividers for phase resolved measurements at the input and output of the matcher. These measurements together with the measured coil temperature allow one to determine matcher and coil losses in order to accurately evaluate rf power dissipated in the plasma. These measurement instruments are connected and controlled through a computer which provides continuous monitoring of discharge characteristics and control of the rf power actually deposited in the plasma. Data that demonstrates the variation of power loss in the matcher and the coil over a wide range of rf power and gas pressure will be presented.

7P12

Ion Temperature Measurements in Helicon Plasmas

Paul Keiter, Matthew Balkey, John Kline, Mark Koepke, Earl Scime and Mike Zintl
West Virginia University, Morgantown, WV

Laser induced fluorescence measurements of the ion temperature in a helicon plasma indicate that the perpendicular ion temperature scales linearly with applied magnetic field. Finite gyroradius effects play a negligible role since at the lowest magnetic fields examined, the ion gyroradius remains much smaller than the chamber diameter. In a cylindrical device, Bohm diffusion across the axial magnetic field leads to a diffusion coefficient which depends inversely on the magnetic field strength. Assuming that the diffusion coefficient determines both the particle and energy confinement times, linear scaling of the ion temperature with magnetic field suggests that the ions are heated by collisions with the electrons. Measurements of the parallel and perpendicular ion temperatures and the electron density versus magnetic field in helicon source will be presented. Ongoing attempts to demonstrate ion cyclotron resonant heating in helicon plasmas will also be discussed and the latest results presented.

7P13

Ion Charge State Distribution in the ECR Source with Pumping by Millimeter-Wave Gyrotron Radiation

S.V. Golubev, S.V. Razin and V.G. Zorin
Institute of Applied Physics of Russian Academy of Science, Nizhny, Novgorod, Russia

Essential increase of ECR multiply charged ion (MCI) source efficiency (that is the increase of the average charge number and current ion beams) connects with possibility to achieve more dense plasma and to transfer to so called quasi gas dynamic regime of the plasma confinement in magnetic traps under the use of pumping with higher frequency. The first results of experimental investigation of ion charge state distribution in a pulse souce of MCI with pumping by millimeter wave radiation of powerful gyrotron are presented here.

Pulse millimeter wave radiation with maximum power $W = 130\ kW$, frequency $F = 37.5\ GHz$ and pulse duration up to $1\ ms$ was focused along magnetic lines into

a mirror *3,3*. Gas pressure was tuned by a pulsed inlet and maintained on level more than 310^{-5} *Torr*. The plasma density measured by cutting off a diagnostic millimeter waves exceeded $2\ 10^{13}\ cm^{-3}$. The ions having flown freely along the axis of the trap were investigated by two-step ion analyzer (magnetic and electrostatic analysis) with mass resolution *3*.

If *W = 130 kW*, the position of the distribution maximum corresponded to argon charge *(+11)=(+12)*, while in the modern CW regime ion sources (with pumping by microwave power of centimeter wavelength) the distribution maximum corresponded to charge *(+8)*. High plasma density (more than order of magnitude exceeded density in the traditional sources) in the such system provides a hope to achieve MCI beams with the record current.

7P14

Boron Doping to Diamond and DLC Using Plasma Immersion Ion Implantation

T. Ikegami*, T. Grotjohn, D. Reinhard and J. Asmussen
Department of Electrical Engineering
Michigan State University, East Lansing, MI 48824-1226

Controlling carriers in diamond by doping is important to realize diamond electronic devices with advanced electrical characteristics. As a doping method the Plasma Immersion Ion Implantation (PIII) has been gathering attention due to its excellence in making shallow, highly doped regions over large areas, and its high dose rate, good dose controllability and isotropic doping properties.

We have begun to investigate boron doping of diamond, silicon and diamond-like carbon films using PIII. As a doping source we use the plasma sputtering of a solid boron carbide (B_4C) target instead of toxic gas source like diborane (B_2H_6)[1]. The B_4C target of 1" diameter and a substrate (Si, diamond or diamond-like carbon film) are located in the downstream region of an ECR plasma produced by the microwave plasma disc reactor (MPDR) filled with 1-5 mTorr Ar gas. In order to sputter the target a negative self bias from -400V to -700V is induced by applying RF (13.56 MHz) power of 50-200W to the target holder. For boron ion implantation, negative pulses of -1kV to -8kV, 1-5μs pulse duration, 1-200Hz repetition rate are applied to the substrate holder using a high voltage pulser which consists of high voltage capacitors and MOSFETs[2].

After thermal treatment of the doped materials their electrical resistivity are measured using the four-probe method. Details of both the PIII source and substrate doping experimental results will be shown at the meeting.

[1] Liu, Gearhart, Booske, ICOPS-96, Conf. Abstracts, **1B05** p. 95, Boston.

[2] I. Nogradi, IEEE Conf. Records of the 1992 Twentieth Power Modulator Symposium, 1992, pp.189-192.

*Visiting from Department of Electrical and Computer Engineering, Kumamoto University, Kumamoto 860, Japan.

7P15

High Current Plasma Electron Emitter[1]

G.Fiksel, D.J. Den Hartog, D, Holly
Sterling Scientific, Inc., Madison, WI
J. Anderson, D. Craig, R. Kendrick,
S. Oliva, J. Sarff, M. Thomas
University of Wisconsin-Madison, Madison, WI

A high current plasma electron emitter based on a miniature plasma source has been developed. The source is characterized by a high electron emission current density and emission current, small size, and low impurity content. The emitting plasma is created by a pulsed high current gas discharge. The source is biased negatively to extract electrons. Electron currents of the order of 1 kA and the emission current density of 1 kA/cm^2 at a bias voltage of about 100V are obtained. The source has a simple design and has proven to be very reliable in operation. Extensive studies of the effect of the source geometry and materials have been conducted. The gas feed through, power dissipation, and impurity content were measured. In particular, spectroscopic measurements revealed that the impurities generated by the source electrodes are trapped inside by the source plasma. A high emission current, small size (3-4 cm in diameter), and low impurity generation make the source attractive for a variety of fusion, general science, and technological applications.

[1]The work was supported by US DOE.

7P16

A High Current Vacuum Arc Ion Source for Heavy Ion Fusion*

N. Qi, S.W. Gensler, R.R. Prasad
and M. Krishnan
Alameda Applied Sciences Corp., 2235 Polvorosa Ave., Suite 230, San Leandro, CA 94577
Fenghua Liu and Ian G. Brown
Lawrence Berkeley National Laboratory University of California at Berkeley, Berkeley, CA 94720

AASC is presently developing a vacuum arc ion source for Heavy Ion Fusion (HIF) and other commercial applications. Induction linear accelerators that produce energetic heavy ion beams are a prime candidate for power-producing fusion reactors. A source of heavy ions with low emittance and low beam noise, 1+ to 3+ charge states, ≈0.5 A current, 5-20 μs pulse widths and ~10 Hz repetition rates is required.

A Gadolinium (A≈158) ion beam with ≈0.12 A beam current, 120 keV beam energy, ≈2.5 cm diameter extraction aperture and 20 μs pulse width has been produced for HIF studies. We have measured that >80% Gd ions were in the 2+ charge state, the beam current fluctuation level (rms) was ≈1.5% and the beam emittance was ≈0.3 π mm mrad (normalized). With ≈8×10^{-5} torr barckground gas pressure, the beam was well space-charge neutralized and good propagation of the 20 μs long Gd ion beams was observed. Details of the work will be presented. The results of the experiment imply that the vacuum arc ion source is a highly promising candidate for HIF applications.

*Work supported by DoE under a Phase I SBIR, Grant #DE-FG03-96ER82116

7P17

Experimental Results of Fluid Flow in Capillary Tubing to Cool Particle and RF Transmission Windows

Robert J. Vidmar
SRI International, Menlo Park, CA

The experimental realization of a capillary-cooled transmission window for energetic particles and radio frequency waves is progressing from a single tube to a multi-tube design, and then to a two-dimensional window. Emperical heat-transfer results using ~100-m inside-diameter capillary tubing and a 28-Mpa (4,000-psi) distilled water hydraulic system are discussed. Details on a high-pressure hydraulic system suitable for cooling a transmission window are quantified. Techniques for assembling multiple capillary tubes into a single manifold are presented.

This work was supported by the Air Force Office of Scientific Research under Contract F49620-95-C-0009.

7P18

Penning Ionization of Cesium by Photoexcited Mercury -- Radiation Transport Effects*

K.R. Stalder and R.J. Vidmar
SRI International, Menlo Park, CA

Following our model of a photoexcited Hg-Cs-N_2-He system previously presented[1] we are now focusing attention on the radiative effects that control the spatial distribution of plasma and the overall system efficiency.

Radiation trapping in mercury vapor at 253.7 nm is significant and frequently presents a great obstacle to excite the bulk of the vapor. It is strongly affected by spectral broadening of both the excitation light source as well as the medium being pumped. In the present case, much of the problem can be overcome by using both isotopically-enriched mercury source lamps and plasma medium. Pressure broadening in the plasma cell causes the effective radiative decay rate to be decreased from the rate for an isolated atom and it also increases the transmission probability for resonant photons to propagate into the medium. Both of these effects are desirable in the present situation.

The results show that significant penetration of the 253.7 nm radiation can be achieved with careful attention being paid to the relative concentrations of ^{196}Hg in the lamp and in the plasma cell. Penning ionization of the cesium by the photoexcited Hg ensures that every photon absorbed results in the formation of a cesium ion.

*Work supported by AFOSR under Contract F49620-95-C-0009

[1] K.R. Stalder and R.J. Vidmar, 1996 ICOPS, paper 3IP14, p.221

7P19

The Negative Hydrogen Ion Source Based on Reflecting Discharge with Metal-Hydride Cathode

I. A. Bitnaya, V.N. Borisko, E.V. Klochko, Yu.V. Sidorenko
Kharkiv State University, Svobody sq.4, 310077, Kharkiv, Ukraine
E-mail: azarenkov@pem.kharkov.ua

The characteristics of plasma sourse of negative hydrogen ions, using the mechanisms of dissotiative attachment low-energy electrons to molecules of worker gas, was studied. Cathodes of plasma producer block was made of metal-hydride *(Zr - V - Fe)* H_x The idea of the use of metal-hydride cathodes was based on the results of the paper [1]. Authors of the paper [1] showed that the hydrogen molecules, desorbed from metal-hydride surface, were in vibrationally excited states and, as a result, the cross section of dissotiative attachment process was increased. We have found that the use of metal-hydride cathode in plasma source of ions allowed to increase the currency and gas effectivity in combination with the simplicity and compactness of the device construction.

1. Yu.F. Shmal'ko et al. Mass-spectrometry determination of vibrationally excited states of molecules of hydrogen desorbed from the surface of metal-hydrides. - Int. Hydrogen Energy. 1995, vol. 20, N5, p. 357-360.

7P20

Special Features of Gas Discharge Characteristics of Magnetron Diode with Metal-Hydride Cathode

I.A. Bitnaya, V.N. Borisko, E.V. Klochko
Kharkiv State University, Svobody sq. 4, 310077, Kharkiv, Ukraine
E-mail: azarenkov@pem.kharkov.ua

The characteristics of gas discharge in planar magnetron was studied. The magnetron cathode was made of metal-hydride based on getter Zr-V alloy. Hydrogen, desorbed from the cathode, was used as worker gas. In the case, when the gas pumping and the gas filling was turned off, the special stationary regime was found. In such regime the control of the worker-gas pressure was carried out by change of the discharge current magnitude only. The pressure dependence for current range of 50-300 mkA was close to linear, and the worker-gas pressure was changed in the range of 70-130 Pa. The presence of such regime was conditioned by the existence of a dynamic balance between the competitive processes of hydrogen sorbtion and desorbtion by metal-hydride cathode.

7P21

Electron Emitter Pulsed-Type Cylindrical IEC

G.H. Miley, Y. Gu, R. Stubbers, R. Zich, J. Sved[1], R. Anderl[2], J. Hartwell[2]
Fusion Studies Lab, University of Illinois, 103 S. Goodwin, Urbana, IL 61801
[1]DASA, Bremmen, Germany
[2]INEL, Idaho Falls, Idaho

A cylindrical version of the single grid Inertial Electrostatic Confinement (IEC) device (termed the C-device) has been developed for use as a 2.5-MeV D-D fusion neutron source for neutron activation analysis[1,2]. The C-device employs a hollow-tube type cathode with similar anodes backed up by "reflector" dishes[1]. The resulting discharge differs from a conventional hollow cathode discharge, by creating an explicit ion beam which is "pinched" in the cathode region. Resulting fusion reactions generate ~10^6 neutron/s. A pulsed version is under development for applications requiring higher fluxes. Several pulsing techniques are under study, including an electron emitter (e-emitter) assisted discharge in a thorated tungsten wire emitter located behind a slotted area in the reflector dishes.

Pulsing is initiated after establishing a low power steady-state discharge by pulsing the e-emitter current using a capacitor switch type circuit. The resulting electron jet, coupled with the discharge by the biased slot array, creates a strong pulse in the pinched ion beam. The pulse length/repetition rate are controlled by the e-emitter pulse circuit. Typical parameters in present studies are ~30μs, 10Hz and 1-amp ion current. Corresponding neutron measurements are an In-foil type activation counter for time averaged rates. Results for a wide variety of operating conditions will be presented.

Supported under DOE Contract DE-AC07-941D13223

1) Y. Gu. et al, "A Portable Cylindrical Electrostatic-Fusion Device for Neutronic Tomography" *Fusion Technol*, 26 **3**, Part 2, 929-232 (1994).

2) G.H. Miley, et al, 3rd Int. Conf. On Dense Z-pinches, AIP Conf. Proc. 299, 675-689 (1994).

7P22

Electron Optics Aspects of X-ray Tube Design

Bill P. Curry
EMSciTek Consulting Co., Glen Ellyn, IL 60137

Since the pioneering work by J.R.M. Vaughan (IEEE Transactions on Electron Devices, Vol. ED-32, No. 3, March, 1985), little has been published concerning the formation of the electron focal spot on the anode target track in an X-ray tube. Electron optical aspects of the cathode cup design are critical in determining the size and shape of the electron focal spot, as well as the beam current distribution across the target. The X-ray focal spot characteristics, in turn, are intimately related to the electron focal spot characteristics.

US and International standards for X-ray focal spot characteristics have recently been tightened on account of the resolution requirements of modern CT scanners. X-ray tube design for desired focal spot characteristics is expedited by use of electron optical codes which can calculate the potential distribution within the region between the electron emitting surface (usually a filament coil) and the rotating anode, as well as the electron trajectories (rays) transversing this region Space charge effects are important for electrons originating near the edges of the cathode slots in which the electron emitting surfaces are embedded, but not for electrons coming from the front of the emitting surface toward the anode. Edge rays are very important to the transverse dimensional of the focal spot; hence, spare charge strongly affects the transverse focal spot size.

In this paper 2-D calculations with self-consistent inclusion of space charge effects and 3-D calculations (without space charge) are presented to show how electron optics codes for PC's can be used to investigate the effect on the electron focal spot characteristics of tube voltage and current, cathode cup geometry, and emitting surface location and geometry. Similar studies can reduce the time (hence, cost) to establish an optimal tube design by minimizing trial and error cathode cup engineering and testing.

7P23

50 Hz Electron Emission from PZT Ferro-Electric Cathodes*

D. Flechtner, Cz. Golkowski, J.D. Ivers, G.S. Kerslick
J.A. Nation and L. Schachter
Cornell University, Ithaca, NY 14850

Ferro-electric cathodes may offer a source of high current density electron beams for applications where the use of conventional field emitters is limited by repetition rate and lifetime. In a ferro-electric cathode, electrons are emitted when the spontaneous polarization is rapidly changed by a pulsed electric field applied across the ferroelectric. When no additional voltage is applied to a planar diode gap, emission current densities are on the order of *1 A/cm²*. When an additional field is applied to the gap, we have measured current densities up to *100 A/cm²*. In a new configuration that permits beam extraction into a drift tube, the cathode is pulsed *10-20kV* negative and electron current densities of *~20 A/cm²* at repetition rates up to *~50 Hz* (power supply limited) have been measured. The one inch diameter ferro-electric cathode is located in the fringing region of a *1.5 kG* solenoid magnetic field *~2.8 cm* from the entrance of a grounded drift tube. A Faraday cup is located several centimeters inside the drift tube and measurements show that repeatable beam current can be extracted from the ferroelectric cathode in this geometry.

*Work supported by AFOSR MURI High Power Microwave Program & USDOE.

7P24

Magnetic Field Topography of the Anode Layer Thruster

Matthew T. Domonkos and Alex C. Gallimore
University of Michigan, Ann Arbor, MI 48109

The anode layer thruster (TAL) built by the Central Scientific Research Institute of Machine Buildings (TsNIMASH) of Kaliningrad, Russia is currently being investigated in the U.S. for both primary and auxiliary spacecraft propulsion. The TAL is a Hall accelerator which consists of an inner electromagnet, three outer electromagnets, an annular anode through which xenon propellant is supplied, and a hollow cathode neutralizer. The radial magnetic field created by the electromagnets crosses with the axial magnetic field to produce an azimuthal drift of electrons. This electron cloud

downstream of the anode establishes the electric field necessary to accelerate the ions. The cathode both supplies the drifting discharge electrons and neutralizes the ion beam. NumerEx of Albuquerque, NM has proposed to model the physical processes within the TAL, and the Plasmadynamics and Electric Propulsion Laboratory (PEPL) at the University of Michigan was contracted to perform very-near-field diagnostics on the thruster to provide data for comparison with the model predictions. The TAL used in this investigation operated at a discharge voltage and current of 300 V and approximately 4.5 A, respectively.

The magnetic field has been mapped using water-cooled Hall probes both while the thruster was operating and with only the vacuum field generated by the electro-magnets. The measured radial magnetic field strength decreased by approximately two-thirds during operation of the thruster. Preliminary estimates to determine the role of the azimuthal electron current indicated that nearly 800 A were required to effect this change. Additional experiments were conducted to examine the error in the Hall probe measurements and to investigate the nature of the decrease in magnetic field strength.

7P25

Plasma Flow In Nonhomogeneous Magnetic Field As A Lens For Focusing Of Ion Beams

V.I. Maslov, I.N. Onishchenko
NSC Kharkiv Institute of Physics & Technology, 310108 Kharkiv, Ukraine

The theoretical investigations of the plasma lens for high-energy ion-beam focusing instead of proposed earlier [1-2] we propose new scheme of focusing effect obtaining due to longitudinal polarization in a plasma motion through the magnetic field of a short coil. Electrons of a plasma flow from a plasma gun when coming upon magnetic barrier are slowing faster comparatively to the ions. Due to the finite radical electric field arises. The estimation of the plasma density, magnetic field etc. are performed for the obtaining of plasma lens with focusing length of 15 cm for focusing of proton beam of 5 MeV energy and 30 mA current.

The work was partly supported by Contract of STCU #298

1. A. Morozov. Dok. Acad. Nauk USSR, 1965, v. 163, No. 1, p.1363

2. H. Lefevre, R. Booth. IEEE Trans. on Nucl. Sci., 1979, NS-26, No. 3, pp.3115-3117

Thursday Morning, 22 May 1997
10:00 a.m. – Rousseau Center

Poster Session 7P26-41:
3.2 Intense Ion and Electron Beams

7P26

Computational and Experimental Studies of the Beam-Target Interaction for High-Dose, Multi-Pulse Radiography

B. G. DeVolder, T. J. T. Kwan, R. D. Fulton, D. C. Moir,
D. M. Oro, D. S. Prono
Los Alamos National Laboratory, Los Alamos, NM 87545

The conversion of an intense relativistic electron beam into x-rays for radiographic imaging is achieved through the bremsstrahlung process of electrons in a target of optimal thickness. To achieve desirable resolution for thick objects, an extremely high-brightness electron beam is used, and a significant amount of beam energy can be deposited in a small area of the target. Vaporization of the target material and expansion of the resultant plasma can occur. In a multi-pulsing design, which will resolve dynamic behavior of the object, the expanding plasma can have an effect on the quality of subsequent electron beam pulses.

The evolution of the plasma was investigated using a two-dimensional Eulerian magnetohydrodynamic code. The driving, or initial, condition for the plasma is the energy deposited in the target by the electron beam. Because the spatial and temporal beam energy deposition profiles can affect the plasma dynamics, several deposition models were tested. Experiments at Los Alamos' Integrated Test Stand (ITS) have characterized the expanding plasma for several target materials using a 5.25-MeV, 3.8-kA, 4-mm-diameter electron beam. Measurements such as axial expansion velocity helped benchmark the code and validate the deposition modes. Using the models that showed best agreement with the ITS experiments, calculations were done for a planned upgraded facility (20-MeV, 4.5-kA beam, spot size reduced by 1/4) to evaluate a multi-pulsing scheme in which the beam is moved to clean sections of the target for subsequent pulses. To minimize electron beam steering, means of confining the target plasma were also explored.

This work was supported by the US Department of Energy.

7P27

Nanostructured Surface Processing by an Intense Pulsed Ion Beam Irradiation

M. Yatsuzuka, T. Masuda, Y. Hashimoto[a], T. Yamasaki, H. Uchida, S. Nobuhara and Y. Yoshihara[b]
Himeji Institute of Technolgy,
Himeji, Hyogo 671-22 Japan
[a]Kobe City College of Technology,
Kobe, Hyogo 651-21, Japan
[b]Nippon Steel Co., Himeji, Hoygo 671-22, Japan

Metal surface modification by irradiating an intense pulsed ion beam (IPIB) with short pulse width has been studied experimentally. An IPIB irradiation to a target leads to rapid heating above its melting point. After the beam is turned off, the heated region is immediately cooled by thermal conduction at a cooling rate of typically 10^{10} K/s. This rapid cooling and resolidification results in generation of nanostructured phase in the top of surface.

The typical hydrogen IPIB parameters are 200 kV of energy, 500 A/cm^2 of current density and 70 ns of pulsewidth. The IPIB was irradiated on a pure titanium to generate nanocrystalline phase. The IPIB-irradiated surface was examined with X-ray diffraction, SEM, and HR-TEM. The randomly oriented lattice fringes as well as a halo diffraction pattern are observed in the HR-TEM micrograph of IPIB-irradiated titanium. The average grain size is found to be 32 nanometers.

7P28

Collision of a High-Energy Plasma Clot with an Obstruction Including Interpenetration and Generation of Electromagnetic Radiation

E.L. Stupitsky, A.Yu. Repin and G.F. Kiuttu
Russian Defense Central Institute of Physics and Technology, Sergiev Posad, Russia
G.F. Kiuttu
Phillips Laboratory, Kirtland AFB, NM

The interaction of high-speed plasma flows and bunches with one another (interpenetration), taking into consideration ionization and radiation processes represents one of the fundamental phenomena in plasma physics and has application to plasma dynamics, astrophysics, and magnetospheric physics. When interpenetration occurs, situations can arise where large current densities are generated over time scales of 1-10 ns.

In this work, we describe the two-dimensional interaction of two counter-flows, initial and reflected from a stationary obstruction.

The dynamics of the interpenetrating flows is described by a system of multispecie magnetohydrodynamic equations. A local Maxwellian approximation is used, taking into account both elastic and inelastic electron collisions. The equations of dynamics, ionization kinetics, and concentration levels are solved. Detailed analysis of resonant and nonresonant recharging was performed for various Z and rate constants for the relevant processes were obtained. On the basis of proper treatment of both dynamics and kinetics, we obtained results for the generation of current density and fields, which were found to be the major characteristics of such interpenetrating flows.

Thus, we have a mathematical vehicle which enables, with a high degree of detail, calculation of all the main features of flows with interpenetration, which is the most difficult, but a the same time, widespread.

7P29

Generation of Secondary Electrons from the Interaction of High-Energy Beams with the Upper Atmosphere

V.V. Kurnosov and E.L. Stupitsky
Russian Defense Central Institute of Physics and Technology, Sergiev Posad, Russia
G.F. Kiuttu
Phillips Laboratory, Kirtland AFB, NM

The injection of beams of neutral and plasma bunches into the atmosphere and magnetosphere is at present an active and fruitful method of researching geophysical phenomena. Such studies have relevance to the functioning of space vehicles (SVs), whose operations are in many respects governed by their resistance to flows of charged particles and electromagnetic fields. Therefore, an urgent problem is the evaluation of the effects of particles and fields on SVs.

We have developed a numerical model based on "large particles," which allows the description of the occurrence and transport of high-energy, low-density electron beams resulting from active experiments in the atmosphere.

The physical model and method of accounting permit the detailed description of fields and currents associated with the injection of charged particles. The model allows the calculation of any space-time characteristics of the

atmosphere under the effect of flows of charged particles. The general principles incorporated into the model permit the description of a wide variety of problems in the upper and middle atmosphere during the passage of high-energy beams.

7P30

Creation of a Monoenergetic Pulsed Positron Beam*

S.J. Gilbert, C. Kurz, R.G. Greaves and C.M. Surko
University of California at Davis, Davis, CA

We have developed a versatile, pulsed source of cold (0.018 eV FWHM), low-energy positrons (E~0--9 eV). Ten microsecond duration pulses of 10^5 positrons are extracted from a thermalized, room temperature positron plasma stored in a Penning trap. The frequency, duration, and amplitude of the pulses can be varied over a wide range. This technique allows for generation of electron pulses by simply inverting the polarity of all electrode potentials. Using this technique, we have also generated quasi steady state electron and positron beams with comparable energy resolution. There are numerous potential applications of such a source of intense, cold positrons. Examples include material surface characterization, such as depth profiling, positron and positronium gas scattering, and annihilation studies.

*Supported by ONR grant N00014-96-10589 and NSF grant PHY-9600407.

7P31

Inclusion of Non-Ideal Effects in 3-D PIC Simulations of Ion Diodes*

T.D. Pointon, R.A. Vesey, T.A. Mehlhorn and M.E. Cuneo
Sandia National Laboratories, Albuquerque, NM 87185

The 3-D particle-in-cell code QUICKSILVER has been used extensively to simulate ion diodes.[1] These simulations use an idealized setup; perfectly azimuthally-symmetric geometric and applied magnetic field, electrons incident on the anode are simply removed from the system, and the entire anode emission region emits only a single ion species—directly from the physical surface throughout the simulation. Results from SABRE experiments exhibit significant differences with such 'ideal' simulations. First, the beam has a time-dependent composition; early in time it is mostly the desired Li^+ ions, but these are rapidly replaced by protons and C^{+n} (the 'parasitic load'). Second, the diode impedance drops rapidly after peak lithium beam power. Third, there are substantial current losses in the diode (i.e., current not carried by the ion beam).

The first two discrepancies may result from formation of dense plasmas on the anode. These are believed to arise from ionization of neutral hydro-carbon impurities desorbed from the anode surface by the intense flux of high-energy electrons from the cathode side. QUICKSILVER has been modified to carefully treat electrons incident on the anode, scattering a fraction back into the diode gap, and updating the local temperature rise from electron deposition. When the temperature of an emission cell exceeds a threshold, emission switches from Li^+ to parasitic ions. The model reproduces the main features of the parasitic load. We have also studied sources of the diode loss currents.

*Funding has been provided by the U.S. DOE under contract DE-AC04-94-AL85000.

1. T.D. Pointon, M.P. Desjarlais, J. Appl. Phys., **80**, 2079 (1996).

7P32

X-Ray Diagnostic Development for Measurement of Electron Deposition to the SABRE Anode

J.S. Lash, M.S. Derzon, M.E. Cuneo, R.A. Vesey and S.E. Lazier
Sandia National Laboratories, Albuquerque, NM 87185

Extraction applied-B ion diodes are under development on the SABRE (6 MV, 250 kA) accelerator at Sandia. We are assessing this technology for the production of high brightness lithium ion beams for inertial confinement fusion. Electron loss physics is a focus of effort since electron sheath physics affects ion beam divergence, ion beam purity, and diode impedance. An x-ray slit-imaging diagnostic is under development for detection of x-rays produced during electron deposition to the anode. This diagnostic will aid in the correlation of electron deposition to ion production to better understand the ion diode physics. The x-ray detector consists of a filter pack, scintillator and optical fiber array that is streaked onto a

CCD camera. Current orientation of the diagnostic provides spatial information across the anode radius at three different azimuths or at three different x-ray energy cuts. The observed x-ray emission spectrum can then be compared to current modeling efforts examining electron deposition to the anode.

Sandia is a multiprogram laboratory operated by Sandia Corporation, a Lockheed Martin Company, for the United States Department of Energy under Contract DE-ACO4-94AL85000.

7P33

Multistage Acceleration of Light Ions for Fusion

Stephen A. Slutz
Sandia National Laboratories, Albuquerque, NM 87185

Theory[1] and experiments[2] indicate that post acceleration can reduce ion divergence. In addition, overall system efficiency should be better in multistage accelerators. Yet even the small step from single-stage to the use of two acceleration stages introduces a significant increase in the system complexity. As an example, the ion beam must remain space-charge-neutral between acceleration stages and the use of a conventional gas cell will result in beam stripping. Diode configurations to circumvent this problem will be presented. Another issue is the effect of diamagnetic pressure on the virtual-cathode of the second stage, which will cause a bending of the magnetic flux surface that defines the virtual cathode. This will result in a focusing of the ions beam. Analytic calculations of this process will be presented. Divergence reduction during post acceleration depends of the level of electromagnetic fluctuations generated by instabilities in both stages. Three dimensional particle-in-cell simulations will be presented to study this process.

1. S. A. Slutz, J. W. Poukey, and T. D. Pointon Phys. Plasmas 1, 2072, 1994

2. T. Lockner and S. Slutz, 11th Int. Conf. on Laser Interaction and Related Phenomenon, Monterey, CA, Oct., 28, 1993

7P34

Bidirectional Pulse Generator System for Linear Induction Accelerators

[1]T. Kobayashi, [1]J. Ohmura, [1]A. Okino, [2]J-H. Park, [2]K-C. Ko and E Hotta
Department of Energy Sciences, Tokyo Institute of Technology, Midori-ku, Yokohama 226, Japan
[1]Department of Electrical and Electronic Engineering, Tokyo Institute of Technology, Meguro-ku, Tokyo 152, Japan
[2]Department of Electrical Engineering, Hanyang University, Seongdong-ku, Seoul 133-791, Korea

In order to generate super-high-power pulsed microwave, the key issues are to develop high-current electron beam sources with high quality and to accelerate the electrons to high energy without spread. For these purposes, two types of high-current linear induction accelerators made from pulse lines, that is, unidirectional and bidirectional pulsers have been already constructed.

The bidirectional pulser made from lines generates a bidirectional output voltage, and the voltage with reverse polarity is used to accelerate a beam. This system needs a cavity made from lines instead of a magnetic core used in the unidirectional pulse generator system in order to transfer the energy initially stored in the pulser to a beam. Using the system , it is possible to make the time integral of the output voltage zero. Thus the final energy stored in the system can be made zero at the end of the pulse, and the system attains the energy transfer efficiency of 100%.

One of the highly efficient bidirectional pulse generators for external pulse injection, which was found by the authors, and a cavity were constructed and tested experimentally. The output impedance of the pulser and the cavity are 5.5 Ω and 11 Ω, respectively and the pulse width for acceleration is 100 ns. The designed maximum charging voltage is 200 kV. The experimentally obtained voltage waveform on the dummy load agreed well with the computed one.

7P35

Electron Flows in a Low Voltage Gap Exposed to an Oblique External Magnetic Field

A.L. Garner*, Y.Y. Lau* and D. Chernin**
*University of Michigan, AnnArbor, MI 48109-2104
**Science Applications International Corporation, McLean, VA 22102

It was recently found that steady-state cycloidal electron flows in a crossed-field gap are easily disrupted to a turbulent state, either by the presence of a small rf electric field across the gap [1], or by a small resistance [2]. Such a collapse is insensitive to the level of the emitted current, and is amenable to a one-dimensional analysis. In the other limit where the external magnetic field is parallel to the gap's electric field, such a collapse is not expected if the emitted current is below the Child-Langmuir value. In this paper, we investigate the general case where the external magnetic field is at an arbitrary angle with respect to the electric field. One-dimensional theories and simulations (PDP1[3]) will be presented on the equilibrium, stability, and turbulent state of electron flows in such a low voltage (non-relativistic) gap. Implications for the noise generation in O-type and M-type electron guns are discussed.

This work was supported by NRL/ONR, NSWC/CRANE and by DoD/AASERT.

1. P.J. Christenson and Y.Y. Lau, Phys. Rev. Lett. **76**, 3324 (1996).

2. P.J. Christenson, D. Chernin, A.L. Garner, and Y.Y. Lau, Phys. Plasmas **3**, 4455 (1996).

3. J.P. Verboncoeur, A.B. Langdon, and T. Gladd, Comput. Phys. Commun. **87**, 199 (1995).

7P36

Characterization of RF Plasma Cleaning Protocols for Removal of Contaminants in High Voltage Beam Diodes*

J.I. Rintamaki#, R.M. Gilgenbach, W.E. Cohen, J.M. Hockman+, R.L. Jaynes, Y.Y. Lau, L.K. Ang, M.E. Cuneo[a] and P.R. Menge[a]
Intense Energy Beam Interaction Laboratory, Nuclear Engineering and Radiological Sciences Dept., University of Michigan, Ann Arbor, MI 48109-2104

Contaminants have been shown to be a contributing factor to parasitic losses in ion beam diodes. Probable primary contaminants are CO, CO_2, H_2O, H_2, and C_nH_m complexes. Experiments are underway at the University of Michigan to characterize effective cleaning protocols for high voltage A-K Gaps. RF cleaning techniques using Ar and Ar/O_2 mixtures are being investigated. Optical emission spectroscopy is being used to view the effects of cleaning on neutral and ion contaminants during the high voltage diode pulse and to characterize the cleaning discharge. Experiments utilize the Michigan Electron Long Beam Accelerator (MELBA) at parameters: V=-0.7 to -1.0 MV, I_{diode}=1-10 kA, and $\tau_{e\text{-}beam}$=0.4-1.0μs. MELBA is used to study thermal and stimulated desorption of contaminants from A-K surfaces due to electron deposition. Pre-analysis and post-analysis of contaminants (e.g., CO, CO_2, H_2), H_2, C_nH_m) is performed using a residual gas analyzer.

---

*Research supported by DoE Contract #DE-AC04-94AL85000 To Sandia National Labs and Sandia Contract No. Al-7553 to University of Michigan

#DoE MFET Graduate Fellowship

+AFOSR Fellowship Recipient

[a]Intense Beam Research Department, Dept. 1231, Sandia National Laboratories, Albuquerque, NM, MS-1193

7P37

Modeling Lithium Plasma Formation by Laser Ionization Based on Resonance Saturation (LIBORS) and Implications for Extreme-Current Ion Sources*

P. Wang and J.J. MacFarlane
University of Wisconsin-Madison, Madison, WI
T.A. Mehlhorn, A.B. Filuk and M.E. Cuneo
Sandia National Laboratories, Albuquerque, NM

Key issues for light ion beam fusion are decreased ion beam divergence with increased ion beam current density. A satisfactory ion source for these kA/cm^2 beams is essential, and we are studying active lithium sources where an independent energy source is used to pre-form a lithium plasma against the anode. We are developing a comprehensive computer code for investigating lighium plasma formation by laser ionization based on resonance saturation (LIBORS) in the presence of large density gradients. In our computer code, a system of time-dependent rate equations, which couples the detailed atomic model with the external radiation field (laser) is solved self-consistently to predict the rapidly-changing

ionization characteristics of the lithium vapor. In particular, 1-D effects will be studied in detail, and time-dependent spectroscopy information will be provided so that the theoretical predictions can be compared with the results of spectroscopy measurement. Details of the physical model and the results will be reported.

*Supported by Sandia National Laboratories and Forschungszentrum, Karlsruhe, Germany.

7P38

Development of a High Brightness, Ohmically Generated Thin Film Lithium Ion Source*

P.R. Menge, M.E. Cuneo, M.A. Bernard, W.E. Fowler
Sandia National Laboratories, Albuquerque, NM

A pure lithium ion source with low source divergence capable of generating high current density beams ($\approx$1000 A/cm^2) is required for pursuing the goal of light ion inertial confinement fusion using pulsed power. It is believed that a uniform fully ionized lithium plasma at the anode surface ($\approx$100 cm^2) created just before arrival of the main power pulse (5-30 MV, 0.1-1 MA, 40-60 ns) will be superior to flashover or field-threshold lithium sources. One method being pursued at Sandia is the development of an ohmically driven thin film lithium source, often termed EMFAPS. The EMFAPS process consists an electrical pulse driven through a thin film coated with or bearing lithium in alloy or compound. The high current flowing through the film increases its temperature and resistivity until the lithium is driven off as vapor. The resistive voltage drop across the film generates a plasma by a gas discharge. Low impedance, fast risetime pulsers provided by NRL (D.D. Hinshelwood) and Pulse Sciences Inc. are being assembled and evaluated as film current drivers for full scale anodes ($\approx$70 cm^2). Smaller scale ($\approx$1 cm^2) tests are underway to optimize film composition, current contact engineering, anode construction, impedance dynamics, and energy disposition. Plasma discharge cleaning, bakeouts, film design and material selection issues are also being characterized to improve ion purity.

*Work supported by DOE contract DE-AC04-94AL85000

7P39

Study of the High Energy Diagnostic Neutral Beam Characteristics of TdeV on its Test Stand*

A.H. Sarkissian and E. Charette
CCFM, Varennes, Quebec, Canada

Development of a high energy (40 kV, 1A) neutral beam injector for diagnostic applications on TdeV is near completion. The beamline together with its differential pumping chamber has been installed on a test stand for characterization. The injector uses a duoPIGatron source[1], and it operates with the source at ground potential and the neutralizer canal at $\leq$–40 kV. The electrons in the neutralizer canal are retained by an electrostatic trap. The residual ions are collected near ground potential. Several diagnostics including calorimetry, visible spectroscopy, infrared imagery and a scanning multi-pin open probe array have been used to study the beam characteristics. We are in the process of characterizing the extracted full beam current, and will present the results at the meeting.

*Supported by AECL, IREQ and INRS.

[1] A.H. Sarkissian et al., Plasma Sources Sci. Technol., 5 (1996), 754

7P40

Electron Beam Generation in Turbulent Plasma of Z-pinch Discharges

V.V. Vikhrev and E.O. Baronova
NFI, RRC Kurchatov Institute, Moscow, 123182, Russia

Numerical modeling of the process of electron beam generation in z-pinch discharges at the current range of 100 kA-10 MA have been done. The proposed model represents the electron generation under turbulent plasma conditions.

Strong inhomogeneity of plasma density distribution and zigzag-like current motion have accounted for the adequate generation process investigation. Z-pinch neck was determined to be the place of electron beam generation. The emerging beam of runaway electrons moves towards the anode.

Numerical approach has shown that beam generation starts directly before the maximal compression and it is terminated at the stage of the pinch expansion. The electron generation rates was chosen corresponding to runaway one taking into account turbulent z-pinch

plasma. The electron beam energy directly depends on the resistance of plasma column. The influence of the energy and electron beam energy was also analyzed.

The dependence of electron beam current and voltage on time and the dependence of plasma electron temperature, density and radius on time are presented.

Theoretical predictions closely agree with experimental results.

7P41

Photofield Emission from Tip Cathodes

Eusebio Garate and Norman Rostoker
Department of Physics and Astronomy
University of California at Irvine, Irvine, CA 92697

We are studying photofield emission from tip cathodes. In photofield emission a cathode is biased to high fields and then irradiated with light. In principle, for fields at the cathode of the order of 0.1 V/Angstrom and greater, the effective work function of the cathode is lowered and the quantum efficiency of photoelectron production increases. In our experiments a cathode of tip radius ~1 micron is biased by applying a pulsed voltage up to 50 kV and pulse duration of up to 200 ns. During the voltage pulse a 25 ns excimer laser pulse is incident on the cathode tip. Typically we have been using XeCl in the excimer which generates a wavelength of 308 nm. In experiments using a tungsten (work function of ~4.5 eV) tip we have generated more than 250 mA in a pulse using the ~3 eV excimer light. Our current experiments on LaB_6 cathodes and field emitter arrays will be discussed.

*This work is supported by the Office of Naval Research under Grant N00014-90-1675

Thursday, 22 May 1997
1:30 p.m. – General Atomics

GENERAL ATOMICS

Tour of the DIII-D Tokamak Facility

Busses Leave From the Front of the
Ctamaran Hotel Conference Area
Promptly at 1:30 p.m.

All Guests Must Register by Tuesday May 20, 1997
at the Registration Desk on the second floor
of the Catamaran Hotel Meeting Rooms

Thursday Afternoon, 22 May 1997
3:00 p.m. – Rousseau Center

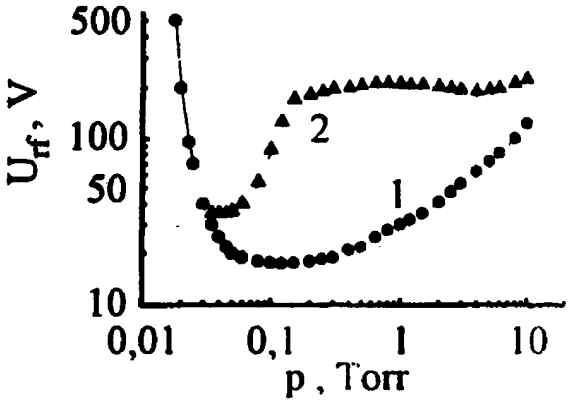
Poster Session 8P42-45:
Unscheduled Papers

8P42

α–γ Transition Properties of an RF Discharge in Argon

V.A. Lisovskiy
Kharkiv State University, pl. Svobody 4, Kharkiv, 310077, Ukraine

This report shows that the α– form range of existence possesses not only the right-hand boundary (conventional one at larger pressures - [Yatsenko N.A.- Zh. Tekh. Fiz., 1981, V. 51, p.1195]) but also a left-hand one (to the left of the RF discharge extinguishing curve minimum). Figure shows the extinguishing curve (1) of the RF discharge in argon (L = 2.2 cm, f = 13.56 Mhz) and the α–γ transition curve (2). At low p secondary electrons fly through the electrode sheath without collisions gaining the energy $\varepsilon_e \approx eU_{sh}$ (U_{sh} is the voltage across the sheath). When $U_{sh} \geq U_i$ (U_i is the ionization potential of the argon atom by an electron impact), a beam of fast electrons penetrates the plasma from the sheath ionizing on its way the gas atoms. The RF discharge transits to a γ– regime. Therefore at low pressures the αγ transition curve coincides with the RF discharge extinguishing curve.

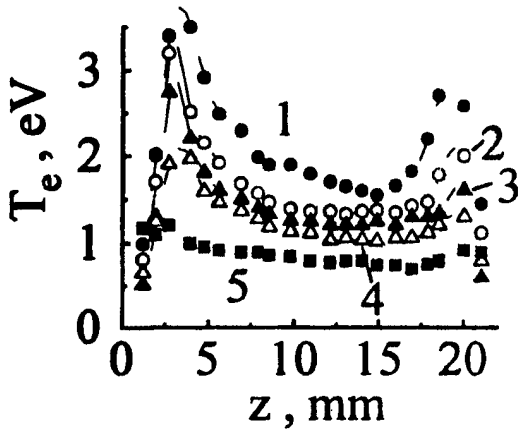


8P43

Electron Temperature Axial Pattern in the RF Discharge

V.A. Lisovskiy, V.S. Boichuk and V.D. Yegorenkov
Kharkiv State University, pl. Svobody 4, Kharkiv, 310077, Ukraine

This report presents the axial profiles of the electron temperature in the RF discharge in argon and air measured by a single probe technique. The pressure range under study was p = 0.1 - 2 Torr, RF field frequency f = 13.56 Mhz, interelectrode spacing was L = 22 mm. Figure shows these profiles $T_e(z)$ under argon pressure p = 1 Torr and the applied RF voltage amplitudes were: 1 - 50 V, 2 - 200, 3 - 225, 4 - 250, 5 - 350 V. The maxima of T_e are observed under intermediate pressures near the electrode sheath boundaries in the broad range of RF voltages. This increase is probably due to the stochastic heating of electrons colliding with oscillating boundaries of electrode sheaths, the phenomenon being known at low pressures ($p \leq 0.1$ Torr).



8P44

Characterization of Radiation Induced Brightness and Darkening in Fiber-Optic Cables at PBFA-Z

S.E. Lazier
Ktech Corporation, Albuquerque, NM 87110-7802

Analog fiber-optic data transmission is required for many diagnostics at the Pulsed Based Fusion Accelerator (PBFA-Z). Radiation-induced brightness and darkening has been characterized in fiber optic cables located at distances ranging from 5 cm to several meters from the target. Spectral measurements of this noise signal have been made to determine which combination of bandpass filtering and shielding is adequate for the diagnostics.

Sandia is a multiprogram laboratory operated by Sandia Corporation, a Lockheed Martin Company, for the United States Department of Energy under Contract DE-AC04-94AL85000.

8P45

Dense-Plasma Emission Pumping of Q-Switched Ti:Sapphire Tube-Laser*

Jae-Tae Seo, Kwang S. Han and Ja H. Lee
Department of Physics, Hampton University
Hampton, VA 23668

Dense argon-plasma emission of a hypocycloidal pinch (HCP) device has been used to pump a Ti:sapphire tube laser.[1] The pumping efficiency was enhanced by using both inner and outer spectrum converters.[2] The HCP plasma had 1.5-eV temperature and $10^{24}/m^3$ density which produced a intense near-UV emission of 1.8-μs risetime. The HCP pumped and Q-switched Ti:sapphire tube laser had 300 kW peak power which was almost 3 times as high as that of the normal oscillation at 820-nm wavelength. It was better than Segawa's experimental result of 1.7 kW peak power, 2.4 times higher than that of normal laser, which was obtained by a conventional flashlamp pumping.[3] The electro-optic Q-switch of HCP pumped-Ti:sapphire tube laser had a quarterwave configuration of which was made by the combination of a rear mirror, a Ti:sapphire tube, a polarizer, a pockels cell, and an output mirror. By this Q-switch, the laser cavity was suddenly opened after blocking for 5-μs to accumulate energy in the Ti:sapphire laser medium, so that the peak power could be increased much higher than that of the normal laser. The Q-switched Ti:sapphire tube laser will be then frequency-doubled by focusing to almost 10 MW/cm^2 power density on a lithium triborate crystal. The most interesting applications of this laser are bathymetry and underwater communications for military and civilian uses.

---

*This work was supported by ONR grant N000-89-J-1653.

1. K.S. Han, J.H. Lee, L. Zhang, and J.T. Seo, "Ti:sapphire Tube Laser by Hyposycloidal-Pinch Plasma Array," 1994 IEEE International Conference on Plasma Science," 178 (1994).

2. Jae-Tae Seo, Kwang S. Han, and Ja H. Lee, "An enhancement of pump efficiency of a Ti:sapphire tube laser with an inner spectrum convertr," Appl. Phys. Lett., 70, 1369 (1997).

3. Y. Segawa, "E/O Q-switching of a flashlamp-pumped Ti:sapphire laser," Adv. Solid-state lasers, 10, 149 (1991.

Index by Author

(The first 9 authors of each abstract are included in the index.)

A

Abbaspour	A.	1C08, 5C09
Abdallah	C.T.	3B08
Abdelrazek	A.	5Q04
Abe	D.K.	6Q15
Abraham-Shrauner	B.	1B05
Acton	D.F.	2P52
Adams	R.G.	3C01
Adamyan	Yu.E.	5P19
Afeyan	B.B.	2P20
Agee	F.J.	7D04
Agi	K.	3B09
Akishev	Yu.S.	1Q05
Akiyama	H.	6Q44
Al-Sharaeh	S.	3A02, 5Q04
Alberts	T.	6Q34
Alexandrovich	B.M.	7P11
Alexeff	I.	4Q16
Allen	K.	3B02-03, 3B04
Aliaga-Rossel	R.	2P65
Allshouse	G.O.	2P51
Amatucci	W.E.	5Q01
Anderl	R.	3A03, 7P21
Anderson	G.K.	7B08
Anderson	H.M.	5D06-07
Anderson	J.	7P15
Anderson	J.P.	4P32, 5B05
Ang	L.K.	4Q23, 4Q24, 7P36
Antonov	V.M.	2E06, 5Q02
Antonsen Jr.	T.M.	3D04, 4P29, 4P30, 4P40, 6Q15, 6Q21, 7A07, 5C08
Anvari	A.	5C08
Apruzese	J.P.	2P47, 2P61
Arad	R.	5P26, 6E06
Arefjev	A.S.	5P22
Arefyev	V.I.	1D03
Arjona	M.R.	6Q13
Arman	M.J.	3B02-03, 5P05, 5P14
Armijo	J.	3C01
Armstrong	C.M.	2D06, 3D01-02, 6A04
Arnott	D.E.	1C04
Arsic	N.	5P21
Asmussen Jr.	J.	1C05, 7P14
Asthana	M.	2P26
Atchinson	W.L.	6B01
Azarenkov	A.N.	1Q28, 1Q29, 2B07
Azizov	E.A.	2P44

B

Baba	K.	2A05
Babineau	M.	6E03
Back	C.A.	1D01-02
Bae	S.	7C08
Bagheri	A.M.	5C09
Bailey	J.E.	1C03, 3C01, 5C05
Baker	K.L.	2P20
Baker	M.C.	3P10
Bakhtiary	M.	2B04, 5EO9
Baksht	R.B.	2P58
Balakirev	V.A.	1P15
Baléo	J.N.	1Q11
Balkcum	A.J.	4P42
Balkey	M.	5Q03, 7P12
Ballew	N.	6Q14
Bandy	S.G.	1E05
Barbee Jr.	T.W.	5C01-02
Bardsley	J.N.	7B05
Barnes	D.C.	7E04
Barnett	L.R.	5B03
Baronova	E.O.	1A04, 2P43, 3P09, 7P40
Barroso	J.	3Q12
Bartlemass	M.	3P10
Bartlett	R.J.	6Q24
Bartnik	A.	3E05
Basten	M.A.	2D07
Baum	C.	1B03, 1B04
Bayless	J.R.	7B05
Bedell	S.	3Q11
Beliaev	V.S.	1D04
Bender	B.A.	2D02
Benford	G.	3B05
Benford	J.N.	3B05, 7A05
Bennett	C.V.	1P02, 6A07
Berezkin	A.N.	5P19
Bernard	M.A.	1C03, 7P38
Bettenhausen	M.H.	1P10, 1P11, 2C03, 3P01, 3P02
Bickes	C.	7D03
Binh	V.T.	1E08
Birdsall	C.K.	5A02, 6Q20, 7P01
Bitnaya	I.A.	7P19, 7P20
Bizyukov	O.A.	1Q28
Black	D.C.	3P07
Blackwell	D.D.	3P05
Blackwood	J.E.	6P31

Blank	M.	4P29, 4P30, 4P33, 5B01-02
Bletzinger	P.	5A06
Bliokh	Yu.P.	1P15
Block	R.C.	1D08
Bobkov	V.V.	1Q20
Bogatov	N.A.	1P09
Bogomaz	A.A.	7D05
Bohnet	M.A.	7E03
Boichuk	V.S.	8P43
Boley	C.D.	2P24, 5E01
Bonuishkin	E.C.	1D06
Booske	J.H.	1C04, 2D07, 3Q03, 3Q11, 6Q18
Borchard	P.	4P33, 6A06
Borisko	V.N.	1Q20, 7P19, 7P20
Borodkin	A.V.	1P15
Borowiecki	M.	2P41
Bortolotti	A.	6D02
Botton	M.	4P31
Bouaziz	M.	6P44
Bourham	M.A.	2P30, 5E07, 7D01, 7D02
Bowers	R.L.	2P46, 6B05-06
Bowles	J.H.	5Q01
Boyer	C.J.	7D01
Brake	M.	4Q26, 4Q27
Brenning	N.	2B05, 2E08, 3P06, 6Q41
Brickman	C.	4Q21
Bridges	J.M.	6P41
Brinkmann	R.P.	5A04
Brodie	I.	1E06
Bromborsky	A.	6Q15
Bromley	B.P.	7P09
Brown	I.G.	3C07, 7P16
Brownell	J.	2P46, 6B05-06
Brownell	J.H.	6Q19
Bruce	R.W.	2D02
Brzosko	J.R.	6D01
Brzosko	J.S.	6D01
Budin	A.V.	7D05
Buie	M.J.	1B06, 4Q27
Bulka	S.	6P53
Burkhart	C.P.	7B05
Burris	R.	1D01-02
Bystritskii	V.M.	1B07, 7B04

C

Cachoncinlle	C.	2P63
Cahalan	P.	6A06
Calame	J.P.	2D01, 4P30, 4P34, 6Q14
Calico	S.E.	3B01, 3B02-03
Calise	F.	6P29
Callis	R.W.	1P04
Camacho	F.	6Q42
Cameron	S.	6Q42
Campbell	R.	6P35
Campbell	R.B.	6P36
Caress	R.W.	5Q05
Carmel	Y.	2D01, 6Q15, 7A07
Carr	A.K.	4Q19, 4Q21
Carroll III	J.J.	1A03, 2E05
Cartwright	K.L.	7P01
Caryotakis	G.	3C07
Castle	M.	4P32
Cauble	R.	5C01-02
Cavazos	T.	1Q16
Cekic	M.	6P38, 6P45
Celliers	P.	5C01-02
Ceperley	P.H.	4P49,. 4P50
Cereceda	C.	3P17
Chacon	L.	7P09
Chan	C.	2A06, 2A07
Chandler	G.A.	2P47, 2P48, 2P51, 6B02-03, 6B05-06
Chang	C.H.	5B 03
Chang	D.-H.	2B03, 2P31
Chang	H-Y.	6Q39
Charbonnier	F.	1E01-02
Charette	E.	7P39
Charrada	K.	6P37
Chase	K.N.	2P18
Chawla	G.K.	1D07
Chen	C.	4P39
Chen	F.F.	1A01-02, 3P03, 3P04, 3P05
Chen	H.Y.	5B03
Chen	K.R.	1A05
Chen	Q.	1P12
Chen	S.	5B07
Chen	S.H.	5B03, 6A03
Chen	W.	1B05
Cheng	J.	6Q14
Chernin	D.	6Q16, 7P35
Chin	P.	6Q14
Ching	C.H.	1C03, 3C01
Chittenden	J.P.	2P65
Chiu	S.	3Q02
Chmielewski	A.G.	6P52, 6P53
Choi	J.H.	6Q28

Choi	J.J.	4P55, 5B04, 5B06
Choi	S.J.	6P36
Chong	C.K.	4P43
Chow	G.-M.	2D02
Chrien	B.E.	5E03
Christenson	P.J.	3P16
Christophorou	L.G.	1Q30
Chu	K.R.	5B03, 6A03
Chu	P.K.	3Q13, 3Q14, 3Q15
Chu	T.S.	6A06
Chun	J.S.	2B03
Chung	H.K.	5C05
Chung	K.H.	1Q19
Chung	K.-S.	2B03, 2P31
Chung	T.H.	1Q12, 1Q22
Ciobanu	S.S.	6Q25
Ciocca	M.	5A07
Cismaru	C.	4Q28
Clark	B.F.	1C03
Clark	M.C.	3B01, 3B02-03
Cluggish	B.P.	3Q01
Coates	D.M.	3C06
Cochran	F.L.	6B07
Coffey	S.K.	5P16, 6B08
Cohen	D.	1C03
Cohen	W.E.	7P36
Coleman	D.	3B02-03
Coleman	P.L.	6B04, 6E01-02
Collins	C.B.	2P63
Comfort	R.H.	2E01-02
Commisso	R.J.	6E01-02, 6E03, 6E05
Connor	K.A.	2P35
Coogan	J.J.	7B08
Cooke	S.J.	4P35, 4P37
Cooke	W.	2D05
Cooper	G.W.	6Q30, 6Q33
Cooperberg	D.J.	5A02
Coppa	G.G.M.	7P06
Cottam	R.	7P02
Courteille	C.	5C06
Coverdale	C.	2P61
Craig	D.	7P15
Cramer	N.F.	3P22
Craven	P.D.	2E01-02
Crowley	T.P.	2P35
Cuneo	M.E.	1C03, 3C01, 3C02-03, 7P31, 7P32, 7P36, 7P37, 7P38
Curry	B.P.	7P22

D

Da Silva	L.B.	5C01-02
Dale	G.E.	5E07
Dalrymple	N.E.	2E04, 7A06
Dangor	A.E.	2P65
Danilov	V.V.	5Q02, 6C02
Danly	B.G.	4P29, 4P30, 4P33, 4P34, 4P35, 5B01-02, 5B04, 5B06, 6A05
Datsko	I.M.	2P58
Davara	G.	2P50
Davies	J.A.	4P39
Davis	H.A.	3C06
Davis	J.	2P47, 2P61, 6B07
Davis	J.L.	1D01-02
Davis	P.R.	6P30, 6P31
Davis	R.	5D04, 5D05
Dawson	J.	2C04
Day	A.C.	1P05
Dayton Jr.	J.A.	2D04, 3D07, 3D09
DeChiara	P.	6D02
Decker	C.D.	1D01-02
Deeney	C.	2P47, 2P48, 2P51, 2P57, 2P59, 2P61, 6B02-03
Degnan	J.H.	5P16, 6B08, 6E07, 6E08
DeMora	J.	3A03
Den Hartog	D.J.	7P15
Deng	B.H.	4P41
Denholm	S.	2A06
Denisenko	I.B.	1Q28, 1Q29
Denisov	G.G.	4P37
Deryuga	V.A.	1Q27
Derzon	M.S.	2P57, 2P62, 6B05-06, 6Q30, 6Q33, 6Q34, 7P32, 8P44
Desiderio	P.	6D02
Desjarlais	M.P.	3C01
Destler	W.W.	6Q15
DeVolder	B.G.	7P26
Dhali	S.K.	1Q08, 4Q17
Dialetis	D.	6Q16
Dickens	J.	3B06
Dikan	D.A.	1P09
Ding	G.	1P10, 1P11, 2C03
Dinh	V.V.	1P02, 4P44
Diyankov	O.V.	2P21, 6C06
Dolliver	D.D.	5E04-05

Domonkos	M.T.	7P24
Dong	X.	1B07
Dong	Y.	2P35
Doranian	D.	5E10
Douglas	M.R.	2P48, 2P53, 2P59, 6B02-03
Drake	R.P.	2P20
Dressman	L.	4P41
Drofa	M.A.	3P23
Drolen	B.L.	2E03
Dussart	R.	2P63
Dyakin	V.M.	3E05

E

Eberhardt	D.S.	6C05
Efremow	N.N.	1E09
El-Habachi	A.	5A07
Elia	M.	5E06
Englebrecht	M.	1Q09
Englert	T.	3B02-03, 3B04
Erofeev	V.I.	2B06
Esarey	E.	2C07, 2P19
Estabrook	K.G.	2P20
Evans	J.D.	3P04
Evtukh	A.A.	1E03, 7A02
Ewig	R.	7E01-02

F

Faehl	R.J.	6B01, 6Q36
Faenov	A.Ya.	2P17, 2P41, 3E05
Failor	B.	2P47, 2P61
Faith	J.C.	2C05
Farber	D.	7C08
Farenik	V.I.	1Q24
Fayet	P.	5C06
Fedorovich,	O.A.	3P13
Fedunin	A.V.	2P58
Fehl	D.L.	2P48, 2P51, 6B02-03, 6Q42
Feicht	J.	6Q23
Felch	K.	4P33, 6A06
Felsner	P.	7D03
Fernandez	A.	6Q13
Fernsler	R.	5A08
Fiedorowicz	H.	3E05
Fievet	C.	6Q25
Fiksel	G.	7P15
Filippov	N.V.	2P37, 2P44, 3E02-03
Filippova	T.I.	2P37
Filuk	A.B.	1C03, 3C01, 7P37
Finnikov	K.A.	6C02
Fischer	R.P.	2D02
Fisher	A.	1D01-02
Fisher	V.	2P50
Flech	K.	6A06
Flechtner	D.	1P06, 7P23
Fleddermann	C.B.	1Q13, 1Q14, 1Q16 7B07
Fleurier	C.	2P63, 6Q25
Fliflet	A.W.	2D02, 4P38
Fochs	S.	2P24, 5E01
Fonash	S.	7C08
Foster	J.E.	6Q40
Fowkes	R.	5P08
Fowler	W.E.	1C03, 3C01, 7P38
Fraenkel	M.	2P17
Frank	J.D.	6P45
Frank	K.	7D03
Freund	H.P.	3D03, 3D08, 4P51
Fridman	B.E.	5P17, 5P18, 6Q31
Friedmann	J.B.	4Q28
Fruchtman	A.	6E06
Fuhr	J.R.	6P41
Fujii	M.	4Q25
Fulton	R.D.	7P26
Furkal	E.	1Q26

G

Gahl	J.M.	3B07, 5P12
Gale	D.G.	5C04, 6B08
Gallagher	D.	2D06, 6A04
Gallimore	A.D.	1C07, 6Q40, 7P24
Gallegoes	R.	3B02-03
Galvez	M.	5D03
Gandel	Y.V.	6Q22
Ganguly	A.K.	4P52
Ganguly	B.N.	5A06
Gannon	B.	3D01-02
Gapon	A.V.	1Q28, 1Q29
Garate	E.	1B07, 7P41
Garcia	M.	1Q10
Garner	A.L.	7P35
Garner	R.C.	6P38
Garrigus	D.	1P05
Garscadden	A.	5A06
Garven	M.	1E04, 1E10, 6P29
Gasilov	V.A.	6B10
Gearhart	S.S.	3Q03, 3Q11
Geis	M.W.	1E08
Gensler	S.W.	5P27, 6Q29, 7P16
Gentils	F.	6Q25
Geren	W.P.	1P05
Gershon	D.	2D01
Gerwin	R.A.	2P60

Ghorannevis	M.	1C08, 2B04, 5C07, 5C08, 5C09, 5E09, 5E10
Gilbert	S.J.	7P30
Gilgenbach	R.M.	1P03, 3C09, 4Q23, 4Q24, 5P01, 5P02, 7P36
Gilligan	J.G.	2P30, 7D01, 7D02
Gilliland	T.	2P47, 2P48, 2P51, 6B02-03
Girka	V.O.	1P01, 2B07, 7A04
Gitlin	M.S.	1P09
Giuliani	J.L.	6P35
Glazyrin	I.V.	2P21, 6C06
Gleizes	A.	6P44
Godyak	V.A.	7P11
Goebel	D.M.	5P20, 6Q23
Goforth	J.H.	6Q26
Gold	S.H.	4P38
Golkowski	Cz.	1P06, 7P23
Golubev	S.V.	7P13
Gomberoff	K.	6E06
Gondarenko	N.A.	2P56
Good	G.R.	1E07, 5B08
Gopinath	V.P.	3P16
Goplen	B.	1E05, 6Q21
Gordillo-Vázquez	F.J.	1Q31
Goryachev	V.L.	6P48, 6P49
Goyer	J.	6E01-02, 6E03
Grabowski	C.	3B07, 5P12
Grafodatsky	O.S.	5Q02
Graham	J.D.	6B08, 6E08
Granatstein	V.L.	4P32, 4P36, 4P51, 5B05, 5B07, 6Q14
Grapperhaus	M.J.	1B01-02, 4Q30
Graves	C.A.	1E04
Greaves	R.G.	7P30
Green	M.C.	1E05
Greenly	J.B.	3C06
Gregoire	D.J.	3D05
Gregor	J.	5A08
Gregorian	L.	2P50
Griesmann	U.	6P41
Grigoriev	V.	1B07
Grimard	D.	4Q27
Groshart	G.	3D01-02
Grossman	J.M.	6E05
Grotjohn	T.A.	1C01-02, 7P14
Groves	K.M.	7A06
Grun	J.	1D01-02
Gu	Y.	7P21
Gueorguiev	L.	3Q12
Guharay	S.K.	3Q09
Guillot	D.	1E08
Gula	W.P.	7P08
Gunell	H.	2B05, 6Q41
Gunin	A.V.	5P13
Guo	H.	5B07
Gurevitch	A.	7B03
Gurin	V.E.	5P16
Guskov	S.Y.	2P27, 2P28
Guzdar	P.N.	3Q09

H

Haaland	P.D.	5A06
Hackett	K.	3B02-03, 3B04
Hafizi	B.	2C07, 4P38
Haill	T.A.	2P62
Haines	M.G.	2P65
Hammer	D.A.	2P52
Hampel	F.	7B03
Han	K.S.	8P45
Han	M.	2P42
Hankins	O.E.	5A01
Hanson	D.L.	3C01
Hardek	T.	2D05
Hargreaves	T.A.	1E07, 5B08
Harper	M.K.	1B03, 1B04
Harris	C.T.	1E04
Harris	S.E.	2C07
Hartemann	F.V.	1P02, 2C08, 6A07
Hartog	D.J.	7P15
Hartwell	J.	3A03, 7P21
Hashimoto	Y.	7P27
Hatfield	L.L.	3B06, 3P10, 5P04, 7D04
Hauser	J.R.	2A03
Haworth	M.	3B02-03, 3B04
Hayashi	Y.	6P50
Hayden	D.B.	1B08, 7P05
Hazelton	R.C.	5P28
Hebner	G.A.	1Q13, 1Q14
Hebron	D.	6Q34
Heinen	V.O.	3D07
Hemmert	D.	3B06
Hendricks	K.	3B02-03, 3B04
Henley	D.	3B04
Hershkowitz	N.	1B03, 1B04, 4Q28
Hinshelwood	D.D.	6E05
Hirose	A.	1Q26, 5E06
Hirshfield	J.L.	4P38, 4P52
Hitchon	W.N.G.	3A05
Hochi	A.	6P40

Hochman	J.M.	5P01, 5P02, 7P36
Hoekstra	R.J.	1B01-02, 4Q32
Hoffman	C.	7E01-02
Hoffmann	D.H.H.	1Q09, 7D03
Hogan	B.	4P32, 6Q14
Holland	C.E.	1E06
Hollenstein	C.	5C06
Hollis	M.A.	1E04, 1E05
Holloway	J.P.	4Q26, 4Q27
Holly	D.	7P15
Hong	D.	2P63, 6Q25
Hong	M.G.	4P47, 4P48
Hong	S.H.	2A08, 4Q18, 6P34
Hooker	J.D.	6P43
Horii	S.	6P40
Hotta	E.	2P29, 7P34
Howling	A.A.	5C06
Hsiao	M.C.	7B05
Hu	W.	4P45
Hu	Y.	1Q17, 6P32
Huang	T.	2C09
Huba	J.D.	6C03
Hubbard	R.F.	2P19
Huh	M.S.	1Q22
Hung	C.L.	5B03
Hur	M.	6P34
Hurt	E.	3D01-02
Hussey	T.W.	6B08
Hutchings	T.	6Q13
Hutchins	J.	3D01-02
Hwang	S.M.	2B03, 6Q28

I

Idzorek	G.C.	2P23, 5E03, 6Q24, 6Q26
Ikegami	T.	7P14
Ikezawa	S.	2A05, 4Q25
Ikhleff	A.	7E06
Il'kaev	R.I.	1D06
Ilgisonis	V.I.	2B09
Iller	E.	6P52
Inaguma	J-I.	2A05, 4Q25
Irion	R.	3P10
Ishihara	O.	3P18, 3P20, 5P11, 5P12
Itoyama	K.	1Q06, 6P50
Ivers	J.D.	1P06, 7P23
Ives	L.	2D03, 7A01

J

Jackson	R.H.	4P51, 6C01, 7P04
Jarboe	T.R.	7E01-02, 7E03
Jarotcki	R.	3E05
Javedani	J.B.	6E07, 6E08
Jaynes	R.L.	5P01, 5P02, 7P36
Jensen	K.L.	1E04, 1E10
Ji	Y.	5D04, 5D05
Jiang	Z.	2A01-02
Jiling	H.	5Q11, 5Q12
Jobe	D.O.	2P47, 2P48, 2P51, 6B02-03
Johnson	D.J.	3C01
Jones	O.S.	6C05
Jones	T.G.	3C05, 6E05, 6Q32
Joshi	C.	2C04, 2C06
Joyce	G.	3A04, 3A06
Juliano	D.R.	1B08, 7P05
Jung	J.K.	1Q19

K

Kaganovich	E.B.	1E03
Kalantar	D.H.	5C01-02
Kalinichenko	A.I.	1Q27
Kalkan	A.	7C08
Kalluri	D.K.	2C09, 3P08
Kando	M.	2A05
Kang	K.D.	6P34
Kang	Y.B.	1Q19
Karasik	M.	1Q01
Kargin	V.I.	5P16
Karpinski	L.	2P41
Kas'anov	Y.S.	2P27, 2P28
Kataev	V.N.	5P16
Katsouleas	T.C.	2C04, 2C06
Katsuki	S.	6Q44
Katsurai	M.	1P12
Kaufman	D.A.	2E03
Kaup	D.J.	6Q17
Kawauchi	T	6Q44
Keefer	D.	6E04
Keinigs	R.K.	6Q36
Keiter	E.R.	4Q31, 5A05
Keiter	P.	5Q03, 7P12
Kelly	K.L.	1P10, 1P11, 2C03
Kelly-Wintenberg	K.	4Q21
Kendrick	R.	7P15
Kerman	A.K.	2C08
Kerslick	G.S.	1P06, 5P03, 7P23
Kharlov	A.V.	1B07
Khebreh	R. Z.	5C09
Kida	K.	2A05, 4Q25
Kikuchi	H.	7E05
Kim	A.A.	2P58
Kim	B.C.	6Q28
Kim	G.H.	2B03

Kim	J.I.	2B03
Kim	K.	6P51
Kim	S.-K.	2P31
Kim	T.Y.	1Q19
Kim	Y.B.	1Q03, 1Q22
Kim	Y.H.	4Q18
Kimmitt	M.F.	6Q19
Kimura	T.	1Q21
King	T.L.	6P51
Kinkead	A.K.	4P38
Kirkici	H.	6P46
Kirkpatrick	R.C.	2P23, 2P60, 5E03
Kishek	R.A.	1P03
Kishimoto	Y.	5E06
Kiuttu	G.F.	2P44, 5P16, 6B08, 6E08, 7P28, 7P29
Klimov	A.I.	5P13
Kline	J.	5Q03, 7P12
Klochko	E.V.	1Q20, 7P19, 7P20
Klyui	N.I.	7A02
Ko	D.K.	1Q19
Ko	K.C.	7P34
Kobayashi	S.	7A07
Kobayashi	T.	7P34
Kodis	M.A.	1E04, 1E10, 6P29, 6Q21
Koepke	M.E.	1A03, 2E05, 7P12
Koh	K.	2A04
Kohno	S.	6Q44
Kokshenev	V.A.	2P58
Kolb	J.	1Q09
Kolgatin	S.N.	5P19
Kolikov	V.A.	7D05
Kolner	B.H.	1P02, 6A07
Komissarov	A.V.	1D05
Kondrashov	D.	3A01
Kong	M.G.	4P46, 4P47, 4P48
Kontar	E.	2E10, 5Q10
Korensowski	G.	5D04
Koretzky	E.	2C05, 4Q22, 6P33
Kornilov	E.A.	1P15
Korolev	P.V.	5P16
Korovin	S.D.	5P06, 5P10, 5P13
Kortbawi	D.	6E01-02, 6E03
Kory	C.L.	2D04, 3D09
Koshelev	S.V.	2P21, 6C06
Koshevoi	M.O.	2P27, 2P28
Kossey	P.	5Q07
Kostecki	J.	3E05
Koval'chuk	B.M.	2P58
Kovalenko	A.V.	3P24
Kovalenko	V.P.	1A09, 3P24
Kovaleski	S.D.	4Q23, 4Q24
Kovpik	O.F.	1P15
Kowalewicz	R.	1Q09
Krainov	V.P.	3P27
Krasik	Ya.E.	5P25, 5P26, 6E06
Kreh	B.B.	6B08
Kreisher	K.E.	4P45
Krishnan	M.	5P27, 6Q29, 7P16
Kristiansen	M.	3B06, 3P10, 5P04, 7D04
Krivosheyev	S.I.	5P19
Krohn	K.E.	1E09
Krompholz	H.	3B06
Kropotov	N.Yu.	1Q24
Kroupp	E.	2P50
Krukovskii	A.Yu.	6B10
Krylov	M.K.	2P44
Kukushkin	A.B.	2P36, 3E04, 5E11
Kunc	J.A.	1Q31
Kuo	S.C.	4Q22, 5Q06
Kuo	S.P.	2C05, 4Q22, 5Q06, 5Q07, 6P33, 7A06
Kuprin	A.G.	7D05
Kurihara	L.K.	2D02
Kurkan	I.K.	5P06
Kurnosov	V.V.	7P29
Kurz	C.	7P30
Kushner	M.J.	1B01-02, 1C04, 4Q29, 4Q30, 4Q31, 4Q32, 5A03, 5A05, 7B06
Kuthi	A.	7B05
Kuz'menkov	L.S.	3P23
Kwan	T.J.T.	7P26
Kwok	T.K.	3Q14, 3Q15
Kyser	R.H.	4P35, 5B04, 5B06

L

L'Eplantier	P.	2P61
Labetsky	A.Yu.	2P58
Lafrance	D.	6Q43
Lai	C.H.	2C04, 2C06
Lai	S.T.	2E07
Lake	P.	1C03
Lam	N.T.	1P10, 1P11
Lam	S.K.	5P23
Lampe	M.	3A04, 3A06
Lan	Y.C.	1Q17, 6P32
Landen	O.L.	1D01-02
Lanford	W.	3Q11
Lapenta	G.	7P06
Lapshin	V.I.	1P01, 2E10

Laroussi	M.	1P13
Lash	J.S.	1C03, 3C01, 4Q24, 7P32, 8P44
Lashintsev	B.V.	1D06
Lasnier	C.J.	5E08
Latham	P.E.	4P29, 4P30, 5B01-02, 6Q13
Lau	Y.Y.	1P03, 3C09, 4Q23, 4Q24, 5P01, 5P02, 5P05, 7P35, 7P36
Laurent	L.L.	1P02, 5P08
Lavernia	E.	1B07
Lawler	J.E.	5D06-07
Lawson	W.	4P30, 4P32, 5B05, 6Q13, 6Q14
Lazier	S.E.	6Q30, 6Q35, 7P32, 8P44
Le Sage	G.P.	1P02, 6A07
Lebedeve	S.	2P65
Lee	D.J.	6P47
Lee	G.S.	6Q28
Lee	H.	2P49
Lee	H.J.	1Q03, 1Q22
Lee	J.H.	8P45
Lee	J.K.	1Q03, 1Q12, 1Q22
Lee	K.-W.	2P31
Lee	M.C.	2E04, 5Q06, 5Q07, 7A06
Lee	S.	2P33, 3Q08
Lehr	F.M.	6B08
Lehr	J.M.	7D04
Lei	J.	2P35
Lemke	R.	3B01, 3B02-03, 3B04
Lemunyan	G.	1Q01
Leou	K.C.	1Q15 1Q17
LePell	P.D.	2P47, 2P61
Leung	W.C.	2E09, 5Q04
Levine	J.S.	7A05
Levush	B.	3D04, 4P29, 4P30, 4P31, 4P33, 4P34, 5B01-02, 5B06, 6A05, 6Q15, 6Q21, 7P03
Lewis III	D.	2D02
Li	H.-S.	2P33, 3Q08
Li	J.	1Q08
Li	J.H.	1Q15
Li	Y.A.	3Q08
Li	Y.M.	6P38
Licki	J.	6P52
Liewer	P.C.	3A01
Lileikis	D.E.	6C04, 6E07, 6E08
Lin	A.T.	2D08, 7A03
Lin	C-C.	2D08, 7A03
Lin	Q.Z.	3Q13
Lin	T.L.	1Q15, 1Q17
Lindemuth	I.R.	2P60, 5E03
Liou	R.	2C04
Lisitisyn	A.G.	6B10
Lisitsyn	I.V.	6Q44
Lisovskiy	V.A.	1Q02, 1Q04, 1Q24, 8P42, 8P43
Litovchenko	V.G.	1E03, 7A02
Liu	A.G.	3Q13, 3Q14, 3Q15
Liu	C.	4P40
Liu	C-Z.	2P39, 2P40, 6D06
Liu	F.	7P16
Liu	H.L.	3Q03, 3Q11
Liu	K.X.	4P40
Lockwood	D.L.	5P24
Loginov	S.V.	2P58
Lohr	J.	1P04
Loring	C.M.	6A06
Lototzky	A.P.	2P44
Louis	L.J.	2D07, 6Q18
Lovberg	R.H.	3C06
Lu	M-F.	2P38, 2P39, 2P40, 2P42, 6D04, 6D05, 6D06
Luchinin	G.A.	1P09
Lucovsky	G.	2A03, 2A04
Luginsland	J.W.	3C09, 5P05, 5P14
Luhmann Jr.	N.C.	1P02, 2C08, 4P41, 4P42, 4P43, 4P44, 6A07
Lund	C.	6B05-06
Luo	C.M.	6D03
Luo	W.	2P33
Lykov	V.A.	2P21
Lysczarz	T.M.	1E09

M

MacDonagh-Dumler	J.	5D06-07
MacFarlane	J.J	2P47, 2P62, 5C05, 7P37
Mackartsev	G.F.	5P16
Mackie	W.A.	1C07, 6P30, 6P31
Maeda	Y.	2P29
Maeyama	M.	2P29
Magni	D.	5C06
Mako	F.	5P07
Malloy	K.J.	3B09
Maloletkov	B.D.	5P22
Malykhina	T.	7A04

Mancusi	J.	7C03
Manheimer	W.M.	3A04, 3A06, 5A08, 5B04, 6A01-02
Mankowski	J.	7D04
Manoilov	E.G.	1E03
Marchenko	R.I.	1E03, 7A02
Marder	B.M.	2P51
Maron	Y.	5P25, 5P26, 6E06
Marrese	C.M.	1C07, 6Q40
Martin	A.K.	7E01-02
Martinez	C.	6Q42
Maslov	V.I.	7P25
Masnavi	M.	5C07, 5E09, 5E10
Masuda	T.	7P27
Mathew	J.	5A08
Mathews	R.H.	1E04
Matsumoto	H.	6P50
Matsuoka	T.	6P40
Mattick	A.T.	7E03
Matuska	W.	2P57, 6B05-06
Matzen	M.K.	2P48, 2P51, 6B02-03, 6B05-06
Maximov	S.G	3P23
Mayo	R.M.	3P07, 5Q05
McCrary	K.E.	1P05
McCollam	K.	7E01-02
McCurdy	A.H.	4P35, 5B04, 5B06
McDermott	D.B.	4P41, 4P42, 4P43, 4P44
McGee	S.	3C09
McGrath	R.T.	7C09
McGuire	G.E.	7C03
McGurn	J.S.	2P47, 2P48, 2P51, 6B02-03
McKenney	J.	1C03
McLenithan	K.	6B05-06
McNeely	M.J.	6Q18
Meger	R.	5A08
Mehlhorn	T.A.	3C01, 3C02-03, 7P31, 7P37
Mel'nik	V.	2E10, 5Q10
Menge	P.R.	1C03, 3C01, 7P36, 7P38
Menniger	W.	3D05
Mentel	J.	1Q32, 6P54
Merritt	B.T.	7B05
Mészáros	M.	2B08, 3P26
Mezzetti	F.	6D02
Michelt	B.	1Q32, 6P54
Mikawa	Y.	2A05, 4Q25
Miklaszewski	R.	2P41, 2P54
Miley	G.H.	3A03, 7P09, 7P21
Miljak	D.G.	3P03
Millard	D.L.	1D08
Miller	S.M.	6Q15
Mirzaei	J.	2B04, 5E09
Mitchell	J.H.	2P65
Miyano	R.	2A05, 4Q25
Moats	A.R.	2P51, 6Q42
Mock	R.C.	2P48, 2P51, 6B02-03, 6B05-06, 6Q30
Moir	D.C.	7P26
Mojahedi	M.	3B09
Mondelli	A.A	3D08
Monfared	M.	5C08
Montie	T.C.	4Q21
Montiero	O.	3C07
Moore	T.E.	2E01-02
Moosman	B.	2P64
Moran	M.J.	5C03
Morel	J.E.	7P08
Morgan	D.V.	6B01, 6B08
Mori	W.B.	2C04, 2C06
Moriarty	D.T.	2E04, 7A06
Morovov	A.P.	1D06
Moschella	J.J.	5P28
Moses	G.A.	2P25, 5C05
Moskowitz	W.P.	5D05, 6P39, 6P42
Mouzouris	Y.	3P01, 3P02
Mozer	F.S.	2E01-02
Muggli	P.	2C04
Murphy	D.	5A08
Murphy	R.A.	1E04
Myers	M.	5A08

N

Na	H.K.	6Q28
Nagatsu	M.	2A05
Nandelstadt	D.	6P54
Napartovich	A.P.	1Q05
Naqvi	S.	5P03
Nardi	V.	6D01, 6D02, 6D03
Nash	T.J.	2P47, 2P48, 2P51, 2P61, 2P62, 6B02-03, 6B05-06
Nation	J.A.	1P06, 5P03, 7P23
Nauka	K.	4Q28
Nebel	R.A.	7E04
Neiger	M.	5D01-02
Neilson	J.	2D03
Nelson	B.A.	7E01-02
Neri	J.M.	3C05
Neuber	A.	3B06

Nezhevenko	O.A.	4P38, 4P52
Ngo	M.T.	1E04, 6P29
Nguyen	K.T.	1E10, 4P33, 4P34, 5B08
Nichipor	H.	6P53
Nielsen	D.	3C01
Niimi	H.	2A04
Nikiforov	A.F.	6B10
Nilsen	J.	3E05
Nishimura	T.	1Q06
Nishiwaki	A.	2A05, 4Q25
Nobuhara	S.	5P09, 5P11, 7P27
Noh	S.J.	1Q19
Noh	T.H.	2B03
Nonaka	S.	2A05
Noonan	W.A.	6Q32
Novikov	V.G.	6B10
Nunnally	W.C.	7C07
Nusinovich	G.	4P36, 5B07, 6A05, 7A07

O

O'Hair	E.	3P10
O'Neill	R.C.	1P04
Oh	B.-H.	2P31
Ohe	K.	1Q21, 6Q37
Ohmura	J.	7P34
Ohnuma	T.	3P25, 5Q08, 7P10
Okamoto	M.	5P09
Okamoto	Y.	2A05
Okino	A.	2P29, 7P34
Oliphant	T.A.	7P08
Oliva	S.	7P15
Oliver	B.V.	3C04, 3C05
Olson	C.L.	3C04, 5C05
Olson	R.	6Q34
Olthoff	J.K.	1Q23, 1Q30
Onishchenko	I.N.	1P15, 7P25
Oona	H.	5E03, 6B05-06, 6Q26
Ordonez	C.A.	1A08, 2P32, 5E04-05
Orlando	T.M.	7B01-02
Oro	D.M.	7P26
Orton	N.P.	7D02
Orvis	D.J.	7E01-02
Oslake	J.M.	6Q20
Osmokrovic	P.	5P21
Osterheld	A.L.	3E05
Otochin	A.A.	6B10
Ottinger	P.F.	3C04, 3C05, 6E03, 6Q32
Overhiser	G.J.	4Q23

P

Palmer	D.	1E05
Palmer	W.D.	1E07, 7C03
Pan	S.C.	1Q15
Pan'kin	M.V.	1Q05
Panarella	E.	2P34, 7E06
Panchenko	V.G.	1A06, 3P11, 3P12, 3P13, 3P14, 3P15
Park	G.S.	4P35
Park	G.T.	3B08
Park	J.H.	7P34
Parker	C.G.	2A03
Parker	G.J.	3A05
Parker	R. K.	5B06
Parks	P.B.	2P25
Parneta	I.M.	1A09
Pavlenko	I.V.	1P01
Pavlenko	V.N.	1A06, 3P11, 3P12, 3P13, 3P14, 3P15
Pavlovski	A.I.	1D06
Pechacek	R.	5A08
Pegel	I.V.	5P06, 5P10, 5P13
Pender	J.T.P.	1B06
Penetrante	B.M.	7B05
Perrin	M.	1C05
Perry	A.J.	7B03
Pershing	D.E.	4P30, 4P34, 4P51
Pert	E.	2D01
Pesensen	D.	3Q10
Peter	W.	5P07
Peterkin	F.E.	7C07
Peterkin Jr.	R.E.	1A08, 1C06, 2P32, 2P53, 6B08, 6E07
Peterson	D.L.	2P48, 2P51, 2P57, 2P62, 6B02-03, 6B05-06
Peterson	G.G.	6Q29
Peterson	R.R.	2P25
Petillo	J.J.	3D08, 4P34
Pfedyokovich	V.N.	6P49
Pfeufer	G.W.	7P08
Philipps	J.	1Q09
Phillips	R.M.	4P42
Pi	T.	3C07
Pickrel	M.M.	7E04
Piejak	R.B.	7P11
Pikar	A.S.	5P16
Pikuz	S.A.	2P41, 2P45, 2P52
Pikuz	T.A.	2P17
Platt	C.L.	6Q19
Platts	D.	6B08, 6Q36

Poeschel R.L. 5P20
Pointon T.D. 3C01, 3C02-03, 7P31
Polevin S.D. 5P10, 5P13
Pollock C.J. 2E01-02
Ponce D. 1P04
Ponomarenko A.G. 2E06, 5Q02
Ponomarev A.G. 1Q27
Ponti E.S. 6Q23
Popkov N.F. 5P16
Popov G.F. 1Q27
Popovic S. 6Q38
Porter J. 6Q42
Pouraslan A. 1C08
Pouvesle J.M. 2P63
Powell C. 6D01, 6D02, 6D03
Prasad R.R 5P27
Prasad R.R. 6Q29, 7P16
Prater R. 1P04
Price D. 7A05
Prono D.S. 7P26
Prucker U. 7D03
Pruka W. 4Q26
Pu W. 3Q04, 3Q05, 3Q06
Puerta J. 3P17
Pulsifer P.E. 2P47
Purcell S.T. 1E08

Q

Qi N. 5P27, 6Q29, 7P16
Qin S. 2A06, 2A07

R

Rader M. 4Q16
Radzimski Z.J. 5A01
Ralph D. 3B02-03, 3B04
Ran J. 2A01-02
Rantsev-Kartinov V.A. 2P36, 3E04, 3P27
Rao M.V.V.S. 1Q23
Rauch J. 6B04
Rauf S. 1B01-02, 4Q29, 5A03
Rayne R.J. 2D02
Razafinimanana M. 6P44
Razin S.V. 7P13
Reass W.A. 3C06
Rees D. 2D05
Reinhard D. 7P14
Reinovsky R.E. 6B01
Reiser M. 4P32, 6Q14
Repin A.Y. 7P28
Rhodes M.A. 2P24, 5E01
Rhodes R. 6E04
Riccardo V. 7P06
Richards J. 2D06, 6A04
Richardson J.L. 4Q19
Riddolls R.J. 2E04, 7A06
Riley R.A. 6E05
Rintamaki J.I. 5P01, 5P02, 7P36
Riordan J.C. 2P47, 2P61
Rix W. 6B04, 6E01-02
Riyopoulos S. 6A08
Roberts J.R. 6P41
Robson A.E. 6P35
Roderick N.F. 2P53, 2P59, 6B05-06
Rodgers J. 5B07
Roerich V. 6B10
Rogers H.H. 2P46
Roitmann A.M. 5P13
Romanova V.M. 2P41, 2P45
Rondeau G. 6Q29
Roquemore L. 1Q01
Roscoe M. 3D01-02
Rose D.V. 3C04, 3C05
Rosenfeld W. 2P63
Rosmej F.B. 2P17
Rostoker N. 7P41
Rostov V.V. 5P06, 5P13
Rosum I.N. 3P14
Roth I.S. 5P23
Roth J.R. 4Q19, 4Q20, 4Q21
Rowlands M.J. 2E04, 7A06
Rozanov V.B. 2P27, 2P28
Rudakov L.I. 6B09
Ruden E.L. 2P53, 5C04, 6B08
Ruden T.E. 6P47
Ruggles L. 6Q42
Ruiz C.L. 6Q30, 6Q33
Rupasov A.A. 2P27, 2P28
Russkikh A.G. 2P58
Rutberg Ph. G. 5P17, 5P18, 6P48, 6P49, 6Q31, 7D05
Ruzic D.N. 1B08, 7P05
Ryabchikov D.L. 1Q20
Ryaslov E.A. 5P16

S

Sadowski M. 2P41, 3E06-07
Safronov A.A. 6P48
Salami M.R. 1C08, 2B04, 5C07, 5C09, 5E09
Sanford T.W.L. 2P47, 2P48, 2P51, 6B02-03, 6B05-06
Santoru J. 5P20
Saraph G.P. 4P32, 5B05, 6Q13, 6Q14

Sarfaty	M.	1B03, 1B04
Sarff	J.	7P15
Sarkisov	G.S.	2P16, 2P45, 2P64
Sarkissian	A.H.	3Q02, 6Q43, 7P39
Sasser	G.E.	5P14
Sato	H.	5Q08
Sato	M.	6A06
Savina	N.P.	6C06
Scafuri	F.	6A04
Scannapieco	T.	6B05-06
Schachter	L.	7P23
Schamiloglu	E.	3B07, 3B08, 3B09, 5P12
Scharer	J.E.	1P10, 1P11, 2C03, 2D07, 3P01, 3P02, 6Q18
Schauer	M.M.	7E04
Schein	J.	6P54
Scheitrum	G.	3C07, 5P08
Schlaug	M.	7D03
Schleinitz	H.M.	3C06
Schmidlapp	F.A.	6Q30, 6Q33
Schoch	P.M.	2P35
Schoen	P.E.	2D02
Schoenbach	K.H.	5A07, 7C07
Scholz	M.	2P41, 2P54
Schone	H.	7C09
Schumann	M.	6P54
Schwandner	A.	7D03
Schweigert	I.V.	2B01-02, 3P19
Schweigert	V.A.	2B01-02, 3P19
Schwoebel	P.R.	1E06
Scime	E.	5Q03, 7P12
Semak	V.	2P22
Seamen	J.F.	2P47, 2P48, 2P51, 6B02-03
Semenovich	V.A.	7A02
Semet	V.	1E08
Sena	M.	3B02-03, 3B04
Seo	J-T.	8P45
Seo	S-H.	6Q39
Seward	C.	7E08
Shah	U.	2P35
Shamamian	V.	6P35
Shamrai	K.P.	1Q18
Shang	Z.	3P28, 3Q07
Shannon	S.C.	4Q26, 4Q27
Shao	J.	2A06
Shapiro	M.	4P45
Sharma	A.S.	3Q09
Sharpe	J.P.	2P30
Shaw	J.	1E04
Sheehey	P.T.	2P60, 5E03
Shelkovenko	T.A.	2P45, 2P52
Sherman	D.M.	4Q20
Shi	W.	5A07
Shiau	J.H.	1Q17
Shiffler	D.	3B02-03, 3B04
Shikanov	A.S.	2P27, 2P28
Shimozuma	T.	6A06
Shin	Y.K.	1Q03
Shiraki	Y.	2A05, 4Q25
Shishlov	A.V.	2P58
Shneerson	G.A.	5E02, 5P19
Shohet	J.L.	1C04, 4Q28
Shpitalnik	R.	6E06
Shumlak	U.	2P53, 6C05, 7E01-02, 7E07
Sidorenko	Yu.V.	1Q20, 7P19
Sielker	R.	1Q32
Sincerny	P.S.	5P23
Singh	N.	2E09, 3A02, 5Q04
Skobelev	I.Yu.	2P17, 3E05
Slavin	V.S.	6C02
Slinker	S.	3A06
Slutz	S.A.	3C01, 7P33
Smith	M.L.	6Q34
Smithe	D.	6Q21
Smolyakov	A.	1Q26
Snavely	R.	5C01-02
Snider	R.T.	6Q27
Snodgrass	T.G.	1C04
Snyder	H.R.	7B07, 7B08
Sobocinski	B.J.	6P29
Soda	H.	7P10
Soderquist	D.	7B03
Solomyannaya	A.D.	6B10
Sommers	W.	6B08
Song	Y.	2P64
Sosipatrov	M.	1Q25
Sotnikov	G.V.	1P15
Souvalian	V.S.	3B08
Spassov	V.A.	3Q12
Spencer	T.A.	3B02-03, 5P01, 5P02, 5P15
Spielman	R.B.	2P47, 2P48, 2P51, 2P61, 6B02-03, 6B05-06, 6Q42
Spindler	H.L.	4Q24
Spindt	C.A.	1E05, 1E06
Sporov	A.	2B07
Sprangle	P.	2C07, 2P19
Stadler	K.R.	7P18
Stamate	E.	6Q37

Stambouli	M.	6P37
Stark	M.A.	3C01
Starostin	A.N.	6B10
Stattel	M.	4P32
Steele	J.	7B03
Stepanov	A.E.	6B10
Stepchenko	A.S.	5P13
Stephens	R.B.	2P25
Stephens II	K.F.	1A08
Stepniewski	W.	2P41, 2P54
Strasik	M.	1P05
Struve	K.W.	2P48, 2P51, 6B02-03
Stubbers	R.A.	3A03, 7P21
Stump	M.D.	5P15
Stupitsky	E.L.	7P28, 7P29
Stygar	W.A.	2P48, 2P51, 6B02-03
Sueda	T.	6Q44
Sukharev	V.	4Q32
Sulzer	M.P.	7A06
Summa	W.J.	5P16
Summers	C.J.	7C01-02
Surko	C.M.	7P30
Suter	L.J.	1D01-02
Svechnikov	S.V.	1E03
Sved	J.	3A03, 7P21
Svensson	A.	3P06
Swanekamp	S.B.	6E05
Sweeney	M.A.	6Q30
Szczurek	M.	3E05
Szydlowski	A.	2P41

T

Taccetti	J.M.	4P51
Tafreshi	A.K.	2B04, 5E09
Takeda	M	6P40
Tanabe	S.	6P50
Tang	B.Y.	3Q13, 3Q14, 3Q15
Tang	C-M.	7C04
Tanigawa	M.	5P09, 5P11
Tarakanov	V.P.	5P10
Temkin	R.J.	4P45
Temple	D.	7C03
Terreault	B.	3Q02
Terry, Jr.	F.	4Q27
Tessnow	T.	7C07
Thomas	G.E.	6Q17
Thomas	M.	7P15
Thompson	J.	6B04, 6E01-02, 6E03
Thornhill	J.	2P61
Tian	X.B.	3Q13
Ting	A.	2P19
Tkachenko	V.	1P08
Torres	J.A.	2P48, 2P51, 6B02-03
Torvén	S.	2B05, 6Q41
Totmeninov	E.M.	5P06
Trebes	J.E.	5C01-02
Treglio	J.	7B03
Trofimovich	E.E.	3P27
Troha	A.L.	1P02, 6A07
Trubnikov	B.A.	5Q09
True	R.B.	1E07, 4P33, 4P38, 6B08
Trushkin	N.I.	1Q05
Tsai	C.H.	1Q15
Tsai	J.L.	1Q15
Tsai	M.-H.	1C01-02
Tsai	P.	4Q16, 4Q21
Tsigutkin	K.	5P26, 6E06
Tucker	E.C.	7D02
Turbin	P.V.	1P08, 1P14, 6Q22
Turchi	P.J.	1C06, 6B08, 6E07, 6E08
Tuszewski	M.G.	3Q10
Twichell	J.C.	1E08
Tyminski	B.	6P52
Tynan	G.	3P04
Tzonev	I.V.	5P27

U

Uchida	H.	7P27
Udrea	B.	6C05, 7E01-02
Ueda	M.	3Q12
Ufimtsev	A.A.	6P49
Uhm	H.S.	2A08
Umstadter	K.R.	1D08
Umstattd	R.	3C07
Ustalov	V.V.	3P13
Uvarov	V.V.	1Q27

V

Vacquie	S.	6P44
Vaden	K.R.	3D07
Vakulenko	M.O.	1A07
Valfells	A.	1P03
Van Brunt	R.J.	1Q23
VanMeter	J.R	1P02, 2C08, 4P41
VanDrie	A.	2P64
Vargas	M.	2P51
Vasilevsky	V.M.	5P19
Veerasingam	R.	6P36, 7C09
Velazco	J.E.	4P49, 4P50
Velikovich	A.L.	2P56, 6B07
Vellenga	D.	7C03
Verboncoeur	J.P.	2B05, 3C08, 6Q20, 7P01

Vesey	R.A.	3C01, 3C02-03, 7P31, 7P32
Vidmar	R.J.	1C09, 2C01-02, 7P17, 7P18
Vignes	M.J.	1Q11
Vikhrev	V.V.	2P43, 7P40
Vilece	K.	7A06
Vladimirov	S.V.	3P18, 3P20, 3P21, 3P22
Vlasov	V.P.	5Q09
Vogler	W.F.	2D03, 7A01
Vogtlin	G.E.	7B05
von Rosenberg Jr.	C.W.	1D07
Vourdas	A.	4P46

W

Wadsworth	L.	4Q16, 4Q21
Walker	D.N.	5Q01
Wallace	R.	1D01-02
Walsh	D.	7C09
Walsh	J.E.	6Q19
Walter	K.C.	7B03
Walter	M.	4P36, 5B07
Walton	A.	7P07
Wan	A.S.	5C01-02
Wang	J.	2E07, 3A01
Wang	P.	1C03, 2P62, 5C05, 7P37
Wang	Q.	5P03
Wang	S.Y.	3Q13
Wang	W.	3Q03, 3Q11
Wang	X.	1Q06
Wang	X.F.	3Q13
Wang	X.X.	2P42
Ware	K.D.	3E01, 5P16
Watkins	R.	6Q23
Weber	B.V.	6E01-02, 6E03, 6E05
Weber	F.	5C01-02
Weingarten	A.	5P25, 6E06
Welch	D.R.	3C04, 5C05
Wells	E.E.	3A02, 5Q04
Wells	J.	7D04
Wenger	D.F.	3C01
Wessel	F.J.	2P64, 3Q10, 7B04
Whaley	D.R.	3D01-02
Whiteson	D.O.	5E03
Whitney	K.G.	2P47, 2P61
Whitton	B.	2P47
Wiese	W.L.	6P41
Wiesmann	H.	5D01-02
Wilkinson	S.P.	4Q20
Williams	R.L.	2P18
Williamson	W.S.	2E01-02, 2E03
Wilson	J.D.	2D04, 3D06
Wintucky	E.G.	1E05
Wong	S.K.	7P07
Wood	B.P.	3Q01, 3Q10, 7B03
Wood	C.H.	6P45
Wood	F.	5B06
Wood	T.	7B04
Woodworth	J.R.	1B05
Woolverton	K.	5P04
Wu	S.L.	1Q15
Wurden	G.A.	1Q01
Wysocki	F.J.	2P60, 5E03

X

Xie	T.	6P30, 6P31
Xu	S.	2P33, 3Q08
Xu	X.	3Q08, 5P08

Y

Yadlowsky	E.J.	2P47, 2P61, 5P28
Yadon	L.	7C03
Yakovlev	V.P.	4P38, 4P51
Yamagiwa	M.	5E06
Yamasaki	T.	7P27
Yang	S.	6D06
Yang	S-Z.	2P39, 2P40, 6D06
Yang	T.C.	2P42
Yang	T.T.	5B03
Yang	Y.	1Q22
Yankelevich	Y.B.	1B07, 7B04
Yanobe	T.	1Q06
Yao	W.W.	7C05-06
Yatsuzuka	M.	5P10, 5P11, 7P27
Yee	D.	7B04
Yegorenkov	V.D.	1Q04, 8P43
Yoon	H.J.	1Q12
Yoon	M.	1Q22
Yoon	N.S.	6Q28
Yoshihara	Y.	7P27
Yoshii	J.	2C06
Yoshioka	T.	4Q25
Young	D.	5P12
Young	F.C.	3C05

Z

Zaginaylov	G.I.	1P14, 6Q22
Zaidman	E.G.	1E10, 3D03, 6Q21
Zakharov	S.V.	2P55, 6B10
Zakharov	Yu.P.	2E06
Zamani Mehr	M.	2B04, 5E09
Zarecki	C.	7C09
Zeng	X.C.	3Q13, 3Q14, 3Q15

Zhang	D.	1P04
Zhang	L.	7E06
Zhang	W.	3P18
Zhdanov	S.K.	5Q09
Zheng	C.	2A01-02
Zhou	Y.	2A06, 2A07
Zich	R.	3A03, 7P21
Zieher	K.W.	1P07
Zigler	A.	2P17
Zimek	Z.	6P52, 6P53
Zintl	M.W.	1A03, 2E05
Zissis	G.	6P37
Zorin	V.G.	7P13
Zorriasatin	S.	1C08
Zuo	Y.	7E09
Zweben	S.J.	1Q01

NOTES

PREVIOUS CONFERENCES

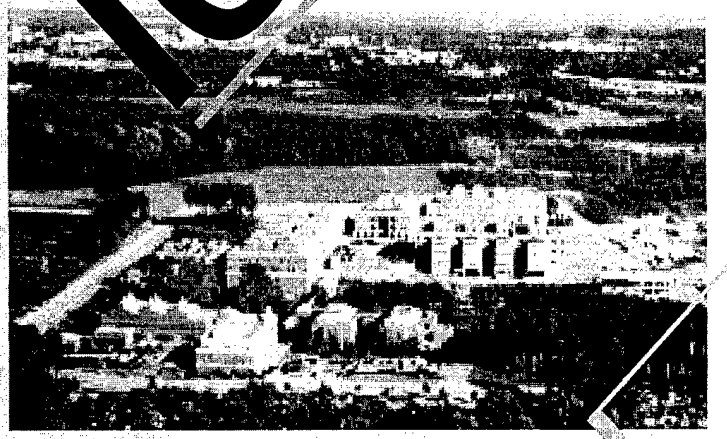
1974	University of Tennessee	Knoxville, TN	I. Alexeff
1975	University of Michigan	Ann Arbor, MI	R. R. Johnson
1976	University of Texas	Austin, TX	E. J. Powers
1977	Rensselaer Polytechnic Institute	Troy, NY	R. L. Hickok
1978	Doubletree Inn	Monterey, CA	R. Schwirzke
1979	Université de Montreal	Montreal, Canada	C. Richard
1980	University of Wisconsin	Madison, WI	J. L. Shohet
1981	Sweeney Convention Center	Santa Fe, NM	S. J. Gitomer
1982	Carleton University	Ottawa, Canada	A. J. Alcock
1983	Sherator Harbor Island Hotel	San Diego, CA	J. L. Luxon
1984	Clarion Hotel	St. Louis, MO	T. J. Menne
1985	Pittsburg Hilton Hotel	Pittsburgh, PA	M. D. Nahemow
1986	Ramada Renaissance Hotel Bessborough Hotel	Saskatoon, Canada	A. Hirose
1987	Hyatt Regency Crystal City	Arlington, VA	F. C. Young
1988	Seattle Sheraton Hotel	Seattle, WA	L. C. Steinhauer
1989	Hyatt Regency	Buffalo, NY	D. M. Benson
1990	Hyatt Regency	Oakland, CA	J. N. Benford
1991	College of William and Mary	Williamsburg, VA	K. H. Schoenbach
1992	Hyatt Regency Westshore	Tampa, FL	N. L. Oleson
1993	Sheraton Landmark Hotel	Vancouver, Canada	A. Ng
1994	Sweeney Convention Center	Santa Fe, NM	A. L. Peratt
1995	University of Wisconsin	Madison, WI	J. E. Scharer
1996	Boston Park Plaza Hotel	Boston, MA	C. Chan

98 ICOPS

Sponsored by the
Plasma Science & Applications Committee
of the IEEE and NC State University

For an information packet, contact

Dr. John G. Gilligan
College of Engineering, Box 7901
Raleigh, North Carolina 27695
(919) 515-3939
gilligan@ncsu.edu



ICOPS will be held in downtown Raleigh, North Carolina, near NC State University and Research Triangle Park.

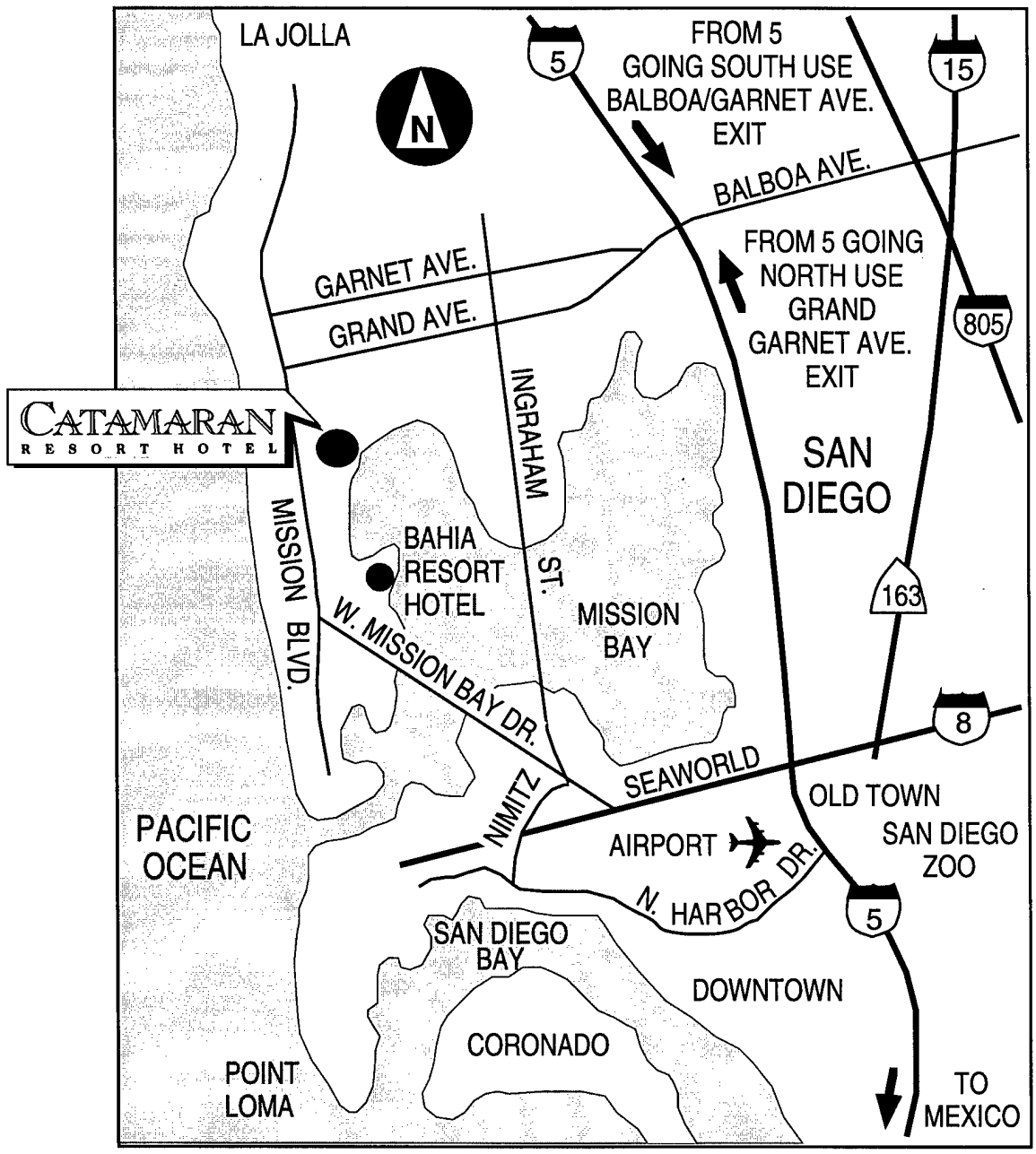
The 25th Anniversary IEEE International Conference On Plasma Science

June 1-3, 1998

Conference Topics

- Basic processes in fully & partially ionized plasmas
- Plasma processing
- Microwave generation & microwave/plasma interactions
- Intense electron & ion beams
- High energy density plasmas
- Industrial & commercial applications of plasma physics
- Plasma diagnostics
- Pulsed power
- Space plasmas

CITY MAP


LA JOLLA
N
5
FROM 5
GOING SOUTH USE
BALBOA/GARNET AVE.
EXIT
15
BALBOA AVE.
FROM 5 GOING
NORTH USE
GRAND
GARNET AVE.
EXIT
805
GARNET AVE.
GRAND AVE.
INGRAHAM ST.
CATAMARAN
RESORT HOTEL
SAN
DIEGO
MISSION BLVD.
BAHIA
RESORT
HOTEL
MISSION
BAY
163
W. MISSION BAY DR.
8
SEAWORLD
NIMITZ
OLD TOWN
SAN DIEGO
ZOO
PACIFIC
OCEAN
AIRPORT
N. HARBOR DR.
5
SAN DIEGO
BAY
DOWNTOWN
CORONADO
POINT
LOMA
TO
MEXICO

SPECIAL EVENTS

Sunday May 18, 1997

Reception: 4:00 pm-8:00 pm—No-host bar with a wide variety of excellent culinary selections.
Kon-Tiki Ballroom, Catamaran Resort Hotel

Monday May 19, 1997

Plenary 1: **Welcome to Conference Participants**—Dr. Jay Hyman, Hughes Research Laboratories, Malibu, CA
8:30 am, Kon-Tiki Ballroom

Changes in the Nature of Plasma Science in the Post-Cold War Era—Professor Roald Z. Sagdeev, University of Maryland, College Park, MD

Plenary 2: **Plasma Propulsion for Deep-Space Missions**—Professor Roald Z. Sagdeev, University of Maryland, College Park, MD
1:30 pm, Kon-Tiki Ballroom

Companion Breakfast—Complimentary in the Companions' Room—*8:30 am to 10:00 am*

San Diego Zoo Tour—*Morning*

Aboard William D. Evans Sternwheeler—Complimentary hors d'oeuvres and drinks with music and a tour of the bay—*Evening*

Tuesday May 20, 1997

Plenary 3: **Trapped Plasmas with a Single Sign of Charge (An Overview)**—Professor Thomas M. O'Neil, University of California at San Diego, La Jolla, CA
8:30 am, Kon-Tiki Ballroom

Plenary 4: **Interaction of Ultra-Intense Lasers with Beams and Plasmas**—Dr. Phillip Sprangle, Naval Research Laboratory, Washington, DC
1:30 pm, Kon-Tiki Ballroom

Special Panel: Changing Career Opportunities in Plasma Science—Dr. Wallace M. Manheimer, Moderator, Naval Research Laboratory, Washington, DC
3:00 pm, Kon-Tiki Ballroom

Nordstrom Complimentary Breakfast—Fashion seminar including "make-up," "make-overs," and personal shoppers—*Morning*

Network Gathering for Women in Plasma Science—*5:00 pm - 6:30 pm*

U.S. Grant Hotel—Cocktails in the Crystal Room and Banquet in the Grand Ballroom—*6:30 pm*

Wednesday May 21, 1997

Plenary 5: **NASA's International Solar Terrestrial Physics Program and the Roadmap Forward**—Dr. Robert L. Carovillano, NASA Headquarters, Washington, DC
8:30 am, Kon-Tiki Ballroom

Plenary 6: **PSAC Prize Address: Science and Applications of Energy Beam Ablation**—Professor Ronald M. Gilgenbach, Director, Intense Energy Beam Interaction Laboratory, University of Michigan, Ann Arbor, MI
1:30 pm, Kon-Tiki Ballroom

Companion Breakfast—Complimentary in the Companions' Room—*8:30 am to 10:00 am*

Guided Tour of Tijuana, Mexico—After breakfast—*All Day*

Thursday May 22, 1997

Plenary 7: **Tokamak Fusion Science Research on the DIII-D Tokamak**—Dr. Thomas C. Simonen, Director, DIII-D Program, General Atomics, La Jolla, CA
8:30 am, Kon-Tiki Ballroom

General Atomics Tour of the DIII-D Tokamak Facility, La Jolla, CA
1:30 pm, Busses leave from the front of the Catamaran Resort Hotel Conference Area

Mini-Course on High-Energy-Density Plasma Diagnostics—Dr. James E. Bailey and Dr. Ramon J. Leeper of Sandia National Laboratories
Catamaran Resort Hotel—Check with the Conference Registration Desk for details

Companion Breakfast—Complimentary in the Companions' Room—Awards Ceremony—*8:30 am to 10:00 am*

Casual No-Host Dinner—*Evening*

Friday May 23, 1997

Mini-Course on High-Energy-Density Plasma Diagnostics—Dr. James E. Bailey and Dr. Ramon J. Leeper of Sandia National Laboratories
Catamaran Resort Hotel—Check with the Conference Registration Desk for details

REPORT DOCUMENTATION PAGE

Form Approved
OMB No. 0704-0188

Public reporting burden for this collection of information is estimated to average 1 hour per response, including the time for reviewing instructions, searching existing data sources, gathering and maintaining the data needed, and completing and reviewing the collection of information. Send comments regarding this burden estimate or any other aspect of this collection of information, including suggestions for reducing this burden, to Washington Headquarters Services, Directorate for Information Operations and Reports, 1215 Jefferson Davis Highway, Suite 1204, Arlington, VA 22202-4302, and to the Office of Management and Budget, Paperwork Reduction Project (0704-0188), Washington, DC 20503.

1. AGENCY USE ONLY *(Leave Blank)*	2. REPORT DATE	3. REPORT TYPE AND DATES COVERED
	1997	Final

4. TITLE AND SUBTITLE
Conference Proceeding for 1997 24th International Conference on Plasma Sciences

5. FUNDING NUMBERS
G

6. AUTHORS
Dr. Julius Hyman

7. PERFORMING ORGANIZATION NAME(S) AND ADDRESS(ES)
Institute of Electrical and Electronics Engineers, Inc.
445 Hoes Lane, PO Box 1331
Piscataway, NJ 08855-1331

8. PERFORMING ORGANIZATION REPORT NUMBER

9. SPONSORING / MONITORING AGENCY NAME(S) AND ADDRESS(ES)
Office of Naval Research
800 North Quincy Street
Arlington, VA 2217-5660

10. SPONSORING / MONITORING AGENCY REPORT NUMBER
N00014-97-1-0401

11. SUPPLEMENTARY NOTES

12a. DISTRIBUTION / AVAILABILITY STATEMENT
Approved for Public release

12b. DISTRIBUTION CODE

13. ABSTRACT *(Maximum 200 words)*

This 360 page softbound publicatioin includes the following major sections. An invitation to ICOPS'97, Catamaran Resort Hotel Floor Plnas, Officers of the IEEE Nuclear and Plasma Sciences Society, Conference Information (including committees, session organizers, mini-course, hotel and travel information, future ICOPS conferences, IEEE membership information, etc.), Summary of Technical Sessions, Conference Record - Abstracts, Index by author, List of Previous Conferences, 1998 Conference, and a map of San Diego.

The Summary of Technical Sessions shows the sessions times and locations and the titles and authors of the presentations. For each presentation, an approximately 200 word abstract is printed in the Conference Record - Abstracts section of this publication.

14. SUBJECT TERMS
ICOPS, Plasma Physics, Plasma Science, Microwave Generation, Microwave/Plasma Interactions, Intense electron Beams, Intense ion Beams, Fusion, Plasma Lighting, Plasma Processing, Plasma Diagnostics, Pulsed Power

15. NUMBER OF PAGES

16. PRICE CODE

17. SECURITY CLASSIFICATION OF REPORT	18. SECURITY CLASSIFICATION OF THIS PAGE	19. SECURITY CLASSIFICATION OF ABSTRACT	20. LIMITATION OF ABSTRACT
Unclassified	Unclassified	Unclassified	UL

	Location	Monday, 19 May 1997		Tuesday, 20 May 1997		Wednesday, 21 May 1997		Thursday, 22 May 1997	
		8:30 a.m.	1:30 p.m.	8:30 a.m.	1:30 p.m.	8:30 a.m.	1:30 p.m.	8:30 a.m.	1:30 p.m.
Plenary	Kon Tiki Ballroom	1) Welcome to Conference Participants 2) Keynote Address: Changes in the Nature of Plasma Science in the Post-Cold War Era	Plasma Propulsion for Deep-Space Missions	Trapped Plasmas with a Single Sign of Charge (An Overview)	Interaction of Ultra-Intense Lasers with Beams and Plasmas	NASA's International Solar Terrestrial Physics Program and the Roadmap Forward	PSAC Prize Address: Science and Applications of Energy Beam Ablation	Tokamak Fusion Science Research on the DIII-D Tokamak	Tour of General Atomics DIII-D Tokamak Facility
	Speaker(s)	1) Dr. Jay Hyman 2) Professor Roald Z. Sagdeev	Professor Roald Z. Sagdeev	Professor Thomas M. O'Neil	Dr. Phillip Sprangle	Dr. Robert L. Carovillano	Professor Ronald M. Gilgenbach	Dr. Thomas C. Simonen	Front of Catamaran Hotel
Oral Sessions	**Location**	**10:00 a.m.**	**3:00 p.m.**	**10:00 a.m.**	**3:00 p.m.**	**10:00 a.m.**	**3:00 p.m.**	**10:00 a.m.**	**3:00 p.m.**
A	Kon Tiki Ballroom	1A 1.1: Basic Processes in Fully Ionized Plasmas–Waves, Instabilities, Plasma Theory, etc. I	2A 5.1: Non-Equilibrium Plasma Processing II	3A 1.4: Computational Plasma Physics I	4A Special Panel Changing Career Opportunities in Plasma Science	5A 1.3: Basic Phenomena in Partially Ionized Gases...	6A 2.2: Fast wave Devices II	7A 2.7: Special Session Microwave Generation and Plasma Interactions	Unscheduled Papers
B	Board Room	1B 5.1: Non-Equilibrium Plasma Processing I	2B 1.1: Basic Processes in Fully Ionized Plasmas-Waves, Instabilities, Plasma Theory, etc. II	3B 2.1: Intense Beam Microwaves	—	5B 2.2: Fast Wave Devices I	6B 4.5: Fast Z-Pinches and X-Ray Lasers	7B 5.5: Environmental/ Energy Issues in Plasma Science	Unscheduled Papers
C	Toucan Room	1C 3.1: Plasma Ion and Electron Sources	2C 2.6: Microwave-Plasma Interactions	3C 3.2: Intense Ion and Electron Beams	—	5C 6: Plasma Diagnostics	6C 1.4: Computational Plasma Physics II	7C 5.4: Flat Panel Displays	Unscheduled Papers
D	Macaw Room	1D 4.1: Laser Produced Plasmas	2D 2.5: Microwave Systems 2.4: Slow Wave Devices I	3D 2.4: Slow Wave Devices II		5D 5.3: Plasma for Lighting	6D 4.4: Dense Plasma Focus II	7D 7.1: MHD and EM/ETH Launchers	Unscheduled Papers
E	Cockatoo Room	1E 2.3: Vacuum Microelectronics	2E 1.2: Space Plasmas	3E 4.4: Dense Plasma Focus I		5E 4.2: Inertial Confinement Fusion 4.3: Magnetic Confinement Fusion	6E 7.3: Fast Opening Switches	7E 4.6: Spherical Configurations / Ball Lightning	Unscheduled Papers
Poster Sessions	**Location**	**10:00 a.m.**	**3:00 p.m.**	**10:00 a.m.**	**3:00 p.m.**	**10:00 a.m.**	**3:00 p.m.**	**10:00 a.m.**	**3:00 p.m.**
P	Rousseau Center	1P 2.5: 1P01-07 2.6: 1P08-15	2P 4.1: 2P16-22 4.2: 2P23-28 4.3: 2P29-35 4.4: 2P36-44 4.5: 2P45-65	3P 1.1: 3P01-28	4P 2.2: 4P29-52	5P 2.1: 5P01-15 7.1: 5P16-19 7.2: 5P20-24 7.3: 5P25-28	6P 2.3: 6P29-32 5.2: 6P33-36 5.3: 6P37-46 5.5: 6P47-54	7P 1.4: 7P01-10 3.1: 7P11-25 3.2: 7P26-41	8P Unscheduled Papers
Q	Multipurpose Room	1Q 1-3a: 1Q01-09 1-3b: 1Q10-20 1-3c: 1Q21-32	—	3Q 5.1-Ia: 3Q01-15	4Q 5.1-IIb: 4Q16-21 5.1-IIc: 4Q22-28 5.1-IId: 4Q-29-32	5Q 1.2: 5Q01-12	6Q 2.2: 6Q13-14 2.4: 6Q15-23 6: 6Q24-44	—	—

Session	Topic	Oral Locations	Poster Locations
1.1 (I &II)	Basic Processes in Fully Ionized Plasmas–Waves, Instabilities, Plasma Theory, etc.	1A-I, 2B-II	3P
1.2	Space Plasmas	2E	5Q
1.3	Basic Phenomena in Partially Ionized Gases–Gaseous Electronics, Electrical Discharges	5A	1Q
1.3-a	Basic Phenomena in Partially Ionized Gases-... (High Pressure Discharges)	5A	1Q
1.3-b	Basic Phenomena in Partially Ionized Gases-... (Plasma Processing & Low Pressure Discharges)	5A	1Q
1.3-c	Basic Phenomena in Partially Ionized Gases-... (Electron & Ion Transport & Fundamental Data)	5A	1Q
1.4 (I & II)	Computational Plasma Physics	3A-I, 6C-II	7P
2.1	Intense Beam Microwaves	3B	5P
2.2 (I & II)	Fast Wave Devices	5B-I, 6A-II	4P, 6Q
2.3	Vacuum Microelectronics	1E	6P
2.4 (I & II)	Slow Wave Devices	2D-I, 3D-II	6Q
2.5	Microwave Systems	2D	1P
2.6	Microwave-Plasma Interactions	2C	1P
2.7	Microwave Generation and Plasma Interactions	7A	—
3.1	Plasma Ion and Electron Sources	1C	7P
3.2	Intense Ion and Electron Beams	3C	7P
4.1	Laser Produced Plasmas	1D	2P
4.2	Inertial Confinement Fusion	5E	2P

Session	Topic	Oral Locations	Poster Locations
4.3	Magnetic Confinement fusion	5E	2P
4.4 (I & II)	Dense Plasma Focus	3E-I, 6D-II	2P
4.5	Fast Z-Pinches and X-Ray Lasers	6B	2P
4.6	Spherical Configurations / Ball Lightning	7E	—
5.1 Ia	Non-Equilibrium Plasma Processing (Ion Implantation)	1B	3Q
5.1 IIb	Non-Equilibrium Plasma Processing (Atmospheric Discharges)	2A	4Q
5.1 IIc	Non-Equilibrium Plasma Processing (Deposition and Etching)	2A	4Q
5.1 IId	Non-Equilibrium Plasma Processing (ICP Modeling)	2A	4Q
5.2	Thermal Plasma Processing	—	6P
5.3	Plasma for Lighting	5D	6P
5.4	Flat Panel Displays	7C	—
5.5	Environmental / Energy Issues in Plasma Science	7B	6P
6	Plasma Diagnostics	5C	6Q
7.1	MHD and EM/ETH Launchers	7D	5P
7.2	Plasma Closing Switches	—	5P
7.3	Fast Opening Switches	6E	5P
8.0	Unscheduled Papers	—	8P

Poster Papers will be displayed all day in the Rousseau Center and Multipurpose Room, 10:00 a.m. - 5:30 p.m. Authors are to be present at their poster session in either the morning or afternoon session as noted in above schedule. Please take down posters at the end of the day. Poster board sizes are approximately 4' x 8'.